

# Development and Validation of the REMP and OO-REMP Hybrid Perturbation Theories

## Dissertation

der Mathematisch-Naturwissenschaftlichen Fakultät  
der Eberhard Karls Universität Tübingen  
zur Erlangung des Grades eines  
Doktors der Naturwissenschaften  
(Dr. rer. nat.)

vorgelegt von  
M.Sc. Stefan Behnle  
aus Filderstadt

Tübingen  
2023

Gedruckt mit Genehmigung der Mathematisch-Naturwissenschaftlichen Fakultät der  
Eberhard Karls Universität Tübingen.

Tag der mündlichen Qualifikation:	17.07.2023
Dekan:	Prof. Dr. Thilo Stehle
1. Berichterstatter:	Prof. Dr. Reinhold F. Fink
2. Berichterstatter:	Prof. Dr. Holger F. Bettinger
3. Berichterstatter:	Prof. Dr. Thorsten Klüner

## Erklärung

Ich erkläre hiermit,

- dass ich die zur Promotion eingereichte Arbeit mit dem Titel: „Development and Validation of the REMP and OO-REMP Hybrid Perturbation Theories“ selbständig verfasst, nur die angegebenen Quellen und Hilfsmittel benutzt und wörtlich oder inhaltlich übernommene Stellen als solche gekennzeichnet habe,
- dass die Richtlinien zur Sicherung guter wissenschaftlicher Praxis der Universität Tübingen (Beschluss des Senats vom 25.5.2000) beachtet wurden,
- dass die eingereichte Arbeit weder vollständig noch in wesentlichen Teilen Gegenstand eines anderen Prüfungsverfahrens gewesen ist,
- dass die vorgelegte Dissertation weder vollständig noch teilweise veröffentlicht wurde,
- dass ich zum Zeitpunkt des Zulassungsantrags an keiner anderen Universität im Promotionsfach als Doktorand angenommen bin.

Ich versichere an Eides statt, dass diese Angaben wahr sind und dass ich nichts verschwiegen habe. Mir ist bekannt, dass die falsche Abgabe einer Versicherung an Eides statt mit Freiheitsstrafe bis zu drei Jahren oder mit Geldstrafe bestraft wird.

Tübingen, den 27.02.2023

---

Stefan Behnle

„Wer es einmal so weit gebracht  
hat, daß er nicht mehr irrt, der  
hat auch zu arbeiten aufgehört.“

---

*(Max Planck)*



## Zusammenfassung

In dieser Arbeit werden die hybriden Störungstheorien REMP und OO-REMP zur Berechnung der elektronischen Korrelationsenergie von Atomen und Molekülen eingeführt und validiert. Es handelt sich dabei um quantenchemische Methoden im Formalismus der Rayleigh-Schrödinger-Störungstheorie, für die hier die Energie 2. Ordnung untersucht wird. Basierend auf den Partitionierungen der Møller-Plesset- (MP) und der Anregungsgraderhaltenden Störungstheorie (Retaining the excitation Degree=RE) wird ein ungestörter Hamiltonoperator mit zugehörigem Störoperator definiert, der sich aus einer gewichteten Summe der vorgenannten Methoden zusammensetzt, wodurch die REMP-Methode definiert ist. Die neuartige Partitionierung nutzt komplementäre Fehler der zugrunde liegenden Methoden zur internen Fehlerkompensation. In dieser Arbeit werden Energien bis zur 2. Ordnung der Störungstheorie untersucht. Es wird gezeigt, dass die REMP-Partitionierung des elektronischen Hamiltonoperators zu systematisch besseren Ergebnissen führt als jede der Einzelmethoden allein, wobei die Parametrisierung der Mischung universell und praktisch systemunabhängig ist. Dies wird am Beispiel unterschiedlicher Typen von Reaktionsenergien und Gleichgewichtsstrukturen, Schwingungswellenzahlen und elektrischen Dipolmomenten kleiner Moleküle demonstriert. Es wird außerdem ein variationelles Energiefunktional definiert, das auf der Hybridpartitionierung basiert. Dabei wird die Form der besetzten Molekülorbitale variiert und so optimiert, dass die Gesamtenergie minimal wird. Die Minimierung dieses Funktionalen bezüglich aller variationellen Parameter liefert Ergebnisse, die die der kanonischen Methode systematisch übertreffen. Die vollständig variationelle Methode zeichnet sich zudem durch hervorragende rechnerische Effizienz bei der Vorhersage molekularer Eigenschaften aus. Es wird gezeigt, dass insbesondere die vollständig variationelle, orbitaloptimierte Variante (OO-REMP) den Kriterien allgemein anwendbarer Quantenchemiemethoden genügt und hochgenaue Ergebnisse produziert. Die Validierungen legen nahe, dass OO-REMP für single-reference-Systeme für die meisten Thermochmie-Testsätze chemische Genauigkeit erreicht (Root mean square-Fehler  $\leq 1$  kcal mol<sup>-1</sup>). Die neu entwickelten Methoden wurden in ein quelloffenes Quantenchemieprogramm implementiert und stehen nun jedermann zur Verfügung.

## Abstract

In this work, the hybrid perturbation theories REMP and OO-REMP for the calculation of electronic correlation energies of atoms and molecules are introduced and validated. These are quantum chemical methods in the framework of Rayleigh-Schrödinger perturbation theory, whose second order energy is investigated here. Based on the partitionings of the Møller-Plesset (MP) and the Retaining the Excitation Degree (RE) perturbation theory, an unperturbed Hamiltonian with a corresponding perturbation operator is defined, which is a weighted sum of the previous methods, thereby defining the REMP method. The novel partitioning has the property to exploit complementary errors of the parent methods for internal error compensation. In this work, energies up to 2<sup>nd</sup> order in perturbation theory are investigated. It is shown that the REMP partitioning of the electronic Hamiltonian leads to systematically better results than each of the original methods, with the important aspect that the parameterization of the mixture is universal and practically independent of the system considered. This is demonstrated with the example various types of reaction energies and equilibrium structures, vibrational wavenumbers, and electric dipole moments of small molecules. Furthermore, a variational energy functional based on the hybrid partitioning is defined. Here, the shape of the occupied molecular orbitals is varied and optimized such, that the total energy becomes minimal. The minimization of this functional with respect to all variational parameters provides results which systematically surpass those of the canonical method. The fully variational method is furthermore characterized by outstanding computational efficiency regarding the prediction of molecular properties. It is shown that especially the fully variational, orbital-optimized variant suffices the criteria of a generally applicable quantum chemical method and does produce highly accurate results. The validations imply that for single-reference systems OO-REMP reaches chemical accuracy (root mean square error  $\leq 1$  kcal mol<sup>-1</sup>) for most of the thermodynamic test sets. The newly developed methods were implemented in an open-source quantum chemistry program package and are now available to everyone.

# Contents

<b>1</b>	<b>Introduction</b>	<b>1</b>
<b>2</b>	<b>Theory</b>	<b>5</b>
2.1	Rayleigh-Schrödinger Perturbation Theory (RSPT)	5
2.2	Configuration State Functions and Their Importance	7
2.3	Normal Order	10
2.4	The Retaining the Excitation Degree PT	11
2.5	The Møller-Plesset PT	17
2.6	The REMP Hybrid Hamiltonian	21
2.7	The Orbital-optimized REMP (OO-REMP) Ansatz	26
2.7.1	Perturbative singles	33
2.8	Analytical Gradients for OO-REMP	34
2.9	Comparison to Other Parameterized Wavefunction Methods	34
2.9.1	Variants of CEPA	34
2.9.2	pCCSD	35
2.9.3	PCPF-MI	35
2.9.4	CCD0	36
2.9.5	Feenberg Scaling	36
2.9.6	OMP2.X	36
2.9.7	$\kappa$ -OMP2	37
2.9.8	Other $\mathcal{O}(n^5)$ and $\mathcal{O}(n^6)$ methods	37
<b>3</b>	<b>Results</b>	<b>39</b>
3.1	Recovered Correlation Energies	39
3.2	Thermochemistry	50
3.3	Noncovalent Interactions	56
3.3.1	The RG18 Benchmark Set	56
3.3.2	The A24 Benchmark Set	60
3.3.3	The O23 Benchmark Set	69
3.3.4	The S22 Benchmark Set	73
3.4	Reaction Energies of Metal-organic Reactions	78
3.5	Equilibrium Structures of Small Molecules	83
3.6	Harmonic Vibrational Frequencies of Small Molecules	88
3.7	Dipole Moments of Small Molecules	91
3.7.1	Main Group Element Molecules	91
3.7.2	A Transition Metal Element Molecule	94
3.8	Performance Summary for Different Properties	98

---

<b>4</b>	<b>Conclusion and Outlook</b>	<b>101</b>
<b>5</b>	<b>List of Papers, Posters, and Talks</b>	<b>105</b>
	<b>Bibliography</b>	<b>107</b>
<b>6</b>	<b>Appendix</b>	<b>128</b>
6.1	Derivation of the OO-REMP working equations . . . . .	128
6.2	Tables . . . . .	142
6.2.1	Tables for the RG18 benchmark set . . . . .	142
6.2.2	Tables for the A24 benchmark set . . . . .	144
6.2.3	Tables for the O23 benchmark set . . . . .	146
6.3	Paper Appendices . . . . .	148

# 1 Introduction

For all but the most simple model systems, the equations which govern the movement of quantum particles – the Dirac equation or the Schrödinger equation – represent many particle problems which cannot be solved exactly analytically in a useful way.<sup>[1–4]</sup> Still chemists and physicists are interested in approximate solutions of these equations as they allow in principle to compute and predict the behaviour of all matter that surrounds us. While solving these equations, one therefore inevitably has to introduce approximations with varying accuracy. Specifically, theoretical chemistry and routine computational chemistry rely on a hierarchy of approximations, which are valid in most cases and whose errors can be estimated and controlled.

When dealing with molecules, the first step is to disentangle the translational and rotational degrees of freedom in the laboratory frame from the internal coordinates.<sup>[5–8]</sup> The total wavefunction can then be expanded in the Born-Huang ansatz<sup>[8]</sup> which involves the complete manifold of electronic states. Discarding the coupling matrix elements between different electronic states – which is justified if they are energetically well separated – leads to the adiabatic approximation and thus to the notion that the nuclei move on a single potential energy surface, but this surface still depends on the nuclear masses.<sup>[6,7]</sup> If also the diagonal corrections – that depend on the nuclear masses – are discarded, one ends up with the famous Born-Oppenheimer approximation,<sup>[5,7,9–11]</sup> where the nuclei move on an electronic potential energy surface that is independent of the nuclear masses. At this stage, the electronic and nuclear motion is completely decoupled. Typically, the nuclei are also not treated as quantum objects anymore but as classical point charges that are fixed in space. Most often, the nuclear spin – if present – is also discarded. The Born-Oppenheimer approximation is one of the cornerstones of theoretical chemistry as it is the most radical way to separate the total wavefunction into disjoint parts for electrons and nuclei, giving rise to the concept of potential energy surfaces and molecular structures.

When starting from a fully relativistic treatment – the Dirac equation<sup>[12,13]</sup> – the approximation that is usually invoked first is that a full four-component treatment is not necessary. By transforming away the "positronic" degrees of freedom, which essentially corresponds to discarding the small component,<sup>[14–16]</sup> one arrives at two-component formalisms which often give excellent results at greatly reduced cost and complexity compared to a four-component treatment. The most drastic approximation concerning relativistic interactions consists in totally discarding relativity by taking the limit of  $c \rightarrow \infty$  upon which one arrives at the Schrödinger equation with a one-component wavefunction. There are then various ways of reintroducing relativity<sup>[7,14,15,17]</sup> e.g. at a perturbative level.<sup>[18–20]</sup>

The third approximation usually applied is that the vast majority of quantum chemi-

cal calculations is performed in a finite set of atom-centered atomic-orbital like basis functions.<sup>[7,17,21,22]</sup> This finite basis set itself represents a systematic approximation which makes quantum-chemical calculations feasible in the first place. At this point, the approximations introduced are already so severe that absolute energies calculated from a single basis set deviate significantly from the true total energy, and applicability is only enabled by error compensation. The exact numerical solution to the Schrödinger equation in a finite basis set can be obtained by the Full Configuration Interaction (FCI) method.<sup>[21,23–25]</sup> FCI however has the drawback that its computational cost still scales exponentially with the system size and is thus only applicable to small molecules and small basis sets.<sup>1</sup> It is therefore necessary to invoke further approximations which allow for an approximate solution of the electronic Schrödinger equation. At this point, one commonly distinguishes between first-principles methods like density functional theory<sup>[31–33]</sup> (DFT) and wavefunction-based *ab initio* methods. Wavefunction-based methods are more rigorous and are typically systematically improvable, sometimes leading to FCI in the ultimate case. In the remaining part of this work DFT will only be used for comparing results.

In many cases, yet another approximation is invoked, namely that a single Slater determinant formed from occupied orbitals (the "reference determinant") provides a qualitatively correct zeroth order description of the system under investigation.<sup>[7,17,21]</sup> The molecular orbitals of this wavefunction are optimized by minimizing its energy expectation value, leading to a Hartree-Fock wavefunction.<sup>[34,35]</sup> Such a wavefunction obeys the Pauli exclusion principle but essentially neglects the correlated motion of the electrons. Instead, it averages out the positions of the other electrons from the point of view of a certain electron. Such a mean-field wavefunction is systematically too high in energy compared to the FCI wavefunction. The energy difference between the energy of a single Slater determinant and the FCI energy is called the *correlation energy*. For accurate prediction of energies and properties, it is absolutely mandatory to recover as much correlation energy and the most important corrections to the wavefunction as possible.

In the realm of the wavefunction methods, the three most commonly encountered approaches to treat the correlation problem are truncated Configuration Interaction (CI), Coupled Cluster Theory (CC) and Perturbation Theory (PT).<sup>[17]</sup> While the former two make use of the complete (Born-Oppenheimer, nonrelativistic) Hamiltonian and ultimately converge to FCI, convergence is not guaranteed for perturbation theory when applied to the electronic correlation problem.

(Rayleigh-Schrödinger) perturbation theory inherently requires further assumptions for partitioning the Hamiltonian into "genuine" and "perturbative" constituents, their attribution being arbitrary and dependent on the design of the method. In other words, one has to decide which constituents are so important that one wants to treat them exactly in the zeroth order solution, and which constituents are less important so that they can be

---

<sup>1</sup>It should be mentioned that there has been considerable effort to construct efficient approximation to FCI like Quantum Monte Carlo FCI<sup>[26–28]</sup> or the ICE-CI approach.<sup>[29,30]</sup>

---

considered to merely be a perturbation compared to the unperturbed part. An important consideration when setting up a partitioning is that the unperturbed problem, i.e. the Schrödinger equation defined by the Hamiltonian of the unperturbed system  $\hat{H}^{(0)}$  has to be solved exactly. The choice of  $\hat{H}^{(0)}$  is therefore strongly limited due to these technical considerations.

The two perturbation theories that constitute the basis for the set of methods investigated in this work are the Møller-Plesset perturbation theory<sup>[36]</sup> (MP-PT, the most established and simple practical member of this kind of methods) and the Retaining the Excitation Degree perturbation theory<sup>[37]</sup> (RE-PT, the most complete useful perturbation theory for the correlation problem). MP and RE differ in the way the two-electron repulsion is partitioned between  $\hat{H}^{(0)}$  and the perturbation  $\hat{H}^{(1)}$ : MP only retains a bare minimum of the two-electron interaction in  $\hat{H}^{(0)}$ , while RE preserves as much as possible (See Sections 2.4 and 2.5 for their respective definitions). The methods investigated here lie in a continuous, smooth range between 100 % MP and 100 % RE, and the results therefore shed some light on the question “how important are different parts of the Hamiltonian for a given target accuracy?” Specifically, a hybrid unperturbed Hamiltonian consisting of a constrained linear combination of the RE and MP counterparts is proposed, which is called the REMP Hamiltonian. Such a hybrid partitioning necessarily implies the approximation inherent to perturbation theory, namely that certain parts of the Hamiltonian are not treated exactly. It furthermore requires the introduction of an additional empirical mixing parameter which smoothly switches between RE and MP by specifying their respective amount in the unperturbed Hamiltonian and the perturbation. Although these assumptions and approximations might seem drastic at first glance, they are not uncommon in the framework of perturbation theory. The Hamiltonian may be partitioned in any reasonable way, and the proposed method will still be a fully-fledged wavefunction method, in contrast to other empirical scaling schemes, which often sacrifice the existence of a proper wavefunction itself or the possibility to obtain higher-order corrections. Additionally, the hybrid partitioning inherits all favourable basic properties of the pure methods, namely that it is rigorously size consistent, size extensive and unitary invariant with respect to rotations within the frozen, correlated occupied and virtual orbitals. As will be shown below, the mixing will come at virtually no additional computational cost compared to the more expensive component (RE) alone. The effect of the mixing parameter at a first-order wavefunction level is twofold: first of all, it balances the treatment of the double excitations of the two perturbation theories. Secondly, it mimics the effects of higher than double excitations on the wavefunction. These excitations would enter the wavefunction at higher orders in perturbation theory and will then directly or indirectly couple to the double excitations. An ideal choice of the mixing parameter will try to approximate the effect of higher-order corrections at the first-order wavefunction level.

The quality of the first-order wavefunction and second order energy can further be improved by iteratively optimizing the orbitals of the reference wavefunction. The unperturbed wavefunction is typically obtained by a mean-field approach (Roothaan-Hall-Hartree-Fock

in the single reference case, MCSCF in a multiconfigurational approach), and is thus often flawed. Better reference wavefunctions and better overall results can be obtained by relaxing the reference under the influence of correlation. This approach termed orbital optimization has been established for a variety of methods.<sup>[38–46]</sup> The inclusion of orbital optimization often turns nonvariational methods into variational ones, thereby greatly simplifying the calculation of properties. It will be demonstrated in this work that the combination of orbital optimization with a hybrid perturbative scheme which mimics higher orders of perturbation theory and higher excitations leads to a method with exceptional predictive power.

In the following, the accuracy of the newly proposed methods are carefully investigated and compared to results of methods with similar or higher computational cost or to experimental data. As quantum chemical methods primarily give access to energies, thermochemical properties were benchmarked with particular care (Sections 3.2 and 3.4). On the other hand, as there is also demand for methods which provide high accuracy for molecular properties at reasonable computational cost, the newly developed methods were validated with respect to molecular equilibrium structures (Section 3.5), harmonic vibrational frequencies (Section 3.6), and static electric dipole moments (Section 3.7).

The method proposed in this work differs from previously proposed approaches in a number of aspects. In contrast to SCS-MP2<sup>[47]</sup> or other *ad hoc* methods, REMP is a fully-fledged perturbation theory and not just an energy recipe. This means that it is in principle possible to calculate energy and wavefunction corrections up to arbitrary orders.<sup>[48]</sup> Compared to other parameterized methods, REMP also features a smaller number of empirical parameters, namely just one, which can unambiguously explained. At least in the case of the orbital-optimized variant, there is also no ambiguity regarding the size of the parameter, instead, there is just a small interval of the parameter space which performs well for various benchmark cases. This is again in contrast to SCS-MP2 where different parameters for different applications were proposed. Comparing pairs of canonical and orbital-optimized methods, one invariably finds that OO-REMP outperforms REMP, contrary to e.g. (OO-)MP2<sup>[43]</sup> or (OO-)CCD/CCSD,<sup>[49]</sup> where the iterative optimization of the occupied orbitals often leads to only mediocre improvements. Section 3.8 summarizes the results of the validations presented in this work and References [50–53] and extracts general estimates for the accuracy reached for the investigated properties. These are put in context with those of other Quantum Chemical methods. Section 6.3 contains complete reprints of the accepted publications related to this work.



## 2 Theory

Throughout this work, the commonly used indexing convention for spin orbitals are used, i.e.  $i, j, k, l$  indicate occupied spin orbitals,  $a, b, c, d$  indicate virtual spin orbitals and  $p, q, r, s$  indicate general spin orbitals (occupied and virtual). The nuclear repulsion  $\widehat{V}_{\text{NN}}$  is ignored throughout this section. The energies are only electronic energies and the nuclear repulsion  $E_{\text{nuc}} = \sum_{I>J} \frac{Z_I Z_J}{r_{IJ}}$  is added at the end to obtain total energies.

The starting point for the construction of the partitioning is the Hamiltonian in second quantization<sup>[54,55]</sup>

$$\widehat{H} = \sum_{pq} h_{pq} \hat{a}_p^\dagger \hat{a}_q + \frac{1}{2} \sum_{pqrs} \langle pq|rs \rangle \hat{a}_p^\dagger \hat{a}_q^\dagger \hat{a}_s \hat{a}_r, \quad (2.1)$$

where  $h_{pq}$  is a matrix element of the one-electron operator (electron kinetic energy and nucleus-electron attraction) in the MO basis,  $\langle pq|rs \rangle$  is a two-electron repulsion integral in Dirac notation, and  $\hat{a}_p^\dagger$  &  $\hat{a}_p$  are electron creation and annihilation operators for spin orbital  $p$ . There is in principle an infinite number of ways how the Hamiltonian in Eq. (2.1) may be partitioned into an unperturbed Hamiltonian and a perturbation, but only few of them lead to actually useful methods.

### 2.1 Rayleigh-Schrödinger Perturbation Theory (RSPT)

Application of Rayleigh-Schrödinger perturbation theory (RSPT) requires a partitioning of the Hamiltonian  $\widehat{H}$  whose eigenfunctions are to be found into an unperturbed part  $\widehat{H}^{(0)}$  (the unperturbed or 0<sup>th</sup> order Hamiltonian) and a perturbation  $\widehat{H}^{(1)}$ <sup>1</sup>

$$\widehat{H} = \widehat{H}^{(0)} + \lambda \widehat{H}^{(1)}, \quad (2.2)$$

where the parameter  $\lambda$  is a measure for the strength of the perturbation.

The (time-independent) Schrödinger equation for the unperturbed Hamiltonian has to be solved exactly

$$\widehat{H}^{(0)} |\Psi_i^{(0)}\rangle = E_i^{(0)} |\Psi_i^{(0)}\rangle, \quad (2.3)$$

---

<sup>1</sup>under certain circumstances, e.g. if there is more than one perturbation, or if there is a perturbation that is not linear in  $\lambda$ , another perturbation,  $\widehat{H}^{(2)}$  is necessary.<sup>[7]</sup> In the context of electronic correlation, only the case  $\lambda = 1$  is considered and a separation of the perturbation thus irrelevant.

i.e. for  $\hat{H}^{(0)}$  the eigenfunction of interest  $|\Psi_i^{(0)}\rangle$  and the corresponding eigenvalues  $E_i^{(0)}$  have to be determined.

The solutions for the total Schrödinger equation and the associated energies are expanded in terms of a power series in the perturbation strength parameter  $\lambda$ <sup>[48,56–58]</sup>

$$|\Psi_i\rangle = \sum_{n=0}^{\infty} \lambda^n |\Psi_i^{(n)}\rangle \quad (2.4)$$

$$E_i = \sum_{n=0}^{\infty} \lambda^n E_i^{(n)} \quad (2.5)$$

$$(\hat{H}^{(0)} + \lambda \hat{H}^{(1)})|\Psi_i\rangle = E_i |\Psi_i\rangle \quad (2.6)$$

$$(\hat{H}^{(0)} + \lambda \hat{H}^{(1)}) \sum_{n=0}^{\infty} \lambda^n |\Psi_i^{(n)}\rangle = \sum_{n=0}^{\infty} \lambda^n E_i^{(n)} \sum_{n=0}^{\infty} \lambda^n |\Psi_i^{(n)}\rangle \quad (2.7)$$

expansion and sorting in different powers of  $\lambda$  and division by them yields

$$\lambda^0 : \quad \hat{H}^{(0)}|\Psi_i^{(0)}\rangle = E^{(0)}|\Psi_i^{(0)}\rangle \quad (2.8)$$

$$\lambda^1 : \quad \hat{H}^{(0)}|\Psi_i^{(1)}\rangle + \hat{H}^{(1)}|\Psi_i^{(0)}\rangle = E^{(1)}|\Psi_i^{(0)}\rangle + E^{(0)}|\Psi_i^{(1)}\rangle \quad (2.9)$$

$$\lambda^2 : \quad \hat{H}^{(0)}|\Psi_i^{(2)}\rangle + \hat{H}^{(1)}|\Psi_i^{(1)}\rangle = E^{(2)}|\Psi_i^{(0)}\rangle + E^{(1)}|\Psi_i^{(1)}\rangle + E^{(0)}|\Psi_i^{(2)}\rangle \quad (2.10)$$

⋮

$$\lambda^n : \quad \hat{H}^{(0)}|\Psi_i^{(n)}\rangle + \hat{H}^{(1)}|\Psi_i^{(n-1)}\rangle = \sum_{m=0}^n E^{(m)}|\Psi_i^{(n-m)}\rangle \quad (2.11)$$

These equations can further be reordered to bring all terms in the same order of the wavefunction to the same side

$$(\hat{H}^{(0)} - E^{(0)})|\Psi_i^{(0)}\rangle = 0 \quad (2.12)$$

$$(\hat{H}^{(0)} - E^{(0)})|\Psi_i^{(1)}\rangle = -(\hat{H}^{(1)} - E^{(1)})|\Psi_i^{(0)}\rangle \quad (2.13)$$

$$(\hat{H}^{(0)} - E^{(0)})|\Psi_i^{(2)}\rangle = -(\hat{H}^{(1)} - E^{(1)})|\Psi_i^{(1)}\rangle + E^{(2)}|\Psi_i^{(0)}\rangle \quad (2.14)$$

Furthermore, a normalized unperturbed wavefunction and intermediate normalization  $\langle \Psi | \Psi^{(0)} \rangle = 1$  are generally imposed. This gives a complete set of equations for the determination of arbitrary orders of energy and wavefunction corrections. Left-projection of Eq. (2.12) with  $\langle \Psi_i^{(0)} |$  recovers the equation for the zeroth order energy and wavefunction. Left-projection of Eq. (2.13) with  $\langle \Psi_i^{(0)} |$  yields an equation for the determination of the first order energy correction  $E^{(1)}$  while left-projection with  $\langle \Psi_i^{(1)} |$  yields the equation for the (iterative) determination of the first order wavefunction correction  $|\Psi_i^{(1)}\rangle$ .

The total wavefunction takes the form

$$|\Psi_i\rangle = |\Psi_i^{(0)}\rangle + \sum_{n=1}^{\infty} \lambda^n |\Psi_i^{(n)}\rangle, \quad (2.15)$$

i.e. it is typically *not* normalized, instead, as  $|\Psi_i^{(0)}\rangle$  is normalized, such a wavefunction is called to possess *intermediate normalization*.

Until now, no assumptions for the form of the wavefunction corrections were made. It is common practice to expand the wavefunction corrections in terms of the excited-state solutions of  $\hat{H}^{(0)}$ . This is especially useful in the case of single-reference electronic structure methods. The unperturbed wavefunction is typically chosen as a single Slater determinant and the wavefunction corrections are expanded in linear combinations of singly, doubly etc. excited Slater determinants or CSFs thereof relative to the reference Slater determinant.

## 2.2 Configuration State Functions and Their Importance

Configuration State Functions (CSFs) are  $n$ -electron wavefunctions that are eigenfunctions of both the  $\hat{S}^2$  and the  $\hat{S}_z$  operator.<sup>[59]</sup> This is in contrast to plain Slater determinants, which are typically eigenfunctions of the  $\hat{S}_z$  operator but not necessarily of  $\hat{S}^2$ , as soon as unpaired electrons are present. Specifically, the components of  $M_S < S$  and  $M_S > -S$  can only be represented by linear combinations of Slater determinants, and the same holds for all open shell singlet states.

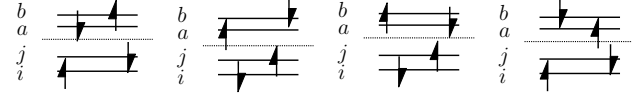
In the context of a perturbation theoretical treatment of the electronic correlation problem, the first order interacting space (FOIS) typically consists of double excitations relative to the reference wavefunction. The most simple case is that the reference is a single closed shell determinant. The FOIS then consists of doubly excited states, and there are at most four unpaired electrons. In general, four unpaired electrons in eight spin orbitals give rise to in total  $\binom{8}{4} = 70$  determinants or CSFs. There are 6 closed shell determinants (no unpaired electrons), yielding 6 singlet states, 48 determinants with two open shells, yielding 12 singlets and 12 triplets, and 16 determinants with four open shells, yielding 1 quintet, 3 triplets and 2 singlets.

As the excited states describing correlation have to preserve the space and spin symmetry of the reference, of all these states of different multiplicity, only the singlet states are relevant here.

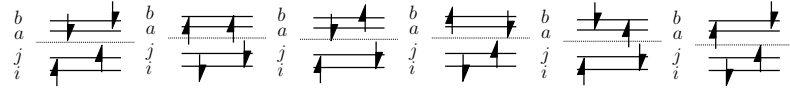
When the Serber CSFs<sup>[59–62]</sup> are employed, the singlet-excited states with up to four open shells are classified into two distinct groups

**Singlet-coupled double excitations (SDE):**

$$\Phi_{ij,S}^{ab} = \frac{1}{2\sqrt{(1+\delta_{ij})(1+\delta_{ab})}} \left( \Phi_{ij}^{\bar{a}b} + \Phi_{ij}^{a\bar{b}} - \Phi_{ij}^{\bar{a}\bar{b}} - \Phi_{ij}^{a\bar{a}} \right) \quad (2.16)$$

**Triplet-coupled double excitations (TDE):**

$$\Phi_{ij,T}^{ab} = \frac{1}{\sqrt{12}} \left( 2\Phi_{ij}^{\bar{a}\bar{b}} + 2\Phi_{ij}^{ab} + \Phi_{ij}^{\bar{a}b} + \Phi_{ij}^{a\bar{b}} + \Phi_{ij}^{\bar{a}\bar{a}} + \Phi_{ij}^{a\bar{a}} \right). \quad (2.17)$$



The names Singlet-coupled double excitations (SDE) and Triplet-coupled double excitations (TDE) arise from the spin-coupling pattern of the involved determinants. The SDEs only contain determinants where the electrons in the orbitals  $i$  and  $j$  are coupled to an  $s = 0$ ,  $m_s = 0$  state, and the signs in the linear combination also couple them to an overall singlet (with fixed  $a/b$  spin). In contrast, the TDEs additionally contain such determinants where the electrons in the occupied and virtual orbitals separately are coupled to a triplet state ( $m_s = 1/ -1$ , the first two determinants). The remaining determinants are also coupled similarly to an  $m_s = 0$  triplet state, while the total linear combination makes this CSF a singlet configuration. The constituting determinants are also depicted below Eqs. (2.16) and (2.17). Although consisting of the same determinants, it has to be noted that the SDE and TDE belonging to a certain  $i, j, a, b$  tuple are mutually orthogonal by construction. The cases where  $i = j$  and/or  $a = b$  are SDEs, so that there are in total more SDEs than TDEs.

In the context of correlated calculations, it is often important to distinguish between these kinds of double excitations. It has been shown that they obey different electron-electron Kato cusp conditions:<sup>[63,64]</sup> The SDE has a cusp in the wavefunction at any point in space where the interelectronic distance  $r_{12}$  becomes zero, and hence has a discontinuous first derivative (Coulomb hole, Eq. (2.18)), while the TDE vanishes if  $r_{12} = 0$  but has a cusp in the first derivative and hence a discontinuous second derivative (Fermi hole, Eq. (2.19))<sup>[63,65–71]</sup>

$$\lim_{r_{12} \rightarrow 0} \frac{1}{\Phi_S} \left( \frac{\partial \Phi_S}{\partial r_{12}} \right) = \frac{1}{2} \quad (2.18)$$

$$\left( \frac{\partial^2 \Phi_T}{\partial r_{12}^2} \right)_{r_{12}=0} = \frac{1}{2} \left( \frac{\partial \Phi_T}{\partial r_{12}} \right)_{r_{12}=0}. \quad (2.19)$$

Double excitations are of particular importance in the context of correlated calculations. First of all, in the case of a restricted closed shell or unrestricted single reference determinant, these are the only excitations that directly enter in the calculation of the correlation energy. Knowledge of the exact doubles therefore suffices to calculate the exact (FCI) correlation energy. Second, the doubles are typically the first excitation class that enters in a perturbative treatment, and they are by far the most important class of excitations. Third, even if there are single excitations that contribute to  $E_{\text{corr}}$ , the doubles still provide an overwhelming portion of the total correlation energy.

It has been shown that the correlation energy contributions of SDEs and TDEs show a distinctly different convergence behaviour with respect to the largest angular momentum of the basis set. In detail, it was shown, that the SDEs roughly converge with  $(L+1)^{-3}$  while the TDEs converge with  $(L+1)^{-5}$  and thus faster with increasing basis set size.<sup>[68,72-74]</sup> It was furthermore shown that the amount of correlation energy that is recovered for the two CSF types is heavily dependent on the method used.<sup>[37,50,65,70,75,76]</sup> Coupled Cluster methods converge rather smoothly to the FCI limit and the fractions of SDE and TDE correlation energy recovered relative to FCI are similar.<sup>[50,70,76]</sup> Truncated CI methods generally converge slower to the FCI limit,<sup>[77,78]</sup> but there is no pronounced imbalance regarding the two kinds of double excitations.

In strong contrast, common perturbation theoretical methods like Møller-Plesset perturbation theory<sup>[36]</sup> or variants thereof like SCS-MP2,<sup>[47]</sup> Epstein-Nesbet perturbation theory<sup>[79,80]</sup> or the Retaining the Excitation Degree perturbation theory<sup>[37]</sup> exhibit significant and systematic errors if the correlation energy is decomposed into the contributions of the SDEs and TDEs separately.<sup>[50,65,70,76,81]</sup> Typically, the contributions by one CSF class are overestimated while those of the other are underestimated, leading to error compensation. This can in turn be attributed to the respective energy denominators.<sup>[70]</sup> As such, this is not a completely new finding. The energy denominator or the EN-PT, e.g., was specifically designed to remedy the shortcomings of the MP energy denominator.<sup>[82]</sup> However, if EN is analyzed in a CSF basis, the results are significantly worse than those from MP.<sup>[70]</sup>

A similar conclusion can be drawn for SCS-MP2<sup>[47]</sup> when it is reformulated in such a way that the actual wavefunction is accessible.<sup>[65,81]</sup> SCS-MP2 itself is also based on an analysis of correlation energy contributions, but of plain “singlet” (opposite-spin pairs, all determinants contributing to Eq. (2.16)) and “triplet” (same-spin pairs, the first two determinants of Eq. (2.17)) excited Slater determinants. Their correlation energy contributions are then rescaled by empirically determined scaling factors. Fink later obtained a relation between the empirical SCS parameters and proper CSF scaling parameters,<sup>[65]</sup> defining the S2-MP method and allowing to rationalize the size of the original parameters. It was further shown that carelessly choosing the SCS-MP2 scaling parameters may even lead to spin contamination of the correlated wavefunction for closed shell references. For the method proposed in this work, such artifacts are excluded by construction.

### 2.3 Normal Order

In the following section, the concept of *normal order* is heavily used. A string of creation- and annihilation operators is said to be in normal order if its expectation value with some reference state vanishes exactly. Normal order can be defined either with respect to the physical vacuum ( $|\rangle$ ) or with respect to the reference Slater determinant, also called *Fermi vacuum*<sup>[55,56]</sup><sup>2</sup>. Normal ordering is usually indicated by curly brackets  $\{\dots\}$  around a string of creation and annihilation operators or with an index N if applied to composed operators. In this text, *normal order* is used synonymous with normal order with respect to the Fermi vacuum. It is furthermore possible to define an excitation degree with respect to the choice of vacuum state for operators, diagrams or vertices. This excitation degree gives the change of the occupation number with respect to some pre-defined orbital space, typically the occupied and virtual orbitals and is marked by  $R$ . For the Fockian  $\widehat{F}$  – an effective one-electron operator – the excitation degree can take the values  $-1/0/+1$ , and for the two-electron operator  $\widehat{W}$  it can take the values  $-2/-1/0/+1/+2$ . By virtue of the definition of the vacuum, the normal ordered Hamiltonian may be defined as difference of the full electronic Hamiltonian  $\widehat{H}$  and the electronic energy of the reference state, here denoted as  $E_{\text{HF}}$  (as mentioned without the  $V_{NN}$  contribution)

$$\widehat{H}_{\text{N}} = \widehat{H} - E_{\text{HF}} \quad (2.20)$$

$$= \widehat{F}_{\text{N}} + \widehat{W}_{\text{N}}. \quad (2.21)$$

This definition can be compared to the partitioning necessary for applying Rayleigh-Schrödinger perturbation theory

$$\widehat{H} = \widehat{H}^{(0)} + \widehat{H}^{(1)} \quad (2.22)$$

$$= \widehat{F}_{\text{N}} + \widehat{W}_{\text{N}} + E_{\text{HF}}. \quad (2.23)$$

The reference energy  $E_{\text{HF}}$ , i.e. the energy of the single reference Slater determinant is obtained via

$$E_{\text{HF}} = \sum_i h_{ii} + \frac{1}{2} \sum_{ij} \langle ij || ij \rangle \quad (2.24)$$

$$= \sum_i f_{ii} - \frac{1}{2} \sum_{ij} \langle ij || ij \rangle. \quad (2.25)$$

---

<sup>2</sup>This is the terminology used by Bartlett and Shavitt; to add some confusion, Kutzelnigg and Mukherjee<sup>[83]</sup> use the terms *genuine vacuum* if  $|\rangle$  and *physical vacuum* if a Slater determinant  $\Phi$  are used as reference point, respectively.

It is furthermore possible to decompose the Fockian into various parts, namely diagonal blocks which contain the occupied-occupied and virtual-virtual blocks and the corresponding off-diagonal blocks

$$\widehat{F} = \sum_{pq} f_{pq} \hat{a}_p^\dagger \hat{a}_q \quad (2.26)$$

$$= \sum_{pq} f_{pq} \{\hat{a}_p^\dagger \hat{a}_q\} + \sum_i f_{ii} \hat{a}_i^\dagger \hat{a}_i \quad (2.27)$$

$$= \widehat{F}_N + \sum_i f_{ii}, \quad (2.28)$$

per Eq. (3.159) of Ref. [56].

$$(2.29)$$

The curly brackets introduced in Eq. (2.27) indicate that the normal-ordered product of the string of creation and annihilation operators is to be used, as noted in Section 2.3.. In an even more general form also suitable for non-canonical orbitals and for such which do not fulfill the Brillouin theorem, the normal-ordered Hamiltonian takes the form<sup>[56]</sup>

$$\begin{aligned} \widehat{H}_N = & \sum_p f_{pp} \{\hat{p}^\dagger \hat{p}\} + \sum_{i \neq j} f_{ij} \{\hat{i}^\dagger \hat{j}\} + \sum_{a \neq b} f_{ab} \{\hat{a}^\dagger \hat{b}\} \\ & + \sum_{a \neq i} f_{ai} \{\hat{a}^\dagger \hat{i}\} + \sum_{i \neq a} f_{ia} \{\hat{i}^\dagger \hat{a}\} + \frac{1}{4} \sum_{pqrs} \langle pq || rs \rangle \{\hat{p}^\dagger \hat{q}^\dagger \hat{s} \hat{r}\}. \end{aligned} \quad (2.30)$$

Eq. (2.30) introduces a shorter notation for creation and annihilation operators ( $\hat{a} = \hat{a}_a$ ,  $\hat{i}^\dagger = \hat{a}_i^\dagger$  etc.). The diagrams that make up the normal-ordered Hamiltonian are shown in Figure 2.1 together with the assigned excitation rank.<sup>[56,84]</sup>

## 2.4 The Retaining the Excitation Degree PT

The Retaining the Excitation Degree (RE) partitioning was developed in 2006 by Reinhold F. Fink.<sup>[37]</sup>

The unperturbed Hamiltonian contains all diagrams with an excitation degree/excitation rank of zero, while all other diagrams are moved to the perturbation

$$\widehat{H}^{(0)} = \widehat{F}_N^d + \widehat{W}_N^d + \underbrace{\langle 0 | \widehat{F}^d | 0 \rangle + \langle 0 | \widehat{W}^d | 0 \rangle}_{=E^{(0)}=E_{\text{ref}}} \quad (2.31)$$

$$\widehat{H}^{(1)} = \widehat{F}^o + \widehat{W}_N^o + \underbrace{\langle 0 | \widehat{W}^o | 0 \rangle}_{=E^{(1)}=0}. \quad (2.32)$$

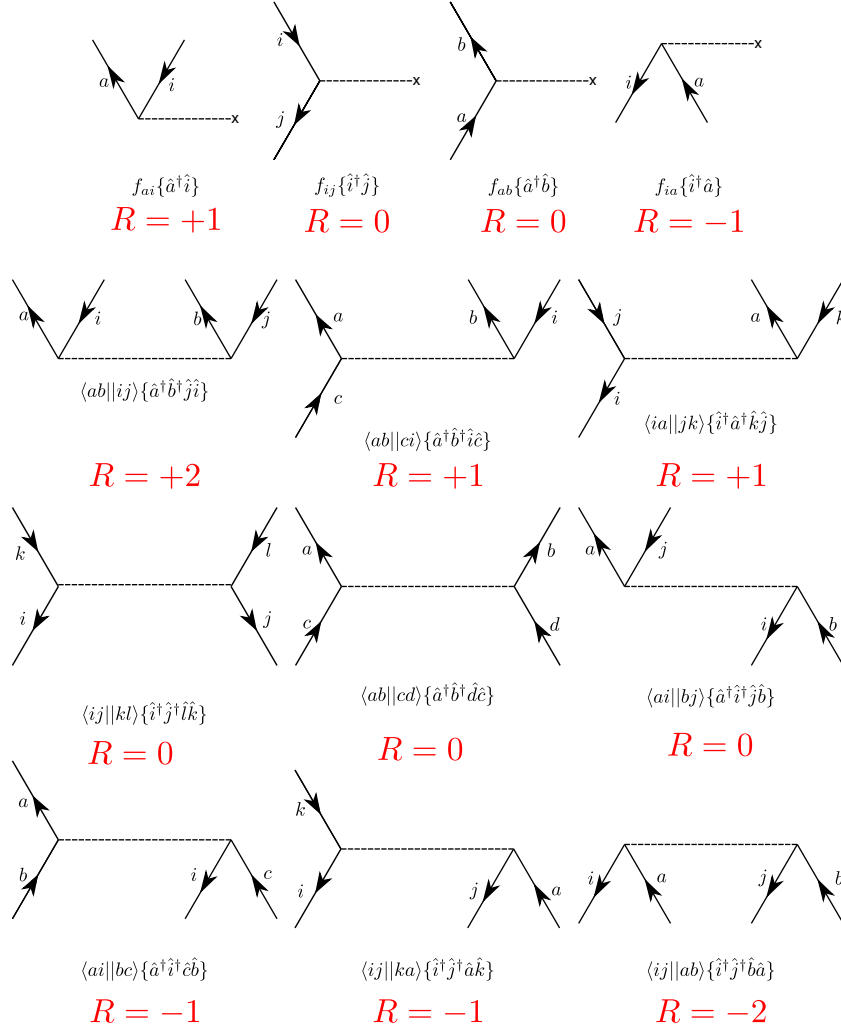


**Figure 2.1:** Antisymmetrized Goldstone diagram fragments that constitute  $\hat{H}_N$ . Given are also the translation into formulae and the excitation rank/excitation degree associated with the diagrams.

The key feature of the RE partitioning is that it includes the maximum number of terms in the unperturbed Hamiltonian as possible while still resulting in working equations where different excitation degrees are decoupled at the level of the unperturbed Hamiltonian. Adding more terms to  $\hat{H}^{(0)}$  would lead to a perturbation theory resembling a CI-type problem where various or in the extreme case all excitation degrees would then be coupled already at the zeroth-order level. This in turn would imply that the wavefunction would have to be truncated at an arbitrary excitation degree. Depending on the wavefunction ansatz, the resulting method resembles a truncated CI ansatz with a potential loss of size consistency (like e.g. CISD), size extensivity or unitary invariance (e.g. CEPA/1).<sup>[85]</sup> In other words, RE shares the property with MP that every order in perturbation theory



naturally adds two excitation degrees to the wavefunction. But in contrast to MP, the perturbers of the newly added excitation rank are fully coupled while MP leaves them uncoupled and introduces couplings only at the next order of wavefunction. RE is the only partitioning which has this property.

$\hat{H}_{\text{RE}}^{(0)}$  has furthermore the property that any Slater determinant is an eigenfunction with the eigenvalue being its expectation value with respect to the total electronic Hamiltonian

$$\hat{H}_{\text{RE}}^{(0)}|\phi\rangle = E|\phi\rangle \quad \text{with} \quad E = \langle\phi|\hat{H}|\phi\rangle. \quad (2.33)$$

In other words, the unperturbed Schrödinger equation is solved exactly by any Slater determinant. Most importantly, a Slater determinant resulting from a Hartree-Fock calculation is already an exact solution of the unperturbed Schrödinger equation, it is therefore not necessary to determine the zeroth order solution separately.

Adding any more terms from  $\hat{H}$  to  $\hat{H}^{(0)}$  would lead to a partitioning where the maximum excitation rank would have to be truncated artificially and whose zeroth order wavefunction equation would not be solved by a single Slater determinant. In other words, if there are terms in  $\hat{H}^{(0)}$  which couple different excitation ranks, then the action of  $\hat{H}^{(0)}$  on a single reference determinant will create excited determinants. The unperturbed Schrödinger equation will then assume the shape of a (truncated) CI problem, so that the maximum excitation rank in the wavefunction expansion would have to be truncated or one ends up with FCI but with an incomplete Hamiltonian. It will then also be impossible to determine the contributions by different excitation ranks of a certain wavefunction correction order separately. Truncated CI methods have the decisive drawback that they are typically neither size consistent nor size extensive. In contrast, perturbation theories that do not include terms in  $\hat{H}^{(0)}$  which couple different excitation ranks have the advantage that the highest excitation rank in the wavefunction is determined by the correction order. If one is interested only in the energy and not in the complete wavefunction, it is often possible to omit the calculation of the corrections with the highest excitation rank.<sup>3</sup> In a sense, RE is thus the most complete practical form of perturbation theory for the electronic correlation problem.

The RE Hamiltonian is also closely related to Dyalls active space Hamiltonian<sup>[82]</sup> as used e.g. in NEVPT.<sup>[86–91]</sup>

At the first order wavefunction/ second order energy, RE is actually only one possibility to derive a method which is known by many names: CEPA/0, OPT-PT, or MBPT( $\infty$ ). In the following, the derivations are sketched:

<sup>3</sup>Prominent examples would be the methods commonly called MP3 and MP4. The MP2 wavefunction belonging to the MP3 energy contains triple and quadruple excitations, but as the triples and quadruples are not coupled to the doubles necessary for calculating the correlation energy, their determination is omitted. An equal argument holds for the fourth order energy correction. Here the aforementioned triples and quadruples of the MP2 wavefunction are necessary as they influence the third order doubles, but the quintuples and hexuples of the third order wavefunction correction are discarded. The very same argument would also apply to RE.

**CEPA/0=LCCD=L-CP-MET** CEPA/0 is obtained from the full CCSD equations by neglecting certain disconnected excitations in the cluster operator that are at least quadratic in the singles excitation operator as well as terms that are quadratic in the doubles excitation operator.<sup>[46,92–97]</sup> CEPA/0(D) is then furthermore obtained by neglecting the singles entirely.

**OPT-PT** OPT-PT<sup>[98,99]</sup> is a generalized form of the Epstein-Nesbet (EN) perturbation theory<sup>[79,80]</sup> which employs level shifts to minimize the energy and give rise to vanishing third-order energy corrections. It was shown that the requirement of a vanishing third order energy leads to a second order energy which equals that of LCCD, i.e. CEPA/0(D) if a Hartree-Fock wavefunction is used as unperturbed wavefunction.

**MBPT( $\infty$ )** MBPT( $\infty$ )<sup>[100–103]</sup> arises from the summation of the correlation energy contributions of only the double excitations in the MP partitioning up to infinite order. This method only provides a correlation energy but not an associated wavefunction.

**XCC(3)** The third-order expectation value Coupled Cluster method<sup>[104]</sup> (XCC(3)) is derived from an expression of the correlation energy as an energy expectation value of a Coupled Cluster wavefunction. Different orders of energies and wavefunctions are derived starting from the normal-ordered Hamiltonian Eq. (2.21) with a partitioning that resembles the MP partitioning of Eqs. (2.42) and (2.43). The second order energy XCC(2) exactly corresponds to the MP2 energy, while the third order energy XCC(3) equals the RE2 energy. XCC differs from conventional perturbation theories insofar as the wavefunctions and energies are not solved order by order, instead, there is only one (projective) working equation per excitation degree.

But while all of these derivations are based on some arbitrary truncations or approximations, RE2 is a stringent perturbation theory leading to these working equations. Of course, the partitioning itself is arbitrary to some degree, but this is a necessity for any RSPT approach to the electron correlation problem.

The first-order wavefunction is expanded in terms of singly and doubly excited determinants relative to the reference determinant (the complete first-order interacting space of the reference determinant)

$$|\Psi^{(1)}\rangle = (\hat{T}_1^{(1)} + \hat{T}_2^{(1)})|\phi_0\rangle = \sum_{ia} t_a^i |\phi_i^a\rangle + \frac{1}{4} \sum_{ijab} t_{ab}^{ij} |\phi_{ab}^{ab}\rangle. \quad (2.34)$$

For obtaining the first-order wavefunction correction, Eqs. (2.31) and (2.32) are inserted into the first-order perturbation equation and projected from left with  $\langle\phi_i^a|$  and  $\langle\phi_{ij}^{ab}|$ , respectively. Higher excitations do not contribute to the first-order perturbation equation

if the reference is chosen as a single Slater determinant. For the single excitations, one obtains

$$\begin{aligned} \langle \phi_i^a | (\widehat{F}_N + \widehat{W}_N + \langle 0 | \widehat{F} | 0 \rangle + \langle 0 | \widehat{W} | 0 \rangle - E^{(0)}) | (\widehat{T}_1^{(1)} + \widehat{T}_2^{(1)}) \phi_0 \rangle \\ = -\langle \phi_i^a | (\widehat{F}_N + \widehat{W}_N - E^{(1)}) | \phi^{(0)} \rangle, \end{aligned} \quad (2.35)$$

where

$$\begin{aligned} E^{(0)} &= \langle 0 | \widehat{F} | 0 \rangle + \langle 0 | \widehat{W} | 0 \rangle = E_{\text{HF}}, \\ E^{(1)} &= \langle 0 | \widehat{F} | 0 \rangle + \langle 0 | \widehat{W} | 0 \rangle = 0, \end{aligned}$$

so that Eq. (2.35) becomes

$$\begin{aligned} \langle \phi_i^a | \{ \widehat{F}_N \widehat{T}_1^{(1)} \}_c | \phi_0 \rangle + \langle \phi_i^a | \{ \widehat{W}_N \widehat{T}_1^{(1)} \}_c | \phi_0 \rangle + \underbrace{\langle \phi_i^a | \{ \widehat{F}_N \widehat{T}_2^{(1)} \}_c | \phi_0 \rangle}_{=0} + \underbrace{\langle \phi_i^a | \{ \widehat{W}_N \widehat{T}_2^{(1)} \}_c | \phi_0 \rangle}_{=0} \\ = -\langle \phi_i^a | \widehat{F}_N | \phi^{(0)} \rangle - \langle \phi_i^a | \widehat{W}_N | \phi^{(0)} \rangle. \end{aligned} \quad (2.36)$$

In contrast to the Møller-Plesset first-order wavefunction, there is now also a two-electron integral diagram which couples the single excitations among each other. In total, the residuum for the first-order RE singles read thus

$$\sigma_a^{i(1)} = f_{ia} + \sum_b f_{ab} t_b^i - \sum_k t_a^k f_{ki} + \sum_{kc} t_c^k (K_{ac}^{ik} - J_{ac}^{ik}) \stackrel{!}{=} 0. \quad (2.37)$$

Eq. (2.37) is trivially solved by  $t_a^{i(1)} = 0 \forall i, a$  if the Brillouin theorem is fulfilled, i.e. if all  $f_{ia}$  are zero.

Left-projection with  $\langle \phi_{ij}^{ab} |$  yields

$$\begin{aligned} \langle \phi_{ij}^{ab} | (\widehat{F}_N + \widehat{W}_N + \langle 0 | \widehat{F} | 0 \rangle + \langle 0 | \widehat{W} | 0 \rangle - E^{(0)}) | (\widehat{T}_1^{(1)} + \widehat{T}_2^{(1)}) \phi_0 \rangle \\ = -\langle \phi_{ij}^{ab} | (\widehat{F}_N + \widehat{W}_N - E^{(1)}) | \phi^{(0)} \rangle \end{aligned} \quad (2.38)$$

$$\begin{aligned} \underbrace{\langle \phi_{ij}^{ab} | \{ \widehat{F}_N \widehat{T}_1^{(1)} \}_c | \phi_0 \rangle}_{=0} + \underbrace{\langle \phi_{ij}^{ab} | \{ \widehat{W}_N \widehat{T}_1^{(1)} \}_c | \phi_0 \rangle}_{=0} + \langle \phi_{ij}^{ab} | \{ \widehat{F}_N \widehat{T}_2^{(1)} \}_c | \phi_0 \rangle + \langle \phi_{ij}^{ab} | \{ \widehat{W}_N \widehat{T}_2^{(1)} \}_c | \phi_0 \rangle \\ = -\langle \phi_{ij}^{ab} | \widehat{F}_N | \phi^{(0)} \rangle - \underbrace{\langle \phi_{ij}^{ab} | \widehat{W}_N | \phi^{(0)} \rangle}_{=0}. \end{aligned} \quad (2.39)$$

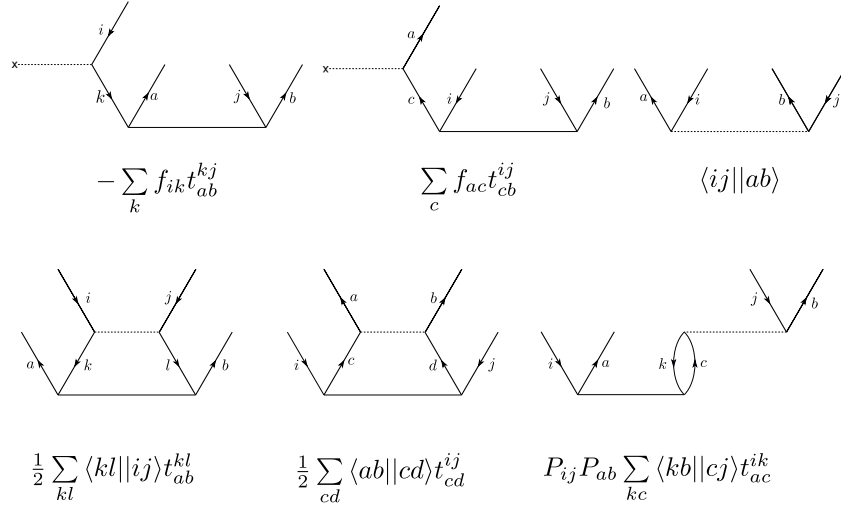


**Figure 2.2:** Diagrams which contribute to the doubles part of the first-order RE wavefunction correction.

The first two terms on the left-hand side vanish as operators with rank zero cannot couple singles to doubles without leaving open lines. The first term on the right-hand side also vanishes as the Fockian diagrams have at most rank  $\pm 1$  and thus cannot couple doubles to the reference.

The third term of the left-hand side yields two diagrams while the fourth term consists of three diagrams. The second term of the right-hand side consists of just one diagram. The three diagrams in the lower row of Figure 2.2 are also known as hole-hole-ladder, particle-particle ladder and ring diagram in coupled cluster theory. Evaluation of all diagrams of Figure 2.2 and insertion in Eq. (2.39) yields

$$\begin{aligned} \sigma_{ab,RE}^{ij} = & \langle ij || ab \rangle + \sum_c (t_{ac}^{ij} f_{bc} - t_{bc}^{ij} f_{ac}) + \sum_k (t_{ab}^{jk} f_{ik} - t_{ab}^{ik} f_{jk}) \\ & + \frac{1}{2} \sum_{kl} t_{ab}^{kl} \langle kl || ij \rangle + \frac{1}{2} \sum_{cd} t_{cd}^{ij} \langle ab || cd \rangle + P_{ij} P_{ab} \sum_{kc} t_{ac}^{ik} \langle kb || cj \rangle, \end{aligned} \quad (2.40)$$

and using  $t_{ab}^{ij} = -t_{ba}^{ij} = -t_{ab}^{ji}$  one obtains

$$\begin{aligned} \sigma_{ab,RE}^{ij} = & K_{ab}^{ij} - K_{ba}^{ij} + \sum_c (t_{ac}^{ij} f_{bc} - t_{bc}^{ij} f_{ac}) + \sum_k (t_{ab}^{jk} f_{ik} - t_{ab}^{ik} f_{jk}) + \sum_{kl} K_{kl}^{ij} t_{ab}^{kl} + \sum_{cd} K_{cd}^{ab} t_{cd}^{ij} \\ & + \sum_{kc} \left( t_{ac}^{ik} (K_{cb}^{kj} - J_{cb}^{kj}) - t_{ac}^{jk} (K_{cb}^{ki} - J_{cb}^{ki}) - t_{bc}^{ik} (K_{ca}^{kj} - J_{ca}^{kj}) + t_{bc}^{jk} (K_{ca}^{ki} - J_{ca}^{ki}) \right). \end{aligned} \quad (2.41)$$

The computational cost of the RE1 singles residuum scales as  $\mathcal{O}(o^2v^2)$  while the most expensive part of the doubles residuum (the external exchange operator<sup>4</sup>) scales as  $\mathcal{O}(o^2v^4)$ . The cost of all other parts (integral transformation ( $\mathcal{O}(on^4)$ ), amplitude update/DIIS ( $\mathcal{O}(o^2v^2)$ ) or parts of the doubles residuum scaling with  $\mathcal{O}(o^3v^3)$  or  $\mathcal{O}(o^4v^2)$ ) is negligible compared to the cost of the EEO with sufficiently complete basis sets.

The equation for calculating the energy is identical to the one used in the Møller-Plesset case (Eq. (2.57)) and is elaborated below.

## 2.5 The Møller-Plesset PT

The Møller-Plesset (MP) perturbation theory<sup>[36]</sup> employs the occupied-occupied and virtual-virtual blocks of the Fock operator (i.e. the mean-field Hamiltonian) as unperturbed Hamiltonian  $\hat{H}^{(0)}$  and the rest (the so-called “fluctuating potential”) as perturbation:

Of the diagrams in Figure 2.1, only the Fock operator diagrams with excitation rank zero, i.e. the diagrams in the middle of the topmost row enter  $\hat{H}^{(0)}$ . In a matrix representation of the Fockian, these correspond to the occupied-occupied and virtual-virtual blocks. A normal-order formulation furthermore excludes the diagonal from  $\hat{H}^{(0)}$  and introduces it by  $E_{\text{HF}}$ . The perturbation is given by all other diagrams. In the canonical RHF and UHF case, the reference determinant only interacts with double excitations, so that the only contribution in  $\hat{H}^{(1)}$  for the first-order wavefunction is given by the diagram with  $R = +2$ . All other diagrams enter only at a later stage where the double and higher excitations are coupled among themselves and with excitations of another rank. Single excitations also do not contribute to the first-order wavefunction in the RHF/UHF case by virtue of the Brillouin theorem. In the ROHF case, on the other hand, single excitations are part of the first-order wavefunction.

The total electronic Hamiltonian of Eq. (2.1) can be partitioned in the following way

$$\hat{H}^{(0)} = \hat{F}_{\text{N}}^{\text{d}} + \underbrace{\langle 0 | \hat{F}^{\text{d}} | 0 \rangle}_{E^{(0)}} \quad (2.42)$$

$$\hat{H}^{(1)} = \hat{V} = \hat{F}^{\text{o}} + \hat{W}_{\text{N}} + \underbrace{\langle 0 | \hat{W} | 0 \rangle}_{E^{(1)}}. \quad (2.43)$$

The unperturbed Hamiltonian contains only the diagonal blocks of the Fockian, i.e. those contributions with  $R = 0$ . The diagrams with  $R = \pm 1$  enter in the perturbation.

Generally, the first-order correction to the wavefunction is computed from

$$(\hat{H}^{(0)} - E^{(0)})|\Psi^{(1)}\rangle = -(\hat{H}^{(1)} - E^{(1)})|\Psi^{(0)}\rangle. \quad (2.44)$$

<sup>4</sup>The external exchange operator (EEO) is the contribution  $K[\mathbf{C}^{ij}]_{ab} = \sum_{cd} K_{cd}^{ab} t_{cd}^{ij}$  to the doubles residuum.

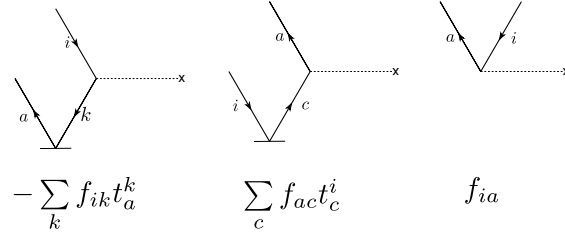


**Figure 2.3:** Diagrams contributing to the single excitations of the first-order Møller-Plesset wavefunction correction.

The reference wavefunction furthermore consists of a single restricted (RHF), restricted open shell (ROHF) or unrestricted (UHF) Slater determinant and the first order correction to the wavefunction contains double excitations at most

$$|\Psi^{(0)}\rangle = |\phi_0\rangle \quad (2.45)$$

$$|\Psi^{(1)}\rangle = (\widehat{T}_1^{(1)} + \widehat{T}_2^{(1)})|\phi_0\rangle = \sum_{i,a} t_a^i |\phi_i^a\rangle + \frac{1}{4} \sum_{ijab} t_{ij}^{ab} |\phi_{ij}^{ab}\rangle. \quad (2.46)$$

Projection from left with  $\langle\phi_i^a|$  provides the equations for determining the singles contributions to the first-order wavefunction

$$\langle\phi_i^a|(\widehat{H}^{(0)} - E^{(0)})|\Psi^{(1)}\rangle = -\langle\phi_i^a|(\widehat{H}^{(1)} - E^{(1)})|\phi^{(0)}\rangle \quad (2.47)$$

$$\langle\phi_i^a|(\widehat{F}_N + \langle 0|\widehat{F}|0\rangle - E^{(0)})|(\widehat{T}_1^{(1)} + \widehat{T}_2^{(1)})\phi_0\rangle = -\langle\phi_i^a|(\widehat{F}_N + \widehat{W}_N + \langle 0|\widehat{W}|0\rangle - E^{(1)})|\phi^{(0)}\rangle. \quad (2.48)$$

Using  $\langle 0|\widehat{F}|0\rangle = E^{(0)}$  and  $\langle 0|\widehat{W}|0\rangle = E^{(1)}$ , this can be rearranged to

$$\langle\phi_i^a|\underbrace{\{\widehat{F}_N \widehat{T}_1^{(1)}\}_c}_{=0 \text{ (excitation rank)}}|\phi_0\rangle + \langle\phi_i^a|\underbrace{\{\widehat{F}_N \widehat{T}_2^{(1)}\}_c}_{f_{ia}}|\phi_0\rangle = -\underbrace{\langle\phi_i^a|\widehat{F}_N|\phi^{(0)}\rangle}_{f_{ia}} - \underbrace{\langle\phi_i^a|\widehat{W}_N|\phi^{(0)}\rangle}_{=0}. \quad (2.49)$$

The second term on the left-hand side vanishes as there is no diagram with excitation rank zero which could couple a doubly excited to a singly excited determinant. The second term on the right-hand side of Eq. (2.49) vanishes exactly as the two-electron part of the normal-ordered Hamiltonian does not contain diagrams which could couple the reference to single excitations (there are no “bubble diagrams” in the normal-ordered Hamiltonian). The subscript  $c$  furthermore indicates that only fully connected diagrams are included, which is necessary for ensuring size-consistency.

The possible contractions of  $\widehat{T}_1^{(1)}$  with  $\widehat{F}_N$  resulting in one open hole and one open particle line are shown in Figure 2.3.

The resulting singles residuum takes the form

$$\sigma_a^{i(1)} = f_{ia} + \sum_b f_{ab} t_b^{i(1)} - \sum_k f_{ik} t_a^{k(1)} \stackrel{!}{=} 0 \quad (2.50)$$

in accordance with Reference [105].

In the case of a restricted Hartree-Fock (RHF) or unrestricted Hartree-Fock (UHF) reference, the Brillouin theorem is fulfilled, i.e. all  $f_{ia}$  are zero, and thus  $t_a^{i(1)} = 0$  trivially solves the first-order singles equation, i.e. there are no single excitations in the first-order wavefunction. The situation is different for a restricted open-shell Hartree-Fock (ROHF) reference, or for any other set of orbitals that do not fulfill the Brillouin theorem, like Kohn-Sham DFT orbitals or iteratively optimized orbitals from an orbital-optimized correlation method like OO-MP2 or OO-CCD. In the latter case, the single excitations are nevertheless mostly ignored as their inclusion would compete with the orbital optimization itself, the reason being that single excitations act as occupied-virtual rotations.<sup>[40,43,44,106]</sup>

For the doubles, one obtains after projection with  $\langle \phi_{ij}^{ab} |$  from left

$$\langle \phi_{ij}^{ab} | \left( \widehat{F}_N + \langle 0 | \widehat{F} | 0 \rangle - E^{(0)} \right) | (\widehat{T}_1^{(1)} + \widehat{T}_2^{(1)}) \phi_0 \rangle = - \langle \phi_{ij}^{ab} | \left( \widehat{F}_N + \widehat{W}_N + \langle 0 | \widehat{W} | 0 \rangle - E^{(1)} \right) | \phi^{(0)} \rangle \quad (2.51)$$

$$\underbrace{\langle \phi_{ij}^{ab} | \{ \widehat{F}_N \widehat{T}_1^{(1)} \}_c | \phi_0 \rangle}_{=0 \text{ (excitation rank)}} + \langle \phi_{ij}^{ab} | \{ \widehat{F}_N \widehat{T}_2^{(1)} \}_c | \phi_0 \rangle = - \underbrace{\langle \phi_{ij}^{ab} | \widehat{F}_N | \phi^{(0)} \rangle}_{=0 \text{ (excitation rank)}} - \underbrace{\langle \phi_{ij}^{ab} | \widehat{W}_N | \phi^{(0)} \rangle}_{=\langle ab || ij \rangle}. \quad (2.52)$$

On the left-hand side,  $\langle 0 | \widehat{F} | 0 \rangle$  and  $E^{(0)}$  again cancel identically, and due to the restriction on the excitation degree, the only surviving contraction is the one of the double excitations with the Fockian, which provides two contributions. On the right-hand side, only the  $R = +2$  diagram of  $\widehat{W}_N$  survives. The contributing contractions and their interpretation are shown in Figure 2.4

One thus obtains

$$\sigma_{ab}^{ij(1)} = K_{ab}^{ij} - K_{ba}^{ij} + \sum_c (t_{ac}^{ij(1)} f_{bc} - t_{bc}^{ij(1)} f_{ac}) + \sum_k (t_{ab}^{jk(1)} f_{ik} - t_{ab}^{ik(1)} f_{jk}) \stackrel{!}{=} 0 \quad (2.53)$$

for the MP2 doubles residuum, in accordance with Ref. [105] and [45]. Eq. (2.53) is valid for any set of orthonormal orbitals and simplifies to

$$t_{ab}^{ij} = \frac{K_{ab}^{ij} - K_{ba}^{ij}}{\varepsilon_a + \varepsilon_b - \varepsilon_i - \varepsilon_j} \quad (2.54)$$

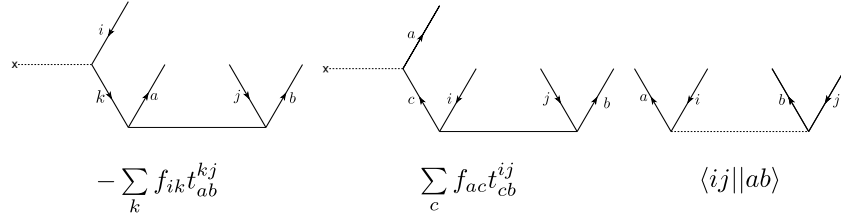


**Figure 2.4:** Diagrams which contribute to the doubles part of the first-order Møller-Plesset wavefunction correction.

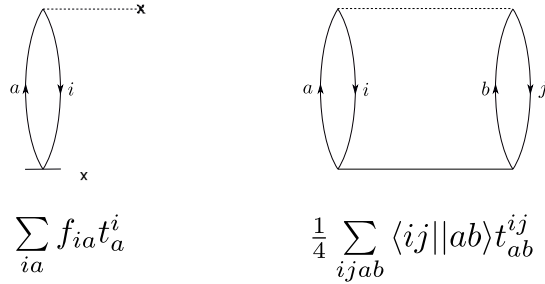


**Figure 2.5:** Diagrams which contribute to the second-order energy correction of MP and RE.

if canonical orbitals are used, i.e if the Fockian is diagonal. This simplified expression is however not applicable for localized orbitals or optimized orbitals, which also tends to introduce off-diagonal elements in the Fockian.

The summed zeroth and first order energies are given by

$$E^{[0]} = E^{(0)} + E^{(1)} = \langle 0 | \hat{H}^{(0)} | 0 \rangle + \langle 0 | \hat{H}^{(1)} | 0 \rangle = \langle 0 | \hat{H} | 0 \rangle = E_{\text{ref}}, \quad (2.55)$$

but  $E_{\text{ref}}$  drops out if normal-ordered operators are used, thus the first actual contribution is the second-order energy correction

$$E^{(2)} = \langle \Psi^{(0)} | \hat{H}^{(1)} | \Psi^{(1)} \rangle. \quad (2.56)$$

The only diagrams which contribute are those which leave no open lines when contracted with the singles and doubles of the first-order wavefunction, respectively, as shown in Figure 2.5. The (projective) second order energy correction thus amounts to

$$E^{(2)} = \sum_{i,a} f_{ia} t_a^{i(1)} + \frac{1}{4} \sum_{ijab} (K_{ab}^{ij} - K_{ba}^{ij}) t_{ab}^{ij(1)}. \quad (2.57)$$

As discussed above, the single excitations do not contribute to the correlation energy in RHF and UHF cases, but they do in case the Brillouin theorem does not hold.

Regarding the computational cost, the MP1 single excitations scale as  $o\mathcal{O}(v^2)$ , the doubles scale as  $\mathcal{O}(o^2v^3)$  for arbitrary orthonormal orbitals and as  $\mathcal{O}(o^2v^2)$  for canonical



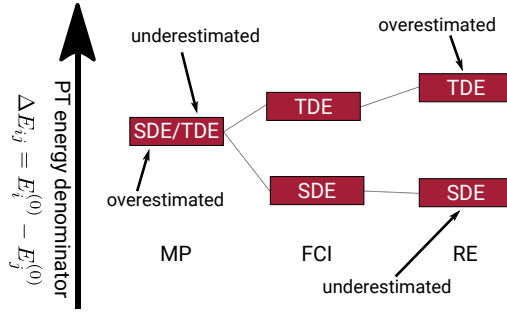


**Figure 2.6:** Schematic representation of the relative alignment of perturbation-theoretical energy denominators of MP and RE compared to back-calculated energy denominators of wavefunctions of (near-)FCI quality.

RHF/UHF orbitals. The correlation energy scales as  $\mathcal{O}(o^2v^2)$ . The most expensive part is the integral transformation step which scales as  $\mathcal{O}(on^4)$ . The computational cost of the Møller-Plesset part is thus negligible compared to that of RE.

## 2.6 The REMP Hybrid Hamiltonian

REMP<sup>[50,76]</sup> consists of a constrained mixture of the unperturbed Hamiltonians of RE (Eq. (2.31)) and MP (Eq. (2.42))

$$\hat{H}_{\text{REMP}}^{(0)} = (1 - A)\hat{H}_{\text{RE}}^{(0)} + A\hat{H}_{\text{MP}}^{(0)}. \quad (2.58)$$

The mixing or scaling parameter  $A$  is the central parameter of the REMP and OO-REMP methods. It determines the amount of Møller-Plesset-type perturbation theory in the total unperturbed Hamiltonian.

The REMP ansatz is inspired by a thorough analysis of the amount of recovered correlation energy by several perturbative wavefunction methods.<sup>[50,70,76]</sup> It was found that RE in second order often recovers more than 100 % of the correlation energy provided by singlet-coupled double excitations, while it recovers significantly less than 100 % of the correlation energy of the triplet-coupled double excitations (see also Section 2.2).

MP in second order, on the other hand, recovers only  $\approx 85\text{--}90\%$  of the SDE correlation energy while it recovers more than 100 % of the TDE correlation energy. The assumption leading to Eq. (2.58) is that a constrained mixture of both theories will lead to an internal error compensation which gives rise to better energies and wavefunctions. The underlying reason for this behavior can be found in the perturbation-theoretical energy denominators

$$\Delta E_{ij}^{ab} = -\frac{\langle \Phi_0 | \hat{H} | \Phi_{ij}^{ab} \rangle}{c_{ij}^{ab}} \quad (2.59)$$

where

$$\Phi_{ij}^{ab} \dots \quad \text{doubly excited CSF (SDE or TDE)} \quad (2.60)$$

$$c_{ij}^{ab} \dots \quad \text{coefficient of this CSF in the wavefunction} \quad (2.61)$$

are vastly different for different perturbation theories. In the Møller-Plesset case, these energy denominators are just made up from orbital energies and are therefore identical for both the SDE and the TDE of a certain  $(i, j, a, b)$  tuple. In other cases such as RE, energy denominators are not directly accessible but have to be back-calculated from the wavefunction according to Eq. (2.59). The same relation is applicable for any wavefunction method which provides CI coefficients, like truncated CI, FCI or coupled cluster. Figure 2.6 shows a schematic comparison of RE1 and MP1 wavefunction energy denominators to FCI ones. It is evident that the energy denominators of a certain  $(i, j, a, b)$  tuple have to differ for the respective SDE and TDE and that RE is already close to the true ratio but overshooting. Hybridizing RE and MP interpolates between their energy denominators and thus gives rise to better wavefunctions than each of the methods alone would achieve.

The mixing parameter  $A$  may now be tuned such that REMP in second order provides better energies and wavefunctions than any of the parent methods. The restriction to second order is not necessary but reasonable due to the already high computational cost of the second-order RE energy. Going to higher orders is possible and has been shown to be successful for the original RE approach.<sup>[37]</sup> However, the resulting methods would be of limited practical use due to the steep computational scaling.

From a comparison of Eqs. (2.31) and (2.42), the action of the mixing may be interpreted as an attenuation of the fluctuating potential in  $\hat{H}^{(0)}$ . At the first-order wavefunction level, the mixing parameter furthermore compensates for the effects of missing higher orders in perturbation theory and especially for the effect of missing singles (in the closed-shell case) and higher excitations. From the perspective of RE, the missing coupling between different excitation ranks is mimicked, from the perspective of MP, also the missing coupling within the latest added excitation rank(s) is mimicked.

The constraint on the unperturbed Hamiltonians ensures that the one-electron part is present exactly once in  $\hat{H}^{(0)}$  which is mandatory for obtaining wavefunctions which obey the Kato cusp conditions.<sup>[63,64,76]</sup> The perturbation is defined by

$$\hat{H}^{(1)} = \hat{H} - \hat{H}^{(0)} \quad (2.62)$$

Insertion of Eq. (2.62) into Eq. (2.13) and using the definitions of  $\widehat{H}_{\text{RE}}^{(0)}$  and  $\widehat{H}_{\text{MP}}^{(0)}$ , one finds for the residuum of the first-order REMP wavefunction

$$\sigma_{a,\text{REMP}}^{i(1)} = f_{ia} + \sum_b f_{ab} t_b^i - \sum_k t_a^k f_{ki} + (1-A) \cdot \sum_{kc} t_c^k (K_{ac}^{ik} - J_{ac}^{ik}) \stackrel{!}{=} 0 \quad (2.63)$$

$$\begin{aligned} \sigma_{ab,\text{REMP}}^{ij(1)} = & K_{ab}^{ij} - K_{ba}^{ij} + \sum_c (t_{ac}^{ij} f_{bc} - t_{bc}^{ij} f_{ac}) + \sum_k (t_{ab}^{jk} f_{ik} - t_{ab}^{ik} f_{jk}) \\ & + (1-A) \cdot \left( \sum_{kl} K_{kl}^{ij} t_{ab}^{kl} + \sum_{cd} K_{cd}^{ab} t_{cd}^{ij} \right. \\ & \left. + \sum_{kc} \left( t_{ac}^{ik} (K_{cb}^{kj} - J_{cb}^{kj}) - t_{ac}^{jk} (K_{cb}^{ki} - J_{cb}^{ki}) - t_{bc}^{ik} (K_{ca}^{kj} - J_{ca}^{kj}) + t_{bc}^{jk} (K_{ca}^{ki} - J_{ca}^{ki}) \right) \right). \end{aligned} \quad (2.64)$$

For closed-shell cases, Eq. (2.64) can further be simplified. The spin can be integrated out and the efficiency of the resulting equations can be improved by the use of the so-called generators of the unitary group instead of plain double excitations.<sup>[107]</sup>

The wavefunction is therefore expanded in terms of nonorthogonal CSFs

$$|\Psi\rangle = |\Phi_0\rangle + \sum_{ia} C_a^i |\Psi_a^i\rangle + \sum_{i>j} \sum_{cd} C_{ab}^{ij} |\Psi_{ab}^{ij}\rangle \quad (2.65)$$

where the singles and doubles CSFs are defined as

$$\Psi_a^i = \widehat{E}_{ia} \Phi_0 = \Phi_a^i + \Phi_{\bar{a}}^{\bar{i}} \quad (2.66)$$

$$\Psi_{ij}^{ab} = \widehat{E}_{jb} \widehat{E}_{ia} \Phi_0 = \Phi_{ij}^{ab} + \Phi_{i\bar{j}}^{\bar{a}\bar{b}} + \Phi_{\bar{i}j}^{\bar{a}\bar{b}} + \Phi_{\bar{i}\bar{j}}^{ab}, \quad i > j \quad (2.67)$$

$$\Psi_{ii}^{ab} = \Phi_{ii}^{ab}. \quad (2.68)$$

$\widehat{E}_{ia} = \hat{a}_a^\dagger \hat{a}_i + \hat{a}_{\bar{a}}^\dagger \hat{a}_{\bar{i}}$  are spin-free excitation or replacement operators,<sup>[55]</sup> and  $\Phi_a^i$  and  $\Phi_{ij}^{ab}$  are plain Slater determinants. The CSFs of Eq. (2.66)–(2.68) are partially nonorthogonal

$$\langle \Psi_{ij}^{ab} | \Psi_{ij}^{ab} \rangle = 2(2 - \delta_{ab}), \quad \langle \Psi_{ij}^{ab} | \Psi_{ij}^{ba} \rangle = 2(2\delta_{ab} - 1), \quad i > j. \quad (2.69)$$

For left-projection, “inverse” or contravariant CSFs are used

$$\widetilde{\Psi}_{ij}^{ab} = \frac{1}{6} \left( \Phi_{ij}^{ab} + \Phi_{i\bar{j}}^{\bar{a}\bar{b}} + 2\Phi_{\bar{i}j}^{\bar{a}\bar{b}} + 2\Phi_{i\bar{j}}^{\bar{a}\bar{b}} - \Phi_{i\bar{j}}^{\bar{a}\bar{b}} - \Phi_{\bar{i}j}^{\bar{a}\bar{b}} \right) \quad (i \neq j) \quad (2.70)$$

$$= \frac{1}{6} (2\widehat{E}_{jb} \widehat{E}_{ia} + \widehat{E}_{ja} \widehat{E}_{ib}) \Phi_0 \quad (2.71)$$

$$\widetilde{\Psi}_{ii}^{ab} = \Phi_{ii}^{ab} \quad (i = j) \quad (2.72)$$

$$\widetilde{\Psi}_i^a = \frac{1}{2} \left( \Phi_i^a + \Phi_{\bar{i}}^{\bar{a}} \right) = \frac{1}{2} \widehat{E}_{ia} \Phi_0. \quad (2.73)$$

The contravariant CSFs are constructed according to  $\langle \widetilde{\Psi}_I | \Psi_J \rangle = \delta_{IJ}$ , where  $I$  and  $J$  are composite orbital indices.

In detail, the generation of the contravariant CSFs works as follows

$$\begin{aligned}
\tilde{\Psi}_{ij}^{ab} &= (2\hat{E}_{jb}\hat{E}_{ia} + \hat{E}_{ja}\hat{E}_{ib})\Phi_0 \\
&= 2(\hat{b}^+ \hat{j} + \hat{b}^+ \hat{j}) (\hat{a}^+ \hat{i} + \hat{a}^+ \hat{i}) \Phi_0 + (\hat{a}^+ \hat{j} + \hat{a}^+ \hat{j}) (\hat{b}^+ \hat{i} + \hat{b}^+ \hat{i}) \Phi_0 \\
&= 2\Phi_{ji}^{ba} + 2\Phi_{ji}^{\bar{b}a} + 2\Phi_{ji}^{b\bar{a}} + 2\Phi_{ji}^{\bar{b}\bar{a}} + \Phi_{ji}^{ab} + \Phi_{ji}^{\bar{a}b} + \Phi_{ji}^{a\bar{b}} + \Phi_{ji}^{\bar{a}\bar{b}} \\
&= 2\Phi_{ij}^{ab} + 2\Phi_{ij}^{a\bar{b}} + 2\Phi_{ij}^{\bar{a}b} + 2\Phi_{ij}^{\bar{a}\bar{b}} - \Phi_{ij}^{ab} - \Phi_{ij}^{\bar{a}b} - \Phi_{ij}^{a\bar{b}} - \Phi_{ij}^{\bar{a}\bar{b}} \\
&= \Phi_{ij}^{ab} + \Phi_{ij}^{a\bar{b}} + 2\Phi_{ij}^{\bar{a}b} + 2\Phi_{ij}^{\bar{a}\bar{b}} - \Phi_{ij}^{\bar{a}b} - \Phi_{ij}^{a\bar{b}}.
\end{aligned}$$

Collecting all necessary bits, the closed-shell REMP doubles residuum is almost identical to the CEPA/0 residuum derived by Wennmohs and Neese<sup>[96]</sup>

$$\begin{aligned}
\sigma_{ab,\text{REMP}}^{ij(1)} &= K_{ab}^{ij} + \left\{ \mathbf{F}^V \mathbf{C}^{ij} + \mathbf{C}^{ij} \mathbf{F}^V \right\}_{ab} \\
&\quad - \sum_k \{ F_{jk} C_{ab}^{ik} + F_{ik} C_{ab}^{kj} \} + \sum_{k,l} K_{kl}^{ij} C_{ab}^{kl} \\
&\quad + (1 - A) \cdot \left( K(\mathbf{C}^{ij})_{ab} \right. \\
&\quad + \sum_k \left\{ \left( 2\mathbf{C}^{ik} - \mathbf{C}^{ik+} \right) \left( \mathbf{K}^{kj} - \frac{1}{2} \mathbf{J}^{kj} \right) + \left( \mathbf{K}^{ik} - \frac{1}{2} \mathbf{J}^{ik} \right) \left( 2\mathbf{C}^{kj} - \mathbf{C}^{kj+} \right) \right\}_{ab} \\
&\quad \left. - \sum_k \left\{ \frac{1}{2} \mathbf{C}^{ik+} \mathbf{J}^{jk+} + \frac{1}{2} \mathbf{J}^{ik} \mathbf{C}^{kj+} + \mathbf{J}^{jk} \mathbf{C}^{ik} + \mathbf{C}^{kj} \mathbf{J}^{ik+} \right\}_{ab} \right) \quad (2.74)
\end{aligned}$$

$$\sigma_{a,\text{REMP}}^{i(1)} = F_a^i + \left\{ \mathbf{F}^V \mathbf{C}^j \right\}_a - \sum_j F_{ij} C_a^j + (1 - A) \cdot \sum_j \left\{ \left( 2\mathbf{K}^{ij} - \mathbf{J}^{ij} \right) \mathbf{C}^j \right\}_a \quad (2.75)$$

with

$$K_{rs}^{pq} = (pr|qs) \quad \mathbf{K}^{pq} \text{ operator matrix element}$$

$$J_{rs}^{pq} = (pq|rs) \quad \mathbf{J}^{pq} \text{ operator matrix element}$$

$$K(\mathbf{C}^{ij})_{ab} = \sum_{cd} (ac|bd) C_{cd}^{ij} \quad \text{external exchange operator}$$

$$\mathbf{F} = \mathbf{h} + \sum_i \left( 2\mathbf{J}^{ii} - \mathbf{K}^{ii} \right) \quad \text{closed-shell Fock matrix}^{[107]}$$

$$\mathbf{F}^V \quad \text{virtual-virtual subblock of the Fock matrix}$$

$$\{\dots\}_{ab} \quad \text{matrix element } (a, b) \text{ of the resulting matrix}$$

$$\{\dots\}_a \quad \text{vector element } (a) \text{ of the resulting vector}$$

$$\langle \mathbf{AB} \rangle = \sum_{p,q} A_{pq} B_{qp} = \text{tr}(\mathbf{AB}) \quad \text{Trace of the product } \mathbf{AB}$$

where  $\mathbf{C}^{ij}$  and  $\mathbf{C}^i$  are now the doubles and singles amplitudes matrices in the basis of the nonorthogonal CSFs.

The calculation of the external exchange operator can be accelerated for large molecules by performing the contraction of amplitudes and integrals in the AO basis and by forming  $\mathbf{K}^+/\mathbf{K}^-$  operators as proposed by Pulay *et al.*<sup>[107–109]</sup> The first step is a partial transformation of the amplitudes/CI coefficients to the AO basis

$$\mathbf{C}_{\text{AO}}^{ij} = \mathbf{U}\mathbf{C}_{\text{MO}}^{ij}\mathbf{U}^+, \quad (2.76)$$

where  $\mathbf{U}$  is the subblock of the virtual MOs of the MO coefficient matrix,  $U(n_{\text{bas}} \times n_{\text{virt}})$ .

Compared to the formation of  $K(\mathbf{C})$  in the MO basis, one already obtains a reduction in floating point operation (FLOP) count as the loops are now driven over integral batches of AO basis integrals which tend to be sparse for large molecules. A further reduction in FLOP count by a factor of two can be achieved by the formation of symmetric and antisymmetric exchange operators:<sup>[57,108,110]</sup>

$$K(\mathbf{C}^{ij})_{\mu\lambda}^{\pm} = \frac{1}{4} \sum_{\nu \geq \sigma} [(\mu\nu|\lambda\sigma) \pm (\mu\sigma|\lambda\nu)](\mathbf{C}_{\nu\sigma}^{ij} \pm \mathbf{C}_{\sigma\nu}^{ij})(2 - \delta_{\nu\sigma}), \quad (2.77)$$

where  $K(\mathbf{C})$  is only formed for  $\lambda \geq \mu$  instead of the full matrix. Together with the restriction on  $\nu$  and  $\sigma$ , this results in a 50% FLOP count saving.

The full exchange operator is then assembled via

$$K(\mathbf{C}^{ij})_{\mu\lambda} = \frac{1}{2}(K(\mathbf{C}^{ij})_{\mu\lambda}^+ + K(\mathbf{C}^{ij})_{\mu\lambda}^-) \quad (2.78)$$

$$K(\mathbf{C}^{ij})_{\lambda\mu} = \frac{1}{2}(K(\mathbf{C}^{ij})_{\mu\lambda}^+ - K(\mathbf{C}^{ij})_{\mu\lambda}^-) \quad (2.79)$$

The back-transformation to the MO basis is achieved via

$$\mathbf{K}(\mathbf{C}^{ij})_{\text{MO}} = \mathbf{U}^+\mathbf{K}(\mathbf{C}^{ij})_{\text{AO}}\mathbf{U}. \quad (2.80)$$

The developed program features both possibilities to form the external exchange operator in the MO or the AO basis.

It is furthermore possible to extend the treatment of the external exchange in the AO basis to also consider the effect of three-external exchange operators as they appear in CISD or in the second-order REMP wavefunction.<sup>[107]</sup> The amplitude matrix is augmented with the single excitations which are then also transformed to the AO basis. The contraction with the AO basis integrals will yield the three- and four external exchange operators in one step. The back-transformation to the MO basis now also has to include the occupied MOs. The contribution of the singles to the doubles residuum is contained in the virtual-virtual block while the contribution of the doubles to the singles is contained

in the occupied-virtual block. Care has to be taken, as the occupied-virtual blocks will also contain contributions from the singles via two-external exchange operators. These have to be subtracted in an  $n^5$  step before the occupied-virtual blocks can be used to calculate the doubles contribution to the singles residuum via three-external exchange operators. As neither the first-order restricted or unrestricted REMP nor the first-order OO-REMP wavefunction do contain single excitations, this will not be discussed in detail, here. The first-order restricted open shell REMP wavefunction contains singles but these do not require three-external exchange operators.

For calculating the correlation energy, the amplitudes are transformed from the nonorthogonal CSF to the contravariant basis

$$\tilde{C}_{ab}^{ij} = \frac{1}{1 + \delta_{ij}} (4C_{ab}^{ij} - 2C_{ba}^{ij}) \quad (2.81)$$

$$\tilde{C}_{ab}^{ii} = C_{ab}^{ii} \quad (2.82)$$

$$\tilde{C}_a^i = 2C_a^i. \quad (2.83)$$

The correlation energy is then given as

$$E_C = \sum_{i \geq j} \sum_{a,b} K_{ab}^{ij} \tilde{C}_{ab}^{ij} + \sum_{i,a} F_{ia} \tilde{C}_a^i \quad (2.84)$$

The idea to mix different unperturbed Hamiltonians is not completely new and was for example also examined by Angeli *et al.* for a mixed MP-EN Hamiltonian for multireference perturbation theory.<sup>[111]</sup> Although the intruder state problem of MR-MP is largely removed, the latter development did not receive much attention as the EN Hamiltonian is lacking size consistency and size extensivity, which is inherited by the mixed method.

## 2.7 The Orbital-optimized REMP (OO-REMP) Ansatz

By comparison of the OO-MP2<sup>[44,112]</sup> and the OCEPA<sup>[46]</sup> energy functional, the following variational energy functional for OO-REMP is derived:

$$\tilde{E}_{\text{REMP}} = \langle 0 | \hat{H} | 0 \rangle + \langle 0 | \{ \widehat{W}_N \widehat{T}_2 \}_c | 0 \rangle + \langle 0 | \{ \widehat{\Lambda}_2 (\widehat{W}_N + (\hat{f}_N + (1 - A) \widehat{W}_N) \widehat{T}_2)_c \}_c | 0 \rangle \quad (2.85)$$

with

$\widehat{W}_N$  ... two-electron operator in normal order

$\widehat{f}_N$  ... effective one-electron operator (Fockian) in normal order

$\widehat{\Lambda}_2$  ... double deexcitation operator, response amplitude, where

$$\widehat{\Lambda}_2 = \frac{1}{4} \sum_{ijab} \lambda_{ij}^{ab} \hat{i}^\dagger \hat{j}^\dagger \hat{b} \hat{a}$$

$A$  ... REMP mixing parameter

$c$  ... *contracted*, i.e. only fully contracted diagrams are considered  
for ensuring size consistency

Furthermore, for parameterizing the orbital change, it is useful to introduce an exponential unitary orbital rotation operator  $\mathbf{U} = e^{\hat{K}}$  which is parameterized by orbital rotation parameters  $\kappa_{pq}$ <sup>[113]</sup>

$$\hat{K} = \sum_{pq} K_{pq} \hat{p}^\dagger \hat{q} = \sum_{p>q} \kappa_{pq} (\hat{p}^\dagger \hat{q} - \hat{q}^\dagger \hat{p}), \quad (2.86)$$

and essentially consists of single orbital replacement operators. By virtue of the Thouless theorem,<sup>[56,114]</sup> any Slater determinant in a given Fock space can be obtained by a linear combination of single orbital replacement operators from any other Slater determinant.

$e^{\hat{K}}$  is a unitary matrix by enforcing  $\kappa$  to be anti-hermitian,<sup>[17]</sup> i.e.  $\kappa_{qp}^* = -\kappa_{pq}$ . As the orbitals are restricted to stay real in this work and as all orbitals are correlated, there are no occupied-occupied or virtual-virtual rotations. i.e. all  $\kappa_{pq}$  are real,  $\kappa_{ij}$  and  $\kappa_{ab}$  are zero and  $\kappa$  is traceless. In practice,  $\mathbf{U}$  is expanded in the Maclaurin series of the exponential function, which is truncated after the quadratic or cubic term and  $\mathbf{U}$  is enforced to be unitary by orthogonalization.

Using the orbital rotation operator, it is possible to express orbitals and operators in a rotated MO basis in terms of unrotated counterparts and rotation parameters<sup>[46]</sup>

$$|\tilde{p}\rangle = e^{\hat{K}} |p\rangle \quad (2.87)$$

$$\hat{p}^\dagger = e^{\hat{K}} \hat{p}^\dagger e^{-\hat{K}} \quad (2.88)$$

$$\hat{p} = e^{\hat{K}} \hat{p} e^{-\hat{K}} \quad (2.89)$$

$$\hat{H}^\kappa = e^{-\hat{K}} \hat{H} e^{\hat{K}} \quad (2.90)$$

$$\hat{H}_N^\kappa = e^{-\hat{K}} \hat{H}_N e^{\hat{K}} \quad (2.91)$$

$$\hat{f}_N^\kappa = e^{-\hat{K}} \hat{f}_N e^{\hat{K}} \quad (2.92)$$

$$\widehat{W}_N^\kappa = e^{-\hat{K}} \widehat{W}_N e^{\hat{K}}. \quad (2.93)$$

With the help of rotated operators, the REMP energy functional can be expressed as function of the orbital rotation parameters:

$$\tilde{E}_{\text{REMP}}^{(2)}(\kappa) = \langle 0 | \hat{H}^\kappa | 0 \rangle + \langle 0 | \{ \hat{W}_N^\kappa \hat{T}_2 \}_c | 0 \rangle + \langle 0 | \{ \hat{\Lambda}_2 (\hat{W}_N^\kappa + (\hat{f}_N^\kappa + (1-A)\hat{W}_N^\kappa) \hat{T}_2)_c \}_c | 0 \rangle \quad (2.94)$$

For obtaining a variational energy, the REMP energy functional Eq. (2.85) is made stationary with respect to both the regular  $t_{ab}^{ij}$  amplitudes as well as the  $\lambda_{ij}^{ab}$  amplitudes and the orbital rotation parameters  $\kappa_{pq}$

$$\frac{\partial \tilde{E}_{\text{REMP}}^{(2)}(\kappa)}{\partial t_{ab}^{ij}} = 0 \quad (2.95)$$

$$\frac{\partial \tilde{E}_{\text{REMP}}^{(2)}(\kappa)}{\partial \lambda_{ij}^{ab}} = 0 \quad (2.96)$$

$$\left. \frac{\partial \tilde{E}_{\text{REMP}}^{(2)}(\kappa)}{\partial \kappa_{pq}} \right|_{\kappa_{pq}=0} = 0 \quad (2.97)$$

by finding solutions which simultaneously fulfill Eqs. (2.95), (2.96) and (2.97).

Eq. (2.94) can be considered as a constrained minimization problem where the energy is minimized under the constraint that the  $t$  amplitude equations are still satisfied. The  $\lambda$  amplitudes serve as Lagrangian multipliers while the rest of the third term corresponds to the first-order wavefunction residuum.

It is furthermore possible to write the total energy in terms of integrals and density matrices<sup>[46,113]</sup>

$$E = \sum_{pq} \gamma_{pq} h_{pq} + \sum_{pqrs} \Gamma_{pqrs} \langle pq || rs \rangle, \quad (2.98)$$

which can be straightforwardly deduced from the second quantization Hamiltonian.  $\gamma_{pq}$  and  $\Gamma_{pqrs}$  are reduced one- and two-particle density matrices (OPDMs and TPDMs). As long as real orbitals are used, the following symmetry properties for the density matrices hold:

$$\gamma_{pq} = \gamma_{qp} \quad (2.99)$$

$$\Gamma_{rspq} = \Gamma_{srqp} = -\Gamma_{rsqp} = -\Gamma_{srpq} \quad (2.100)$$

$$= \Gamma_{pqrs} = \Gamma_{qpsr} = -\Gamma_{qprs} = -\Gamma_{pqsr} \quad (2.101)$$



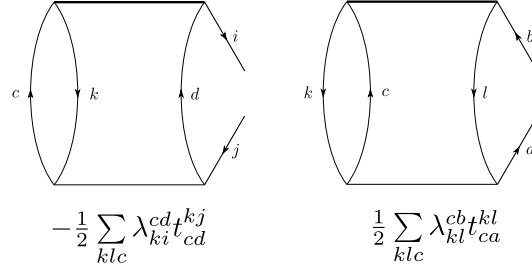


**Figure 2.7:** Diagrams representing the correlation contribution to the one-particle density matrix (OPDM). Left-hand side:  $\gamma_{ij}$ , right-hand-side:  $\gamma_{ab}$ .

Density matrices can again be formulated in a normal-ordered fashion which establishes the connection to a diagrammatic construction. Application of the Wick theorem yields<sup>[56]</sup>

$$\begin{aligned} \gamma_{pq} &= \underbrace{(\gamma_{\text{N}})_{pq}}_{\gamma^{\text{corr}}} + \underbrace{\delta_{ip}\delta_{jq}}_{\gamma_{pq}^{\text{ref}}} \quad (2.102) \\ \Gamma_{rspq} &= \underbrace{(\Gamma_{\text{N}})_{rspq}}_{\Gamma_{rspq}^{\text{corr}}} \\ &\quad + \underbrace{\delta_{pi}\delta_{ri}(\gamma_{\text{N}})_{sq} + \delta_{qi}\delta_{si}(\gamma_{\text{N}})_{rp} - \delta_{pi}\delta_{si}(\gamma_{\text{N}})_{rq} - \delta_{qi}\delta_{ri}(\gamma_{\text{N}})_{sp}}_{\Gamma_{rspq}^{\text{sep}}} \\ &\quad + \underbrace{\delta_{pi}\delta_{ri}\delta_{qj}\delta_{sj} - \delta_{pi}\delta_{si}\delta_{qj}\delta_{rj}}_{\Gamma_{rspq}^{\text{ref}}} \quad (2.103) \end{aligned}$$

The latter arises from the application of the Wick theorem, namely that a string of creation and annihilation operators (which the density essentially is) can be represented by its normal product form and all possible contractions.

From a comparison of Eqs. (2.94) and (2.98), and using the decomposition of the density matrices into reference, separable and correlation contributions, expressions for the REMP density matrices can be derived. In fact, the raw density matrices are identical to the OCEPA density matrices,<sup>[46]</sup> but when orbital gradients are formed, certain two-particle densities are multiplied by  $1 - A$ .

A graphical/diagrammatic derivation of the correlation part of the OPDMs and TPDMs is given in Figure 2.7 and 2.8. The OPDM diagrams have two open lines for contraction with  $h_{pq}$  while the TPDM diagrams have four open lines for contraction with  $\langle pq||rs \rangle$ .

The diagrammatic interpretation of the densities can be accomplished by inserting an auxiliary vertex consisting e.g. of a hatched doublebar and connecting the open lines with this vertex.<sup>[56]</sup> The labels of the densities are then

$$\gamma_{\text{in|out}} \quad (2.104)$$

$$\Gamma_{\text{left in|right in|left out|right out}} \quad (2.105)$$

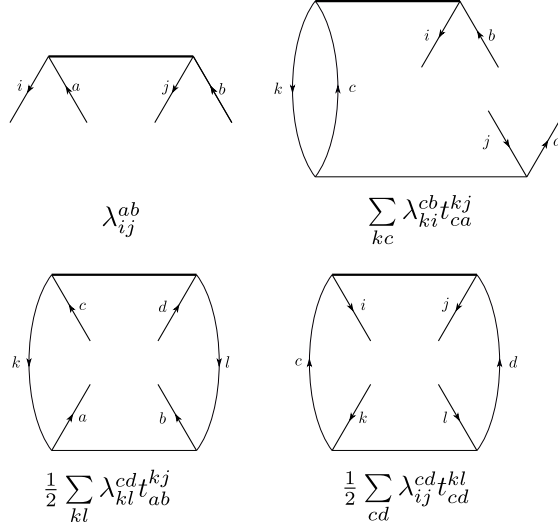


**Figure 2.8:** Diagrams representing the correlation contribution to the two-particle density matrix (TPDM). Upper left:  $\Gamma_{ijab}$ , upper right:  $\Gamma_{iajb}$ , lower left:  $\Gamma_{abcd}$ , lower right:  $\Gamma_{ijkl}$ .

The interpretation of the diagrams in Figure 2.7 yields

$$\gamma_{ij}^{\text{corr}} = -\frac{1}{2} \sum_{kcd} \lambda_{ki}^{cd} t_{cd}^{kj} \quad (2.106)$$

$$\gamma_{ab}^{\text{corr}} = \frac{1}{2} \sum_{klc} \lambda_{lk}^{cb} t_{ca}^{kl} = \frac{1}{2} \sum_{klc} \lambda_{kl}^{bc} t_{ac}^{kl} \quad (2.107)$$

With no single excitations and no orbital relaxation contributions ( $z$  vector / orbital response equations<sup>[115–118]</sup>), there are no  $\gamma_{ia}$  and  $\gamma_{ai}$  contributions.<sup>[46,112]</sup>

The diagrams in Figure 2.8 yield the following nonzero TPDMs:

$$G_{ijkl} = \frac{1}{2} \sum_{cd} \lambda_{ij}^{cd} t_{cd}^{kl} \quad (2.108)$$

$$G_{abcd} = \frac{1}{2} \sum_{kl} \lambda_{kl}^{cd} t_{ab}^{kl} \quad (2.109)$$

$$G_{iabj} = \sum_{kc} \lambda_{ki}^{cb} t_{ca}^{kj} = -G_{iajb} \quad (2.110)$$

$$G_{ijab} = \lambda_{ab}^{ij} \quad (2.111)$$

The factor of  $\frac{1}{4}$  originating from unrestricted summation over two-electron integrals still needs to be included somehow for use with Eq. (2.98). Bozkaya *et al.*<sup>[46]</sup> decided to absorb the additional factor  $\frac{1}{4}$  into the definition of the two-particle density matrices. This factor

does not emerge from the diagrammatic construction of the density matrices. The final expressions for the OPDMs and TPDMs then become

$$\gamma_{pq} = \gamma_{pq}^{\text{ref}} + \gamma_{pq}^{\text{corr}} \quad (2.112)$$

where

$$\gamma_{pq}^{\text{ref}} = \delta_{pq}^{\text{occ}} \quad (2.113)$$

$$\gamma_{ij}^{\text{corr}} = -\frac{1}{2} \sum_m^{\text{occ}} \sum_{ef}^{\text{virt}} t_{ef}^{im} \lambda_{jm}^{ef} \quad (2.114)$$

$$\gamma_{ab}^{\text{corr}} = \frac{1}{2} \sum_{mn}^{\text{occ}} \sum_e^{\text{virt}} t_{be}^{mn} \lambda_{mn}^{ae} \quad (2.115)$$

$$\Gamma_{pqrs} = \Gamma_{pqrs}^{\text{ref}} + \Gamma_{pqrs}^{\text{sep}} + \Gamma_{pqrs}^{\text{corr}} \quad (2.116)$$

where

$$\Gamma_{pqrs}^{\text{ref}} = \frac{1}{4} (\delta_{pr}^{\text{occ}} \delta_{qs}^{\text{occ}} - \delta_{ps}^{\text{occ}} \delta_{qr}^{\text{occ}}) \quad (2.117)$$

$$\Gamma_{pqrs}^{\text{sep}} = \frac{1}{4} (\delta_{pr}^{\text{occ}} \gamma_{qs} + \delta_{qs}^{\text{occ}} \gamma_{pr} - \delta_{qr}^{\text{occ}} \gamma_{ps} - \delta_{ps}^{\text{occ}} \gamma_{qr}) \quad (2.118)$$

$$\Gamma_{ijkl}^{\text{corr}} = \frac{1}{8} \sum_{cd} \lambda_{kl}^{cd} t_{cd}^{ij} \quad (2.119)$$

$$\Gamma_{ijab}^{\text{corr}} = \frac{1}{4} t_{ab}^{ij} \quad (2.120)$$

$$\Gamma_{iajb}^{\text{corr}} = -\frac{1}{4} \sum_{kc} \lambda_{jk}^{ac} t_{bc}^{ik} \quad (2.121)$$

$$\Gamma_{abcd}^{\text{corr}} = \frac{1}{8} \sum_{kl} \lambda_{kl}^{cd} t_{ab}^{kl} \quad (2.122)$$

An important aspect of Hermitian methods like MP2 and CEPA(0) is that the  $t$  amplitudes directly solve the  $\lambda$  amplitude equations, i.e. that<sup>[46,118]</sup>

$$\widehat{\Lambda}_2 = \widehat{T}_2^\dagger \quad (2.123)$$

and thus<sup>[119–121]</sup> (see also Eq. (6.4))

$$\lambda_{ij}^{ab} = t_{ab}^{ij*}. \quad (2.124)$$

Therefore, it is not necessary to explicitly solve the lambda equations resulting from Eq. (2.95), instead, the  $\lambda$  amplitudes may be substituted by the  $t$  amplitudes in all density matrices.

The orbital gradient  $w_{pq}$  is obtained from the asymmetry of the generalized Fock matrix  $F_{pq}$

$$w_{pq} = F_{pq} - F_{qp} \quad (2.125)$$

where

$$F_{pq} = \sum_r h_{pr} \gamma_{rq} + 2 \sum_{rst} \langle rs || tp \rangle \Gamma_{rstq} \quad (2.126)$$

The orbital gradient of the  $n^{\text{th}}$  iteration will furthermore be labeled  $\mathbf{w}^n$ .

From the orbital gradient  $\mathbf{w}^n$ , a set of orbital rotation parameters  $\kappa_{pq}^n$  is obtained as damped (diagonal hessian) step in the opposite direction of the orbital gradient<sup>5</sup>

$$\kappa_{pq}^n = -\frac{w_{pq}^n}{2(f_{aa}^n - f_{ii}^n)}, \quad (2.127)$$

where  $f_{aa}^n$  and  $f_{ii}^n$  are diagonal elements of the MO basis Fockian of the  $n^{\text{th}}$  orbital iteration.

From the orbital rotation parameters  $\kappa_{pq}^n$ , the orbital rotation matrix  $\mathbf{K}^n$  is constructed as

$$\mathbf{K} = \text{skew}(\kappa) \quad (2.128)$$

$$K_{pq} = \begin{cases} \kappa_{pq} & p > q \\ -\kappa_{pq} & p < q \\ 0 & p = q \end{cases} \quad (2.129)$$

The orbitals of iteration  $n$ ,  $\mathbf{C}_n$ , are obtained by subsequently applying the orbital rotations of all  $n$  iterations to the initial orbitals  $\mathbf{C}_0$

$$\mathbf{C}_n = \mathbf{C}_0 e^{\mathbf{K}_1} e^{\mathbf{K}_2} \dots e^{\mathbf{K}_n} \quad (2.130)$$

In practice, the orbital rotations  $e^{\mathbf{K}^n}$  of each iteration are summed up to a total orbital rotation  $e^{\bar{\mathbf{K}}^n}$ , and the new orbitals are obtained by applying this total orbital rotation to the initial set of orbitals

$$\bar{\kappa}^n = \sum_{i=1}^n \kappa^i \quad (2.131)$$

$$\bar{\mathbf{K}}^n = \text{skew}(\bar{\kappa}^n) \quad (2.132)$$

$$\mathbf{C}_n = \mathbf{C}_0 e^{\bar{\mathbf{K}}^n}. \quad (2.133)$$

---

<sup>5</sup>reminder: the gradient points in the direction of the steepest ascend, thus the step has to follow the opposite direction.

The reason is that only then a DIIS extrapolation for the orbital rotation can be applied. DIIS in theory needs a common basis for the different vectors of the quantity to be extrapolated. This common basis is given by the initial set of orbitals<sup>6</sup>.

The matrix exponentials of the orbital rotations are obtained by applying the Taylor series of the exponential function and terminating the series after the second-order term

$$\mathbf{U} = e^{\bar{\mathbf{K}}_n} = \sum_{i=0}^{\infty} \frac{(\bar{\mathbf{K}}_n)^i}{i!} = \mathbf{1} + \bar{\mathbf{K}}_n + \frac{1}{2}(\bar{\mathbf{K}}_n)^2 + \dots \quad (2.134)$$

The unitary matrix  $\mathbf{U}$  is subsequently orthonormalized using a modified Gram-Schmidt procedure<sup>[122]</sup> to remove any residual nonorthogonality by numerical noise. Without this step, the MOs would soon lose their orthogonality, resulting in instability and a runaway of the energy. It was furthermore tested whether it is beneficial to go beyond the quadratic term in Eq. (2.134), but no noticeable difference in convergence behavior was observed.

It should be stressed again that OO-REMP is a variational method, i.e. that the energy is minimized with respect to all variational parameters (orbital coefficients and amplitudes). The mixing parameter itself is not a variational parameter but belongs to the Hamiltonian. In the current formulation, OO-REMP is still subject to the constraint that the orbitals and the amplitudes are real.

### 2.7.1 Perturbative singles

During the orbital-optimization procedure, single excitations are excluded completely. This choice has been made by other authors, too,<sup>[39,42,43,46]</sup> e.g. in the case of OCEPA, OO-MP2 or OCCD, as the single excitations compete with the orbital rotation parameters, essentially acting as orbital rotations. Formally, the singles equations are not fulfilled by setting the single excitations to zero as the Fockian will contain non-zero elements in the virtual-occupied block as soon as occupied-virtual unitary transformations to the orbitals are applied. In other words, as soon as the orbitals are optimized, the Brillouin theorem is not fulfilled anymore. After convergence of the orbital iterations, it seems desirable to estimate the effect of the discarded single excitations. A singles correction to the correlation energy can be obtained by solving the REMP singles equations Eq. (2.63) with the converged optimized orbitals and operators calculated therefrom. Such an optional singles correction has also been implemented and was assessed for several benchmark sets (see Section 3.2). However, it turned out that such a singles correction is not beneficial and should not be applied. This aspect has already been discussed by Neese *et al.* in the context of OO-MP2<sup>[43]</sup> where it was found that the result do not benefit from *a posteriori* singles. Nevertheless, it was necessary to also show this for REMP and not to just assume that OO-MP2 results are transferable to OO-REMP.

<sup>6</sup>In practice, one often observes deviations from this rule. A combined extrapolation for orbitals and amplitudes necessarily uses a different basis for the amplitudes in each iteration (the current MOs), but in practice, no severe problems were observed.

This is in contrast to the Brueckner Coupled cluster method<sup>[123–126]</sup> (B-CCD or BD) where the orbitals are optimized such that the coupled cluster singles amplitudes vanish exactly on convergence.

## 2.8 Analytical Gradients for OO-REMP

Analytical gradients for OO-REMP were implemented in PSI4 as extension of the OCC and the DF0CC module. The analytical gradient engine of PSI4 needs the relaxed one-particle density, the relaxed two-particle density, and the generalized Fock matrix.<sup>[46]</sup> With these quantities at hand, the engine calculates the gradient integrals, namely the derivatives of  $h_{pq}$ ,  $\langle pq||rs\rangle$  and the derivative of the overlap matrix for the nuclear positions. The densities and the generalized Fock matrix are transformed to the AO basis and contracted with the respective integral derivatives to yield the electronic contribution to the nuclear gradient:

$$\frac{dE}{dx} = \sum_{\mu\nu} \gamma_{\mu\nu} h_{\mu\nu}^x + \sum_{\mu\nu\lambda\sigma} \Gamma_{\mu\nu\lambda\sigma} \langle \mu\nu||\lambda\sigma\rangle^x - \sum_{\mu\nu} F_{\mu\nu} S_{\mu\nu}^x \quad (2.135)$$

As all quantities except the derivative integrals are available after an OO-REMP calculation, the calculation of gradients is cheap compared to the initial OO-REMP calculation. The transformation of  $\gamma_{\mu\nu}$  and  $F_{\mu\nu}$  scales as  $\mathcal{O}(N^3)$ , the transformation of  $\Gamma_{\mu\nu\lambda\sigma}$  scales as  $\mathcal{O}(N^5)$  analogous to the ERIs, but can be done in batches. The calculation of the derivative integrals scales at most as  $\mathcal{O}(N^4)$  and is thus also negligible compared to the preceding calculation<sup>7</sup>.

## 2.9 Comparison to Other Parameterized Wavefunction Methods

There is a number of methods which are conceptually similar to the REMF approach. Hence it seems instructive to highlight the similarities and differences as well as the accuracy which can be achieved by these methods.

### 2.9.1 Variants of CEPA

The coupled electron pair approximation (CEPA, in former days also know as self-consistent electron pairs (SCEP) approximation) dates back to Kelly<sup>[127,128]</sup> and Meyer.<sup>[94,129–132]</sup> Originally, it was derived as an approximation to Čížeks coupled cluster method<sup>[93,133]</sup> (at that time called coupled-pair many-electron theory, CP-MET). CEPA(0), also called

<sup>7</sup>One might think that the ERI derivatives scale as  $\mathcal{O}(N^4 \cdot n_{\text{nuc}})$ , but this is a worst-case estimate. In the AO basis, the additional prefactor is limited to the three Cartesian directions and the four nuclei involved in the ERI.

LCCD or L-CP-MET, can actually be rationalized by linearizing terms in the CCSD residuum.<sup>[96]</sup> Principally, all CEPA methods were derived by introducing approximations to the CCSD approach with more or less hand-waving arguments. Koch and Kutzelnigg<sup>[134]</sup> later added CEPA(4) and CEPA(5) to the already existing set of CEPA(0)-CEPA(3). Pulay and Sæbø later added a variational version of CEPA.<sup>[135]</sup> ACPF,<sup>[136]</sup> AQCC<sup>[137]</sup> and other coupled-pair functionals belong also to this family of methods. Owing to the fact that many of them are not unitary invariant, the availability of efficient coupled cluster codes, and with the advent of density functional theory in the late 80ies, the CEPA methods fell into oblivion.

It was only in 2008 that Wennmohs and Neese<sup>[96]</sup> published efficient working equations and energy shifts for a large number of old and new coupled-pair type methods. Kollmar, Heßelmann and Neese<sup>[138-140]</sup> also worked out variational and unitary invariant alternatives to the classical CEPA methods.

The “classical” coupled-pair type methods are typically not parameterized with empirical scaling factors but by introducing rational factors, pair energies or by manipulating the denominator of an energy functional with e.g. shifts that depend on the number of correlated electrons.<sup>[96]</sup>

### 2.9.2 pCCSD

Parameterized Coupled Cluster with singles and doubles (pCCSD) was devised by Nooijen and coworkers.<sup>[103,141,142]</sup> The idea is to apply scaling factors to terms arising from diagrams that describe disconnected triple and quadruple excitations. The parameters can be determined such that the method is exact for two-electron cases. With only two electrons, certain diagrams have to cancel exactly, which is achieved by restricting the parameter space. The property of being rigorously exact for two-electron systems is what makes pCCSD different from REMP. As shown in Section 3.1, the latter is only approximately exact. A further direct comparison between REMP and pCCSD is not appropriate, as pCCSD is built upon the exponential CC ansatz, while REMP originates from a CI-type ansatz. The terms that are scaled in pCCSD originate from  $\hat{T}_1\hat{T}_2$  and  $\hat{T}_2^2$ . Such terms are not present in the first order REMP wavefunction, instead, they are implicitly taken care of by virtue of the mixing parameter  $A$ . In higher orders, they would enter as connected triples and quadruples. It is therefore also not obvious how to directly relate the parameters of the pCCSD ansatz to the REMP mixing parameter. In terms of accuracy, it has been shown<sup>[50]</sup> that canonical REMP performs similar to the variants pCCSD/1a and pCCSD/1b. No OO-REMP calculations were performed for this set.

### 2.9.3 PCPF-MI

The parameterized Coupled pair functional PCPF-MI<sup>[143]</sup> is a generalization of ACPF<sup>[136]</sup> and AQCC.<sup>[137]</sup> It introduces three parameters that modify the energy shifts of the

coupled-pair functional. The three parameters act separately on the same-spin doubles, the opposite spin doubles and the singles. The set of parameters was specifically optimized with regard to noncovalent interactions and indeed provides quite impressive results, surpassing several CEPA variants, ACPF, AQCC and CCSD. Unfortunately, there were never any results apart from noncovalent interactions, hence the general applicability remains questionable.

#### 2.9.4 CCD0

CCD0<sup>[144,145]</sup> and CCSD0 (Singlet-paired coupled cluster) are approximation to CCD and CCSD which entirely eliminate the TDEs from the doubles excitations manifold. They are hence still exact in the two-electron case. It is furthermore claimed that these methods are much more robust when multireference cases are encountered and that they are able to describe bond dissociation when full CCSD fails. The loose connections to the REMP ansatz are that these are also methods that include at most double excitations and that the different behaviour of the two doubles singlet CSFs are exploited.

#### 2.9.5 Feenberg Scaling

Feenberg scaling<sup>[146–148]</sup> departs from a partitioning of  $\hat{H}$  in  $\hat{H}^{(0)}$  and  $\hat{H}^{(1)}$ , but then introduces an additional repartitioning parameter  $\mu$

$$\hat{H}^{(0)'} = \frac{1}{\mu} \hat{H}^{(0)} \quad (2.136)$$

$$\hat{H}^{(1)'} = \hat{H}^{(1)} + \frac{\mu - 1}{\mu} \hat{H}^{(0)}. \quad (2.137)$$

The repartitioning parameter  $\mu$  is now determined such that the third order perturbative energy correction becomes zero. An important variant of Feenberg scaling is OPT-PT proposed by Szabados and Surján<sup>[98,99]</sup> where individual Feenberg parameters were introduced for every excited configuration. Upon optimization of these parameters, this approach is identical to RE2 or RE3 as well as to CEPA(0)/D.

As the third order energy correction of RE is already zero with an RHF reference,<sup>[37,75]</sup> RE can be regarded as optimal in this sense. There is also a connection between spin-component scaled methods and Feenberg scaling.<sup>[65,81]</sup> A relation to REMP can be seen in the necessity of one scaling or mixing parameter which moves parts of the total Hamiltonian between  $\hat{H}^{(0)}$  and  $\hat{H}^{(1)}$ .

#### 2.9.6 OMP2.X

The MP2.X and OMP2.X methods<sup>[149]</sup> are hybrids between MP2(OO-MP2) and MP3(OO-MP3). It was recognized that MP2 tends to overestimate noncovalent interaction energies



while MP3 tends to underestimate them.<sup>[150]</sup> In the spirit of the current work, it was investigated whether some hybrid will lead to better noncovalent interaction energies with the result that systematically better results are obtained when only 50% of the third order MP energy correction are used (MP2.5)<sup>[151]</sup> or a basis-dependent MP3 fraction (MP2.X).<sup>[152]</sup> The same reasoning was used by Bozkaya and Sherrill to design the OMP2.5 method which works by iteratively optimizing the MP2.5 energy functional.<sup>[153]</sup> While MP2.5 often only modestly improves upon MP2, there was always a substantial improvement found by optimizing the reference determinant. Quite like in the case of RE and MP, it was also found that OMP2.5 consistently improves upon its parent methods OMP2 and OMP3, not only for noncovalent interactions but also for structures and general thermochemistry.<sup>[154,155]</sup> The obvious connection to REMP and OO-REMP is the mixing parameter and the large impact of orbital optimization.

### 2.9.7 $\kappa$ -OMP2

The already good results of OO-MP2 can be further improved by introducing an additional regularization of the MP2 energy denominators<sup>[156–159]</sup>

$$E(\kappa)_{\kappa\text{-MP2}} = -\frac{1}{4} \sum_{ijab} \frac{|\langle ij|ab\rangle|^2}{\Delta_{ij}^{ab}} (1 - e^{-\kappa\Delta_{ij}^{ab}})^2 \quad (2.138)$$

where  $\Delta_{ab}^{ij}$  is the MP energy denominator and  $\kappa$  is an empirical regularization parameter. The regularization is parameterized and orbital-energy dependent, and mainly has the effect of increasing too small MP energy denominators. Quite like REMP, it is an approach to cure the problem of inappropriate energy denominators.

The regularized ansatz was additionally combined with orbital optimization and the idea underlying MP2.5, in that a variable portion of the MP3 energy is added to the  $\kappa$ -OOMP2 energy, leading to MP2.8: $\kappa$ -OOMP2. This leads to impressive results<sup>[160]</sup> at the cost of two empirical parameters and a computational scaling of  $n^6$  owing to the MP3 part. Unfortunately, the available literature presents no evidence that the method is size-consistent and unitary invariant. Owing to the nonvariational nature of the scaled MP3 contribution, the implementation and calculation of analytic gradients is more involved than for variational methods like OO-REMP. In addition, recent investigations have shown that the originally promoted value for the regularization parameter was too large, especially if transition metals are involved, and that presumably a globally optimal value does not exist.<sup>[161]</sup>

### 2.9.8 Other $\mathcal{O}(n^5)$ and $\mathcal{O}(n^6)$ methods

There exists a number of methods with a computational scaling of  $\mathcal{O}(n^5)$  or  $(n^6)$  which try to improve upon MP2 or CCSD at no additional cost.

OS-CCSD-SPT(2)<sup>[162]</sup> adds a second-order correction to OS-CCSD that can be determined

from the first-order wavefunction of a similarity-transformed Hamiltonian. It was shown to significantly improve upon CCSD but is clearly still inferior to CCSD(T). It was also shown that the use of PBE0 orbitals provides better results than HF orbitals, showing that the method is strongly dependent on a proper reference wavefunction.

Spin-ratio scaled MP2<sup>[163]</sup> (SRS-MP2) is another method primarily aimed at the calculation of noncovalent interactions energies. It works by rescaling the correlation energy contribution of same-spin and opposite-spin pairs to the interaction energy with separate factors. The method has the drawbacks that it is only applicable to complexes, that the scaling coefficients are basis set dependent and that the results deteriorate towards the CBS limit. There are furthermore different scaling factors required depending on the character of the dominating interaction.

Correlation energies can furthermore be calculated from the random phase approximation<sup>[164–167]</sup> (RPA). There exists a number of ways to derive the RPA correlation energy expression,<sup>[168]</sup> but from a technical point of view, it can be regarded as an approximation to Coupled Cluster Doubles<sup>[169]</sup> (CCD). As such, it is not exact for two-electron cases. In recent years, RPA has gained some popularity in replacing MP2 correlation in double hybrid functionals.<sup>[170,171]</sup> With no further approximations, the RPA correlation energy scales as  $\mathcal{O}(n^6)$ ,<sup>[172]</sup> but this can be brought down to  $\mathcal{O}(n^5)$  for the integral transformation and  $\mathcal{O}(n^4)$  for the iterations just like MP2, and further savings are possible by local approximations.<sup>[173]</sup>

### 3 Results

The REMP and OO-REMP working equations were implemented in the wavel suite of programs<sup>[174–181]</sup> as well as in the open source quantum chemistry program PSI4.<sup>[182–184]</sup> Both implementations also contain the necessary code for calculating electric multipole moments. The implementation in PSI4 furthermore is able to calculate analytical structural gradients for OO-REMP and numerical gradients for both REMP and OO-REMP. While the implementation in wavel only uses unapproximated, conventional two-electron integrals, the PSI4 implementation also features the resolution of identity approximation.<sup>[185–189]</sup> Two-electron integrals can be reconstructed either from three-center integrals employing a conventional auxiliary basis<sup>[49,120,183,184,190–199]</sup> set or from Cholesky factors obtained from an incomplete Cholesky decomposition<sup>[200–203]</sup> of the exact two-electron integral tensor.<sup>[121,155,204,205]</sup> The implementations in wavel and PSI4 are both parallelized with the OpenMP<sup>[206]</sup> shared memory parallelization. Optimized level-2 and level-3 BLAS routines are used for matrix-vector and matrix-matrix operations whenever possible. Both programs can be linked against any BLAS library that support the standard set of operations<sup>[207,208]</sup> and both the Intel<sup>®</sup> MKL<sup>[209]</sup> and the OpenBLAS<sup>[210]</sup> library were successfully used with both programs.

#### 3.1 Recovered Correlation Energies

In previous assessments of the REMP<sup>[50,76]</sup> and S2REMP<sup>[211]</sup> methods, the primary measure for the quality of the method originated from a direct comparison of the wavefunctions in terms of the CI coefficients to high-quality coupled cluster wavefunctions. Only as secondary measures, the amount of recovered correlation energy or reaction energy benchmarks were considered. The employed methodology relies on the MO coefficients to be exactly the same in all calculations, which is of course not the case anymore in orbital-optimized calculations. The direct comparison of wavefunctions of orbital-optimized and canonical calculations would require a tedious transformation to a common basis. Orbital-optimized methods alter the reference orbitals beyond unitary transformations of only the occupied-occupied or virtual-virtual block. The energy of the reference determinant subsequently also changes, and while the total energy is minimized variationally, the energy of the reference determinant increases, meaning that part of the previous Hartree-Fock energy is now recovered as correlation energy.

The comparison of one- and two-particle densities – derived from the respective wavefunctions – in the AO basis is another possibility, but, first, one can then equally well compare properties calculated from these densities, and, second, due to the still missing REMP  $z$ -vector equations, there is no access to relaxed canonical REMP densities.

The only quantity which is thus available for canonical REMP, OO-REMP, and near-full CI wavefunctions is the correlation energy, which is defined as the total energy minus the energy of the corresponding SCF (RHF or UHF) calculation. A further breakdown into spin-components or CSF contributions is not easily possible anymore as soon as orbital optimization is active. It is of course possible to calculate the contributions of such terms, but it is not reasonable, because as soon as the orbitals are optimized iteratively, a part of the reference energy is “transferred” to the correlation energy, and it is impossible to determine how much of each calculated energy is actually correlation and how much should be subtracted as “stolen” reference energy. Furthermore, a direct comparison to higher level wavefunction methods would require programs which are able to use orbitals which do not satisfy the Brillouin theorem. It is unclear to which extent `mrcc` is capable of doing so but usually, the validity of the Brillouin theorem is assumed to keep the code simple and efficient. As there is still no implementation of OO-REMP based on exact two-electron integrals which can make use of frozen core orbitals, also the reference near-Full CI calculations have to be performed with all electrons correlated which causes a very rapid increase of the computational cost with system size.

All REMP and OO-REMP calculations were performed using a development version of the `wavels` suite of programs while CCSD, CCSD(T), CCSDT and CCSDTQ calculations were done using `mrcc` version 2022-03-18.<sup>[77,78,212,213]</sup> All calculations were converged to better than  $1 \cdot 10^{-10}$  both in energy and residuum for obtaining results that are free from numerical noise. Hartree-Fock (SCF) and canonical MP2 energies were compared between `wavels` and `mrcc` and verified to coincide reasonably.

The most simple yet relevant test systems are those with only two electrons. With only two electrons, Full CI is trivially accessible via CISD or CCSD. It is also highly desirable that a method relying on (single and) double excitations is at least (nearly) exact for two-electron systems. For testing this property, a set consisting of  $\text{H}^-$ ,  $\text{H}_2$ ,  $\text{H}_3^+$ , and the He atom was compiled (the  $\text{Li}^+$  cation and other Helium-like cations were not considered as they are already too different from the other examples and require special core-polarized basis sets).

The average recovered correlation energy in comparison to Full CI is drawn in Figure 3.1, and the mixing ratios leading to results closest to 100% correlation energy are listed in Table 3.1. Due to the small number of entries in all sets of this section, no tests for normal distribution or outliers were performed. In the analysis, no truncated CI methods were included as they are known to lack size consistency.

One finds that for these simple two-electron systems, RE2 and OO-RE2 mostly overestimate the true correlation energy, while MP2 and OO-MP2 drastically underestimate it. Figure 3.1 thus clearly recovers one of the working hypotheses of the REMP approach, namely that RE2 overestimates the contribution by singlet-coupled pairs while MP2 underestimates it (in closed-shell two-electron systems, there is only one singlet pair). This trend carries over to the orbital-optimized variant. Generally, OO-REMP recovers slightly more correlation energy than canonical REMP, in line with the variational nature

**Table 3.1:** Møller-Plesset fractions  $A$  in percent where the amount of recovered correlation energy of the two-electron systems  $\text{H}^-$ ,  $\text{H}_2$ ,  $\text{H}_3^+$  and  $\text{He}$  approaches 100%. Taken from Figure 3.1 and visually estimated to 0.5%.

basis set	REMP	OO-REMP
cc-pVDZ	2.5	4.0
cc-pVTZ	4.0	5.5
cc-pVQZ	5.0	6.0
aug-cc-pVTZ	6.0	8.0
aug-cc-pVQZ	6.0	8.0

of the method. The graphs in Figure 3.1 are cut at  $A = 0.30$  for the sake of clarity, as the amount of recovered correlation energy decreases to  $\approx 80\%$  for  $A = 1.0$  in all cases. This is no new result for canonical REMP<sup>[76,211]</sup> while for OO-REMP no such analysis has been performed so far. Quite interestingly, one finds similar trends with REMP and OO-REMP. The optimal mixing ratio is slightly basis set dependent, it increases with increasing basis set size and converges to  $A_{\text{opt}} \approx 0.06$ . OO-REMP consistently requires larger MP fractions and converges to  $A_{\text{opt}} \approx 0.08$ . This finding is qualitatively in line with the results of closed-shell thermochemistry benchmarks<sup>[51]</sup> ( $A_{\text{opt}} \approx 0.15$  for REMP vs.  $A_{\text{opt}} \approx 0.20$  for OO-REMP), although the actual optimal values are distinctly different. Quite interestingly, one finds that OO-REMP is – apart of the cc-pVDZ basis set – not more precise than canonical REMP. In contrast, with increasing basis set size the mixing ratio with the smallest standard deviation moves away from the mixture which recovers 100% correlation energy. and also moves outside a region of 1% correlation energy error. This behavior is especially prominent for the augmented basis sets. It should also be noted that the  $\text{H}^-$  is rather peculiar in the sense that it is not bound at all at the SCF level and that at the FCI level it is also only bound with the cc-pVQZ, aug-cc-pVTZ and aug-cc-pVQZ basis, i.e. with sufficiently diffuse basis sets.

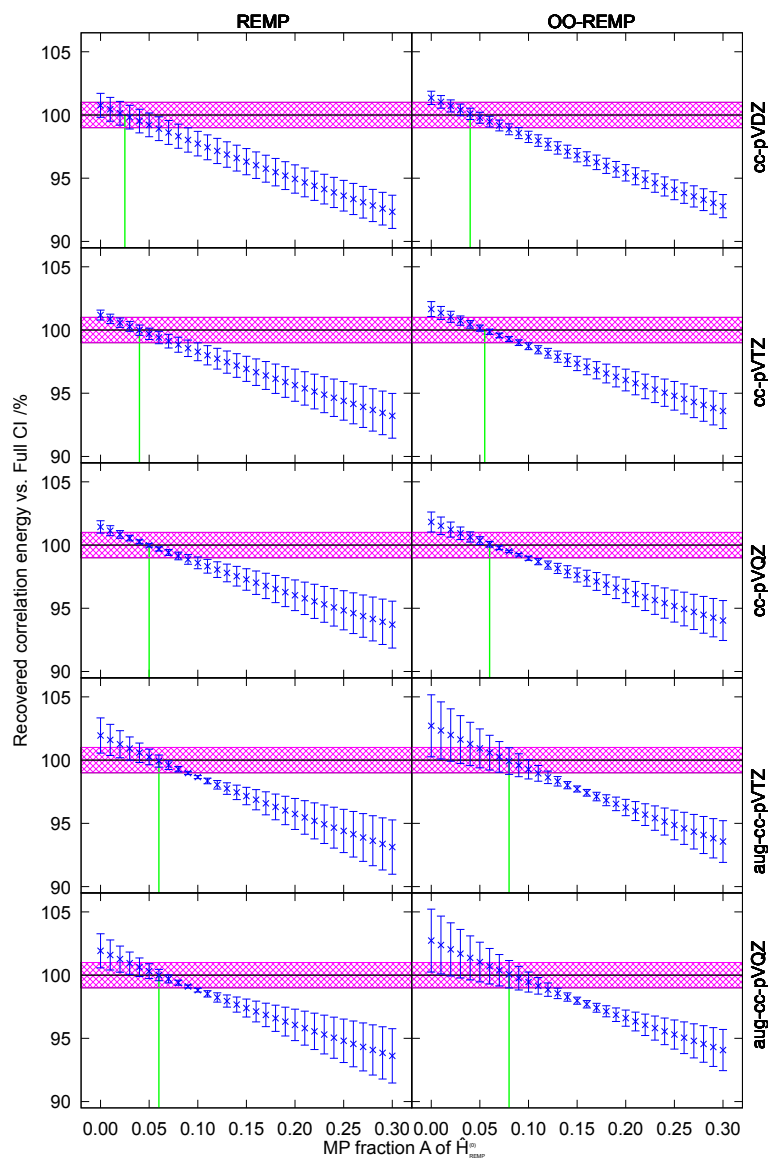


**Figure 3.1:** Graphical representation of the recovered correlation energy for four two-electron systems ( $H^-$ ,  $H_2$ ,  $H_3^+$ ,  $He$ ). Error bars indicate one standard deviation, green vertical bars indicate the mixing ratio at which roughly 100 % of the FCI correlation energy is recovered. The hatched area spans the region of  $(100 \pm 1)$  % correlation energy. Perturbative correlation energies correspond to second order in energy.

The amount of recovered correlation energy was further tested with a set of small main-group compounds, consisting of both closed- and open-shell systems. The set features the two pseudo-two-electron cases  $\text{Li}_2$  and the Be atom where the behavior for two-electron cases is recovered.

**Table 3.2:** Møller-Plesset fractions  $A$  in percent where the amount of recovered correlation energy approaches 100 %. Taken from Figure 3.2 and visually estimated to 0.5 %.

basis set	REMP	OO-REMP
cc-pVDZ	6.0	7.5
cc-pVTZ	4.0	5.5
cc-pVQZ	2.0	4.5
aug-cc-pVTZ	2.0	4.0
aug-cc-pVQZ	1.0	3.5

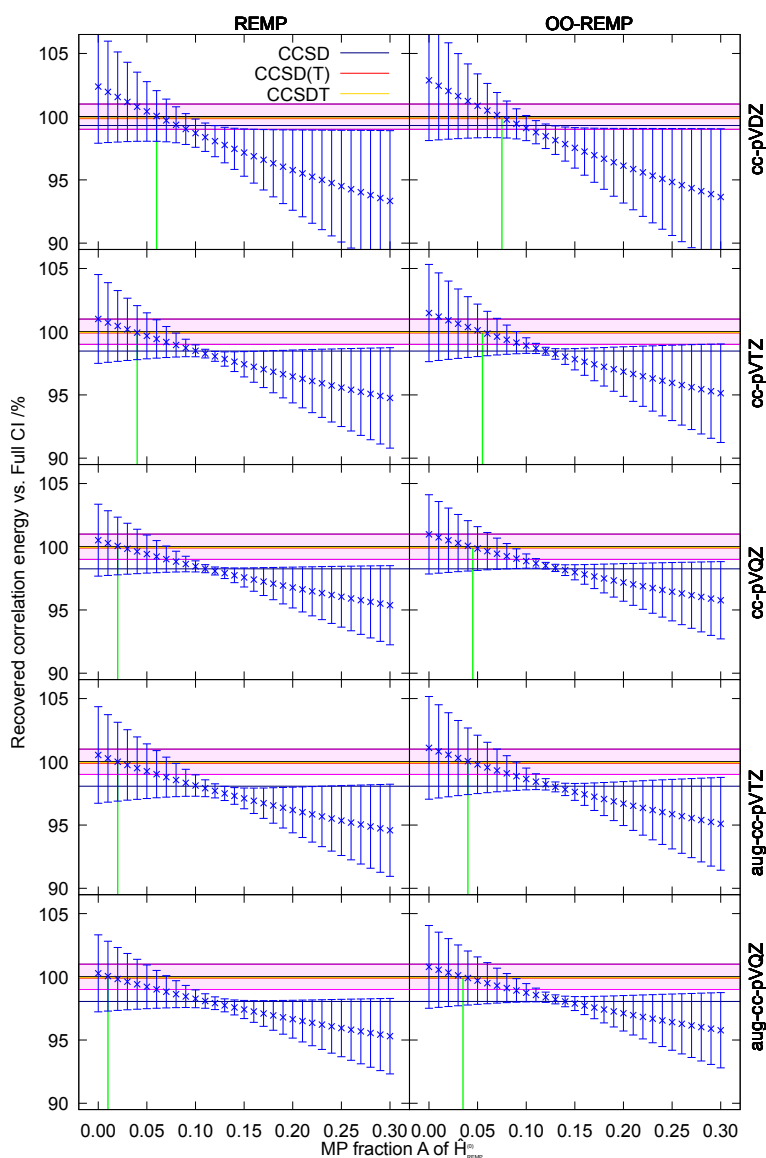
From the assessment of many-electron systems, quite different conclusions can be drawn than from two-electron systems. Figure 3.2 and Table 3.2 in comparison to Figure 3.1 and Table 3.1 show that the behavior with respect to basis size increase is partially reversed. With increasing basis set size, the  $A$  value which leads to 100 % recovery of  $E_{\text{corr}}$  now decreases for both REMP and OO-REMP. The behavior that OO-REMP tends to require larger  $A$  values than REMP with fixed basis size is however preserved. Figure 3.2 also shows the amount of correlation energy recovered by CCSD, CCSD(T) and CCSDT.

Table 3.3 lists the average recovered correlation energy for ten small molecules. With respect to the basis set size, one finds the same key results as before:<sup>[76]</sup>

- Increasing the basis set size leads to a sharp increase of the correlation energy recovered by MP2. This is more pronounced when the cardinal number is increased but also noticeable when the basis set is augmented with diffuse functions.
- RE2 on the other hand experiences a decrease of the recovered correlation energy, also both with increase of the basis cardinal number and the augmentation.
- Orbital optimization always leads to an average increase of the recovered correlation energy compared to the canonical methods, but the gain is always clearly below 1 %. At the same time, the uncertainty of the recovered correlation energy almost always increases.
- The key finding underlying the REMP concept – namely that RE overestimates the correlation energy and that MP2 underestimates it – persists also if core correlation is considered.
- For this set of molecules, the series  $\text{CCSD} \rightarrow \text{CCSDT} \rightarrow \text{CCSDTQ}$  converges strictly monotonic from above regarding the correlation energy. As the underlying distribution is one-sided capped, it might not be completely justified to use the standard deviation as measure for the uncertainty.

- 
- CCSD becomes worse with increasing basis set size. The recovered correlation energy drops from more than 99 % to 98 % when going from cc-pVDZ to aug-cc-pVQZ. At the same time, the uncertainty increases.
  - The REMP mixtures which lead to minimal standard deviation are almost equal both with and without orbital optimization. In case they are not exactly equal, the orbital-optimized variant demands slightly larger MP fractions. As with the parent methods, the orbital-optimized variants recover slightly more correlation energy than the canonical ones. In contrast to the parent methods, the minimal standard deviations achieved with OO-REMP are always smaller than those obtained with REMP.
  - CCSD(T) always delivers excellent results, recovering 99.9 % of the CCSDTQ correlation energy with uncertainties of mostly less than 0.1 %.
  - CCSDT is only slightly superior to CCSD(T). For all basis sets, it recovers at least 0.03 % more correlation energy than CCSD(T) with similar errors.
  - Although the results are not fully converged, meaningful results can be obtained from the cc-pVTZ and especially the aug-cc-pVTZ basis set.





**Figure 3.2:** Graphical representation of the recovered correlation energy for ten many-electron systems (OH, OH<sup>-</sup>, Ne, BeH<sub>2</sub>, Be, HF, F<sup>-</sup>, F, LiH, Li<sub>2</sub>). Error bars indicate one standard deviation, green vertical bars indicate the mixing ratio at which roughly 100% of the CCSDTQ correlation energy is recovered. The hatched area spans the region of (100±1)% correlation energy. Perturbative correlation energies correspond to second order in energy. The errors of CCSD, CCSD(T) and CCSDT are indicated as horizontal dark blue, red and yellow lines.

**Table 3.3:** Amount of recovered correlation energy from several methods and basis sets, average over ten molecules (OH, OH<sup>-</sup>, Ne, BeH<sub>2</sub>, Be, HF, F<sup>-</sup>, F, LiH, Li<sub>2</sub>). The REMP/OO-REMP mixture selected is that with the smallest standard deviation. All errors refer to CCSDTQ with the respective basis set.

method	average	$\sigma$	median	min	max
cc-pVDZ					
RE2	102.38	4.48	100.57	99.41	111.30
REMP2(0.10)	98.70	1.12	98.93	96.85	100.58
MP2	82.72	15.06	85.20	58.43	97.89
OO-RE2	102.87	4.76	100.85	99.66	111.80
OO-REMP2(0.11)	98.77	0.92	99.01	97.07	100.04
OO-MP2	82.94	15.03	85.42	58.60	97.90
CCSD	99.30	0.50	99.33	98.58	99.97
CCSD(T)	99.85	0.12	99.82	99.69	100.00
CCSDT	99.90	0.10	99.92	99.75	100.00
cc-pVTZ					
RE2	101.01	3.51	99.09	98.42	108.65
REMP2(0.11)	98.27	0.34	98.25	97.87	98.87
MP2	87.45	11.54	92.52	65.89	98.26
OO-RE2	101.48	3.84	99.45	98.78	110.16
OO-REMP2(0.12)	98.46	0.31	98.54	97.91	98.94
OO-MP2	87.85	11.67	93.00	66.17	98.73
CCSD	98.47	0.92	98.36	97.09	99.83
CCSD(T)	99.90	0.07	99.91	99.78	99.97
CCSDT	99.95	0.05	99.97	99.85	100.00
cc-pVQZ					
RE2	100.52	2.84	99.00	98.10	106.21
REMP2(0.12)	98.09	0.32	98.12	97.65	98.67
MP2	89.36	9.48	93.40	72.78	98.50
OO-RE2	100.98	3.13	99.34	98.49	107.56
OO-REMP2(0.12)	98.50	0.26	98.50	98.12	98.89
OO-MP2	89.82	9.64	93.89	73.11	99.14
CCSD	98.25	1.00	98.18	96.66	99.75
CCSD(T)	99.90	0.06	99.91	99.81	99.97
CCSDT	99.95	0.05	99.97	99.84	100.00
aug-cc-pVTZ					
RE2	100.54	3.82	98.80	96.93	108.50
REMP2(0.12)	97.70	0.56	97.83	96.63	98.40
MP2	87.92	11.33	92.45	66.48	98.79
OO-RE2	101.10	4.06	99.23	97.61	110.03
OO-REMP2(0.13)	98.02	0.39	97.99	97.37	98.71
OO-MP2	88.67	11.81	93.08	66.76	100.66
CCSD	98.07	1.35	98.05	95.76	99.81
CCSD(T)	99.88	0.08	99.90	99.77	99.97
CCSDT	99.94	0.07	99.97	99.77	100.00
aug-cc-pVQZ					
RE2	100.28	3.05	98.90	97.15	106.20
REMP2(0.12)	97.91	0.50	98.05	96.92	98.58
MP2	89.71	9.48	93.51	72.99	99.00
OO-RE2	100.79	3.27	99.28	97.76	107.55
OO-REMP2(0.13)	98.22	0.36	98.22	97.60	98.82
OO-MP2	90.40	9.90	94.07	73.30	100.66
CCSD	98.05	1.25	98.08	95.86	99.75
CCSD(T)	99.90	0.06	99.91	99.80	99.98
CCSDT	99.93	0.07	99.96	99.76	100.00

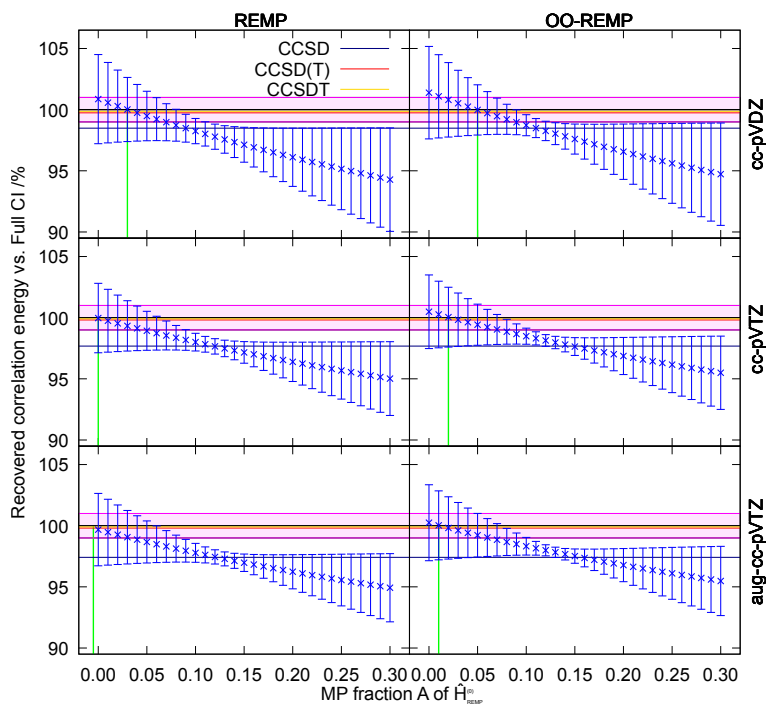


**Figure 3.3:** Graphical representation of the recovered correlation energy for 19 many-electron systems (OH, OH<sup>-</sup>, Ne, BeH<sub>2</sub>, Be, HF, F<sup>-</sup>, F, LiH, Li<sub>2</sub>, LiF, N<sub>2</sub>, CO, <sup>1</sup>CH<sub>2</sub> (<sup>1</sup>A<sub>1</sub>), <sup>3</sup>CH<sub>2</sub> (<sup>3</sup>B<sub>1</sub>), H<sub>2</sub>O, BH<sub>3</sub>, NH<sub>3</sub>, CH<sub>4</sub>). Error bars indicate one standard deviation, green vertical bars indicate the mixing ratio at which roughly 100 % of the CCSDTQ correlation energy is recovered. The hatched area spans the region of (100±1) % correlation energy. Perturbative correlation energies correspond to second order in energy.

The set was successively augmented with nine more larger molecules for which it is impossible to obtain CCSDTQ/aug-cc-pVQZ results in reasonable time but for which CCSDTQ/cc-pVTZ and CCSDTQ/aug-cc-pVTZ numbers are available (LiF, N<sub>2</sub>, CO, <sup>1</sup>CH<sub>2</sub> (treated as <sup>1</sup>A<sub>1</sub>-symmetric closed-shell singlet), <sup>3</sup>CH<sub>2</sub> (<sup>3</sup>B<sub>1</sub>), H<sub>2</sub>O, BH<sub>3</sub>, NH<sub>3</sub>, CH<sub>4</sub>).

**Table 3.4:** Amount of recovered correlation energy from several methods and basis sets, average over 19 molecules (OH, OH<sup>-</sup>, Ne, BeH<sub>2</sub>, Be, HF, F<sup>-</sup>, F, LiH, Li<sub>2</sub>, LiF, N<sub>2</sub>, CO, <sup>1</sup>CH<sub>2</sub>, <sup>3</sup>CH<sub>2</sub>, H<sub>2</sub>O, BH<sub>3</sub>, NH<sub>3</sub>, CH<sub>4</sub>). The REMP/OO-REMP mixture selected is that with the smallest standard deviation. All errors refer to CCSDTQ with the respective basis set.

method	average	$\sigma$	median	min	max
cc-pVDZ					
RE2	100.86	3.64	99.85	97.34	111.30
REMP2(0.11)	98.02	0.99	98.00	96.39	99.68
MP2	85.99	12.08	90.26	58.43	98.41
OO-RE2	101.39	3.78	100.10	98.49	111.80
OO-REMP2(0.11)	98.49	0.78	98.60	97.07	100.04
OO-MP2	86.51	12.29	90.66	58.60	100.13
CCSD	98.49	1.15	98.58	95.88	99.97
CCSD(T)	99.74	0.16	99.72	99.37	100.00
CCSDT	99.86	0.12	99.87	99.55	100.00
cc-pVTZ					
RE2	99.97	2.84	98.99	97.15	108.65
REMP2(0.12)	97.65	0.63	97.73	96.36	98.71
MP2	88.91	9.17	92.27	65.89	98.26
OO-RE2	100.48	3.01	99.43	98.12	110.16
OO-REMP2(0.12)	98.14	0.48	98.18	97.16	98.94
OO-MP2	89.53	9.42	92.81	66.17	99.02
CCSD	97.68	1.24	97.55	95.17	99.83
CCSD(T)	99.81	0.14	99.84	99.42	99.97
CCSDT	99.91	0.09	99.93	99.62	100.00
aug-cc-pVTZ					
RE2	99.68	2.96	98.71	96.93	108.50
REMP2(0.13)	97.29	0.57	97.42	96.35	98.39
MP2	89.23	8.97	92.47	66.48	98.79
OO-RE2	100.24	3.10	99.22	97.61	110.03
OO-REMP2(0.13)	97.83	0.42	97.77	96.93	98.71
OO-MP2	90.05	9.42	93.13	66.76	100.66
CCSD	97.41	1.33	97.25	95.11	99.81
CCSD(T)	99.81	0.14	99.81	99.42	99.97
CCSDT	99.90	0.10	99.92	99.61	100.00

Table 3.4 shows that the inclusion of larger and electronically more demanding molecules changes the outcome slightly. Instead of more than 100 %, RE2 now recovers slightly less than 100 % correlation energy. The same decrease is found for OO-RE2, but the latter still recovers more than 100 % correlation energy. MP2 and OO-MP2, on the other hand,

recover 1.5 % more correlation energy for the larger set compared to the smaller set. The effect on the optimal REMP mixture is however minimal as the mixing ratio  $A$  exhibiting the smallest error changes by 1 % at most and the amount of correlation energy recovered by those mixtures changes by 0.6 % at most. The general trend of CCSD to recover less correlation energy with increasing basis size is also present for the larger set, additionally, one finds that the general amount of correlation energy is smaller and the uncertainty is larger in case of the larger set. Also in the case of CCSD(T) and CCSDT, the amount of recovered correlation energy decreases and the uncertainty increases, although to a much smaller extent. It should however be mentioned that the decrease of recovered correlation energy is not related to missing size consistency. All investigated methods are strictly size-consistent, size-extensive and unitary invariant. Therefore, the differences between Tables 3.2 and 3.4 are related to the choice of molecules rather than missing size consistency.

The finding that both RE2 and MP2 recover less than 100 % correlation energy is insofar interesting as that – assuming a linear interpolation – it is now not possible anymore to arrive at a mixed method which recovers 100 % of the FCI (or CCSDTQ) correlation energy. OO-RE on the other hand still recovers slightly more than 100 % of the CCSDTQ correlation energy, making it in principle possible to construct a method which reproduces the FCI correlation energy. This can also be seen in Figure 3.3 which shows that the points where 100 % correlation energy are recovered are shifted significantly compared to Figure 3.2.

In general, the hierarchy of the investigated methods does not change after considering the larger set of molecules. Including even larger molecules and/or larger basis sets was not possible with the available computational resources and programs. The CCSDTQ/aug-cc-pVQZ calculation for the hydroxide ion took already 1873 h CPU time on a JUSTUS2 compute node (9½ days of wall clock time) to reach a convergence of  $1 \cdot 10^{-10}$  in both energy and residuum. Given the results from Table 3.4, one can rank the investigated methods as follows:  $MP2 < OO-MP2 < RE2 < OO-RE2 < CCSD \approx REMP < OO-REMP < CCSD(T) < CCSDT$ . OO-REMP is superior to CCSD insofar as it can reach a much narrower distribution of the recovered correlation energy and at the same time recovers a larger amount of correlation energy. CCSD(T) seems to be useful as total correlation energy reference as it recovers 99.8(1) % of the CCSDTQ correlation energy for the investigated set of molecules. At the same time, CCSD(T) would not be useful for an analysis which breaks down the correlation energy in terms of configuration state functions, as the associated wavefunction is not easily accessible.

Tables 3.3 and 3.4 also list the median and the lower and upper extremes as additional statistical quantity. In all cases, the average and the median agree reasonably well, thus corroborating the previous statements. The REMP methods with the smallest standard deviation also do not exhibit serious outliers, indicating that REMP and especially OO-REMP with appropriate mixing parameters provide a much more balanced and uniform description of the electronic correlation than any of the parent methods alone. Given that the statistical population is not overly large, the median is only of limited significance. It

is however noteworthy that in all cases the median is slightly smaller than the arithmetic mean. In case of the larger basis sets, the median of all REMP and OO-REMP mixtures is below 100 %, indicating that no mixture is able to reproduce the FCI correlation energy.

As such an analysis is only possible for small molecules and not too large basis sets, the remaining analysis focuses on the performance for larger systems where other measures for the quality of the calculation are taken into account. An analysis of the total correlation energy recovered is furthermore only of limited significance regarding the quality of a method. As has been e.g. the case with SCS-MP2, a method may deliver a decent total correlation energy whereas the breakdown into CSF class contributions reveals large errors and heavily flaws in the associated wavefunction.

A potentially interesting subject for further studies would be to investigate which choice for  $A$  provides the best results if the reference and the correlation energies are extrapolated to the CBS limit.

### 3.2 Thermochemistry

*The results discussed in this section were already published in References [50–52].*

Getting basic thermochemistry right is one of the most indispensable requirements for any generally applicable quantum chemical method.

REMP and OO-REMP were parameterized and tested on a number of closed and open shell thermochemistry benchmark sets. The first benchmark set that REMP and OO-REMP were applied to is a subset of the reactions that were used by Grimme to parameterize SCS-MP2,<sup>[47]</sup> hence this set will be referred to as the “SCS-MP2” set. From the original set, all open-shell reactions and the transition states were removed. The reasons for choosing this set were that all molecules are of modest size so that it was possible to run all calculations with the first version of the newly written REMP program, furthermore, as SCS-MP2 was regarded as competitor to REMP, it was directly possible to compare to SCS-MP2 results. Additionally, a very similar set was used by Bozkaya and coworkers to benchmark OCEPA,<sup>[214]</sup> OMP2, OMP2.5, OMP3,<sup>[154]</sup> and several spin-component-scaled derivatives thereof.<sup>[215]</sup> When the first REMP results were generated, there were only QCISD(T) reference numbers available, hence it was also necessary to generate proper CCSD(T) reaction energies. As result of the SCS-MP2 set, it was found that the MAD of REMP averaged over all reactions becomes minimal with  $A = 0.12$  and amounts to  $1.18 \text{ kcal mol}^{-1}$  (RMSD= $1.88 \text{ kcal mol}^{-1}$ ). For comparison, SCS-MP2 scored an MAD of  $1.82 \text{ kcal mol}^{-1}$  on its own calibration set and CCSD yielded  $1.99 \text{ kcal mol}^{-1}$ .

For running OO-REMP calculations, the set further had to be pruned, and on the basis of this set, it was found that OO-REMP(0.25) achieves an MAD of  $0.48 \text{ kcal mol}^{-1}$  (RMSD= $0.65 \text{ kcal mol}^{-1}$ ) while the performance of REMP was hardly changed. REMP(0.13) yields an MAD of  $1.16 \text{ kcal mol}^{-1}$  (RMSD= $1.73 \text{ kcal mol}^{-1}$ ). These results show that OO-REMP has the potential to deliver results with chemical accuracy, but such a bold statement has to be verified by further benchmark sets for more diverse chemistry.

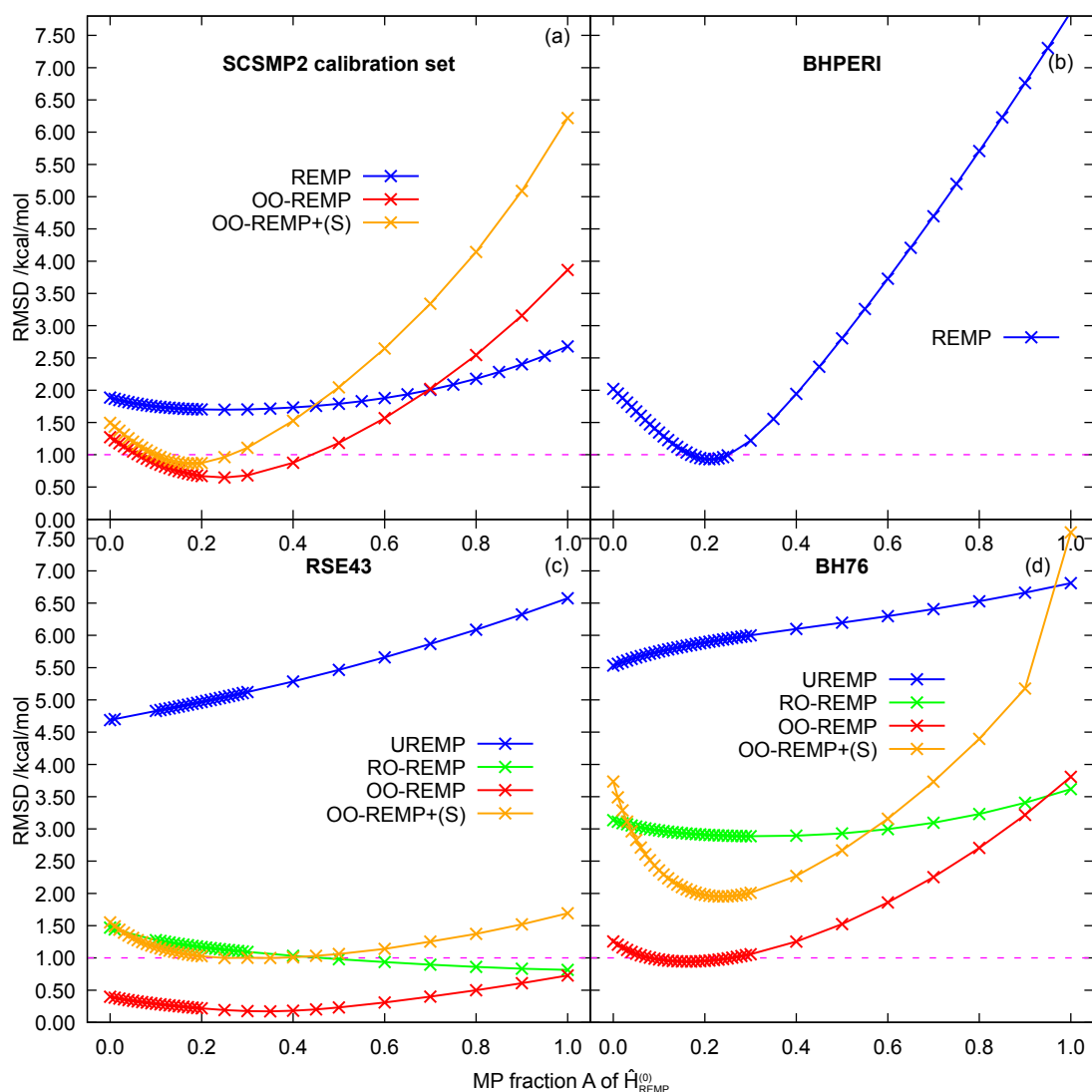


**Figure 3.4:** Graphical representation of the RMSD for four different benchmark sets and different REMP flavors (a) the (pruned) SCS-MP2 calibration set (b) the (incomplete) BHPERI set (c) the RSE43 benchmark set (d) the BH76 benchmark set.

REMP and OO-REMP were subsequently tested on a number of benchmark sets covering a broad scope of main group reactivity: The RSE43 benchmark set<sup>[43,216]</sup> is dedicated to the stability of doublet radicals, namely, it tests the ability of a method to predict the relative stability of such radical species. On average, the reaction energies are not large, it is thus easy to obtain a “chemically accurate” result for this set. Canonical REMP was tested in both the spin-unrestricted and the restricted-open shell variant. It turned out that the restricted formulation provides significantly better results as some of the UHF reference determinants suffer from severe spin contamination. It was also shown that

the error of the UREMP results correlates fairly well with the spin contamination of the reference. One can thus conclude that for such systems it is desirable to use methods which try to yield spin-pure wavefunctions. As shown in Figure 3.4, OO-REMP performs well for this benchmark set and clearly outperforms its canonical counterpart. Part of the success of OO-REMP for this benchmark set is rooted in the ability of orbital-optimized methods to provide approximately spin-pure wavefunctions.<sup>[43,120,217]</sup> Compared to other methods (especially DFT), OO-REMP performs outstandingly well for the RSE43 benchmark set.

The BHPERI<sup>[216,218–221]</sup> benchmark set consists of the barrier heights of 26 pericyclic reactions, and in contrast to the first benchmark set, this set now tests the ability to predict transition state energies and reaction barrier heights. Transition states are generally more demanding than minimum structures due to the typically elongated bonds and the potential open shell character. From the original set, reactions 9 and 10 were excluded from the full scan due to the large size of the constituting molecules. All remaining systems were treated at the restricted closed shell level. For the excluded reactions, selected points in the  $A$  range were calculated to show that they follow the general trend<sup>1</sup>. So far, no OO-REMP data are available for the BHPERI set.

The BH76 set<sup>[216,221–223]</sup> consists of two subsets, namely the HTBH38<sup>[222]</sup> and the NHTBH38<sup>[223]</sup> set, describing barrier heights for hydrogen and non-hydrogen atom transfer reactions. Almost all of these reactions are of open shell character, the whole set is thus only tractable with a program capable of using a restricted open shell or an unrestricted reference determinant. Calculations for the BH76 set were done with UHF and ROHF reference as well as using orbital optimization. Similar to the other cases, it was found that OO-REMP performs better than the canonical counterparts and also better than OO-REMP including perturbative singles (OO-REMP+(S)).

Figure 3.4 shows a graphical representation of the RMSDs for the four benchmark sets. The RMSD was chosen as it is a more rigorous statistical measure than the MAD. As can be seen, OO-REMP yields in all cases an RMSD close to or below  $1 \text{ kcal mol}^{-1}$ . The variant which includes perturbative singles [OO-REMP+(S)] performs consistently worse, although it shows virtually the same trends. Whenever there is data for both UREMP and RO-REMP, one finds that RO-REMP performs significantly better. Yet, the results achieved for the BH76 set still render it unreliable. UREMP, finally, leads to no improvement over pure RE, and on an absolute scale the results obtained for RSE43 and BH76 show that it should not be used. Already from the data presented in Figure 3.4 it is safe to conclude that orbital optimization is mandatory for open shell cases and definitely an improvement for closed shell cases. It is furthermore quite satisfying that the minima of the OO-REMP curves are always located close to  $A \approx 0.20$ . The unrestricted REMP variant shows no minima at all, instead, pure RE is always the choice of  $A$  which still performs best. The restricted-closed shell variant behaves rather like the closed shell

---

<sup>1</sup>with the computational resources acquired since these calculations were performed, it should now also be possible to run the remaining calculations.



variant, but given that the errors are still large, it can hardly be regarded as a useful method.

Until now, all thermochemistry benchmark sets used CCSD(T) as reference method. CCSD(T) is often called the “gold standard” for computational chemistry of single reference cases and it is the *de facto* standard for benchmarking density functional methods, but even CCSD(T) is not free of errors. It is therefore desirable to use at least one benchmark set with a reference level of theory better than CCSD(T). Such a benchmark set is the W4-11<sup>[224]</sup> set of Karton *et al.* The set primarily consists of atomization energies, but there are four additional benchmark sets derived from the primary set. In detail, the derived benchmark sets cover heavy atom transfer reactions, bond dissociation reactions, isomerizations, and substitution reactions. The reference reaction energies were calculated at the W4 composite level of theory<sup>[225]</sup> which aims to reach the relativistic CCSDTQ5/CBS limit and is claimed to provide sub  $\text{kJ mol}^{-1}$  accuracy. Said reference numbers are also available in an electronic-energy only fashion, discarding all relativistic and ZPVE corrections, making comparisons between electronic structure methods more easy.<sup>[224]</sup> The atomization reactions were furthermore categorized by the amount of perturbative triples correlation energy as measure for the multireference character of the involved species. Here, all molecules falling into the fourth category with the largest multireference character (“Systems dominated by severe nondynamical correlation effects”) were excluded from the statistical evaluation, leaving 124 atomization reactions, 504 heavy atom transfer reactions, 83 bond dissociation reactions, 18 isomerization reactions and 13 substitution reactions. This is justified by the fact that after all, REMP and OO-REMP are single reference methods, and not meant to be able to treat multireference cases. For many of the excluded molecules, severe convergence issues were observed. The resulting non-multireference set was proposed by Karton *et al.*<sup>[224]</sup> and is designated as TAE\_nonMR124. The collection of the non-multireference atomization energies and the derived non-multireference reactions is called W4-11\_nonMR here.

Figure 3.5 shows a graphical representation of the RMSDs achieved with UREMP, RO-REMP, and OO-REMP for the W4-11\_nonMR set and its derived sets together with the respective results for CCSD and CCSD(T). As reference reaction energies the purely electronic part of the W4-11 reference energies was used. Due to the experience gathered on the other benchmark sets, no OO-REMP+(S) calculations were performed. As can be seen, the various subsets are more or less challenging, and they differ in their dependence on the mixing parameter  $A$ . But while most of the RMSD curves in Fig. 3.5 exhibit minima, their location is only in the case of OO-REMP consistent across different subsets. CCSD shows rather poor performance, being sometimes better than the canonical REMP flavors, sometimes even significantly worse, e.g. for the atomization energies. The canonical REMP variants UREMP and RO-REMP exhibit minima in most cases, but even the respective best-performing mixtures are often off by several  $\text{kcal mol}^{-1}$ . OO-REMP provides very accurate results at the minima located at  $A \approx 0.20$ . In fact, the RMSD of OO-REMP is only above  $1 \text{ kcal mol}^{-1}$  in case of the atomization energies ( $1.15 \text{ kcal mol}^{-1}$  @  $A = 0.23$ ) and the heavy atom transfer reactions ( $2.15 \text{ kcal mol}^{-1}$  @  $A = 0.20$ ). In the

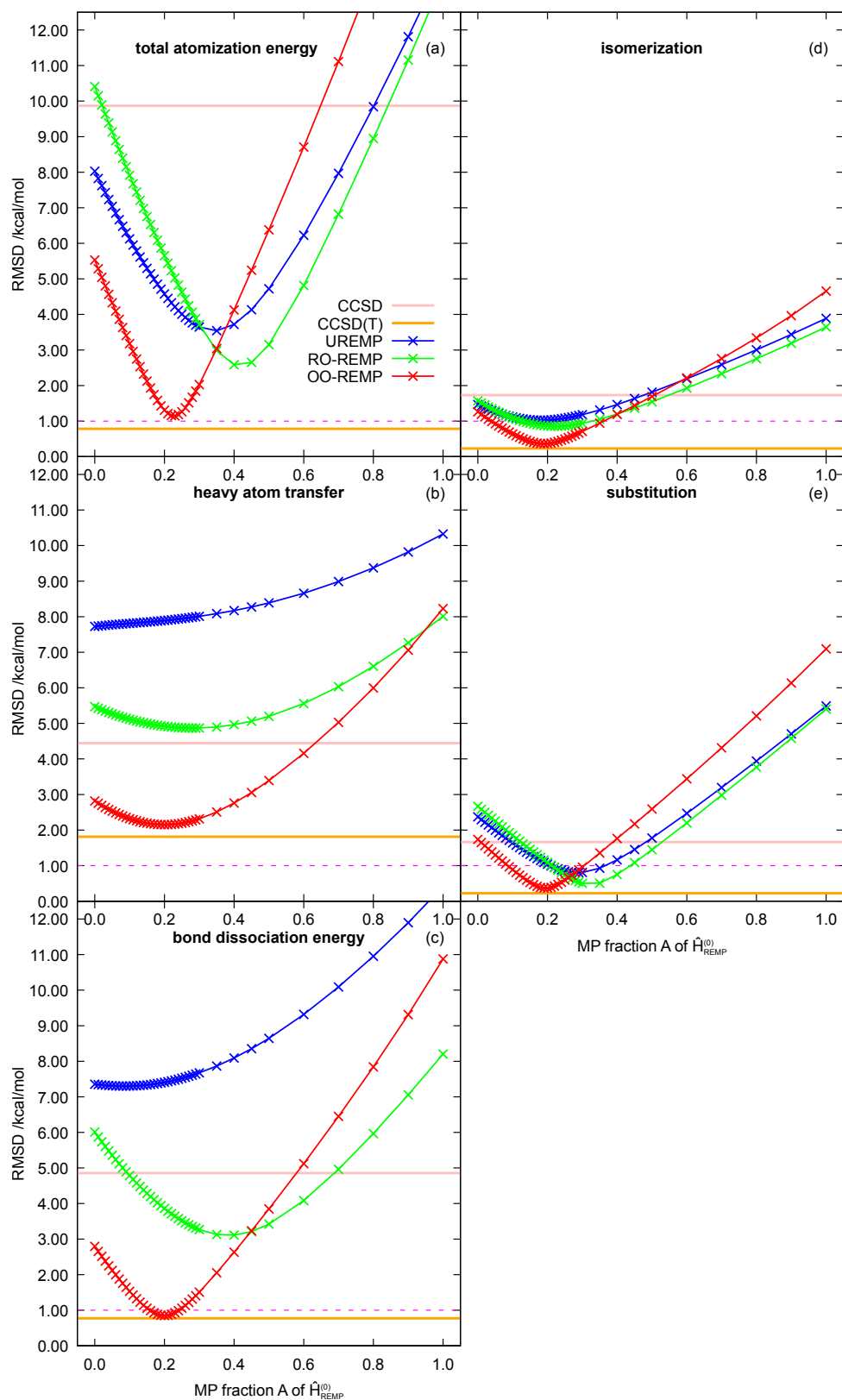


**Figure 3.5:** Graphical representation of the RMSD for the W4-11\_nonMR set and its derived subsets as function of the mixing parameter  $A$ . Average over (a) total atomization energies ( $n = 124$ ) (b) heavy atom transfer reactions ( $n = 504$ ) (c) bond dissociation energies ( $n = 83$ ) (d) isomerization energies ( $n = 18$ ) (e) substitution reactions ( $n = 13$ ). All energies were extrapolated to the CBS limit from the aug-cc-pwCVTZ and aug-cc-pwCVQZ basis sets. See Reference [52] for further results.

latter case, it is quite comforting that CCSD(T) fails comparably badly with an RMSD of  $1.81 \text{ kcal mol}^{-1}$ . In the remaining cases, both CCSD(T) and OO-REMP(0.20) manage to achieve an RMSDs below  $1 \text{ kcal mol}^{-1}$ . It is additionally noteworthy that neither OO-RE2 nor OO-MP2 provides an RMSD below  $1 \text{ kcal mol}^{-1}$  for any of the subsets. In the case of the atomization energies, e.g. OO-REMP(0.23) improves upon OO-RE2 by a factor of five, and compared to OO-MP2 the improvement is even much larger and amounts roughly to a factor of 15(!). It is thus fair to say that REMP hybridization turns two barely useful parent methods into a very powerful approach.

Other basis set combinations were also tested,<sup>[52]</sup> but they turned out to be insufficient. Both alternative basis set combinations tested (def2-[T/Q]ZVPPD and aug-cc-pV[T/Q]Z) are lacking core correlation functions. Moreover, the Ahlrichs type basis sets are excellent basis sets for DFT calculations but were not constructed with the aim of systematic extrapolability.<sup>[226]</sup> <sup>2</sup> Results obtained without CBS extrapolation, i.e. from a single basis set, turned out to be a complete disaster in most cases (see Ref. [52] for further details). Depending on the basis set, the RMSD of the atomization energies amounts to at least  $2 \text{ kcal mol}^{-1}$  (QZ basis sets are still better than TZ basis sets), the optimal  $A$  varies wildly with the basis set, and goes up to 0.6–0.8 in the case of TZ basis sets (with RMSDs larger than  $5 \text{ kcal mol}^{-1}$ ). In the case of the radical substitution and especially the isomerization reactions, the results are much more consistent across different basis sets, as the electronic structure changes not too much when going from the reactants to the products of the reaction. There is thus much more error compensation possible and the basis set needs to be less flexible as there are no large changes in the formal oxidation state. The results for the atomization energies (cf. Figure 1 of Reference [52]) however show that it would be foolish to simply rely on error compensation in difficult cases.

To conclude, one finds that canonical REMP works for closed-shell main group covalent thermochemistry and provides an RMSD slightly larger than  $1 \text{ kcal mol}^{-1}$  with  $0.15 \leq A \leq 0.25$ . The canonical unrestricted generalization hardly provides any improvement and can mostly be considered useless while the high-spin restricted open-shell generalization in principle works but provides only modest improvement. In contrast, the orbital-optimized variant consistently delivers outstanding accuracy for both closed and open shell systems, with the optimal mixing ratio being located at  $A \approx 0.20$  regardless of the character of the benchmark set. The orbital optimized variant has the drawback that it fails for multireference cases, this could however also be considered as a “feature”, as it is generally not advisable to treat multireference species like  $\text{O}_3$ ,  $\text{C}_2$  or  $\text{S}_4$  at a single reference level. It can however be expected that such species will be accessible as soon as a proper multiconfigurational reference is used.

---

<sup>2</sup>The plain def2-XZVP basis sets – optimized by minimizing the atomic HF energy – are only recommended for HF and DFT; for correlation treatment, the doubly polarized basis sets – optimized by maximizing the absolute MP2 correlation energy from an additional set of polarization functions – are recommended.<sup>[227]</sup> The diffuse def2-XZVPPD basis sets<sup>[228]</sup> are explicitly advertised as “property optimized” and are obtained by maximizing the atomic Hartree-Fock polarizability. The def2 basis sets furthermore have the disadvantage that there are no 5Z and 6Z basis sets necessary for extreme accuracy

### 3.3 Noncovalent Interactions

*Disclaimer: A part of the results presented here was generated by Julian Schöckle during his bachelor thesis<sup>[229]</sup> under the supervision of the present author.*

Noncovalent interactions are an important and wide field of chemical research<sup>[230]</sup> and an essential aspect of supramolecular chemistry.<sup>[231–234]</sup> They are especially relevant in condensed matter, specifically in biological material<sup>[235–238]</sup> and other soft matter. In organisms, they are relevant for the secondary structure of proteins as well as for keeping cell membranes together. Noncovalent interactions are furthermore responsible for the structure, stability and function of double-stranded DNA<sup>[237–239]</sup> and are thus indispensable for all higher forms of life as we know it. This is reflected by the presence of Watson-Crick nucleobase pairs in many intermolecular interaction benchmark sets like S22.

Noncovalent complexes can be classified by the contributing interactions as e.g. being dominated by electrostatic interactions, dispersion driven or mixed, typically on the basis of DFT-SAPT calculations.<sup>[151,240–245]</sup> For a generally applicable quantum chemical method, it is of paramount importance to be able to describe these kinds of interactions accurately and unbiased. MP2, e.g., is known to perform very well for electrostatic interactions while it is unreliable for dispersion-dominated complexes.<sup>[151]</sup> These findings are completely recovered by the results for the A24 benchmark set shown in Section 3.3.2.

#### 3.3.1 The RG18 Benchmark Set

The RG18 benchmark set<sup>[216]</sup> consists of 18 complexes of rare gas atoms (either rare gas oligomers or complexes with small molecules). The structures were used as available from the GMTKN55 database together with the CCSD(T)/CBS reference interaction energies which were given with a precision of  $0.01 \text{ kcal mol}^{-1}$ .

This set is interesting as it combines “regular” main group molecules and rare gases. While main group molecules tend to have well-localizable and spatially separated electron pairs where SDEs are important, rare gases (except helium) do have rather crowded electron pairs and as a consequence, TDEs become more important.<sup>[70,246]</sup> Rare gases thus can be arranged in between main group elements and transition metals.

For obtaining accurate noncovalent interaction energies, an extrapolation to the complete basis set (CBS) limit and often also a BSSE correction (counterpoise correction) is mandatory.<sup>[247]</sup> While both methods work quite differently, they have the same goal, namely to eliminate shortcomings of a finitely large orbital basis set

The same basis set selection and CBS extrapolation technique as in the case of the reference numbers were used:<sup>[216]</sup> All homo- and heterodimers use the aug-cc-pVTZ and aug-cc-pVQZ bases and are counterpoise-corrected while all higher oligomers of noble gases use the aug-cc-pwCVTZ and aug-cc-pwCVQZ bases but no counterpoise correction.

In accordance with the reference calculations, chemical core electrons were frozen for the dimers and heterocomplexes while all electrons were correlated for the trimers, tetramers and hexamers. The energies were first extrapolated to the CBS limit, only afterward the CP correction was applied while calculating interaction energies. In the case of krypton, the  $h$  functions were stripped from the aug-cc-pwCVQZ basis set as wavel is not capable to compute integrals over basis functions with  $L > 4$ . The resulting differences are expected to be insignificantly small.

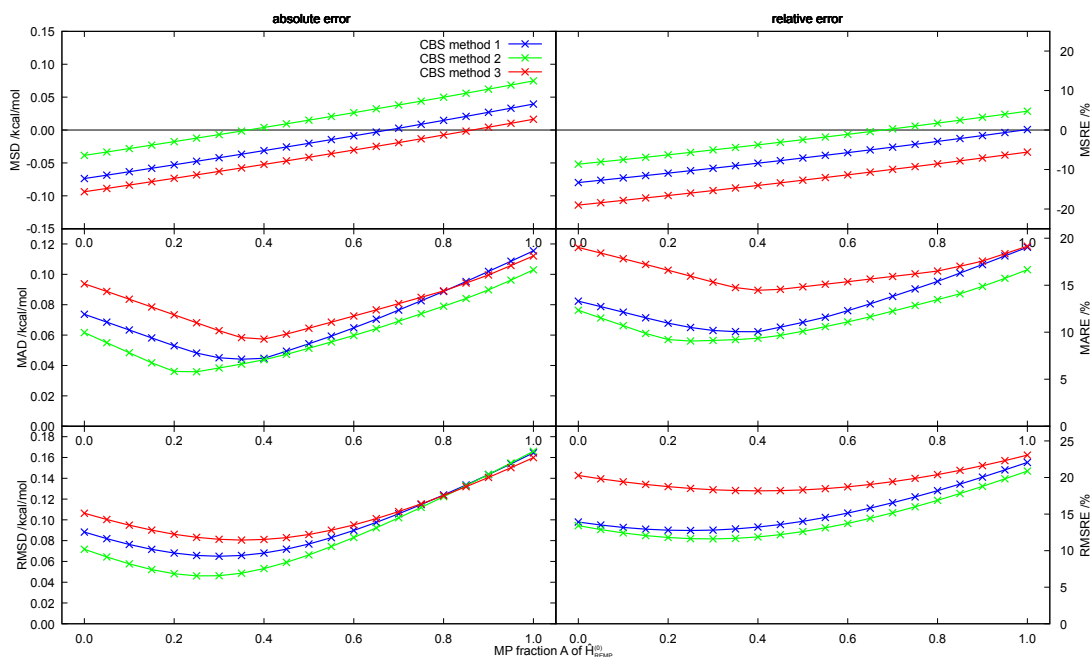


**Figure 3.6:** Statistical descriptors for the RG18 benchmark set as function of the REMP scaling parameter  $A$ . Absolute errors on the left, relative errors on the right.

Originally, two different schemes for the CBS extrapolation were tested<sup>[229]</sup> and it was found that the optimal mixing parameter slightly depends on the choice of the extrapolation scheme as well as on the chosen error descriptor (MAE vs. RMSD). In this work, a third extrapolation scheme was added.

As CBS extrapolation and BSSE correction are crucial for obtaining accurate noncovalent interaction energies, three different CBS extrapolation schemes were applied and compared (see also the more detailed elaboration in Section 3.3.2):

- The first scheme is based on

$$E_{\text{Ref}}(X) = E_{\text{Ref,CBS}} + A \cdot e^{-\alpha\sqrt{X}} \quad (3.1)$$

$$E_{\text{Corr}}(X) = E_{\text{Corr,CBS}} + X^{-\beta} \quad (3.2)$$

where  $X$  is the basis cardinal number and  $\alpha$  and  $\beta$  are parameters either determined from fitting to results from at least three basis sets for the system under consideration

or determined by fitting to a large number of molecules. It is commonly attributed to Petersson and coworkers.<sup>[226,248]</sup> Here, the parameters determined by Neese and Valeev<sup>[226]</sup> for aug-cc-pV[T,Q]Z were used ( $\alpha = 5.79$ ,  $\beta = 3.05$ ).

- The second scheme is based on

$$E_{\text{Ref}}(X) = E_{\text{Ref,CBS}} + A \cdot e^{-\alpha X} \quad (3.3)$$

$$E_{\text{Corr}}(X) = E_{\text{Corr,CBS}} + X^{-\beta} \quad (3.4)$$

It was introduced by Helgaker *et al.*<sup>[249–253]</sup> Also for this scheme, a fixed parameter set was used, namely the universally applied choice  $\alpha = 1.63$  and  $\beta = 3.05$ .

- The third scheme applied (focal point analysis<sup>[254,255]</sup>) is the one that is commonly used to approximate the correlation energy of a large basis and an expensive method from MP2 calculations:

$$E_{\text{REMP,large}} \approx E_{\text{MP2,large}} + E_{\text{REMP,small}} - E_{\text{MP2,small}} \quad (3.5)$$

This scheme is not as accurate as actual CBS extrapolation schemes but the method of choice when expensive calculations with large basis sets are not affordable.

Figure 3.6 shows the mean signed deviation, the mean absolute deviation and the root mean square deviation as well as their relative counterparts for REMP based on canonical orbitals. The reference reaction energies are expressed as dissociation energies. RE2 thus slightly underbinds noncovalent complexes while MP2 tends to slightly overbind them (absolute errors) or is on average right on spot (relative errors). MAD and RMSD however reveal that both the absolute and relative error are improved by REMP. Quite interestingly, the position of the minimum and its depth slightly depend on the choice of CBS extrapolation technique. Method 2 delivers the best results, closely followed by method 1. Method 3 is not competitive and exhibits significantly larger errors. There might however be a bias towards method 2 as it can be safely assumed that it was also used for the reference numbers. The smallest MAD achieved with REMP amounts to  $0.036 \text{ kcal mol}^{-1}$  at  $A = 0.25$ , corresponding to a relative error of 9.1%. This is in reasonable agreement with the other thermochemistry results, but shows that noncovalent interactions tend to require rather large  $A$  values. Method 1 has its minimum in the MAD at  $A = 0.35$  ( $0.044 \text{ kcal mol}^{-1}$ )

It should be noted that there is a broad range in  $A$  where both method 1 and 2 yield noncovalent interaction energies with errors smaller than  $0.1 \text{ kcal mol}^{-1}$  and relative errors smaller than 10%. Extrapolation method 3 also has errors mostly below  $0.1 \text{ kcal mol}^{-1}$ , but the relative errors are mostly larger than 15%.

Table 3.5 lists the RE and MP statistics as well as the best performing mixture for both extrapolation methods along with some representative DFT results. As the DFT results were obtained with a different basis set (def2-QZVP), this comparison should not be overinterpreted. On the other hand, def2-QZVP is a very good basis set for DFT, as

**Table 3.5:** Absolute errors for the RG18 benchmark set, all in kcal mol<sup>-1</sup>. REMP energies were extrapolated from aug-cc-pV[T/Q]Z for dimers and aug-cc-pwCV[T/Q]Z for higher aggregates as described above. DFT errors were taken from Reference [256] without modification.

A	MSD	MAD	stdev	RMSD	min	max
method 1						
0.00	-0.074	0.074	0.050	0.088	-0.174	-0.006
0.30	-0.042	0.045	0.051	0.065	-0.212	0.015
1.00	0.040	0.115	0.164	0.164	-0.296	0.384
method 2						
0.00	-0.039	0.062	0.062	0.072	-0.125	0.117
0.25	-0.012	0.036	0.046	0.046	-0.101	0.081
1.00	0.075	0.103	0.152	0.166	-0.064	0.392
DFT results (selection, obtained with the def2-QZVP basis, taken from Ref. [256])						
revTPSS, D3(BJ)	0.029	0.057	0.074	0.078	-0.130	0.200
revTPSSh, D3(BJ)	0.027	0.061	0.075	0.078	-0.170	0.160
BLYP, D3(BJ)	0.005	0.055	0.082	0.080	-0.130	0.210
APFD	0.053	0.071	0.085	0.098	-0.070	0.230
B2PLYP, D3(0)	-0.059	0.153	0.180	0.185	-0.410	0.240
B3LYP, D3(BJ)	-0.077	0.133	0.185	0.196	-0.620	0.250
DSD-PBEB95, D3(BJ)	0.097	0.171	0.274	0.283	-0.300	0.830
M062X, no D	-0.033	0.231	0.315	0.308	-0.590	0.800
BP86, D3(0)	-0.524	0.554	0.700	0.859	-2.790	0.170

DFT generally has different basis set requirements than wavefunction methods.<sup>[7]</sup> The fact that a completely different basis set was used than for the reference calculations probably explains the surprising ranking of the DFT methods. Specifically, it was found that mGGA and hybrid functionals perform better than double hybrids. Given the usually outstanding performance of double hybrid functionals, this is probably the result of fortunate error cancellation. These considerations apart, REMP clearly outperforms all tested density functional for the RG18 benchmark set. The supposedly best density functional – revTPSS-D3(BJ) – achieves an RMSD of 0.08 kcal mol<sup>-1</sup>. The hybrid variant – revTPSSh-D3(BJ) – is essentially on par, closely followed by BLYP-D3(BJ). The best double hybrid, B2PLYP-D3(0), exhibits an RMSD which is twice as large. The mediocre performance of the double hybrid functionals may be due to the MP2 correlation contribution, which might require some form of CBS extrapolation for sub-0.1 kcal mol<sup>-1</sup> performance.<sup>[257–260]</sup> REMP(0.25) in conjunction with the second extrapolation method, on the other hand, achieves an RMSD of merely 0.05 kcal mol<sup>-1</sup>, with the MSD being only -0.01 kcal mol<sup>-1</sup>. Considering that the reference energies were given with 0.01 kcal mol<sup>-1</sup> precision, a part of the REMP error may even be ascribed to reference round-off errors. On the first glance this is an impressive result, therefore it should be kept in mind that the average reaction energy of the RG18 set amounts to merely 0.58 kcal mol<sup>-1</sup>. An analysis of the relative errors therefore is advisable, too. As has been shown above, REMP achieves a mean absolute relative error clearly below 10%. A comparison of the respective

DFT results (cf. Table 6.3) shows that none of the selected DFT methods is capable of achieving an MARE below 10%. Also in this respect, REMP is clearly superior to DFT.

Due to time and resource limitations, it was not possible to obtain OO-REMP results for the RG18 benchmark set. As OO-REMP in various tests turned out to be at least as accurate as REMP, it can be expected that OO-REMP would further improve upon the REMP results for this set.

### 3.3.2 The A24 Benchmark Set

The A24 set<sup>[261]</sup> consists of 24 noncovalent interactions of small closed-shell molecules for which highly accurate reference numbers are available. The reference numbers include electronic energies up to CCSDT(Q), core corrections, and optionally relativistic corrections.<sup>[262,263]</sup> The reference numbers used here are a best estimate for CCSDT(Q)/CBS without relativity, constructed from

- The CCSD(T)/CBS estimate by Sirianni, Burns and Sherrill<sup>[264]</sup> (A24B)
- The  $\Delta$ core correlation correction by Rezak *et al.*<sup>[261,263]</sup>
- The best-estimate  $\Delta$ CCSDT(Q) correction by Burns *et al.*<sup>[262]</sup> whenever available, otherwise the aVDZ correction from the same source (HCN dimer and formaldehyde dimer)

The reference interaction energies obtained by this composite approach are listed in Table 3.6 together with the dominant kind of interaction .

Again, the question emerges how to best extrapolate to the CBS limit, especially if one wants to compare achieve extreme accuracy for comparing to CCSDT(Q) data. In the following, four different procedures were tested and are compared to each other:

- 1) **Full CBS extrapolation,  $\beta = 3.00$ :** The SCF energy is extrapolated from aug-cc-pVTZ and aug-cc-pVQZ with the Petersson formula<sup>[248,265–268]</sup> and a fixed exponent  $\alpha = 5.79$  as proposed by Neese and Valeev.<sup>[226]</sup> The correlation energy is extrapolated from aug-cc-pVTZ and aug-cc-VQZ with the Halkier-Helgaker formula<sup>[252,253]</sup> and a fixed exponent of  $\beta = 3.0$  (the literature default<sup>[226]</sup>).
- 2) **Full CBS extrapolation,  $\beta = 3.05$ :** The SCF energy is extrapolated from aug-cc-pVTZ and aug-cc-VQZ with the Petersson formula and a fixed exponent  $\alpha = 5.79$ . The correlation energy is extrapolated from aug-cc-pVTZ and aug-cc-VQZ with the Halkier-Helgaker formula and a fixed exponent of  $\beta = 3.05$  as proposed by Neese and Valeev for this basis set combination.<sup>[226]</sup>
- 3)  **$\Delta$ MP2,  $\beta = 3.00$ :** The SCF energy is taken from RHF/aug-cc-pV5Z, the MP2 correlation energy is extrapolated from aug-cc-pVTZ and aug-cc-pVQZ with a fixed exponent of  $\beta = 3.00$ . Finally, the correlation energy difference of OO-REMP and MP2 calculated with the aug-cc-pVQZ basis is added, where the OO-REMP



**Table 3.6:** Reference interaction energies and interaction characterization for the A24 benchmark set, best estimate for CCSDT(Q)/CBS + core correlation. All energies in kcal mol<sup>-1</sup>. HB: hydrogen-bonded, DD: dispersion dominated, MX: mixed character. The assignment to dominating interaction characters is based on SAPT2+3(CCD)/aTZ calculations and was inferred from Figure 1 of Reference [262]. Note that it slightly differs from Řezáč and Hobza’s original assignment.<sup>[261]</sup>

#	system	est. CCSDT(Q)/CBS	character
1	water··· ammonia	-6.559	HB
2	water dimer	-5.057	HB
3	HCN dimer	-4.767	HB
4	HF dimer	-4.534	HB
5	ammonia dimer	-3.171	HB
6	HF··· methane	-1.692	MX
7	ammonia··· methane	-0.785	MX
8	water··· methane	-0.677	MX
9	formaldehyde dimer	-4.533	MX
10	water··· ethene	-2.590	MX
11	formaldehyde··· ethene	-1.642	MX
12	ethyne dimer	-1.542	MX
13	ammonia··· ethene	-1.396	MX
14	ethene dimer	-1.115	DD
15	methane··· ethene	-0.517	DD
16	borane··· methane	-1.530	MX
17	methane··· ethane	-0.843	DD
18	methane··· ethane	-0.616	DD
19	methane dimer	-0.542	DD
20	Ar··· methane	-0.412	DD
21	Ar··· ethene	-0.361	DD
22	ethene··· ethyne	0.784	DD
23	ethene dimer	0.894	DD
24	ethyne dimer	1.080	DD
average		-1.755±2.025	
abs. average		1.985	
median		-1.255	

correlation energy is taken as difference of the OO-REMP/aug-cc-pVQZ and the RHF/aug-cc-pVQZ energy (hybrid of the conventional CBS scheme and the focal point scheme<sup>[244,262,269,270]</sup>).

- 4)  **$\Delta$ MP2,  $\beta$  fitted:** The SCF energy is taken from RHF/aug-cc-pV5Z<sup>3</sup>, the MP2 correlation energy is extrapolated from aug-cc-pVTZ, aug-cc-pVQZ and aug-cc-pV5Z with a free fitted exponent. Finally, the correlation energy difference of OO-REMP and MP2 calculated with the aug-cc-pVQZ basis is added, where the

<sup>3</sup>aug-cc-pV[T/Q/5]Z calculations were performed with ORCA as wawels is not able to treat the  $h$  functions present in the 5Z basis.

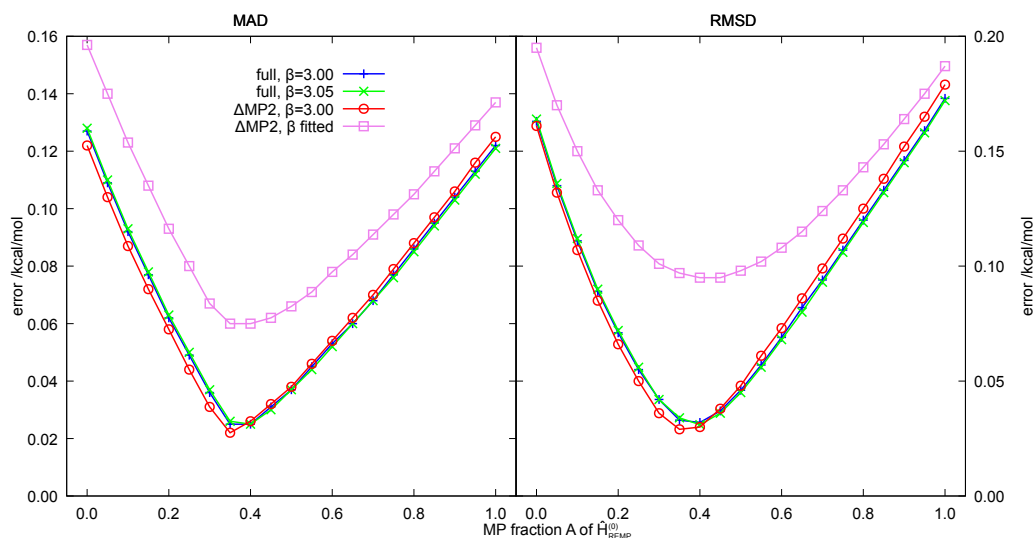


**Figure 3.7:** Comparison of different CBS extrapolation schemes for the A24 benchmark set. Left-hand panel: MAD, right-hand panel: RMSD. See test for further explanations. Errors are calculated with respect to the reference interaction energies listed in Table 3.6.

OO-REMP correlation energy is taken as difference of the OO-REMP/aug-cc-pVQZ and the RHF/aug-cc-pVQZ energy.

In principle, many more combinations are possible, the SCF energy could be extrapolated using a recipe, a different basis set could be used for the  $\Delta$ MP2 correction etc.

Figure 3.7 shows a comparison of the aforementioned extrapolation schemes. The most striking observations are that OO-RE and OO-MP2 results are of virtually the same quality (with OO-MP2 being even slightly superior) while in between, there is an improvement by up to a factor of six upon the parent method! This will be discussed later, the focus here is on the extrapolation technique. As can be seen, while there is almost no difference between the first three methods, the last one where the CBS MP2 correlation energy is fitted to three basis sets clearly falls behind.

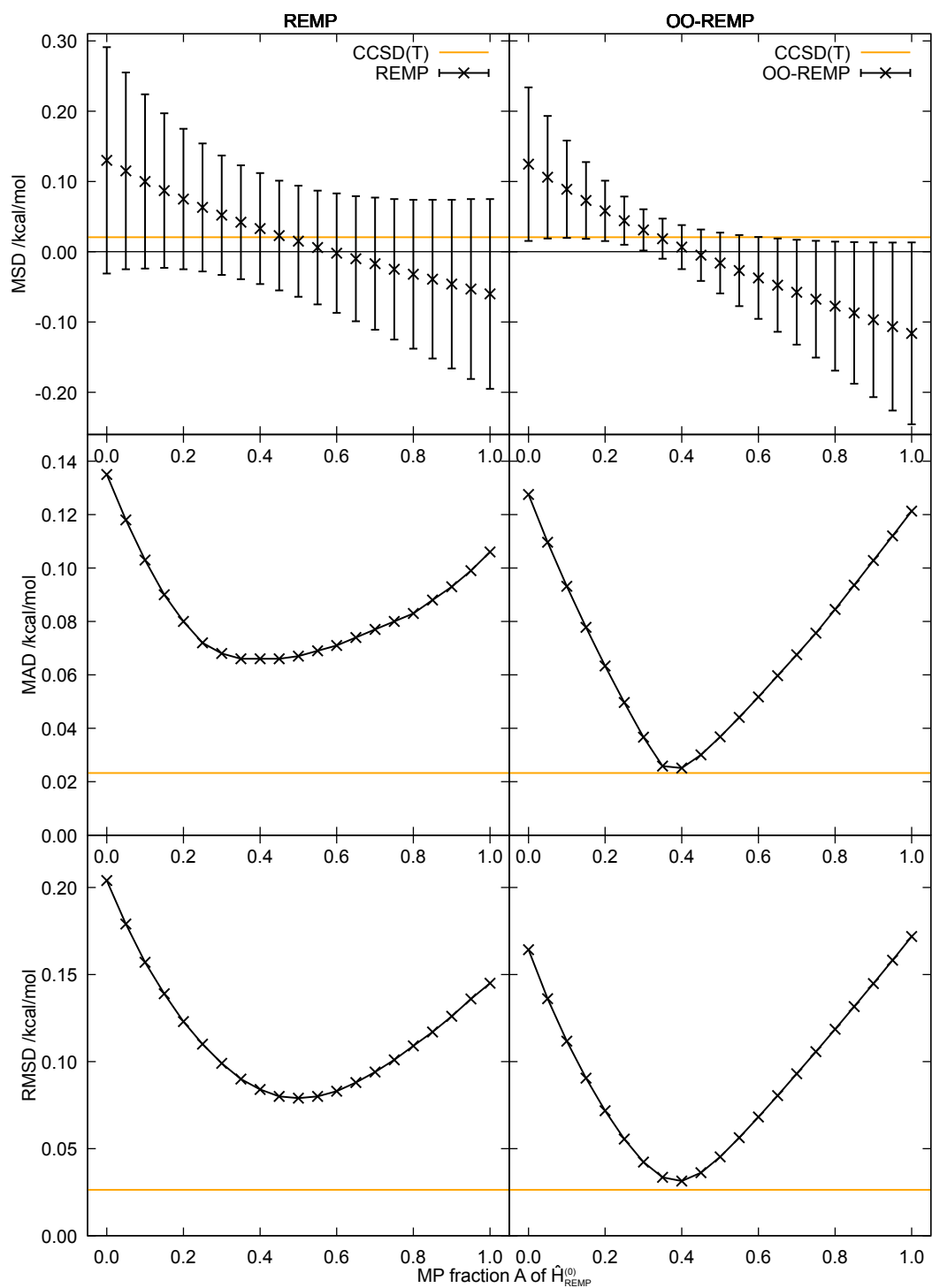
A comparison of the first two extrapolation recipes reveals no significant differences, thus either choice for the correlation energy exponent is fine. Judged by the MAD, the results using a  $\Delta$ MP2 scheme and a large-basis SCF energy are even better by  $\approx 0.005 \text{ kcal mol}^{-1}$  up to  $A = 0.35$  and barely noticeable worse above. The results where the CBS MP2 correlation energy is fitted with a free exponent are worse by  $0.01\text{--}0.04 \text{ kcal mol}^{-1}$  compared to the best results, on the other hand, they are still impressively accurate and interestingly, the ideal value for  $A$  is practically the same as for the other schemes. From the RMSD plot, essentially the same conclusions can be drawn. As the RMSD is more sensitive to outliers, the absolute numbers are larger and the difference between the good and the bad extrapolation schemes is larger. The comparison of different

extrapolation schemes shows that if sufficiently large basis sets and validated extrapolation schemes are employed, it is possible to arrive at almost identical results from different schemes. The aug-cc-pVTZ basis set used in scheme 4 is probably too small and should be replaced by aug-cc-pV6Z for freely fitting the exponent. Inspection at the single reaction level shows that in case of scheme 4, the vast majority of the error is caused by reactions 20 and 21 (Ar $\cdots$ methane and Ar $\cdots$ ethane), each systematically being off by at least 0.2 kcal mol $^{-1}$ . Given that these reactions behave inconspicuously with other extrapolation schemes and that MP2 is not the method of choice for rare gases, it might well be that the free-exponent CBS correlation energy is severely off if rare gases are involved. For the remaining discussion, extrapolation scheme 2 will be used, as it is the most sound one.

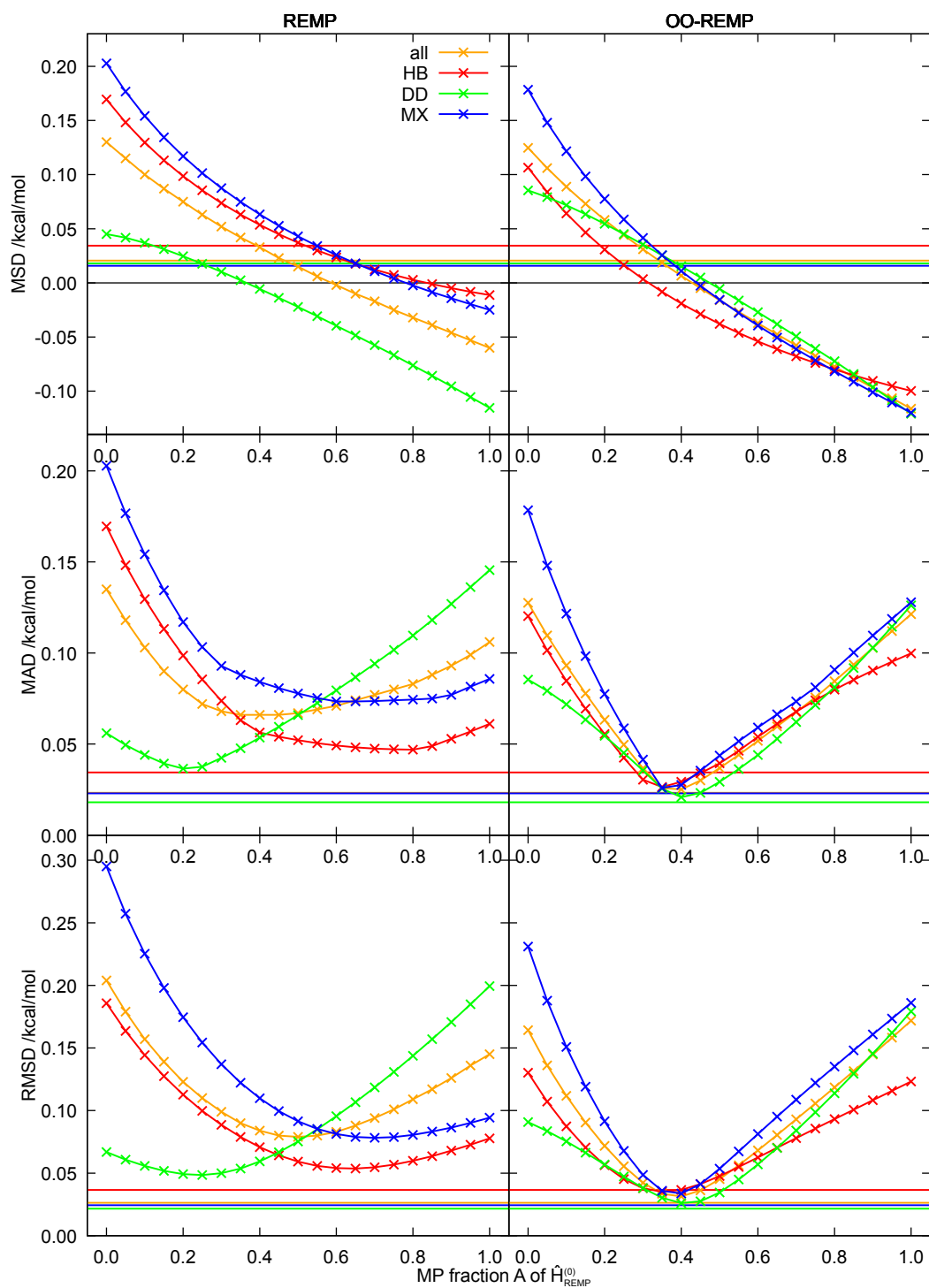
Figure 3.8 shows the MSD, MAD and RMSD obtained with REMP and OO-REMP averaged over all members of the A24 benchmark set in comparison to the CCSD(T)/CBS result and using the CCSDT(Q)/CBS+core results from Table 3.6 as reference. Both REMP and OO-REMP exhibit minima in the MAD and RMSD curves, but OO-REMP clearly outperforms canonical REMP. Quite interestingly, one finds that MP2 performs quite well and yields better results than pure RE, OO-RE and OO-MP2. Concerning REMP, the flat minimum of the MAD curve is located at  $A \approx 0.35$  while the RMSD becomes minimal at  $A \approx 0.50$ . OO-REMP on the other hand exhibits rather steep minima for both MAD and RMSD which are located at  $A \approx 0.40$ . The REMP(0.35) results are already impressively accurate with an MAD below 0.07 kcal mol $^{-1}$ , but they are still inferior to the best OO-REMP result, which is virtually on par to CCSD(T) with an MAD slightly larger than 0.02 kcal mol $^{-1}$  (see Table 6.4). OO-REMP also outperforms REMP in the whole range  $0.20 \leq A \leq 0.60$ .

Figure 3.9 reveals why OO-REMP performs so much better for the A24 benchmark set than canonical REMP: While different dominating interactions require significantly different optimal  $A$  values, the minima in the right-hand panel are almost on top of each other, meaning that when orbital optimization is operational, there is a single value for  $A$  which performs best regardless of the kind of dominating interaction. In the case of canonical REMP, the overall smallest RMSD is obtained at around  $A = 0.50$  while the DD systems require  $A = 0.25$ , the HB systems require  $A = 0.65$  and the MX systems need  $A = 0.70$ . This also indicates that in case of the mixed systems, the hydrogen-bonded part clearly dominates the error, being usually larger. Despite the inconsistency between different subsets, it should be noted that e.g. the results obtained for HB and MX systems at the DD minimum, and vice versa, are still rather good with RMSDs below 0.15 kcal mol $^{-1}$  at the “foreign” minima. On the other hand, none of the minima comes even close to the performance of CCSD(T)/CBS.

Turning to OO-REMP, one finds that all three subsets exhibit their minima around  $A \approx 0.35$ – $0.40$ . Both the MAD and the RMSD are clearly below 0.05 kcal mol $^{-1}$  in total and for the three subsets individually. In case of the HB systems, the minimum is even below the CCSD(T)/CBS value and in all other cases, the difference between OO-REMP and CCSD(T) amounts to less than 10 cal mol $^{-1}$ . So unless the CCSD(T)/CBS values



**Figure 3.8:** MSD, MAD and RMSD for the A24 benchmark set. Error bars indicate one standard deviation. Left panel: REMP, right panel: OO-REMP. Errors are calculated wrt. approximate CCSDT(Q)/CBS. See Table 6.4 for numerical data.



**Figure 3.9:** Absolute error breakdown of the A24 set into interaction classes. Crosses indicate REMP (left) or OO-REMP (right) results, respectively, horizontal lines indicate the CCSD(T)/CBS part of the reference results. Errors are wrt. estimated CCSDT(Q)/CBS. HB: hydrogen-bonded, DD: dispersion-dominated, MX: mixed character.

are not systematically lacking some important contributions compared to the OO-REMP, results, OO-REMP suggests itself as cost efficient alternative to CCSD(T) for such problems. If moving towards the mixing parameter value that turned out to be best in other scenarios ( $A \approx 0.25$ ), the accuracy decreases, but MAD and RMSD are still  $0.10 \text{ kcal mol}^{-1}$  in total and for every subset individually.

Again, a look at relative errors seems appropriate. Figure 3.10 shows relative errors for REMP and OO-REMP relative to CCSDT(Q)/CBS and in comparison to CCSD(T)/CBS. The conclusions that can be drawn from the relative errors are essentially the same as with the absolute errors. On a relative scale, one finds that both REMP and OO-REMP as well as CCSD(T) tend to underestimate noncovalent interactions (which is in contrast to the absolute errors; in the case of the relative errors, a few systems with very small reference interaction energy may easily change the sign of an unregularized relative error). In terms of the MARE and the RMSRE, the trends that have been found before, are essentially confirmed. Canonical REMP now performs best with  $A = 0.35$  (RMSRE=6.2 %), which is less than the best-performing  $A$  from absolute errors. OO-REMP achieves an RMSRE of 3.0 % at  $A = 0.45$ , in fairly good agreement with the best  $A$  from absolute errors.

Figure 3.11 shows the decomposition of the relative error in terms of the three subsets. One finds that the HB subset with its potentially larger interaction energies is nearly insensitive to variations in  $A$  and exhibits the by far smallest relative errors. The DD systems, on the other hand, which have rather small interaction energies show the largest relative errors. The overall relative error is therefore dominated by the DD and the mixed systems.

Again, one finds some distinctive differences between REMP and OO-REMP. While the HB systems are insensitive to a change in  $A$ , the shallow minima in the RMSRE are located at  $A = 0.65$  (REMP, 1.17 %) and  $A = 0.40$  (OO-REMP, 0.82 %), respectively. The sensitive DD systems have minima in the RMSRE at  $A = 0.30$  (REMP, 7.43 %) and  $A = 0.45$  (OO-REMP, 3.90 %). The mixed systems, finally, exhibit minima at  $A = 0.60$  (REMP, 5.38 %) and  $A = 0.45$  (OO-REMP, 2.55 %). OO-REMP is thus much more consistent, the range in  $A$  where an RMSRE below 10 % for all subsets is reached, is much broader, and it is the only method capable of achieving an RMSRE below 5 % for all subsets separately. Compared to CCSD(T)/CBS, the relative errors of OO-REMP are slightly larger, on the other hand, CCSD(T)/CBS shows the same order for the errors (HB<MX<DD) as OO-REMP. As a side-note, it should be kept in mind that the RMSRE is below 10 % in the  $A$  parameter range favored by other benchmark sets ( $0.15 \leq A \leq 0.25$ ), so that there is no need for finding a different optimal parameter for noncovalent interactions.

The rather large optimal  $A$  value is unusual and might be a side-effect of an insufficiently large basis set combination and further effects. As the reference includes a core-correlation correction, it seems appropriate to repeat the calculation with the aug-cc-pwCV[T,Q]Z combination to verify that the unusually large mixing parameter choice does not simply compensate for an insufficiently large basis set. The role of the counterpoise correction

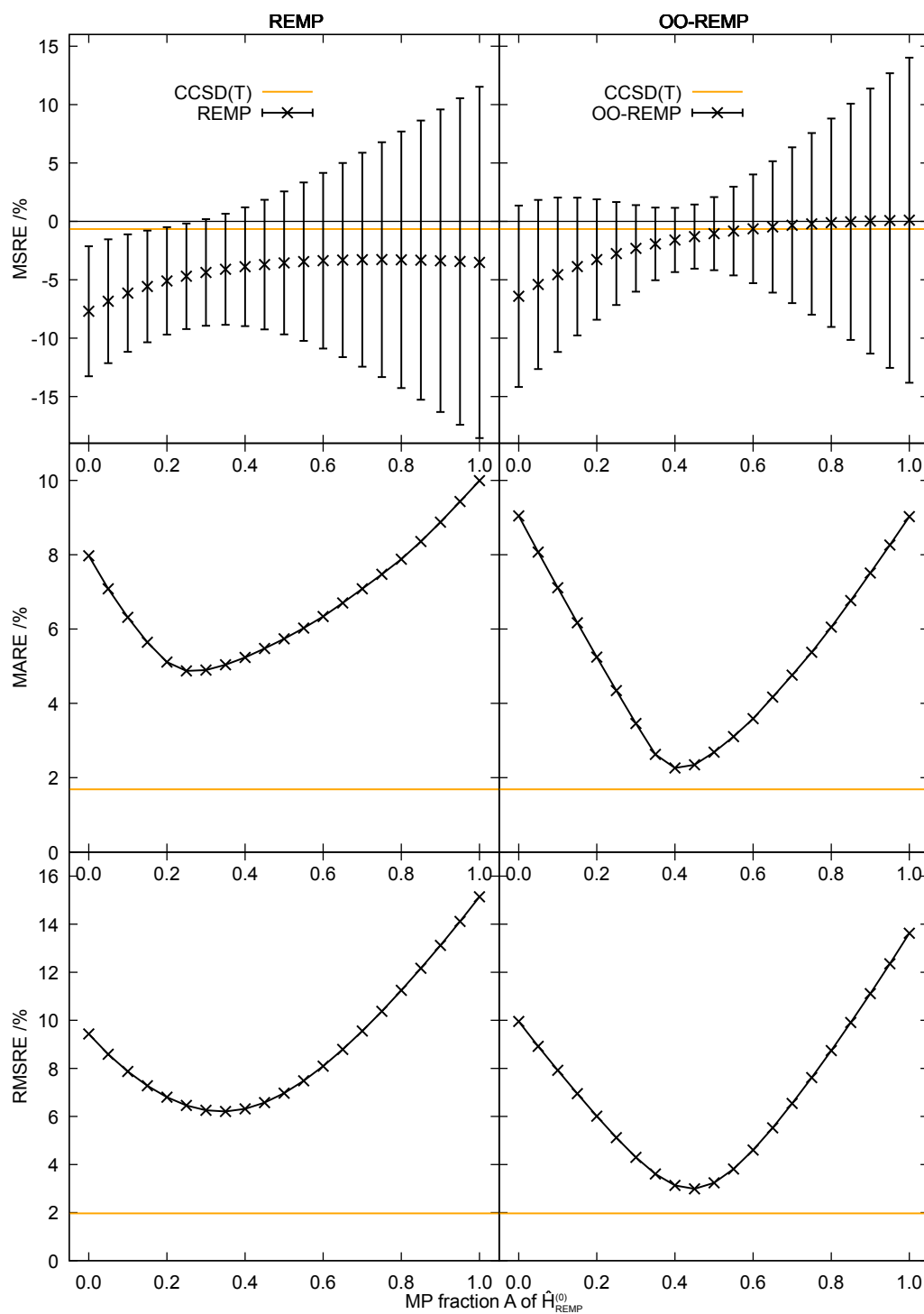


**Figure 3.10:** MSRE, MARE and RMSRE for the A24 benchmark set. Error bars indicate one standard deviation. Left panel: REMP, right panel: OO-REMP. Errors are calculated wrt. approximate CCSDT(Q)/CBS. See Table 6.5 for numerical data.

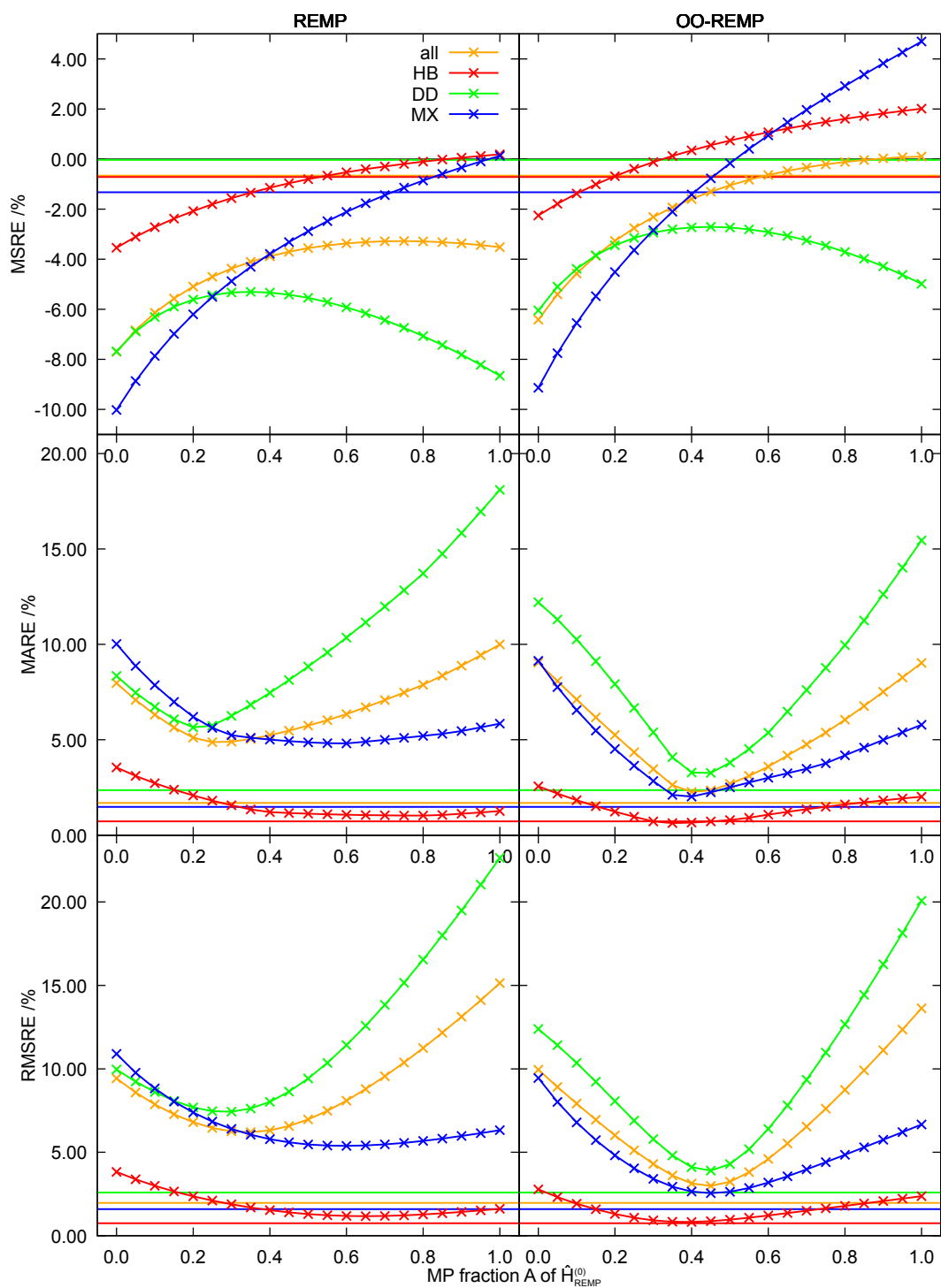


**Figure 3.11:** Relative error breakdown of the A24 set into interaction classes. Crosses indicate REMP (left) or OO-REMP (right) results, respectively, horizontal lines indicate the CCSD(T)/CBS part of the reference results. Errors are wrt. estimated CCSDT(Q)/CBS. HB: hydrogen-bonded, DD: dispersion-dominated, MX: mixed character.



might also need a critical reevaluation. It is often claimed that the Boys-Bernardi correction tends to overshoots the BSSE,<sup>[7,271]</sup> and as MP2 systematically overbinds all complexes, one might hypothesize that the unusually large optimal  $A$  value compensates for an overshooting BSSE correction (see Section 3.3.3 for a more detailed discussion of this matter).

To summarize these results, one finds that REMP provides some systematic improvement over the parent methods, but at a rather unusual, large value for the mixing parameter. OO-REMP further improves on REMP with average relative errors clearly below 5%, almost on par with CCSD(T).

### 3.3.3 The O23 Benchmark Set

*Results for the O23 benchmark set were already published in Reference [51].*

The O23 benchmark set is a set originally consisting of 23 open-shell noncovalent interaction energies constructed by Bozkaya and coworkers.<sup>[121,272]</sup> The reference energies were obtained at the CCSD(T)/CBS + counterpoise correction<sup>[273]</sup> level of theory<sup>[121]</sup> (CBS extrapolation done from aug-cc-pV[T/Q]Z, all electrons correlated). From the original set, later the Ar $\cdots$ NO system (reaction 12) was removed as it exhibited convergence issues at the OCEPA level of theory (orbital iterations do not converge for  $A \lesssim 0.1$ <sup>4</sup>). The average absolute reaction energy of this set amounts to 8.60 kcal mol<sup>-1</sup>, spanning from 0.00 kcal mol<sup>-1</sup> (He $\cdots$ Li) to -65.22 kcal mol<sup>-1</sup> (H<sub>2</sub>O $\cdots$ Be<sup>+</sup>).

OO-REMP calculations were performed for the O23 benchmark set with the same basis set combination as in the case of the reference results, and the CBS extrapolation has been performed with the same formulae and parameters. A counterpoise correction was applied to account for the remaining basis set superposition error. UREMP and RO-REMP were not tested as they were expected to be not competitive for this set.

During the review phase of Reference [52], it was noted that a slightly unusual value for the parameter  $\alpha$  of the SCF extrapolation procedure (the two-point fixed-exponent formula according to Halkier *et al.*<sup>[253]</sup> was used with  $\alpha = 1.60$  instead of  $\alpha = 1.63$ ). The results presented here use the accepted literature exponent ( $\alpha = 1.63$ ), showing that the results do not significantly depend on the last decimal place of the exponent.

Figure 3.12 shows a graphical representation of absolute and relative errors obtained with OO-REMP for the O23 benchmark set. Quite interestingly, the conclusions that can be drawn from comparing the absolute and the relative errors<sup>5</sup> could hardly be more different. Probably the most important finding is that both the MAD and the RMSD are below 1 kcal mol<sup>-1</sup> throughout the whole range. For relatively weak noncovalent interactions,

<sup>4</sup>A number of cases from the O23 set was used in Ref. [204], but compared to the original set, the open-shell noncovalent interaction benchmark set in the latter reference is remarkably pruned.

<sup>5</sup>The He $\cdots$ Li was excluded for calculating relative errors as its reference interaction energy was given as 0.00 kcal mol<sup>-1</sup>, leading to a diverging relative error.

this is of course the bare minimum to be expected and not overwhelming. Looking into the results in more detail, one finds that the MAD exhibits a minimum at  $A = 0.45$  ( $0.10 \text{ kcal mol}^{-1}$ ), while the RMSD (being sensitive top outliers) becomes minimal at  $A = 0.35$  ( $0.18 \text{ kcal mol}^{-1}$ ). Those results do not completely agree, but as in the whole range of  $0.20 \geq A \geq 0.45$  the RMSD is below  $0.2 \text{ kcal mol}^{-1}$ , the exact choice is probably not that critical. Judged by the relative error,  $A = 0.05$  would be the optimal choice. And while the MARE stays below 10 % up to  $A = 0.60$ , the RMSRE steeply increases with increasing  $A$ , reaching already more than 10 % at  $A = 0.15$ . In detail, one finds that the relative errors are dominated mostly by the triplet Lithium atom dimer, having a reference interaction energy of solely  $-0.97 \text{ kcal mol}^{-1}$ . Issues with small reference numbers leading to large relative errors are often countered by calculating regularized relative errors. This however requires a reasonable choice for the regularization parameter, for which no example in the literature was found related to noncovalent interactions.

**Table 3.7:** Absolute error measures for the O23 benchmark set. All in  $\text{kcal mol}^{-1}$ . OO-REMP/CBS(aug-cc-pV[T/Q]Z), all electrons correlated, reference numbers: CCSD(T)/CBS(aug-cc-pV[T/Q]Z), all electrons correlated, taken from Ref. [121].

A	MSD	MAD	stdev	RMSD	min	max
0.00	0.198	0.214	0.286	0.342	-0.150	1.037
0.25	0.123	0.126	0.143	0.186	-0.035	0.464
0.45	0.086	0.100	0.182	0.197	-0.104	0.661
0.50	0.077	0.113	0.208	0.217	-0.112	0.703
1.00	-0.009	0.384	0.670	0.655	-1.927	1.562
MP2	0.182	0.681	1.464	1.444	-5.450	3.550
MP3	0.287	0.594	1.159	1.170	-2.730	4.350
CCSD	0.362	0.379	0.493	0.603	-0.200	1.590
OMP2.5	0.065	0.120	0.212	0.217	-0.210	0.780
OMP3	0.143	0.234	0.411	0.427	-0.500	1.610

All in all, and also compared to the competing methods in Table 6.6, it can be concluded that OO-REMP performs outstandingly well for the O23 benchmark set. As expected, MP2 and MP3 (UMP2 & UMP3) are completely unreliable for open shell noncovalent interactions, with RMSDs larger than  $1 \text{ kcal mol}^{-1}$ . CCSD and OMP3 are better than the former methods but are inferior to the best OO-REMP mixture. OMP2.5 – being conceptually somewhat related to OO-REMP – provides competitive results that are only slightly worse than the best OO-REMP results. Currently, there are no DFT results available for the O23 benchmark set, and it was out of the scope of this work to generate these numbers.

Regarding the optimal REMP mixing ratio, it is quite interesting that the choice of  $A$  which provides the best results differs significantly from the one that provides correlation energies closest to 100 % or the smallest possible scatter of the correlation energy (cf. Sec. 3.1). The reason for this is unclear, especially as the amount of recovered correlation

energy decreases with increasing  $A$ . Both the OO-REMP and the reference CCSD(T) calculations employ identical basis sets, CBS extrapolation schemes and an identical counterpoise correction. Errors resulting from basis set incompleteness are therefore expected to cancel out. On the other hand, these results are perfectly in line with those for the RG18 benchmark set (cf. Sec. 3.3.1), insofar as noncovalent interactions tend to require rather large values for  $A$ , the outcome for the O23 set is consistent with the previous findings. Moreover, while there is a minimum in the MAD and the RMSD at quite large values of  $A$ , the results obtained with  $0.15 \geq A \geq 0.25$  are not bad at all and for sure useful.

There are two hypotheses for the unusually large optimal mixing parameter value for noncovalent interactions. Calculations of noncovalent interactions typically employ basis set extrapolation and counterpoise correction. The Boys-Bernardi scheme is often claimed to slightly overshoot the true BSSE<sup>6</sup>, and it is not entirely clear whether (OO-)REMP and CCSD(T) are affected in the same way so that these effects cancel out. The second hypothesis is that TDEs are especially important for accurately describing the correlation in noncovalently bound systems. As MP2 typically overestimates their contribution, a larger MP fraction in  $\hat{H}^{(0)}$  would lead to a larger amount of correlation energy being recovered and thus provide a better description of these systems. To confirm this hypothesis, one would need a detailed breakdown of the correlation part of the interaction energy in terms of SDEs and TDEs. The reference numbers for such an analysis would have to be generated at least at the CCSDT level of theory. If the reason for the unusual high mixing parameter value is rooted in the extraordinary importance of the TDEs, then the S2REMP ansatz might lead to further improvements as it was shown to get both the SDEs and the TDEs right without sacrificing much of the correlation energy. In conjunction with the CBS extrapolation, again the question emerges whether SDEs and TDEs converge at the same rate and with the same functional dependence to the CBS limit. The W4 composite level of theory e.g. employs different exponents for extrapolating the SDE and TDE components of the RCCSD correlation energy<sup>[225]</sup> based on a proposal by Klopper<sup>[276]</sup> (see also references therein for context and competing schemes). It has furthermore been shown by Klopper that already for the smallest noncovalently bound system, the helium dimer, great care has to be taken when extrapolating to the CBS limit.<sup>[68]</sup> Such effects are expected to be not important and cancel out for the current benchmark set as the reference CCSD(T) energies were also generated with a simple extrapolation. For future investigations it might be important to keep this in mind, as REMP is constructed with the idea to get both kinds of double excitations right, providing an ideal starting point for separate extrapolation (i.e. using different exponents for SDEs and TDEs).

---

<sup>6</sup>see e.g. Reference [271]; in recent times, this point of view has however been questioned,<sup>[274]</sup> Sherrill and coworkers recently advocated for using half-corrected energies,<sup>[262]</sup> and Martin and coworkers found that it depends on the method and basis set<sup>[275]</sup>

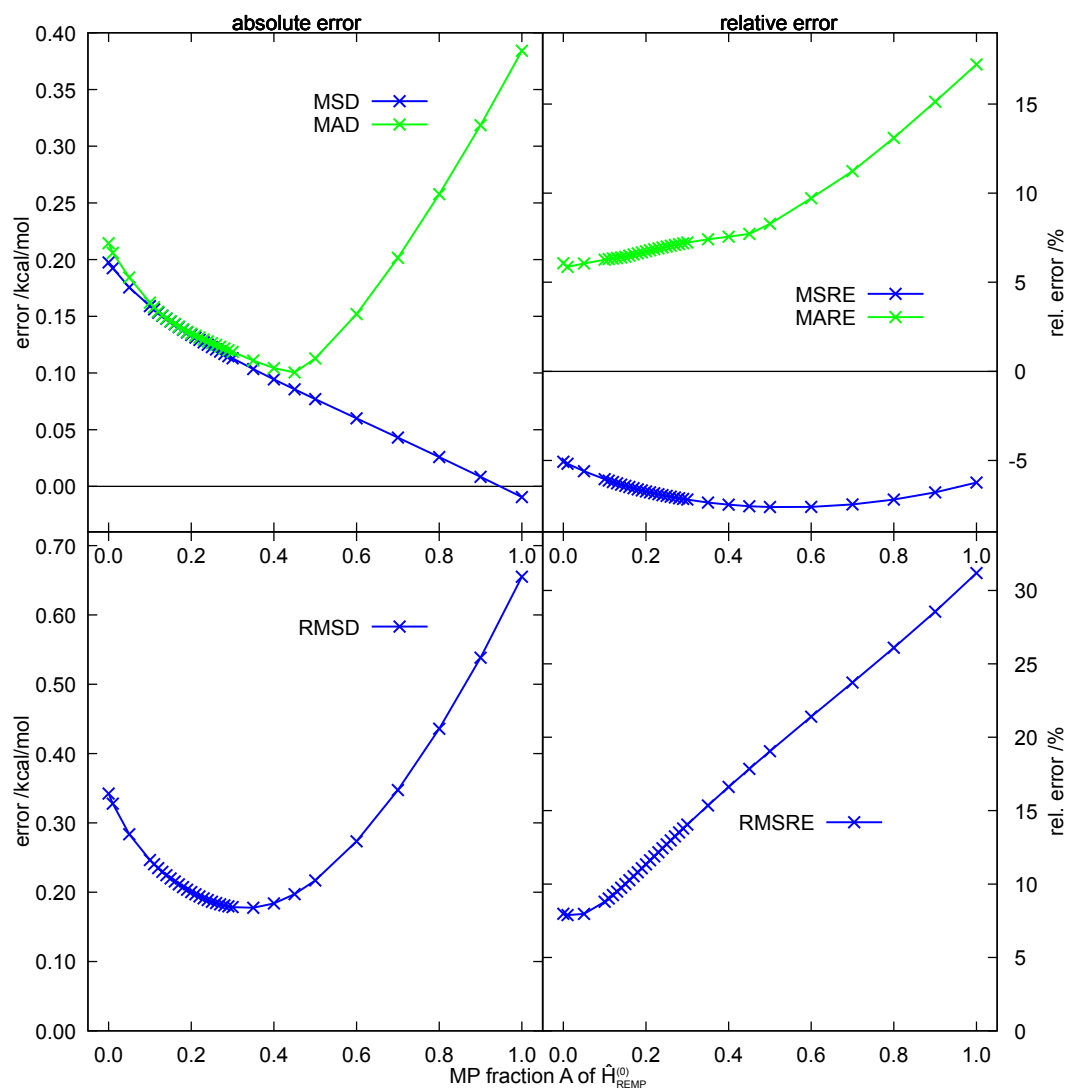


**Figure 3.12:** Graphical representation of absolute and relative errors for the O23 open-shell noncovalent interaction benchmark, OO-REMP/CBS(aug-cc-pV[T/Q]Z). Reference: CCSD(T)/CBS(aug-cc-pV[T/Q]Z). See Tables 6.6 and 6.7 for numerical values. The He...Li system was excluded for calculating relative errors.

### 3.3.4 The S22 Benchmark Set

The S22 benchmark set<sup>[277]</sup> goes back to Hobza and coworkers and is probably the most famous benchmark set for noncovalent interactions. The reference interaction energies have been revised several times<sup>[269,278]</sup> and it was investigated in countless studies.<sup>[244,264,279]</sup> The currently accepted best-estimate reference values are the S22B interaction energies of Marshall *et al.*<sup>[216,269]</sup> These reference calculations either directly extrapolate large-basis CCSD(T) calculations for the small systems or use MP2/CBS+ $\Delta_{\text{MP2}}^{\text{CCSD(T)}}$  composite schemes and are thus of approximate CCSD(T)/CBS quality.

The S22 set features a broad variety of systems, from small dominantly hydrogen-bonded water dimers to Watson-Crick base pairs and dispersion-dominated benzene dimers. Whereas the smaller systems are easily computationally accessible, the larger systems are quite demanding and calculations beyond triple- $\zeta$  basis sets are hardly possible with steep-scaling wavefunction methods. This makes it difficult to treat all systems at an equal footing. In an earlier stage,<sup>[229]</sup> various extrapolation techniques were assessed for the S22 set in conjunction with REMP. For the sake of brevity, only one protocol will be presented here, namely a focal-point scheme:<sup>[254,255]</sup>

- The MP2/CBS energy is extrapolated from aug-cc-pVTZ and aug-cc-pVQZ with the Petersson extrapolation<sup>[268]</sup> with fixed exponents of  $\alpha = 5.79$  and  $\beta = 3.05$  as in Section 3.3.2. Core electrons are kept frozen.
- The MP2/CBS energy is augmented with a  $\Delta_{\text{REMP-MP2}}$  correction as regularly done with CCSD(T). The REMP correction is calculated from the largest feasible basis set for each system which allows REMP calculations to be performed within reasonable time employing standard high-performance gear<sup>7</sup>. Again, core electrons were kept frozen.

With this computational compound protocol, it is possible to obtain approximate REMP/CBS interaction energies at reasonable cost. The MP2/CBS energies, e.g. can all be obtained in a few hours of wall clock time using ORCA on modern hardware.

For computing the  $\Delta_{\text{REMP-MP2}}$  correction, the largest feasible aug-cc-pVXZ basis set was used (see Table 3.8). Core electrons were kept frozen during correlation treatment.

Figure 3.13 shows the results obtained for the S22 benchmark set with the composite extrapolation scheme described above. As has been the case before, there is an obvious

---

<sup>7</sup>In a heroic and reckless attempt, it was possible to converge the REMP/aug-cc-pVTZ wavefunction for the Adenine-Thymine Watson-Crick complex for a single  $A$  value ( $A = 0.15$ ) on one of the old chem compute nodes, wasting at least 8000 h of CPU time (the calculation had to be restarted at least twice) and using  $\approx 242$  GB RAM. Even if it is taken into account that the program has since been improved and adapted to get along with less RAM, and that e.g. the compute nodes of the JUSTUS2 cluster are vastly more powerful, each scan point will still easily burn 1–2 weeks of wall clock time on one compute node. Such calculations are thus in principle technically feasible, but the effort is disproportionate to the insight gained. After finding an appropriate mixing ratio  $A$ , it is of course possible to run production calculations for a single fixed mixing ratio, but complete  $A$  range scans are prohibitively expensive.

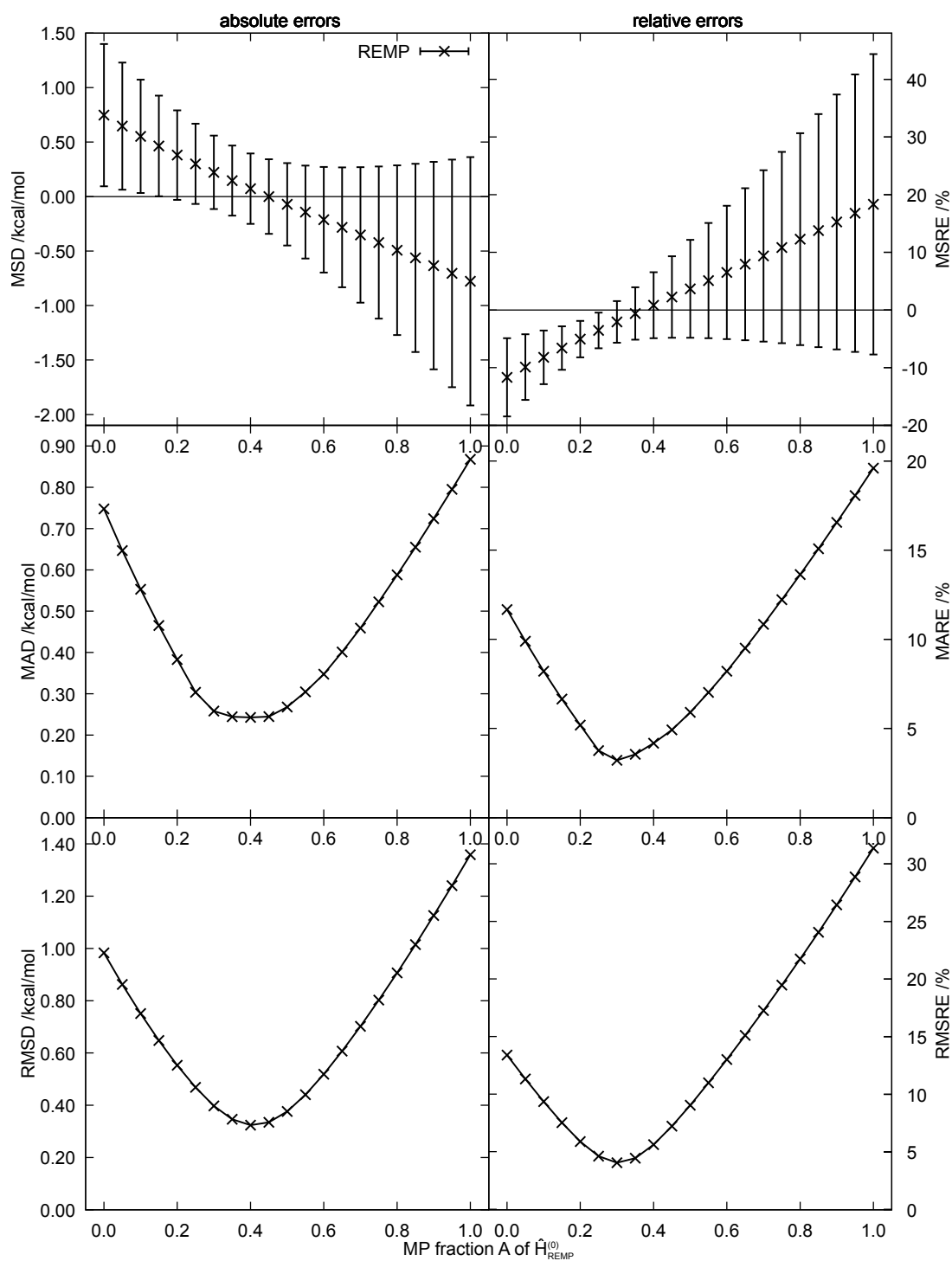


**Figure 3.13:** Absolute (left panel) and relative (right panel) errors for the S22 benchmark set. Data collected from  $\text{MP2/CBS} + \Delta_{\text{REMP-MP2}}$  (see text for details). Errors are with respect to the S22B benchmark results by Marshall *et al.*<sup>[269]</sup> Error bars indicate one standard deviation.

**Table 3.8:** Basis sets used for calculating the  $\Delta_{\text{REMP-MP2}}$  correction for the S22 benchmark set and interaction classification according to Ref. [269].

1	HB	ammonia dimer	aug-cc-pVQZ
2	HB	water dimer	aug-cc-pVQZ
3	HB	formic acid dimer	aug-cc-pVQZ
4	HB	formamide dimer	aug-cc-pVQZ
5	HB	uracil dimer h-bond	aug-cc-pVDZ
6	HB	2-pyridone 2-aminopyridine complex	aug-cc-pVDZ
7	HB	adenine thymine Watson-Crick	aug-cc-pVDZ
8	DD	methane dimer	aug-cc-pVQZ
9	DD	ethene dimer	aug-cc-pVQZ
10	DD	benzene methane complex	aug-cc-pVTZ
11	DD	benzene dimer parallel displaced stack	aug-cc-pVTZ
12	DD	pyrazine dimer	aug-cc-pVTZ
13	MX	uracil dimer stack	aug-cc-pVDZ
14	DD	indole benzene stack	aug-cc-pVDZ
15	MX	adenine thymine complex stack	aug-cc-pVDZ
16	MX	ethene ethyne complex	aug-cc-pVQZ
17	MX	benzene water complex	aug-cc-pVTZ
18	MX	benzene ammonia complex	aug-cc-pVTZ
19	MX	benzene HCN complex	aug-cc-pVTZ
20	DD	benzene dimer T-shape	aug-cc-pVTZ
21	MX	indole benzene T-shape	aug-cc-pVDZ
22	MX	phenol dimer	aug-cc-pVDZ

improvement upon mixing the parent methods. The results are furthermore qualitatively in line with the findings for the A24 basis set, especially concerning the optimal RE/MP mixing ratio. The best results are again obtained in the range of  $0.30 \leq A \leq 0.45$ . This is larger than the thermochemistry optimum but consistent with the other noncovalent interaction benchmark sets. The reasons for this discrepancy were already discussed in the context of the A24 benchmark set.

The present results for the S22 set should not be considered to be authoritative as the employed basis sets and the extrapolation procedure give room for improvement. Nevertheless, even with rather small basis sets, the outcome can be considered to be at least a partial success. The MAD and RMSD are clearly below  $0.5 \text{ kcal mol}^{-1}$  with an optimal mixing parameter choice ( $A \approx 0.4$ ,  $0.24 \text{ kcal mol}^{-1}$  and  $0.32 \text{ kcal mol}^{-1}$ , respectively) and the MARE and RMSRE are brought below 5%.

Burns *et al.*<sup>[244]</sup> tested a large number of model chemistries for noncovalent interactions. Their results will not be repeated here, it is just noted that their MP2/aug-cc-pVTQZ result was exactly reproduced. In essence, they found that with large enough basis sets, MP2C,<sup>[280,281]</sup> MP2.5<sup>[150]</sup> and SCS(MI)-CCSD<sup>[282,283]</sup> provide results with MADs of  $\approx 0.2 \text{ kcal mol}^{-1}$  or below. None of the DFT methods they tested (using the aug-cc-pVTZ basis set) reached such an accuracy.

**Table 3.9:** Absolute error statistics for the S22 benchmark set. All errors are relative to the S22B reference interaction energies<sup>[269]</sup> and in kcal mol<sup>-1</sup>.

	A	MSD	MAD	STDEV	RMSD	min	max
	0.00	0.75	0.75	0.65	0.98	0.05	2.44
	0.15	0.46	0.47	0.46	0.65	-0.01	1.63
	0.20	0.38	0.38	0.41	0.55	-0.02	1.37
	0.25	0.30	0.30	0.37	0.47	-0.04	1.11
	0.30	0.22	0.26	0.34	0.40	-0.12	0.88
	0.35	0.15	0.24	0.32	0.35	-0.34	0.80
	0.40	0.07	0.24	0.32	0.32	-0.56	0.72
	0.45	0.00	0.24	0.34	0.33	-0.78	0.66
	0.50	-0.07	0.27	0.38	0.38	-1.01	0.59
	0.55	-0.14	0.30	0.43	0.44	-1.24	0.53
	0.60	-0.21	0.35	0.48	0.52	-1.48	0.48
	1.00	-0.78	0.87	1.14	1.36	-3.59	0.27
<hr/>							
MP2/aug-cc-pVTQZ <sup>a)</sup>			0.87				
MP2C/aug-cc-pVTQZ <sup>a)</sup>			0.16				
MP2C/[aVTQZ; $\delta$ aTZ] <sup>b)</sup>			0.16				
MP2.5/[aVTQZ; $\delta$ aTZ] <sup>b)</sup>			0.19				
CCSD/[aVTQZ; $\delta$ aTZ] <sup>b)</sup>			0.90				
SCS(MI)-CCSD/[aVTQZ; $\delta$ aTZ] <sup>b)</sup>			0.09				
SCS-PCPF-MI/[aVTQZ; $\delta$ aDZ] <sup>c)</sup>			0.09				
<hr/>							
BP86-D3(BJ)/def2-QZVP <sup>d)</sup>	0.39		0.51		0.70		
B3LYP-D3(BJ)/def2-QZVP <sup>d)</sup>	0.29		0.31		0.43		
$\omega$ B97X-D3(0)/def2-QZVP <sup>d)</sup>	0.07		0.21		0.29		
B2GPPLYP-D3(BJ)/def2-QZVP <sup>d)</sup>	0.09		0.14		0.20		

<sup>a)</sup> Taken from Table VI of Ref. [244]

<sup>b)</sup> Taken from Table VII of Ref. [244]

<sup>c)</sup> Taken from Table 3 of Ref. [143]

<sup>d)</sup> Taken from Ref. [284]

When inspecting the numbers in Table 3.9, it should be considered that at least SCS(MI)-CCSD was trained on the S22 set. The same holds for SCS-PCPF-MI, which was trained on a subset of S22. Regarding the computational cost, MP2.5, (SCS)-CCSD, and SCS-PCPF-MI exhibit the same computational scaling as REMP ( $\mathcal{O}(n^6)$ ). A direct comparison of the numbers in Table 3.9 is furthermore problematic as the REMP results mix several basis sets for calculating the  $\delta aXZ$  correction. One furthermore finds that DFT especially with certain double hybrids and large enough basis sets is fairly accurate for the S22 set.

Figure 3.14 shows a comparison for the three subsets hydrogen-bonded, mixed character, and dispersion dominated (see Table 3.8 for the assignment). The three subsets behave essentially as their counterparts from the A24 set (cf. Figures 3.9 and 3.11). The dispersion-dominated subset is best described with  $A \approx 0.25$ , while the hydrogen-bonded systems demand  $A \approx 0.70 - 0.80$ . The mixed systems are interesting insofar as they are right in the middle between HB and DD in the case of S22. In the case of the A24 set,



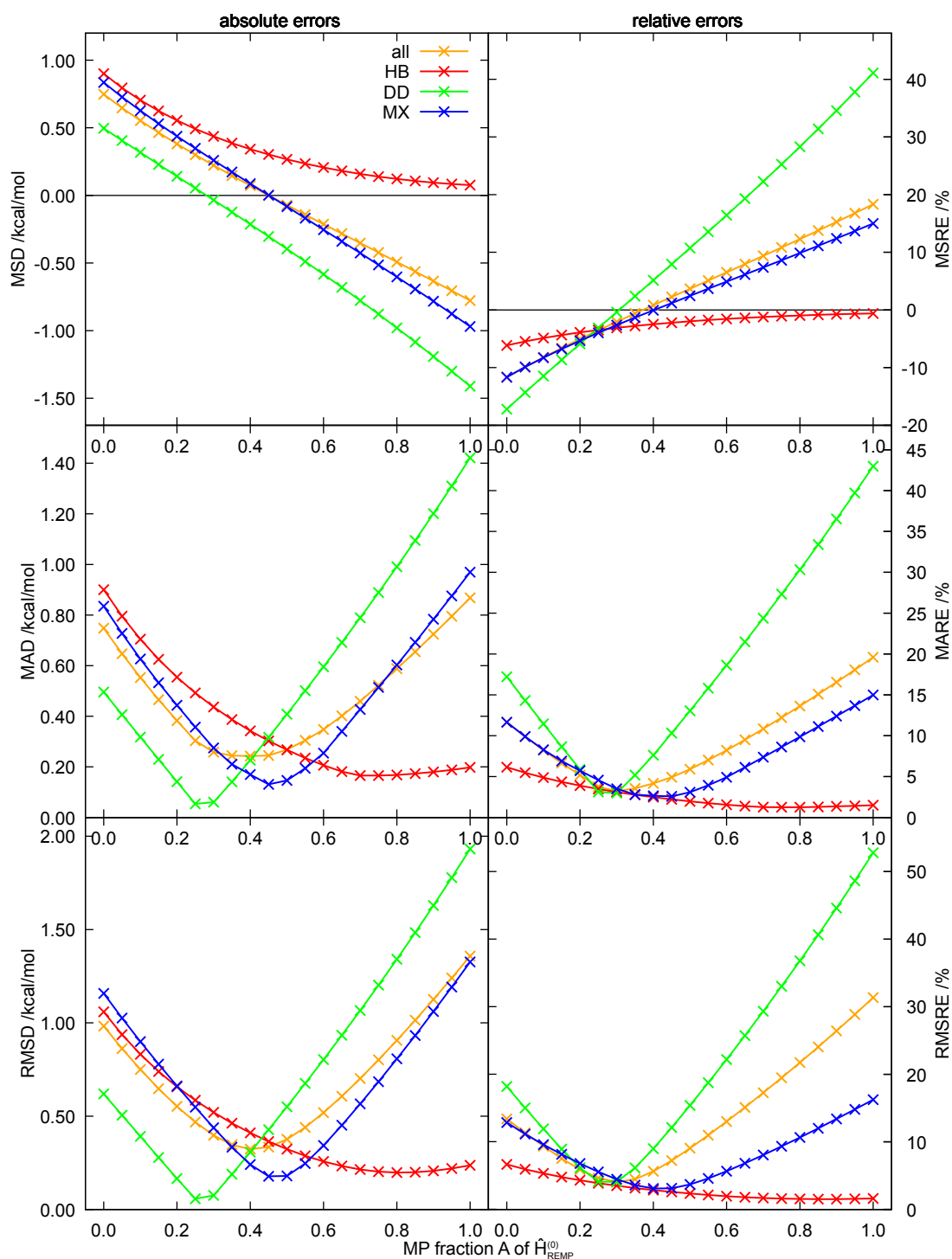


**Figure 3.14:** Absolute (left panel) and relative (right panel) errors for the HB, MX and DD subsets of the S22 benchmark set. Data collected from MP2/CBS+ $\Delta_{\text{REMP-MP2}}$  (see text for details). Errors are with respect to the S22B benchmark results by Marshall *et al.*<sup>[269]</sup> Error bars indicate one standard deviation.

the mixed systems behave rather similar to the hydrogen-bonded systems. The obvious difference between A24 and S22 is that the mixed systems of S22 are on average fairly large, featuring more dispersion interactions than the average mixed system of A24. The relative errors of the S22 set exhibit the same trends as the A24 set regarding the minima position. The positions of the minima of the relative errors are furthermore in good agreement with those of the absolute errors. Another common feature of A24 and S22 is that the smallest average absolute error is found in the set of dispersion-dominated systems, while the smallest average relative error is encountered in the set of hydrogen-bonded systems.

So far, no complete set of results obtained with OO-REMP is available. OO-REMP has the drawback that the current canonical implementations do not allow to freeze core electrons during the iterative orbital optimization, which makes calculations especially for larger molecules considerably more costly. Given that OO-REMP clearly outperformed canonical REMP in case of the A24 set and that it led to much more consistent results, it can be envisaged that the same will hold for the S22 set, considering the striking similarity of the canonical REMP S22 and A24 results. A possible cost-efficient alternative to full large-basis OO-REMP calculations for all systems would be to employ the composite scheme that was successfully applied for canonical REMP.

There is furthermore the S22x5 benchmark set<sup>[151]</sup> derived from S22. In addition to S22, it features structures at 0.9, 1.2, 1.5, and 2.0 times the equilibrium distance along the direction of the noncovalent interaction. The S22x5 benchmark set therefore also allows to test for non-parallelism errors and for correct dissociation of noncovalent interactions. Some preliminary data for S22x5 was so far gathered,<sup>[229]</sup> but no complete set of results exists (both for REMP and OO-REMP).

A topic which has not been considered so far at all are three-body noncovalent interactions.<sup>[285]</sup> These turned out to be challenging for dispersion-corrected DFT,<sup>[286]</sup> hence it would be interesting to test REMP and OO-REMP on this still rather unexplored terrain.

### 3.4 Reaction Energies of Metal-organic Reactions

So far, all benchmark sets were exclusively constructed from first- and second row (main group) elements. A quantum-chemical method with a broad scope of applicability should however be applicable to the whole periodic table and not only to the easy part. This is especially true as transition metal chemistry and transition metal catalysis is still an important and ever-growing field.

On the other hand, there are only a few high-quality benchmark sets for transition metal chemistry like the 3dMLBE20 set,<sup>[287]</sup> a set by Cheng *et al.*,<sup>[288]</sup> a set of bond dissociation energies by Fang *et al.*,<sup>[289]</sup> or the ccCA-TM/11 set.<sup>[290,291]</sup> The main reason is that transition metals often exhibit a distinctively different electronic structure than main-group elements, with unpaired electrons and crowded electron pairs. Often the

electronic structure is of multiconfigurational nature, making it difficult to obtain accurate reference energies even with sophisticated single-reference wavefunction methods.<sup>[292]</sup>

For reaching reasonable quantitative agreement between calculated and (hard to obtain) experimental bond dissociation energies, scalar-relativistic coupled cluster methods with core-valence correction and higher-order excitation corrections are necessary,<sup>[288]</sup> and the standard tool for generating computational benchmark data – CCSD(T)/CBS – is – despite of different claims<sup>[289]</sup> – of limited use in these cases.<sup>[287,292]</sup> The question whether single-reference CCSD(T) is an appropriate reference method crucially depends on the amount of multiconfigurational/multireference character of the species involved.<sup>[292]</sup> Post-CCSD(T) effects can either be covered by going up to CCSDTQ (neglecting even higher excitations) or by using multireference correlation methods. Unfortunately, all available *a posteriori* single reference diagnostics for multireference character do not correlate sufficiently well with the actual size of the multireference correction found in the case of transition metal compounds,<sup>[292]</sup> so that there is still room for improvement.

The current formulations of REMP and OO-REMP are strictly limited to single reference Slater determinants, making the treatment of multireference systems unreliable.<sup>8</sup> When looking for suitable benchmark sets, the selection thus has to be limited to such sets which are tractable at the single reference level. Such a set is e.g. the MOR41 set by Dohm *et al.*<sup>[293]</sup> which is composed of real-life examples of various kinds of closed-shell transition metal reactions. The absence of strong multireference character was warranted by calculating the  $T_1$  diagnostic and by inspecting FOD plots for signs of multireference character for all molecules. The MOR41 set thus only contains reactions where it is safe to assume that CCSD(T)/CBS or in this case DLPNO-CCSD(T)/CBS(def2-[T/Q]ZVPP) will provide reasonable reference electronic reaction energies. Moreover, the authors argue that their reference reaction energies are only correct to a safety margin of  $\pm 2$  kcal mol<sup>-1</sup>.

RI-REMP and RI-OO-REMP (PSI4 designation: RI-OREMP) calculations were performed for as many reactions of the MOR41 set as possible. These calculations make use of the REMP implementation in the DF-OCC code of PSI4, which has the capability to freeze core electrons during the orbital optimization procedure as well as (experimental) support for effective core potentials which is vital for calculations starring 4d and 5d metals. At a late stage, it was found that PSI4 uses different default frozen core electron numbers for transition metals than wavel or the reference ORCA calculations. This gives of course rise to some additional deviations apart from the RI error. Unfortunately, it was too late to rerun all calculations when this problem was recognized. But as it was so far not possible to obtain REMP results with two consecutive basis for doing a CBS extrapolation, all comparisons are rather qualitative than quantitative anyway.

<sup>8</sup>Care has to be taken with the nomenclature here. The attribution of single- or multireference character always depends on the chosen basis. The basis chosen in this work are plain Slater determinants, but it could also be configurations or configuration state functions. There are known cases whose reference is e.g. well described by a single open shell low-spin configuration state function. In a CSF picture, this would be a single reference case, in a determinant picture, this would still be a multireference case.

The def2-TZVPP basis set was chosen for all calculations. The RI-REMP and RI-OREMP calculations additionally use the def2-universal-jkfit auxiliary basis (the “universal” or def2/JK) as JK fitting basis for the Hartree-Fock calculation and the reference determinant of the RI-OREMP calculation, and the def-TZVPP-RIFIT (the def2-TZVPP cbas or def2-TZVPP/C) auxiliary basis set as correlation fitting basis set, i.e. as auxiliary basis for two-, three-, and four-external exchange integrals. The details of the implementation can be found in Ref. [204].

The canonical REMP code in PSI4 constructs the external exchange operator by first transforming exact ERIs from the AO to the MO basis, requiring up to  $n_{\text{virt}}^4/8$  doubles for storing transformed ERIs. These are then contracted with the amplitudes to form the EEO, optionally using symmetry up to  $D_{2h}$ . Such an algorithm is efficient for small molecules and with enough storage at hand. It also has the advantage that the actual formation of the EEO scales as  $\mathcal{O}(n_{\text{occ}}^2 n_{\text{virt}}^4)$ , that symmetry can conveniently be used, and that the contraction of amplitudes and integrals can be done very efficiently using level 3 BLAS routines. The drawback is that the sparsity of the ERI tensor is lost. The formation of the EEO in the AO basis has the drawback that it formally scales as  $\mathcal{O}(n_{\text{occ}}^2 n_{\text{bas}}^4)$ , but this is usually overcompensated by the sparsity of the ERI tensor. When an efficient prescreening is used, and when only contractions which integrals that are actually nonzero are performed, this is usually the most efficient choice for larger molecules, as long as no virtual space truncation is performed.

Using the RI approximation for the two-electron integrals (TEI) / electron repulsion integrals (ERI) has the advantage that not all ERIs in the AO basis have to be calculated and transformed to the MO basis, thus saving the CPU time for recalculating all ERIs in each iteration, or saving memory (disk or RAM) needed for storing AO/MO basis exact ERIs. Instead, three-index ERIs are calculated, which are easier to store on disk or in memory. From the three-index ERIs, the four-index-integrals are reconstructed and contracted with the amplitudes to form the EEO. In principle, this can again be done in either the AO or the MO basis. Unfortunately, there is no gain in terms of efficiency from using the RI approximation compared to exact ERIs<sup>9</sup> in the case of coupled cluster/coupled pair type methods. The reconstructed ERIs still need to be processed in the same way as the exact ERIs, and there is only a gain in efficiency when the reconstruction of the four-index ERIs from three-index ERIs is faster than their exact calculation (or reading them from disk). The current PSI4 implementation in the DFOCC module furthermore has the drawback that there is neither symmetry no batching implemented, i.e. the program needs  $n_{\text{virt}}^2 n_{\text{aux}}/2 + n_{\text{virt}}^4/8$  doubles of RAM for the reconstruction of the ERIs. This limits the size of the systems tractable at the moment to molecules with  $\approx 1000$  AO basis functions and  $\approx 2000$  JK or C auxiliary basis functions before the memory demand becomes unsustainably large. But already this modes number of basis functions required some fixes in the code, namely replacing

---

<sup>9</sup>also see this explanation by Frank Neese in the ORCA users forum: <https://orcaforum.kofo.mpg.de/viewtopic.php?f=8&t=7646&p=33016&hilit=integral#p33016>

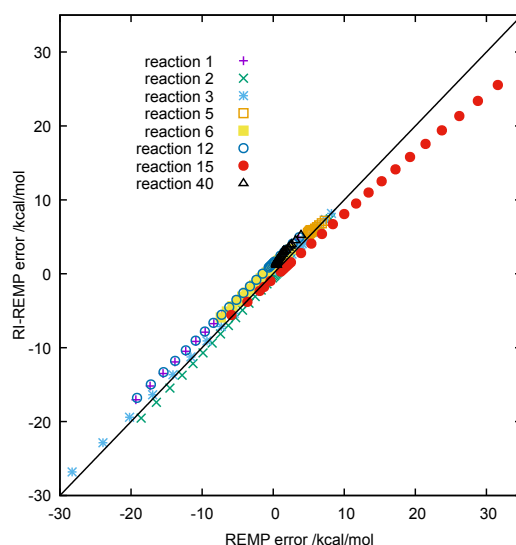


**Figure 3.15:** Correlation between the errors of RI-REMP and canonical REMP for a selection of reactions of the MOR41 benchmark set. Points of the same type belong to different values of the mixing parameter  $A$ . Errors were calculated wrt. the original MOR41 reference reaction energies.

many 32 bit (four byte) integers by 64 bit (eight byte, `long long int`) integers, before any production calculation was possible.

Running all calculations of the MOR41 benchmark set with the currently available (OO-)REMP programs is clearly out of scope. The authors of Ref. [293] state that running the largest DLPNO-CCSD(T)/def2-QZVPP necessary ( $>100$  atoms,  $\approx 5000$  basis functions) took 3 weeks of (wall clock) time on not further specified hardware. As soon as there is a DLPNO version of REMP, such calculations are of course possible, but until then, it would require a massively parallel (MPI) implementation of REMP. Given that (canonical) REMP is trivially implemented on top of an existing CEPA/0 program (which is in turn an approximation to CCD), this should be fairly easy as soon as one has a working DLPNO-CCSD (or PNO-LCCSD) code at hand.

Figure 3.15 shows a comparison between the errors of RI-REMP and the errors of canonical REMP for a limited set of reactions. All in all, the agreement is reasonably good, and the residual inconsistency can be attributed to the different frozen core settings. This shows that the RI error is sufficiently small and that RI-REMP is an adequate approximation to canonical REMP similar to other RI-accelerated methods.

It was possible to obtain raw DLPNO-CCSD(T)/def2-TZVPP data for most reactants of the MOR41 benchmark set, which allow for a more sound comparison to RI-REMP/def2-

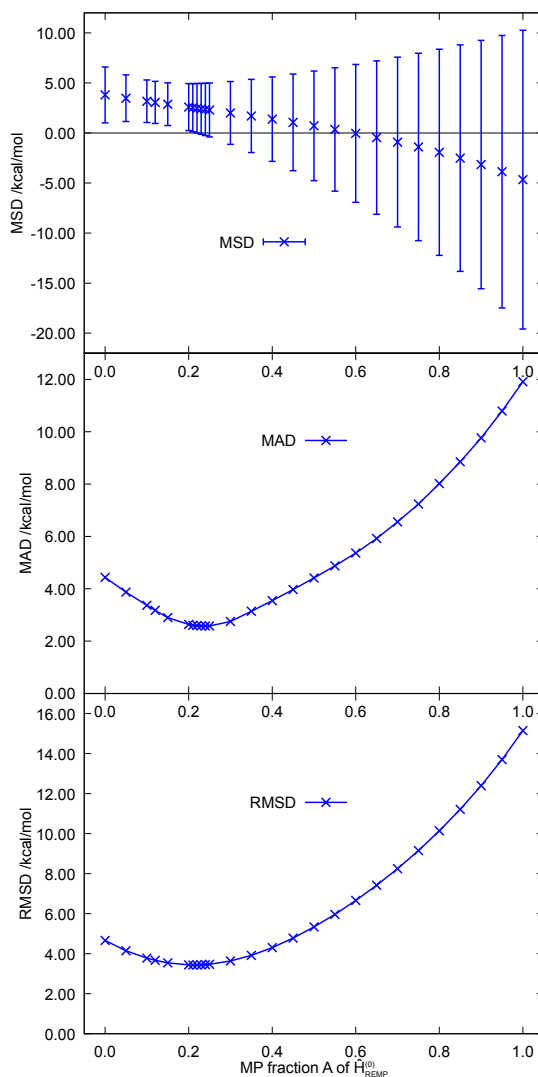


**Figure 3.16:** Statistics for the 15 smallest systems of the MOR41 benchmark set, RI-REMP/def2-TZVPP. Reference data: DLPNO-CCSD(T)/def2-TZVPP. Error bars indicate one standard deviation.

TZVPP results. In total, there is complete DLPNO-CCSD(T) and RI-REMP data for a total of 15 reactions.<sup>10</sup>

Figure 3.16 shows a statistical evaluation for this subset. The performance provided by RI-REMP is admittedly not great but also not terrible. RE, i.e. CEPA(0)/D, exhibits a reasonable performance with an MAD of 4.4 kcal mol<sup>-1</sup>. MP2, on the other hand, has

<sup>10</sup>reaction 1, reaction 2, reaction 3, reaction 6, reaction 12, reaction 13, reaction 15, reaction 18, reaction 19, reaction 20, reaction 23, reaction 29, reaction 36, reaction 39, and reaction 40 as defined in Ref. [293].

an MAD of almost  $12 \text{ kcal mol}^{-1}$ , being unacceptably large for any application. REMP hybridization leads to a considerable improvement upon both RE and MP, specifically the MAD reaches a minimum with REMP(0.24) of  $2.6 \text{ kcal mol}^{-1}$ , bringing down the RE error by almost one half. The corresponding RMSD is  $3.5 \text{ kcal mol}^{-1}$ . On an absolute scale, this is still an alarmingly large error. On the other hand, this result has to be put into relation to results of competing methods. Furthermore, it should again be stressed that the reference reaction energies themselves are provided with a safety margin of  $2 \text{ kcal mol}^{-1}$ . None of the wavefunction methods tested in Ref. [293] reaches this accuracy for the full set, and only a hand full of the more expensive hybrid and double hybrid density functionals perform equally well or better. It is furthermore quite satisfying that the range in  $A$  where REMP performs best is again between an MP fraction of 15 and 25 %, being qualitatively in line with all other covalent thermochemistry benchmark sets. Furthermore, the subset used here could be biased in the sense that in case of the smaller systems, the central transition metal atom makes up a larger portion of the molecule compared to the big molecules neglected here. It has been shown before that isolated transition metal atoms and ions demand different REMP mixing ratios than main group elements<sup>[76]</sup> judged by the amount of recovered correlation energy and the wavefunction error. It is however unclear to which extent this is transferable to transition metal organometallics.

There is also a number of preliminary results from RI-OO-REMP, but the size of the systems that can be treated is currently even more limited than in the case of RI-REMP. As OO-REMP so far turned out to be clearly superior to REMP in any aspect, developments and investigation in this direction propose themselves.

### 3.5 Equilibrium Structures of Small Molecules

*The results presented in this section were already published in Reference [53], the vast majority of the raw data was generated by Robert Richter<sup>[294]</sup> and Luca Völk<sup>[295]</sup>*

So far, all investigations were exclusively concerned with thermochemistry, preferably of molecular structures claimed to be minima on the potential energy surface (PES). This section now deals with finding minima on the potential energy surface and the question how well REMP performs for this task. Finding minimum structures of molecules is one of the most basic tasks of computational chemistry and typically one of the first steps of any computational study. Nature tends to minimize the free energy, and molecules therefore tend to spend most of their time near to a local minimum on the PES. The vast number of experimental analytical techniques furthermore assumes that the object of study initially is in a ground state minimum. For any meaningful comparison of calculation and experiment, it is therefore of utmost importance to be able to accurately predict molecular equilibrium structures. This is especially true for methods that claim universal applicability.

It turns out that the accurate experimental determination of equilibrium structures with sub-pm accuracy is quite involved and requires the exact measurement of rotational spectra and often calculations for obtaining further corrections for rotation-vibration couplings.<sup>[296]</sup> For instance, it was only in 2018 when it was possible to obtain a really accurate equilibrium structure for the hydrogen peroxide molecule,<sup>[297]</sup> and for other molecules like the dichlorine molecule, even today no structure with asserted sub-pm accuracy is available.

In order to test the ability of REMP and OO-REMP for predicting equilibrium molecular structures, a set consisting of 59 bond lengths of 50 small closed and open shell main group molecules was compiled. This set is inspired by the work of Bak *et al.*,<sup>[298]</sup> Coriani *et al.*<sup>[299]</sup> as well as Tentscher *et al.*<sup>[300]</sup> Their sets of molecules were merged, and the reference data was updated to the latest/best available experimental estimate (which changes significantly in some cases). Furthermore, problematic cases (e.g. F<sub>2</sub>) were removed from the set and further small molecules missing so far (e.g. O<sub>2</sub>) were added. The primary criteria for inclusion into the set was that the structure is an (empirical) experimental equilibrium structure, i.e. that the anharmonicity, the centrifugal distortion, and the rotation-vibration coupling were properly taken care of, and that the uncertainty of the bond length is below 0.1 pm. Furthermore, the data should be generated from several isotopologues to remove isotope effects.<sup>11</sup> At first glance, the requirement of an uncertainty below 0.1 pm seems to be an overly strict criterion, given that there is not so much data available fulfilling it. These criteria furthermore completely rule out the use of solid state X-ray structures, as these typically correspond to the position expectation value of the zeroth vibrational level  $r_0$  instead of the distance belonging to the minimum of the PES  $r_e$ . Already in the presence of weak anharmonicity, the difference between  $r_0$  and  $r_e$  may reach some tenth of a picometer. Neglecting such details may lead to systematically too large, false positive errors for very accurate methods: It was shown that there are computational methods which are actually capable of predicting equilibrium bond lengths with an accuracy of 0.1 pm.<sup>[301]</sup>

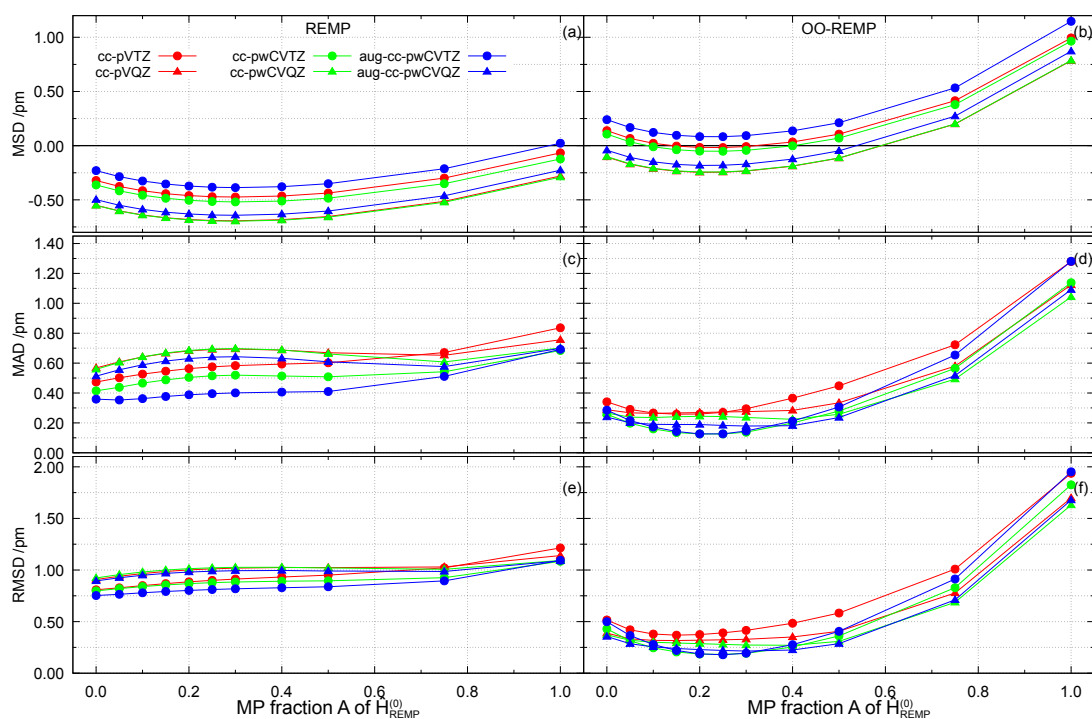
As it soon turned out to be vital to also correlate the core electrons for accurate results, no frozen core approximation is applied throughout this section.

Figure 3.17 shows the essence of the bond length benchmark for REMP and OO-REMP. Depending on the basis set, one finds that canonical REMP systematically underestimates main group bond lengths. And while canonical MP2 is on average quite accurate (smallest MSD), it exhibits the largest uncertainty (largest MAD and RMSD), making it unreliable with mean absolute errors of at least 0.6 pm. The most accurate method of the canonical REMP series is RE (i.e. CEPA(0)/D). In between, one finds that the bond lengths do first systematically decrease up to  $A \approx 0.35$ , then they start to increase again. The MAD and especially the RMSD are largely unaffected, varying only slowly between  $0 \leq A \leq 0.6$ . Quite interestingly, one finds that REMP exhibits the smallest errors in conjunction with

---

<sup>11</sup>the minimum of the Born-Oppenheimer potential energy surface corresponding to the equilibrium structure does not depend on the isotopic composition.





**Figure 3.17:** Statistics for the bond length benchmark set, average over 59 bond lengths. Reference: best available experimental/semiempirical bond length.

the aug-cc-pwCVTZ basis set ( $\text{MAD} \approx 0.4$  pm), indicating a Pauling point. With the even larger aug-cc-pwCVQZ basis set the results clearly become worse. This results also implies that REMP will not benefit from a CBS extrapolation of the gradients, as all [T/Q] basis combinations shown in Figure 3.17 exhibit shorter bond length with the larger basis. In conclusion, one can say that canonical REMP regardless of the mixing parameter is not a useful method for structural optimizations. It is not much more accurate than MP2, but has a prohibitively large computational cost for crude survey calculations. Approximating the 95 % confidence interval with  $2 \times$  the RMSD,<sup>[302,303]</sup> one finds a 95 % CI of almost 1.5 pm. Such an accuracy might be sufficient for survey calculations, but not for high-quality in-depth calculations.

Turning to OO-REMP, one finds some notable differences compared to the canonical variant. The most striking difference is that now on average the bonds are  $\approx 0.5$  pm longer, while the general basis set trends are preserved. Instead of a systematic underestimation, one finds that within  $0 \leq A \leq 0.5$ , the signed average bond length errors are in a narrow interval of  $\pm 0.25$  pm. Again one finds that triple zeta basis sets predict longer bonds than quadruple zeta basis sets, but the former now tend to be slightly too large while the latter tend to be too small. The MAD and the RMSD show unambiguous minima in the range between  $A = 0.15$  and  $A = 0.40$ , depending on the basis set. In any case the minima are

rather flat and the precise value of  $A$  is less important than the basis set. Contrary to canonical REMP, the cc-pwCVTZ, aug-cc-pwCVTZ and aug-cc-pwCVQZ basis sets lead to almost identical RMSDs of  $\approx 0.20$  pm (0.18, 0.18, and 0.22 pm for the three basis sets at their respective minima). This in turn implies a 95 % confidence interval of less than 0.5 pm, probably well suited for high-quality, predictive calculations.

It was also possible to obtain fixed-basis CCSD(T) results for the same basis sets as listed in Figure 3.17 using ORCA and numerical gradient techniques. CCSD(T) was found to deliver even more accurate results than OO-REMP at the drawback of a significantly larger computational cost. In fact, CCSD(T)/aug-cc-pwCVQZ achieved an MAD of 0.08 pm and an RMSD of 0.12 pm. This result is qualitatively in line with that of Pawłowski *et al.*,<sup>[304]</sup> who found an MAD of  $\approx 0.1$  pm using CCSD(T) and different basis sets.

The above result shows that the scrupulous selection of reference data is mandatory for rigorous validations. Otherwise, poor reference data may artificially spoil the performance of a good method. Given the accuracy of CCSD(T), one would ideally demand an even smaller uncertainty for the reference data as it is already now hardly possible to discriminate between the reference uncertainty and the tested methods uncertainty. This is also backed by a second set of bond lengths tested, where the reference data is of inferior quality. The low quality set contains  $r_e$  values with large experimental uncertainty, but it also contains  $r_0$  values, as this is often the only quantity available. The statistical indicators for this set are worse for both OO-REMP and CCSD(T), a result which can be attributed to the poor quality of the reference data (see Ref. [53]).

Figure 3.18 shows some arbitrarily selected bond length error examples calculated at the REMP/aug-cc-pwCVTZ and OO-REMP/aug-cc-pwCVTZ level of theory. This particular basis set was chosen as it led to the best performance for both REMP and OO-REMP. As it can be seen, there is good reason to exclude the  $F_2$  molecule from the benchmark set, although there is highly reliable reference data available. The pronounced multireference character of this molecule leads to a wild variation of the results with changes in  $A$ , and it furthermore leads to convergence issues and finally a diverging bond for OO-REMP below  $A = 0.15$ , hence there are not data points for  $A < 0.15$ . Figure 3.19 furthermore shows that MP2 and OO-MP2 exhibit the largest error spread with some bond lengths being underestimated and others being overestimated. RE2 and OO-RE2 on the other hand lead to a small scatter but a consistent overestimation of almost all bond lengths. In between at  $A \approx 0.20$  there is a region with small scatter and bond length centered somewhat around zero. One furthermore finds that OO-REMP quite consistently predicts slightly longer bond lengths than REMP and that OO-REMP is not in all cases more accurate than REMP. The results shown in Figure 3.19 are also interesting insofar as one finds that choosing  $A \approx 0.20$  provides not only good results for well-behaved single reference molecules (and close to zero error for the two-electron system  $H_2$ ), but also reasonable results for complicated systems like PN or OF which supposed multireference character.

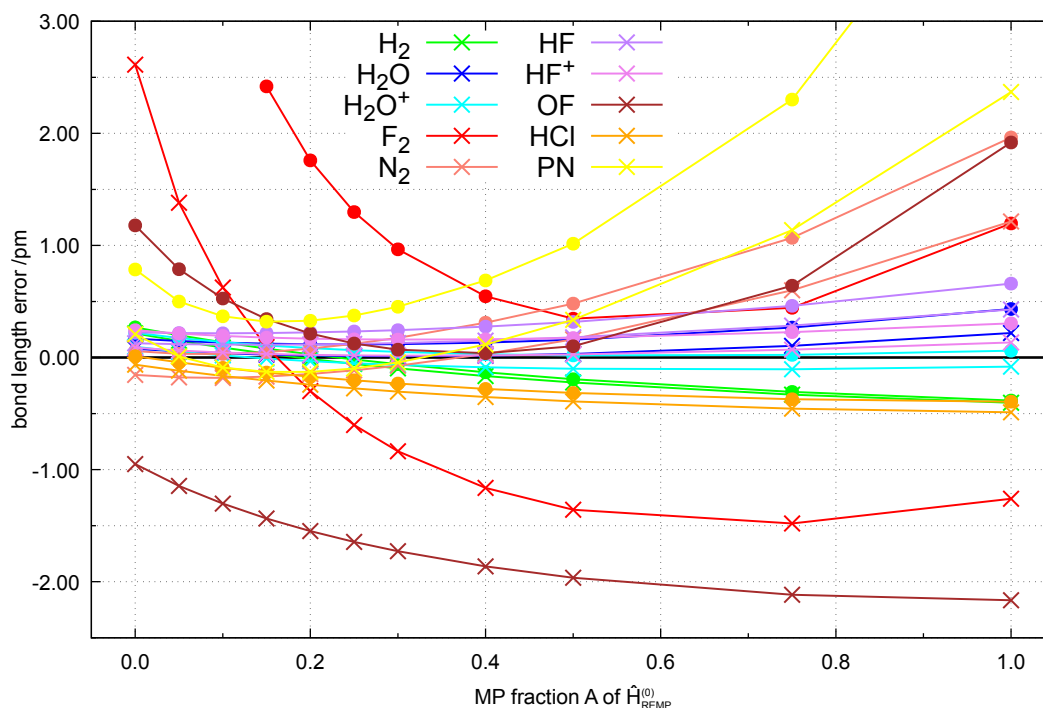


**Figure 3.18:** Some examples for bond length errors calculated with REMP and OO-REM. Crosses indicate canonical REMP, dots indicate OO-REM. Basis set: aug-cc-pwCVTZ.

For further ranking of the REMP and OO-REM results, there need to be data from other methods like DFT or different coupled cluster excitation levels. For a smaller set of molecules, Karton and Martin<sup>[301]</sup> found that CCSD(T)/CBS provides an MAD of 0.17 pm, which is in line with our results. They furthermore found that the inclusion of connected quadruples is mandatory for reliably achieving sub-pm accuracy as is done in the W4<sup>[225,305]</sup> composite approach. The obvious drawback of such composite approaches (“layered extrapolation”) is that there are typically no analytical gradients available, making the calculation of equilibrium structures cumbersome and expensive.

The structure benchmark data collection also contains two sets of equilibrium bond angle sets. Bond angles and especially proper dihedral angles are generally even harder to obtain experimentally than bond lengths. Angles are more flexible and even more prone to anharmonic effects than bonds, which is generally reflected in the larger relative uncertainties. Furthermore, a molecule needs at least three atoms to have a bond angle, causing that an exact structure determination becomes very involved. The bond angle benchmark largely corroborates the bond length analysis, but one finds a significantly smaller dependence of the results on the mixing parameter  $A$ .

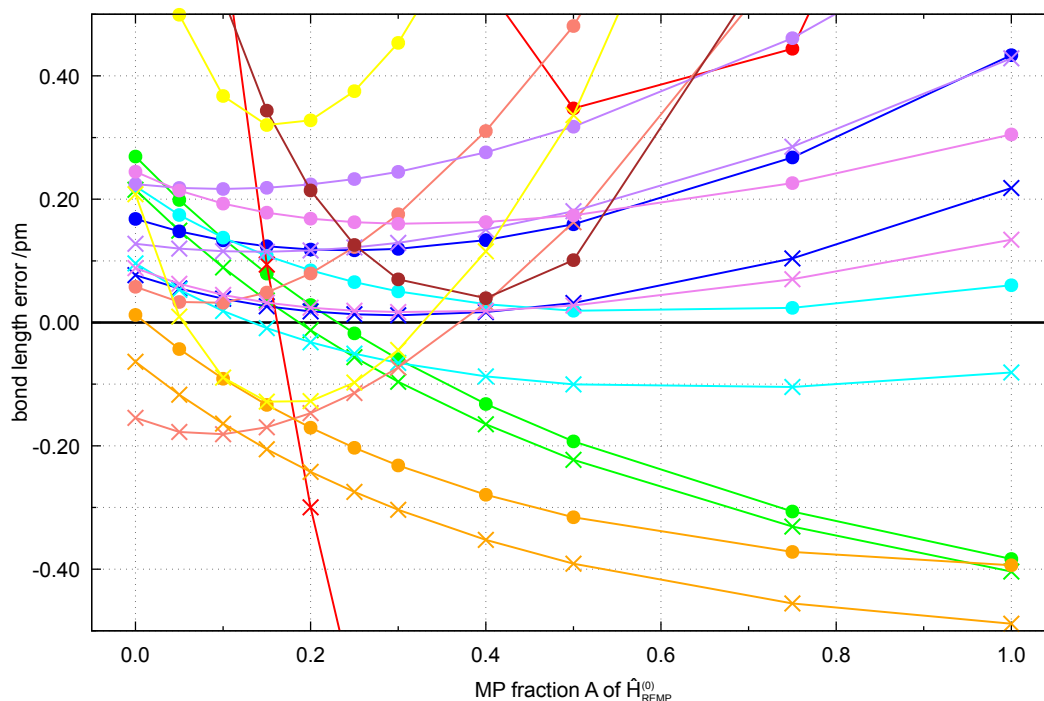


**Figure 3.19:** Zoom into the interesting region of Figure 3.18. See the caption of Figure 3.18 for details.

### 3.6 Harmonic Vibrational Frequencies of Small Molecules

*The results presented in this section were already published in Reference [53], the majority of the raw data was generated by Paul Idzko.<sup>[306]</sup>*

The set of equilibrium structures of the previous section was used to create yet another benchmark set. For a subset of molecules, experimental harmonic vibrational wavenumbers were available, i.e. true  $\tilde{\nu}_e$  numbers that have been corrected for rotational distortion and anharmonicity by measuring several overtones and combination bands. Such data is only available from precise gas-phase measurements or measurements in rare gas matrices, hence the size of molecules is rather limited. For the harmonic vibrational wavenumbers, no precision criterion was applied. Typically, the precision of such data is assumed to be much better than what can be achieved by quantum chemical methods.<sup>12</sup>

The use of frequencies that were properly extrapolated to the harmonic limit is crucial, as the following example shows: In the case of the  $^{12}\text{C}^{16}\text{O}$  molecule, e.g., the hypothetical<sup>13</sup>

<sup>12</sup>If uncertainties are provided, they are typically significantly smaller than  $0.1\text{ cm}^{-1}$ .

<sup>13</sup>the Q branch itself at  $2143\text{ cm}^{-1}$  is forbidden due to angular momentum conservation and thus not observed experimentally in the gas phase, only the P and R branches bracketing it.

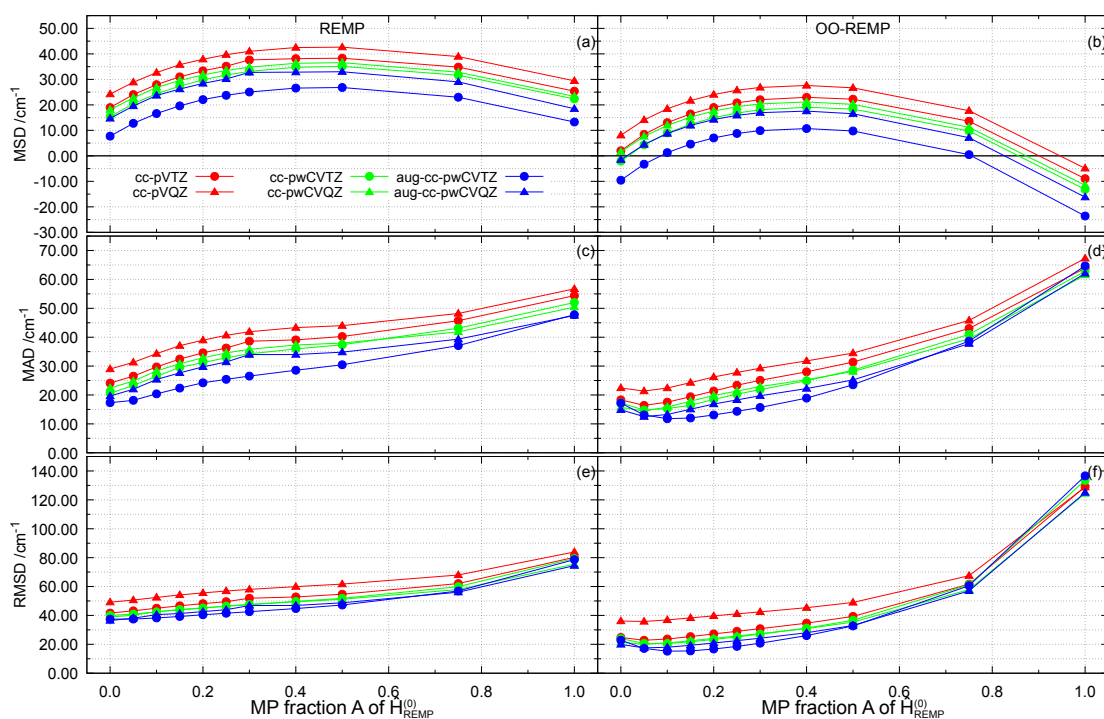


**Figure 3.20:** Statistics for the vibrations benchmark set, average over 81 harmonic vibrational modes of 43 molecules. Reference: best available experimental harmonic vibrational wavenumbers.

pure vibrational, anharmonic  $0 \rightarrow 1$  transition has a wavenumber of  $2143 \text{ cm}^{-1}$ ,<sup>[307]</sup> while the extrapolated harmonic vibrational wavenumber amounts to  $2169.8 \text{ cm}^{-1}$ .<sup>[308]</sup> The difference between the harmonic vibrational wavenumber typically calculated and the corresponding experimental value by a coarse experiment thus amounts to more than  $25 \text{ cm}^{-1}$ . As is well known and as will be shown below, this difference is significantly larger than the typical uncertainty of high-level quantum-chemical methods. The use of harmonic vibrational frequencies as proper reference is therefore mandatory.

Great care has to be taken to select proper nuclear masses as vibrational wavenumbers are mass-dependent. Quantum-chemical calculations primarily yield the partial second derivatives of the potential energy surface with respect to two nuclear coordinates at a given point (the Hessian), which corresponds to force constants. The nuclear masses are then introduced by mass-weighting the Hessian prior to diagonalization. If calculated harmonic frequencies shall be compared to experimental data, it is often necessary to manually specify the atomic masses as quantum chemistry programs often use averaged atomic masses instead of the mass of the most abundant isotope. The benchmark set also contains data from molecules for which data for more than one isotopologue was available, e.g. AlH&AlD, H<sub>2</sub>, HD & D<sub>2</sub> etc. The Hessian was always calculated at the respective minimum geometry provided by the tested method to remove any ambiguity regarding

the choice of the structure. The vibrational frequencies benchmark set therefore contains molecules for which no precise experimental equilibrium structure data was available but good harmonic frequencies data. The Hessian was constructed from a five-point numerical differentiation of energies (REMP) or gradients (OO-REMP), respectively, as implemented in PSI4. For this benchmark set, so far no CCSD(T) data or results for other methods exists.

Figure 3.20 shows a graphical representation of the statistical descriptors for the vibrational frequencies benchmark. Overall, one finds trends comparable to the structure benchmark. Both REMP and OO-REMP again seem to have a basis set Pauling point with the aug-cc-pwCVTZ basis set. The REMP data furthermore shows that for this benchmark set, there is no improvement by hybridization, analogously to the equilibrium structures. Pure RE/aug-cc-pwCVTZ provides the best vibrational frequencies with an MAD of  $17.3 \text{ cm}^{-1}$  (RMSD= $37.4 \text{ cm}^{-1}$ ). With increasing MP2 fraction, the MAD and RMSD increase steadily until the MAD surpassed  $45 \text{ cm}^{-1}$  with pure MP2. It can be noticed that on average all REMP frequencies are too high, indicating that REMP predicts bonds as too stiff. OO-REMP/aug-cc-pwCVTZ, on the other hand, exhibits shallow minima in the MAD and the RMSD at  $0.10 < A < 0.20$  (OO-REMP(0.10) yields an MAD of  $11.8 \text{ cm}^{-1}$  and an RMSD of  $15.3 \text{ cm}^{-1}$ ). Compared to canonical REMP, the mean signed deviation is also smaller, with OO-REMP(0.10)/aug-cc-pwCVTZ being almost spot-on. Lastly, the dramatically smaller RMSD:MAD ratio of OO-REMP indicates that it is less plagued by outliers than canonical REMP. In conclusion, the bonds predicted by OO-REMP are thus on average not only slightly longer than their corresponding REMP counterparts (cf. Figure 3.17) but also less rigid, which is a result of the improved description of the electronic correlation.

As there is currently no data available from other methods, it is difficult to rank REMP and OO-REMP compared to other methods, especially CCSD(T) and common density functionals. The latter comparison would be particularly interesting as DFT is routinely used in thermochemistry protocols to calculate the ZPVE correction.<sup>14</sup> From an absolute point of view, an MAD of  $12 \text{ cm}^{-1}$  seems impressive. If the 95 % CI is again approximated with  $2 \times$  the RMSD, one obtains a 95 % CI of  $\approx 30 \text{ cm}^{-1}$ . Wennmohs and Neese assessed the performance of a large number of coupled-pair type methods on a small number of molecules.<sup>[96]</sup> They found an MAD of  $8.5 \text{ cm}^{-1}$  for CCSD(T), and MAD of  $25.6 \text{ cm}^{-1}$  for NCPF/1 (their best coupled-pair method), and an MAD of  $56.4 \text{ cm}^{-1}$  (data from Table 4 of Ref. [96]). Although their set of molecules is smaller and differs a bit from the one used here, the performance of MP2 is comparable (cf. Fig. 3.20). Tentscher *et al.*<sup>[300]</sup> also assessed the capability of a large number of methods to predict harmonic vibrational wavenumbers of small radicals. They found that at least RO-CCSD(T) including core correlation and large (core-polarized) basis sets are necessary to reach an MAD below

<sup>14</sup>Of course it will not be as simple as just substituting DFT with something “better”, because part of the success of DFT is rooted in the error compensation of wrongly predicted harmonic frequencies and the effect of anharmonicity, leading to scale factors close to unity.<sup>[309]</sup> Additionally, it might be necessary to determine scaling factors for OO-REMP, too, for obtaining good ZPE corrections.

$10\text{ cm}^{-1}$ . UCCSD(T) and also CC3 turned out to be insufficient with MADs larger than  $30\text{ cm}^{-1}$ . Tew *et al.*<sup>[310]</sup> found a MAD of  $6.2\text{ cm}^{-1}$  for frozen core CCSD(T)/aug-cc-pVQZ compared to the basis set limit, and have shown that for reaching quantitative agreement with the experiment, corrections beyond perturbative triples, core correlation corrections, and also relativistic corrections are necessary. While some of these tend to cancel each other, each of these corrections may amount to several  $\text{cm}^{-1}$ . Martin<sup>[311]</sup> also found a slight overestimation by CCSD(T) at the CBS limit. Pawłowski *et al.*<sup>[304]</sup> also estimate the error of CCSD(T) with QZ basis sets to be  $\approx 9\text{ cm}^{-1}$ . Karton and Martin<sup>[301]</sup> found similar results, and only after the inclusion of corrections beyond CCSDTQ, i.e. with the full W4 model, they were able to achieve an MAD below  $1\text{ cm}^{-1}$ . From this point of view, the performance of OO-REMP, yielding MADs below  $20\text{ cm}^{-1}$  with various basis sets, is even more impressive. All in all, the quality of the results is quite promising.

## 3.7 Dipole Moments of Small Molecules

### 3.7.1 Main Group Element Molecules

*The results presented in this section were already published in Reference [53], a part of the data was generated by André Förstner.<sup>[312]</sup>*

The static dipole moment is the most simple electric multipole moment (apart from total charges, which are actually monopoles), and play a crucial role in noncovalent interactions and the mutual orientation of molecules. Electric dipole moments are furthermore proper observables and if the system under investigation has net zero charge, they are gauge invariant.<sup>15</sup> Molecular electric dipole moments can be measured rather precisely,<sup>[316]</sup> typical measurements make use of the Stark effect, i.e. the splitting of degenerate lines under the action of an external electric field. In the gas phase, the dipole moment can be deduced from pure rotational spectra (microwave spectra) with additional external fields with an accuracy of 1% or better. An alternative technique is molecular beam electric resonance with a claimed uncertainty of 0.02% and a precision clearly better than 1%.<sup>16</sup> As will be shown below, the experimental uncertainty is smaller than the typical computational uncertainty, the number of significant digits is thus sufficient to make valid judgments of the predictive performance of the investigated methods. The calculation of molecular dipole moments is straightforward, either fully analytically (if a

<sup>15</sup>Multipole moments correspond to the expansion of the charge distribution in a basis of spherical harmonics. Generally, only the lowest non-vanishing expansion coefficient is independent of the choice of the origin (i.e. the dipole for neutral molecules and the center of charge for ions). All higher moments will depend on the choice of the origin<sup>[313]</sup> and the only thing that can be done about it is to choose the origin reasonably as e.g. the center of mass. Dipole moments of ions are also considerably more difficult to measure than those of neutral molecules.<sup>[314,315]</sup>

<sup>16</sup>Molecular beam electric resonance (MBER) dipole moments are typically reported with at least three significant decimals, often even more, see e.g. Refs. [317–320]. The uncertainty of these numbers is thus clearly below 1%. Ref. [319] describes a typical MBER apparatus as it has been built 50 years ago.

(relaxed) one-particle density is available), or as numerical derivative of the energy with respect to external electric fields. As such, the dipole moment can serve as substitute for assessing the quality of the one-particle density itself, which in turn is related to the quality of the wavefunction.

The ability to predict molecular dipole moments was assessed with two different benchmark sets: The smaller set consists of 20 small, formally closed shell singlet and single reference molecules for which experimental dipole moments are available,<sup>[194]</sup> the larger set consists of 150 closed and open shell molecules, where CCSD(T) was taken as reference.<sup>[321]</sup> In both cases, the CCSD(T) structures provided with the benchmark data were used. For

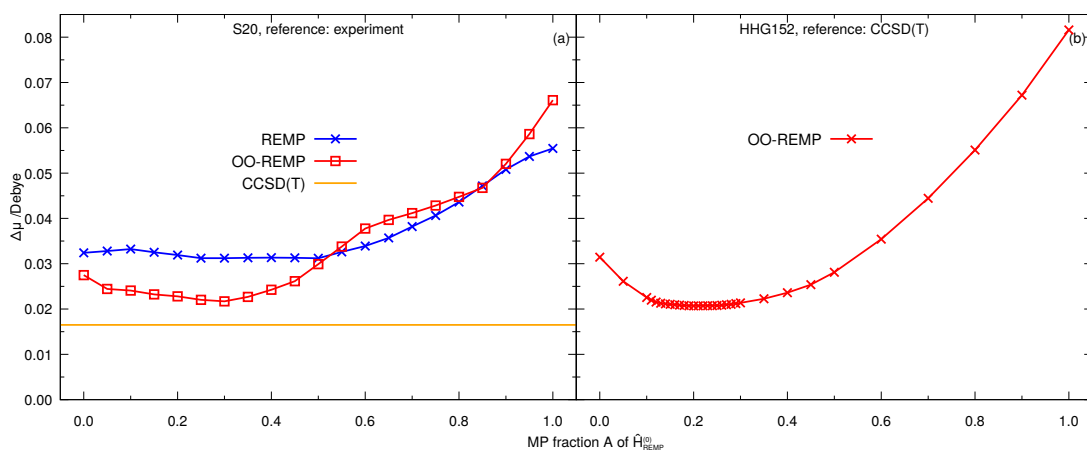


**Figure 3.21:** Mean absolute deviations of computed dipole moments from the respective reference. Left-hand panel (a): S20 set,<sup>[194]</sup> REMP and OO-REMP calculations performed with the aug-cc-pV5Z(-h) basis set, reference: best available experimental value; right-hand panel: HHG152 set<sup>[321]</sup> excluding singlet methylene and ozone, OO-REMP/aug-cc-pVQZ, reference: CCSD(T)/aug-cc-pVQZ. See Ref. [53] for further details.

the small S20 set,<sup>[194]</sup> it was found that both REMP and OO-REMP improve on their parent methods. REMP systematically overestimates dipole moments by  $\approx 0.03$  D and the MAD and RMSD have both shallow minima around  $A = 0.30$ , see Fig. 3.21(a). This corresponds to a mean absolute relative error of  $\approx 4\%$ . OO-REMP performs significantly better, the MAD and the RMSD become minimal between  $0.25 \leq A \leq 0.30$ , and the MAD amounts to 0.022 D. The relative error becomes minimal in the same region and amounts to 2.7%. For comparison, CCSD(T) achieved an MAD of 0.016 D corresponding to an MARE of 1.95%. CCSD(T) is thus still slightly better than REMP and OO-REMP and can thus serve as reference method for dipole moments, but the distance especially to OO-REMP is small, so results obtained with CCSD(T) as reference should not be overinterpreted. For this set, also a number of DFT results were available, but none of the tested functionals came even close to REMP.

The second set originally consisted of 152 closed and open shell molecules and noncovalent complexes,<sup>[321]</sup> but  $\text{O}_3$  and singlet  $\text{CH}_2$  had to be excluded.  $\text{O}_3$  exhibited the known



problem that for  $A < 0.17$  the orbital optimization did not converge.  $^1\text{CH}_2$  had the problem that the initial broken symmetry determinant either did not lead to convergence or collapsed to a closed shell singlet, depending on  $A$ . In either case, the CCSD(T) reference numbers are questionable, anyway. For  $\text{O}_3$ , it has been shown that there are sizable post-(T) contributions,<sup>[224]</sup> invalidating CCSD(T) as reference method. The CCSD(T) calculation for  $^1\text{CH}_2$  builds upon a broken-symmetry determinant with  $\langle \hat{S}^2 \rangle = 0.72$ , being a mixture of the open shell singlet and the  $m_s = 0$  component of the triplet. It can safely be expected that UCCSD(T) cannot compensate for such an amount of spin contamination. The given reference dipole moment might thus serve as reference for methods building upon the same ill-defined spin state, but not as adequate reference for spin-pure singlet methylene. The set contains some other molecules with UHF unstable singlets, but quite fortunately, they did not give rise to convergence issues if a broken symmetry determinant obtained from a stability analysis was used to seed the orbital optimization.<sup>17</sup>

It has been shown before that OO-REMP performs remarkably well also for electronically more complicated open shell systems. On the other hand, canonical REMP struggles for these systems, and as analytical dipole moments currently are only available for OO-REMP, only OO-REMP has been applied to the larger benchmark set. For the larger set, no experimental data is available in all cases, therefore CCSD(T) has been used as reference. As shown above, CCSD(T) is assumed to be still a bit more accurate than OO-REMP and hence acceptable as reference method for lack of alternatives.

For OO-REMP, one finds a shallow minimum in the range of  $0.15 < A < 0.30$  where the MAD amounts to 0.02 D, corresponding to a relative error of 2.5–2.8 % (see Fig. 3.21(b)). For comparison, MP2 and CCSD yield 0.2 D (0.04 D) corresponding to an MARE of 27 % (7.5 %). OO-REMP thus outperforms CCSD by a factor of 2 at virtually the same computational cost. A further breakdown of the set into UHF stable closed shell singlets and unstable singlets or higher multiplicities shows that OO-REMP performs better for the closed shell cases (MAD  $\approx$  0.01 D) and worse for the open shell cases (MAD  $\approx$  0.3 D), but the minimum is in both case located around  $A \approx 0.20$  and the difference in performance is not dramatic. All figures of merit regarding relative errors furthermore improve if regularized relative errors instead of plain relative errors are computed. OO-REMP(0.20) then scores an RMSRE of 2.1 %, which is clearly superior to all methods reported in Reference [321] (ignoring the different choice of basis sets). Only some double hybrid functionals are able to compete yielding RMSREs in the 3.x % range.

For a small set of molecules, Karton and Martin<sup>[301]</sup> were able to calculate dipole moments at the W4 level. Surprisingly, they found that dipole moments are practically converged at the CCSD(T)/CBS level and that the remaining difference between W4 and available reference data (MAD of 0.038 a.u.) is significantly larger than the residual difference

---

<sup>17</sup>wavels itself is currently still not capable of performing any kind of stability analysis. The respective calculations were performed with ORCA, subsequently the resulting broken-symmetry orbitals were extracted from the output file, transferred to the wavels start orbital format and used to seed a UHF calculation.

between CCSD(T) and W4 (MAD of 0.004 a.u.). This again justifies the use of CCSD(T) as reference level of theory, at least for single reference molecules.

The outcome of the dipole moments investigation is quite interesting. On one hand, one finds again that REMP and OO-REMP improve upon their parent methods, and that the minima with respect to the mixing parameter  $A$  are in the same range as in most other cases (structures and covalent thermochemistry). On the other hand, one finds a clear disagreement with the recovered correlation energy investigation (Section 3.1). This is important as both the amount of recovered correlation energy and the dipole moment can be regarded as proxy measure for the quality of the wavefunction. The seeming contradiction can be resolved by considering that both quantities apply some kind of weighting to the wavefunction: for calculating the correlation energy, the excited configuration coefficients are contracted with  $\hat{H}$  matrix elements, while for calculating the dipole moment, the density calculated from the wavefunction is contracted with dipole matrix elements. The energy criterion thus weights those excited configurations larger which provide the most correlation energy, while the dipole moment places emphasis on those configurations which have the largest influence on the charge distribution in the molecule.

A non-weighted measure for the wavefunction quality would be the overlap criterion<sup>[50]</sup> originally used for assessing the REMP wavefunction quality. As has been discussed above, the wavefunction overlap of OO-REMP wavefunctions with e.g. Coupled Cluster wavefunctions is not easily available, one therefore has to resort to some replacement measure.

### 3.7.2 A Transition Metal Element Molecule

It is instructive to not only investigate simple main group element molecules but to also consider at least one example of a transition metal species. Due to its approximate closed-shell singlet nature, CuF is still tractable at a single reference level of theory.

Figure 3.22 shows the dipole moment of CuF calculated at the RHF and OO-REMP level with two different basis sets. Furthermore, two experimental reference values are shown. An experimental equilibrium bond length of 1.744 922 Å was used for all calculations.<sup>[322]</sup> The comparison between aug-cc-pwCVQZ and aug-cc-pwCV5Z(-hi) shows that the dipole moment is practically converged at that basis set saturation level.<sup>18</sup>

There are currently (at least) two experimental dipole moments available, one rather unreliable value of  $5.77 \pm 0.20$  D<sup>[322]</sup> (Hoeft *et al.*, 1970) and one rather accurate value

<sup>18</sup>aug-cc-pwCV5Z(-hi) calculations were performed using wawels. The  $h$  and  $i$  functions had to be stripped from the basis set due to limitations of the integral engine. aug-cc-pwCVQZ calculations were performed using PSI4. The analytical dipole moment implementation in PSI4 was not yet thoroughly verified, but close agreement between both results indicates that the implementation is indeed correct. Moreover, also for PSI4 either  $i$  functions would have to be stripped, or the the integral library would have to be recompiled from scratch.

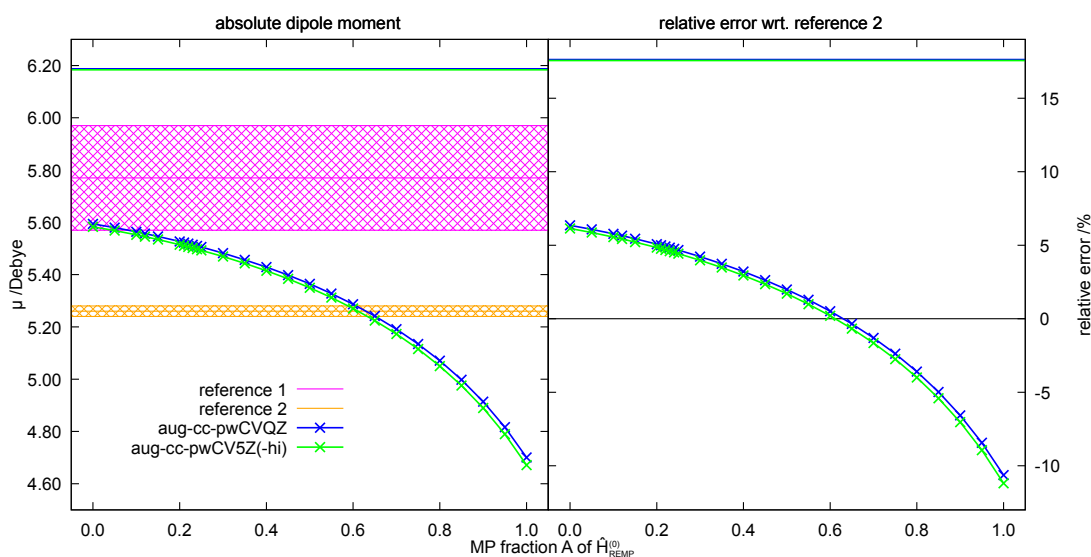


**Figure 3.22:** Calculated permanent electric dipole moment of CuF and comparison to experimental reference data. Computational method: OO-REMP or RHF and basis set as indicated. Horizontal blue and green lines indicate RHF dipole moments, crosses indicate OO-REMP values. Reference 1 is taken from Ref. [322], reference 2 is taken from Ref. [323]. Hatched areas indicate  $\pm$ one experimental standard deviation.

of  $5.26 \pm 0.02 \text{ D}^{[323]}$  (Wang *et al.*, 2010). The newer value is compatible with the old one at a  $3\sigma$  or 95% CI level, but not vice versa. Generally, it is assumed that the newer experimental value is more reliable. The older value is listed nevertheless, as a number of theoretical studies use it as reference.<sup>[324,325]</sup>

Figure 3.22 and Table 3.10 show that OO-REMP in the regularly best-performing region predicts the dipole moment  $\approx 5\%$  too large. The most probable explanation is the neglect of (scalar-)relativistic effects. A comparison between MRCI and MRCI+DKH2 shows that inclusion of relativistic effects significantly lowers the dipole moment. This is further corroborated by the close agreement of scalar-relativistic CCSD(T) calculations with the newer experimental result. Unsurprisingly, RHF predicts a way too large dipole moment, i.e. it predicts the bond to be too ionic. DFT, on the other hand, predicts systematically too small dipole moments.<sup>[325]</sup>

In order to test the hypothesis whether relativistic effects are responsible for the lower dipole moment, additional calculations including scalar-relativistic corrections were performed. The second-order Douglas-Kroll-Hess Hamiltonian<sup>[326–332]</sup> (DKH2) was chosen as it is implemented both in PSI4<sup>[331]</sup> and ORCA.<sup>[331,333–335]</sup> It is originally a two-component formalism,<sup>[336]</sup> but it is common practice to further neglect parts of it: The implementations used in this work, e.g., drop the spin-dependent terms, so that the DKH Hamiltonian effectively acts as a perturbative correction to the one-electron matrix elements, introducing scalar-relativistic corrections. Spin-orbit terms are neglected entirely.<sup>[337]</sup> DKH2 in this

**Table 3.10:** Comparison of experimental and theoretical dipole moments for the CuF molecule in its  $X^1\Sigma^+$  ground state. All values in Debye.

RHF/aug-cc-pwCV5Z(-hi)	6.18
OO-REMP(0.00)/aug-cc-pwCV5Z(-hi)	5.58
OO-REMP(0.20)/aug-cc-pwCV5Z(-hi)	5.51
OO-REMP(0.55)/aug-cc-pwCV5Z(-hi)	5.31
OO-REMP(1.00)/aug-cc-pwCV5Z(-hi)	4.67
Dirac-Coulomb 4C HF /large basis <sup>[325]</sup>	6.13
Dirac-Coulomb 4C CAM-B3-LYP /large basis <sup>[325]</sup>	5.11
scalar-relativistic CCSD(T)/CBS <sup>[325]</sup>	5.29
MRCI/5Z <sup>[324]</sup>	5.93
MRCI+DKH2/5Z <sup>[324]</sup>	5.64
RCCSD(T)+DKH2/5Z <sup>[324]</sup>	5.31
experiment (1970) <sup>[322]</sup>	5.77±0.20
experiment (2010) <sup>[323]</sup>	5.26±0.02

form has the advantage that it is a simple correction to the one-electron integrals<sup>[331,334]</sup> as long as only energies are concerned and the correction comes at a negligible computational cost. Typically, DKH calculations are performed with scalar-relativistic reconstructions of common basis sets. When assigning changes in an expectation value upon a modification of the Hamiltonian, it is advisable to ensure that the change is due to a change in the Hamiltonian and not due to a change in the basis set. Not all basis sets are available as scalar-relativistically recontracted version, they are available for a considerably lower number of elements, different programs feature different basis sets in their built-in library and even less basis sets are available from [basissetexchange.org](http://basissetexchange.org).

The calculation of static electric dipole moments including the DKH correction is straightforward: The new density is just contracted with the dipole matrix elements as in the nonrelativistic case. DKH2 will not add any correction to the dipole matrix elements.<sup>[330]</sup>

Figure 3.23 depicts the dipole moments that are obtained upon inclusion of the DKH2 treatment compared to a nonrelativistic treatment. Similar to the MRCI results in Table 3.10, one finds that scalar-relativistic results lower the dipole moment by  $\approx 0.2$  D. Importantly, this is almost independent of the basis set used, i.e. the use of a relativistically recontracted basis set is not absolutely mandatory here. The corrections introduced by the DKH2 one-electron Hamiltonian turned out to be vastly more important than the choice of the basis set. DKH2-OO-REMP dramatically improves upon OO-REMP considering this example. The mixing ratio where the error becomes minimal shifts from 55–65 % MP2 to  $\approx 40$  % and the relative error of DKH2-OO-REMP(0.20)/aug-cc-pwCVQZ-DK amounts to only 2.3 % compared to 5.1 % from OO-REMP(0.20)/aug-cc-pwCVQZ. Upon inclusion of basic scalar-relativistic corrections, the relative error for transition-metal species is hence not larger than for main-group molecules (see Sec. 3.7.1).

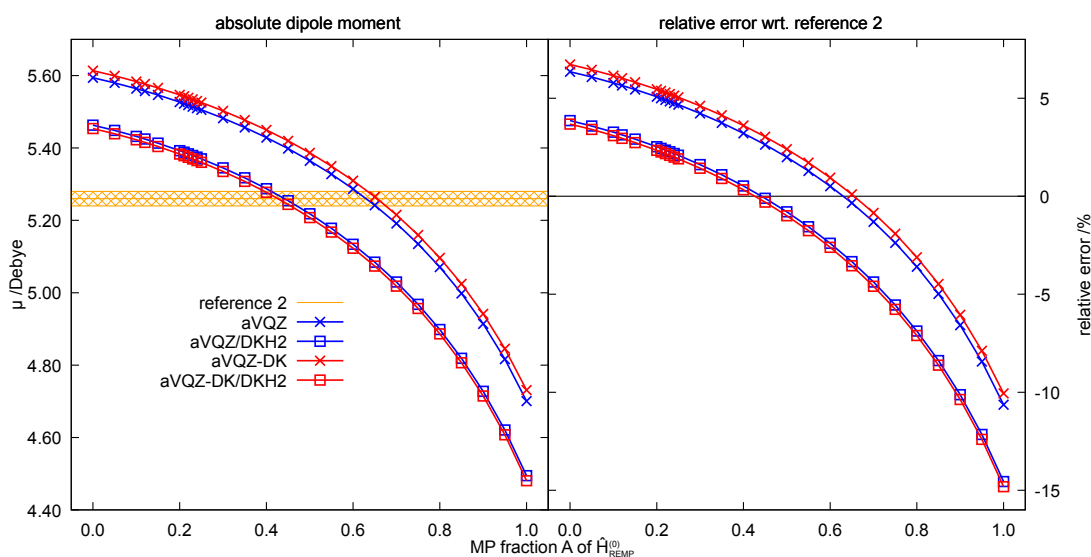


**Figure 3.23:** Comparison of the electric dipole moment of CuF computed with OO-REMP and different basis sets depending on the relativistic treatment. Crosses indicate a strictly nonrelativistic treatment, squares indicate inclusion of scalar-relativistic effects at the one-electron level by the DKH2 ansatz. Blue symbols indicate the aug-cc-pwCVQZ basis, red symbols indicate the combination Cu:aug-cc-pwCVQZ-DK/F:aug-cc-pCVQZ-DK. The left panel shows the absolute dipole moment, the right panel shows the relative error with respect to Ref. [323].

**Table 3.11:** Comparison of electric dipole moments of CuF computed with different basis sets and with or without DKH2 relativistic corrections. All values in Debye.

basis set	non-relativistic	DKH2
	RHF	
aug-cc-pwCV5Z	6.184	6.103
Cu:aug-cc-pwCV5Z-DK/F:cc-pV5Z-DK	6.187	6.093
OO-CEPA(0)/D		
aug-cc-pwCV5Z	5.595	5.464
Cu:aug-cc-pwCV5Z-DK/F:cc-pV5Z-DK	5.591	5.435

Table 3.11 shows the dipole moment of CuF calculated with different methods, different basis sets<sup>19</sup> and different levels of relativistic treatment. All calculations in Table 3.11 were performed with ORCA 5.0.3. This serves as independent check to verify the PSI4

<sup>19</sup>The unconventional basis combination arises from the unavailability of better “-DK” basis sets in the ORCA basis library for fluorine.

results by an independent DKH2 implementation.<sup>20</sup> Overall, the previous findings are almost quantitatively reproduced despite the differing basis sets. At the RHF level, scalar-relativistic effects decrease the dipole moment by  $\approx 0.1$  D (being still too large), while at the OCEPA level, the correction amounts to almost 0.2 D. The correction is in both cases larger with the recontracted basis. Given that the numbers in Table 3.11 and the (DKH)-OO-REMP(0.00) results in Figure 3.23 do agree almost quantitatively, it can be assumed that the DKH-OO-REMP dipole moments are technically correct. The interpretation of the results in Table 3.11 is not straightforward. Half of the relativistic shift is contributed by the reference determinant, the other half is due to correlation. A possible explanation would be that the relativistic orbital contraction is stronger at the copper atom, making it more electronegative. This especially affects the Cu 4s orbital which participates in the bonding, making the Cu-F bond slightly less polar. There is of course also significant contribution of Cu 3d orbitals in the bond, and these are known to slightly expand. On the other hand, the Cu-*d*-F-*p*- $\pi$  bonding and antibonding orbitals are filled, so that their effect should cancel. The fluorine atom is also affected by relativity, but to a lesser extent. Correlation also involves virtual orbitals, and as the orbitals into which correlation takes place were not determined, no conclusive explanation can be given. One possible explanation would be enhanced correlation from fluorine into vacant Cu-*p* orbitals which are energetically lowered by scalar-relativistic effects, but a detailed analysis is out of scope, here.

The dipole moment of CuF is of course just a single example and no statistically sound data collection. More data needs to be gathered to corroborate the findings. Nevertheless, it shows that OO-REMP might be also a useful method for transition metal systems.

Ironically, these last results close the circle to the introduction where it was stated that relativistic effects are ignored in the vast majority of cases. The example of the dipole moment of a seemingly simple molecule show that all too often basic assumptions turn out to become invalid when the scope is extended. Every now and then established assertions should be questioned and checked against unbiased facts.

### 3.8 Performance Summary for Different Properties

The preceding sections have shown that REMP and OO-REMP are able to deliver very accurate results and that there is almost always an improvement observable with an appropriate choice of the mixing parameter *A*. Table 3.12 shows a summary of the previously presented results and a comparison how REMP and OO-REMP perform for various properties compared to other methods. The data listed in Table 3.12 was mostly generated in this work or in related works that use the same benchmark sets, as indicated. In some cases, however, no data for the same benchmark set was available, it was then

---

<sup>20</sup>Well, actually not completely independent. The DKH implementation used in PSI4 is the one by B. A. Hess, M. Reiher and A. Wolf, linked in as optional module. The DKH implementation in ORCA is due to F. Neese, but the output mentions help by Hess, Reiher and Wolf. There is thus a nonzero possibility that both implementations share common mistakes.

necessary to resort to reasonably comparable datasets. A mixing ratio of 80:20 (RE:MP) was chosen for Table 3.12 as it is close to the optimum mixing in the majority of cases and a choice that can generally be recommended.

As can be seen, REMP and OO-REMP in most cases improve upon the results of their respective parent methods with respect to almost all considered properties. One further finds that orbital optimization often leads to only a minor improvement for RE and hardly any improvement for MP. In contrast, orbital optimization invariably leads to an improvement for REMP. OO-REMP(0.20) is found to provide significantly better results than CCSD at formally the same computational cost and only slightly inferior results compared to CCSD(T) (whenever CCSD(T) was not used as reference). Table 3.12 also lists results from the widely popular B3-LYP functional and the prototypical double hybrid, B2-PLYP. In contrast to OO-REMP, none of the two functionals achieves an accuracy of  $1 \text{ kcal mol}^{-1}$  for thermochemical applications. Quite interestingly, it also turned out that in the case of the benchmark sets and density functionals listed in Table 3.12, the inclusion of an empirical dispersion correction worsens the results.

Unfortunately, no extensive comparison to the most recent range-separated, dispersion corrected, spin-component scaled double-hybrid functionals<sup>[338]</sup> ( $\omega$ DSD or xDSD functionals) is possible. Such functionals typically have at least half a dozen adjustable empirical parameters. It is now common practice to parameterize new functionals on large databases like e.g. the GMTKN55, warranting statistically significant results for thermochemistry. At the same time, there is typically no data on how well such functionals perform for other properties like molecular structures. An interesting and logical development in this direction is the inclusion of MP3 correlation<sup>[339]</sup> leading to DSD3 functionals. The improved correlation comes at the expense of yet another parameter and a formal computational cost of  $n^6$  while achieving only modest improvements.

**Table 3.12:** Overview of the average performance for various kinds of reaction types and properties. Given are mean absolute deviations or mean absolute relative errors. Values are in kcal mol<sup>-1</sup> or percent as indicated. *ref.* indicates that the respective method was used as reference. Canonical REMP refers to either the restricted closed shell or the unrestricted variant. Basis sets are either reasonably large or a CBS extrapolation was performed. If not specified otherwise, no dispersion correction was applied to DFT methods.

	Closed-shell thermochemistry /kcal mol <sup>-1</sup>	Transfer reaction /kcal mol <sup>-1</sup>	Atomization barrier heights /kcal mol <sup>-1</sup>	Atomization energies /kcal mol <sup>-1</sup>	Bond dissociation energies /kcal mol <sup>-1</sup>	Isomerization energies /kcal mol <sup>-1</sup>	Bond lengths /pm	Bond angles /°	Dipole moments /%
REMP(0.20)	1.2	4.2	3.3	3.7	0.8	0.39	0.4	5.3	
OO-REMP(0.20)	0.5	0.8	1.1	0.6	0.4	0.13	0.2	3.0	
RE2	1.4	3.9	6.4	4.8	1.1	0.36	0.3	9.3	
OO-RE	1.0	0.9	4.4	2.3	1.3	0.29	0.3	6.7	
MP2	2.0	4.4	10.9	9.8	3.1	0.69	0.3	14.0	
OO-MP2	2.6	2.9	15.3	8.8	4.7	1.28	0.5	15.7	
CCSD	1.4 <sup>a)</sup>	–	8.4	3.8	1.7	≈ 0.4 – 0.5 <sup>b)</sup>	≈ 0.3 <sup>c)</sup>	9.2 <sup>d)</sup>	
CCSD(T)	<i>ref.</i>	<i>ref.</i>	0.6	0.5	0.2	0.08	0.2	2.0 <sup>d)</sup>	
B3-LYP	2.7 <sup>e)</sup>	4.9 <sup>f)</sup>	3.2 <sup>g)</sup>	3.2 <sup>h)</sup>	1.7 <sup>i)</sup>	0.68 <sup>j)</sup>	–	6.2 <sup>d)</sup>	
B2-PLYP	–	2.3 <sup>f)</sup>	1.9 <sup>g)</sup>	2.1 <sup>h)</sup>	1.8 <sup>i)</sup>	0.30 <sup>j)</sup>	–	– <sup>k)</sup>	
$\omega$ DSD <sub>72</sub> -PBEP86-D4	–	0.9 <sup>l)</sup>	2.2 <sup>l)</sup>	–	–	–	–	–	

<sup>a)</sup> Recalculated from Table 1 of Ref. [215] with those reactions included here

<sup>b)</sup> Inferred from Table IV of Ref. [298], Table III of Ref. [299], and Table 4 of Ref. [300]

<sup>c)</sup> taken from Table VII of Ref. [299]

<sup>d)</sup> Calculated from Table 2 of Ref. [194]

<sup>e)</sup> Taken from Table II of Ref. [47] (larger set, QCISD(T) as reference)

<sup>f)</sup> Taken from Ref [340]

<sup>g)</sup> Taken from Table 6 of Ref. [224] (nonMR)

<sup>h)</sup> Taken from Table 7 of Ref. [224] (all 99 reactions including MR)

<sup>i)</sup> Taken from Table 9 of Ref. [224]

<sup>j)</sup> Taken from Table 4 of Ref. [300] (B2-PLYP-D, B3-LYP without D)

<sup>k)</sup> No data is available for the S20 benchmark set, but B2-PLYP outperformed B3-LYP on the benchmark set of Ref. [321] (RMSE of 5.31% vs. 6.98%)

<sup>l)</sup> Taken from Table S5 of Ref. [338],  $\omega = 0.13$ ; entry “W4-11” is assumed to be the set of atomization energies including the MR cases



## 4 Conclusion and Outlook

In this work, the REMP and OO-REMP classes of methods have been introduced and benchmarked. It has been shown that – as hypothesized – the hybrid methods lead to results that improve over both parent methods and that promising accuracy is achieved so that at least the orbital-optimized variant may become a routine method. It has furthermore been shown that the ideal mixing is nearly independent of the molecule and property under consideration, so that a globally optimal mixing ratio can be established.

To take up the lines from the introduction, it has been shown that the instantaneous two-electron interaction is indeed an important component of the Hamiltonian which cannot completely be treated as a perturbation. The RE perturbation theory which includes the instantaneous two-electron repulsion for all perturbers of the same excitation degree in the unperturbed Hamiltonian  $\hat{H}^{(0)}$  leads to significantly more accurate results than MP-PT. At the same time, it was found that RE in low orders tends to overshoot on the correlation energy and that this can be corrected by damping the two-electron operator in  $\hat{H}^{(0)}$ . The results provided by REMP and OO-REMP generally show better agreement with reference results and exhibit a sharper error distributions, which implies both smaller systematic and statistical errors. It is especially important that it was possible to achieve chemical accuracy for a variety of well-established benchmark sets. REMP and OO-REMP are thus not just yet another proof-of-principle or toy methods but potential methods for routine application when a higher accuracy is required than the one provided by typical density functional methods. In particular, the combination of easily available analytical gradients, high accuracy,  $\mathcal{O}(n^6)$  scaling and easy-to-implement working equations is a unique feature of OO-REMP. The only method for routine calculations which has an even higher accuracy – CCSD(T) – has a steeper scaling of  $\mathcal{O}(n^7)$  and is generally computationally more demanding. Additionally, analytical gradients are hardly available owing to their difficult nature.

The (OO-)REMP approach allows for further possible improvements. As has been shown, for several applications, and if no very high accuracy is required, already canonical REMP provides reasonably accurate results. It is therefore desirable to also derive and implement analytical first derivatives for REMP. Bozkaya and Sherrill derived the  $z$ -vector equations for CEPA/0,<sup>[46]</sup> it should thus not be too complicated to implement the REMP orbital response equations, especially as the MP2  $z$ -vector equations are known for a long time.<sup>[341]</sup> Combining these to yield  $z$ -vector equations for REMP will give access to relaxed first-order properties.

Introducing more degrees of freedom into the Hamiltonian by using different scaling factors for different configuration state function classes (see Section 2.2) leads to the

S2REMP approach. The S2REMP approach was extensively evaluated by Marc Edelmann in his master thesis.<sup>[211]</sup> It was shown that already one additional independent parameter leads to significant improvements over the REMP ansatz with one parameter. Specifically, it was found that of the three parameters  $S$  (scaling the SDE-SDE interaction),  $A$  (scaling the SDE-TDE interaction) and  $T$  (scaling the TDE-TDE interaction),  $S$  and  $T$  may be constrained to the same value. It was furthermore shown that the choice of  $A = 0.25$ ,  $S = 0.05$ ,  $T = 0.05$  provides the best overall results, leading to a significant improvement both with respect to the amount of recovered correlation energy and with respect to the quality of the doubles-part of the wavefunction (all values specifying the amount of  $\hat{H}_{\text{MP}}^{(0)}$  in  $\hat{H}^{(0)}$ ). As such, these findings are very promising, and with this choice for a test set of 44 molecules,  $100.1 \pm 0.6\%$  of the CCSDTQ correlation energy was recovered. Further validation, however, will require a much faster implementation than the current one, which is based on a CI program operating with explicit matrix representations of the Hamiltonians. This implies that sigma vector equations like Eq. (2.74) in a Serber CSF basis (see Section 2.2) need to be derived and implemented. The S2REMP approach has the clear drawback that the mixing parameters are tied to specific CSFs and their interaction, making a generalization to higher orders nontrivial, as more open shells will require even a larger number of parameters. The generalization to open shell cases will be nontrivial, too, as at least in the ROHF case, the first-order wavefunction will contain single excitations, eventually requiring yet another parameter. The S2REMP approach may also be coupled to orbital optimization, although it can be expected that the working equations will be fairly complex and complicated to derive.

In terms of speed-up, the combination of REMP and pair natural orbital (PNO) techniques seems promising. Pioneered by Meyer<sup>[94,95,132]</sup> and Taylor,<sup>[342]</sup> and later by Staemmler and Fink,<sup>[181]</sup> this method was recently revived by Neese *et al.*<sup>[343–352]</sup> with notable contributions by Werner *et al.*<sup>[353–361]</sup> and Kállay *et al.*<sup>[362,363]</sup> Usage of PNOs allows to drastically shrink the virtual space of calculations and eventually leads to linear scaling. In the case of canonical REMP, the implementation and application will be straightforward, given that a PNO machinery is available, as usage of PNOs has been demonstrated for both MP2<sup>[347,349,353,354,364]</sup> and CEPA/0.<sup>[176,343,345,346,365]</sup> In the case of OO-REMP, the situation is considerably more difficult, as every orbital macroiteration will invalidate the current set of PNOs. To the best of the knowledge of the author, this is still an unsolved problem.

The most important extension of the REMP approach would be a generalization to multiconfigurational reference wavefunctions. It has recently been shown that the uncontracted multireference RE approach performs better than any other second order MRPT approach and is even capable of quantitatively describing the chromium dimer,<sup>[366,367]</sup> a system which is notoriously difficult to model due to the large number of active orbitals and electrons, the presence of both large static and large dynamic correlation and hence an extremely bad zeroth order description by CASSCF. The character of the wavefunction additionally changes with increasing bond distance from various low spin configurations to a high-spin atomic configuration. Given that the REMP approach leads to a significant

---

improvement in the closed-shell singlet case, it can be anticipated that there will be at least some improvement if MRRE is combined with some multireference Møller-Plesset derivative like MRMP2<sup>[368–371]</sup> or NEVPT2.<sup>[86–89]</sup> There is already some interesting work by Saitow and Yanai<sup>[372]</sup> who combined CASPT2 and a CEPA/0-like treatment for different spaces with PNOs.

There is more work to be done with respect to benchmarking REMP and OO-REMP for additional properties: The current implementation allows for the calculation of electric multipole moments up to hexadecapoles with arbitrary origin. Given that higher order multipole moments were for a long time claimed to be decisive for the structure of noncovalent aggregates, it seems worthy to build up a benchmark set for these properties. However, as they are not easily accessible experimentally and plagued by arbitrariness of the gauge origin,<sup>[313]</sup> the majority of the data will have to be calculated by high-level methods with the advantage that the origin will be well-defined. Static dipole polarizabilities, hyperpolarizabilities<sup>[301,373–375]</sup> and higher moment polarizabilities are accessible by numerical differentiation of energies obtained with finite external electric fields. The necessary code is available and operational but due to time and resource restrictions, it was so far not possible to perform such calculations. The performance for the dipole moment of CuF and some preliminary results for the MOR41 set not shown in this work indicate that at least OO-REMP might be also useful for single-reference transition metal systems. Further investigations in this direction seem worthwhile and promising.

A very interesting and potentially useful long-term goal would be the derivation and implementation of excitation energies and other properties via response theory.<sup>[376]</sup> MP2 is not useful for computing excitation energies,<sup>[377]</sup> and to the best knowledge of the author, there have so far not been any attempts to compute excitation energies from CEPA/0, OO-MP2 or OCEPA from a response theory formalism. There has, however, recently been some effort towards TD-OOMP2<sup>[378–380]</sup> and TD-OCEPA.<sup>[381]</sup> All ingredients for a TD-OO-REMP ansatz are therefore in principle available and only need to be wired together. This will give access to optical properties like optical absorption spectra, frequency-dependent polarizabilities or hyperpolarizabilities, that can be used to simulate e.g. higher harmonic generation effects.<sup>[382–384]</sup> It has been shown that TD-OO-MP2 provides results that are comparable in quality to TDCC2 and TDCCSD as well as their linear response counterparts.<sup>[378–380]</sup> The advantage of real-time time-dependent methods is that they are typically easier to derive and implement than their linear-response counterparts and that they also work when the linear response approximation breaks down. Their disadvantage is that they often require the time-dependent wavefunction to be propagated for tens of thousands of time steps, with specific pulse shapes for a specific property.<sup>[379]</sup> Given that the OO-REMP ground state wavefunction seems to be of decent quality and that OO-REMP turned out to be superior to both parent methods, attempts in this direction seem to be promising.

The methodology developed in this thesis is now publicly available to everyone via <https://psicode.org> or <https://github.com/psi4/psi4/> both as source code and

starting from version 1.7 (released on 2022-12-06) also in the precompiled binaries of PSI4. As the code base of the df-occ subprogram recently underwent further changes<sup>1</sup>, it can be expected that also the RI-accelerated REMP variants (df-REMP and df-OREMP) will gain some speedup.

---

<sup>1</sup>Improvements in the external exchange operator by Yavuz Alagöz and Uğur Bozkaya not yet merged to the master branch

## 5 List of Papers, Posters, and Talks

### List of peer-reviewed publications related to this work:

- S. Behnle & R. F. Fink: “REMP: A hybrid perturbation theory providing improved electronic wavefunctions and properties”, *J. Chem. Phys.*, **150** (2019), 124107, doi: 10.1063/1.5086168
- S. Behnle & R. F. Fink: “OO-REMP: Approaching Chemical Accuracy with Second-Order Perturbation Theory”, *J. Chem. Theory Comput.* **17** (2021), 3259-3266, doi: 10.1021/acs.jctc.1c00280
- S. Behnle & R. F. Fink: “UREMP, RO-REMP, and OO-REMP: Hybrid perturbation theories for open-shell electronic structure calculations”, *J. Chem. Phys.* **156** (2022), 124103, doi: 10.1063/5.0081285
- S. Behnle, R. Richter, L. Völkl, P. Idzko, A. Förstner, U. Bozkaya & R. F. Fink: “Accurate property prediction by second order perturbation theory: The REMF and OO-REMP hybrids” *J. Chem. Phys.* **157** (2022), 104111, doi: 10.1063/5.0105628

### List of peer-reviewed publications coauthored but unrelated to this work:

- M. Müller, S. Behnle, C. Maichle-Mössmer & H. F. Bettinger: “Boron–nitrogen substituted perylene obtained through photocyclisation”, *Chem. Commun.* **50** (2014), 7821-7823, doi: 10.1039/C4CC01424C
- J. Banerjee, S. Behnle, M. C. E. Galbraith, V. Settels, B. Engels, R. Tonner & R. F. Fink: “Comparison of the periodic slab approach with the finite cluster description of metal–organic interfaces at the example of PTCDA on Ag(110)”, *J. Comput. Chem.* **39** (2018) 844-852, doi: 10.1002/jcc.25159
- J. Henrichsmeyer, M. Thelen, M. Bröckel, M. Fadel, S. Behnle, M. Sekkal-Rahal & R. F. Fink: “Rationalizing Aggregate Structures with Orbital Contributions to the Exchange-Repulsion Energy”, *ChemPhysChem* (2023), e202300097, accepted for publication, doi: 10.1002/cphc.202300097

### List of conference talks:

- STC 2021: “The Orbital Optimized REMF Hybrid Perturbation Theory - Accurate Thermochemistry and Structures from 2<sup>nd</sup> Order PT” (contributed talk)

### List of conference posters:

- STC 2018: “REMP: A New Hybrid Perturbation Theory With Improved Prediction Capabilities”

- MQM 2019: “REMP: A Hybrid Perturbation Theory With Improved Predictive Capabilities”
- STC 2019: “OO-REMP: Reaching Chemical Accuracy using Perturbation Theory?”
- STC 2021: “OO-REMP: Accurate Energies and Properties From Second Order Perturbation Theory”
- STC 2022: “Knocking at CCSD(T)’s Door: How far can 2<sup>nd</sup> Order Perturbation Theory be Pushed?”

## Bibliography

- [1] F. S. Levin, *An Introduction to Quantum Theory*, Cambridge University Press, **2002**, 808 pp., ISBN: 0521598419, DOI: 10.1017/CB09781139164177.
- [2] H. Poincaré, *Acta Math.* **1890**, *13*, 1–270, eprint: <https://archive.org/download/actamathematica071efgoog/actamathematica071efgoog.pdf>.
- [3] W. Qiu-Dong, *Celestial Mech. Dyn. Astr.* **1990**, *50*, 73–88, DOI: 10.1007/BF00048987.
- [4] L. K. Babadzanjanz, *Celestial Mech. Dyn. Astr.* **1993**, *56*, 427–449, DOI: 10.1007/BF00691812.
- [5] B. Sutcliffe in *Adv. Chem. Phys.* John Wiley & Sons, Ltd, **2000**, pp. 1–121, ISBN: 9780470141731, DOI: 10.1002/9780470141731.ch1.
- [6] L. Piela, *Ideas of Quantum Chemistry*, Elsevier Science & Technology Books, Amsterdam, **2013**, p. 1078, ISBN: 978-0-444-59436-5, eprint: <https://www.elsevier.com/books/ideas-of-quantum-chemistry/piela/978-0-444-59436-5>.
- [7] F. Jensen, *Introduction to Computational Chemistry*, Third Edition, Wiley, **2017**, 664 pp., ISBN: 978-1-118-82599-0.
- [8] M. Born, K. Huang, *Dynamical Theory of Crystal Lattices*, Oxford University Press, **1954**, 432 pp., ISBN: 0-19-850369-5.
- [9] M. Born, R. Oppenheimer, *Ann. Phys.* **1927**, *389*, 457–484, DOI: 10.1002/andp.19273892002.
- [10] W. Kolos, L. Wolniewicz, *J. Chem. Phys.* **1964**, *41*, 3663–3673, DOI: 10.1063/1.1725796.
- [11] W. Kutzelnigg, *Einführung in die Theoretische Chemie*, Wiley-VCH, **2002**, 936 pp., ISBN: 978-3-527-30609-1.
- [12] P. A. M. Dirac, R. H. Fowler, *Proc. R. Soc. London A.* **1928**, *117*, 610–624, DOI: 10.1098/rspa.1928.0023.
- [13] P. A. M. Dirac, R. H. Fowler, *Proc. R. Soc. London A.* **1928**, *118*, 351–361, DOI: 10.1098/rspa.1928.0056.
- [14] T. Saue, *ChemPhysChem* **2011**, *12*, 3077–3094, DOI: 10.1002/cphc.201100682.
- [15] M. Reiher, A. Wolf, *Relativistic Quantum Chemistry: The Fundamental Theory of Molecular Science*, Second Edition, Wiley-VCH Verlag GmbH, Weinheim, **2015**, 750 pp., ISBN: 9783527334155, DOI: 10.1002/9783527667550.

- [16] W. Liu, *J. Chem. Phys.* **2020**, *152*, 180901, DOI: 10.1063/5.0008432.
- [17] T. Helgaker, P. Jørgensen, J. Olsen, *Molecular Electronic-Structure Theory*, Repr., Wiley, Weinheim, **2004**, 908 pp., ISBN: 0-471-96755-6, DOI: 10.1002/9781119019572.
- [18] S. Stopkowicz, J. Gauss, *J. Chem. Phys.* **2008**, *129*, 164119, DOI: 10.1063/1.2998300.
- [19] S. Stopkowicz, J. Gauss, *J. Chem. Phys.* **2011**, *134*, 064114, DOI: 10.1063/1.3522766.
- [20] S. Stopkowicz, J. Gauss, *J. Chem. Phys.* **2011**, *134*, 204106, DOI: 10.1063/1.3587633.
- [21] A. Szabo, N. S. Ostlund, *Modern Quantum Chemistry: Introduction to Advanced Electronic Structure Theory*, Dover Publications, Inc., **1996**, 480 pp., ISBN: 0-486-69186-1.
- [22] C. J. Cramer, *Essentials of Computational Chemistry: Theories and Models*, 2. ed., Wiley, Chichester, **2004**, 596 pp., ISBN: 0-470-09182-7.
- [23] P. Saxe, H. F. Schaefer III., N. C. Handy, *Chem. Phys. Lett.* **1981**, *79*, 202–204, DOI: 10.1016/0009-2614(81)80187-X.
- [24] P. Knowles, N. Handy, *Chem. Phys. Lett.* **1984**, *111*, 315–321, DOI: 10.1016/0009-2614(84)85513-X.
- [25] P. J. Knowles, N. C. Handy, *Comput. Phys. Commun.* **1989**, *54*, 75–83, DOI: 10.1016/0010-4655(89)90033-7.
- [26] G. H. Booth, A. J. W. Thom, A. Alavi, *J. Chem. Phys.* **2009**, *131*, 054106, DOI: 10.1063/1.3193710.
- [27] G. H. Booth, A. Alavi, *J. Chem. Phys.* **2010**, *132*, 174104, DOI: 10.1063/1.3407895.
- [28] D. Cleland, G. H. Booth, A. Alavi, *J. Chem. Phys.* **2010**, *132*, 041103, DOI: 10.1063/1.3302277.
- [29] V. G. Chilkuri, F. Neese, *J. Chem. Theory Comput.* **2021**, *17*, 2868–2885, DOI: 10.1021/acs.jctc.1c00081.
- [30] V. G. Chilkuri, F. Neese, *J. Comput. Chem.* **2021**, *42*, 982–1005, DOI: 10.1002/jcc.26518.
- [31] P. Hohenberg, W. Kohn, *Phys. Rev.* **1964**, *136*, B864–B871, DOI: 10.1103/PhysRev.136.B864.
- [32] R. G. Parr, Y. Weitao, *Density-Functional Theory of Atoms and Molecules*, Oxford University Press, USA, **1994**, 352 pp., ISBN: 9780195092769.
- [33] W. Koch, M. C. Holthausen, *A Chemist's Guide to Density Functional Theory*, Wiley-VCH Verlag GmbH, **2001**, 313 pp., ISBN: 3-527-30372-3, eprint: <https://onlinelibrary.wiley.com/doi/epub/10.1002/3527600043>.



- [34] C. C. J. Roothaan, *Rev. Mod. Phys.* **1951**, *23*, 69–89, DOI: 10.1103/RevModPhys.23.69.
- [35] C. C. J. Roothaan, *Rev. Mod. Phys.* **1960**, *32*, 179–185, DOI: 10.1103/RevModPhys.32.179.
- [36] C. Møller, M. S. Plesset, *Phys. Rev.* **1934**, *46*, 618–622, DOI: 10.1103/PhysRev.46.618.
- [37] R. F. Fink, *Chem. Phys. Lett.* **2006**, *428*, 461–466, DOI: 10.1016/j.cplett.2006.07.081.
- [38] G. E. Scuseria, H. F. Schaefer, *Chem. Phys. Lett.* **1987**, *142*, 354–358, DOI: 10.1016/0009-2614(87)85122-9.
- [39] A. I. Krylov, C. D. Sherrill, E. F. C. Byrd, M. Head-Gordon, *J. Chem. Phys.* **1998**, *109*, 10669–10678, DOI: 10.1063/1.477764.
- [40] C. D. Sherrill, A. I. Krylov, E. F. C. Byrd, M. Head-Gordon, *J. Chem. Phys.* **1998**, *109*, 4171–4181, DOI: 10.1063/1.477023.
- [41] S. R. Gwaltney, C. D. Sherrill, M. Head-Gordon, A. I. Krylov, *J. Chem. Phys.* **2000**, *113*, 3548–3560, DOI: 10.1063/1.1286597.
- [42] R. C. Lochan, M. Head-Gordon, *J. Chem. Phys.* **2007**, *126*, 164101, DOI: 10.1063/1.2718952.
- [43] F. Neese, T. Schwabe, S. Kossmann, B. Schirmer, S. Grimme, *J. Chem. Theory Comput.* **2009**, *5*, 3060–3073, DOI: 10.1021/ct9003299.
- [44] U. Bozkaya, J. M. Turney, Y. Yamaguchi, H. F. Schaefer, C. D. Sherrill, *J. Chem. Phys.* **2011**, *135*, 104103, DOI: 10.1063/1.3631129.
- [45] U. Bozkaya, *J. Chem. Phys.* **2011**, *135*, 224103, DOI: 10.1063/1.3665134.
- [46] U. Bozkaya, C. D. Sherrill, *J. Chem. Phys.* **2013**, *139*, 054104, DOI: 10.1063/1.4816628.
- [47] S. Grimme, *J. Chem. Phys.* **2003**, *118*, 9095–9102, DOI: 10.1063/1.1569242.
- [48] P. Knowles, K. Somasundram, N. Handy, K. Hirao, *Chem. Phys. Lett.* **1985**, *113*, 8–12, DOI: 10.1016/0009-2614(85)85002-8.
- [49] U. Bozkaya, A. Ünal, Y. Alagöz, *J. Chem. Phys.* **2020**, *153*, 244115, DOI: 10.1063/5.0035811.
- [50] S. Behnle, R. F. Fink, *J. Chem. Phys.* **2019**, *150*, 124107, DOI: 10.1063/1.5086168.
- [51] S. Behnle, R. F. Fink, *J. Chem. Theory Comput.* **2021**, *17*, 3259–3266, DOI: 10.1021/acs.jctc.1c00280.
- [52] S. Behnle, R. F. Fink, *J. Chem. Phys.* **2022**, *156*, 124103, DOI: 10.1063/5.0081285.
- [53] S. Behnle, R. Richter, L. Völkl, P. Idzko, A. Förstner, U. Bozkaya, R. F. Fink, *J. Chem. Phys.* **2022**, *157*, 104111, DOI: 10.1063/5.0105628.

- [54] V. Fock, *Z. Phys* **1932**, *75*, 622–647, DOI: 10.1007/BF01344458.
- [55] P. R. Surján, *Second quantized approach to quantum chemistry: an elementary introduction*, Springer, Berlin, **1989**, 184 pp., ISBN: 3-540-51137-7.
- [56] I. Shavitt, R. J. Bartlett, *Many-Body Methods in Chemistry and Physics: MBPT and Coupled-Cluster Theory*, Cambridge University Press, **2009**, 532 pp., ISBN: 978-0-521-81832-2, DOI: 10.1017/CB09780511596834.
- [57] S. Saebø, P. Pulay, *J. Chem. Phys.* **1987**, *86*, 914–922, DOI: 10.1063/1.452293.
- [58] N. C. Handy, P. J. Knowles, K. Somasundram, *Theor. Chim. Acta* **1985**, *68*, 87–100, DOI: 10.1007/BF00698753.
- [59] R. Pauncz, *Spin Eigenfunctions*, Plenum Press (Springer), New York, **1979**, 370 pp., ISBN: 978-1-4684-8528-8, DOI: 10.1007/978-1-4684-8526-4.
- [60] R. Serber, *J. Chem. Phys.* **1934**, *2*, 697–710, DOI: 10.1063/1.1749377.
- [61] R. Serber, *Phys. Rev.* **1934**, *45*, 461–467, DOI: 10.1103/PhysRev.45.461.
- [62] R. Pauncz, *Int. J. Quantum Chem.* **1977**, *12*, 369–382, DOI: 10.1002/qua.560120213.
- [63] T. Kato, *Commun. Pure Appl. Math.* **1957**, *10*, 151–177, DOI: 10.1002/cpa.3160100201.
- [64] R. T. Pack, W. B. Brown, *J. Chem. Phys.* **1966**, *45*, 556–559, DOI: 10.1063/1.1727605.
- [65] R. F. Fink, *J. Chem. Phys.* **2010**, *133*, 174113, DOI: 10.1063/1.3503041.
- [66] P. J. Reynolds, D. M. Ceperley, B. J. Alder, W. A. J. Lester, *J. Chem. Phys.* **1982**, *77*, 5593–5603, DOI: 10.1063/1.443766.
- [67] Z. Sun, P. J. Reynolds, R. K. Owen, W. A. Lester, *Theor. Chim. Acta* **1989**, *75*, 353–368, DOI: 10.1007/BF00526694.
- [68] W. Klopper, *J. Chem. Phys.* **2001**, *115*, 761–765, DOI: 10.1063/1.1379577.
- [69] C. Hättig, W. Klopper, A. Köhn, D. P. Tew, *Chem. Rev.* **2012**, *112*, 4–74, DOI: 10.1021/cr200168z.
- [70] R. F. Fink, *J. Chem. Phys.* **2016**, *145*, 184101, DOI: 10.1063/1.4966689.
- [71] S. Fournais, M. Hoffmann-Ostenhof, T. Hoffmann-Ostenhof, T. Ø. Sørensen, *Comm. Math. Phys.* **2005**, *255*, 183–227, DOI: 10.1007/s00220-004-1257-6.
- [72] W. Kutzelnigg, J. D. Morgan, *J. Chem. Phys.* **1992**, *96*, 4484–4508, DOI: 10.1063/1.462811.
- [73] W. Kutzelnigg, J. D. Morgan, *J. Chem. Phys.* **1992**, *97*, 8821–8821, DOI: 10.1063/1.463358.
- [74] C. Schwartz, *Phys. Rev.* **1962**, *126*, 1015–1019, DOI: 10.1103/PhysRev.126.1015.
- [75] R. F. Fink, *Chem. Phys.* **2009**, *356*, 39–46, DOI: 10.1016/j.chemphys.2008.10.004.

- [76] S. Behnle, MA thesis, Mathematisch-Naturwissenschaftliche Fakultät der Eberhardt-Karls Universität Tübingen, Tübingen, **2018**.
- [77] M. Kállay, P. R. Surján, *J. Chem. Phys.* **2000**, *113*, 1359–1365, DOI: 10.1063/1.481925.
- [78] M. Kállay, P. R. Surján, *J. Chem. Phys.* **2001**, *115*, 2945–2954, DOI: 10.1063/1.1383290.
- [79] P. S. Epstein, *Phys. Rev.* **1926**, *28*, 695–710, DOI: 10.1103/PhysRev.28.695.
- [80] R. K. Nesbet, *Proc. R. Soc. London Ser. A* **1955**, *230*, 312, DOI: 10.1098/rspa.1955.0134.
- [81] S. Grimme, L. Goerigk, R. F. Fink, *WIREs Comput. Mol. Sci.* **2012**, *2*, 886–906, DOI: 10.1002/wcms.1110.
- [82] K. G. Dyall, *J. Chem. Phys.* **1995**, *102*, 4909–4918, DOI: 10.1063/1.469539.
- [83] W. Kutzelnigg, D. Mukherjee, *J. Chem. Phys.* **1997**, *107*, 432–449, DOI: 10.1063/1.474405.
- [84] J. Gauss, Coupled-Cluster Theory: Lecture Material for the Modern Wavefunction Methods Summer School, Gelsenkirchen, **2018**.
- [85] W. Kutzelnigg in *Methods of Electronic Structure Theory*, (Ed.: H. F. Schaefer), Springer US, Boston, MA, **1977**, pp. 129–188, ISBN: 978-1-4757-0887-5, DOI: 10.1007/978-1-4757-0887-5\_5.
- [86] C. Angeli, R. Cimiraglia, S. Evangelisti, T. Leininger, J.-P. Malrieu, *J. Chem. Phys.* **2001**, *114*, 10252–10264, DOI: 10.1063/1.1361246.
- [87] C. Angeli, R. Cimiraglia, J.-P. Malrieu, *Chem. Phys. Lett.* **2001**, *350*, 297–305, DOI: 10.1016/S0009-2614(01)01303-3.
- [88] C. Angeli, R. Cimiraglia, J.-P. Malrieu, *J. Chem. Phys.* **2002**, *117*, 9138–9153, DOI: 10.1063/1.1515317.
- [89] C. Angeli, S. Borini, M. Cestari, R. Cimiraglia, *J. Chem. Phys.* **2004**, *121*, 4043–4049, DOI: 10.1063/1.1778711.
- [90] C. Angeli, M. Pastore, R. Cimiraglia, *Theor. Chem. Acc.* **2007**, *117*, 743–754, DOI: 10.1007/s00214-006-0207-0.
- [91] C. Angeli, B. Bories, A. Cavallini, R. Cimiraglia, *J Chem Phys* **2006**, *124*, 054108, DOI: 10.1063/1.2148946.
- [92] J. Čížek, *J. Chem. Phys.* **1966**, *45*, 4256–4266, DOI: 10.1063/1.1727484.
- [93] J. Čížek in *Advances in Chemical Physics*, Vol. 14, (Eds.: R. Lefebvre, C. Moser), Wiley-Blackwell, **1969**, pp. 35–89, ISBN: 9780470143599, DOI: 10.1002/9780470143599.ch2.
- [94] W. Meyer, *Int. J. Quantum Chem.* **1971**, *5*, 341–348, DOI: 10.1002/qua.560050839.

- [95] W. Meyer, *J Chem Phys* **1973**, *58*, 1017–1035, DOI: 10.1063/1.1679283.
- [96] F. Wennmohs, F. Neese, *Chem. Phys.* **2008**, *343*, 217–230, DOI: 10.1016/j.chemphys.2007.07.001.
- [97] R. J. Bartlett, *Annu. Rev. Phys. Chem.* **1981**, *32*, 359–401, DOI: 10.1146/annurev.pc.32.100181.002043.
- [98] Á. Szabados, P. Surján, *Chem. Phys. Lett.* **1999**, *308*, 303–309, DOI: 10.1016/S0009-2614(99)00647-8.
- [99] P. R. Surján, Á. Szabados, *J. Chem. Phys.* **2000**, *112*, 4438–4446, DOI: 10.1063/1.481006.
- [100] R. J. Bartlett, I. Shavitt, *Chem. Phys. Lett.* **1977**, *50*, 190–198, DOI: 10.1016/0009-2614(77)80161-9.
- [101] R. J. Bartlett, I. Shavitt, *Chem. Phys. Lett.* **1978**, *57*, 157–158, DOI: 10.1016/0009-2614(78)80374-1.
- [102] G. D. Purvis, R. J. Bartlett, *J. Chem. Phys.* **1978**, *68*, 2114–2124, DOI: 10.1063/1.436023.
- [103] V. Rishi, A. Perera, R. J. Bartlett, *Mol. Phys.* **2019**, *117*, 2201–2216, DOI: 10.1080/00268976.2018.1492748.
- [104] R. J. Bartlett, J. Noga, *Chem. Phys. Lett.* **1988**, *150*, 29–36, DOI: 10.1016/0009-2614(88)80392-0.
- [105] T. D. Crawford, H. F. Schaefer, T. J. Lee, *J. Chem. Phys.* **1996**, *105*, 1060–1069, DOI: 10.1063/1.471951.
- [106] A. Köhn, J. Olsen, *J. Chem. Phys.* **2005**, *122*, 084116, DOI: 10.1063/1.1850918.
- [107] P. Pulay, S. Saebø, W. Meyer, *J. Chem. Phys.* **1984**, *81*, 1901–1905, DOI: 10.1063/1.447863.
- [108] T. Janowski, A. R. Ford, P. Pulay, *J. Chem. Theory Comput.* **2007**, *3*, 1368–1377, DOI: 10.1021/ct700048u.
- [109] R. Kobayashi, A. P. Rendell, *Chem. Phys. Lett.* **1997**, *265*, 1–11, DOI: 10.1016/S0009-2614(96)01387-5.
- [110] T. Janowski, P. Pulay, *J. Chem. Theory Comput.* **2008**, *4*, 1585–1592, DOI: 10.1021/ct800142f.
- [111] C. Angeli, R. Cimiraglia, J.-P. Malrieu, *Chem. Phys. Lett.* **2000**, *317*, 472–480, DOI: 10.1016/S0009-2614(99)01458-X.
- [112] U. Bozkaya, C. D. Sherrill, *J. Chem. Phys.* **2013**, *138*, 184103, DOI: 10.1063/1.4803662.
- [113] P. E. M. Siegbahn, J. Almlöf, A. Heiberg, B. O. Roos, *J. Chem. Phys.* **1981**, *74*, 2384–2396, DOI: 10.1063/1.441359.
- [114] D. Thouless, *Nucl. Phys.* **1960**, *21*, 225–232, DOI: 10.1016/0029-5582(60)90048-1.

- [115] P. Jørgensen, J. Simons, *J. Chem. Phys.* **1983**, *79*, 334–357, DOI: 10.1063/1.445528.
- [116] N. C. Handy, H. F. Schaefer, *J. Chem. Phys.* **1984**, *81*, 5031–5033, DOI: 10.1063/1.447489.
- [117] G. W. Trucks, E. Salter, C. Sosa, R. J. Bartlett, *Chem. Phys. Lett.* **1988**, *147*, 359–366, DOI: 10.1016/0009-2614(88)80249-5.
- [118] E. A. Salter, G. W. Trucks, R. J. Bartlett, *J. Chem. Phys.* **1989**, *90*, 1752–1766, DOI: 10.1063/1.456069.
- [119] U. Bozkaya, *J. Chem. Phys.* **2013**, *139*, 104116, DOI: 10.1063/1.4820877.
- [120] U. Bozkaya, *J. Chem. Theory Comput.* **2014**, *10*, 4389–4399, DOI: 10.1021/ct500634s.
- [121] U. Bozkaya, *J. Chem. Theory Comput.* **2014**, *10*, 2371–2378, DOI: 10.1021/ct500231c.
- [122] J. Stoer, *Numerische Mathematik 1*, Achte, neu bearbeitete und erweiterte Auflage, Springer, Berlin Heidelberg New York, **2002**, 371 pp., ISBN: 3-540-66154-9.
- [123] K. A. Brueckner, *Phys. Rev.* **1954**, *96*, 508–516, DOI: 10.1103/PhysRev.96.508.
- [124] R. A. Chiles, C. E. Dykstra, *J. Chem. Phys.* **1981**, *74*, 4544–4556, DOI: 10.1063/1.441643.
- [125] N. C. Handy, J. A. Pople, M. Head-Gordon, K. Raghavachari, G. W. Trucks, *Chem. Phys. Lett.* **1989**, *164*, 185–192, DOI: 10.1016/0009-2614(89)85013-4.
- [126] C. Hampel, K. A. Peterson, H.-J. Werner, *Chem. Phys. Lett.* **1992**, *190*, 1–12, DOI: 10.1016/0009-2614(92)86093-W.
- [127] H. P. Kelly, A. M. Sessler, *Phys Rev* **1963**, *132*, 2091–2095, DOI: 10.1103/PhysRev.132.2091.
- [128] H. P. Kelly, *Phys. Rev.* **1964**, *134*, A1450–A1453, DOI: 10.1103/PhysRev.134.A1450.
- [129] W. Meyer, *J. Chem. Phys.* **1973**, *58*, 1017–1035, DOI: 10.1063/1.1679283.
- [130] W. Meyer, *Theor. Chim. Acta* **1974**, *35*, 277–292, DOI: 10.1007/BF00548478.
- [131] W. Meyer, *J. Chem. Phys.* **1976**, *64*, 2901–2907, DOI: 10.1063/1.432551.
- [132] W. Meyer in *Methods of Electronic Structure Theory*, (Ed.: H. F. Schaefer), Springer US, Boston, MA, **1977**, pp. 413–446, ISBN: 978-1-4757-0887-5, DOI: 10.1007/978-1-4757-0887-5\_11.
- [133] J. Čížek, J. Paldus, *Int. J. Quantum Chem.* **1971**, *5*, 359–379, DOI: 10.1002/qua.560050402.
- [134] S. Koch, W. Kutzelnigg, *Theor. Chim. Acta* **1981**, *59*, 387–411, DOI: 10.1007/BF02402402.

- [135] P. Pulay, S. Sæbø, *Chem. Phys. Lett.* **1985**, *117*, 37–41, DOI: 10.1016/0009-2614(85)80400-0.
- [136] R. J. Gdanitz, R. Ahlrichs, *Chem. Phys. Lett.* **1988**, *143*, 413–420, DOI: 10.1016/0009-2614(88)87388-3.
- [137] P. G. Szalay, R. J. Bartlett, *Chem. Phys. Lett.* **1993**, *214*, 481–488, DOI: 10.1016/0009-2614(93)85670-J.
- [138] C. Kollmar, F. Neese, *Mol. Phys.* **2010**, *108*, 2449–2458, DOI: 10.1080/00268976.2010.496743.
- [139] C. Kollmar, A. Heßelmann, *Theor. Chem. Acc.* **2010**, *127*, 311–325, DOI: 10.1007/s00214-009-0719-5.
- [140] C. Kollmar, F. Neese, *J. Chem. Phys.* **2011**, *135*, 084102, DOI: 10.1063/1.3624567.
- [141] L. M. J. Huntington, M. Nooijen, *J. Chem. Phys.* **2010**, *133*, 184109–184127, DOI: 10.1063/1.3494113.
- [142] L. M. J. Huntington, A. Hansen, F. Neese, M. Nooijen, *J. Chem. Phys.* **2012**, *136*, 064101–064117, DOI: 10.1063/1.3682325.
- [143] D. R. Nascimento, A. E. DePrince, *J. Chem. Theory Comput.* **2014**, *10*, 4324–4331, DOI: 10.1021/ct500462p.
- [144] I. W. Bulik, T. M. Henderson, G. E. Scuseria, *J. Chem. Theory Comput.* **2015**, *11*, 3171–3179, DOI: 10.1021/acs.jctc.5b00422.
- [145] J. A. Gomez, T. M. Henderson, G. E. Scuseria, *J. Chem. Phys.* **2016**, *144*, 244117, DOI: 10.1063/1.4954891.
- [146] E. Feenberg, *Phys. Rev.* **1956**, *103*, 1116–1119, DOI: 10.1103/PhysRev.103.1116.
- [147] P. Goldhammer, E. Feenberg, *Phys. Rev.* **1956**, *101*, 1233–1234, DOI: 10.1103/PhysRev.101.1233.
- [148] A. T. Amos, *J. Chem. Phys.* **1970**, *52*, 603–605, DOI: 10.1063/1.1673029.
- [149] R. Sedlak, K. E. Riley, J. Řezáč, M. Pitoňák, P. Hobza, *ChemPhysChem* **2013**, *14*, 698–707, DOI: <https://doi.org/10.1002/cphc.201200850>.
- [150] M. Pitoňák, P. Neogrády, J. Černý, S. Grimme, P. Hobza, *ChemPhysChem* **2009**, *10*, 282–289, DOI: 10.1002/cphc.200800718.
- [151] L. Gráfová, M. Pitoňák, J. Řezáč, P. Hobza, *J. Chem. Theory Comput.* **2010**, *6*, 2365–2376, DOI: 10.1021/ct1002253.
- [152] K. E. Riley, J. Řezáč, P. Hobza, *Phys. Chem. Chem. Phys.* **2011**, *13*, 21121–21125, DOI: 10.1039/C1CP22525A.
- [153] U. Bozkaya, C. D. Sherrill, *J. Chem. Phys.* **2014**, *141*, 204105, DOI: 10.1063/1.4902226.
- [154] E. Soydaş, U. Bozkaya, *J. Chem. Theory Comput.* **2015**, *11*, 1564–1573, DOI: 10.1021/ct501184w.

- [155] U. Bozkaya, *J. Chem. Theory Comput.* **2016**, *12*, 1179–1188, DOI: 10.1021/acs.jctc.5b01128.
- [156] J. Lee, M. Head-Gordon, *J. Chem. Theory Comput.* **2018**, *14*, 5203–5219, DOI: 10.1021/acs.jctc.8b00731.
- [157] L. W. Bertels, J. Lee, M. Head-Gordon, *J. Phys. Chem. Lett.* **2019**, *10*, 4170–4176, DOI: 10.1021/acs.jpcllett.9b01641.
- [158] A. Rettig, D. Hait, L. W. Bertels, M. Head-Gordon, *J. Chem. Theory Comput.* **2020**, *16*, 7473–7489, DOI: 10.1021/acs.jctc.0c00986.
- [159] E. Keller, T. Tsatsoulis, K. Reuter, J. T. Margraf, *J. Chem. Phys.* **2022**, *156*, 024106, DOI: 10.1063/5.0078119.
- [160] M. Loipersberger, L. W. Bertels, J. Lee, M. Head-Gordon, *J. Chem. Theory Comput.* **2021**, *17*, 5582–5599, DOI: 10.1021/acs.jctc.1c00469.
- [161] A. Rettig, J. Shee, J. Lee, M. Head-Gordon, *J. Chem. Theory Comput.* **2022**, *18*, 5382–5392, DOI: 10.1021/acs.jctc.2c00641.
- [162] D. W. Small, *J. Chem. Theory Comput.* **2020**, *16*, 4014–4020, DOI: 10.1021/acs.jctc.0c00244.
- [163] S. Tan, S. Barrera Acevedo, E. I. Izgorodina, *J. Chem. Phys.* **2017**, *146*, 064108, DOI: 10.1063/1.4975326.
- [164] L. Hedin, *Phys. Rev.* **1965**, *139*, A796–A823, DOI: 10.1103/PhysRev.139.A796.
- [165] D. Langreth, J. Perdew, *Solid State Commun.* **1975**, *17*, 1425–1429, DOI: 10.1016/0038-1098(75)90618-3.
- [166] D. L. Freeman, *Phys. Rev. B* **1977**, *15*, 5512–5521, DOI: 10.1103/PhysRevB.15.5512.
- [167] D. C. Langreth, J. P. Perdew, *Phys. Rev. B* **1977**, *15*, 2884–2901, DOI: 10.1103/PhysRevB.15.2884.
- [168] H. Eshuis, J. E. Bates, F. Furche, *Theor. Chem. Acc.* **2012**, *131*, 1084, DOI: 10.1007/s00214-011-1084-8.
- [169] G. E. Scuseria, T. M. Henderson, D. C. Sorensen, *J. Chem. Phys.* **2008**, *129*, 231101, DOI: 10.1063/1.3043729.
- [170] P. D. Mezei, G. I. Csonka, A. Ruzsinszky, M. Kállay, *J. Chem. Theory Comput.* **2015**, *11*, 4615–4626, DOI: 10.1021/acs.jctc.5b00420.
- [171] S. Grimme, M. Steinmetz, *Phys. Chem. Chem. Phys.* **2016**, *18*, 20926–20937, DOI: 10.1039/C5CP06600J.
- [172] F. Furche, *J. Chem. Phys.* **2008**, *129*, 114105, DOI: 10.1063/1.2977789.
- [173] M. Kállay, *J. Chem. Phys.* **2015**, *142*, 204105, DOI: 10.1063/1.4921542.
- [174] V. Staemmler, *Theor. Chim. Acta* **1977**, *45*, 89–94, DOI: 10.1007/BF00552543.
- [175] M. Jungen, *Theor. Chim. Acta* **1981**, *60*, 369–377, DOI: 10.1007/BF00549280.

- [176] V. Staemmler, R. Jaquet, *Theor. Chim. Acta* **1981**, *59*, 487–500, DOI: 10.1007/BF02394652.
- [177] U. Meier, V. Staemmler, *Theor. Chim. Acta* **1989**, *76*, 95–111, DOI: 10.1007/BF00532127.
- [178] J. Wasilewski, *Int. J. Quantum Chem.* **1989**, *36*, 503–524, DOI: 10.1002/qua.560360406.
- [179] R. Fink, Dissertation, Ruhr-Universität Bochum, D-44780 Bochum, Germany, **1991**.
- [180] J. Wasilewski, *Int. J. Quantum Chem.* **1991**, *39*, 649–656, DOI: 10.1002/qua.560390502.
- [181] R. Fink, V. Staemmler, *Theor. Chim. Acta* **1993**, *87*, 129–145, DOI: 10.1007/BF01113534.
- [182] J. M. Turney, A. C. Simmonett, R. M. Parrish, E. G. Hohenstein, F. A. Evangelista, J. T. Fermann, B. J. Mintz, L. A. Burns, J. J. Wilke, M. L. Abrams, N. J. Russ, M. L. Leininger, C. L. Janssen, E. T. Seidl, W. D. Allen, H. F. Schaefer, R. A. King, E. F. Valeev, C. D. Sherrill, T. D. Crawford, *WIREs Comput. Mol. Sci.* **2012**, *2*, 556–565, DOI: 10.1002/wcms.93.
- [183] R. M. Parrish, L. A. Burns, D. G. A. Smith, A. C. Simmonett, A. E. DePrince, E. G. Hohenstein, U. Bozkaya, A. Y. Sokolov, R. Di Remigio, R. M. Richard, J. F. Gonthier, A. M. James, H. R. McAlexander, A. Kumar, M. Saitow, X. Wang, B. P. Pritchard, P. Verma, H. F. Schaefer, K. Patkowski, R. A. King, E. F. Valeev, F. A. Evangelista, J. M. Turney, T. D. Crawford, C. D. Sherrill, *J. Chem. Theory Comput.* **2017**, *13*, 3185–3197, DOI: 10.1021/acs.jctc.7b00174.
- [184] D. G. A. Smith, L. A. Burns, A. C. Simmonett, R. M. Parrish, M. C. Schieber, R. Galvelis, P. Kraus, H. Kruse, R. Di Remigio, A. Alenaizan, A. M. James, S. Lehtola, J. P. Misiewicz, M. Scheurer, R. A. Shaw, J. B. Schriber, Y. Xie, Z. L. Glick, D. A. Sirianni, J. S. O'Brien, J. M. Waldrop, A. Kumar, E. G. Hohenstein, B. P. Pritchard, B. R. Brooks, H. F. Schaefer, A. Y. Sokolov, K. Patkowski, A. E. DePrince, U. Bozkaya, R. A. King, F. A. Evangelista, J. M. Turney, T. D. Crawford, C. D. Sherrill, *J. Chem. Phys.* **2020**, *152*, 184108, DOI: 10.1063/5.0006002.
- [185] B. I. Dunlap, J. W. D. Connolly, J. R. Sabin, *J. Chem. Phys.* **1979**, *71*, 3396–3402, DOI: 10.1063/1.438728.
- [186] O. Vahtras, J. Almlöf, M. Feyereisen, *Chem. Phys. Lett.* **1993**, *213*, 514–518, DOI: 10.1016/0009-2614(93)89151-7.
- [187] M. Feyereisen, G. Fitzgerald, A. Komornicki, *Chem. Phys. Lett.* **1993**, *208*, 359–363, DOI: 10.1016/0009-2614(93)87156-W.
- [188] R. Bauernschmitt, M. Häser, O. Treutler, R. Ahlrichs, *Chem. Phys. Lett.* **1997**, *264*, 573–578, DOI: 10.1016/S0009-2614(96)01343-7.
- [189] F. Neese, G. Olbrich, *Chem. Phys. Lett.* **2002**, *362*, 170–178, DOI: 10.1016/S0009-2614(02)01053-9.



- [190] U. Bozkaya, *J. Chem. Phys.* **2014**, *141*, 124108, DOI: 10.1063/1.4896235.
- [191] U. Bozkaya, *J. Chem. Phys.* **2014**, *141*, 219901, DOI: 10.1063/1.4903269.
- [192] U. Bozkaya, C. D. Sherrill, *J. Chem. Phys.* **2016**, *144*, 174103, DOI: 10.1063/1.4948318.
- [193] U. Bozkaya, C. D. Sherrill, *J. Chem. Phys.* **2017**, *147*, 044104, DOI: 10.1063/1.4994918.
- [194] U. Bozkaya, E. Soydaş, B. Filiz, *J. Comput. Chem.* **2020**, *41*, 769–779, DOI: 10.1002/jcc.26126.
- [195] A. Ünal, U. Bozkaya, *J. Chem. Theory Comput.* **2022**, *18*, 1489–1500, DOI: 10.1021/acs.jctc.1c01000.
- [196] K. Eichkorn, O. Treutler, H. Öhm, M. Häser, R. Ahlrichs, *Chem. Phys. Lett.* **1995**, *242*, 652–660, DOI: 10.1016/0009-2614(95)00838-U.
- [197] K. Eichkorn, O. Treutler, H. Öhm, M. Häser, R. Ahlrichs, *Chem. Phys. Lett.* **1995**, *240*, 283–290, DOI: 10.1016/0009-2614(95)00621-A.
- [198] K. Eichkorn, F. Weigend, O. Treutler, R. Ahlrichs, *Theor. Chim. Acta* **1997**, *97*, 119–124, DOI: 10.1007/s002140050244.
- [199] F. Weigend, M. Häser, H. Patzelt, R. Ahlrichs, *Chem. Phys. Lett.* **1998**, *294*, 143–152, DOI: 10.1016/S0009-2614(98)00862-8.
- [200] N. H. F. Beebe, J. Linderberg, *Int. J. Quantum Chem.* **1977**, *12*, 683–705, DOI: 10.1002/qua.560120408.
- [201] I. Røeggen, E. Wisløff-Nilssen, *Chem. Phys. Lett.* **1986**, *132*, 154–160, DOI: 10.1016/0009-2614(86)80099-9.
- [202] H. Koch, A. Sánchez de Merás, T. B. Pedersen, *J. Chem. Phys.* **2003**, *118*, 9481–9484, DOI: 10.1063/1.1578621.
- [203] W. H. Press, S. A. Teukolsky, W. T. Vetterling, B. P. Flannery, *Numerical Recipes: The Art of Scientific Computing*, 3rd Edition: Cambridge University Press, **2007**, 1235 pp., ISBN: 978-0-521-88407-5.
- [204] U. Bozkaya, *Phys. Chem. Chem. Phys.* **2016**, *18*, 11362–11373, DOI: 10.1039/C6CP00164E.
- [205] U. Bozkaya, *J. Chem. Theory Comput.* **2019**, *15*, 4415–4429, DOI: 10.1021/acs.jctc.9b00378.
- [206] The OpenMP Architecture Review Board, OpenMP: Enabling HPC since 1997, **2023**, <https://www.openmp.org/> (visited on 02/23/2023).
- [207] The BLAS (Basic Linear Algebra Subprograms) netlib reference implementation, <https://netlib.org/blas/> (visited on 02/16/2023).
- [208] L. S. Blackford, J. Demmel, J. Dongarra, I. Duff, S. Hammarling, G. Henry, M. Heroux, L. Kaufman, A. Lumsdaine, A. Petitet, R. Pozo, K. Remington, R. C. Whaley, *ACM Trans. Math. Softw.* **2002**, *28*, 135–151, DOI: 10.1145/567806.567807.

- [209] Intel® oneAPI Math Kernel Library, <https://www.intel.com/content/www/us/en/developer/tools/oneapi/onemkl.html> (visited on 02/16/2023).
- [210] Z. Xianyi, W. Qian, W. Saar, OpenBLAS: An optimized BLAS library, **2023**, <http://www.openblas.net/> (visited on 02/16/2023).
- [211] M. Edelmann, MA thesis, Eberhard-Karls-Universität Tübingen, **2022**, 41 pp.
- [212] M. Kállay, P. R. Nagy, D. Mester, Z. Rolik, G. Samu, J. Csontos, J. Csóka, P. B. Szabó, L. Gyevi-Nagy, B. Hégyel, I. Ladjánszki, L. Szegedy, B. Ladóczki, K. Petrov, M. Farkas, P. D. Mezei, Á. Ganyecz, *J. Chem. Phys.* **2020**, *152*, 074107, DOI: 10.1063/1.5142048.
- [213] MRCC, a quantum chemical program suite written by M. Kállay, P. R. Nagy, D. Mester, L. Gyevi-Nagy, J. Csóka, P. B. Szabó, Z. Rolik, G. Samu, J. Csontos, B. Hégyel, Á. Ganyecz, I. Ladjánszki, L. Szegedy, B. Ladóczki, K. Petrov, M. Farkas, P. D. Mezei, and R. A. Horváth. See [www.mrcc.hu](http://www.mrcc.hu). **2022**.
- [214] E. Soydaş, U. Bozkaya, *J. Comput. Chem.* **2014**, *35*, 1073–1081, DOI: 10.1002/jcc.23592.
- [215] E. Soydaş, U. Bozkaya, *J. Chem. Theory Comput.* **2013**, *9*, 1452–1460, DOI: 10.1021/ct301078q.
- [216] L. Goerigk, A. Hansen, C. Bauer, S. Ehrlich, A. Najibi, S. Grimme, *Phys. Chem. Chem. Phys.* **2017**, *19*, 32184–32215, DOI: 10.1039/C7CP04913G.
- [217] A. I. Krylov, *J. Chem. Phys.* **2000**, *113*, 6052–6062, DOI: 10.1063/1.1308557.
- [218] T. C. Dinadayalane, R. Vijaya, A. Smitha, G. N. Sastry, *J. Phys. Chem. A* **2002**, *106*, 1627–1633, DOI: 10.1021/jp013910r.
- [219] V. Guner, K. S. Khuong, A. G. Leach, P. S. Lee, M. D. Bartberger, K. N. Houk, *J. Phys. Chem. A* **2003**, *107*, 11445–11459, DOI: 10.1021/jp035501w.
- [220] D. H. Ess, K. N. Houk, *J. Phys. Chem. A* **2005**, *109*, 9542–9553, DOI: 10.1021/jp052504v.
- [221] L. Goerigk, S. Grimme, *J. Chem. Theory Comput.* **2010**, *6*, 107–126, DOI: 10.1021/ct900489g.
- [222] Y. Zhao, B. J. Lynch, D. G. Truhlar, *Phys. Chem. Chem. Phys.* **2005**, *7*, 43–52, DOI: 10.1039/B416937A.
- [223] Y. Zhao, N. González-García, D. G. Truhlar, *J. Phys. Chem. A* **2005**, *109*, 2012–2018, DOI: 10.1021/jp045141s.
- [224] A. Karton, S. Daon, J. M. Martin, *Chem. Phys. Lett.* **2011**, *510*, 165–178, DOI: 10.1016/j.cplett.2011.05.007.
- [225] A. Karton, E. Rabinovich, J. M. L. Martin, B. Ruscic, *J. Chem. Phys.* **2006**, *125*, 144108, DOI: 10.1063/1.2348881.
- [226] F. Neese, E. F. Valeev, *J. Chem. Theory Comput.* **2011**, *7*, 33–43, DOI: 10.1021/ct100396y.

- [227] F. Weigend, R. Ahlrichs, *Phys. Chem. Chem. Phys.* **2005**, *7*, 3297–3305, DOI: 10.1039/B508541A.
- [228] D. Rappoport, F. Furche, *J. Chem. Phys.* **2010**, *133*, 134105–134115, DOI: 10.1063/1.3484283.
- [229] J. Schöckle, BA thesis, Eberhard-Karls-Universität Tübingen, **2020**, 44 pp.
- [230] K. Müller-Dethlefs, P. Hobza, *Chem. Rev.* **2000**, *100*, 143–168, DOI: 10.1021/cr9900331.
- [231] K. E. Riley, P. Hobza, *WIREs Comput. Mol. Sci.* **2011**, *1*, 3–17, DOI: 10.1002/wcms.8.
- [232] E. G. Hohenstein, C. D. Sherrill, *WIREs Comput. Mol. Sci.* **2012**, *2*, 304–326, DOI: 10.1002/wcms.84.
- [233] J.-M. Lehn, *Supramolecular Chemistry: Concepts and Perspectives*, Wiley-VCH Verlag GmbH, Weinheim, **1995**, 281 pp., ISBN: 3-527-29312-4, DOI: 10.1002/3527607439.
- [234] S. Kubik, *Supramolecular Chemistry*, De Gruyter, Berlin, Boston, **2021**, 597 pp., ISBN: 9783110595611, DOI: 10.1515/9783110595611.
- [235] J. Černý, P. Hobza, *Phys. Chem. Chem. Phys.* **2007**, *9*, 5291–5303, DOI: 10.1039/B704781A.
- [236] L. M. Salonen, M. Ellermann, F. Diederich, *Angew. Chem. Int. Ed.* **2011**, *50*, 4808–4842, DOI: 10.1002/anie.201007560.
- [237] M. Kolář, T. Kubař, P. Hobza, *J. Phys. Chem. B* **2011**, *115*, 8038–8046, DOI: 10.1021/jp202878d.
- [238] O. A. Stasyuk, D. Jakubec, J. Vondrášek, P. Hobza, *J. Chem. Theory Comput.* **2017**, *13*, 877–885, DOI: 10.1021/acs.jctc.6b00775.
- [239] J. Poater, M. Swart, F. M. Bickelhaupt, C. Fonseca Guerra, *Org. Biomol. Chem.* **2014**, *12*, 4691–4700, DOI: 10.1039/C4OB00427B.
- [240] A. Heßelmann, G. Jansen, *Chem. Phys. Lett.* **2002**, *357*, 464–470, DOI: 10.1016/S0009-2614(02)00538-9.
- [241] A. Heßelmann, G. Jansen, *Chem. Phys. Lett.* **2002**, *362*, 319–325, DOI: 10.1016/S0009-2614(02)01097-7.
- [242] J. Řezáč, K. E. Riley, P. Hobza, *J. Chem. Theory Comput.* **2011**, *7*, 2427–2438, DOI: 10.1021/ct2002946.
- [243] J. Řezáč, K. E. Riley, P. Hobza, *J. Chem. Theory Comput.* **2014**, *10*, 1359–1360, DOI: 10.1021/ct5000692.
- [244] L. A. Burns, M. S. Marshall, C. D. Sherrill, *J. Chem. Phys.* **2014**, *141*, 234111, DOI: 10.1063/1.4903765.
- [245] B. Jeziorski, R. Moszynski, K. Szalewicz, *Chem. Rev.* **1994**, *94*, 1887–1930, DOI: 10.1021/cr00031a008.

- [246] D. Cremer, *WIREs Comput. Mol. Sci.* **2011**, *1*, 509–530, DOI: 10.1002/wcms.58.
- [247] F. Jensen, *Introduction to Computational Chemistry*, Wiley-VCH, **2000**, 600 pp., ISBN: 978-0-470-01187-4.
- [248] S. Zhong, E. C. Barnes, G. A. Petersson, *J. Chem. Phys.* **2008**, *129*, 184116, DOI: 10.1063/1.3009651.
- [249] T. Helgaker, W. Klopper, H. Koch, J. Noga, *J. Chem. Phys.* **1997**, *106*, 9639–9646, DOI: 10.1063/1.473863.
- [250] D. Feller, *J. Chem. Phys.* **1992**, *96*, 6104–6114, DOI: 10.1063/1.462652.
- [251] D. Feller, *J. Chem. Phys.* **1993**, *98*, 7059–7071, DOI: 10.1063/1.464749.
- [252] A. Halkier, T. Helgaker, P. Jørgensen, W. Klopper, H. Koch, J. Olsen, A. K. Wilson, *Chem. Phys. Lett.* **1998**, *286*, 243–252, DOI: 10.1016/S0009-2614(98)00111-0.
- [253] A. Halkier, T. Helgaker, P. Jørgensen, W. Klopper, J. Olsen, *Chem. Phys. Lett.* **1999**, *302*, 437–446, DOI: 10.1016/S0009-2614(99)00179-7.
- [254] A. L. L. East, W. D. Allen, *J. Chem. Phys.* **1993**, *99*, 4638–4650, DOI: 10.1063/1.466062.
- [255] A. G. Császár, W. D. Allen, H. F. Schaefer, *J. Chem. Phys.* **1998**, *108*, 9751–9764, DOI: 10.1063/1.476449.
- [256] Reference data and DFT results for the RG18 benchmark set, <http://www.thch.uni-bonn.de/tc.old/downloads/GMTKN/GMTKN55/RG18.html> (visited on 10/12/2022).
- [257] Y.-Y. Chuang, S.-M. Chen, *J. Comput. Chem.* **2011**, *32*, 1671–1679, DOI: 10.1002/jcc.21745.
- [258] B. Chan, L. Radom, *Theor. Chem. Acc.* **2013**, *133*, 1426, DOI: 10.1007/s00214-013-1426-9.
- [259] P. Kraus, *J. Chem. Theory Comput.* **2020**, *16*, 5712–5722, DOI: 10.1021/acs.jctc.0c00684.
- [260] A. Tarnopolsky, A. Karton, R. Sertchook, D. Vuzman, J. M. L. Martin, *J. Phys. Chem. A* **2008**, *112*, 3–8, DOI: 10.1021/jp710179r.
- [261] J. Řezáč, P. Hobza, *J. Chem. Theory Comput.* **2013**, *9*, 2151–2155, DOI: 10.1021/ct400057w.
- [262] L. A. Burns, M. S. Marshall, C. D. Sherrill, *J. Chem. Theory Comput.* **2014**, *10*, 49–57, DOI: 10.1021/ct400149j.
- [263] J. Řezáč, M. Dubecký, P. Jurečka, P. Hobza, *Phys. Chem. Chem. Phys.* **2015**, *17*, 19268–19277, DOI: 10.1039/C5CP03151F.
- [264] D. A. Sirianni, L. A. Burns, C. D. Sherrill, *J. Chem. Theory Comput.* **2017**, *13*, 86–99, DOI: 10.1021/acs.jctc.6b00797.
- [265] D. G. Truhlar, *Chem. Phys. Lett.* **1998**, *294*, 45–48, DOI: 10.1016/S0009-2614(98)00866-5.

- [266] W. Klopper, W. Kutzelnigg, *J. Mol. Struct. THEOCHEM* **1986**, *135*, 339–356, DOI: 10.1016/0166-1280(86)80068-9.
- [267] W. Kutzelnigg, *Int. J. Quantum Chem.* **1994**, *51*, 447–463, DOI: 10.1002/qua.560510612.
- [268] A. Karton, J. M. L. Martin, *Theor. Chem. Acc.* **2006**, *115*, 330–333, DOI: 10.1007/s00214-005-0028-6.
- [269] M. S. Marshall, L. A. Burns, C. D. Sherrill, *J. Chem. Phys.* **2011**, *135*, 194102, DOI: 10.1063/1.3659142.
- [270] C. E. Warden, D. G. A. Smith, L. A. Burns, U. Bozkaya, C. D. Sherrill, *J. Chem. Phys.* **2020**, *152*, 124109, DOI: 10.1063/5.0004863.
- [271] Ł. M. Mentel, E. J. Baerends, *J. Chem. Theory Comput.* **2014**, *10*, 252–267, DOI: 10.1021/ct400990u.
- [272] E. Soydaş, U. Bozkaya, *J. Chem. Theory Comput.* **2013**, *9*, 4679–4683, DOI: 10.1021/ct4008124.
- [273] S. Boys, F. Bernardi, *Mol. Phys.* **1970**, *19*, 553–566, DOI: 10.1080/00268977000101561.
- [274] M. Gray, P. E. Bowling, J. M. Herbert, *J. Chem. Theory Comput.* **2022**, *18*, 6742–6756, DOI: 10.1021/acs.jctc.2c00883.
- [275] B. Brauer, M. K. Kesharwani, J. M. L. Martin, *J. Chem. Theory Comput.* **2014**, *10*, 3791–3799, DOI: 10.1021/ct500513b.
- [276] W. Klopper, *Mol. Phys.* **2001**, *99*, 481–507, DOI: 10.1080/00268970010017315.
- [277] P. Jurečka, J. Šponer, J. Černý, P. Hobza, *Phys. Chem. Chem. Phys.* **2006**, *8*, 1985–1993, DOI: 10.1039/B600027D.
- [278] T. Takatani, E. G. Hohenstein, M. Malagoli, M. S. Marshall, C. D. Sherrill, *J. Chem. Phys.* **2010**, *132*, 144104, DOI: 10.1063/1.3378024.
- [279] N. N. Dutta, K. Patkowski, *J. Chem. Theory Comput.* **2018**, *14*, 3053–3070, DOI: 10.1021/acs.jctc.8b00204.
- [280] A. Heßelmann, *J. Chem. Phys.* **2008**, *128*, 144112, DOI: 10.1063/1.2905808.
- [281] M. Pitoňák, A. Heßelmann, *J. Chem. Theory Comput.* **2010**, *6*, 168–178, DOI: 10.1021/ct9005882.
- [282] T. Takatani, E. G. Hohenstein, C. D. Sherrill, *J. Chem. Phys.* **2008**, *128*, 124111, DOI: 10.1063/1.2883974.
- [283] M. Pitoňák, J. Řezáč, P. Hobza, *Phys. Chem. Chem. Phys.* **2010**, *12*, 9611–9614, DOI: 10.1039/C0CP00158A.
- [284] DFT results for the S22 benchmark set, <http://www.thch.uni-bonn.de/tc.old/software/GMTKN/GMTKN55/S22.html> (visited on 11/02/2022).
- [285] J. Řezáč, Y. Huang, P. Hobza, G. J. O. Beran, *J. Chem. Theory Comput.* **2015**, *11*, 3065–3079, DOI: 10.1021/acs.jctc.5b00281.

- [286] W. Jankiewicz, R. Podeszwa, H. A. Witek, *J. Chem. Theory Comput.* **2018**, *14*, 5079–5089, DOI: 10.1021/acs.jctc.8b00167.
- [287] X. Xu, W. Zhang, M. Tang, D. G. Truhlar, *J. Chem. Theory Comput.* **2015**, *11*, 2036–2052, DOI: 10.1021/acs.jctc.5b00081.
- [288] L. Cheng, J. Gauss, B. Ruscic, P. B. Armentrout, J. F. Stanton, *J. Chem. Theory Comput.* **2017**, *13*, 1044–1056, DOI: 10.1021/acs.jctc.6b00970.
- [289] Z. Fang, M. Vasiliu, K. A. Peterson, D. A. Dixon, *J. Chem. Theory Comput.* **2017**, *13*, 1057–1066, DOI: 10.1021/acs.jctc.6b00971.
- [290] W. Jiang, M. L. Laury, M. Powell, A. K. Wilson, *J. Chem. Theory Comput.* **2012**, *8*, 4102–4111, DOI: 10.1021/ct300455e.
- [291] W. Jiang, N. J. DeYonker, J. J. Determan, A. K. Wilson, *J. Phys. Chem. A* **2012**, *116*, 870–885, DOI: 10.1021/jp205710e.
- [292] Y. A. Aoto, A. P. de Lima Batista, A. Köhn, A. G. S. de Oliveira-Filho, *J. Chem. Theory Comput.* **2017**, *13*, 5291–5316, DOI: 10.1021/acs.jctc.7b00688.
- [293] S. Dohm, A. Hansen, M. Steinmetz, S. Grimme, M. P. Checinski, *J. Chem. Theory Comput.* **2018**, *14*, 2596–2608, DOI: 10.1021/acs.jctc.7b01183.
- [294] R. Richter, Validating the predictional capacity of REMP and OO-REMP for bond lengths and bond angles, Internship report, Eberhard Karls Universität Tübingen, **2021**, 81 pp.
- [295] L. Völkl, BA thesis, Eberhard-Karls-Universität Tübingen, **2021**, 43 pp.
- [296] F. Pawłowski, P. Jørgensen, J. Olsen, F. Hegelund, T. Helgaker, J. Gauss, K. L. Bak, J. F. Stanton, *J. Chem. Phys.* **2002**, *116*, 6482–6496, DOI: 10.1063/1.1459782.
- [297] J. H. Baraban, P. B. Changala, J. F. Stanton, *J. Mol. Spectrosc.* **2018**, *343*, 92–95, DOI: 10.1016/j.jms.2017.09.014.
- [298] K. L. Bak, J. Gauss, P. Jørgensen, J. Olsen, T. Helgaker, J. F. Stanton, *J. Chem. Phys.* **2001**, *114*, 6548–6556, DOI: 10.1063/1.1357225.
- [299] S. Coriani, D. Marchesan, J. Gauss, C. Hättig, T. Helgaker, P. Jørgensen, *J. Chem. Phys.* **2005**, *123*, 184107, DOI: 10.1063/1.2104387.
- [300] P. R. Tentscher, J. S. Arey, *J. Chem. Theory Comput.* **2012**, *8*, 2165–2179, DOI: 10.1021/ct300194x.
- [301] A. Karton, J. M. L. Martin, *J. Chem. Phys.* **2010**, *133*, 144102, DOI: 10.1063/1.3489113.
- [302] B. Ruscic, *Int. J. Quantum Chem.* **2014**, *114*, 1097–1101, DOI: 10.1002/qua.24605.
- [303] A. Karton, *WIREs Comput. Mol. Sci.* **2016**, *6*, 292–310, DOI: 10.1002/wcms.1249.
- [304] F. Pawłowski, A. Halkier, P. Jørgensen, K. L. Bak, T. Helgaker, W. Klopper, *J. Chem. Phys.* **2003**, *118*, 2539–2549, DOI: 10.1063/1.1533032.

- [305] A. Karton, P. R. Taylor, J. M. L. Martin, *J. Chem. Phys.* **2007**, *127*, 064104, DOI: 10.1063/1.2755751.
- [306] P. Idzko, BA thesis, Eberhard-Karls-Universität Tübingen, **2021**, 33 pp.
- [307] N. Mina-Camilde, C. Manzanares I., J. F. Caballero, *J. Chem. Educ.* **1996**, *73*, 804, DOI: 10.1021/ed073p804.
- [308] K. K. Irikura, *J. Phys. Chem. Ref. Data* **2007**, *36*, 389–397, DOI: 10.1063/1.2436891.
- [309] M. K. Kesharwani, B. Brauer, J. M. L. Martin, *J. Phys. Chem. A* **2015**, *119*, 1701–1714, DOI: 10.1021/jp508422u.
- [310] D. P. Tew, W. Klopper, M. Heckert, J. Gauss, *J. Phys. Chem. A* **2007**, *111*, 11242–11248, DOI: 10.1021/jp070851u.
- [311] J. M. Martin, *Chem. Phys. Lett.* **1998**, *292*, 411–420, DOI: 10.1016/S0009-2614(98)00683-6.
- [312] A. Förstner, BA thesis, Eberhard-Karls-Universität Tübingen, **2021**, 31 pp.
- [313] A. D. Buckingham, *Q. Rev. Chem. Soc.* **1959**, *13*, 183–214, DOI: 10.1039/QR9591300183.
- [314] K. B. Laughlin, G. A. Blake, R. C. Cohen, D. C. Hovde, R. J. Saykally, H.-J. Foth, E. Hirota, T. Oka, *Philos. Trans. R. Soc. Lond. A* **1988**, *324*, 109–119.
- [315] B. J. Mount, M. Redshaw, E. G. Myers, *Phys. Rev. A* **2012**, *85*, 012519, DOI: 10.1103/PhysRevA.85.012519.
- [316] R. D. Nelson Jr., D. R. Lide Jr., A. A. Maryott, Selected Values of Electric Dipole Moments for Molecules in the Gas Phase, U.S. Department of Commerce, National Bureau of Standards, **1967**, <https://nvlpubs.nist.gov/nistpubs/Legacy/NSRDS/nbsnsrcs10.pdf> (visited on 12/07/2022).
- [317] E. W. Kaiser, *J. Chem. Phys.* **1970**, *53*, 1686–1703, DOI: 10.1063/1.1674245.
- [318] J. Raymonda, W. Klemperer, *J. Chem. Phys.* **1971**, *55*, 232–233, DOI: 10.1063/1.1675513.
- [319] J. S. Muenter, *J. Chem. Phys.* **1972**, *56*, 5409–5412, DOI: 10.1063/1.1677052.
- [320] R. L. DeLeon, J. S. Muenter, *J. Chem. Phys.* **1985**, *82*, 1702–1704, DOI: 10.1063/1.448402.
- [321] D. Hait, M. Head-Gordon, *J. Chem. Theory Comput.* **2018**, *14*, 1969–1981, DOI: 10.1021/acs.jctc.7b01252.
- [322] J. Hoelt, F. Lovas, E. Tiemann, T. Törring, *Z. Naturforsch. A* **1970**, *25*, 35–39, DOI: 10.1515/zna-1970-0106.
- [323] F. Wang, T. C. Steimle, *J. Chem. Phys.* **2010**, *132*, 054301, DOI: 10.1063/1.3292606.
- [324] C. Koukounas, A. Mavridis, *J. Phys. Chem. A* **2008**, *112*, 11235–11250, DOI: 10.1021/jp805034w.

- [325] E. Goll, H. Stoll, C. Thierfelder, P. Schwerdtfeger, *Phys. Rev. A* **2007**, *76*, 032507, DOI: 10.1103/PhysRevA.76.032507.
- [326] M. Douglas, N. M. Kroll, *Ann. Phys.* **1974**, *82*, 89–155, DOI: 10.1016/0003-4916(74)90333-9.
- [327] G. Jansen, B. A. Hess, *Phys. Rev. A* **1989**, *39*, 6016–6017, DOI: 10.1103/PhysRevA.39.6016.
- [328] M. Reiher, A. Wolf, *J. Chem. Phys.* **2004**, *121*, 2037–2047, DOI: 10.1063/1.1768160.
- [329] M. Reiher, A. Wolf, *J. Chem. Phys.* **2004**, *121*, 10945–10956, DOI: 10.1063/1.1818681.
- [330] K. G. Dyall, *J. Chem. Phys.* **2001**, *115*, 9136–9143, DOI: 10.1063/1.1413512.
- [331] A. Wolf, M. Reiher, B. A. Hess, *J. Chem. Phys.* **2002**, *117*, 9215–9226, DOI: 10.1063/1.1515314.
- [332] M. Barysz, A. J. Sadlej, *J. Mo. Struct. Theochem* **2001**, *573*, 181–200, DOI: 10.1016/S0166-1280(01)00542-5.
- [333] F. Neese, A. Wolf, T. Fleig, M. Reiher, B. A. Hess, *J. Chem. Phys.* **2005**, *122*, 204107, DOI: 10.1063/1.1904589.
- [334] B. Sandhoefer, S. Kossmann, F. Neese, *J. Chem. Phys.* **2013**, *138*, 104102, DOI: 10.1063/1.4792362.
- [335] B. Sandhoefer, F. Neese, *J. Chem. Phys.* **2012**, *137*, 094102, DOI: 10.1063/1.4747454.
- [336] T. Nakajima, K. Hirao, *Chem. Rev.* **2012**, *112*, 385–402, DOI: 10.1021/cr200040s.
- [337] D. Aravena, M. Atanasov, A. A. Auer, U. Becker, G. Bistoni, D. Bykov, V. G. Chilkuri, D. Datta, A. K. Dutta, S. Ehlert, D. Ganyushin, M. Garcia, Y. Guo, A. Hansen, B. Helmich-Paris, L. Huntington, R. Izsák, M. Kettner, C. Kollmar, S. Kossmann, M. Krupička, L. Lang, M. Lechner, D. Lenk, D. G. Liakos, D. Manganas, D. A. Pantazis, A. Papadopoulos, T. Petrenko, P. Pinski, P. Pracht, C. Reimann, M. Retegan, C. Riplinger, T. Risthaus, M. Roemelt, M. Saitow, B. Sandhöfer, I. Schapiro, A. Sen, K. Sivalingam, B. de Souza, G. Stoychev, W. V. den Heuvel, B. Wezislá, M. Kállay, S. Grimme, E. Valeev, G. Chan, J. Pittner, M. Brehm, L. Goerigk, V. Åsgeirsson, L. Ungur, W. Schneider, Manual for the Quantum Chemistry Program Package ORCA, Version 5.0.3, Max-Planck-Institut für Kohlenforschung, Mülheim a. d. Ruhr, **2022**, 1329 pp.
- [338] G. Santra, M. Cho, J. M. L. Martin, *J. Phys. Chem. A* **2021**, *125*, 4614–4627, DOI: 10.1021/acs.jpca.1c01294.
- [339] G. Santra, E. Semidalas, J. M. L. Martin, *J. Phys. Chem. A* **2021**, *125*, 4628–4638, DOI: 10.1021/acs.jpca.1c01295.



- [340] DFT data for BH76 from the GMTKN55 homepage, <http://www.thch.uni-bonn.de/tc.old/downloads/GMTKN/GMTKN55/BH76.html> (visited on 2020-01-09).
- [341] T. Helgaker, P. Jørgensen, N. C. Handy, *Theor. Chim. Acta* **1989**, *76*, 227–245, DOI: 10.1007/BF00532006.
- [342] P. R. Taylor, *J. Chem. Phys.* **1981**, *74*, 1256–1270, DOI: 10.1063/1.441186.
- [343] F. Neese, F. Wennmohs, A. Hansen, *J. Chem. Phys.* **2009**, *130*, 114108, DOI: 10.1063/1.3086717.
- [344] F. Neese, A. Hansen, D. G. Liakos, *J. Chem. Phys.* **2009**, *131*, 064103, DOI: 10.1063/1.3173827.
- [345] A. Hansen, D. G. Liakos, F. Neese, *J. Chem. Phys.* **2011**, *135*, 214102, DOI: 10.1063/1.3663855.
- [346] D. G. Liakos, A. Hansen, F. Neese, *J. Chem. Theory Comput.* **2011**, *7*, 76–87, DOI: 10.1021/ct100445s.
- [347] P. Pinski, C. Riplinger, E. F. Valeev, F. Neese, *J. Chem. Phys.* **2015**, *143*, 034108, DOI: 10.1063/1.4926879.
- [348] Y. Guo, K. Sivalingam, E. F. Valeev, F. Neese, *J. Chem. Phys.* **2016**, *144*, 094111, DOI: 10.1063/1.4942769.
- [349] F. Pavošević, P. Pinski, C. Riplinger, F. Neese, E. F. Valeev, *J. Chem. Phys.* **2016**, *144*, 144109, DOI: 10.1063/1.4945444.
- [350] C. Riplinger, P. Pinski, U. Becker, E. F. Valeev, F. Neese, *J. Chem. Phys.* **2016**, *144*, 024109, DOI: 10.1063/1.4939030.
- [351] F. Pavošević, C. Peng, P. Pinski, C. Riplinger, F. Neese, E. F. Valeev, *J. Chem. Phys.* **2017**, *146*, 174108, DOI: 10.1063/1.4979993.
- [352] M. Saitow, U. Becker, C. Riplinger, E. F. Valeev, F. Neese, *J. Chem. Phys.* **2017**, *146*, 164105, DOI: 10.1063/1.4981521.
- [353] Q. Ma, H.-J. Werner, *J. Chem. Theory Comput.* **2015**, *11*, 5291–5304, DOI: 10.1021/acs.jctc.5b00843.
- [354] H.-J. Werner, G. Knizia, C. Krause, M. Schwilk, M. Dornbach, *J. Chem. Theory Comput.* **2015**, *11*, 484–507, DOI: 10.1021/ct500725e.
- [355] M. Schwilk, Q. Ma, C. Köppl, H.-J. Werner, *J. Chem. Theory Comput.* **2017**, *13*, 3650–3675, DOI: 10.1021/acs.jctc.7b00554.
- [356] Q. Ma, M. Schwilk, C. Köppl, H.-J. Werner, *J. Chem. Theory Comput.* **2017**, *13*, 4871–4896, DOI: 10.1021/acs.jctc.7b00799.
- [357] Q. Ma, M. Schwilk, C. Köppl, H.-J. Werner, *J. Chem. Theory Comput.* **2018**, *14*, 6750–6750, DOI: 10.1021/acs.jctc.8b01099.
- [358] Q. Ma, H.-J. Werner, *J. Chem. Theory Comput.* **2018**, *14*, 198–215, DOI: 10.1021/acs.jctc.7b01141.

- [359] C. Krause, H.-J. Werner, *J. Chem. Theory Comput.* **2019**, *15*, 987–1005, DOI: 10.1021/acs.jctc.8b01012.
- [360] Q. Ma, H.-J. Werner, *J. Chem. Theory Comput.* **2020**, *16*, 3135–3151, DOI: 10.1021/acs.jctc.0c00192.
- [361] Q. Ma, H.-J. Werner, *J. Chem. Theory Comput.* **2021**, *17*, 902–926, DOI: 10.1021/acs.jctc.0c01129.
- [362] P. R. Nagy, G. Samu, M. Kállay, *J. Chem. Theory Comput.* **2018**, *14*, 4193–4215, DOI: 10.1021/acs.jctc.8b00442.
- [363] P. R. Nagy, M. Kállay, *J. Chem. Theory Comput.* **2019**, *15*, 5275–5298, DOI: 10.1021/acs.jctc.9b00511.
- [364] G. L. Stoychev, A. A. Auer, J. Gauss, F. Neese, *J. Chem. Phys.* **2021**, *154*, 164110, DOI: 10.1063/5.0047125.
- [365] D. G. Liakos, F. Neese, *J. Phys. Chem. A* **2012**, *116*, 4801–4816, DOI: 10.1021/jp302096v.
- [366] H. R. Larsson, H. Zhai, K. Gunst, G. K.-L. Chan, *J. Chem. Theory Comput.* **2022**, *18*, 749–762, DOI: 10.1021/acs.jctc.1c00957.
- [367] H. R. Larsson, H. Zhai, C. J. Umrigar, G. K.-L. Chan, *J. Am. Chem. Soc.* **2022**, *144*, 15932–15937, DOI: 10.1021/jacs.2c06357.
- [368] K. Hirao, *Chem. Phys. Lett.* **1992**, *190*, 374–380, DOI: 10.1016/0009-2614(92)85354-D.
- [369] K. Hirao, *Chem. Phys. Lett.* **1992**, *196*, 397–403, DOI: 10.1016/0009-2614(92)85710-R.
- [370] J. P. Finley, K. Hirao, *Chem. Phys. Lett.* **2000**, *328*, 60–66, DOI: 10.1016/S0009-2614(00)00920-9.
- [371] J.-P. Malrieu, J.-L. Heully, A. Zaitsevskii, *Theor. Chim. Acta* **1995**, *90*, 167–187, DOI: 10.1007/BF01113846.
- [372] M. Saitow, T. Yanai, *J. Chem. Phys.* **2020**, *152*, 114111, DOI: 10.1063/1.5142622.
- [373] H. Sekino, Y. Maeda, M. Kamiya, K. Hirao, *J. Chem. Phys.* **2007**, *126*, 014107, DOI: 10.1063/1.2428291.
- [374] L. Xu, A. Kumar, B. M. Wong, *J. Comput. Chem.* **2018**, *39*, 2350–2359, DOI: 10.1002/jcc.25519.
- [375] C. Holzer, Y. J. Franzke, M. Kehry, *J. Chem. Theory Comput.* **2021**, *17*, 2928–2947, DOI: 10.1021/acs.jctc.1c00203.
- [376] T. Helgaker, S. Coriani, P. Jørgensen, K. Kristensen, J. Olsen, K. Ruud, *Chem. Rev.* **2012**, *112*, 543–631, DOI: 10.1021/cr2002239.
- [377] C. Hättig in *Computational Nanoscience: Do It Yourself!*, Publication Series of the John von Neumann Institute for Computing (NIC), Forschungszentrum Jülich, Jülich, **2006**, pp. 245–278, ISBN: 3-00-017350-1.

- [378] H. Pathak, T. Sato, K. L. Ishikawa, *J. Chem. Phys.* **2020**, *153*, 034110, DOI: 10.1063/5.0008789.
- [379] H. E. Kristiansen, B. S. Ofstad, E. Hauge, E. Aurbakken, Ø. S. Schøyen, S. Kvaal, T. B. Pedersen, *J. Chem. Theory Comput.* **2022**, *18*, 3687–3702, DOI: 10.1021/acs.jctc.1c01309.
- [380] H. E. Kristiansen, B. S. Ofstad, E. Hauge, E. Aurbakken, Ø. S. Schøyen, S. Kvaal, T. B. Pedersen, *J. Chem. Theory Comput.* **2022**, *18*, 5755–5757, DOI: 10.1021/acs.jctc.2c00830.
- [381] H. Pathak, T. Sato, K. L. Ishikawa, *J. Chem. Phys.* **2020**, *152*, 124115, DOI: 10.1063/1.5143747.
- [382] P. A. Franken, A. E. Hill, C. W. Peters, G. Weinreich, *Phys. Rev. Lett.* **1961**, *7*, 118–119, DOI: 10.1103/PhysRevLett.7.118.
- [383] M. W. Walser, C. H. Keitel, A. Scrinzi, T. Brabec, *Phys. Rev. Lett.* **2000**, *85*, 5082–5085, DOI: 10.1103/PhysRevLett.85.5082.
- [384] X. Li, N. Govind, C. Isborn, A. E. I. I. DePrince, K. Lopata, *Chem. Rev.* **2020**, *120*, 9951–9993, ISSN: 0009-2665, DOI: 10.1021/acs.chemrev.0c00223.
- [385] SymPy secondquant: Second quantization operators and states for bosons, <https://github.com/sympy/sympy/blob/master/sympy/physics/secondquant.py> (visited on 10/14/2022).
- [386] Second Quantization, <https://docs.sympy.org/latest/modules/physics/secondquant.html> (visited on 10/14/2022).
- [387] M. Hjorth-Jensen, Many-body Hamiltonians, basic linear algebra and Second Quantization, <https://nucleartalent.github.io/ManyBody2018/doc/pub/secondquant/html/secondquant-bs.html> (visited on 10/14/2022).

## 6 Appendix

### 6.1 Derivation of the OO-REMP working equations

The starting point for the derivation is the REMF energy functional Eq. (2.85):

$$\tilde{E}_{\text{REMP}}^{(2)}(\kappa) = \langle 0 | \hat{H}^\kappa | 0 \rangle + \langle 0 | (\widehat{W}_N^\kappa \hat{T}_2)_c | 0 \rangle + \langle 0 | (\hat{\Lambda}_2 (\widehat{W}_N^\kappa + (\hat{f}_N^\kappa + (1 - A) \widehat{W}_N^\kappa) \hat{T}_2)_c) | 0 \rangle \quad (6.1)$$

Derivation of Eq. (6.1) for  $t_{ab}^{ij}$  yields

$$\frac{\partial \tilde{E}_{\text{REMP}}^{(2)}(\kappa)}{\partial t_{ab}^{ij}} = \langle 0 | (\widehat{W}_N^\kappa \hat{a}^\dagger \hat{b}^\dagger \hat{j} \hat{i})_c | 0 \rangle + \langle 0 | (\hat{\Lambda}_2 \hat{f}_N^\kappa \hat{a}^\dagger \hat{b}^\dagger \hat{j} \hat{i})_c | 0 \rangle + (1 - A) \langle 0 | (\hat{\Lambda}_2 (\widehat{W}_N^\kappa \hat{a}^\dagger \hat{b}^\dagger \hat{j} \hat{i})_c) | 0 \rangle, \quad (6.2)$$

derivation for  $\lambda_{ij}^{ab}$  yields

$$\frac{\partial \tilde{E}_{\text{REMP}}^{(2)}(\kappa)}{\partial \lambda_{ij}^{ab}} = \langle 0 | (\hat{i}^\dagger \hat{j}^\dagger \hat{b} \hat{a} \widehat{W}_N^\kappa)_c | 0 \rangle + \langle 0 | (\hat{i}^\dagger \hat{j}^\dagger \hat{b} \hat{a} \hat{f}_N^\kappa \hat{T}_2)_c | 0 \rangle + (1 - A) \langle 0 | (\hat{i}^\dagger \hat{j}^\dagger \hat{b} \hat{a} (\widehat{W}_N^\kappa \hat{T}_2)_c) | 0 \rangle. \quad (6.3)$$

Eq. (6.2) and (6.3) are just the Hermitian conjugate of each other, it is immediately clear that – in contrast to coupled cluster theory – the solutions of the regular amplitude equations also solve the  $\lambda$  equations via

$$\lambda_{ij}^{ab} = t_{ab}^{ij*}. \quad (6.4)$$

In case of real orbitals, this is furthermore simplified to  $\lambda_{ij}^{ab} = t_{ab}^{ij}$ .

Derivation of Eq. (6.1) for  $\kappa_{pq}$  around  $\kappa_{pq} = 0$  yields the orbital gradient:

$$\left. \frac{\partial \tilde{E}_{\text{REMP}}^{(2)}(\kappa)}{\partial \kappa_{pq}} \right|_{\kappa_{pq}=0} = w_{pq} \stackrel{!}{=} 0. \quad (6.5)$$

Deriving in the vicinity of  $\kappa_{pq} = 0$  is not strictly necessary but it keeps the resulting expressions somewhat manageable. The assumption that the orbital gradient and thus the orbital rotation parameters are small is valid in many cases and this approximation will become even better when convergence is approached. On the other hand, it will

probably be invalid if the orbital gradient is very large. This might actually be one of the reasons for failing orbital convergence in nasty cases.

For performing the derivative, the definitions of the rotated operators (Eqs. (2.90), (2.92), (2.93)) are inserted in Eq. (6.1). Subsequently, the exponentials are expanded in the Taylor series (Maclaurin series to be precise) of the exponential function. The approximation of a vanishing orbital rotation is the used to eliminate the exponential functions from the expressions

$$\begin{aligned}
\tilde{E}_{\text{REMP}}^{(2)}(\kappa) &= \langle 0 | e^{-\hat{K}} \hat{H} e^{\hat{K}} | 0 \rangle \\
&+ \langle 0 | (e^{-\hat{K}} \widehat{W}_N e^{\hat{K}} \widehat{T}_2)_c | 0 \rangle \\
&+ \langle 0 | (\widehat{\Lambda}_2 e^{-\hat{K}} \widehat{W}_N e^{\hat{K}})_c | 0 \rangle \\
&+ \langle 0 | (\widehat{\Lambda}_2 (e^{-\hat{K}} \hat{f}_N e^{\hat{K}} \widehat{T}_2)_c) | 0 \rangle \\
&+ (1 - A) \langle 0 | (\widehat{\Lambda}_2 (e^{-\hat{K}} \widehat{W}_N e^{\hat{K}} \widehat{T}_2)_c) | 0 \rangle
\end{aligned} \tag{6.6}$$

where

$$\hat{K} = \sum_{pq} K_{pq} \hat{p}^\dagger \hat{q} = \sum_{p>q} \kappa_{pq} (\hat{p}^\dagger \hat{q} - \hat{q}^\dagger \hat{p}) \tag{6.7}$$

and

$$e^{\hat{K}} = e^{\sum_{p>q} \kappa_{pq} (\hat{p}^\dagger \hat{q} - \hat{q}^\dagger \hat{p})} = 1 + \sum_{p>q} \kappa_{pq} (\hat{p}^\dagger \hat{q} - \hat{q}^\dagger \hat{p}) + \frac{1}{2} (\sum_{p>q} \kappa_{pq} (\hat{p}^\dagger \hat{q} - \hat{q}^\dagger \hat{p}))^2 + \dots \tag{6.8}$$

$$e^{-\hat{K}} = e^{-\sum_{p>q} \kappa_{pq} (\hat{p}^\dagger \hat{q} - \hat{q}^\dagger \hat{p})} = 1 - \sum_{p>q} \kappa_{pq} (\hat{p}^\dagger \hat{q} - \hat{q}^\dagger \hat{p}) + \frac{1}{2} (\sum_{p>q} \kappa_{pq} (\hat{p}^\dagger \hat{q} - \hat{q}^\dagger \hat{p}))^2 - \dots \tag{6.9}$$

Deriving Eq. (6.6) for the orbital rotation parameters  $\kappa_{pq}$  and subsequently setting the remaining  $\kappa_{pq}$  to zero yields

$$\begin{aligned}
\left. \frac{\partial \tilde{E}_{\text{REMP}}^{(2)}(\kappa)}{\partial \kappa_{pq}} \right|_{\kappa_{pq}} &= - \langle 0 | (\hat{p}^\dagger \hat{q} - \hat{q}^\dagger \hat{p}) \hat{H} | 0 \rangle + \langle 0 | \hat{H} (\hat{p}^\dagger \hat{q} - \hat{q}^\dagger \hat{p}) | 0 \rangle \\
&\quad - \langle 0 | ((\hat{p}^\dagger \hat{q} - \hat{q}^\dagger \hat{p}) \widehat{W}_N \widehat{T}_2)_c | 0 \rangle + \langle 0 | (\widehat{W}_N (\hat{p}^\dagger \hat{q} - \hat{q}^\dagger \hat{p}) \widehat{T}_2)_c | 0 \rangle \\
&\quad - \langle 0 | (\widehat{\Lambda}_2 (\hat{p}^\dagger \hat{q} - \hat{q}^\dagger \hat{p}) \widehat{W}_N)_c | 0 \rangle + \langle 0 | (\widehat{\Lambda}_2 \widehat{W}_N (\hat{p}^\dagger \hat{q} - \hat{q}^\dagger \hat{p}))_c | 0 \rangle \\
&\quad - \langle 0 | (\widehat{\Lambda}_2 ((\hat{p}^\dagger \hat{q} - \hat{q}^\dagger \hat{p}) \hat{f}_N \widehat{T}_2)_c)_c | 0 \rangle + \langle 0 | (\widehat{\Lambda}_2 (\hat{f}_N (\hat{p}^\dagger \hat{q} - \hat{q}^\dagger \hat{p}) \widehat{T}_2)_c)_c | 0 \rangle \\
&\quad - (1 - A) \langle 0 | (\widehat{\Lambda}_2 ((\hat{p}^\dagger \hat{q} - \hat{q}^\dagger \hat{p}) \widehat{W}_N \widehat{T}_2)_c)_c | 0 \rangle + (1 - A) \langle 0 | (\widehat{\Lambda}_2 (\widehat{W}_N (\hat{p}^\dagger \hat{q} - \hat{q}^\dagger \hat{p}) \widehat{T}_2)_c)_c | 0 \rangle \\
&\hspace{15em} (6.10) \\
&= \underbrace{\langle 0 | [\widehat{H}, (\hat{p}^\dagger \hat{q} - \hat{q}^\dagger \hat{p})] | 0 \rangle}_{\textcircled{1}} \\
&\quad + \underbrace{\langle 0 | ([\widehat{W}_N, (\hat{p}^\dagger \hat{q} - \hat{q}^\dagger \hat{p})] \widehat{T}_2)_c | 0 \rangle}_{\textcircled{2}} \\
&\quad + \underbrace{\langle 0 | (\widehat{\Lambda}_2 [\widehat{W}_N, (\hat{p}^\dagger \hat{q} - \hat{q}^\dagger \hat{p})])_c | 0 \rangle}_{\textcircled{3}} \\
&\quad + \underbrace{\langle 0 | (\widehat{\Lambda}_2 ([\hat{f}_N, (\hat{p}^\dagger \hat{q} - \hat{q}^\dagger \hat{p})] \widehat{T}_2)_c)_c | 0 \rangle}_{\textcircled{4}} \\
&\quad + (1 - A) \underbrace{\langle 0 | (\widehat{\Lambda}_2 ([\widehat{W}_N, (\hat{p}^\dagger \hat{q} - \hat{q}^\dagger \hat{p})] \widehat{T}_2)_c)_c | 0 \rangle}_{\textcircled{5}} \\
&\hspace{15em} (6.11)
\end{aligned}$$

i.e. from the exponentials only the leading term ( $e^0 = 1$ ) survives. The first term is also well known as orbital gradient or variational condition from Hartree-Fock theory.<sup>[17]</sup> The resulting matrix element will therefore be no surprise.

Eq. (6.11) is now suitable for being evaluated with second quantization programs.

In this work, the python package `secondquant` from the sympy collection (`sympy.physics.secondquant`) was used.<sup>[385,386]</sup> The scripts used here were inspired by the second quantization tutorial by Morten Hjorth-Jensen.<sup>[387]</sup>

The involved operators are defined as follows:

$$\widehat{W} = \frac{1}{4} v_{tu}^{rs} \hat{r}^\dagger \hat{s}^\dagger \hat{u} \hat{t} \quad (6.12)$$

$$\widehat{W}_N = \frac{1}{4} v_{tu}^{rs} \{ \hat{r}^\dagger \hat{s}^\dagger \hat{u} \hat{t} \} \quad (6.13)$$

where  $v_{tu}^{rs}$  is the antisymmetrized two-electron integral defined as

$$v_{tu}^{rs} = \langle rs||tu \rangle = \langle rs|tu \rangle - \langle rs|ut \rangle = -v_{tu}^{sr} = -v_{ut}^{rs} = v_{ut}^{sr} \quad (6.14)$$

$$\hat{f} = f_s^r \hat{r}^\dagger \hat{s} \quad (6.15)$$

$$\hat{h} = h_s^r \hat{r}^\dagger \hat{s} \quad (6.16)$$

$$\hat{f}_N = f_s^r \{\hat{r}^\dagger \hat{s}\} \quad (6.17)$$

$$\hat{H} = h_s^r \hat{r}^\dagger \hat{s} + \frac{1}{4} v_{tu}^{rs} \hat{r}^\dagger \hat{s}^\dagger \hat{u} \hat{t} \quad (6.18)$$

$$\hat{H}_N = h_s^r \{\hat{r}^\dagger \hat{s}\} + \frac{1}{4} v_{tu}^{rs} \{\hat{r}^\dagger \hat{s}^\dagger \hat{u} \hat{t}\} \quad (6.19)$$

$$\hat{T}_2 = \frac{1}{4} t_{ab}^{ij} \hat{a}^\dagger \hat{b}^\dagger \hat{j} \hat{i} \quad (6.20)$$

$$\hat{\Lambda}_2 = \frac{1}{4} \lambda_{kl}^{cd} \hat{k}^\dagger \hat{l}^\dagger \hat{d} \hat{c} \quad (6.21)$$

where  $\{\}$  indicates the normal-ordered product, i.e. that the operators are to be brought to normal order but that no contractions inside are made. Furthermore, when contractions with other operators are formed, no contractions inside the normal-ordered operators are made.  $i, j, k, l, a, b, c, d, r, s, t, u$  are dummy indices that can be summed over and replaced while the target indices  $p$  and  $q$  of the orbital gradient are no dummies and must not be replaced. The symbols  $a, b, c, d$  are restricted to refer to orbitals above the Fermi level while  $i, j, k, l$  are restricted to be below the Fermi level.  $p, q, r, s, t, u$  are not restricted a priori, but restrictions will occur naturally from contractions. All indices in the following refer to spin orbitals.

Part ① is just the orbital gradient of the reference determinant, which is simply the Fockian. For the first commutator, one obtains the following nonzero contractions:

$$\begin{aligned} & \langle 0 | [\hat{H}, (\hat{p}^\dagger \hat{q} - \hat{q}^\dagger \hat{p})] | 0 \rangle \\ &= -\delta_{as} \delta_{ir} \delta_{rp} \delta_{sq} h_r^s + \delta_{as} \delta_{ir} \delta_{rq} \delta_{sp} h_r^s \\ & \quad + \delta_{at} \delta_{ir} \delta_{js} \delta_{ru} \delta_{sp} \delta_{tq} v_{rs}^{tu} - \delta_{at} \delta_{ir} \delta_{js} \delta_{ru} \delta_{sq} \delta_{tp} v_{rs}^{tu} \\ & \quad + \delta_{ap} \delta_{ir} \delta_{jq} \delta_{rs} \delta_{tp} \delta_{uq} v_{rt}^{su} + \delta_{ap} \delta_{iq} \delta_{rp} \delta_{sq} h_r^s \\ & \quad - \delta_{aq} \delta_{ir} \delta_{jp} \delta_{rs} \delta_{tp} \delta_{uq} v_{ru}^{st} - \delta_{aq} \delta_{ip} \delta_{rp} \delta_{sq} h_s^r \end{aligned} \quad (6.22)$$

by resolving  $\delta$ 's over repeated indices and unifying dummy indices, one obtains

$$\begin{aligned} &= +\delta_{ap} \delta_{iq} h_q^p - \delta_{ip} \delta_{aq} h_p^q + \delta_{ap} \delta_{iq} h_p^q - \delta_{ip} \delta_{aq} h_q^p \\ & \quad + \delta_{aq} \delta_{ir} \delta_{jp} \delta_{ru} v_{rp}^{qu} - \delta_{ap} \delta_{ir} \delta_{jq} \delta_{ru} v_{rq}^{pu} \\ & \quad + \delta_{ap} \delta_{ir} \delta_{jq} \delta_{rs} v_{rp}^{sq} - \delta_{aq} \delta_{ir} \delta_{jp} \delta_{rs} v_{rq}^{sp} \end{aligned} \quad (6.23)$$

by resolving  $\delta_{jr}$  and  $\delta_{rs}$ , and applying a more conventional notation, one obtains

$$\begin{aligned}
&= + \delta_{ap}\delta_{iq}h_{pq} - \delta_{ip}\delta_{aq}h_{pq} + \delta_{ap}\delta_{iq}h_{pq} - \delta_{ip}\delta_{aq}h_{pq} \\
&\quad - \delta_{aq}\delta_{ip} \sum_j^{\text{occ}} \langle qj||pj \rangle + \delta_{ap}\delta_{iq} \sum_j^{\text{occ}} \langle pj||qj \rangle \\
&\quad + \delta_{ap}\delta_{iq} \sum_j^{\text{occ}} \langle qj||pj \rangle - \delta_{aq}\delta_{ip} \sum_j^{\text{occ}} \langle pj||qj \rangle
\end{aligned} \tag{6.24}$$

$$= 2(\widehat{P}_-(p, q)(\delta_{ap}\delta_{iq}h_{pq} + \delta_{ap}\delta_{iq}\langle pj||qj \rangle)) \tag{6.25}$$

$$= 2(\delta_{ap}\delta_{iq}f_{pq} - \delta_{aq}\delta_{ip}f_{qp}) \tag{6.26}$$

stating that

- the contribution of the reference to the orbital gradient is given by the asymmetry of the MO basis Fock matrix and that
- there are only contributions from the occupied-virtual and virtual-occupied block, as expected.

For further use, this result can be expressed in terms of the reference contribution of the one- and two-particle density matrices  $\gamma_{pq}^{\text{ref}}$  and  $\Gamma_{pqrs}^{\text{ref}}$ :

$$\gamma_{pq}^{\text{ref}} = \delta_{pq}^{\text{occ}} \tag{6.27}$$

$$\Gamma_{pqrs}^{\text{ref}} = \frac{1}{4}(\delta_{pr}^{\text{occ}}\delta_{qs}^{\text{occ}} - \delta_{ps}^{\text{occ}}\delta_{qr}^{\text{occ}}) \tag{6.28}$$

so that the reference orbital gradient can be expressed as part of a generalized Fock matrix  $F_{pq}$ :

$$w_{pq}^{\text{ref}} = 2(F_{pq}^{\text{ref}} - F_{qp}^{\text{ref}}) = 2\widehat{P}_-(p, q)F_{pq} \tag{6.29}$$

$$= 2\left(\sum_r h_{pr}\gamma_{rq}^{\text{ref}} + 2\sum_{rst} \langle rs||tp \rangle \Gamma_{rstq}^{\text{ref}} - \sum_r h_{qr}\gamma_{rp}^{\text{ref}} - 2\sum_{rst} \langle rs||tq \rangle \Gamma_{rstp}^{\text{ref}}\right) \tag{6.30}$$

$$= 2\widehat{P}_-(p, q) \left( \sum_r h_{pr}\gamma_{rq}^{\text{ref}} + 2\sum_{rst} \langle rs||tp \rangle \Gamma_{rstq}^{\text{ref}} \right) \tag{6.31}$$



By inserting Eqs. (6.27) and (6.28) in Eq. (6.30), it can be shown that this definition indeed recovers the Fockian formed from the reference determinant:

$$F_{pq}^{\text{ref}} = \sum_r h_{pr} \delta_{rq}^{\text{occ}} + 2 \sum_{rst} \langle rs || tp \rangle \frac{1}{4} (\delta_{rt}^{\text{occ}} \delta_{sq}^{\text{occ}} - \delta_{rq}^{\text{occ}} \delta_{st}^{\text{occ}}) \quad (6.32)$$

$$= \sum_r h_{pr} \delta_{rq}^{\text{occ}} + 2 \left( \frac{1}{4} \sum_s \sum_j \langle js || jp \rangle \delta_{sq}^{\text{occ}} - \frac{1}{4} \sum_r \sum_j \langle rj || jp \rangle \delta_{rq}^{\text{occ}} \right) \quad (6.33)$$

$$= \sum_r h_{pr} \delta_{rq}^{\text{occ}} + 2 \left( \frac{1}{4} \sum_s \sum_j \langle js || jp \rangle \delta_{sq}^{\text{occ}} + \frac{1}{4} \sum_s \sum_j \langle sj || pj \rangle \delta_{sq}^{\text{occ}} \right) \quad (6.34)$$

$$= \sum_r h_{pr} \delta_{rq}^{\text{occ}} + \sum_s \sum_j \langle js || jp \rangle \delta_{sq}^{\text{occ}} \quad (6.35)$$

$$= \begin{cases} p \in \{\text{occ}\}, q \in \{\text{occ}\} & f_{ij} \\ p \in \{\text{virt}\}, q \in \{\text{occ}\} & f_{ai} \\ p \in \{\text{occ}\}, q \in \{\text{virt}\} & 0 \\ p \in \{\text{virt}\}, q \in \{\text{virt}\} & 0 \end{cases} \quad (6.36)$$

If  $p$  and  $q$  both belong to the set of occupied orbitals, their contributions to the orbital gradient cancel exactly and  $w_{pq}$  is zero as expected. The orbital gradient furthermore vanishes if  $p$  and  $q$  both are virtual orbitals. If either  $p$  or  $q$  is a virtual index, Eq. (6.26) is recovered and  $w_{qp} = -w_{pq}$  is fulfilled. The definition Eq. (6.28) ensures that the TPDM has the correct exchange symmetry.

For part ②, one obtains

$$\begin{aligned} & \langle 0 | ([\widehat{W}_N, (\hat{p}^\dagger \hat{q} - \hat{q}^\dagger \hat{p})] \widehat{T}_2)_c | 0 \rangle \\ &= \frac{1}{2} (-\delta_{bp} \delta_{cq} v_{ac}^{ij} - \delta_{bp} \delta_{kq} v_{ak}^{ij} + \delta_{bp} \delta_{cp} v_{ac}^{ij} + \delta_{bq} \delta_{kp} v_{ak}^{ij} \\ & \quad - \delta_{cp} \delta_{jq} v_{ab}^{ci} + \delta_{cq} \delta_{jp} v_{ab}^{ci} - \delta_{jp} \delta_{kq} v_{ab}^{ik} + \delta_{jq} \delta_{kp} v_{ab}^{ik}) t_{ab}^{ij} \end{aligned} \quad (6.37)$$

and after expansion, one obtains

$$\begin{aligned} &= \frac{1}{2} (\delta_{cp} \delta_{bq} v_{ac}^{ij} t_{ab}^{ij} - \delta_{cq} \delta_{bp} v_{ac}^{ij} t_{ab}^{ij} + \delta_{kp} \delta_{bq} v_{ak}^{ij} t_{ab}^{ij} - \delta_{kq} \delta_{bp} v_{ak}^{ij} t_{ab}^{ij} \\ & \quad + \delta_{cp} \delta_{jq} v_{ab}^{ic} t_{ab}^{ij} - \delta_{cq} \delta_{jp} v_{ab}^{ic} t_{ab}^{ij} + \delta_{kp} \delta_{jq} v_{ab}^{ik} t_{ab}^{ij} - \delta_{kq} \delta_{jp} v_{ab}^{ik} t_{ab}^{ij}) \end{aligned} \quad (6.38)$$

Part ③ yields

$$\begin{aligned} & \langle 0 | (\widehat{\Lambda}_2 [\widehat{W}_N, (\hat{p}^\dagger \hat{q} - \hat{q}^\dagger \hat{p})])_c | 0 \rangle \\ &= \frac{1}{2} (-\delta_{bp} \delta_{cq} v_{ij}^{ac} - \delta_{bp} \delta_{kq} v_{ij}^{ak} + \delta_{bp} \delta_{cp} v_{ij}^{ac} + \delta_{bq} \delta_{kp} v_{ij}^{ak} \\ & \quad - \delta_{cp} \delta_{jq} v_{ci}^{ab} + \delta_{cq} \delta_{jp} v_{ci}^{ab} - \delta_{jp} \delta_{kq} v_{ik}^{ab} + \delta_{jq} \delta_{kp} v_{ik}^{ab}) \lambda_{ij}^{ab} \\ &= \frac{1}{2} (\delta_{cp} \delta_{bq} v_{ij}^{ac} \lambda_{ij}^{ab} - \delta_{cq} \delta_{bp} v_{ij}^{ac} \lambda_{ij}^{ab} + \delta_{kp} \delta_{bq} v_{ij}^{ak} \lambda_{ij}^{ab} - \delta_{kq} \delta_{bp} v_{ij}^{ak} \lambda_{ij}^{ab} \\ & \quad + \delta_{cp} \delta_{jq} v_{ic}^{ab} \lambda_{ij}^{ab} - \delta_{cq} \delta_{jp} v_{ic}^{ab} \lambda_{ij}^{ab} + \delta_{kp} \delta_{jq} v_{ik}^{ab} \lambda_{ij}^{ab} - \delta_{kq} \delta_{jp} v_{ik}^{ab} \lambda_{ij}^{ab}) \end{aligned} \quad (6.39)$$

Again, the Einstein summation convention is applied, i.e.  $i, j, a$  are indices that are summed over. By recalling that  $t_{ab}^{ij} = \lambda_{ij}^{ab}$ , Eqs. (6.38) and (6.39) can be merged into a single contribution to the orbital gradient by defining the two-particle density matrix  $\Gamma_{ijab}$  as

$$\Gamma_{ijab} = \frac{1}{4}t_{ab}^{ij} = \frac{1}{4}\lambda_{ab}^{ij} = \Gamma_{abij}. \quad (6.40)$$

The orbital gradient resulting from Eqs. (6.38) and (6.39) can then just be expressed as equivalent to Eq. (6.30). Summing Eqs. (6.38) and (6.39) yields

$$\begin{aligned} & \langle 0 | ([\widehat{W}_N, (\hat{p}^\dagger \hat{q} - \hat{q}^\dagger \hat{p})] \widehat{T}_2)_c | 0 \rangle + \langle 0 | (\widehat{\Lambda}_2 [\widehat{W}_N, (\hat{p}^\dagger \hat{q} - \hat{q}^\dagger \hat{p})])_c | 0 \rangle \\ &= \frac{1}{2} (\delta_{cp} \delta_{bq} v_{ac}^{ij} t_{ab}^{ij} - \delta_{cq} \delta_{bp} v_{ac}^{ij} t_{ab}^{ij} + \delta_{kp} \delta_{bq} v_{ak}^{ij} t_{ab}^{ij} - \delta_{kq} \delta_{bp} v_{ak}^{ij} t_{ab}^{ij} \\ & \quad + \delta_{cp} \delta_{jq} v_{ab}^{ic} t_{ab}^{ij} - \delta_{cq} \delta_{jp} v_{ab}^{ic} t_{ab}^{ij} + \delta_{kp} \delta_{jq} v_{ab}^{ik} t_{ab}^{ij} - \delta_{kq} \delta_{jp} v_{ab}^{ik} t_{ab}^{ij} \\ & \quad + \delta_{cp} \delta_{bq} v_{ij}^{ac} \lambda_{ij}^{ab} - \delta_{cq} \delta_{bp} v_{ij}^{ac} \lambda_{ij}^{ab} + \delta_{kp} \delta_{bq} v_{ij}^{ak} \lambda_{ij}^{ab} - \delta_{kq} \delta_{bp} v_{ij}^{ak} \lambda_{ij}^{ab} \\ & \quad + \delta_{cp} \delta_{jq} v_{ic}^{ab} \lambda_{ij}^{ab} - \delta_{cq} \delta_{jp} v_{ic}^{ab} \lambda_{ij}^{ab} + \delta_{kp} \delta_{jq} v_{ik}^{ab} \lambda_{ij}^{ab} - \delta_{kq} \delta_{jp} v_{ik}^{ab} \lambda_{ij}^{ab}) \end{aligned} \quad (6.41)$$

$$\stackrel{(6.40)}{=} 4 (\delta_{cp} \delta_{bq} v_{ac}^{ij} \Gamma_{ijab} - \delta_{cq} \delta_{bp} v_{ac}^{ij} \Gamma_{ijab} + \delta_{kp} \delta_{bq} v_{ak}^{ij} \Gamma_{ijab} - \delta_{kq} \delta_{bp} v_{ak}^{ij} \Gamma_{ijab} \\ + \delta_{cp} \delta_{jq} v_{ab}^{ic} \Gamma_{ijab} - \delta_{cq} \delta_{jp} v_{ab}^{ic} \Gamma_{ijab} + \delta_{kp} \delta_{jq} v_{ab}^{ik} \Gamma_{ijab} - \delta_{kq} \delta_{jp} v_{ab}^{ik} \Gamma_{ijab}) \quad (6.42)$$

$$= 4 \widehat{P}_-(p, q) \left( \delta_{kp} \delta_{jq} v_{ik}^{ab} \Gamma_{abij} + \delta_{kp} \delta_{bq} v_{ak}^{ij} \Gamma_{ijab} + \delta_{cp} \delta_{jq} v_{ic}^{ab} \Gamma_{abij} + \delta_{cp} \delta_{bq} v_{ac}^{ij} \Gamma_{ijab} \right) \quad (6.43)$$

$$= 2 \widehat{P}_-(p, q) \left( \sum_{rst} 2 \langle rs || tp \rangle \Gamma_{rstq} \right) \quad (6.44)$$

$$= 2 (F_{pq}^{2\text{el}} - F_{qp}^{2\text{el}}) \quad (6.45)$$

where

$$F_{pq}^{\text{el}} = \sum_{rst} 2 \langle rs || tp \rangle \Gamma_{rstq} \quad (6.46)$$

which can be generalized to coincide with the second part of Eq. (6.31).

Part ④ provides the following lengthy contribution to the orbital gradient (again, the Einstein convention is applied):

$$\begin{aligned}
& \langle 0 | (\widehat{\Lambda}_2([\widehat{f}_N, \widehat{p}^\dagger \widehat{q}]\widehat{T}_2)_c) | 0 \rangle \\
&= \frac{\delta_{ap} \delta_{iq} f_i^a \lambda_{jk}^{bc} t_{bc}^{jk}}{4} + \frac{\delta_{ap} \delta_{iq} f_a^i \lambda_{jk}^{bc} t_{bc}^{jk}}{4} \\
&+ \frac{\delta_{ap} \delta_{kq} f_i^a \lambda_{ij}^{bc} t_{bc}^{jk}}{2} + \frac{\delta_{ap} \delta_{kq} f_a^i \lambda_{jk}^{bc} t_{bc}^{ij}}{2} \\
&- \frac{\delta_{aq} \delta_{ip} f_i^a \lambda_{jk}^{bc} t_{bc}^{jk}}{4} - \frac{\delta_{aq} \delta_{ip} f_a^i \lambda_{jk}^{bc} t_{bc}^{jk}}{4} \\
&- \frac{\delta_{aq} \delta_{kp} f_i^a \lambda_{ij}^{bc} t_{bc}^{jk}}{2} - \frac{\delta_{aq} \delta_{kp} f_a^i \lambda_{jk}^{bc} t_{bc}^{ij}}{2} \\
&- \frac{\delta_{bp} \delta_{dq} f_b^a \lambda_{ij}^{ac} t_{cd}^{ij}}{2} - \frac{\delta_{bp} \delta_{dq} f_a^b \lambda_{ij}^{cd} t_{ac}^{ij}}{2} \\
&+ \frac{\delta_{bq} \delta_{dp} f_b^a \lambda_{ij}^{ac} t_{cd}^{ij}}{2} + \frac{\delta_{bq} \delta_{dp} f_a^b \lambda_{ij}^{cd} t_{ac}^{ij}}{2} \\
&+ \frac{\delta_{cp} \delta_{iq} f_i^a \lambda_{jk}^{ab} t_{bc}^{jk}}{2} + \frac{\delta_{cp} \delta_{iq} f_a^i \lambda_{jk}^{bc} t_{ab}^{jk}}{2} \\
&- \frac{\delta_{cq} \delta_{ip} f_i^a \lambda_{jk}^{ab} t_{bc}^{jk}}{2} - \frac{\delta_{cq} \delta_{ip} f_a^i \lambda_{jk}^{bc} t_{ab}^{jk}}{2} \\
&+ \frac{\delta_{jp} \delta_{lq} f_j^i \lambda_{kl}^{ab} t_{ab}^{ik}}{2} + \frac{\delta_{jp} \delta_{lq} f_i^j \lambda_{ik}^{ab} t_{ab}^{kl}}{2} \\
&- \frac{\delta_{jq} \delta_{lp} f_j^i \lambda_{kl}^{ab} t_{ab}^{ik}}{2} - \frac{\delta_{jq} \delta_{lp} f_i^j \lambda_{ik}^{ab} t_{ab}^{kl}}{2} \tag{6.47}
\end{aligned}$$

From the raw output of sympy, the first and third row in Eq. (6.47) may actually be discarded as they are not fully contracted (summation runs only over indices of  $t$  and  $\lambda$ , forming closed loops over these vertices and leaving the vertex corresponding to the Fockian unconnected). In the remaining terms, the  $t$  and  $\lambda$  vertices are all connected via three lines per pair. By introducing the correlation contribution to the one-particle density

$$\gamma_{ij}^{\text{corr}} = -\frac{1}{2} \sum_{kcd} t_{cd}^{ik} \lambda_{jk}^{cd} = \frac{1}{2} \sum_{kcd} t_{cd}^{ki} \lambda_{jk}^{cd} \quad \text{etc.} \tag{6.48}$$

$$\gamma_{ab}^{\text{corr}} = \frac{1}{2} \sum_{klc} t_{bc}^{kl} \lambda_{kl}^{ac} = -\frac{1}{2} \sum_{klc} t_{cb}^{kl} \lambda_{kl}^{ac} \quad \text{etc.} \tag{6.49}$$

(note the antisymmetry of the one-particle density upon swapping the order of arguments of the amplitudes) the remaining terms can be simplified considerably as

$$\begin{aligned}
& \langle 0 | (\widehat{\Lambda}_2([\widehat{f}_N, \widehat{p}^\dagger \widehat{q}]\widehat{T}_2)_c) | 0 \rangle \\
&= 2(\delta_{ap} \delta_{kq} f_a^i \gamma_{ik}^{\text{corr}} - \delta_{aq} \delta_{kp} f_i^a \gamma_{ki}^{\text{corr}} + \delta_{bp} \delta_{dq} f_b^a \gamma_{ad}^{\text{corr}} - \delta_{bq} \delta_{dp} f_a^b \gamma_{da}^{\text{corr}} \\
&- \delta_{cp} \delta_{iq} f_a^i \gamma_{ca}^{\text{corr}} + \delta_{cq} \delta_{ip} f_i^a \gamma_{ac}^{\text{corr}} + \delta_{jp} \delta_{lq} f_j^i \gamma_{il}^{\text{corr}} - \delta_{jq} \delta_{lp} f_i^j \gamma_{li}^{\text{corr}}) \tag{6.50}
\end{aligned}$$

In case of REMP, we can assume that  $f_{pq} = f_{qp}$  and  $\gamma_{pq} = \gamma_{qp}$  (real orbitals, structure of amplitude equations). Furthermore, the dummy indices can be made more convenient:

$$= 2\hat{P}_-(p, q) \left( \delta_{ip}\delta_{jq}f_{ik}\gamma_{kj}^{\text{corr}} + \delta_{ip}\delta_{aq}f_{ic}\gamma_{ca}^{\text{corr}} + \delta_{ap}\delta_{iq}f_{ak}\gamma_{ki}^{\text{corr}} + \delta_{ap}\delta_{bq}f_{ac}\gamma_{cb}^{\text{corr}} \right) \quad (6.51)$$

Eq. (6.51) already resembles the structure known from the reference orbital gradient. By inserting the definition of the Fockian, it can be decomposed further

$$f_{pq} = h_{pq} + \sum_k^{\text{occ}} J_{kk}^{pq} - K_{kk}^{pq} = h_{pq} + \sum_k^{\text{occ}} \langle pk||qk \rangle \quad (6.52)$$

It is immediately clear that the one-electron contribution to the orbital gradient can be generalized as

$$w_{pq} = 2\hat{P}_-(p, q) \left( \sum_r h_{pr}\gamma_{rq}^{\text{corr}} \right). \quad (6.53)$$

The two-electron contribution yields

$$2\hat{P}_-(p, q) \left( \delta_{ip}\delta_{jq} \sum_k^{\text{occ}} \sum_l^{\text{occ}} \langle il||kl \rangle \gamma_{kj}^{\text{corr}} + \delta_{ip}\delta_{aq} \sum_c^{\text{occ}} \sum_l^{\text{occ}} \langle il||cl \rangle \gamma_{ca}^{\text{corr}} \right. \\ \left. + \delta_{ap}\delta_{iq} \sum_k^{\text{occ}} \sum_l^{\text{occ}} \langle al||kl \rangle \gamma_{ki}^{\text{corr}} + \delta_{ap}\delta_{bq} \sum_c^{\text{occ}} \sum_l^{\text{occ}} \langle al||cl \rangle \gamma_{cb}^{\text{corr}} \right) \quad (6.54)$$

where the summations have been written out explicitly. Next, another formal summation is introduced for the two-electron integral indices that are equal. Additionally, the permutational symmetry of the TEIs is used for reordering them in a more convenient form:

$$= 2\hat{P}_-(p, q) \left( \delta_{ip}\delta_{jq} \sum_k^{\text{occ}} \sum_{lm}^{\text{occ}} \langle lk||mi \rangle \delta_{lm} \gamma_{kj}^{\text{corr}} + \delta_{ip}\delta_{aq} \sum_c^{\text{occ}} \sum_{lm}^{\text{occ}} \langle lc||mi \rangle \delta_{lm} \gamma_{ca}^{\text{corr}} \right. \\ \left. + \delta_{ap}\delta_{iq} \sum_k^{\text{occ}} \sum_{lm}^{\text{occ}} \langle lk||ma \rangle \delta_{lm} \gamma_{ki}^{\text{corr}} + \delta_{ap}\delta_{bq} \sum_c^{\text{occ}} \sum_{lm}^{\text{occ}} \langle lc||ma \rangle \delta_{lm} \gamma_{cb}^{\text{corr}} \right) \quad (6.55)$$

The two-electron contribution of ④ my thus be covered by introducing the separable two-particle density matrix as

$$\Gamma_{rstq}^{\text{sep}} = \delta_{rt}^{\text{occ}} \gamma_{sq}$$

Such a definition would however destroy the exchange symmetry of the TPDM. It is thus better to evenly distribute the OPDM contributions:

$$\Gamma_{rstq}^{\text{sep}} = \frac{1}{4} (\delta_{rt}^{\text{occ}} \gamma_{sq} + \delta_{sq}^{\text{occ}} \gamma_{rt} - \delta_{st}^{\text{occ}} \gamma_{rq} - \delta_{rq}^{\text{occ}} \gamma_{st}) \quad (6.56)$$

or with more convenient indices

$$\Gamma_{pqrs}^{\text{sep}} = \frac{1}{4}(\delta_{pr}^{\text{occ}} \gamma_{qs} + \delta_{qs}^{\text{occ}} \gamma_{pr} - \delta_{qr}^{\text{occ}} \gamma_{ps} - \delta_{ps}^{\text{occ}} \gamma_{qr}) \quad (6.57)$$

which now obeys the exchange symmetry but leads to an identical result. From a computational point of view, it is irrelevant whether the contribution of ③ to the orbital gradient is formed from Eq. (6.51) or by separating the one- and two-electron contributions. Both the direct contraction and the formation of the separable TPDM scale as  $n^3$  and are thus insignificant compared to other parts.

Part ⑤ results in the following raw result:

$$\begin{aligned} & \langle 0 | \widehat{\Lambda}_2 [ \widehat{W}_N, (\widehat{p}^+ \widehat{q} - \widehat{q}^+ \widehat{p}) ] \widehat{T}_2 | 0 \rangle \\ &= \frac{1}{4} (4\delta_{bp} \delta_{dq} t_{ac}^{ik} v_{cj}^{dk} - \delta_{bp} \delta_{eq} t_{cd}^{ij} v_{cd}^{ae} - \delta_{bp} \delta_{kq} t_{cd}^{ij} v_{cd}^{ak} - 4\delta_{bp} \delta_{lq} t_{ac}^{ik} v_{cj}^{kl} \\ &\quad - 4\delta_{bq} \delta_{dp} t_{ac}^{ik} v_{cj}^{dk} + \delta_{bq} \delta_{ep} t_{cd}^{ij} v_{cd}^{ae} + \delta_{bq} \delta_{kp} t_{cd}^{ij} v_{cd}^{ak} + 4\delta_{bq} \delta_{lp} t_{ac}^{ik} v_{cj}^{kl} \\ &\quad + 4\delta_{cp} \delta_{dq} t_{ac}^{ik} v_{dj}^{bk} - \delta_{cp} \delta_{jq} t_{ab}^{kl} v_{ci}^{kl} + 2\delta_{cp} \delta_{lq} t_{ab}^{ik} v_{jl}^{ck} + 2\delta_{cp} \delta_{lq} t_{ab}^{ik} v_{cj}^{kl} \\ &\quad - 4\delta_{cp} \delta_{lq} t_{ac}^{ik} v_{jl}^{bk} - \delta_{cp} \delta_{lq} t_{ab}^{kl} v_{ij}^{ck} - 4\delta_{cq} \delta_{dp} t_{ac}^{ik} v_{dj}^{bk} + \delta_{cq} \delta_{jp} t_{ab}^{kl} v_{ci}^{kl} \\ &\quad - 2\delta_{cq} \delta_{lp} t_{ab}^{ik} v_{jl}^{ck} - 2\delta_{cq} \delta_{lp} t_{ab}^{ik} v_{cj}^{kl} + 4\delta_{cq} \delta_{lp} t_{ac}^{ik} v_{jl}^{bk} + \delta_{cq} \delta_{lp} t_{ab}^{kl} v_{ij}^{ck} \\ &\quad - \delta_{dp} \delta_{eq} t_{cd}^{ij} v_{ce}^{ab} - 4\delta_{dp} \delta_{jq} t_{ac}^{ik} v_{cd}^{bk} + 2\delta_{dp} \delta_{kq} t_{ac}^{ij} v_{ck}^{bd} + 2\delta_{dp} \delta_{kq} t_{ac}^{ij} v_{cd}^{bk} \\ &\quad - \delta_{dp} \delta_{kq} t_{cd}^{ij} v_{ck}^{ab} - 4\delta_{dp} \delta_{kq} t_{ac}^{ik} v_{cj}^{bd} + \delta_{dq} \delta_{ep} t_{cd}^{ij} v_{ce}^{ab} + 4\delta_{dq} \delta_{jp} t_{ac}^{ik} v_{cd}^{bk} \\ &\quad - 2\delta_{dq} \delta_{kp} t_{ac}^{ij} v_{ck}^{bd} - 2\delta_{dq} \delta_{kp} t_{ac}^{ij} v_{cd}^{bk} + \delta_{dq} \delta_{kp} t_{cd}^{ij} v_{ck}^{ab} + 4\delta_{dq} \delta_{kp} t_{ac}^{ik} v_{cj}^{bd} \\ &\quad + 4\delta_{jp} \delta_{lq} t_{ac}^{ik} v_{cl}^{bk} - \delta_{jp} \delta_{mq} t_{ab}^{kl} v_{im}^{kl} - 4\delta_{jq} \delta_{lp} t_{ac}^{ik} v_{cl}^{bk} + \delta_{jq} \delta_{mp} t_{ab}^{kl} v_{im}^{kl} \\ &\quad + 4\delta_{kp} \delta_{lq} t_{ac}^{ik} v_{cj}^{bl} - 4\delta_{kq} \delta_{lp} t_{ac}^{ik} v_{cj}^{bl} - \delta_{lp} \delta_{mq} t_{ab}^{kl} v_{ij}^{km} + \delta_{lq} \delta_{mp} t_{ab}^{kl} v_{ij}^{km}) \lambda_{ij}^{ab} \end{aligned} \quad (6.58)$$

and with  $\lambda$  multiplied out

$$\begin{aligned} &= \frac{1}{4} (4\delta_{bp} \delta_{dq} v_{cj}^{dk} t_{ac}^{ik} \lambda_{ij}^{ab} - \delta_{bp} \delta_{eq} v_{cd}^{ae} t_{cd}^{ij} \lambda_{ij}^{ab} - \delta_{bp} \delta_{kq} v_{cd}^{ak} t_{cd}^{ij} \lambda_{ij}^{ab} - 4\delta_{bp} \delta_{lq} v_{cj}^{kl} t_{ac}^{ik} \lambda_{ij}^{ab} \\ &\quad - 4\delta_{bq} \delta_{dp} v_{cj}^{dk} t_{ac}^{ik} \lambda_{ij}^{ab} + \delta_{bq} \delta_{ep} v_{cd}^{ae} t_{cd}^{ij} \lambda_{ij}^{ab} + \delta_{bq} \delta_{kp} v_{cd}^{ak} t_{cd}^{ij} \lambda_{ij}^{ab} + 4\delta_{bq} \delta_{lp} v_{cj}^{kl} t_{ac}^{ik} \lambda_{ij}^{ab} \\ &\quad + 4\delta_{cp} \delta_{dq} v_{dj}^{bk} t_{ac}^{ik} \lambda_{ij}^{ab} - \delta_{cp} \delta_{jq} v_{ci}^{kl} t_{ab}^{kl} \lambda_{ij}^{ab} + 2\delta_{cp} \delta_{lq} v_{jl}^{ck} t_{ab}^{ik} \lambda_{ij}^{ab} + 2\delta_{cp} \delta_{lq} v_{cj}^{kl} t_{ab}^{ik} \lambda_{ij}^{ab} \\ &\quad - 4\delta_{cp} \delta_{lq} v_{jl}^{bk} t_{ac}^{ik} \lambda_{ij}^{ab} - \delta_{cp} \delta_{lq} v_{ij}^{ck} t_{ab}^{kl} \lambda_{ij}^{ab} - 4\delta_{cq} \delta_{dp} v_{dj}^{bk} t_{ac}^{ik} \lambda_{ij}^{ab} + \delta_{cq} \delta_{jp} v_{ci}^{kl} t_{ab}^{kl} \lambda_{ij}^{ab} \\ &\quad - 2\delta_{cq} \delta_{lp} v_{jl}^{ck} t_{ab}^{ik} \lambda_{ij}^{ab} - 2\delta_{cq} \delta_{lp} v_{cj}^{kl} t_{ab}^{ik} \lambda_{ij}^{ab} + 4\delta_{cq} \delta_{lp} v_{jl}^{bk} t_{ac}^{ik} \lambda_{ij}^{ab} + \delta_{cq} \delta_{lp} v_{ij}^{ck} t_{ab}^{kl} \lambda_{ij}^{ab} \\ &\quad - \delta_{dp} \delta_{eq} v_{ce}^{ab} t_{cd}^{ij} \lambda_{ij}^{ab} - 4\delta_{dp} \delta_{jq} v_{cd}^{bk} t_{ac}^{ik} \lambda_{ij}^{ab} + 2\delta_{dp} \delta_{kq} v_{ck}^{bd} t_{ac}^{ij} \lambda_{ij}^{ab} + 2\delta_{dp} \delta_{kq} v_{cd}^{bk} t_{ac}^{ij} \lambda_{ij}^{ab} \\ &\quad - \delta_{dp} \delta_{kq} v_{ck}^{ab} t_{cd}^{ij} \lambda_{ij}^{ab} - 4\delta_{dp} \delta_{kq} v_{cj}^{bd} t_{ac}^{ik} \lambda_{ij}^{ab} + \delta_{dq} \delta_{ep} v_{ce}^{ab} t_{cd}^{ij} \lambda_{ij}^{ab} + 4\delta_{dq} \delta_{jp} v_{cd}^{bk} t_{ac}^{ik} \lambda_{ij}^{ab} \\ &\quad - 2\delta_{dq} \delta_{kp} v_{ck}^{bd} t_{ac}^{ij} \lambda_{ij}^{ab} - 2\delta_{dq} \delta_{kp} v_{cd}^{bk} t_{ac}^{ij} \lambda_{ij}^{ab} + \delta_{dq} \delta_{kp} v_{ck}^{ab} t_{cd}^{ij} \lambda_{ij}^{ab} + 4\delta_{dq} \delta_{kp} v_{cj}^{bd} t_{ac}^{ik} \lambda_{ij}^{ab} \\ &\quad + 4\delta_{jp} \delta_{lq} v_{cl}^{bk} t_{ac}^{ik} \lambda_{ij}^{ab} - \delta_{jp} \delta_{mq} v_{im}^{kl} t_{ab}^{kl} \lambda_{ij}^{ab} - 4\delta_{jq} \delta_{lp} v_{cl}^{bk} t_{ac}^{ik} \lambda_{ij}^{ab} + \delta_{jq} \delta_{mp} v_{im}^{kl} t_{ab}^{kl} \lambda_{ij}^{ab} \\ &\quad + 4\delta_{kp} \delta_{lq} v_{cj}^{bl} t_{ac}^{ik} \lambda_{ij}^{ab} - 4\delta_{kq} \delta_{lp} v_{cj}^{bl} t_{ac}^{ik} \lambda_{ij}^{ab} - \delta_{lp} \delta_{mq} v_{ij}^{km} t_{ab}^{kl} \lambda_{ij}^{ab} + \delta_{lq} \delta_{mp} v_{ij}^{km} t_{ab}^{kl} \lambda_{ij}^{ab}) \end{aligned} \quad (6.59)$$

Compared to the raw result of (4), there are no uncontracted terms in the sympy output. Eq. (6.58) can be simplified in various ways. The first possible simplification is that it is possible to identify the one-particle densities already defined in Eqs. (6.48) and (6.49). The remaining part can be simplified by introducing correlated two-particle density matrices:

$$\Gamma_{ijkl} = \frac{1}{8} \sum_{cd} \lambda_{kl}^{cd} v_{cd}^{ij} \quad (6.60)$$

$$\Gamma_{abcd} = \frac{1}{8} \sum_{kl} \lambda_{kl}^{cd} v_{ab}^{kl} \quad (6.61)$$

$$\Gamma_{iajb} = -\frac{1}{4} \sum_{kc} \lambda_{jk}^{ac} t_{bc}^{ik} \quad (6.62)$$

It will soon be clear why this sign and prefactor convention is reasonable. After inserting the density matrix definitions, one obtains

$$\langle 0 | \widehat{\Lambda}_2 [\widehat{W}_N, (\hat{p}^+ \hat{q} - \hat{q}^+ \hat{p})] \widehat{T}_2 | 0 \rangle \quad (6.63)$$

insert density definitions

$$\begin{aligned} &= \frac{1}{4} (-16\delta_{bp}\delta_{dq}v_{cj}^{dk}\Gamma_{kbjc} - 8\delta_{bp}\delta_{eq}v_{cd}^{ae}\Gamma_{cdab} - 8\delta_{bp}\delta_{kq}v_{cd}^{ak}\Gamma_{cdab} + 16\delta_{bp}\delta_{lq}v_{cj}^{kl}\Gamma_{kbjc} \\ &\quad + 16\delta_{bq}\delta_{dp}v_{cj}^{dk}\Gamma_{kbjc} + 8\delta_{bq}\delta_{ep}v_{cd}^{ae}\Gamma_{cdab} + 8\delta_{bq}\delta_{kp}v_{cd}^{ak}\Gamma_{cdab} - 16\delta_{bq}\delta_{lp}v_{cj}^{kl}\Gamma_{kbjc} \\ &\quad - 16\delta_{cp}\delta_{dq}v_{dj}^{bk}\Gamma_{kbjc} - 8\delta_{cp}\delta_{jq}v_{ci}^{kl}\Gamma_{klij} - 4\delta_{cp}\delta_{lq}v_{jl}^{ck}\gamma_{kj} - 4\delta_{cp}\delta_{lq}v_{cj}^{kl}\gamma_{kj} \\ &\quad + 16\delta_{cp}\delta_{lq}v_{jl}^{bk}\Gamma_{kbjc} - 8\delta_{cp}\delta_{lq}v_{ij}^{ck}\Gamma_{klij} + 16\delta_{cq}\delta_{dp}v_{dj}^{bk}\Gamma_{kbjc} + 8\delta_{cq}\delta_{jp}v_{ci}^{kl}\Gamma_{klij} \\ &\quad + 4\delta_{cq}\delta_{lp}v_{jl}^{ck}\gamma_{kj} + 4\delta_{cq}\delta_{lp}v_{cj}^{kl}\gamma_{kj} - 16\delta_{cq}\delta_{lp}v_{jl}^{bk}\Gamma_{kbjc} + 8\delta_{cq}\delta_{lp}v_{ij}^{ck}\Gamma_{klij} \\ &\quad - 8\delta_{dp}\delta_{eq}v_{ce}^{ab}\Gamma_{cdab} + 16\delta_{dp}\delta_{jq}v_{cd}^{bk}\Gamma_{kbjc} + 4\delta_{dp}\delta_{kq}v_{ck}^{bd}\gamma_{bc} + 4\delta_{dp}\delta_{kq}v_{cd}^{bk}\gamma_{bc} \\ &\quad - 8\delta_{dp}\delta_{kq}v_{ck}^{ab}\Gamma_{cdab} + 16\delta_{dp}\delta_{kq}v_{cj}^{bd}\Gamma_{kbjc} + 8\delta_{dq}\delta_{ep}v_{ce}^{ab}\Gamma_{cdab} - 16\delta_{dq}\delta_{jp}v_{cd}^{bk}\Gamma_{kbjc} \\ &\quad - 4\delta_{dq}\delta_{kp}v_{ck}^{bd}\gamma_{bc} - 4\delta_{dq}\delta_{kp}v_{cd}^{bk}\gamma_{bc} + 8\delta_{dq}\delta_{kp}v_{ck}^{ab}\Gamma_{cdab} - 16\delta_{dq}\delta_{kp}v_{cj}^{bd}\Gamma_{kbjc} \\ &\quad - 16\delta_{jp}\delta_{lq}v_{cl}^{bk}\Gamma_{kbjc} - 8\delta_{jp}\delta_{mq}v_{im}^{kl}\Gamma_{klij} + 16\delta_{jq}\delta_{lp}v_{cl}^{bk}\Gamma_{kbjc} + 8\delta_{jq}\delta_{mp}v_{im}^{kl}\Gamma_{klij} \\ &\quad - 16\delta_{kp}\delta_{lq}v_{cj}^{bl}\Gamma_{kbjc} + 16\delta_{kq}\delta_{lp}v_{cj}^{bl}\Gamma_{kbjc} - 8\delta_{lp}\delta_{mq}v_{ij}^{km}\Gamma_{klij} + 8\delta_{lq}\delta_{mp}v_{ij}^{km}\Gamma_{klij}) \quad (6.64) \end{aligned}$$

subsequently, the terms are reordered so that terms belonging to each other stand next to each other:

$$\begin{aligned}
&= 2\delta_{mp}\delta_{lq}v_{km}^{ij}\Gamma_{ijkl} - 2\delta_{mq}\delta_{lp}v_{km}^{ij}\Gamma_{ijkl} + 2\delta_{mp}\delta_{jq}v_{im}^{kl}\Gamma_{klij} - 2\delta_{mq}\delta_{jp}v_{im}^{kl}\Gamma_{klij} \\
&\quad + 2\delta_{cp}\delta_{jq}v_{ic}^{kl}\Gamma_{klij} - 2\delta_{cq}\delta_{jp}v_{ic}^{kl}\Gamma_{klij} + 2\delta_{cp}\delta_{lq}v_{kc}^{ij}\Gamma_{ijkl} - 2\delta_{cq}\delta_{lp}v_{kc}^{ij}\Gamma_{ijkl} \\
&\quad + 4\delta_{lp}\delta_{kq}v_{bl}^{cj}\Gamma_{cjbk} - 4\delta_{lq}\delta_{kp}v_{bl}^{cj}\Gamma_{cjbk} + 4\delta_{lp}\delta_{bq}v_{kl}^{cj}\Gamma_{cjk b} - 4\delta_{lq}\delta_{bp}v_{kl}^{cj}\Gamma_{cjk b} \\
&\quad + 4\delta_{lp}\delta_{cq}v_{jl}^{bk}\Gamma_{bkjc} - 4\delta_{lq}\delta_{cp}v_{jl}^{bk}\Gamma_{bkjc} + 4\delta_{dp}\delta_{kq}v_{bd}^{cj}\Gamma_{cjk b} - 4\delta_{dq}\delta_{kp}v_{bd}^{cj}\Gamma_{cjk b} \\
&\quad + 4\delta_{dp}\delta_{jq}v_{cd}^{bk}\Gamma_{bkcj} - 4\delta_{dq}\delta_{jp}v_{cd}^{bk}\Gamma_{bkcj} + 4\delta_{dp}\delta_{bq}v_{kd}^{cj}\Gamma_{cjk b} - 4\delta_{dq}\delta_{bp}v_{kd}^{cj}\Gamma_{cjk b} \\
&\quad + 4\delta_{dp}\delta_{cq}v_{jd}^{kb}\Gamma_{kbjc} - 4\delta_{dq}\delta_{cp}v_{jd}^{kb}\Gamma_{kbjc} + 4\delta_{lp}\delta_{jq}v_{cl}^{bk}\Gamma_{bkcj} - 4\delta_{lq}\delta_{jp}v_{cl}^{bk}\Gamma_{bkcj} \\
&\quad + 2\delta_{kp}\delta_{bq}v_{ak}^{cd}\Gamma_{cdab} - 2\delta_{kq}\delta_{bp}v_{ak}^{cd}\Gamma_{cdab} + 2\delta_{kp}\delta_{dq}v_{ck}^{ab}\Gamma_{abcd} - 2\delta_{kq}\delta_{dp}v_{ck}^{ab}\Gamma_{abcd} \\
&\quad + 2\delta_{ep}\delta_{bq}v_{ae}^{cd}\Gamma_{cdab} - 2\delta_{eq}\delta_{bp}v_{ae}^{cd}\Gamma_{cdab} + 2\delta_{ep}\delta_{dq}v_{ce}^{ab}\Gamma_{abcd} - 2\delta_{eq}\delta_{dp}v_{ce}^{ab}\Gamma_{abcd} \\
&\quad + \delta_{lp}\delta_{cq}v_{jl}^{ck}\gamma_{kj} - \delta_{cp}\delta_{lq}v_{jl}^{ck}\gamma_{kj} + \delta_{lp}\delta_{cq}v_{cj}^{kl}\gamma_{kj} - \delta_{cp}\delta_{lq}v_{cj}^{kl}\gamma_{kj} \\
&\quad + \delta_{dp}\delta_{kq}v_{ck}^{bd}\gamma_{bc} - \delta_{dq}\delta_{kp}v_{ck}^{bd}\gamma_{bc} + \delta_{dp}\delta_{kq}v_{cd}^{bk}\gamma_{bc} - \delta_{dq}\delta_{kp}v_{cd}^{bk}\gamma_{bc}
\end{aligned} \tag{6.65}$$

identical terms can now be merged by unifying summation dummy indices; by swapping the summation dummies  $j/k$  and  $b/c$  in the OPDM contributions, these can be simplified, too as  $\gamma_{kj} = \gamma_{jk}$

$$\begin{aligned}
&= + 4\delta_{mp}\delta_{lq}v_{km}^{ij}\Gamma_{ijkl} - 4\delta_{mq}\delta_{lp}v_{km}^{ij}\Gamma_{ijkl} + 4\delta_{cp}\delta_{lq}v_{kc}^{ij}\Gamma_{ijkl} - 4\delta_{cq}\delta_{lp}v_{kc}^{ij}\Gamma_{ijkl} \\
&\quad + 4\delta_{lp}\delta_{kq}v_{bl}^{cj}\Gamma_{cjbk} - 4\delta_{lq}\delta_{kp}v_{bl}^{cj}\Gamma_{cjbk} + 4\delta_{lp}\delta_{bq}v_{kl}^{cj}\Gamma_{cjk b} - 4\delta_{lq}\delta_{bp}v_{kl}^{cj}\Gamma_{cjk b} \\
&\quad + 4\delta_{lp}\delta_{cq}v_{jl}^{bk}\Gamma_{bkjc} - 4\delta_{lq}\delta_{cp}v_{jl}^{bk}\Gamma_{bkjc} + 4\delta_{dp}\delta_{kq}v_{bd}^{cj}\Gamma_{cjk b} - 4\delta_{dq}\delta_{kp}v_{bd}^{cj}\Gamma_{cjk b} \\
&\quad + 4\delta_{dp}\delta_{jq}v_{cd}^{bk}\Gamma_{bkcj} - 4\delta_{dq}\delta_{jp}v_{cd}^{bk}\Gamma_{bkcj} + 4\delta_{dp}\delta_{bq}v_{kd}^{cj}\Gamma_{cjk b} - 4\delta_{dq}\delta_{bp}v_{kd}^{cj}\Gamma_{cjk b} \\
&\quad + 4\delta_{dp}\delta_{cq}v_{jd}^{kb}\Gamma_{kbjc} - 4\delta_{dq}\delta_{cp}v_{jd}^{kb}\Gamma_{kbjc} + 4\delta_{lp}\delta_{jq}v_{cl}^{bk}\Gamma_{bkcj} - 4\delta_{lq}\delta_{jp}v_{cl}^{bk}\Gamma_{bkcj} \\
&\quad + 4\delta_{kp}\delta_{dq}v_{ck}^{ab}\Gamma_{abcd} - 4\delta_{kq}\delta_{dp}v_{ck}^{ab}\Gamma_{abcd} + 4\delta_{ep}\delta_{dq}v_{ce}^{ab}\Gamma_{abcd} - 4\delta_{eq}\delta_{dp}v_{ce}^{ab}\Gamma_{abcd} \\
&\quad + 2\delta_{lp}\delta_{cq}v_{jl}^{ck}\gamma_{kj} - 2\delta_{cp}\delta_{lq}v_{jl}^{ck}\gamma_{kj} + 2\delta_{dp}\delta_{kq}v_{ck}^{bd}\gamma_{bc} - 2\delta_{dq}\delta_{kp}v_{ck}^{bd}\gamma_{bc}
\end{aligned} \tag{6.66}$$

now, the permutation operator can again be introduced

$$\begin{aligned}
&= 2\hat{P}_-(p, q)(2\delta_{mp}\delta_{lq}v_{km}^{ij}\Gamma_{ijkl} + 2\delta_{cp}\delta_{lq}v_{kc}^{ij}\Gamma_{ijkl} + 2\delta_{lp}\delta_{kq}v_{bl}^{cj}\Gamma_{cjbk} + 2\delta_{lp}\delta_{bq}v_{kl}^{cj}\Gamma_{cjk b} \\
&\quad + 2\delta_{lp}\delta_{cq}v_{jl}^{bk}\Gamma_{bkjc} + 2\delta_{dp}\delta_{kq}v_{bd}^{cj}\Gamma_{cjk b} + 2\delta_{dp}\delta_{jq}v_{cd}^{bk}\Gamma_{bkcj} + 2\delta_{dp}\delta_{bq}v_{kd}^{cj}\Gamma_{cjk b} \\
&\quad + 2\delta_{dp}\delta_{cq}v_{jd}^{kb}\Gamma_{kbjc} + 2\delta_{lp}\delta_{jq}v_{cl}^{bk}\Gamma_{bkcj} + 2\delta_{kp}\delta_{dq}v_{ck}^{ab}\Gamma_{abcd} + 2\delta_{ep}\delta_{dq}v_{ce}^{ab}\Gamma_{abcd} \\
&\quad + \delta_{lp}\delta_{cq}v_{jl}^{ck}\gamma_{kj} + \delta_{dp}\delta_{kq}v_{ck}^{bd}\gamma_{bc})
\end{aligned} \tag{6.67}$$

so that the contributions by two-particle densities can be generalized as

$$= 2\hat{P}_-(p, q)(2\sum_{rst} v_{tp}^{rs}\Gamma_{rstq}^{\text{CORR}}) = 2\hat{P}_-(p, q)(2\sum_{rst} \langle rs || tp \rangle \Gamma_{rstq}^{\text{CORR}}) \tag{6.68}$$

Regarding the OPDM contributions ( $\delta_{lp}\delta_{cq}v_{jl}^{ck}\gamma_{kj} + \delta_{dp}\delta_{kq}v_{ck}^{bd}\gamma_{bc}$ ), it was not possible to elucidate their origin and nature. Such terms are not present in the OCEPA formulation of Bozkaya and Sherrill. It is not possible to rewrite them in the scheme of the separable TPDMs, as both  $p$  and  $q$  occur in the ERI part while the OPDM part does not contain any target index. Furthermore, writing these contributions as separable TPDM would require one- and three-external TPDMs which are needed nowhere else. The only possibility is that these contributions are not fully contracted in nature and thus can and should be discarded entirely.

Due to the contraction pattern of integrals and densities (first three indices are contracted, must share the occupation pattern), there are only 12 different combinations of occupied and virtual indices possible with the densities present in the last part:

$rstp$	$rstq$
oooo	oooo
oooo	ooov
ovoo	ovov
ovov	ovov
ovvo	ovvo
ovvv	ovvo
vooo	voov
voov	voov
vovo	vovo
vovv	vovo
vvvo	vvvv
vvvv	vvvv

all of these are present in Eq. (6.67), thus it is possible to also generalize the last part in the same way as before.

It was furthermore impossible to reproduce where Bozkaya and Sherrill got the additional factor 2 in their orbital gradient from (e.g. Eq. (37) in Ref. [46]).

On the other hand, as the orbital gradient is a property which is brought to zero, a missing factor 2 just means that the convergence criterion has to be tightened by that factor.

Collecting all contributions from ①–⑤, the orbital gradient may be written as

$$w_{pq} = 2F_{pq} - 2F_{qp} = 2\hat{P}_- F_{pq} \quad (6.69)$$

where the generalized Fock matrix  $F_{pq}$  is defined as

$$F_{pq} = \sum_r h_{pr}\gamma_{rq} + 2 \sum_{rst} \langle rs || tp \rangle \Gamma_{rstq} \quad (6.70)$$



with the one-particle density matrix (OPDM)  $\gamma_{pq}$  and the two-particle density matrix (TPDM)  $\Gamma_{pqrs}$  being defined as

$$\gamma_{pq} = \gamma_{pq}^{\text{ref}} + \gamma_{pq}^{\text{corr}} \quad (6.71)$$

where

$$\gamma_{pq}^{\text{ref}} = \delta_{pq}^{\text{occ}} \quad \text{from ①, Eq. (6.27)} \quad (6.72)$$

$$\gamma_{ij}^{\text{corr}} = -\frac{1}{2} \sum_m^{\text{occ}} \sum_{ef}^{\text{virt}} t_{ef}^{im} \lambda_{jm}^{ef} \quad \text{from ②, Eq. (6.48)} \quad (6.73)$$

$$\gamma_{ab}^{\text{corr}} = \frac{1}{2} \sum_{mn}^{\text{occ}} \sum_e^{\text{virt}} t_{be}^{mn} \lambda_{mn}^{ae} \quad \text{from ②, Eq. (6.49)} \quad (6.74)$$

$$\Gamma_{pqrs} = \Gamma_{pqrs}^{\text{ref}} + \Gamma_{pqrs}^{\text{sep}} + \Gamma_{pqrs}^{\text{corr}} \quad (6.75)$$

where

$$\Gamma_{pqrs}^{\text{ref}} = \frac{1}{4} (\delta_{pr}^{\text{occ}} \delta_{qs}^{\text{occ}} - \delta_{ps}^{\text{occ}} \delta_{qr}^{\text{occ}}) \quad \text{from ①, Eq. (6.28)} \quad (6.76)$$

$$\Gamma_{pqrs}^{\text{sep}} = \frac{1}{4} (\delta_{pr}^{\text{occ}} \gamma_{qs} + \delta_{qs}^{\text{occ}} \gamma_{pr} - \delta_{qr}^{\text{occ}} \gamma_{ps} - \delta_{ps}^{\text{occ}} \gamma_{qr}) \quad \text{from ④, Eq. (6.57)} \quad (6.77)$$

$$\Gamma_{ijkl}^{\text{corr}} = \frac{1}{8} \sum_{cd} \lambda_{kl}^{cd} t_{cd}^{ij} \quad \text{from ⑤, Eq. (6.60)} \quad (6.78)$$

$$\Gamma_{ijab}^{\text{corr}} = \frac{1}{4} t_{ab}^{ij} \quad \text{from ② \& ③, Eq. (6.40)} \quad (6.79)$$

$$\Gamma_{iajb}^{\text{corr}} = -\frac{1}{4} \sum_{kc} \lambda_{jk}^{ac} t_{bc}^{ik} \quad \text{from ⑤, Eq. (6.62)} \quad (6.80)$$

$$\Gamma_{abcd}^{\text{corr}} = \frac{1}{8} \sum_{kl} \lambda_{kl}^{cd} t_{ab}^{kl} \quad \text{from ⑤, Eq. (6.61)} \quad (6.81)$$

The REMF scaling factor  $A$  for  $\Gamma_{ijkl}^{\text{corr}}$ ,  $\Gamma_{iajb}^{\text{corr}}$ , and  $\Gamma_{abcd}^{\text{corr}}$  can be either included in the densities (as has been done in both the wavel and the PSI4 implementation) or only added when the generalized Fock matrix is constructed.

*The latter one should be the preferred way of treating the TPDMs in later developments. The densities  $\Gamma_{ijkl}$ ,  $\Gamma_{iajb}$  and  $\Gamma_{abcd}$  or course also do exist for MP2, they are just not needed for calculating the orbital gradient. They **are** needed when two-electron properties (like  $\langle \hat{S}^2 \rangle$ ) are calculated, however, and in this case, they should also not be scaled.*

The currently available implementations of OO-REMP are correct, but the scaling of the TPDMs should nevertheless be moved to the generalized Fock matrix code.

## 6.2 Tables

### 6.2.1 Tables for the RG18 benchmark set

**Table 6.1:** Absolute errors for the RG18 benchmark set, all in kcal mol<sup>-1</sup>. Energies were extrapolated from aug-cc-pV[T/Q]Z for dimers and aug-cc-pwCV[T/Q]Z for higher aggregates as described in Section 3.3.1.

A	MSD	MAD	stdev	RMSD	min	max
method 1						
0.00	-0.074	0.074	0.050	0.088	-0.174	-0.006
0.15	-0.058	0.058	0.043	0.072	-0.191	-0.003
0.20	-0.053	0.053	0.044	0.068	-0.198	0.001
0.25	-0.048	0.048	0.047	0.066	-0.205	0.006
0.30	-0.042	0.045	0.051	0.065	-0.212	0.015
0.35	-0.037	0.044	0.056	0.066	-0.218	0.040
0.40	-0.031	0.045	0.062	0.068	-0.225	0.064
0.45	-0.026	0.049	0.069	0.072	-0.231	0.089
0.50	-0.020	0.054	0.076	0.077	-0.237	0.115
1.00	0.040	0.115	0.164	0.164	-0.296	0.384
method 2						
0.00	-0.039	0.062	0.062	0.072	-0.125	0.117
0.15	-0.023	0.042	0.048	0.052	-0.109	0.095
0.20	-0.018	0.036	0.046	0.048	-0.105	0.088
0.25	-0.012	0.036	0.046	0.046	-0.101	0.081
0.30	-0.007	0.038	0.047	0.046	-0.099	0.074
0.35	-0.002	0.041	0.050	0.049	-0.096	0.071
0.40	0.004	0.044	0.054	0.053	-0.093	0.094
0.45	0.009	0.047	0.060	0.059	-0.091	0.117
0.50	0.015	0.051	0.066	0.066	-0.088	0.140
1.00	0.075	0.103	0.152	0.166	-0.064	0.392
method 3						
0.00	-0.094	0.094	0.052	0.106	-0.194	-0.020
0.15	-0.079	0.079	0.046	0.090	-0.217	-0.021
0.20	-0.073	0.073	0.047	0.086	-0.224	-0.021
0.25	-0.068	0.068	0.049	0.083	-0.232	-0.019
0.30	-0.063	0.063	0.053	0.081	-0.239	-0.013
0.35	-0.058	0.058	0.058	0.081	-0.246	0.007
0.40	-0.052	0.057	0.064	0.081	-0.254	0.027
0.45	-0.047	0.061	0.070	0.083	-0.261	0.048
0.50	-0.041	0.065	0.077	0.086	-0.268	0.069
1.00	0.016	0.112	0.164	0.160	-0.335	0.329

**Table 6.2:** Relative errors for the RG18 benchmark set, all in percent. Energies were extrapolated from aug-cc-pV[T/Q]Z for dimers and aug-cc-pwCV[T/Q]Z for higher aggregates as described in Section 3.3.1.

A	MSRE	MARE	rel. stdev	RMSRE	min	max
method 1						
0.00	-13.3	13.3	4.2	13.9	-22.5	-4.6
0.15	-11.5	11.5	6.0	12.9	-25.5	-1.0
0.20	-10.9	11.0	6.9	12.8	-26.5	0.4
0.25	-10.3	10.5	7.7	12.8	-27.5	1.8
0.30	-9.7	10.2	8.6	12.8	-28.4	3.2
0.35	-9.0	10.1	9.6	13.0	-29.3	4.7
0.40	-8.4	10.1	10.5	13.2	-30.3	6.1
0.45	-7.7	10.5	11.5	13.6	-31.2	8.0
0.50	-7.1	11.0	12.4	14.0	-32.0	10.2
1.00	0.1	19.0	22.7	22.1	-40.4	34.2
method 2						
0.00	-8.7	12.3	10.6	13.4	-23.6	11.5
0.15	-6.9	9.9	10.2	12.1	-26.7	9.2
0.20	-6.3	9.2	10.3	11.8	-27.7	8.5
0.25	-5.7	9.1	10.5	11.6	-28.6	7.9
0.30	-5.0	9.1	10.8	11.6	-29.6	7.3
0.35	-4.4	9.2	11.1	11.7	-30.5	6.7
0.40	-3.8	9.4	11.6	11.9	-31.4	7.0
0.45	-3.1	9.7	12.1	12.2	-32.3	8.7
0.50	-2.4	10.1	12.7	12.6	-33.2	11.0
1.00	4.8	16.6	20.9	20.9	-41.6	35.0
method 3						
0.00	-19.0	19.0	7.2	20.3	-38.1	-10.9
0.15	-17.2	17.2	8.4	19.1	-40.3	-6.1
0.20	-16.6	16.6	9.0	18.8	-41.0	-4.5
0.25	-16.0	16.0	9.6	18.5	-41.7	-2.8
0.30	-15.3	15.3	10.3	18.3	-42.4	-1.1
0.35	-14.7	14.7	11.1	18.2	-43.1	0.6
0.40	-14.0	14.5	11.9	18.2	-43.8	2.3
0.45	-13.4	14.6	12.7	18.2	-44.5	4.1
0.50	-12.7	14.8	13.6	18.3	-45.1	5.8
1.00	-5.6	19.1	23.0	23.1	-51.7	29.4

**Table 6.3:** Relative errors of DFT methods for the RG18 benchmark set, all in percent. Energies were retrieved from Reference [256] and used without modification. The def2-QZVP basis set was used in all cases. All errors in percent.

A	MSRE	MARE	rel. stdev	RMSRE	min	max
DFT/def2-QZVP						
revTPSS, D3(BJ)	12.8	15.1	19.5	22.9	-8.6	66.7
revTPSSh, D3(BJ)	8.3	13.1	15.7	17.4	-15.0	50.0
BLYP, D3(BJ)	5.2	11.5	16.4	16.8	-12.1	47.8
APFD	13.9	15.7	15.5	20.5	-4.6	47.8
B2PLYP, D3(0)	-12.2	32.7	39.7	40.5	-77.8	100.0
B2PLYP, D3(BJ)	-19.9	31.5	32.3	37.2	-74.1	47.8
DSD-PBEB95, D3(BJ)	13.1	27.5	33.7	35.3	-63.0	72.2
M062X, no D	5.8	44.4	53.8	52.6	-62.5	112.5
BP86, D3(0)	-111.4	115.9	108.5	153.4	-337.5	23.6

## 6.2.2 Tables for the A24 benchmark set

**Table 6.4:** Absolute error measures for REMP, OO-REMP and CCSD(T) for the A24 benchmark set, all errors wrt. approximate CCSDT(Q)/CBS results from Ref.[262]. All values in kcal mol<sup>-1</sup>. REMP and OO-REMP are extrapolated from aug-cc-pV[T,Q]Z, CCSD(T) is taken from Ref. [264]. See Section 3.3.2 for computational details.

A	MSD	MAD	stdev	RMSD	min	max
REMP						
0.00	0.130	0.135	0.161	0.204	-0.047	0.784
0.05	0.115	0.118	0.140	0.179	-0.034	0.680
0.10	0.100	0.103	0.124	0.157	-0.028	0.592
0.15	0.087	0.090	0.110	0.139	-0.026	0.515
0.20	0.075	0.080	0.100	0.123	-0.029	0.449
0.25	0.063	0.072	0.091	0.110	-0.035	0.391
0.30	0.052	0.068	0.085	0.099	-0.049	0.339
0.35	0.042	0.066	0.081	0.090	-0.064	0.293
0.40	0.033	0.066	0.079	0.084	-0.085	0.252
0.45	0.023	0.066	0.078	0.080	-0.108	0.215
0.50	0.015	0.067	0.079	0.079	-0.132	0.181
0.55	0.006	0.069	0.081	0.080	-0.157	0.150
0.60	-0.002	0.071	0.085	0.083	-0.183	0.122
0.65	-0.010	0.074	0.089	0.088	-0.210	0.109
0.70	-0.017	0.077	0.094	0.094	-0.238	0.103
0.75	-0.025	0.080	0.100	0.101	-0.267	0.098
0.80	-0.032	0.083	0.106	0.109	-0.296	0.094
0.85	-0.039	0.088	0.113	0.117	-0.326	0.089
0.90	-0.046	0.093	0.120	0.126	-0.358	0.086
0.95	-0.053	0.099	0.128	0.136	-0.390	0.082
1.00	-0.060	0.106	0.135	0.145	-0.423	0.079
OO-REMP						
0.00	0.125	0.128	0.109	0.164	-0.035	0.566
0.05	0.106	0.110	0.087	0.136	-0.044	0.451
0.10	0.089	0.093	0.069	0.112	-0.051	0.353
0.15	0.073	0.078	0.055	0.090	-0.057	0.268
0.20	0.058	0.063	0.043	0.072	-0.062	0.193
0.25	0.044	0.050	0.034	0.056	-0.065	0.126
0.30	0.031	0.037	0.029	0.042	-0.067	0.096
0.35	0.019	0.026	0.029	0.034	-0.068	0.082
0.40	0.007	0.025	0.031	0.031	-0.068	0.070
0.45	-0.005	0.030	0.037	0.036	-0.084	0.058
0.50	-0.016	0.037	0.043	0.045	-0.127	0.047
0.55	-0.027	0.044	0.051	0.056	-0.167	0.036
0.60	-0.037	0.052	0.058	0.068	-0.205	0.031
0.65	-0.048	0.060	0.066	0.080	-0.241	0.029
0.70	-0.058	0.068	0.075	0.093	-0.276	0.026
0.75	-0.068	0.076	0.083	0.106	-0.310	0.024
0.80	-0.077	0.085	0.092	0.119	-0.342	0.023
0.85	-0.087	0.094	0.101	0.132	-0.374	0.022
0.90	-0.097	0.103	0.110	0.145	-0.405	0.022
0.95	-0.106	0.112	0.120	0.158	-0.436	0.021
1.00	-0.116	0.121	0.129	0.172	-0.467	0.021
CCSD(T)/CBS/FC	0.021	0.023	0.017	0.026	-0.032	0.053

**Table 6.5:** Relative error measures for REMP, OO-REMP and CCSD(T) for the A24 benchmark set, all errors wrt. approximate CCSDT(Q)/CBS results from Ref.[262]. All values in kcal mol<sup>-1</sup>. REMP and OO-REMP are extrapolated from aug-cc-pV[T,Q]Z, CCSD(T) is taken from Ref. [264]. See Section 3.3.2 for computational details.

<i>A</i>	MSRE	MARE	rel. stdev	RMSRE	min	max
REMP						
0.00	-7.7	8.0	5.6	9.4	-17.3	3.3
0.05	-6.8	7.1	5.3	8.6	-15.0	2.9
0.10	-6.1	6.3	5.0	7.9	-14.0	2.1
0.15	-5.6	5.6	4.8	7.3	-13.0	0.9
0.20	-5.1	5.1	4.6	6.8	-12.4	0.2
0.25	-4.7	4.9	4.5	6.5	-12.1	0.8
0.30	-4.4	4.9	4.6	6.3	-11.8	2.0
0.35	-4.1	5.0	4.8	6.2	-11.5	3.3
0.40	-3.9	5.2	5.1	6.3	-11.3	4.6
0.45	-3.7	5.5	5.6	6.6	-12.5	6.0
0.50	-3.6	5.7	6.1	7.0	-14.8	7.4
0.55	-3.4	6.0	6.8	7.5	-17.2	8.8
0.60	-3.4	6.3	7.5	8.1	-19.8	10.2
0.65	-3.3	6.7	8.3	8.8	-22.4	11.6
0.70	-3.3	7.1	9.2	9.6	-25.1	13.0
0.75	-3.3	7.5	10.1	10.4	-27.9	14.5
0.80	-3.3	7.9	11.0	11.2	-30.8	15.9
0.85	-3.3	8.4	12.0	12.2	-33.8	17.4
0.90	-3.4	8.9	13.0	13.1	-36.8	18.9
0.95	-3.4	9.4	14.0	14.1	-39.9	20.3
1.00	-3.5	10.0	15.0	15.1	-43.1	21.8
OO-REMP						
0.00	-6.4	9.0	7.8	10.0	-15.1	11.9
0.05	-5.4	8.1	7.2	8.9	-13.6	11.9
0.10	-4.6	7.1	6.6	7.9	-12.0	11.1
0.15	-3.9	6.2	5.9	7.0	-10.6	9.9
0.20	-3.3	5.2	5.2	6.0	-9.8	8.3
0.25	-2.8	4.3	4.4	5.1	-9.2	6.4
0.30	-2.3	3.5	3.7	4.3	-8.5	4.5
0.35	-1.9	2.6	3.1	3.6	-7.9	3.1
0.40	-1.6	2.3	2.8	3.1	-7.4	1.5
0.45	-1.3	2.3	2.7	3.0	-6.8	2.8
0.50	-1.0	2.7	3.1	3.2	-6.3	4.1
0.55	-0.8	3.1	3.8	3.8	-8.4	5.5
0.60	-0.6	3.6	4.7	4.6	-11.3	6.8
0.65	-0.5	4.2	5.6	5.5	-14.3	8.1
0.70	-0.3	4.8	6.7	6.5	-17.4	9.3
0.75	-0.2	5.4	7.8	7.6	-20.6	10.6
0.80	-0.1	6.1	8.9	8.7	-23.9	11.8
0.85	0.0	6.8	10.1	9.9	-27.3	13.3
0.90	0.0	7.5	11.4	11.1	-30.7	15.1
0.95	0.1	8.3	12.6	12.4	-34.3	16.9
1.00	0.1	9.0	13.9	13.6	-38.0	18.7
CCSD(T)/CBS/FC	-0.7	1.7	1.9	2.0	-2.5	4.3

## 6.2.3 Tables for the O23 benchmark set

**Table 6.6:** Absolute error measures for the O23 benchmark set. All in kcal mol<sup>-1</sup>. OO-REMP/CBS(aug-cc-pV[T/Q]Z), all electrons correlated, reference numbers: CCSD(T)/CBS(aug-cc-pV[T/Q]Z), all electrons correlated from Ref. [121].

<i>A</i>	MSD	MAD	stdev	RMSD	min	max
0.00	0.198	0.214	0.286	0.342	-0.150	1.037
0.01	0.192	0.206	0.272	0.328	-0.138	0.957
0.05	0.175	0.184	0.228	0.284	-0.092	0.727
0.10	0.159	0.162	0.193	0.246	-0.031	0.681
0.11	0.156	0.158	0.187	0.240	-0.018	0.670
0.12	0.153	0.154	0.182	0.235	-0.005	0.658
0.13	0.151	0.151	0.177	0.230	-0.004	0.646
0.14	0.148	0.148	0.173	0.225	-0.004	0.633
0.15	0.145	0.146	0.169	0.220	-0.004	0.620
0.16	0.143	0.143	0.165	0.215	-0.004	0.607
0.17	0.140	0.141	0.161	0.211	-0.004	0.593
0.18	0.138	0.138	0.158	0.207	-0.004	0.578
0.19	0.136	0.136	0.155	0.204	-0.004	0.563
0.20	0.134	0.135	0.153	0.200	-0.008	0.548
0.21	0.131	0.133	0.150	0.197	-0.014	0.532
0.22	0.129	0.131	0.148	0.194	-0.019	0.516
0.23	0.127	0.130	0.146	0.191	-0.025	0.499
0.24	0.125	0.128	0.145	0.189	-0.030	0.482
0.25	0.123	0.126	0.143	0.186	-0.035	0.464
0.26	0.121	0.125	0.142	0.184	-0.040	0.458
0.27	0.119	0.123	0.142	0.182	-0.045	0.471
0.28	0.117	0.122	0.141	0.181	-0.050	0.483
0.29	0.115	0.120	0.141	0.180	-0.054	0.496
0.30	0.113	0.119	0.142	0.179	-0.058	0.508
0.35	0.103	0.111	0.148	0.178	-0.077	0.564
0.40	0.094	0.104	0.161	0.184	-0.092	0.615
0.45	0.086	0.100	0.182	0.197	-0.104	0.661
0.50	0.077	0.113	0.208	0.217	-0.112	0.703
0.60	0.060	0.152	0.273	0.273	-0.381	0.778
0.70	0.043	0.201	0.353	0.347	-0.704	0.934
0.80	0.026	0.258	0.445	0.436	-1.066	1.132
0.90	0.008	0.319	0.551	0.538	-1.472	1.341
1.00	-0.009	0.384	0.670	0.655	-1.927	1.562

**Table 6.7:** Relative error measures for the O23 benchmark set. All in percent. OO-REMP/CBS(aug-cc-pV[T/Q]Z), all electrons correlated, reference numbers: CCSD(T)/CBS(aug-cc-pV[T/Q]Z), all electrons correlated from Ref. [121].

A	MSRE	MARE	rel. stdev	RMSRE	min	max
0.00	-5.1	6.1	6.3	8.0	-20.4	7.0
0.01	-5.2	5.9	6.1	7.9	-20.3	6.5
0.05	-5.6	6.0	5.8	8.0	-19.6	4.6
0.10	-6.0	6.3	6.5	8.8	-20.9	2.2
0.11	-6.1	6.3	6.8	9.0	-22.9	1.8
0.12	-6.2	6.3	7.0	9.2	-24.8	1.3
0.13	-6.3	6.4	7.3	9.5	-26.7	0.8
0.14	-6.4	6.4	7.6	9.7	-28.5	0.4
0.15	-6.4	6.4	7.9	10.0	-30.3	0.0
0.16	-6.5	6.5	8.1	10.3	-32.1	-0.1
0.17	-6.6	6.6	8.4	10.5	-33.8	0.0
0.18	-6.6	6.6	8.7	10.8	-35.4	0.0
0.19	-6.7	6.7	9.0	11.1	-37.0	0.0
0.20	-6.7	6.7	9.4	11.3	-38.6	0.0
0.21	-6.8	6.8	9.7	11.6	-40.1	0.1
0.22	-6.8	6.8	10.0	11.9	-41.6	0.1
0.23	-6.9	6.9	10.3	12.2	-43.1	0.1
0.24	-6.9	7.0	10.6	12.4	-44.5	0.1
0.25	-7.0	7.0	10.9	12.7	-45.9	0.1
0.26	-7.0	7.0	11.2	13.0	-47.2	0.2
0.27	-7.1	7.1	11.5	13.2	-48.5	0.2
0.28	-7.1	7.1	11.8	13.5	-49.8	0.2
0.29	-7.2	7.2	12.1	13.8	-51.1	0.2
0.30	-7.2	7.2	12.4	14.0	-52.3	0.2
0.35	-7.4	7.4	13.8	15.3	-58.1	0.3
0.40	-7.5	7.6	15.2	16.6	-63.4	0.4
0.45	-7.6	7.7	16.6	17.8	-68.1	0.5
0.50	-7.6	8.3	17.9	19.0	-72.5	2.6
0.60	-7.6	9.7	20.5	21.4	-80.2	10.3
0.70	-7.5	11.2	23.1	23.7	-86.7	19.0
0.80	-7.2	13.1	25.7	26.1	-92.5	28.7
0.90	-6.8	15.1	28.4	28.6	-97.5	39.7
1.00	-6.2	17.2	31.3	31.2	-102.0	51.9

### 6.3 Paper Appendices

All papers are reprinted with permission of the respective copyright owners:

- Paper 1: Reproduced from S. Behnle and R. F. Fink, *J. Chem. Phys.* **150** (2019) 124107, <https://doi.org/10.1063/1.5086168> or <https://aip.scitation.org/doi/10.1063/1.5086168>, with the permission of AIP Publishing.
- Paper 2: Reprinted with permission from S. Behnle and R. F. Fink, *J. Chem. Theory Comput.* **17** (2021) 3259–3266, <https://doi.org/10.1021/acs.jctc.1c00280> or <https://pubs.acs.org/doi/10.1021/acs.jctc.1c00280>. Copyright 2021 American Chemical Society.
- Paper 3: Reproduced from S. Behnle and R. F. Fink, *J. Chem. Phys.* **156** (2022) 124103, <https://doi.org/10.1063/5.0081285> or <https://aip.scitation.org/doi/10.1063/5.0081285>, with the permission of AIP Publishing.
- Paper 4: Reproduced from S. Behnle, R. Richter, L. Völkl, P. Idzko, A. Förstner, U. Bozkaya, and R. F. Fink, *J. Chem. Phys.* **157** (2022) 104111, <https://doi.org/10.1063/5.0105628> or <https://aip.scitation.org/doi/10.1063/5.0105628>, with the permission of AIP Publishing.



# REMP: A hybrid perturbation theory providing improved electronic wavefunctions and properties

Cite as: J. Chem. Phys. **150**, 124107 (2019); <https://doi.org/10.1063/1.5086168>

Submitted: 18 December 2018 . Accepted: 03 March 2019 . Published Online: 27 March 2019

Stefan Behnle , and Reinhold F. Fink 



View Online



Export Citation



CrossMark



Where in the **world** is AIP Publishing?  
*Find out where we are exhibiting next*



# REMP: A hybrid perturbation theory providing improved electronic wavefunctions and properties

Cite as: J. Chem. Phys. 150, 124107 (2019); doi: 10.1063/1.5086168

Submitted: 18 December 2018 • Accepted: 3 March 2019 •

Published Online: 27 March 2019



View Online



Export Citation



CrossMark

Stefan Behnle<sup>a)</sup>  and Reinhold F. Fink<sup>b)</sup> 

## AFFILIATIONS

Institute of Physical and Theoretical Chemistry, Eberhard Karls Universität Tübingen, 72076 Tübingen, Germany

<sup>a)</sup>Electronic mail: [stefan.behnle@uni-tuebingen.de](mailto:stefan.behnle@uni-tuebingen.de).

<sup>b)</sup>Electronic mail: [reinhold.fink@uni-tuebingen.de](mailto:reinhold.fink@uni-tuebingen.de).

## ABSTRACT

We propose a new perturbation theoretical approach to the electron correlation energy by choosing the zeroth order Hamiltonian as a linear combination of the corresponding “Retaining the Excitation degree” (RE) and the Møller-Plesset (MP) operators. In order to fulfill Kato cusp conditions, the RE and MP contributions are chosen to sum up to one.  $15\% \pm 5\%$  MP contribution is deduced to be in an optimal range from a fit of the first order REMP wavefunction to near full configuration interaction reference data. For closed shell systems, the same range of MP weights shows best performance for equilibrium bond distances and vibrational wavenumbers of diatomic molecules, the reaction energies in the spin component scaled MP2 fit set, the transition energies of the BHPERI test set, and the parameterized coupled cluster with singles and doubles (pCCSD) fit set. For these properties, REMP outperforms all other tested perturbation theories at second order and shows equal performance as the best coupled pair approaches or pCCSD methods as well as the best double hybrid density functionals. Furthermore, REMP is shown to fulfill all required fundamental boundary conditions of proper wavefunction based quantum chemical methods (unitary invariance and size consistency).

Published under license by AIP Publishing. <https://doi.org/10.1063/1.5086168>

## I. INTRODUCTION

The oldest but still most used perturbation theoretical (PT) approach to the electron correlation energy is the Møller-Plesset (MP) method<sup>1,2</sup> which is defined by setting the unperturbed Hamiltonian to the Fock-operator. MP-PT has the advantage of being size consistent,<sup>3,4</sup> invariant with respect to any unitary transformation of the occupied or virtual orbitals<sup>5</sup> and extensible to unrestricted and multireference cases.<sup>6–9</sup> Formally, the computational effort of MP2 scales with the fifth power of the system size which renders MP2 still useful for large systems. Furthermore, a multitude of efficient MP2 approximations have been proposed that allow the application whenever it is possible to generate a suitable reference wavefunction;<sup>10–13</sup> see also the introduction of Ref. 14.

Known drawbacks of MP-PT are its poor performance for systems with clustering of electron pairs<sup>2</sup> like late transition metals or even the neon atom for which the perturbation series was shown

to diverge!<sup>15</sup> To overcome these shortcomings, several modifications of MP-PT were proposed. The most successful variants are spin component scaled MP2 (SCS-MP2)<sup>16–18</sup> and orbital-optimized MP2 (OO-MP2).<sup>14,19–21</sup> The SCS-MP2 model was proposed as an *ad hoc* parameterization of the same-spin and opposite-spin components of the MP2 correlation energy. The parameter choice was motivated by the aim to mostly retain the total MP2 correlation energy and to correct that MP2 underestimates the correlation energy of two electron systems like helium or H<sub>2</sub>. The actual parameters were fitted by minimizing the least square deviation for a set of reaction energies. Further theoretical considerations allowed us to motivate the SCS-MP2 parameterization and to turn SCS-MP2 in the second order energy of a fully fledged perturbation theory.<sup>18,22</sup> OO-MP2 minimizes the MP2 energy by varying the occupied orbitals of the reference wavefunction. This is most successful if the reference wavefunction is severely damaged, e.g., by spin contamination.<sup>14</sup>

The Møller-Plesset partitioning is not the only possible partitioning of the electronic Hamiltonian. The “Retaining the Excitation degree” (RE) partitioning which has been developed by one of the authors<sup>23,24</sup> is a competing scheme which includes a more complex unperturbed Hamiltonian than MP. It is based on the idea that the configurations in an  $N$ -electron wavefunction basis can be assigned an excitation degree relative to the predefined orbital sets. The zeroth order Hamiltonian accounts for all interactions between configurations that have the same number of electrons in these subsets. For closed-shell singlet reference cases, RE2 is identical to the simplest coupled electron pair approach (CEPA) termed CEPA/0(D)<sup>25,26</sup> which belongs to the set of coupled-pair type methods<sup>27,28</sup> and dates back to Kelly.<sup>29–31</sup> CEPA/0(D) can be derived in various ways and is equivalent to linearized coupled-cluster with doubles (LCCD)<sup>32–34</sup> originally named linearized coupled-pair many-electron theory (LCP-MET),<sup>35,36</sup> many body perturbation theory with all orders in double-excitation diagrams [MBPT-D( $\infty$ )],<sup>37,38</sup> or optimized partitioning perturbation theory (OPT-PT).<sup>39,40</sup>

Recently, one of the present authors identified systematic errors in first order wavefunctions of different PT methods.<sup>41</sup> Accordingly, RE2 has a slight tendency to overestimate the correlation energy due to configuration state functions (CSFs) that are of singlet-coupled doubly excited (SDE) type. Simultaneously, it underestimates correlation contributions from triplet-coupled doubly excited (TDE) CSFs to a somewhat larger degree. On the other hand, MP2 overestimates the contributions of the TDEs and underestimates those of the SDEs substantially. Based on the observation of the inverted trends of wavefunction errors in the first order wavefunction, we investigate in the following whether it is possible to set up a perturbation theory termed “REMP” where these errors cancel by design. Hereby, the ultimate but ambitious goal is to develop an “ideal PT”<sup>41</sup> that reproduces the full configuration interaction (FCI) double coefficients in the first order perturbed wavefunction and thus the FCI energy with the second order PT-energy.

The paper is structured as follows: In Sec. II, the REMP approach is proposed and our implementation is described. Additionally, an approach that allows us to judge the quality of a wavefunction by means of an overlap criterion is developed. In Sec. III, computational details are described as well as the performance of REMP wavefunctions in comparison to high level coupled-cluster calculations with up to quadruple excitations as well as other approaches. Furthermore, the performance of REMP for molecular and thermochemical properties is investigated in Sec. IV where we try to obtain an unbiased assessment of our new method by validating it with benchmark sets that were used before for alternative approaches like SCS-MP2,<sup>16</sup> CEPA,<sup>42,43</sup> or parameterized coupled cluster with singles and doubles (pCCSD).<sup>44,45</sup> Conclusions and an outlook are given in Sec. V.

## II. THEORY

### A. REMP perturbation theory

Throughout this article, the indices  $i, j, k, l$  represent occupied orbitals, while  $a, b, c, d$  are used for virtual and  $p, q, r, s$  for arbitrary orbitals.

Rayleigh-Schrödinger perturbation theory<sup>46</sup> can be used to incorporate electron correlation into electronic wavefunctions.<sup>47,48</sup>

The electronic Hamiltonian  $\hat{H}$  is partitioned into an unperturbed part  $\hat{H}^{(0)}$  for which

$$\hat{H}^{(0)}\Psi^{(0)} = E^{(0)}\Psi^{(0)} \quad (1)$$

is exactly fulfilled and a perturbation  $\hat{H}^{(1)}$ .

In the formalism of second quantization, the electronic Hamiltonian reads<sup>48–50</sup>

$$\hat{H} = \sum_{p,q} h_{pq} \hat{a}_p^\dagger \hat{a}_q + \frac{1}{2} \sum_{pqrs} \langle pq|rs \rangle \hat{a}_p^\dagger \hat{a}_q^\dagger \hat{a}_s \hat{a}_r, \quad (2)$$

where  $h_{pq}$  is a matrix element of the one-electron Hamiltonian,  $\langle pq|rs \rangle = \int \phi_p^*(1) \phi_q^*(2) \frac{1}{r_{12}} \phi_r(1) \phi_s(2) dr$  is a two-electron repulsion integral (ERI) in Dirac notation, and  $\hat{a}/\hat{a}^\dagger$  are the annihilation/creation operators of the second quantization formalism. The MP partitioning uses the Fock operator,  $\hat{F}$ , as unperturbed zeroth order Hamiltonian

$$\hat{H}_{\text{MP}}^{(0)} = \hat{F} = \sum_{p,q} F_{pq} \hat{a}_p^\dagger \hat{a}_q. \quad (3)$$

Using the second quantization Hamiltonian [Eq. (2)], RE-PT can be defined by grouping the spin orbitals in orbital spaces. In this work, two such spaces are chosen: (i) the occupied and (ii) the virtual orbitals in the closed shell Hartree-Fock reference wavefunction. Now we can define an excitation degree,  $n_{\text{ex}}$ , which is in our case the number of electrons in the virtual orbital space. The zeroth order Hamiltonian includes all terms of the second quantization Hamiltonian that do not change the excitation degree

$$\hat{H}_{\text{RE}}^{(0)} = \sum_{\substack{p,q; \\ \Delta n_{\text{ex}}=0}} h_{pq} \hat{a}_p^\dagger \hat{a}_q + \frac{1}{2} \sum_{\substack{p,q,r,s; \\ \Delta n_{\text{ex}}=0}} \langle pq|rs \rangle \hat{a}_p^\dagger \hat{a}_q^\dagger \hat{a}_s \hat{a}_r. \quad (4)$$

We define the REMP method by setting the unperturbed Hamiltonian to a constrained mixture of corresponding RE and MP counterparts as

$$\hat{H}_{\text{REMP}}^{(0)} = (1 - A) \cdot \hat{H}_{\text{RE}}^{(0)} + A \cdot \hat{H}_{\text{MP}}^{(0)}. \quad (5)$$

Note that every linear combination of  $\hat{H}_{\text{RE}}^{(0)}$  and  $\hat{H}_{\text{MP}}^{(0)}$  fulfills the zeroth order perturbation equation [Eq. (1)] which is required for the perturbation theory. We choose the constraint that their contributions sum up to unity to guarantee that the exact REMP wavefunctions obey the electron-electron Kato cusp conditions.<sup>51,52</sup> The latter result from the balance between kinetic and electron-electron repulsion energies in the short distance limit. In a PT approach, this requires that the unscaled kinetic energy operator appears in  $\hat{H}^{(0)}$  since the full electron-electron repulsion operator is contained in  $\hat{H}^{(1)}$ .<sup>18</sup> Loosening this constraint leads to models that are related to the Feenberg-Goldhammer scaling method.<sup>53–55</sup>

In this work, we investigate the performance of REMP at second order for electronic energies which means that  $A = 0$  corresponds to RE2 and  $A = 1$  corresponds to MP2 energies. Furthermore, if wavefunctions are considered, these are first order in PT. The choice of  $\hat{H}^{(0)}$  is motivated by our previous study<sup>41</sup> where it was found that for the water molecule in a cc-pVDZ<sup>56</sup> basis, RE2 recovers 100.2% of the correlation energy resulting from singlet-coupled double excitations (SDEs, see Sec. II C for the definition) and 97.7% of the correlation energy resulting from triplet-coupled

double excitations (TDEs), whereas MP2 provides 86.3% of the SDE correlation energy and 116.6% of the TDE correlation energy. A linear interpolation of these correlation energy contributions allows us to estimate that at  $A \approx 0.1$  the amount of recovered SDE and TDE correlation energies amounts to about 99%, this corresponds to a 90:10 mixture of RE and MP. Similar considerations of further systems studied in Ref. 41 lead to the conclusion that  $A$  should be in the range between 0.1 and 0.2. As REMP with  $A = 0.15$  showed a balanced performance for the various tests described below and as a fixed mixing ratio is required for reasonable applications, REMP(0.15) results are presented for all cases discussed below.

The primary implementation of REMP was done as an extension of an arbitrary order determinantal CI program.<sup>57,58</sup> The same code already was used for the evaluation of REN.<sup>24</sup> For REMP, one additionally needs the matrix representation of  $\widehat{H}_{MP}^{(0)}$  which is diagonal for canonical orbitals. In the routine which solves the perturbation equations,<sup>59</sup> the appropriate linear combination of these  $\mathbf{H}^{(0)}$  matrices is determined. This program allows us to determine arbitrary orders of perturbation theory if the configuration space allows us to treat the FCI problem. The obvious drawback of this implementation is that the non-zero matrix elements of  $\widehat{H}$  and  $\widehat{H}^{(0)}$  are individually determined and stored which limits the application range to expansions with about  $10^6$  doubly excited determinants.

If one restricts the perturbation to second order, it is possible to reformulate REMP in a much more efficient way by making use of the fact that RE2 for closed-shell singlets just coincides with CEPA/0(D).<sup>24</sup> The whole formalism can then be treated by the direct CI framework developed by Roos<sup>60</sup> where storing the Hamiltonian matrix is avoided completely. According to Pulay, Saebø, and Meyer,<sup>61</sup> the direct CI problem can be cast into a set of highly efficient matrix equations (see also Refs. 43, 62, and 63). Inserting the doubles shift for CEPA/0(D) ( $\Delta^{ij} = 0$ ) into the doubles residuum equation, we obtain the RE part of the REMP residuals

$$\begin{aligned} \sigma_{ab,RE2}^{ij} &= \left( \widetilde{\Psi}_{ij}^{ab} \left| \widehat{H} - E_0 \right| \Psi \right) \\ &= K_{ab}^{ij} + \left\{ \mathbf{F}^V \mathbf{C}^{ij} + \mathbf{C}^{ij} \mathbf{F}^V \right\}_{ab} - \sum_{k=1}^{n_{occ}} \left( F_{jk} C_{ab}^{ik} + F_{ik} C_{ab}^{kj} \right) + K(\mathbf{C}^{ij})_{ab} \\ &\quad + \sum_{k,l=1}^{n_{occ}} K_{kl}^{ij} C_{ab}^{kl} + \sum_{k=1}^{n_{occ}} \left\{ (2\mathbf{C}^{ik} - \mathbf{C}^{ik+}) \left( \mathbf{K}^{kj} - \frac{1}{2} \mathbf{J}^{kj} \right) \right. \\ &\quad \left. + \left( \mathbf{K}^{ik} - \frac{1}{2} \mathbf{J}^{ik} \right) \left( 2\mathbf{C}^{kj} - \mathbf{C}^{kj+} \right) \right\}_{ab} - \sum_{k=1}^{n_{occ}} \left\{ \frac{1}{2} \mathbf{C}^{ik+} \mathbf{J}^{jk+} + \frac{1}{2} \mathbf{J}^{ik} \mathbf{C}^{kj+} \right. \\ &\quad \left. + \mathbf{J}^{jk} \mathbf{C}^{ik} + \mathbf{C}^{kj} \mathbf{J}^{ik+} \right\}_{ab}, \end{aligned} \quad (6)$$

where  $K_{rs}^{pq} = (pr|qs)$ ,  $J_{rs}^{pq} = (pq|rs)$ , and  $K(\mathbf{C}^{ij})_{ab} = \sum_{c,d} K_{cd}^{ab} C_{cd}^{ij}$ .  $\mathbf{F}^V$  represents the virtual-virtual sub-block of the Fock matrix and the braces  $\{\}_{ab}$  indicate that the  $(ab)$  element of the matrix that results from this operation shall be taken.

This matrix representation of the doubles correlation problem makes use of non-orthogonal CSFs (see Ref. 61 for further details) where the right-hand side (ket) wavefunctions are given by  $\Psi = \Phi_0 + \sum_{i \geq j} \sum_{ab} C_{ab}^{ij} \Psi_{ab}^{ij}$  with the doubly excited configurations  $\Psi_{ij}^{ab} = \Phi_{ij}^{ab} + \Phi_{ij}^{\bar{a}\bar{b}} + \Phi_{ij}^{\bar{a}b} + \Phi_{ij}^{a\bar{b}}$  for  $i > j$  and  $\Psi_{ii}^{ab} = \Phi_{ii}^{\bar{a}\bar{b}}$  for  $i = j$  where, e.g.,  $\Phi_{ij}^{\bar{a}\bar{b}}$  is the Slater determinant that results if the alpha spin orbital  $i$  is substituted

by  $a$  and the beta spin orbital  $j$  by  $b$ . The left-hand side configurations are given by  $\widetilde{\Psi}_{ij}^{ab} = \frac{1}{6} \left( \Phi_{ij}^{ab} + \Phi_{ij}^{\bar{a}\bar{b}} + 2\Phi_{ij}^{\bar{a}b} + 2\Phi_{ij}^{a\bar{b}} - \Phi_{ij}^{\bar{a}b} - \Phi_{ij}^{a\bar{b}} \right)$  for  $i > j$  and  $\widetilde{\Psi}_{ii}^{ab} = \Phi_{ii}^{\bar{a}\bar{b}}$  for  $i = j$ .

The equivalent residuum equation for MP2 has been derived by Pulay and Saebø<sup>64</sup> as

$$\sigma_{ab,MP2}^{ij} = K_{ab}^{ij} + \left\{ \mathbf{F}^V \mathbf{C}^{ij} + \mathbf{C}^{ij} \mathbf{F}^V \right\}_{ab} - \sum_k \left( F_{ik} C_{ab}^{kj} + F_{kj} C_{ab}^{ik} \right). \quad (8)$$

As the terms in the MP2 residuum are identical to the first three terms in the RE2 residuum,

$$\sigma_{ab,REMP}^{ij} = (1 - A) \sigma_{ab,RE2}^{ij} + A \sigma_{ab,MP2}^{ij} \quad (9)$$

can be obtained by multiplying the fourth to seventh terms in Eq. (7) by  $(1 - A)$ . Therefore, REMP2 can be easily implemented in any matrix oriented CI or CEPA code. Amplitude update is done with the perturbative estimate

$$C_{ab}^{ij}(n+1) = C_{ab}^{ij}(n) - \frac{\sigma_{ab}^{ij}}{F_{aa} + F_{bb} - F_{ii} - F_{jj} + \delta_{ls}}, \quad (10)$$

where, e.g.,  $F_{ii}$  is a diagonal element of the Fock matrix in the MO basis and  $\delta_{ls}$  is an adjustable level shift parameter. The perturbative update scheme is coupled with a standard direct inversion in the iterative subspace (DIIS) extrapolation scheme of the amplitudes using the residuum vectors  $\sigma^{ij}$  as DIIS error vectors.<sup>63,65-67</sup> Level shifting and DIIS extrapolation may influence the rate of convergence but do not affect the converged amplitudes. In conjunction with OpenMP<sup>68</sup> shared-memory parallelization and an efficient basic linear algebra subprograms (BLAS) library,<sup>69</sup> our implementation allows us to perform conventional configuration interaction with singles and doubles (CISD) calculations with  $500 \times 10^6$  configurations on a single high performance compute node within about 4 days.

Briefly we note that the introduction of mixing/scaling parameters into the residuum equations is not unprecedented but also used, e.g., in the framework of the parameterized CCSD (pCCSD) model.<sup>44,45</sup>

## B. Choice of the zeroth order wavefunction

Whenever perturbation theory is used, the question of the unperturbed zeroth order wavefunction arises. In the case of REMP, this is especially interesting as we are hybridizing different unperturbed Hamiltonians. A closed shell singlet Hartree-Fock reference wavefunction is a natural choice for the unperturbed wavefunction as it is an eigenfunction of both  $\widehat{H}_{RE}^{(0)}$  and  $\widehat{H}_{MP}^{(0)}$ . This is our choice for the present investigation while extensions to unrestricted or multireference wavefunctions shall be investigated in subsequent studies.

## C. Configuration state functions

All analyses of wavefunctions in this contribution have been performed in the basis of the Serber Configuration State Functions (CSFs).<sup>70,71</sup> In contrast to determinants, these are always eigenfunctions of the  $\widehat{S}^2$  operator and therefore better suited for analyzing systematic trends. Serber CSFs therefore provide a more natural and compact representation of the wavefunction. This partitioning of the

doubly excited manifold of the wavefunction has been used already in a previous study by one of us<sup>41</sup> and has proven to be meaningful. The Serber CSFs give rise to two different kinds of doubly excited singlet states, namely, the singlet coupled double excitations (SDEs)

$$\Psi_{ij,\text{SDE}}^{ab} = \frac{1}{2\sqrt{(1+\delta_{ij})(1+\delta_{ab})}} \left( \Phi_{ij}^{\bar{a}b} + \Phi_{ij}^{a\bar{b}} - \Phi_{ij}^{\bar{a}b} - \Phi_{ij}^{a\bar{b}} \right), \quad (11)$$

and the triplet coupled double excitations (TDEs)<sup>41,70,71</sup>

$$\Psi_{ij,\text{TDE}}^{ab} = \frac{1}{\sqrt{12}} \left( 2\Phi_{ij}^{\bar{a}b} + 2\Phi_{ij}^{ab} + \Phi_{ij}^{\bar{a}b} + \Phi_{ij}^{\bar{a}b} + \Phi_{ij}^{ab} + \Phi_{ij}^{ab} \right). \quad (12)$$

The definition of the SDEs includes the cases where two electrons are excited out of the same spatial orbital or into the same spatial orbital. Using Serber CSFs instead of determinants has furthermore the big advantage that the Hamiltonian matrix is partly decoupled: All matrix elements between SDEs and TDEs are zero except those between CSFs that differ by at most one occupied and one virtual index.

#### D. Wavefunction error analysis

Commonly, empirical parameters in quantum chemical models are determined on the basis of energies or properties, that is, the parameters are varied until the model predicts some ten to a few hundred reference values as good as possible. As REMP is a parameterized wavefunction-based method, we propose to find reliable parameters by comparing the resulting wavefunctions with accurate reference wavefunctions. As the wavefunction of a quantum mechanical system ultimately contains all information about this system, we think that such a criterion can deliver additional information for assessing accurate general purpose approaches.

As a reasonable, albeit non-unique, indicator of the wavefunction error of a given method  $M$ , we chose the squared norm of the difference between the wavefunction obtained with this method,  $\Psi(M)$ , and a reference wavefunction,  $\Psi(R)$ ,

$$d_M(X) = \langle |\Psi(M) - \Psi(R)|_X^2 \rangle. \quad (13)$$

In the first order perturbed wavefunctions considered in the following, only doubly excited configurations are included. Thus, we restrict the wavefunction difference in Eq. (13) to the space  $X$  of all doubly excited (ADE) configuration. As the spin-coupling within double excitations has been identified to behave differently, the SDE and TDE configuration spaces are also briefly considered. As rather accurate and still tractable approximation to FCI,  $\Psi(R)$  was obtained at the coupled cluster with singles, doubles, triples and quadruples (CCSDTQ)/cc-pVQZ level of theory and intermediate normalization was used for both wavefunctions. With these definitions, the wavefunction error indicator can be conveniently evaluated by

$$d_M(X) = \sum_{ijab} \left( c_{ab,X}^{ij}(M) - c_{ab,X}^{ij}(R) \right)^2, \quad (14)$$

where  $c_{ij,X}^{ab}(M)$  represents the double excitation CI-coefficient of the configuration space  $X$  with the method  $M$  and the orbital indices run over all possible values for  $X$ .

We mention that Pape and Hanrath defined a related wavefunction variance and further measures that can also be used to assess

approximate wavefunctions on the basis of FCI counterparts.<sup>72</sup> Furthermore, we investigated other wavefunction error indicators and one of our referees pointed out that reduced density matrices may also be utilized to assess errors related to wavefunctions. As all our considerations lead to similar results, we keep the present work concise and limit our investigations to the criterion defined in Eq. (13).

### III. RESULTS

#### A. Computational details

All REMP calculations have been performed using a development version of the Bochum-Basel *ab initio* suite of programs. One version explicitly stores the matrix elements of the Hamiltonian and the unperturbed Hamiltonian and has been implemented as an extension of the existing RE-PT program<sup>17,18,24,41</sup> which is based on an open-ended determinantal CI program.<sup>57,58,73,74</sup> Furthermore, a matrix oriented REMP version was implemented as an extension of the MC-CEPA program<sup>75,76</sup> and is inspired by the matrix-driven CI program of ORCA (`mdci`). All CCSDTQ, CCSDT, and CCSD calculations were performed using the arbitrary order Coupled Cluster program MRCC<sup>77</sup> version 2017-09-25 by Kállay and Surján.<sup>78,79</sup> All CCSD(T) calculations were performed using ORCA 4.0.1.2.<sup>80,81</sup> For the comparison of the wavefunctions, `mrcc` has been interfaced with our programs to ensure that integrals, MOs, signs, etc., are identical. In all other cases where comparisons between programs were made, it was ensured that the basis definitions used are exactly the same. Experimental geometries were obtained from the NIST Computational Chemistry Comparison and Benchmark Database (CCCBDB),<sup>82-85</sup> and atomic weights were retrieved from the NIST Atomic Weights Database.<sup>86</sup> Basis sets were used as stored in the TurboMole 6.5<sup>87</sup> basis set library. If not available there, they were taken from the EMSL basis set exchange website.<sup>88-90</sup>

#### B. Unitary invariance and size consistency

For closed-shell singlet reference functions, REMP results are invariant with respect to any unitary rotation of the occupied and/or virtual orbitals as the unperturbed Hamiltonians of the respective parent methods (RE- and MP-PT) are not affected by these operations. The corresponding proof for RE-PT is given in Ref. 24 in Eq. (13) and the following paragraph (see also Refs. 91 and 92). Unitary invariance of the Fockian can be demonstrated with similar arguments (see also Ref. 5). Due to this unitary invariance, size consistency<sup>47</sup> of REMP is proven by the following argument: if the total system consists of non-interacting closed-shell subsystems with localized orbitals, then the unperturbed Hamiltonian breaks into distinct and uncoupled parts of the subsystems by the following argument: if the total system consists of non-interacting closed-shell subsystems with localized orbitals, then the unperturbed Hamiltonian breaks into distinct and uncoupled parts of the subsystems (see also Refs. 3, 5, 24, 91, and 92). That is, REMP is size consistent whenever the underlying reference wavefunction has this property.

Unitary invariance and size consistency of REMP2 were also tested numerically. For that purpose, calculations on water, methane, ethane, and a neon dimer were performed with both



canonical and Foster-Boys<sup>93</sup> localized molecular orbitals. In all cases, the converged energies of both calculations agree within a few picohartrees.

For testing size consistency, the water dimer of the SCS-MP2 fit set (see below) was chosen and the distance between both monomers was increased by  $10\,000a_0$ . The resulting energy agrees with the sum of the energies of the separated monomers within a few picohartree. The same result holds for the neon dimer (def2-TZVP basis, distance  $10\,000a_0$ ). The remaining energy differences can be explained by finite convergence criteria as well as the limited precision and numerical noise produced by double precision (64 bit) floating point arithmetics.

### C. Assessment of the REMP wavefunction

We performed REMP and CCSDTQ calculations with the cc-pVQZ basis set for 30 main group systems and three transition metal systems (see captions of Figs. 2 and 3, respectively; see also the [supplementary material](#) for corresponding atomic coordinates). The systems considered here are reasonably described by single configuration reference wavefunctions, and CCSDTQ usually accounts for more than 99.95% of the correlation energy which seems sufficient. CC calculations with higher excitation degrees proved to be hardly possible due to their high computational demand.

As in the previous study,<sup>41</sup> the CC amplitudes were converted to CI coefficients for determinants

$$c_{ab}^{ij} = t_{ab}^{ij} + t_a^i t_b^j - t_b^i t_a^j \quad (15)$$

which were transformed to CI coefficients for the Serber CSFs using Eqs. (11) and (12). REMP wavefunctions were obtained for  $A$  in the range between 0.00 and 0.20 (0.50 for the CO molecule) in steps of 0.01. These were compared with the CCSDTQ wavefunctions providing  $d_{\text{REMP}}(X)$  values for all double excitations ( $X = \text{ADE}$ ), as well as for the SDE and TDE subgroups.

Figure 1 shows  $d_{\text{REMP}}$  values as a function of the REMP parameter  $A$  for the CO molecule (numerical values are collected in Table S1 of the [supplementary material](#)). The best agreement of the REMP wavefunction with the ADE portion of its CCSDTQ counterpart is

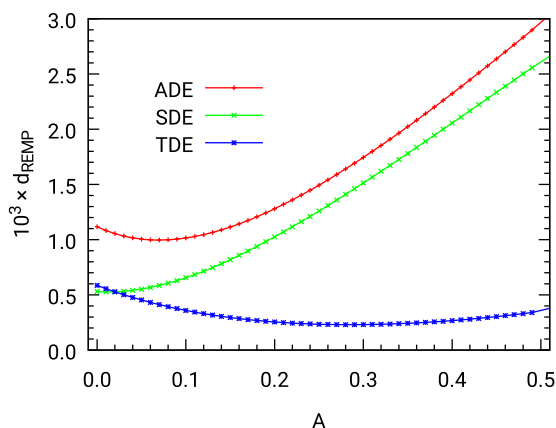


FIG. 1. Wavefunction error  $d_{\text{REMP}}$  as a function of  $A$  for the CO molecule with the cc-pVQZ basis.

found at  $A = 0.07$ . The corresponding  $d_{\text{REMP}}(\text{ADE})$ -value of  $1.0 \cdot 10^{-3}$  should be compared with the corresponding numbers of CCSD ( $1.2 \cdot 10^{-3}$ ), MP2 ( $6.5 \cdot 10^{-3}$ ), CISD ( $4.7 \cdot 10^{-3}$ ), and CCSDT ( $7.0 \cdot 10^{-6}$ ). Obviously, and as expected, the CCSDT wavefunction is in excellent agreement with the CCSDTQ reference while the REMP  $d$ -value indicates a slightly improved performance upon CCSD and a substantial better wavefunction than the MP and CISD counterparts. We note that breaking up the total error into separate parts for SDEs and TDEs reveals additional information. The delicate differences in the spin coupling of the electrons in the two singlet CSF types lead to remarkably different preferences for the MP fraction of the REMP Hamiltonian. While a low  $A$  value of about 0.02 is optimal for the SDEs, the TDE configurations are best represented with  $A = 0.28$ .

To get an impression of the systematical behavior upon variation of  $A$ , a set of closed shell species was investigated comprising 30 main group systems and three transition metal systems. The averaged wavefunction errors of the main group systems are plotted in Fig. 2, while those of the transition metal systems are depicted in Fig. 3. The systems are listed in the respective figure captions of Figs. 2 and 3 and their coordinates, as well as the numerical values of the wavefunction errors are collected in the [supplementary material](#).

Figure 2 shows that the averaged wavefunction errors of the main group elements behave similar to those of the CO molecule discussed above. The minimum of the ADE curve is more distinct than in the corresponding data of the CO molecule, but it is found at almost the same MP contribution (about 8%). An inspection of the individual systems shows that the best REMP wavefunctions are generally obtained for  $A$ -values between 0.02 and 0.12. However, the wavefunctions of systems with double and triple bonds as well as systems with crowded electron pairs like  $\text{F}_2$ , the Ne atom,  $\text{F}^-$ , NP, or MgO are best described with  $A$ -values around 0.1.

In Ref. 41, it was observed that RE- and MP-perturbation theories perform distinctly different for main group and transition metal systems. Thus, we also considered the wavefunction errors of the

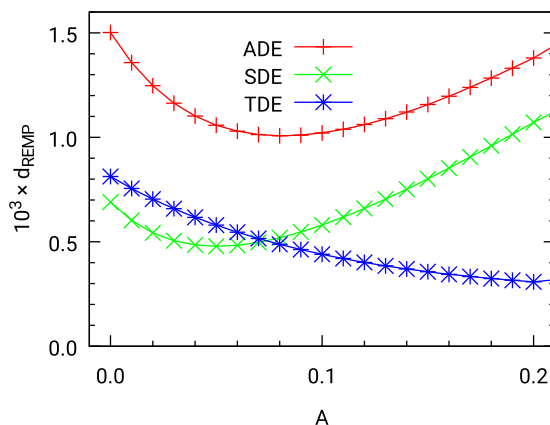
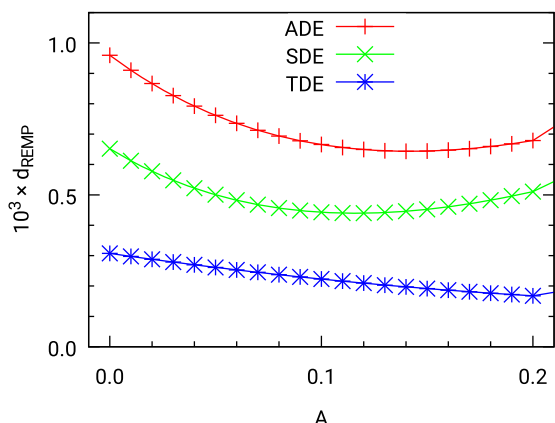


FIG. 2. Graphical representation of the wavefunction errors  $d_{\text{REMP}}$  averaged over the main group systems  $\text{H}_2$ ,  $\text{H}^-$ , LiH, He, Ne, Ar,  $\text{BeH}_2$ ,  $\text{BH}_3$ ,  $\text{BH}_4^-$ ,  $\text{CH}_2(^1A_1)$ ,  $\text{CH}_3^+$ ,  $\text{CH}_3^-$ ,  $\text{CH}_4$ ,  $\text{H}_2\text{O}$ , HF,  $\text{F}^-$ , LiF, BeO, BF, CO,  $\text{N}_2$ ,  $\text{NO}^+$ ,  $\text{CN}^-$ ,  $\text{F}_2$ , HCl,  $\text{Cl}^-$ , MgO, NP, SiO, and  $\text{C}_2\text{H}_2$  (ethyne). Basis set: cc-pVQZ. See Table S2 of the [supplementary material](#) for numerical values.



**FIG. 3.** Wavefunction error  $d_{\text{REMP}}$  averaged over the transition metal systems Zn,  $\text{Zn}^{2+}$ , and  $\text{Cu}^+$ .

metal systems (Zn,  $\text{Zn}^{2+}$ , and  $\text{Cu}^+$ ). The resulting averaged  $d_{\text{REMP}}(X)$  graphs are shown in Fig. 3 (see Table S3 of the [supplementary material](#) for numerical values). For the very strongly crowded electron pairs in these systems, even larger MP contributions of about 14% give rise to the average best wavefunctions.

In conclusion, for most of the more demanding systems, an MP contribution in the REMP-Hamiltonian in the order of 0.08–0.14 provides wavefunctions with smallest  $d_{\text{REMP}}(X)$  indicator. An individual inspection of the singlet- and triplet-coupled doubly excited configurations shows that smaller  $A$ -values of 0.02–0.12 are preferred for the SDEs, while the TDE contribution to the wavefunction is better represented with  $A > 0.2$ .

#### D. Geometrical parameters of main group diatomics

The nine main group diatomics AlH, BF, BH,  $\text{Cl}_2$ , CO, CS,  $\text{F}_2$ , HF, and  $\text{N}_2$  have been used by Wennmohs and Neese to benchmark coupled pair type methods for predicting equilibrium bond lengths  $r_e$  and equilibrium harmonic wavenumbers  $\tilde{\nu}_e$ .<sup>43</sup> In this work, only the valence electrons were correlated here, and the QZVP basis was used.<sup>94</sup> We tried to reproduce the numbers of Ref. 43 as close as possible; unfortunately, no exact protocol was given. Therefore, we describe our protocol as close as possible to facilitate future reproduction. Deviations between our results and those of Ref. 43 can be explained by different numbers and positions of sampling points and especially by different reduced masses.

The potential energy surface (PES) was scanned at 21 sampling points equally spaced around the experimental equilibrium geometry  $r_e$  reaching from  $r_e - 2x_0$  to  $r_e + 2x_0$ , where  $x_0 = \sqrt{\hbar/2\pi c\mu\tilde{\nu}_{e,\text{exp}}}$  is the classical turning point of the harmonic oscillator at its zero point energy with  $\hbar$ ,  $c$ , and  $\mu$  being the reduced Planck constant, the speed of light, and the reduced mass, respectively. As we are not only interested in  $r_e$  but also in  $\tilde{\nu}_e$ , the sampled area has been chosen such that at least the part of the PES which is relevant for the ground state vibrational wave function is covered sufficiently. The analysis was performed for isotopically pure species composed of the majority isotopes, and isotopic masses have been retrieved from the NIST Atomic Weights Database.<sup>86</sup> A Morse potential<sup>95</sup> was subsequently

fitted to the data points for obtaining  $r_e$  and  $\tilde{\nu}_e$

$$V_{\text{Morse}}(r) = \frac{\hbar\omega_e}{4x_e} \cdot \left(1 - e^{-\sqrt{\frac{2\mu x_e \omega_e}{\hbar}} \cdot (r-r_e)}\right)^2 + T_e. \quad (16)$$

Specifically, the Morse potential of Eq. (16) was used which directly delivers  $r_e$ ,  $\omega_e = 2\pi\tilde{\nu}_e c$ , and the anharmonicity  $x_e$ . Additionally, the uncertainties of the determined parameters can be estimated from the respective fit errors. The fit error of  $r_e$  was in all cases negligibly small and exceeded in almost no case 0.02 pm, except for  $\text{F}_2/\text{CEPA}/0(\text{SD})$  where the minimum was outside the sampled area. The fit error of  $\tilde{\nu}_e$  was at most  $\approx 4 \text{ cm}^{-1}$ . Errors of that size occurred however only for large anharmonicities, and in most cases, the uncertainty of  $\tilde{\nu}_e$  was well below  $1 \text{ cm}^{-1}$ . All data necessary for reproducing the PES scan can be found in Table S4 of the [supplementary material](#).

Table I impressively shows that REMP performs well for equilibrium bond distances and harmonic vibrational frequencies. In particular, all mixtures presented surpass their parent methods with respect to both measures. The results closest to the experiment are obtained with MP fractions of 10%–20%. Compared to the other coupled-pair type methods, REMP performs remarkably well. Out of 18 coupled pair functionals, CEPA/1(SD)<sup>25,26,42,96</sup> and the coupled pair functional (CPF) named CPF/1 have previously been identified as the most accurate coupled pair approaches for this test set.<sup>43</sup> With respect to  $r_e$ , REMP(0.15) is as accurate as these methods. We did not reevaluate CPF/1 as it has been shown to deliver virtually identical

**TABLE I.** Mean absolute errors of selected REMP mixing ratios and competing wave function methods relative to experimental data. All REMP results are based on second order energies. The numbers in brackets indicate the MP fraction. Basis: def2-QZVP. For post-HF methods, standard frozen core settings are used. Molecules: AlH, BF, BH,  $\text{Cl}_2$ , CO, CS,  $\text{F}_2$ , HF, and  $\text{N}_2$ .

Method	$r_e$ (pm)	$\tilde{\nu}_e$ ( $\text{cm}^{-1}$ )
REMP2(0.00) $\cong$ CEPA/0(D)	0.62	54.6
REMP2(0.10)	0.32	42.9
REMP2(0.15)	0.28	39.9
REMP2(0.20)	0.30	39.5
REMP2(0.25)	0.32	39.6
REMP2(0.50)	0.38	45.9
REMP2(0.75)	0.50	50.6
REMP2(1.00) $\cong$ MP2	0.64	61.2
CISD	1.18	97.6
CEPA/0(SD)	1.86	89.1
CEPA/1(SD)	0.30	27.5
MP3	0.92	96.3
SCS-MP2	0.40	46.0
CCSD	0.47	53.1
CCSD(T)	0.34	11.0
SCF	2.61	207.2
BP86 <sup>a</sup>	1.31	62.0
B3LYP <sup>a</sup>	0.71	30.7
B2-PLYP <sup>a</sup>	0.39	21.8

<sup>a</sup>Integration grid size 7.

results as CEPA/1 which is conceptually closer to our method. Furthermore, the best REMP mixture also outperforms SCS-MP2 with standard scaling parameters.

The performance of REMP for harmonic frequencies is a bit worse than that of CEPA/1 but still acceptable especially when compared to competing methods with the same formal  $n^6$  scaling. Briefly we note that Wennmohs and Neese obviously omitted the SCF result of  $F_2$  for averaging which is for sure theoretically justifiable. As mentioned before, CEPA/0 performs significantly poorer if single excitations are included, i.e., CEPA/0(D) is better than CEPA/0(SD).

Furthermore, for this set REMP(0.15) performs better than the common generalized gradient approximation (GGA) and hybrid density functionals BP86<sup>97,98</sup> and B3LYP,<sup>99-103</sup> respectively, and about as good as B2-PLYP.<sup>104</sup> Finally, we note that the informative value of the numbers in Table I is limited due to systematic errors in the combination of the QZVP basis set with the considered valence correlation. Thus, the available information does not allow to differentiate between the performance of REMP(0.15), CEPA/1(SD), CCSD(T), and B2-PLYP for bond distances, while CCSD(T) clearly predicts vibrational wavenumbers more accurately than CEPA/1(SD) and B2-PLYP which may be slightly more accurate than the REMP(0.15) values. In any case, the four approaches mentioned above outperform the other methods in Table I for  $r_e$  and  $\tilde{\nu}_e$  values.

To elucidate the error related to missing core correlation, we additionally performed the aforementioned calculations

**TABLE II.** Mean absolute errors of selected REMP mixing ratios and competing wave function methods relative to experimental data. All REMP results are based on second order energies. The numbers in brackets indicate the MP fraction. Basis: cc-pwCVQZ (H: cc-pVQZ). All electrons were active during the correlation treatment. Molecules: AlH, BF, BH, Cl<sub>2</sub>, CO, CS, F<sub>2</sub>, HF, and N<sub>2</sub>.

Method	$r_e$ (pm)	$\tilde{\nu}_e$ (cm <sup>-1</sup> )
REMP2(0.00) $\cong$ CEPA/0(D)	0.72	60.4
REMP2(0.10)	0.48	48.8
REMP2(0.15)	0.50	45.9
REMP2(0.20)	0.53	46.9
REMP2(0.25)	0.58	49.5
REMP2(0.50)	0.70	51.9
REMP2(0.75)	0.75	55.1
REMP2(1.00) $\cong$ MP2	0.82	63.0
CISD	1.92	123.2
CEPA/0(SD)	1.59	84.3
CEPA/1(SD)	0.40	35.1
MP3	1.21	102.6
SCS-MP2	0.49	47.4
CCSD	0.79	61.8
CCSD(T)	0.15	15.4
SCF	2.62	207.3
BP86 <sup>a</sup>	1.27	61.3
B3LYP <sup>a</sup>	0.78	39.2
B2-PLYP <sup>a</sup>	0.36	23.0

<sup>a</sup>Integration grid size 7.

without frozen cores for all post-HF methods (including B2PLYP) and appropriate basis sets (cc-pwCVQZ). The respective results are listed in Table II. As REMP now tends to systematically underestimate bond lengths (see Table S6 of the [supplementary material](#) for absolute numbers), the statistical descriptors are slightly worse than without core correlation. This is however not a unique feature of REMP, but applies to all coupled-pair type methods, CISD and CCSD. The only method which seems to benefit significantly from inclusion of core correlation is CCSD(T). In essence, only including core correlation even deteriorates the results obtained from coupled pair-type model chemistries. Other possible sources of systematic error are basis set incompleteness and missing relativistic effects. As these are effects that are commonly neglected in routine model chemistries, we did not investigate corrections for both.

#### IV. PERFORMANCE FOR THERMOCHEMICAL PROPERTIES

Prediction of thermodynamic and kinetic data is one of the most important and successful applications of computational chemistry. Therefore, the performance of REMP for the prediction of reaction energies and transition energies is investigated in Secs. IV A–IV C.

##### A. The SCS-MP2 calibration set

As SCS-MP2 is probably the best performing single reference perturbation theory, we decided to use the calibration set of SCS-MP2 to benchmark REMP. From the original set of reactions,<sup>16</sup> we omitted the reaction involving triplet methylene (42) as of now, our programs are restricted to closed shell singlet cases and the transition states [reactions (39)–(41)] because these are tested in the BHPERI test set (see below). The reference reaction energies have been recalculated at the CCSD(T) level of theory which leads to deviations of up to several kcal mol<sup>-1</sup> with respect to the original QCISD(T) results. We performed all calculations with both the cc-pVQZ and the def2-QZVP bases. However, the results are nearly the same; therefore, only the def2-QZVP results are presented.

Table III lists the results for all considered reactions for CCSD, SCS-MP2, REMP(0.12), and REMP(0.15). REMP shows the smallest errors for  $A = 0.12$ . Statistical measures for these methods are collected in Table IV (all evaluated data are shown in Table S7 of the [supplementary material](#)). With respect to the mean absolute deviation (MAD) and the root mean square (RMS) deviation, REMP(0.12) and REMP(0.15) clearly beat SCS-MP2 on its own calibration set. We note that REMP is particularly accurate for the isomerization reactions (28)–(34) and the noncovalent dimerization reactions (49)–(51).

While the CCSD and the SCS-MP2 error seem to be completely uncorrelated, there is a reasonable correlation between errors of CCSD and REMP(0.12) with a slope less than one. The largest reaction energy errors of REMP(0.12) involve either ozone [reactions (3) and (23)] or HNO<sub>2</sub> (reaction 10) and amount to  $-7.02$ ,  $-4.46$ , and  $-5.59$  kcal mol<sup>-1</sup>. For these reactions, CCSD shows even larger errors ( $-14.11$ ,  $-12.61$ , and  $-7.00$  kcal mol<sup>-1</sup>).

In order to track down the reason for the failure of REMP and CCSD for certain reactions, we computed the D1(MP2),<sup>105</sup>



TABLE III. Comparison of calculated reaction energies in kcal mol<sup>-1</sup>. Errors ( $\Delta\Delta E$ ) refer to CCSD(T). Basis: def2-QZVP.

	Reaction	$\Delta E$		$\Delta\Delta E$		
		CCSD(T)	CCSD	SCS-MP2	REMP(0.12)	REMP(0.15)
1	$F_2 + H_2 \rightarrow 2 HF$	-135.07	-2.98	-2.77	-0.48	-1.00
2	$F_2O + H_2 \rightarrow F_2 + H_2O$	-69.01	-2.74	-2.09	-2.69	-2.80
3	$O_3 + 3 H_2 \rightarrow 3 H_2O$	-225.14	-14.11	3.28	-7.02	-7.33
4	$H_2O_2 + H_2 \rightarrow 2H_2O$	-87.30	-1.92	-1.69	-1.04	-1.28
5	$CO + H_2 \rightarrow H_2CO$	-4.86	-0.10	0.77	-0.78	-0.83
6	$CO + 3 H_2 \rightarrow CH_4 + H_2O$	-64.51	-1.50	2.07	-2.56	-2.72
7	$N_2 + 3 H_2 \rightarrow 2 NH_3$	-38.96	-1.55	4.43	-1.70	-1.86
8	$^1CH_2 + H_2 \rightarrow CH_4$	-128.71	0.98	-1.98	-0.24	-0.71
9	$N_2O + H_2 \rightarrow N_2 + H_2O$	-81.47	-5.64	1.36	-3.97	-3.76
10	$HNO_2 + 3 H_2 \rightarrow 2 H_2O + NH_3$	-130.92	-7.00	1.47	-5.59	-5.62
11	$C_2H_2$ (ethyne) + $H_2 \rightarrow C_2H_4$	-49.38	-0.85	2.45	-0.82	-0.76
12	$H_2C=C=O + 2 H_2 \rightarrow H_2CO + CH_4$	-43.19	-2.16	0.77	-1.68	-1.58
13	Benzene + 3 $H_2 \rightarrow$ cyclohexane (chair)	-69.57	-4.34	2.91	-0.93	-0.96
14	$BH_3 + 3 HF \rightarrow BF_3 + 3 H_2$	-92.29	1.16	0.46	2.12	2.04
15	$HCOOH \rightarrow CO_2 + H_2$	2.33	1.22	-3.03	1.49	1.39
16	$CO + H_2O \rightarrow CO_2 + H_2$	-6.11	2.30	-1.86	2.31	2.06
17	$C_2H_2$ (ethyne) + $HF \rightarrow C_2H_3F$	-26.82	-0.16	2.84	0.06	0.15
18	$HCN + H_2O \rightarrow CO + NH_3$	-12.17	-0.70	1.73	0.52	0.59
19	$HCN + H_2O \rightarrow HCONH_2$	-21.44	0.31	2.60	1.05	0.94
20	$HCONH_2 + H_2O \rightarrow HCOOH + NH_3$	0.83	0.07	0.30	0.28	0.32
21	$HCN + NH_3 \rightarrow N_2 + CH_4$	-37.72	-0.66	-0.63	-0.34	-0.27
22	$CO + CH_4 \rightarrow H_3CCHO$	3.14	0.70	1.06	-0.15	-0.25
23	$O_3 + CH_4 \rightarrow 2 H_2O + CO$	-160.63	-12.61	1.21	-4.46	-4.61
24	$N_2 + F_2 \rightarrow N_2F_2$	17.12	1.84	4.73	2.22	2.07
25	$BH_3 + 2 F_2 \rightarrow BF_3 + 3 HF$	-249.35	-4.89	-2.50	0.73	-0.04
26	$2BH_3 \rightarrow B_2H_6$	-43.33	2.80	3.68	1.34	1.21
27	$2^1CH_2 \rightarrow C_2H_4$	-199.47	3.45	-4.06	0.47	-0.36
28	$H_3CONO \rightarrow H_3NO_2$	-3.52	1.05	-2.61	0.02	-0.21
29	$H_2C=C$ : (vinylidene) $\rightarrow C_2H_2$ (ethyne)	-44.90	1.38	-4.70	0.08	-0.25
30	Allene $\rightarrow$ propyne	-1.35	-0.31	-2.78	0.18	0.01
31	Cyclopropene $\rightarrow$ propyne	-23.35	-0.33	-1.11	0.35	0.34
32	Oxirane $\rightarrow H_3CCHO$	-26.28	-0.21	0.14	0.56	0.60
33	Vinyl alcohol $\rightarrow H_3CCHO$	-10.65	-0.23	-1.09	0.61	0.57
34	Cyclobutene $\rightarrow$ (E)-1,3-butadiene	-11.30	0.32	0.79	-0.02	0.14
35	$C_2H_4 + ^1CH_2 \rightarrow$ cyclopropane	-107.42	1.57	-2.88	-0.19	-0.83
36	$C_2H_2 + C_2H_4 \rightarrow$ cyclobutene	-32.45	0.33	1.40	-0.38	-0.53
37	(E)-1,3-butadiene + $C_2H_4 \rightarrow$ cyclohexene	-44.89	-0.31	-0.13	0.08	-0.26
38	$3C_2H_2$ (ethyne) $\rightarrow$ benzene	-153.24	2.03	4.44	-1.46	-1.74
43	$HF + H^+ \rightarrow H_2F^+$	-122.20	-0.43	0.11	-0.38	-0.34
44	$H_2O + H^+ \rightarrow H_3O^+$	-172.23	-0.78	-0.03	-0.55	-0.50
45	$NH_3 + H^+ \rightarrow NH_4^+$	-212.38	-0.88	-0.43	-0.47	-0.42
46	$F^- + H^+ \rightarrow HF$	-383.22	-0.73	1.33	-0.64	-0.53
47	$OH^- + H^+ \rightarrow H_2O$	-405.17	-1.29	1.35	-0.93	-0.81
48	$NH_2^- + H^+ \rightarrow NH_3$	-419.60	-1.66	0.39	-0.90	-0.81
49	$2NH_3 \rightarrow (NH_3)_2$	-3.12	0.30	0.41	0.15	0.14
50	$2H_2O \rightarrow (H_2O)_2$	-5.02	0.31	0.44	0.19	0.18
51	$2HF \rightarrow (HF)_2$	-4.64	0.21	0.40	0.15	0.14

**TABLE IV.** Statistics for the SCS-MP2 sets in kcal mol<sup>-1</sup>. Errors ( $\Delta\Delta E$ ) refer to CCSD(T). Basis: def2-QZVP.

	CCSD	SCS-MP2	REMP(0.12)	REMP(0.15)
Considering all reactions in Table III				
MAD	1.99	1.82	1.18	1.21
RMSD	3.46	2.26	1.88	1.91
Max	14.11	4.73	7.02	7.33
Excluding reactions involving O <sub>3</sub> (3 and 23)				
MAD	1.48	1.80	0.97	1.00
RMSD	2.13	2.25	1.47	1.47
Max	7.00	4.73	5.59	5.62

D2(MP2),<sup>106</sup> and T1(CCSD)<sup>107</sup> diagnostics for the molecules in Table III. The most unfavorable parameters were obtained for O<sub>3</sub> with D1(MP2)/D2(MP2)/T1(CCSD) = 0.055/0.261/0.027, while HNO<sub>2</sub> provides 0.053/0.201/0.020. In these cases, the diagnostic parameters are clearly above the respective warning thresholds (0.040/0.18/0.02). Further critical molecules are N<sub>2</sub>O (0.045/0.181/0.020) and F<sub>2</sub>O (0.032/0.173/0.016) which show the next largest errors of REMP(0.12). In these cases, the diagnostic parameters indicate that the Hartree-Fock determinant is no longer an appropriate zeroth order wavefunction. Thus, REMP (as well as CCSD) fails in cases where poor performance can be expected.

As ozone exhibits a strong multireference character, all reactions with this molecule were excluded from the test set in Ref. 14. If we do so, the mean absolute deviations of REMP(0.12) and REMP(0.15) reach the 1 kcal mol<sup>-1</sup> value of chemical accuracy, while the SCS-MP2 value is essentially unaffected. REMP also seems to be superior to commonly used density functionals. For plain B3LYP and the original set, Grimme<sup>16</sup> found a MAD of 2.7 kcal mol<sup>-1</sup>.

## B. The BHPERI set

In order to test the performance for transition states, we selected the BHPERI test set contained in the GMTKN24 benchmark set collection.<sup>108</sup> The BHPERI set consists of 26 activation barriers for pericyclic reactions of closed-shell molecules. We selected those 24 reactions whose constituents were tractable by our current program, i.e., we excluded reactions (9) and (10). We chose again the def2-QZVP basis set and did not consider core excitations. The reference activation barriers were taken from a recent publication by Karton and Goerigk<sup>109</sup> who found the original CBS-QB3 activation barriers to be quite inaccurate. Table V lists statistical descriptors for the performance of several REMP mixing ratios, for SCS-MP2, and density functional theory (DFT) for typical generalized gradient approximation (GGA) functionals, hybrid functionals, and the best double hybrid functionals.

Pure RE overestimates the activation barriers systematically. This is a well-known shortcoming of CEPA type methods.<sup>33</sup> MP2, on the other hand, drastically underestimates the activation energies of the BHPERI set. It should therefore be possible to find one or more values for  $A$  which give rise to zero mean deviation.

**TABLE V.** Statistical errors of different REMP mixtures averaged over 24 reactions of the BHPERI set; errors refer to the reference values of Ref. 109. Basis set: def2-QZVP. Values are in kcal mol<sup>-1</sup>. For comparison, a selection of commonly used density functionals is also included.

Method	MD	MAD	RMS	Max. error
REMP(0.00)≅CEPA/0(D)	1.68	1.79	2.02	4.03
REMP(0.10)	0.96	1.12	1.34	3.49
REMP(0.12)	0.80	1.00	1.23	3.38
REMP(0.14)	0.64	0.89	1.12	3.26
REMP(0.15)	0.56	0.84	1.08	3.20
REMP(0.16)	0.48	0.79	1.03	3.14
REMP(0.18)	0.32	0.70	0.97	3.03
REMP(0.20)	0.15	0.63	0.94	2.91
REMP(0.22)	-0.02	0.64	0.93	2.79
REMP(0.23)	-0.10	0.68	0.94	2.73
REMP(0.25)	-0.27	0.78	0.99	2.60
REMP(1.00)≅MP2	-7.48	7.48	7.86	11.03
SCS-MP2	-0.70	1.16	1.40	2.93
BP86 <sup>a</sup>	-6.71	6.71	6.96	10.00
B3LYP <sup>a</sup>	-0.68	1.06	1.32	2.70
PW6B95 <sup>a</sup>	-0.07	1.10	1.32	3.00
M06-2X <sup>a</sup>	0.55	1.24	1.63	4.40
B2-PLYP <sup>a</sup>	-1.62	1.64	1.78	3.10
B2GP-PLYP <sup>a</sup>	-1.53	1.53	1.70	3.20
PWPB95 <sup>a</sup>	-0.05	0.84	0.95	1.80

<sup>a</sup>Data taken from the supplementary material of Ref. 109. All functionals include a D3 or D3(BJ) dispersion correction, averaging was done only over those 24 reactions considered in this paper, and therefore the statistics slightly deviate from those of Ref. 109.

In the case of the BHPERI set, a larger MP fraction than before (20% instead of 12%) was found to give the best agreement with the reference activation barriers. Also REMP(0.15) performs quite well. Furthermore, SCS-MP2 is outperformed by REMP with respect to all measures for  $A = 0.20$ .

Nevertheless, this results of course from the compensation of various errors, namely, basis set incompleteness, missing core correlation, missing single excitations, missing higher excitations, and the intended cancellation of energy denominator errors. The ideal mixing ratios are therefore best characterized as “Pauling Points” in the parameter space.

For the BHPERI set, there are results for a multitude of density functionals available.<sup>108,109</sup> When the results of Table V are compared to those of Tables 5 and 6 of Ref. 109, it is found that on average the best REMP mixing beats all available functional classes. For this specific set, REMP(0.20) shows a slightly smaller MAD (0.63 kcal mol<sup>-1</sup>) than all the six double hybrid density functionals (DHDFs) investigated in Ref. 109. With an MAD of 0.84 kcal mol<sup>-1</sup>, REMP(0.15) performs equally well as the best performing DHDF PWPB95.

## C. The pCCSD calibration set

When looking for competing methods with the same formal scaling as REMP ( $n^6$ ), the parameterized coupled cluster methods<sup>44,45</sup> are probably the theoretically most sound. We therefore

**TABLE VI.** Statistical error descriptors of different REMP mixtures averaged over 36 reactions of the pCCSD calibration set; errors refer to the CCSD(T) reference values of Ref. 45. Basis set: def2-QZVPP. Values are in kcal mol<sup>-1</sup>. Total energies can be found in Table S10 of the [supplementary material](#).

Method	MD	MAD	SD	RMS	Max. error
REMP(0.00)	0.20	1.19	1.89	1.88	6.04
REMP(0.10)	-0.20	0.82	1.27	1.27	4.86
REMP(0.11)	-0.23	0.80	1.24	1.25	5.01
REMP(0.12)	-0.27	0.78	1.22	1.24	5.16
REMP(0.13)	-0.30	0.76	1.21	1.23	5.30
REMP(0.14)	-0.34	0.75	1.20	1.23	5.44
REMP(0.15)	-0.37	0.75	1.21	1.24	5.58
REMP(0.16)	-0.40	0.77	1.21	1.26	5.71
REMP(0.17)	-0.43	0.80	1.23	1.28	5.84
REMP(0.18)	-0.46	0.82	1.25	1.31	5.97
REMP(0.19)	-0.49	0.85	1.27	1.35	6.09
REMP(0.20)	-0.52	0.88	1.30	1.38	6.21
REMP(1.00)	-1.87	3.61	5.49	5.73	19.53
CCSD <sup>a</sup>		1.17	1.56	1.71	5.67
pCCSD/1a <sup>a</sup>		0.86	1.25	1.23	3.57
pCCSD/1b <sup>a</sup>		0.83	1.18	1.17	2.70
CEPA/1 <sup>a</sup>		0.85	1.20	1.18	3.30
B3LYP <sup>a</sup>		2.63	3.29	3.44	9.45

<sup>a</sup>Table I of Ref. 45.

decided to benchmark REMP against the first set that was used in Ref. 45 to calibrate pCCSD/1a and pCCSD/1b. This set consists of 36 reaction energies of 44 small closed shell molecules and partly overlaps with the SCS-MP2 calibration set. Table VI contains the statistical error descriptors for the pCCSD set for selected REMP mixtures. In excellent agreement with the previous results, we find again that a mixture of about 15% MP and 85% RE yields results that are closest to CCSD(T). The overall performance of REMP(0.15) is comparable to that of pCCSD/1b. We note that the REMP(0.15) MAD value of 0.75 kcal mol<sup>-1</sup> is slightly smaller than the best parameterized CCSD result (pCCSD/1b) of 0.83 kcal mol<sup>-1</sup>. However, the largest REMP error is bigger than the pCCSD value. Specifically, this error always occurs for reaction (34) (NF<sub>3</sub> + 3H<sub>2</sub> → NH<sub>3</sub> + 3HF). If this reaction was excluded from the set, also the largest error would be comparable to that of pCCSD/1b. Interestingly, for this reaction, CCSD is also off by -6.5 kcal mol<sup>-1</sup>, which indicates that it is crucial to explicitly account for triple excitations in this case. For this set, plain B3LYP is clearly inferior to all tested CCSD and CEPA variants.

## V. SUMMARY AND OUTLOOK

We have proposed and investigated a new type of hybrid perturbation theory termed REMP that emerges from mixing the unperturbed Hamiltonians of RE and MP-PT. Using only a single empirical parameter, systematic errors of the first-order wavefunctions have been minimized for a set of molecules. The obtained mixing ratio of 10%-20% MP contribution to the unperturbed Hamiltonian is consistent with qualitative estimates.

Compared to its parent methods, REMP delivers better wavefunctions and provides more accurate geometries and reaction energies. In contrast to some of the competing schemes, it is the first (useful) member of a well-defined perturbation series and still obeys all fundamental boundary conditions. From its parent methods, REMP inherits the important features of being strictly size consistent, size extensive, and unitary invariant. This was shown analytically and also confirmed numerically up to picohartree accuracy. Finally, the implementation of the second order PT is straightforward in existing CISD codes.

Performance of the REMP method was tested with a wavefunction error indicator and test sets for equilibrium bond distances, equilibrium vibrational wavenumbers, reaction energies, and activation barriers that have been taken from previous studies in order to avoid a biased sample selection. We found that a mixing ratio of 15% MP- and 85% RE-contribution to the unperturbed Hamiltonian performs best on average and we recommend to use this in further applications of the method. REMP(0.15) outperforms SCS-MP2 as well as all GGA and hybrid DFT approaches for all investigated properties with the exception of B3LYP for the case of equilibrium wavenumbers  $\tilde{\nu}_e$ . For thermochemical test sets, typical errors are close to or better than 1 kcal mol<sup>-1</sup>. This performance is similar to that of CEPA/1 and parameterized coupled cluster theory (pCCSD/1b), as the best coupled pair type approaches, as well as the best double hybrid density functionals. Large errors are observed only in those cases where single reference correlation methods are expected to fail. While these results are very promising, further tests are needed to explore the general applicability of REMP.

As an original wavefunction based approach, REMP can be extended in several directions. In particular, it can be applied in multi-configuration perturbation theory where the RE partitioning has shown promising performance.<sup>23,32,110,111</sup> Given the success of orbital-optimized methods (OO-MP2<sup>4,21</sup> and OO-CEPA<sup>112</sup>), the implementation of OO-REMP looks promising. In particular, we believe this to be fruitful for open shell systems. Moreover, yet another improvement of the unperturbed Hamiltonian seems to be possible by defining different mixings for the two doubly excited CSF classes analogous to S2-PT.<sup>18</sup> Work on these topics is in progress in our laboratory.

## SUPPLEMENTARY MATERIAL

See [supplementary material](#) for all structures used for the wavefunction analysis of Sec. III C and numerical data for all plots in this paper.

## ACKNOWLEDGMENTS

We are indebted to Mihály Kállay (Budapest University of Technology and Economics) for making the MRCC program package available as well as for comprehensive support. Furthermore, we thank Frank Neese (MPI für Kohlenforschung Mülheim/Ruhr) and the ORCA development team for providing the ORCA program package free of charge. We thank Lucien Caspers (now Universität Bremen) who contributed to this work at an early stage. The major part of the computations were performed at the computational resources of the light induced sensor and analytics (LISA+)

compute cluster at the University of Tübingen. We are indebted to Dr. Jihène Jerbi and Maximilian Winkler for valuable comments on this manuscript.

The authors declare no conflict of interest.

## REFERENCES

- <sup>1</sup>C. Møller and M. S. Plesset, *Phys. Rev.* **46**, 618 (1934).
- <sup>2</sup>D. Cremer, *Wiley Interdiscip. Rev.: Comput. Mol. Sci.* **1**, 509 (2011).
- <sup>3</sup>K. A. Brueckner, *Phys. Rev.* **100**, 36 (1955).
- <sup>4</sup>R. J. Bartlett, *Annu. Rev. Phys. Chem.* **32**, 359 (1981).
- <sup>5</sup>T. D. Crawford, H. F. Schaefer, and T. J. Lee, *J. Chem. Phys.* **105**, 1060 (1996).
- <sup>6</sup>K. Andersson, P.-Å. Malmqvist, B. O. Roos, A. J. Sadlej, and K. Wolinski, *J. Phys. Chem.* **94**, 5483 (1990).
- <sup>7</sup>K. Hirao, *Chem. Phys. Lett.* **190**, 374 (1992).
- <sup>8</sup>K. Hirao, *Chem. Phys. Lett.* **196**, 397 (1992).
- <sup>9</sup>S. Chattopadhyay, R. K. Chaudhuri, U. S. Mahapatra, A. Ghosh, and S. S. Ray, *Wiley Interdiscip. Rev.: Comput. Mol. Sci.* **6**, 266 (2016).
- <sup>10</sup>F. Weigend and M. Häser, *Theor. Chem. Acc.* **97**, 331 (1997).
- <sup>11</sup>F. Weigend, M. Häser, H. Patzelt, and R. Ahlrichs, *Chem. Phys. Lett.* **294**, 143 (1998).
- <sup>12</sup>P. Pinski, C. Riplinger, E. F. Valeev, and F. Neese, *J. Chem. Phys.* **143**, 034108 (2015).
- <sup>13</sup>F. Pavošević, P. Pinski, C. Riplinger, F. Neese, and E. F. Valeev, *J. Chem. Phys.* **144**, 144109 (2016).
- <sup>14</sup>F. Neese, T. Schwabe, S. Kossmann, B. Schirmer, and S. Grimme, *J. Chem. Theory Comput.* **5**, 3060 (2009).
- <sup>15</sup>O. Christiansen, J. Olsen, P. Jørgensen, H. Koch, and P.-Å. Malmqvist, *Chem. Phys. Lett.* **261**, 369 (1996).
- <sup>16</sup>S. Grimme, *J. Chem. Phys.* **118**, 9095 (2003).
- <sup>17</sup>S. Grimme, L. Goerigk, and R. F. Fink, *Wiley Interdiscip. Rev.: Comput. Mol. Sci.* **2**, 886 (2012).
- <sup>18</sup>R. F. Fink, *J. Chem. Phys.* **133**, 174113 (2010).
- <sup>19</sup>R. C. Lochan and M. Head-Gordon, *J. Chem. Phys.* **126**, 164101 (2007).
- <sup>20</sup>U. Bozkaya, J. M. Turney, Y. Yamaguchi, H. F. Schaefer III, and C. D. Sherrill, *J. Comput. Phys.* **135**, 104103 (2011).
- <sup>21</sup>E. Soydaş and U. Bozkaya, *J. Chem. Theory Comput.* **9**, 4679 (2013).
- <sup>22</sup>Á. Szabados, *J. Chem. Phys.* **125**, 214105 (2006).
- <sup>23</sup>R. F. Fink, *Chem. Phys.* **356**, 39 (2009).
- <sup>24</sup>R. F. Fink, *Chem. Phys. Lett.* **428**, 461 (2006).
- <sup>25</sup>W. Kutzelnigg, "Pair correlation theories," in *Modern Theoretical Chemistry*, edited by H. F. Schaefer III (Plenum Press, 1977), pp. 129–188.
- <sup>26</sup>R. Ahlrichs, *Comput. Phys. Commun.* **17**, 31 (1979).
- <sup>27</sup>W. Meyer, *J. Chem. Phys.* **64**, 2901 (1976).
- <sup>28</sup>H.-J. Werner, *Theor. Chem. Acc.* **103**, 322 (2000).
- <sup>29</sup>H. P. Kelly, *Phys. Rev.* **131**, 684 (1963).
- <sup>30</sup>H. P. Kelly and A. M. Sessler, *Phys. Rev.* **132**, 2091 (1963).
- <sup>31</sup>H. P. Kelly, *Phys. Rev.* **134**, A1450 (1964).
- <sup>32</sup>S. Sharma and A. Alavi, *J. Chem. Phys.* **143**, 102815 (2015).
- <sup>33</sup>A. G. Taube and R. J. Bartlett, *J. Chem. Phys.* **130**, 144112 (2009).
- <sup>34</sup>R. J. Bartlett and M. Musial, *Rev. Mod. Phys.* **79**, 291 (2007).
- <sup>35</sup>J. Čížek, *J. Chem. Phys.* **45**, 4256 (1966).
- <sup>36</sup>J. Čížek, *Adv. Chem. Phys.* **14**, 35 (1969).
- <sup>37</sup>R. J. Bartlett and I. Shavitt, *Chem. Phys. Lett.* **50**, 190 (1977).
- <sup>38</sup>R. J. Bartlett and I. Shavitt, *Chem. Phys. Lett.* **57**, 157 (1978).
- <sup>39</sup>A. Szabados and P. Surján, *Chem. Phys. Lett.* **308**, 303 (1999).
- <sup>40</sup>P. R. Surján and A. Szabados, *J. Chem. Phys.* **112**, 4438 (2000).
- <sup>41</sup>R. F. Fink, *J. Chem. Phys.* **145**, 184101 (2016).
- <sup>42</sup>W. Meyer, *J. Chem. Phys.* **58**, 1017 (1973).
- <sup>43</sup>F. Wennmohs and F. Neese, *Chem. Phys.* **343**, 217 (2008).
- <sup>44</sup>L. M. J. Huntington and M. Nooijen, *J. Chem. Phys.* **133**, 184109 (2010).
- <sup>45</sup>L. M. J. Huntington, A. Hansen, F. Neese, and M. Nooijen, *J. Chem. Phys.* **136**, 064101 (2012).
- <sup>46</sup>E. Schrödinger, *Ann. Phys.* **385**, 437 (1926).
- <sup>47</sup>A. Szabo and N. S. Ostlund, *Modern Quantum Chemistry: Introduction to Advanced Electronic Structure Theory* (Dover Publications, Inc., 1996).
- <sup>48</sup>T. Helgaker, P. Jørgensen, and J. Olsen, *Molecular Electronic-Structure Theory* (Wiley, Chichester, New York Weinheim, 2004).
- <sup>49</sup>V. Fock, *Z. Phys.* **75**, 622 (1932).
- <sup>50</sup>P. R. Surján, *Second Quantized Approach to Quantum Chemistry: An Elementary Introduction* (Springer, Berlin, Heidelberg, 1989).
- <sup>51</sup>T. Kato, *Commun. Pure Appl. Math.* **10**, 151 (1957).
- <sup>52</sup>R. T. Pack and W. B. Brown, *J. Chem. Phys.* **45**, 556 (1966).
- <sup>53</sup>P. Goldhammer and E. Feenberg, *Phys. Rev.* **101**, 1233 (1956).
- <sup>54</sup>E. Feenberg, *Phys. Rev.* **103**, 1116 (1956).
- <sup>55</sup>C. Schmidt, M. Warken, and N. C. Handy, *Chem. Phys. Lett.* **211**, 272 (1993).
- <sup>56</sup>T. H. J. Dunning, *J. Chem. Phys.* **90**, 1007 (1989).
- <sup>57</sup>J. Wasilewski, *Int. J. Quantum Chem.* **36**, 503 (1989).
- <sup>58</sup>J. Wasilewski, *Int. J. Quantum Chem.* **39**, 649 (1991).
- <sup>59</sup>P. Knowles, K. Somasundram, N. Handy, and K. Hirao, *Chem. Phys. Lett.* **113**, 8 (1985).
- <sup>60</sup>B. Roos, *Chem. Phys. Lett.* **15**, 153 (1972).
- <sup>61</sup>P. Pulay, S. Saebø, and W. Meyer, *J. Chem. Phys.* **81**, 1901 (1984).
- <sup>62</sup>G. E. Scuseria, C. L. Janssen, and H. F. Schaefer III, *J. Chem. Phys.* **89**, 7382 (1988).
- <sup>63</sup>C. Hampel, K. A. Peterson, and H.-J. Werner, *Chem. Phys. Lett.* **190**, 1 (1992).
- <sup>64</sup>P. Pulay and S. Saebø, *Theor. Chim. Acta* **69**, 357 (1986).
- <sup>65</sup>P. Pulay, *Chem. Phys. Lett.* **73**, 393 (1980).
- <sup>66</sup>P. Pulay, *J. Comput. Chem.* **3**, 556 (1982).
- <sup>67</sup>G. D. I. Purvis and R. J. Bartlett, *J. Chem. Phys.* **75**, 1284 (1981).
- <sup>68</sup>See <https://www.openmp.org/> for OpenMP: Enabling HPC since 1997, The OpenMP Architecture Review Board; visited last 26 November 2018.
- <sup>69</sup>See <https://www.openblas.net/> for OpenBLAS: An optimized BLAS library, developed by Z. Xianyi, W. Qian, and W. Saar; visited last 26 November 2018.
- <sup>70</sup>R. Serber, *J. Chem. Phys.* **2**, 697 (1934).
- <sup>71</sup>R. Serber, *Phys. Rev.* **45**, 461 (1934).
- <sup>72</sup>D. Pape and M. Hanrath, *Chem. Phys.* **401**, 157 (2012).
- <sup>73</sup>V. Staemmler, *Theor. Chim. Acta* **45**, 89 (1977).
- <sup>74</sup>U. Meier and V. Staemmler, *Theor. Chim. Acta* **76**, 95 (1989).
- <sup>75</sup>R. Fink and V. Staemmler, *Theor. Chim. Acta* **87**, 129 (1993).
- <sup>76</sup>R. Fink, "Entwicklung eines Mehrkonfigurations-CEPA-Programms unter Benutzung von PNO's und Anwendung auf organisch chemische Fragestellungen," Doctoral dissertation (Ruhr-Universität Bochum, Bochum, Germany 1991).
- <sup>77</sup>MRCC, a quantum chemical program suite written by M. Kállay, Z. Rolik, J. Csontos, P. Nagy, G. Samu, D. Mester, I. Ladjánszki, L. Szegedy, B. Ladóczki, K. Petrov, M. Farkas, and B. Hégyel, See also Z. Rolik, L. Szegedy, I. Ladjánszki, B. Ladóczki, and M. Kállay, *J. Chem. Phys.* **139**, 094105 (2013) as well as: [www.mrcc.hu](http://www.mrcc.hu).
- <sup>78</sup>M. Kállay and P. R. Surján, *J. Chem. Phys.* **113**, 1359 (2000).
- <sup>79</sup>M. Kállay and P. R. Surján, *J. Chem. Phys.* **115**, 2945 (2001).
- <sup>80</sup>F. Neese, *Wiley Interdiscip. Rev.: Comput. Mol. Sci.* **2**, 73 (2012).
- <sup>81</sup>F. Neese, *Wiley Interdiscip. Rev.: Comput. Mol. Sci.* **8**, e1327 (2018).
- <sup>82</sup>*NIST Computational Chemistry Comparison and Benchmark DataBase, NIST Standard Reference Database Number 101, Release 19*, edited by R. D. Johnson III (National Institute of Standards and Technology, 2018), <http://cccbdb.nist.gov/>; visited last 02 November 2018.
- <sup>83</sup>See <http://cccbdb.nist.gov/expdiatomicx.asp> for Experimental Diatomic Data, National Institute of Standards and Technology; visited last 27 December 2017.
- <sup>84</sup>See <http://cccbdb.nist.gov/diatomicexpbondx.asp> for List of Experimental Diatomic Bond Lengths, National Institute of Standards and Technology; visited last 27 December 2017.
- <sup>85</sup>See <http://cccbdb.nist.gov/expgeom1x.asp> for Experimental Geometry Data, National Institute of Standards and Technology; visited last 27 December 2017.

- <sup>86</sup>J. S. Coursey, D. J. Schwab, J. J. Tsai, and R. A. Dragoset, *Atomic Weights and Isotopic Compositions with Relative Atomic Masse* (NIST Physical Measurement Laboratory, 2017), <https://www.nist.gov/pml/atomic-weights-and-isotopic-compositions-relative-atomic-masses>; visited last 27 December 2017.
- <sup>87</sup>TURBOMOLE V6.5 2013, a development of University of Karlsruhe and Forschungszentrum Karlsruhe GmbH, 1989-2007, TURBOMOLE GmbH, since 2007; available from <http://www.turbomole.com>.
- <sup>88</sup>See <https://bse.pnl.gov/bse/portal> for EMSL Basis Set Exchange v1.2.2; visited last 19 July 2018.
- <sup>89</sup>D. Feller, *J. Comput. Chem.* **17**, 1571 (1996).
- <sup>90</sup>K. L. Schuchardt, B. T. Didier, T. Elsethagen, L. Sun, V. Gurumoorthi, J. Chase, J. Li, and T. L. Windus, *J. Chem. Inf. Model.* **47**, 1045 (2007).
- <sup>91</sup>C. Angeli, R. Cimiraglia, S. Evangelisti, T. Leininger, and J.-P. Malrieu, *J. Chem. Phys.* **114**, 10252 (2001).
- <sup>92</sup>K. G. Dyall, *J. Chem. Phys.* **102**, 4909 (1995).
- <sup>93</sup>J. M. Foster and S. F. Boys, *Rev. Mod. Phys.* **32**, 300 (1960).
- <sup>94</sup>F. Weigend, F. Furche, and R. Ahlrichs, *J. Chem. Phys.* **119**, 12753 (2003).
- <sup>95</sup>P. M. Morse, *Phys. Rev.* **34**, 57 (1929).
- <sup>96</sup>W. Meyer, *Int. J. Quantum Chem.* **5**, 341 (1971).
- <sup>97</sup>J. P. Perdew, *Phys. Rev. B* **33**, 8822 (1986).
- <sup>98</sup>A. D. Becke, *Phys. Rev. A* **38**, 3098 (1988).
- <sup>99</sup>J. C. Slater, *Phys. Rev.* **81**, 385 (1951).
- <sup>100</sup>S. H. Vosko, L. Wilk, and M. Nusair, *Can. J. Phys.* **58**, 1200 (1980).
- <sup>101</sup>C. Lee, W. Yang, and R. G. Parr, *Phys. Rev. B* **37**, 785 (1988).
- <sup>102</sup>A. D. Becke, *J. Chem. Phys.* **98**, 5648 (1993).
- <sup>103</sup>P. J. Stephens, F. J. Devlin, C. F. Chabalowski, and M. J. Frisch, *J. Phys. Chem.* **98**, 11623 (1994).
- <sup>104</sup>S. Grimme, *J. Chem. Phys.* **124**, 034108 (2006).
- <sup>105</sup>C. L. Janssen and I. M. Nielsen, *Chem. Phys. Lett.* **290**, 423 (1998).
- <sup>106</sup>I. M. Beck Nielsen and C. L. Janssen, *Chem. Phys. Lett.* **310**, 568 (1999).
- <sup>107</sup>T. J. Lee and P. R. Taylor, *Int. J. Quantum Chem.* **36**, 199 (1989).
- <sup>108</sup>L. Goerigk and S. Grimme, *J. Chem. Theory Comput.* **6**, 107 (2010).
- <sup>109</sup>A. Karton and L. Goerigk, *J. Comput. Chem.* **36**, 622 (2015).
- <sup>110</sup>S. Sharma, G. Jeanmairet, and A. Alavi, *J. Chem. Phys.* **144**, 034103 (2016).
- <sup>111</sup>G. Jeanmairet, S. Sharma, and A. Alavi, *J. Chem. Phys.* **146**, 044107 (2017).
- <sup>112</sup>U. Bozkaya and C. D. Sherrill, *J. Chem. Phys.* **139**, 054104 (2013).





# OO-REMP: Approaching Chemical Accuracy with Second-Order Perturbation Theory

Stefan Behnle\* and Reinhold F. Fink\*

Cite This: *J. Chem. Theory Comput.* 2021, 17, 3259–3266

Read Online

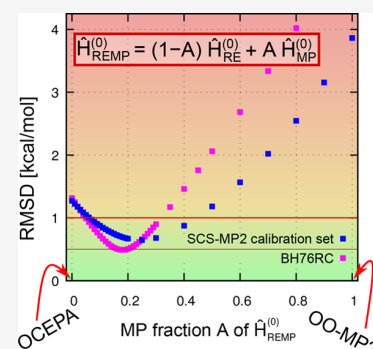
ACCESS |

Metrics & More

Article Recommendations

Supporting Information

**ABSTRACT:** We present a perturbation theory (PT) providing second-order energies that reproduce main group chemistry benchmark sets for reaction energies, barrier heights, and atomization energies with mean absolute deviations below 1 kcal mol<sup>-1</sup>. The PT is defined as a constrained mixture of the unperturbed Hamiltonians of the Retaining the Excitation degree (RE) and the Møller–Plesset (MP) PTs. The orbitals of the reference wave function, a single unrestricted Slater determinant, are iteratively optimized to minimize the total energy. For all benchmark sets, good and near optimal performance of OO-REMP was observed for an unperturbed Hamiltonian consisting of 25% MP and 75% RE contributions.



Peterson et al.<sup>1</sup> pointed out that the computational chemistry literature frequently identifies “chemical accuracy” with a mean absolute deviation (MAD) error estimate below 1 kcal mol<sup>-1</sup>, while an experimentalist’s definition would be typically a 95% confidence interval corresponding rather to a root-mean-square deviation (RMSD) below 0.5 kcal mol<sup>-1</sup>. The only quantum chemical methods which have been broadly shown to meet this requirement for chemically relevant properties like reaction and transition state energies are Coupled-Cluster (CC) approaches explicitly including up to triple or higher excitations.<sup>2,3</sup> So far, perturbation theory (PT), the alternative class of generally applicable wave function based methods, failed to reach a comparable level of accuracy; however, very successful and accurate combinations with CC methods have been proposed<sup>4,5</sup>—most notably the “Gold Standard” of quantum chemistry, coupled-cluster with single, double, and perturbative triple excitations [CCSD(T)].<sup>6</sup> Nevertheless, the conceptually simple and computationally efficient Møller–Plesset second- and third-order approaches (MP2 and MP3) have been widely applied and validated.<sup>7–9</sup> Substantially better performance than MP2 at the same computational cost was found by Grimme for spin-component scaling (SCS)-MP2<sup>10,11</sup> where terms of the correlation energy expression corresponding to same- and opposite-spin double-excitations are scaled empirically. Grimme achieved further improvements with SCS-MP3<sup>12</sup> by adding the MP3 energy contribution with a prefactor of 0.25 to the SCS-MP2 energy. Fractional perturbation theories like MP2.X—which is the MP3 energy contribution multiplied by 0.X added to the MP2 energy—have been proposed, and in particular, MP2.5 proved very successful for nonbonded interaction energies.<sup>13,14</sup>

One of the present authors identified that MP2 systematically underestimates correlation effects of singlet coupled electron pairs, while it overestimates those from triplet pairs.<sup>15</sup> This work also showed that the Retaining the Excitation degree (RE) PT<sup>16,17</sup> behaves essentially the other way around, while providing more accurate first-order wave functions. In order to balance these systematic errors of RE- and MP-PT, a hybrid method where the unperturbed Hamiltonian is a linear combination of the RE and MP ones was designed and implemented by the present authors.<sup>18</sup> This approach, named REMP, was shown to provide more accurate first-order wave functions and to outperform the MP2 and RE2 parent methods for reaction energies and molecular properties.<sup>18</sup>

For open-shell cases, the definition of PT is straightforward for unrestricted Hartree–Fock (UHF) reference wave functions. However, the latter tend to become inaccurate due to spin-contamination errors.<sup>19</sup> Orbital-optimized (OO)-MP2 was developed and shown to perform substantially better for these cases.<sup>20–22</sup> Similar observations were made for OO-MP2.X and its SCS variants<sup>23</sup> and for OCEPA.<sup>24,25</sup> The latter is the OO variant of coupled electron pair approximation zero with doubles [CEPA(0)D] which is identical to RE2 for unrestricted HF reference wave functions.<sup>16</sup> The concept of orbital optimization, i.e., minimizing the total energy with respect to

Received: March 22, 2021

Published: May 19, 2021



orbitals and the CI-coefficients/amplitudes, has been developed originally for multiconfiguration self-consistent field<sup>26,27</sup> and for coupled-cluster theory.<sup>28</sup> Orbital optimization for spin-opposite-scaled (SOS)-MP2 was introduced by Head-Gordon et al.<sup>20</sup> and generalized to SCS-MP2 by Neese et al.<sup>21</sup> Later, Bozkaya and Sherrill<sup>23,29,30</sup> developed extensions to higher orders in perturbation theory and analytic energy gradients.

To our knowledge, the best performing OO-PT methods are the recently proposed OO-MP2.5<sup>31,32</sup> (also named OMP2.5) and MP2.8:κ-OOMP2<sup>33</sup> approaches which reproduce reactions and transition energies of the HTBH38 test set with root-mean-square deviations (RMSDs) of about 1 kcal mol<sup>-1</sup>. MP2.8:κ-OOMP2 is the MP2.8 energy obtained with the spin-unrestricted determinant of the OO regularized MP2 approach. In the latter, the MP2-correlation energy term is empirically modified as to avoid failure of the PT if the energy denominator approaches zero.

Inspired by the success of the orbital-optimized PTs, we implemented an orbital-optimized variant of REMP2 termed "OO-REMP". In the following, we describe this approach and its performance for the benchmark sets used in the recently proposed OO-MP2.5<sup>31,32</sup> and MP2.8:κ-OOMP2<sup>33</sup> methods. As in these works, results of OO-MP2, OCEPA, and CCSD are also shown. The aim of the present work is to provide a realistic and unbiased assessment of OO-REMP in the context of recent developments of orbital-optimized PTs.

The prerequisite for applying (Rayleigh–Schrödinger) PT to electronic wave functions and energies is the definition of an unperturbed Hamiltonian,  $\hat{H}^{(0)}$ , that fulfills the zeroth-order perturbation equation

$$\hat{H}^{(0)}|\Phi^{(0)}\rangle = E^{(0)}|\Phi^{(0)}\rangle \quad (1)$$

exactly. In this work, a single (spin-unrestricted) Slater determinant is used for the unperturbed wave function,  $|\Phi^{(0)}\rangle$ . The unperturbed Hamiltonian for RE-PT is defined<sup>16</sup> as a part of the second quantization<sup>34</sup> Hamiltonian

$$\hat{H}_{\text{RE}}^{(0)} = \sum_{pq}^{\Delta n_{\text{ex}}=0} h_{pq} \hat{a}_p^\dagger \hat{a}_q + \frac{1}{2} \sum_{pqrs}^{\Delta n_{\text{ex}}=0} \langle pq|rs \rangle \hat{a}_p^\dagger \hat{a}_q^\dagger \hat{a}_s \hat{a}_r \quad (2)$$

Here  $p, q, r,$  and  $s$  are spin-orbital indices,  $h_{pq}$  is a matrix element of the one-electron Hamiltonian,  $\langle pq|rs \rangle = \int \phi_p^*(1) \phi_q^*(2) \frac{1}{r_{12}} \phi_r(1) \phi_s(2) d\tau$  represents an electron repulsion integral (ERI) in Dirac notation, and  $\hat{a}_p$  ( $\hat{a}_p^\dagger$ ) is the annihilation (creation) operator of the spin orbital  $p$ . The excitation degree restriction ( $\Delta n_{\text{ex}} = 0$ ) on the sums indicates that only those terms are retained where the number of annihilated and created electrons in the occupied spin orbitals in  $|\Phi^{(0)}\rangle$  is identical. In other words, the creator-annihilator combination does not change the excitation degree (number of electrons in occupied spin orbitals) of any Slater determinant it is applied to. With this definition,  $\hat{H}_{\text{RE}}^{(0)}$  fulfills eq 1 independent of the choice of the occupied orbitals in  $|\Phi^{(0)}\rangle$ .

The unperturbed MP-Hamiltonian is generally set to the Fock operator  $\hat{F} = \hat{h} + \hat{J} - \hat{K}$  which means that eq 1 is only fulfilled if  $|\Phi^{(0)}\rangle$  is a HF wave function. As the latter is not the case for OO-MP,  $\hat{H}^{(0)}$  has to be modified either with a projector or in a form resembling eq 2

$$\hat{H}_{\text{MP}}^{(0)} = \sum_{pq}^{\Delta n_{\text{ex}}=0} F_{pq} \hat{a}_p^\dagger \hat{a}_q \quad (3)$$

Using the above definitions, the orbital-independent unperturbed Hamiltonian of REMP-PT is given by<sup>18</sup>

$$\hat{H}_{\text{REMP}}^{(0)} = (1 - A) \hat{H}_{\text{RE}}^{(0)} + A \hat{H}_{\text{MP}}^{(0)} \quad (4)$$

$$= \sum_{pq}^{\Delta n_{\text{ex}}=0} [h_{pq} + A(J_{pq} - K_{pq})] \hat{a}_p^\dagger \hat{a}_q + (1 - A) \frac{1}{2} \sum_{pqrs}^{\Delta n_{\text{ex}}=0} \langle pq|rs \rangle \hat{a}_p^\dagger \hat{a}_q^\dagger \hat{a}_s \hat{a}_r \quad (5)$$

where  $A$ , the MP-amount in the unperturbed Hamiltonian, is the REMP parameter that was estimated to be about 0.1–0.2.<sup>18</sup> Note that  $\hat{H}_{\text{REMP}}^{(0)}$  contains the complete one-electron Hamiltonian for any choice of  $A$ , as this is required to guarantee that the perturbed wave functions fulfill Kato's cusp conditions.<sup>35</sup> The idea of REMP-PT is to tune  $A$  such that the first-order perturbed wave function approximates the first-order interacting part of the exact wave function as close as possible.<sup>18</sup>

For the description of the orbital optimization, we adopt a Coupled-Cluster style notation. As the present approach can be seen as a combination of MP2 with CEPA(0)D, orbital optimization can and was implemented as described by Bozkaya and Sherrill for these approaches.<sup>24,36</sup> Briefly, the first-order wave function is given by

$$|\Psi^{(1)}\rangle = \hat{T}_2^{(1)} |\Phi^{(0)}\rangle \quad (6)$$

where  $|\Phi^{(0)}\rangle$  is the (single) reference Slater determinant, and  $\hat{T}_2$  denotes the doubles cluster operator. Singly excited configurations are neglected as in all other OO-PTs known to the authors.<sup>20,21,31,36</sup>

Using the concept of normal ordering,<sup>37</sup> the total electronic Hamiltonian in second quantization<sup>34</sup> can be written as

$$\hat{H} = \hat{F}_N^d + \langle \Phi^{(0)} | \hat{F}^d | \Phi^{(0)} \rangle + \hat{F}^o + \hat{W}_N + \langle \Phi^{(0)} | \hat{W} | \Phi^{(0)} \rangle \quad (7)$$

where  $N$  indicates normal order with respect to the Fermi vacuum,<sup>37</sup>  $d$  designates the diagonal (occupied-occupied and the virtual-virtual) parts of the respective operator,  $o$  is the off-diagonal part (occupied-virtual/virtual-occupied), and  $\hat{W}$  is that part of the two-electron repulsion operator which is not included in the Fockian ("fluctuation potential").

Using the representation of eq 7, it is possible to rewrite the unperturbed Hamiltonians and the perturbation of MP and RE in a way suitable for diagrammatic evaluation

$$\hat{H}_{\text{MP}}^{(0)} = \hat{F}_N^d + \langle \Phi^{(0)} | \hat{F}^d | \Phi^{(0)} \rangle \quad (8)$$

$$\hat{H}_{\text{MP}}^{(1)} = \hat{F}^o + \hat{W}_N + \langle \Phi^{(0)} | \hat{W} | \Phi^{(0)} \rangle \quad (9)$$

$$\hat{H}_{\text{RE}}^{(0)} = \hat{F}_N^d + \sum_{R=0} \hat{W}_N + \langle \Phi^{(0)} | \hat{F}^d | \Phi^{(0)} \rangle + \sum_{R=0} \langle \Phi^{(0)} | \hat{W} | \Phi^{(0)} \rangle \quad (10)$$

$$\hat{H}_{\text{RE}}^{(1)} = \hat{F}^o + \sum_{R \neq 0} \hat{W}_N + \sum_{R \neq 0} \langle \Phi^{(0)} | \hat{W} | \Phi^{(0)} \rangle \quad (11)$$

where  $R$  denotes the excitation degree of the terms/diagrams included. Every diagram used in the context of electron correlation can be assigned an excitation degree; there is thus an intimate connection between the concept of excitation degrees used in (single reference) RE and diagrammatic



techniques. For single reference cases, the partitioning defined by eqs 8 and 9 and eqs 10 and 11 is identical to the one defined by eqs 2 and 3, respectively. If a canonical RHF or UHF determinant is chosen as  $|\Phi^{(0)}\rangle$  and  $|\Psi^{(1)}\rangle$  is expanded in the respective doubly substituted determinants, one obtains REMP and UREMP, respectively. A systematic assessment of the canonical unrestricted REMP variant will be presented elsewhere.<sup>38</sup>

The OO-REMP energy and wave function are obtained by minimizing the second-order REMP energy functional

$$\begin{aligned} \tilde{E}_{\text{REMP}}^{(2)} = & \langle \Phi^{(0)} | \hat{H} | \Phi^{(0)} \rangle + \langle \Phi^{(0)} | \{ \hat{W}_N \hat{T}_2^{(1)} \}_c | \Phi^{(0)} \rangle \\ & + \langle \Phi^{(0)} | [ \hat{\Lambda}_2^{(1)} \{ \hat{W}_N + \hat{F}_N \hat{T}_2^{(1)} + (1 - A) \hat{W}_N \hat{T}_2^{(1)} \}_c ] | \Phi^{(0)} \rangle \end{aligned} \quad (12)$$

with respect to the  $\hat{T}_2$  amplitudes and the MO coefficients  $c_{\mu i}$  of the reference determinant  $|\Phi^{(0)}\rangle$ .<sup>39</sup> The derivation follows the lines of OCEPA,<sup>24</sup> and the actual working equations are very similar to the OCEPA equations differing only by the insertion of  $(1 - A)$  in front of those residuum contributions and density matrix contributions which exclusively appear in OCEPA.

Using the energy representation in eq 12, orbital optimization for REMP2 was implemented as described for the parent methods OO-MP2 and OCEPA by Bozkaya et al.<sup>24,36</sup> who use an exponential unitary orbital rotation operator  $e^{\hat{k}}$ .<sup>40</sup> More details on the implementation and further results will be presented in an upcoming publication.<sup>38</sup> The expectation value of the  $\hat{S}^2$  operator which can be used as a measure for the quality of the wave function was implemented according to eq 13 of ref 41.

All OO-REMP calculations have been performed using a development version of our local *ab initio* suite of programs (wawels). The OO-REMP implementation is an extension of the MCCEPA program<sup>42</sup> and is inspired by the matrix-driven CI program of ORCA<sup>43,44</sup> and the orbital-optimized coupled-cluster code (OCC)<sup>24,25</sup> of PSI4.<sup>45</sup> All CCSD(T) calculations were performed using ORCA 4.2.0.

Besides, the MAD and RMSD statistical error estimates mentioned at the beginning, in the following, we also use Mean Signed Deviation (MSD), the standard deviation ( $\sigma$ ), and the error spread ( $\Delta_{\text{min-max}}$ ) which is the largest positive minus the largest negative error.

Table 1 shows OO-REMP error descriptors for a set of closed-shell reactions used before by Soydaş and Bozkaya.<sup>32</sup> This set is mostly a subset of the reactions employed by Grimme to parametrize SCS-MP2.<sup>10</sup> Precisely, the intersecting set of the closed-shell reactions of refs 10, 21, 46, and 32 was used with Grimme's structures (see the Supporting Information for an explicit list of the reactions considered, additional data on reactions not contained in the test set of Soydaş and Bozkaya,<sup>32</sup> and evidence for the reliability of the employed basis sets). Reference reaction energies were recomputed at the CCSD(T)/def2-QZVP level of theory with all electrons being correlated. Table 1 collects the resulting error descriptors as well as those from REMP2/def2-QZVP results with a canonical RHF reference wave function with respect to CCSD(T)/def2-QZVP where core electrons had been frozen.

As has been found before,<sup>21</sup> OO-MP2 (OO-REMP with  $A = 1$ ) does not improve on MP2 (REMP2 with  $A = 1$ ) for the closed-shell reaction energies considered there. Furthermore, as also observed before,<sup>24,25,47</sup> OO-RE2 or OCEPA (OO-REMP with  $A = 0$ ) performs only slightly better than RE2 [CEPA(0)D] for these closed-shell systems. However, OO-REMP does quite

**Table 1. Error Descriptors of OO-REMP/def2-QZVP with Respect to CCSD(T)/def2-QZVP (All Electrons Correlated) as well as REMP2/def2-QZVP with an HF Reference Wave Function with Respect to CCSD(T)/def2-QZVP (Frozen Core) for the SCS-MP2 Calibration Set<sup>d</sup>**

A	MSD	MAD	$\Delta_{\text{min-max}}$	$\sigma$	RMSD
OO-REMP/def2-QZVP					
0.00	0.26	0.97	6.08	1.27	1.27
0.15	-0.06	0.56	3.45	0.76	0.75
0.20	-0.13	0.51	3.15	0.67	0.67
0.25	-0.18	0.48	3.02	0.63	0.65
0.30	-0.22	0.49	2.87	0.65	0.68
1.00	0.23	2.57	19.21	3.92	3.86
REMP2/def2-QZVP					
0.00	0.04	1.36	8.57	1.92	1.89
0.15	-0.31	1.17	7.69	1.72	1.72
0.20	-0.39	1.20	7.53	1.68	1.70
0.25	-0.46	1.21	7.34	1.66	1.70
0.30	-0.52	1.23	7.10	1.65	1.70
1.00	-0.51	1.97	12.32	2.68	2.68
OO-SCS-MP2 <sup>a</sup>	-0.17	1.79	11.90	2.38	2.35
SCS-OMP3 <sup>b</sup>	0.45	1.31	6.50	1.74	1.77
OMP2.5/CBS <sup>c</sup>	0.59	1.03	4.50	1.29	1.40

<sup>a</sup>Taken from ref 21. Errors are with respect to Grimme's original QCISD(T) reference reaction energies which do not include core correlation. <sup>b</sup>Taken from ref 46. Reference: CCSD(T)/cc-pCVTZ. <sup>c</sup>Taken from ref 32. Reference: CCSD(T)/CBS(cc-pV[T/Q]Z). <sup>d</sup>All values are in kcal mol<sup>-1</sup>. See Table S8 for a list of the reactions. Statistics for OO-SCS-MP2, SCS-OMP3, and OMP2.5 were recomputed for the subset of reactions considered here. The average absolute reaction energy of this set amounts to 32.65 kcal mol<sup>-1</sup>.

significantly improve upon both OO-RE2 and OO-MP2 as well as the respective REMP2 variants without orbital optimization. For  $A \approx 0.25$ , OO-REMP shows the lowest RMSD of 0.65 kcal mol<sup>-1</sup> indicating that the best OO-REMP parameter is slightly larger than that for REMP2 ( $A \approx 0.12-0.20$ ).<sup>18</sup> One furthermore finds that the error spread  $\Delta_{\text{min-max}}$  and the standard deviation decrease toward the optimal mixing parameter indicating less serious outliers and an overall sharper-peaked error distribution. As shown in Table 1 for these closed-shell reaction energies, REMP2, OO-SCS-MP2, SCS-OMP3, and OMP2.5 are outperformed by OO-REMP with  $A = 0.25$ . In the remaining discussion, we will focus on the latter choice [designated as OO-REMP(0.25)], as it turns out to be near to optimal for all investigated benchmark sets. We note that OO-REMP is a quantum chemical method containing a parameter. General applicability of such an approach requires that a good description of different properties is obtained for a single value of this parameter. This is the case if error estimates of all properties of particular interest are minimal or near to minimal for the recommended parameter choice. We will show that this holds for OO-REMP(0.25) by presenting results for OO-REMP with  $A$  between 0.15 and 0.30.

As the next benchmark, we consider the BH76 set<sup>48</sup> which consists of 76 barrier heights for chemical reactions in the gas phase involving neutral and ionic as well as closed- and open-shell species. It is composed of the HTBH38<sup>49</sup> and the NHTBH38<sup>50</sup> subsets which collect Barrier-Heights for Hydrogen-Transfer and Non-Hydrogen (larger atoms and functional groups)-Transfer reactions. In all cases, the forward and backward reactions are included.

The nondegenerate reactions provide a set of reaction energies, the BH76RC set, which is also discussed below. As we wanted to make our results comparable to those of the remarkably well performing MP2.8: $\kappa$ -OOMP2 approach of Bertels et al.,<sup>33</sup> we used the same basis set (aug-cc-pVTZ) and reference method [CCSD(T) with all electrons correlated] as in their work.

Figure 1 shows the root-mean-square deviation of the HTBH38 and the NHTBH38 subsets of BH76 if the full A

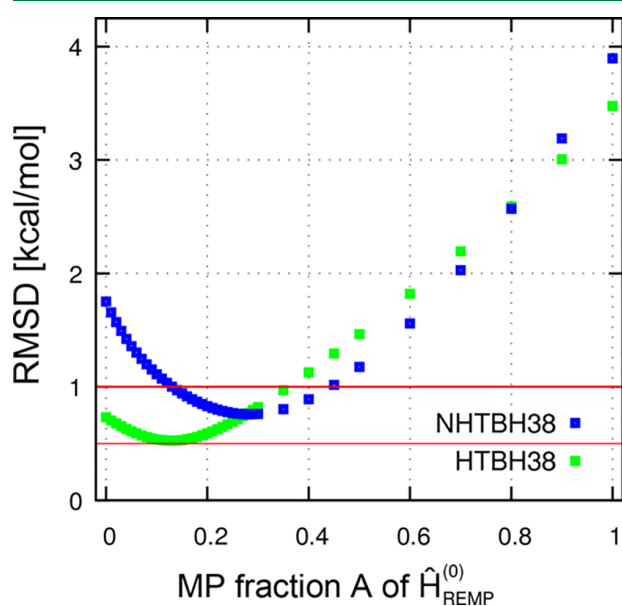


**Figure 1.** Root-mean-square deviations of OO-REMP/aug-cc-pVTZ with respect to CCSD(T)/aug-cc-pVTZ for the HTBH38 and the NHTBH38 benchmark sets versus A, the MP fraction of the unperturbed REMP-Hamiltonian.

parameter range is sampled (see the Supporting Information for the corresponding data).

Table 2 lists error descriptors for the HTBH38 subset obtained with OO-REMP. It is clearly visible that REMP hybridization leads to a significant improvement compared to the parent methods OCEPA and OO-MP2. For A values

**Table 2.** Error Descriptors in kcal mol<sup>-1</sup> for the HTBH38 Subset of the BH76 Benchmark Set<sup>c</sup>

A	MSD	MAD	min	max	$\sigma$	RMSD
0.00	0.42	0.66	-1.47	1.29	0.61	0.73
0.15	0.48	0.51	-0.34	0.73	0.23	0.53
0.20	0.47	0.54	-0.70	1.16	0.37	0.59
0.25	0.44	0.56	-1.07	1.73	0.54	0.69
0.30	0.40	0.60	-1.44	2.28	0.73	0.82
1.00	-0.95	2.77	-7.15	8.57	3.39	3.48
CCSD <sup>a</sup>	1.88	1.92	-0.78	4.15	1.17	2.21
MP2.8: $\kappa$ -OOMP2 <sup>a</sup>	-0.12	0.58	-1.42	1.30	0.71	0.71
OOMP2.5 <sup>b</sup>		1.30	-5.20	4.30	1.80	

<sup>a</sup>Taken from ref 33. <sup>b</sup>Taken from ref 32. Using the reference energies of Zhao et al.,<sup>50</sup> basis: CBS(cc-pV[T/Q]Z). <sup>c</sup>OO-REMP/aug-cc-pVTZ, all electrons correlated. Reference reaction energies: CCSD(T)/aug-cc-pVTZ taken from ref 33. The average absolute reaction energy amounts to 12.79 kcal mol<sup>-1</sup>.

between 0 and 0.3, OO-REMP provides an RMSD clearly below 1 kcal mol<sup>-1</sup>. However, the barriers are systematically overestimated by  $\approx 0.44 \pm 0.04$  kcal mol<sup>-1</sup>. For OO-REMP(0.25), the largest error found (1.7 kcal mol<sup>-1</sup>) belongs to reaction 56 which is the abstraction of the hydrogen atom of HF by another hydrogen atom. The canonical counterpart, UREMP(0.25), performs much poorer overestimating this barrier by 3.9 kcal mol<sup>-1</sup>. Moreover, while OO-REMP delivers practically spin-pure wave functions<sup>41</sup> ( $\langle \hat{S}^2 \rangle = 0.752$  for the transition state), the first-order UREMP wave function of the transition state is somewhat spin-contaminated ( $\langle \hat{S}^2 \rangle = 0.757$ ).

Table 2 also lists results for CCSD and MP2.8: $\kappa$ -OOMP2 taken from ref 33. For A = 0.25, OO-REMP clearly outperforms CCSD and OOMP2.5. Furthermore, its RMSD (0.69 kcal mol<sup>-1</sup>) is slightly smaller than that of MP2.8: $\kappa$ -OOMP2 (0.71 kcal mol<sup>-1</sup>).

Table 3 lists the results for the NHTBH38 subset. REMP hybridization again provides a systematic improvement over the

**Table 3.** Error Descriptors in kcal mol<sup>-1</sup> for the NHTBH38 Subset of the BH76 Benchmark Set<sup>b</sup>

A	MSD	MAD	min	max	$\sigma$	RMSD
0.00	0.24	1.30	-6.22	2.55	1.76	1.75
0.15	0.55	0.79	-2.18	1.75	0.78	0.94
0.20	0.55	0.72	-1.62	1.47	0.63	0.83
0.25	0.53	0.70	-1.25	1.17	0.57	0.77
0.30	0.48	0.69	-1.53	1.23	0.60	0.76
1.00	-1.64	2.62	-18.48	2.32	3.58	3.90
CCSD <sup>a</sup>	2.07	2.07	0.13	7.65	1.49	2.53
MP2.8: $\kappa$ -OOMP2 <sup>a</sup>	0.27	0.64	-0.95	1.58	0.72	0.76

<sup>a</sup>Taken from ref 33. <sup>b</sup>OO-REMP/aug-cc-pVTZ, all electrons correlated. Reference reaction energies: CCSD(T)/aug-cc-pVTZ taken from ref 33. The average absolute reaction energy amounts to 23.52 kcal mol<sup>-1</sup>.

parent methods. The MSD, MAD, and RMSD error measures obtained for OO-REMP(0.25) are consistently below 1 kcal mol<sup>-1</sup>.

The largest error belongs to the reaction "HF + F  $\rightarrow$  HF...F<sup>‡</sup>" (reaction 10) whose barrier is underestimated by 1.25 kcal mol<sup>-1</sup>. UREMP(0.25) overestimates this barrier by as much as 23 kcal mol<sup>-1</sup>. Again, while the OO-REMP wave functions are practically spin-pure ( $\langle \hat{S}^2 \rangle = 0.750$  for the HF...F transition state), the first-order UREMP wave function of the transition state is heavily spin-contaminated ( $\langle \hat{S}^2 \rangle = 1.10$ ). Bertels and Head-Gordon<sup>33</sup> report the MP2.8: $\kappa$ -OOMP2 method to reproduce the NHTBH38 set with RMSD and MAD values of 0.76 kcal mol<sup>-1</sup> and 0.64 kcal mol<sup>-1</sup> which are only marginally lower than the OO-REMP(0.25) results (0.77 kcal mol<sup>-1</sup> and 0.70 kcal mol<sup>-1</sup>). However, the error spread of OO-REMP(0.25), indicated by the standard deviation of 0.57 kcal mol<sup>-1</sup>, is clearly smaller than the MP2.8: $\kappa$ -OOMP2 counterpart (0.72 kcal mol<sup>-1</sup>). The opposite trend holds for the average error indicated by the MSD value of OO-REMP(0.25) (0.53 kcal mol<sup>-1</sup>) which is almost twice as large as that of MP2.8: $\kappa$ -OOMP2 (0.27 kcal mol<sup>-1</sup>).

Finally turning to the reaction energies of the BH76RC set (Table 4), one finds a surprisingly accurate result with OO-REMP. The MSD is close to zero, and the RMSD values for A between 0.12 and 0.30 are all lower than 1 kcal mol<sup>-1</sup> (see the Supporting Information for an extended table). For A = 0.25,

**Table 4. Error Descriptors in kcal mol<sup>-1</sup> for the BH76RC Benchmark Set<sup>b</sup>**

A	MSD	MAD	min	max	$\sigma$	RMSD
0.00	-0.01	0.93	-4.51	3.02	1.34	1.32
0.15	-0.01	0.31	-1.33	1.93	0.54	0.53
0.20	0.01	0.36	-0.83	1.78	0.51	0.51
0.25	0.03	0.52	-1.27	1.71	0.67	0.66
0.30	0.05	0.70	-1.88	1.88	0.91	0.90
1.00	0.83	3.96	-10.01	20.48	5.55	5.52
CCSD <sup>a</sup>	-0.65	1.21	-7.18	1.98	1.82	1.91
MP2.8: $\kappa$ -OOMP2 <sup>a</sup>	-0.14	0.65	-1.47	1.53	0.84	0.84

<sup>a</sup>Taken from ref 33. <sup>b</sup>OO-REMP/aug-cc-pVTZ, all electrons correlated. Reference reaction energies: CCSD(T)/aug-cc-pVTZ taken from ref 33. The average absolute reaction energy amounts to 21.40 kcal mol<sup>-1</sup>.

OO-REMP provides an RMSD of only 0.66 kcal mol<sup>-1</sup>, clearly better than CCSD (1.91 kcal mol<sup>-1</sup>) and well below the MP2.8: $\kappa$ OOMP2 value of 0.84 kcal mol<sup>-1</sup>.

As the BH76 test set has been intensively investigated as a difficult case for DFT approaches,<sup>48,50</sup> a comparison with OO-REMP seems to be of interest. For the most demanding NHTBH38 subset of the BH76 test set, Goerigk et al. report an RMSD value of 6.23 kcal mol<sup>-1</sup> for the frequently used B3LYP-D3 hybrid functional, while 2.67 kcal mol<sup>-1</sup> is obtained with the best double-hybrid functional for this test set (DSD-BLYP-D3<sup>51</sup>).

As an additional test for properties other than regular reaction energies, the O23 set<sup>22,31,47,53</sup> of Bozkaya is considered. This set consists of 23 small open-shell noncovalent interactions. Noncovalent interaction energies are BSSE corrected<sup>54</sup> and were calculated from CBS-extrapolated total energies. The latter follows the CBS(3/4,aug-CC) recipe which uses a two-point Halkier procedure<sup>55</sup> from aug-cc-pVTZ and aug-cc-pVQZ basis sets with  $\alpha = 1.6$  and  $\beta = 3$ . As SCF energy, the UHF energy was used, and as correlation energy, the difference between UHF and the OO-REMP total energy was used.

Table 5 shows that OO-REMP also performs very well for these open-shell noncovalent interactions. The ideal MP2

**Table 5. Error Descriptors in kcal mol<sup>-1</sup> for the O23 Benchmark Set<sup>a</sup>**

A	MSD	MAD	min	max	$\sigma$	RMSD
0.00 <sup>a</sup>	0.20	0.21	-0.15	1.04	0.29	0.34
0.15	0.14	0.14	-0.00	0.62	0.17	0.21
0.20	0.13	0.13	-0.01	0.55	0.15	0.20
0.25	0.12	0.12	-0.04	0.46	0.14	0.18
0.30	0.11	0.11	-0.06	0.51	0.14	0.17
1.00	-0.02	0.37	-1.93	1.56	0.65	0.64
CCSD <sup>b</sup>	0.36	0.38	-0.20	1.59	0.49	0.60
OMP3 <sup>b</sup>	0.14	0.23	-0.50	1.61	0.41	0.43
SCS-OMP3-VDW <sup>b</sup>	0.34	0.34	0.00	1.41	0.44	0.55
OMP2.5 <sup>c</sup>	0.07	0.12	-0.21	0.78	0.21	0.22

<sup>a</sup>Excluding reaction 12 as the orbital optimization did not converge for  $A \leq 5\%$ . <sup>b</sup>Taken from ref 22. <sup>c</sup>Taken from ref 31. <sup>d</sup>OO-REMP/CBS(3/4,aug-CC), all electrons correlated. Reference reaction energies: CCSD(T)/CBS(3/4,aug-CC) taken from ref 53. The average absolute reaction energy amounts to 8.60 kcal mol<sup>-1</sup>.

fraction for this set is 35%, but OO-REMP(0.25) performs only slightly worse providing an RMSD of 0.19 kcal mol<sup>-1</sup> which is even slightly lower than for OMP2.5 (RMSD = 0.22 kcal mol<sup>-1</sup>). This is particularly remarkable due to the excellent performance of OMP2.5 for noncovalent interactions seen in the MAD of 0.12 kcal mol<sup>-1</sup> which is a little bit lower than the OO-REMP value (MAD = 0.13 kcal mol<sup>-1</sup>). However, OO-REMP(0.25) is superior to OMP2.5 with respect to outliers.

As a final benchmark, we consider the non-multireference subset of the W4-11 thermochemistry set that Bertels et al. used to parametrize MP2.8: $\kappa$ -OOMP2.<sup>33</sup> Table 6 lists error estimates

**Table 6. Error Descriptors in kcal mol<sup>-1</sup> for the 124 W4-11-nonMR Heats of Formation (Negative Atomization Energies)<sup>b</sup>**

A	MSD	MAD	min	max	$\sigma$	RMSD
0.00	4.68	4.68	-2.15	13.44	3.24	5.69
0.15	1.95	1.95	-1.71	5.88	1.14	2.26
0.20	1.07	1.19	-1.81	4.24	0.92	1.41
0.25	0.20	0.96	-3.06	3.78	1.23	1.25
0.30	-0.67	1.49	-5.06	4.25	1.81	1.92
1.00	-13.31	14.49	-48.74	10.80	12.50	18.22
CCSD <sup>a</sup>	8.01	8.01	0.00	20.34	4.82	9.34
MP2.8: $\kappa$ -OOMP2 <sup>a</sup>	-0.52	1.65	-5.83	5.24	2.03	2.09

<sup>a</sup>Data taken from the SI of ref 33 for the first 124 reactions. <sup>b</sup>OO-REMP/aug-cc-pVTZ, all electrons correlated. Reference reaction energies: CCSD(T)/aug-cc-pVTZ taken from ref 33. The average absolute reaction energy amounts to 326.68 kcal mol<sup>-1</sup>.

for average electronic heats of formation (negative atomization energies) for the 124 non-multireference cases of the W4-11 benchmark set<sup>56</sup> (TAE140). For this rather demanding test set, the RMSD of OO-REMP(0.25) (1.25 kcal mol<sup>-1</sup>) lies above 1 kcal mol<sup>-1</sup>, while the less stringent MAD (0.96 kcal mol<sup>-1</sup>) is just below this threshold. As before, the performance of OO-REMP(0.25) exceeds CCSD, OO-MP2, and OCEPA by far, and outperforms even MP2.8: $\kappa$ -OOMP2 which provides an RMSD of only 1.59 kcal mol<sup>-1</sup>.

Table 7 summarizes results obtained for the full set of 746 non-multireference reactions from the W4-11-derived sets TAE140, BDE99, HAT707, SN13, and ISOMERIZATION20

**Table 7. Error Descriptors in kcal mol<sup>-1</sup> for the 746 W4-11-nonMR Reactions<sup>b</sup>**

A	MSD	MAD	min	max	$\sigma$	RMSD
0.00	1.38	2.50	-5.84	13.44	3.00	3.30
0.15	0.34	1.02	-3.61	5.88	1.30	1.34
0.20	0.05	0.72	-3.35	4.24	0.96	0.96
0.25	-0.22	0.74	-3.25	3.78	0.95	0.97
0.30	-0.48	1.02	-5.06	4.25	1.26	1.35
1.00	-3.50	7.98	-48.74	17.86	10.24	10.81
CCSD <sup>a</sup>	1.49	3.62	-8.60	20.34	4.71	4.94
MP2.8: $\kappa$ -OOMP2 <sup>a</sup>	-0.45	1.25	-5.83	5.24	1.53	1.59

<sup>a</sup>Data taken from the SI of ref 33. <sup>b</sup>OO-REMP/aug-cc-pVTZ, all electrons correlated. Reference reaction energies: CCSD(T)/aug-cc-pVTZ taken from ref 33. The average absolute reaction energy amounts to 107.52 kcal mol<sup>-1</sup>.



that were used to parametrize MP2.8: $\kappa$ -OOMP2. Nevertheless, its MAD and RMSD values (1.25 kcal mol<sup>-1</sup> and 1.59 kcal mol<sup>-1</sup>)<sup>57</sup> are outperformed by the OO-REMP(0.25) counterparts (0.74 kcal mol<sup>-1</sup> and 0.97 kcal mol<sup>-1</sup>).

According to the results presented above, orbital-optimized REMP (OO-REMP) performs best with about 25% MP-contribution in the unperturbed Hamiltonian ( $A = 0.25$ ). OO-REMP improves upon all parent methods MP2, OMP2, CEPA(0)D, and OCEPA as well as on CCSD. Its performance is better or at least on par with that of OO-MP2.5 and MP2.8: $\kappa$ -OOMP2 which are—to the best of our knowledge—the best performing PT derived approaches proposed so far. As shown for other PTs before, orbital optimization is a convenient way to further improve the already fairly accurate results of the REMP approach for closed-shell reference cases while it is crucial for open-shell systems.<sup>20,21,24,25,31,32</sup>

OO-REMP(0.25) reproduces all considered test sets of reaction energies and reaction barrier heights of closed- and open-shell main-group systems with RMSD values below 1 kcal mol<sup>-1</sup>. For the rather demanding atomization energies of the W4-11-nonMR test set, this threshold is met for the less stringent MAD error estimate. Very good performance is also observed for the noncovalent interaction energies of the O23 test set. Thus, OO-REMP emerges as a quantum chemical approach which solely includes the first-order interacting space (i.e., no explicit triple or higher excitations) and meets the challenging criterion of being chemically accurate for the considered benchmark sets in its common definition in the computational chemistry literature.<sup>1</sup> We note, that the experimentalist's definition of chemical accuracy (RMSD = 0.5 kcal mol<sup>-1</sup>) is not but almost met by OO-REMP(0.25) for the chemically relevant reaction energy and barrier height benchmark sets.

Considering the computational scaling, OO-REMP, OO-MP2.5, MP2.8: $\kappa$ -OO-MP2, and the related PT scale as  $O(n^6)$  with the system size. OO-REMP is an iterative  $O(n^6)$  procedure requiring the same computational effort as OCEPA and about the same as CCSD. The latter does not need orbital macroiterations but requires evaluation of disconnected diagrams (some characteristic wall clock timings are collected in the Supporting Information). SCS-OMP3 and OMP2.5 exhibit iterative  $O(n^6)$  steps in the determination of the first-order wave function correction and some two-particle densities. MP2.8: $\kappa$ -OOMP2 scales as  $O(n^5)$  during the orbital iterations, and only a single energy evaluations scales as  $O(n^6)$ . OO-(SCS)-MP2, finally, only exhibits iterative  $O(n^5)$  scaling.

As OO-REMP provides relaxed densities as a Hylleraas-like energy functional is minimized with respect to the forms of the orbitals, it allows for fast analytical property evaluation.<sup>24</sup> Further improvement of the method seems possible by modifying the unperturbed Hamiltonian, e.g., by spin-component scaling<sup>35</sup> or by moving to higher order or fractional perturbation theories. Extensions to multireference cases are also possible as multireference RE approaches have been derived, implemented, and successfully applied.<sup>17,58–60</sup> Combination of these methods with any of the Fock-type operators commonly used in multireference PT<sup>58</sup> should lead to multireference REMP in a relatively straightforward manner.

While the results shown above are promising, further validation is required to obtain a more complete picture of the performance of OO-REMP. In particular, transition metal

system (e.g., TMC151<sup>61</sup> or MOR41<sup>62</sup>) and larger molecule benchmark sets as contained in the GMTKN55<sup>63</sup> shall be investigated. As these benchmark sets are not accessible with conventional codes like ours, it seems worth implementing (OO-)REMP variants with reduced prefactor or scaling as has already been demonstrated for OCEPA.<sup>47</sup>

Further details about our OO-REMP implementation as well as extensions of REMP to canonical open-shell reference wave functions will be reported in an upcoming publication.<sup>38</sup>

## ■ ASSOCIATED CONTENT

### Supporting Information

The Supporting Information is available free of charge at <https://pubs.acs.org/doi/10.1021/acs.jctc.1c00280>.

SCF, CCSD, and CCSD(T) total energies and new reference energies for SCS-MP2 set, OO-REMP total energies for all single point calculations involved, and some representative timings for OO-REMP in comparison to other methods (PDF)

Structures provided as TURBOMOLE coord file and OO-REMP total energies for all single point calculations involved (ZIP)

## ■ AUTHOR INFORMATION

### Corresponding Authors

Stefan Behnle – Eberhard Karls Universität, 72076 Tübingen, Germany; [orcid.org/0000-0003-3797-7272](https://orcid.org/0000-0003-3797-7272);

Email: [stefan.behnle@uni-tuebingen.de](mailto:stefan.behnle@uni-tuebingen.de)

Reinhold F. Fink – Eberhard Karls Universität, 72076 Tübingen, Germany; [orcid.org/0000-0002-8288-924X](https://orcid.org/0000-0002-8288-924X);

Email: [reinhold.fink@uni-tuebingen.de](mailto:reinhold.fink@uni-tuebingen.de)

Complete contact information is available at: <https://pubs.acs.org/doi/10.1021/acs.jctc.1c00280>

### Notes

The authors declare no competing financial interest.

## ■ ACKNOWLEDGMENTS

The authors are grateful for access to the computational resources provided by the LISA+ collaboration, the bwHPC project of the state of Baden-Württemberg, and by the bwForClusters JUSTUS and JUSTUS 2 that were supported by the Deutsche Forschungsgemeinschaft (DFG) through grant nos. INST 40/467-1 and INST 40/575-1.

## ■ REFERENCES

- (1) Peterson, K. A.; Feller, D.; Dixon, D. A. Chemical accuracy in ab initio thermochemistry and spectroscopy: current strategies and future challenges. *Theor. Chem. Acc.* **2012**, *131*, 1079.
- (2) Harding, M. E.; Vazquez, J.; Gauss, J.; Stanton, J. F.; Kállay, M. Towards highly accurate ab initio thermochemistry of larger systems: Benzene. *J. Chem. Phys.* **2011**, *135*, 044513.
- (3) Karton, A. A computational chemist's guide to accurate thermochemistry for organic molecules. *WIREs Comput. Mol. Sci.* **2016**, *6*, 292–310.
- (4) Bomble, Y. J.; Stanton, J. F.; Kállay, M.; Gauss, J. Coupled-cluster methods including noniterative corrections for quadruple excitations. *J. Chem. Phys.* **2005**, *123*, 054101.
- (5) Gwaltney, S. R.; Sherrill, C. D.; Head-Gordon, M.; Krylov, A. I. Second-order perturbation corrections to singles and doubles coupled-cluster methods: General theory and application to the valence optimized doubles model. *J. Chem. Phys.* **2000**, *113*, 3548–3560.

- (6) Raghavachari, K.; Trucks, G. W.; Pople, J. A.; Head-Gordon, M. A fifth-order perturbation comparison of electron correlation theories. *Chem. Phys. Lett.* **1989**, *157*, 479–483.
- (7) Cremer, D. Møller-Plesset perturbation theory: from small molecule methods to methods for thousands of atoms. *WIREs Comput. Mol. Sci.* **2011**, *1*, 509–530.
- (8) He, Y.; Cremer, D. Molecular Geometries at Sixth Order Møller-Plesset Perturbation Theory. At What Order Does MP Theory Give Exact Geometries? *J. Phys. Chem. A* **2000**, *104*, 7679–7688.
- (9) Helgaker, T.; Gauss, J.; Jørgensen, P.; Olsen, J. The prediction of molecular equilibrium structures by the standard electronic wave functions. *J. Chem. Phys.* **1997**, *106*, 6430–6440.
- (10) Grimme, S. Improved second-order Møller–Plesset perturbation theory by separate scaling of parallel- and antiparallel-spin pair correlation energies. *J. Chem. Phys.* **2003**, *118*, 9095–9102.
- (11) Grimme, S.; Goerigk, L.; Fink, R. F. Spin-component-scaled electron correlation methods. *WIREs Comput. Mol. Sci.* **2012**, *2*, 886–906.
- (12) Grimme, S. Improved third-order Møller-Plesset perturbation theory. *J. Comput. Chem.* **2003**, *24*, 1529–1537.
- (13) Pitonak, M.; Neogady, P.; Cerny, J.; Grimme, S.; Hobza, P. Scaled MP3 Non-Covalent Interaction Energies Agree Closely with Accurate CCSD(T) Benchmark Data. *ChemPhysChem* **2009**, *10*, 282–289.
- (14) Sedlak, R.; Janowski, T.; Pitoňák, M.; Řezáč, J.; Pulay, P.; Hobza, P. Accuracy of Quantum Chemical Methods for Large Noncovalent Complexes. *J. Chem. Theory Comput.* **2013**, *9*, 3364–3374.
- (15) Fink, R. F. Why does MP2 work? *J. Chem. Phys.* **2016**, *145*, 184101.
- (16) Fink, R. F. Two new unitary-invariant and size-consistent perturbation theoretical approaches to the electron correlation energy. *Chem. Phys. Lett.* **2006**, *428*, 461–466.
- (17) Fink, R. F. The multi-reference retaining the excitation degree perturbation theory: A size-consistent, unitary invariant, and rapidly convergent wavefunction based ab initio approach. *Chem. Phys.* **2009**, *356*, 39–46.
- (18) Behnle, S.; Fink, R. F. REMP: A hybrid perturbation theory providing improved electronic wavefunctions and properties. *J. Chem. Phys.* **2019**, *150*, 124107.
- (19) Knowles, P. J.; Andrews, J. S.; Amos, R. D.; Handy, N. C.; Pople, J. A. Restricted Møller–Plesset theory for open-shell molecules. *Chem. Phys. Lett.* **1991**, *186*, 130–136.
- (20) Lochan, R. C.; Head-Gordon, M. Orbital-optimized opposite-spin scaled second-order correlation: An economical method to improve the description of open-shell molecules. *J. Chem. Phys.* **2007**, *126*, 164101.
- (21) Neese, F.; Schwabe, T.; Kossmann, S.; Schirmer, B.; Grimme, S. Assessment of Orbital-Optimized, Spin-Component Scaled Second-Order Many-Body Perturbation Theory for Thermochemistry and Kinetics. *J. Chem. Theory Comput.* **2009**, *5*, 3060–3073.
- (22) Soydaş, E.; Bozkaya, U. Accurate Open-Shell Noncovalent Interaction Energies from the Orbital-Optimized Møller–Plesset Perturbation Theory: Achieving CCSD Quality at the MP2 Level by Orbital Optimization. *J. Chem. Theory Comput.* **2013**, *9*, 4679–4683.
- (23) Bozkaya, U. Orbital-optimized third-order Møller-Plesset perturbation theory and its spin-component and spin-opposite scaled variants: Application to symmetry breaking problems. *J. Chem. Phys.* **2011**, *135*, 224103.
- (24) Bozkaya, U.; Sherrill, C. D. Orbital-optimized coupled-electron pair theory and its analytic gradients: Accurate equilibrium geometries, harmonic vibrational frequencies, and hydrogen transfer reactions. *J. Chem. Phys.* **2013**, *139*, 054104.
- (25) Soydaş, E.; Bozkaya, U. Assessment of the orbital-optimized coupled-electron pair theory for thermochemistry and kinetics: Improving on CCSD and CEPA(1). *J. Comput. Chem.* **2014**, *35*, 1073–1081.
- (26) Roos, B. In *Ab Initio Methods in Quantum Chemistry, part II*; Advances in Chemical Physics, Lawley, K., Ed.; John Wiley & Sons, Inc.: 1987; Vol. LXIX, pp 399–446.
- (27) Werner, H.-J. Matrix-Formulated Direct Multiconfiguration Self-Consistent Field and Multiconfiguration Reference Configuration-Interaction Methods. *Adv. Chem. Phys.* **1987**, *11*, 1–62.
- (28) Scuseria, G. E.; Schaefer, H. F. The optimization of molecular orbitals for coupled cluster wavefunctions. *Chem. Phys. Lett.* **1987**, *142*, 354–358.
- (29) Bozkaya, U. Analytic energy gradients for the orbital-optimized third-order Møller–Plesset perturbation theory. *J. Chem. Phys.* **2013**, *139*, 104116.
- (30) Bozkaya, U.; Sherrill, C. D. Analytic energy gradients for the orbital-optimized second-order Møller–Plesset perturbation theory. *J. Chem. Phys.* **2013**, *138*, 184103.
- (31) Bozkaya, U.; Sherrill, C. D. Orbital-optimized MP2.5 and its analytic gradients: Approaching CCSD(T) quality for noncovalent interactions. *J. Chem. Phys.* **2014**, *141*, 204105.
- (32) Soydaş, E.; Bozkaya, U. Assessment of Orbital-Optimized MP2.5 for Thermochemistry and Kinetics: Dramatic Failures of Standard Perturbation Theory Approaches for Aromatic Bond Dissociation Energies and Barrier Heights of Radical Reactions. *J. Chem. Theory Comput.* **2015**, *11*, 1564–1573.
- (33) Bertels, L. W.; Lee, J.; Head-Gordon, M. Third-Order Møller–Plesset Perturbation Theory Made Useful? Choice of Orbitals and Scaling Greatly Improves Accuracy for Thermochemistry, Kinetics, and Intermolecular Interactions. *J. Phys. Chem. Lett.* **2019**, *10*, 4170–4176.
- (34) Surján, P. R. *Second quantized approach to quantum chemistry: an elementary introduction*; Springer: Berlin, Heidelberg, 1989; DOI: 10.1007/978-3-642-74755-7.
- (35) Fink, R. F. Spin-component-scaled Møller–Plesset (SCS-MP) perturbation theory: A generalization of the MP approach with improved properties. *J. Chem. Phys.* **2010**, *133*, 174113.
- (36) Bozkaya, U.; Turney, J. M.; Yamaguchi, Y.; Schaefer, H. F.; Sherrill, C. D. Quadratically convergent algorithm for orbital optimization in the orbital-optimized coupled-cluster doubles method and in orbital-optimized second-order Møller-Plesset perturbation theory. *J. Chem. Phys.* **2011**, *135*, 104103.
- (37) Kutzelnigg, W.; Mukherjee, D. Normal order and extended Wick theorem for a multiconfiguration reference wave function. *J. Chem. Phys.* **1997**, *107*, 432–449.
- (38) Behnle, S.; Fink, R. manuscript in preparation.
- (39) Derivation of eq 12 for  $\lambda_{ij}^{ab}$  yields the usual  $t$  amplitude equations, while derivation for  $t_{ab}^{ij}$  yields the  $\lambda$  amplitude equations. The  $\lambda$  amplitudes serve as Lagrangian multipliers enforcing the constraint that the  $t$  amplitude equations are still solved if the orbitals are modified. As in the case of OO-CEPA and OO-MP2, the equality  $\lambda_{ij}^{ab} = t_{ab}^{ij}$  holds for OO-REMP; it is therefore not necessary to explicitly solve the  $\lambda$  equations.
- (40) Helgaker, T.; Jørgensen, P.; Olsen, J. *Molecular Electronic-Structure Theory*; Wiley: Chichester, New York, Weinheim, 2000; DOI: 10.1002/9781119019572.
- (41) Chen, W.; Schlegel, H. B. Evaluation of S2 for correlated wave functions and spin projection of unrestricted Møller–Plesset perturbation theory. *J. Chem. Phys.* **1994**, *101*, 5957–5968.
- (42) Fink, R.; Staemmler, V. A multi-configuration reference CEPA method based on pair natural orbitals. *Theor. Chim. Acta* **1993**, *87*, 129–145.
- (43) Hansen, A.; Liakos, D. G.; Neese, F. Efficient and accurate local single reference correlation methods for high-spin open-shell molecules using pair natural orbitals. *J. Chem. Phys.* **2011**, *135*, 214102.
- (44) Neese, F. Software update: the ORCA program system, version 4.0. *WIREs Comput. Mol. Sci.* **2018**, *8*, e1327–e1327.
- (45) Smith, D. G. A.; Burns, L. A.; Simmonett, A. C.; Parrish, R. M.; Schieber, M. C.; Galvelis, R.; Kraus, P.; Kruse, H.; Remigio, R. D.; Alenaizan, A.; James, A. M.; Lehtola, S.; Misiewicz, J. P.; Scheurer, M.; Shaw, R. A.; Schriber, J. B.; Xie, Y.; Glick, Z. L.; Sirianni, D. A.; O'Brien, J. S.; Waldrop, J. M.; Kumar, A.; Hohenstein, E. G.; Pritchard, B. P.; Brooks, B. R.; Schaefer, H. F.; Sokolov, A. Y.; Patkowski, K.; DePrince, A. E.; Bozkaya, U.; King, R. A.; Evangelista, F. A.; Turney, J. M.; Crawford, T. D.; Sherrill, C. D. Psi4 1.4: Open-source software for high-throughput quantum chemistry. *J. Chem. Phys.* **2020**, *152*, 184108.

(46) Soydaş, E.; Bozkaya, U. Assessment of Orbital-Optimized Third-Order Møller–Plesset Perturbation Theory and Its Spin-Component and Spin-Opposite Scaled Variants for Thermochemistry and Kinetics. *J. Chem. Theory Comput.* **2013**, *9*, 1452–1460.

(47) Bozkaya, U. Orbital-optimized linearized coupled-cluster doubles with density-fitting and Cholesky decomposition approximations: an efficient implementation. *Phys. Chem. Chem. Phys.* **2016**, *18*, 11362–11373.

(48) Goerigk, L.; Hansen, A.; Bauer, C.; Ehrlich, S.; Najibi, A.; Grimme, S. A look at the density functional theory zoo with the advanced GMTKN55 database for general main group thermochemistry, kinetics and noncovalent interactions. *Phys. Chem. Chem. Phys.* **2017**, *19*, 32184–32215.

(49) Lynch, B. J.; Truhlar, D. G. What Are the Best Affordable Multi-Coefficient Strategies for Calculating Transition State Geometries and Barrier Heights? *J. Phys. Chem. A* **2002**, *106*, 842–846.

(50) Zhao, Y.; González-García, N.; Truhlar, D. G. Benchmark Database of Barrier Heights for Heavy Atom Transfer, Nucleophilic Substitution, Association, and Unimolecular Reactions and Its Use to Test Theoretical Methods. *J. Phys. Chem. A* **2005**, *109*, 2012–2018.

(51) Kozuch, S.; Gruzman, D.; Martin, J. M. L. DSD-BLYP: A General Purpose Double Hybrid Density Functional Including Spin Component Scaling and Dispersion Correction. *J. Phys. Chem. C* **2010**, *114*, 20801–20808.

(52) The error estimates for the NHTBH38 subset were calculated from the results provided in ref 63.

(53) Bozkaya, U. Orbital-Optimized Second-Order Perturbation Theory with Density-Fitting and Cholesky Decomposition Approximations: An Efficient Implementation. *J. Chem. Theory Comput.* **2014**, *10*, 2371–2378.

(54) Boys, S.; Bernardi, F. The calculation of small molecular interactions by the differences of separate total energies. Some procedures with reduced errors. *Mol. Phys.* **1970**, *19*, 553–566.

(55) Halkier, A.; Helgaker, T.; Jørgensen, P.; Klopper, W.; Koch, H.; Olsen, J.; Wilson, A. K. Basis-set convergence in correlated calculations on Ne, N<sub>2</sub>, and H<sub>2</sub>O. *Chem. Phys. Lett.* **1998**, *286*, 243–252.

(56) Karton, A.; Daon, S.; Martin, J. M. W4–11: A high-confidence benchmark dataset for computational thermochemistry derived from first-principles W4 data. *Chem. Phys. Lett.* **2011**, *510*, 165–178.

(57) Slight deviations from Table 1 of ref 33 for OO-MP2 probably result from convergence to different states and decimal rounding errors as reference numbers were provided with only two decimal places.

(58) Roca-Sanjuan, D.; Aquilante, F.; Lindh, R. Multiconfiguration second-order perturbation theory approach to strong electron correlation in chemistry and photochemistry. *WIREs Comput. Mol. Sci.* **2012**, *2*, 585–603.

(59) Sharma, S.; Alavi, A. Multireference linearized coupled cluster theory for strongly correlated systems using matrix product states. *J. Chem. Phys.* **2015**, *143*, 102815.

(60) Saitow, M.; Yanai, T. A multireference coupled-electron pair approximation combined with complete-active space perturbation theory in local pair-natural orbital framework. *J. Chem. Phys.* **2020**, *152*, 114111.

(61) Chan, B.; Gill, P. M. W.; Kimura, M. Assessment of DFT Methods for Transition Metals with the TMC151 Compilation of Data Sets and Comparison with Accuracies for Main-Group Chemistry. *J. Chem. Theory Comput.* **2019**, *15*, 3610–3622.

(62) Dohm, S.; Hansen, A.; Steinmetz, M.; Grimme, S.; Chęcinski, M. P. Comprehensive Thermochemical Benchmark Set of Realistic Closed-Shell Metal Organic Reactions. *J. Chem. Theory Comput.* **2018**, *14*, 2596–2608.

(63) GMTKN55 - A database for general main group thermochemistry, kinetics, and non-covalent interactions. <https://www.chemie.uni-bonn.de/pctc/mulliken-center/software/GMTKN/gmtkn55> (accessed 2021-01-20).

# UREMP, RO-REMP, and OO-REMP: Hybrid perturbation theories for open-shell electronic structure calculations

Cite as: J. Chem. Phys. **156**, 124103 (2022); <https://doi.org/10.1063/5.0081285>

Submitted: 08 December 2021 • Accepted: 21 February 2022 • Accepted Manuscript Online: 22 February 2022 • Published Online: 22 March 2022

 Stefan Behnle and  Reinhold F. Fink



View Online



Export Citation



CrossMark

## ARTICLES YOU MAY BE INTERESTED IN

[Efficient and automated quantum chemical calculation of rovibrational nonresonant Raman spectra](#)

The Journal of Chemical Physics **156**, 124102 (2022); <https://doi.org/10.1063/5.0087359>

[Cavity quantum-electrodynamical time-dependent density functional theory within Gaussian atomic basis. II. Analytic energy gradient](#)

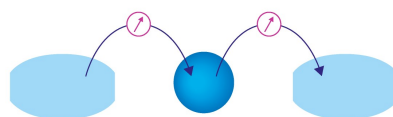
The Journal of Chemical Physics **156**, 124104 (2022); <https://doi.org/10.1063/5.0082386>

[H<sub>2</sub>O inside the fullerene C<sub>60</sub>: Inelastic neutron scattering spectrum from rigorous quantum calculations](#)

The Journal of Chemical Physics **156**, 124101 (2022); <https://doi.org/10.1063/5.0086842>

Webinar

Interfaces: how they make  
or break a nanodevice



March 29th – Register now

 Zurich  
Instruments



# UREMP, RO-REMP, and OO-REMP: Hybrid perturbation theories for open-shell electronic structure calculations

Cite as: J. Chem. Phys. 156, 124103 (2022); doi: 10.1063/5.0081285

Submitted: 8 December 2021 • Accepted: 21 February 2022 •

Published Online: 22 March 2022



View Online



Export Citation



CrossMark

Stefan Behnle<sup>a)</sup>  and Reinhold F. Fink<sup>b)</sup> 

## AFFILIATIONS

Institute for Physical and Theoretical Chemistry, Eberhard Karls University Tübingen, Auf der Morgenstelle 18, 72076 Tübingen, Germany

<sup>a)</sup>Electronic mail: [stefan.behnle@uni-tuebingen.de](mailto:stefan.behnle@uni-tuebingen.de)

<sup>b)</sup>Author to whom correspondence should be addressed: [reinhold.fink@uni-tuebingen.de](mailto:reinhold.fink@uni-tuebingen.de)

## ABSTRACT

An accurate description of the electron correlation energy in closed- and open-shell molecules is shown to be obtained by a second-order perturbation theory (PT) termed REMP. REMP is a hybrid of the Retaining the Excitation degree (RE) and the Møller–Plesset (MP) PTs. It performs particularly encouragingly in an orbital-optimized variant (OO-REMP) where the reference wavefunction is given by an unrestricted Slater determinant whose spin orbitals are varied such that the total energy becomes a minimum. While the approach generally behaves less satisfactorily with unrestricted Hartree–Fock references, reasonable performance is observed for restricted Hartree–Fock and restricted open-shell Hartree–Fock references. Inclusion of single excitations to OO-REMP is investigated and found—as in similar investigations—to be dissatisfying as it deteriorates performance. For the non-multireference subset of the accurate W4-11 benchmark set of Karton *et al.* [Chem. Phys. Lett. 510, 165–178 (2011)], OO-REMP predicts most atomization and reaction energies with chemical accuracy (1 kcal mol<sup>-1</sup>) if complete-basis-set extrapolation with augmented and core-polarized basis sets is used. For the W4-11 related test-sets, the error estimates obtained with the OO-REMP method approach those of coupled-cluster with singles, doubles and perturbative triples [CCSD(T)] within 20%–35%. The best performance of OO-REMP is found for a mixing ratio of 20%:80% MP:RE, which is essentially independent of whether radical stabilization energies, barrier heights, or reaction energies are investigated. Orbital optimization is shown to improve the REMP approach for both closed and open shell cases and outperforms coupled-cluster theory with singles and doubles (CCSD), spin-component scaled Møller–Plesset theory at second order (SCS-MP2), and density functionals, including double hybrids in all the cases considered.

Published under an exclusive license by AIP Publishing. <https://doi.org/10.1063/5.0081285>

## I. INTRODUCTION

Rayleigh–Schrödinger perturbation theory<sup>1</sup> is a standard method for introducing electron correlation into the electronic wavefunction.<sup>2–5</sup> This requires to partition the Hamiltonian  $\hat{H}$  into an unperturbed Hamiltonian  $\hat{H}^{(0)}$  and a perturbation  $\hat{H}^{(1)} = \hat{H} - \hat{H}^{(0)}$  and to identify an unperturbed (zeroth order) wavefunction  $\Psi^{(0)}$ , also termed reference wavefunction. The standard approach is the Møller–Plesset<sup>2,4,6</sup> (MP) method, which utilizes the Hartree–Fock (HF) determinant as an unperturbed wavefunction and the corresponding Fockian as  $\hat{H}^{(0)}$ . While MP fulfills all criteria for generally applicable wavefunction theories, such as

size consistency, unitary invariance, systematic improvability, and others, its predictational capacity for typical chemical problems is unsatisfactory. Improved performance was achieved by (i) empirically modifying the correlation energy expression as in spin-component scaled (SCS)-MP2,<sup>7,8</sup> SCS-MP3,<sup>9</sup> or regularized MP variants;<sup>10,11</sup> (ii) introducing fractional order perturbed energies as in MP2.5,<sup>12</sup> MP2.X,<sup>13</sup> or MP3.5;<sup>14</sup> (iii) choosing another unperturbed Hamiltonian as the, however, generally unsatisfactory Epstein–Nesbet (EN)<sup>15–18</sup> one, Feenberg scaling,<sup>19–21</sup> the Feenberg scaled SCS-MP2 variant,<sup>22</sup> the S2-MP approach,<sup>23</sup> or the optimized perturbation theory (OPT-PT);<sup>18,24,25</sup> and (iv) modifying the reference wavefunction by orbital optimization, as has been demonstrated for OO-MP2,<sup>26,27</sup> OB-MP2,<sup>28</sup> OO-MP3,<sup>29,30</sup>



OCID,<sup>31,32</sup> or OCCD.<sup>33–36</sup> It was shown to be particularly effective to employ several of these improvements simultaneously, as in OO-SOS-MP2,<sup>37,38</sup> OMP2.5,<sup>39–41</sup> OCEPA(0),<sup>42–44</sup> and the orbital-optimized and regularized MP-PT approaches  $\kappa$ - or  $\sigma$ -OOMP2<sup>11</sup> and MP2.8: $\kappa$ -OOMP2.<sup>10</sup>

The “Retaining the Excitation Degree” (RE)<sup>45,46</sup> method is an alternative partitioning of the Hamiltonian proposed by one of the present authors. The zeroth-order Hamiltonian contains all contributions of the second-quantization Hamiltonian that do not change the number of electrons in the occupied or virtual orbitals. It is related to Dyall’s active space Hamiltonian.<sup>47</sup> The general concept behind RE is to maximize the number of terms in  $\widehat{H}^{(0)}$  and minimize the number of terms in  $\widehat{H}^{(1)}$ . The unperturbed Hamiltonian couples all configurations of the same excitation degree, while the perturbation exclusively couples configurations of different excitation degrees.

In the present work, we shall describe and validate several implementations of the REMP hybrid perturbation theory for open-shell systems. REMP is defined by setting  $\widehat{H}^{(0)}$  to a weighted mixture of the unperturbed Hamiltonians of the MP and RE methods.<sup>48</sup> The idea to mix the perturbation methods RE and MP emerges from a systematic investigation of the errors of the respective first-order wavefunctions in terms of proper configuration state functions (CSFs) by one of the authors.<sup>49</sup> Accordingly, MP2 has a clear and systematic tendency to strongly underestimate correlation energy contributions of singlet-coupled doubly excited (SDE) CSFs, while the corresponding triplet-coupled doubly excited (TDE) CSF contributions are overestimated. To a lesser degree, RE behaves essentially in the opposite way by overestimating SDE and underestimating TDE contributions. The mixed approach REMP is designed as to ameliorate these errors. In an earlier contribution,<sup>48</sup> it was shown that forming a mixed unperturbed Hamiltonian, indeed, leads to an improved wavefunction itself. REMP, therefore, has the potential to provide the right answer for the right reason albeit at the cost of one empirical parameter.

While coupled-cluster with singles, doubles and perturbative triples [CCSD(T)]<sup>2,50</sup> is still the *de facto* gold standard for correlated single reference calculations, in recent years, a number of methods emerged that circumvent the necessity to explicitly calculate triple excitations while exhibiting almost competitive performance. Like PCPF-MI,<sup>51</sup> pCCSD,<sup>52,53</sup> or OS-CCSD-SP(2),<sup>54</sup> these are mostly coupled pair or coupled cluster-type methods, which either introduce some scaling in the amplitude expression or add perturbative corrections with  $n^6$  scaling to the CCSD energy. Within the realm of perturbation theory, comparable performance was demonstrated for some of the above-mentioned Møller–Plesset variants, which combine orbital optimization with empirical scaling of higher-order perturbative contributions while preserving an  $n^6$  scaling. Examples for this class of methods are OMP2.5,<sup>39–41</sup> MP2.8: $\kappa$ -OOMP2,<sup>10</sup> and the orbital-optimized variant of REMP (OO-REMP), which was recently presented in a letter by the present authors.<sup>55</sup> In the following, we provide a more complete report on the latter methodology. Furthermore, we describe the REMP approach for unrestricted and restricted open-shell reference wavefunctions. We also consider the effect of adding single excitations within the OO-REMP approach. The performance of these methods is validated with reaction energy and activation barrier benchmark sets.

## II. THEORY

### A. REMP perturbation theory

Throughout this work, the commonly used indexing scheme for spin orbitals is used, i.e.,  $i, j, k, l, m, n$  are used for occupied,  $a, b, c, d, e, f$  are used for virtual, and  $p, q, r, s$  are used for arbitrary spin-orbitals.  $\hat{a}_i$  denotes an annihilation operator from spin orbital  $i$ , while  $\hat{a}_i^\dagger$  denotes its adjoint creation operator.

For applying Rayleigh–Schrödinger perturbation theory to the electron correlation problem,<sup>1,2,56</sup> the electronic Hamiltonian  $\widehat{H}$  is partitioned into a perturbation  $\widehat{H}^{(1)}$  and an unperturbed part  $\widehat{H}^{(0)}$  for which the unperturbed (zeroth order) Schrödinger equation

$$\widehat{H}^{(0)}|\Psi^{(0)}\rangle = E^{(0)}|\Psi^{(0)}\rangle \quad (1)$$

must be exactly fulfilled.

In the formalism of second quantization,<sup>2,57,58</sup> the electronic Hamiltonian reads

$$\widehat{H} = \sum_{p,q} h_{pq} \hat{a}_p^\dagger \hat{a}_q + \frac{1}{2} \sum_{pqrs} \langle pq|rs \rangle \hat{a}_p^\dagger \hat{a}_q^\dagger \hat{a}_s \hat{a}_r, \quad (2)$$

where  $h_{pq}$  is a matrix element of the one-electron Hamiltonian and  $\langle pq|rs \rangle = \int \phi_p^*(1) \phi_q^*(2) \frac{1}{r_{12}} \phi_r(1) \phi_s(2) d\tau$  is a two-electron repulsion integral in the Dirac notation.

The MP partitioning uses the Fock operator as the unperturbed zeroth-order Hamiltonian. Starting from Hartree–Fock theory, this is the most natural choice,

$$\widehat{H}_{\text{MP}}^{(0)} = \widehat{F} = \widehat{h} + \widehat{J} - \widehat{K} \quad (3)$$

$$= \sum_{p,q} f_{pq} \hat{a}_p^\dagger \hat{a}_q = \sum_{p,q} \delta_{pq} \epsilon_p \hat{a}_p^\dagger \hat{a}_q, \quad (4)$$

where the last equality only holds in the case of canonical MOs.  $f_{pq}$  denotes a matrix element of the Fockian in the MO basis,  $\epsilon_p$  denotes an eigenvalue of the Fockian (“orbital energy”), and  $\delta_{pq}$  is the Kronecker delta. Within a matrix representation of the Hamiltonian in a configuration interaction (CI) basis,  $\widehat{H}_{\text{MP}}^{(0)}$  contains only diagonal matrix elements.<sup>59</sup>

The Fock operator does only fulfill Eq. (1) for Hartree–Fock orbitals. For any other set of orbitals, the Fock operator is no more a valid choice of the unperturbed Hamiltonian and must be amended as, e.g.,

$$\widehat{F}^{\text{d}} = \sum_{ij} f_{ij} \hat{a}_i^\dagger \hat{a}_j + \sum_{a,b} f_{ab} \hat{a}_a^\dagger \hat{a}_b. \quad (5)$$

The combination of an annihilation operator and a creation operator represents a single excitation, and the single excitations in Eq. (5) do not change the excitation degree (the number of electrons in the virtual orbitals). Thus, the diagonal Fock operator may be written as

$$\widehat{F}^{\text{d}} = \sum_{\substack{p,q; \\ \Delta n_{\text{ex}}=0}} f_{pq} \hat{a}_p^\dagger \hat{a}_q, \quad (6)$$

where  $\Delta n_{\text{ex}}$  designates the change in the excitation degree due to the respective excitation operator.

The RE perturbation theory<sup>45,46,60</sup> is defined by applying such an excitation degree restriction to the Hamiltonian in second quantization, Eq. (2). The zeroth order Hamiltonian includes all terms that do not change the excitation degree

$$\widehat{H}_{\text{RE}}^{(0)} = \sum_{\substack{p,q; \\ \Delta n_{\text{ex}}=0}} h_{pq} \hat{a}_p^\dagger \hat{a}_q + \frac{1}{2} \sum_{\substack{p,q,r,s; \\ \Delta n_{\text{ex}}=0}} \langle pq|rs \rangle \hat{a}_p^\dagger \hat{a}_q^\dagger \hat{a}_s \hat{a}_r. \quad (7)$$

For RHF (closed-shell singlet) references, the RE second-order energy correction coincides with the CEPA(0)<sup>61,62</sup> correlation energy, also known as linearized coupled cluster with doubles (LCCD),<sup>63–65</sup> linearized coupled-pair many-electron-theory (L-CP-MET),<sup>66,67</sup> all orders in double excitation diagrams many-body perturbation theory [MBPT-D( $\infty$ )],<sup>68,69</sup> or optimized perturbation theory (OPT-PT).<sup>24,25</sup>

The REMP method is defined by setting the unperturbed Hamiltonian to a constrained mixture of the Møller–Plesset- and the RE-PTs,

$$\widehat{H}_{\text{REMP}}^{(0)} = (1 - A) \cdot \widehat{H}_{\text{RE}}^{(0)} + A \cdot \widehat{H}_{\text{MP}}^{(0)}. \quad (8)$$

The mixing parameter  $A$  represents the Møller–Plesset amount of the unperturbed Hamiltonian. Energies and wavefunctions obtained with it are denoted as REMP( $A$ ). Further details on the motivation of REMP and the closed shell implementation can be found in our preceding publication.<sup>48</sup>

The focus of this work was to implement the OO-REMP approach into an efficient code, which does not introduce approximations beyond the basis set expansion and a threshold value for two electron integrals. Thus, we limited ourselves to the second-order energy and the first-order wavefunction, which allows for an efficient implementation in a direct CI fashion. In the following, the orbital optimization approach is described where we adopt a coupled cluster style notation.<sup>3</sup>

The open-shell generalization uses plain excited Slater determinants to express the first-order perturbed wavefunction as

$$|\Psi^{(1)}\rangle = (\widehat{T}_1^{(1)} + \widehat{T}_2^{(1)})|\phi_0\rangle, \quad (9)$$

where  $\widehat{T}$  denotes the usual cluster operator and  $|\phi_0\rangle$  is the (single) reference Slater determinant. Using the formalism of second quantization<sup>57</sup> and the concept of normal order (with respect to the Fermi vacuum),<sup>3,70–72</sup> the total electronic Hamiltonian can be rewritten as

$$\widehat{H} = \widehat{F}_N^d + \langle \phi_0 | \widehat{F}^d | \phi_0 \rangle + \widehat{F}^o + \widehat{W}_N + \langle \phi_0 | \widehat{W} | \phi_0 \rangle, \quad (10)$$

where  $N$  indicates normal order with respect to the Fermi vacuum,  $d$  implies that only the block-diagonal part,<sup>73</sup> i.e., only the occupied–occupied and the virtual–virtual part, are included,  $o$  indicates that only the off-diagonal part (occupied–virtual/virtual–occupied) is included, and  $\widehat{W}$  is that part of the two-electron repulsion operator that is not included in the Fockian (“fluctuation potential”).

Using the representation of Eq. (10), it is possible to rewrite the unperturbed Hamiltonians and the perturbation of MP and RE in a way suitable for diagrammatic evaluation,

$$\widehat{H}_{\text{MP}}^{(0)} = \widehat{F}_N^d + \underbrace{\langle \phi_0 | \widehat{F}^d | \phi_0 \rangle}_{E_{\text{MP}}^{(0)}}, \quad (11)$$

$$\widehat{H}_{\text{MP}}^{(1)} = \widehat{F}^o + \underbrace{\langle \phi_0 | \widehat{W} | \phi_0 \rangle}_{E_{\text{MP}}^{(1)}}, \quad (12)$$

$$\widehat{H}_{\text{RE}}^{(0)} = \widehat{F}_N^d + \widehat{W}_{R=0} + \underbrace{\langle \phi_0 | \widehat{F}^d | \phi_0 \rangle + \langle \phi_0 | \widehat{W}_{R=0} | \phi_0 \rangle}_{=E_{\text{RE}}^{(0)}=E_{\text{HF}}}, \quad (13)$$

$$\widehat{H}_{\text{RE}}^{(1)} = \widehat{F}^o + \widehat{W}_{R \neq 0} + \underbrace{\langle \phi_0 | \widehat{W}_{R \neq 0} | \phi_0 \rangle}_{=E_{\text{RE}}^{(1)}=0}, \quad (14)$$

where  $R$  denotes the excitation degree of the terms/diagrams included. Every diagram used in the context of electron correlation can be assigned an excitation degree; there is thus an intimate connection between the concept of excitation degrees used in (single-reference) RE and diagrammatic techniques. The partitioning defined by Eqs. (11) and (12) for MP and Eqs. (13) and (14) for RE is fully consistent with the partitioning used in the closed-shell case, the MP partitioning for unrestricted Hartree–Fock (UHF) references, and the so-called RMP (“Restricted Møller–Plesset”) theory partitioning for ROHF references.<sup>71,72,74</sup> The RE first-order doubles residuum derived from this partitioning is again identical to CEPA/0(D) for UHF references.<sup>75,76</sup> If Eqs. (9) and (11)–(14) are inserted into the equation determining the first-order perturbed wavefunction and left-projected with  $\langle \phi_{ij}^{ab} |$  or  $\langle \phi_i^a |$ , one obtains the following (spin-orbital) residuum equations for RE and MP, respectively (assuming orthonormal orbitals):

$$\begin{aligned} \sigma_{ab,\text{RE1}}^{ij} = & K_{ab}^{ij} - K_{ba}^{ij} + \sum_c (t_{ac}^{ij} f_{bc} - t_{bc}^{ij} f_{ac}) + \sum_k (t_{ab}^{ik} f_{ik} - t_{ab}^{ik} f_{jk}) \\ & + \sum_{kl} K_{kl}^{ij} t_{ab}^{kl} + \sum_{cd} K_{ab}^{cd} t_{cd}^{ij} + \sum_{kc} (t_{ac}^{ik} (K_{cb}^{kj} - J_{cb}^{kj}) \\ & - t_{ac}^{jk} (K_{cb}^{ki} - J_{cb}^{ki}) - t_{bc}^{ik} (K_{ca}^{kj} - J_{ca}^{kj}) + t_{bc}^{jk} (K_{ca}^{ki} - J_{ca}^{ki})), \quad (15) \end{aligned}$$

$$\sigma_{a,\text{RE1}}^i = f_{ia} + \sum_b f_{ab} t_b^i - \sum_k t_a^k f_{ki} + \sum_{kc} t_c^k (K_{ac}^{ik} - J_{ac}^{ik}), \quad (16)$$

$$\sigma_{ab,\text{MP1}}^{ij} = K_{ab}^{ij} - K_{ba}^{ij} + \sum_c (t_{ac}^{ij} f_{bc} - t_{bc}^{ij} f_{ac}) + \sum_k (t_{ab}^{ik} f_{ik} - t_{ab}^{ik} f_{jk}), \quad (17)$$

$$\sigma_{a,\text{MP1}}^i = f_{ia} + \sum_b f_{ab} t_b^i - \sum_k f_{ik} t_a^k. \quad (18)$$

As for the closed shell case,<sup>48</sup> the MP1 residuum is completely contained in the RE1 residuum. For obtaining spin-integrated equations, the sums have to be expanded in terms of spin orbitals and the spin has to be integrated out, which eliminates certain terms. Note that Eqs. (15)–(18) do not assume canonical orbitals but are valid for any set of orthonormal orbitals.

### 1. UREMP

The generalization to unrestricted reference determinants is straightforward. Appropriate residuum equations for UREMP are obtained from Eqs. (15)–(18) by simply keeping the parts that occur in both the MP and the RE residuum and by scaling those parts by  $1 - A$ , which only occur in the RE residuum. If (canonical or localized) UHF orbitals are used, the Brillouin theorem is fulfilled, and consequently, the single excitations vanish exactly. In the case of UHF references, the second order energy correction of RE is again identical to CEPA/0(D). It will here be denoted as URE2.

### 2. RO-REMP

The extension of REMP to restricted open-shell reference determinants is not as straightforward as in the UHF case. The main obstacle is that there exist at least seven possibilities to formulate the MP2 energy for an ROHF reference.<sup>71</sup> Furthermore, there exist several parameterizations of ROHF, which lead to the same wavefunction but to different orbitals and orbital energies.<sup>77</sup> The ROHF orbitals used in this work diagonalize the effective Fock operator described by Jungen in Ref. 78. They correspond to the scheme described by Fægri and Manne,<sup>79</sup> which is also the ROHF parameterization used in TURBOMOLE. Some of the ROMP2 variants proposed in the literature are not invariant with respect to the choice of ROHF flavor<sup>80</sup> or can only be applied for one specific ROHF parameterization.<sup>71,77</sup> To keep things as simple as possible, we decided to use the RMP variant for Møller–Plesset treatment. RMP has the advantage that the residuum equations for the restricted open-shell case are the same as in the UHF case. On the other hand, RMP has the disadvantage that effectively different orbitals for different spins (DODS) are introduced, which ultimately destroys the exact  $\langle S^2 \rangle$  properties. When building operators from integrals and orbitals, densities are formed with different numbers of  $\alpha$  and  $\beta$  spin electrons, resulting in different operators for  $\alpha$  and  $\beta$  spin orbitals. This becomes even more obvious if semicanonical orbitals<sup>72</sup> are constructed. Using semicanonical orbitals for RMP2 has the advantage that in this basis, the Fock operators become block-diagonal again. Thus, energies and amplitudes can be computed from a sum-over-states expression. For the RE partitioning, on the other hand, semicanonical orbitals provide no advantage as the scaling of the most expensive step (the external exchange operator) is not affected by the choice of the canonicalization. Using semicanonical orbitals, furthermore, introduces some ambiguity as soon as core or high-lying virtual orbitals are excluded from the correlation treatment: the usual procedure is to first block-diagonalize the Fockians in the full MO basis, then to recalculate all necessary operators, and then to freeze unwanted orbitals. However, original ROHF orbitals with the same number of frozen core orbitals provide results distinctly different from those obtained after semicanonicalization. The reason is that the semicanonicalization is not a unitary transformation within the frozen or active space but is allowed to

mix frozen and active orbitals. Our program is able to use any kind of orthonormal orbitals. As we do not see any benefit from using semicanonical orbitals for REMP, we decided to directly use the Fægri–Manne ROHF orbitals resulting from the ROHF-SCF procedure for all RO-REMP calculations. It is important to note that our results for 100% MP thus may slightly deviate from frozen core RMP2 results obtained with other programs, such as ORCA,<sup>97,98</sup> GAMESS-US,<sup>116</sup> or PSI4,<sup>117</sup> which use semicanonical orbitals by default.

As the Brillouin theorem is generally not fulfilled for ROHF, the first-order wavefunction correction will contain single excitations. They are treated like the double excitations; residuum vector elements occurring in Eq. (16) but not in Eq. (18) are scaled by  $1 - A$ .

The similarity of RE to CEPA/0 partially breaks down for ROHF. The equations that determine the first order singles and doubles amplitudes are decoupled for RE, while they are coupled for CEPA/0(SD).

The second-order RE energy with a restricted open-shell reference will be denoted as RORE2, while the second-order REMP energy will be denoted as RO-REMP( $A$ ) according to the chosen value of the mixing parameter  $A$ .

### B. Orbital-optimized REMP

The Orbital-Optimized REMP (OO-REMP) method is inspired by its relative Orbital-Optimized MP2 (abbreviated as OO-MP2<sup>27,81</sup> or OMP2<sup>35</sup> by different authors) and Orbital Optimized CEPA [OO-CEPA or OCEPA(0)<sup>44</sup>]. The concept of adjusting the orbitals of the reference determinant such that the total energy of a correlated method becomes minimal with respect to all parameters has been pioneered by Scuseria and Schaefer<sup>33</sup> in the context of coupled cluster theory. This has later been extended by Krylov *et al.*<sup>82,83</sup> Orbital optimization for SOS-MP2 was introduced by Head-Gordon *et al.*<sup>37,84</sup> and extended to SCS-MP2 by Neese *et al.*<sup>27,85</sup> Later, Bozkaya and Sherrill<sup>26,29,30,39,86–88</sup> introduced analytic gradients and extensions to higher orders in perturbation theory. The same authors also developed the OCEPA(0)<sup>44</sup> model, an orbital-optimized variant of CEPA(0)/D and an approximation to full OO-CCD. The orbital-optimized REMP model closely follows the lines of OCEPA(0).

From a comparison of Eq. (68) of Ref. 35 and Eq. (7) of Ref. 44, the second order REMP energy functional is given by

$$\begin{aligned} \tilde{E}_{\text{REMP}}^{(2)} = & \langle \phi_0 | \hat{H} | \phi_0 \rangle + \langle \phi_0 | \{ \widehat{W}_N \widehat{T}_2^{(1)} \}_c | \phi_0 \rangle \\ & + \left\langle \phi_0 \left[ \widehat{\Lambda}_2^{(1)} \{ \widehat{W}_N + \widehat{f}_N \widehat{T}_2^{(1)} + (1 - A) \widehat{W}_N \widehat{T}_2^{(1)} \}_c \right] \phi_0 \right\rangle, \end{aligned} \quad (19)$$

where

$$\widehat{T}_2^{(1)} = \frac{1}{4} \sum_{ij} \sum_{a,b} t_{ab}^{ij(1)} \hat{a}_a^\dagger \hat{a}_b^\dagger \hat{a}_j \hat{a}_i$$

is the first order doubles cluster operator and

$$\widehat{\Lambda}_2^{(1)} = \frac{1}{4} \sum_{ij} \sum_{a,b} \lambda_{ij}^{ab(1)} \hat{a}_i^\dagger \hat{a}_j^\dagger \hat{a}_b \hat{a}_a$$

is the doubles deexcitation operator with the  $\lambda$  amplitudes serving as Lagrangian multipliers.  $\widehat{f}_N$  and  $\widehat{W}_N$  are the normal-ordered Fockian and the two-electron component of the normal ordered Hamiltonian, respectively.<sup>3,89</sup>

As in the case of OCEPA(0), this functional is made stationary with respect to all parameters, namely, the  $t_2$  amplitudes, the  $\lambda_2$  amplitudes, and the MO coefficients  $c_{\mu i}$ . As usual, the  $\lambda$  amplitudes serve as Lagrangian multipliers, enforcing the constraint that the usual amplitude equations are still solved if the orbitals are modified. The derivation of Eq. (19) for  $\lambda_{ij}^{ab}$  thus yields the usual amplitude equations,

$$\frac{\partial \widetilde{E}_{\text{REMP}}^{(2)}}{\partial \lambda_{ij}^{ab}} = \langle \phi_{ij}^{ab} | \widehat{W}_N | \phi_0 \rangle + \langle \phi_{ij}^{ab} | \{ \widehat{f}_N \widehat{T}_2^{(1)} + (1-A) \widehat{W}_N \widehat{T}_2^{(1)} \}_c | \phi_0 \rangle \stackrel{!}{=} 0. \quad (20)$$

The derivation of Eq. (19) with respect to  $t_{ab}^{ij}$  yields the lambda amplitude equations,

$$\frac{\partial \widetilde{E}_{\text{REMP}}^{(2)}}{\partial t_{ab}^{ij}} = \langle \phi_0 | \widehat{W}_N | \phi_{ij}^{ab} \rangle + \langle \phi_0 | \{ \widehat{\Lambda}_2^{(1)} (\widehat{f}_N + (1-A) \widehat{W}_N) \}_c | \phi_{ij}^{ab} \rangle \stackrel{!}{=} 0. \quad (21)$$

From a comparison of Eqs. (20) and (21), it is obvious that  $\widehat{\Lambda}_2^{(1)} = \widehat{T}_2^{(1)\dagger}$  and thus  $\lambda_{ij}^{ab} = t_{ab}^{ij\dagger}$  holds for REMP. This is also the case for OCEPA(0) and OO-MP2 and in contrast to coupled cluster theory. It is therefore not necessary to explicitly solve the  $\Lambda$  equations.<sup>44,87,90</sup>

For the parameterization of the orbital change, we follow the methodology of Bozkaya *et al.*<sup>26,29,30,35,42-44,88</sup> who used an exponential unitary orbital rotation operator<sup>2</sup>  $e^{\widehat{K}}$ . The orbitals and operators can now be expressed as functions of orbital rotation parameters,

$$|\tilde{p}\rangle = e^{\widehat{K}} |p\rangle, \quad (22)$$

$$\tilde{a}_p^\dagger = e^{\widehat{K}} \hat{a}_p^\dagger e^{-\widehat{K}}, \quad (23)$$

$$\tilde{a}_p = e^{\widehat{K}} \hat{a}_p e^{-\widehat{K}}, \quad (24)$$

$$\widehat{H}^\kappa = e^{-\widehat{K}} \widehat{H} e^{\widehat{K}}, \quad (25)$$

$$\widehat{H}_N^\kappa = e^{-\widehat{K}} \widehat{H}_N e^{\widehat{K}}, \quad (26)$$

$$\widehat{f}_N^\kappa = e^{-\widehat{K}} \widehat{f}_N e^{\widehat{K}}, \quad (27)$$

$$\widehat{W}_N^\kappa = e^{-\widehat{K}} \widehat{W}_N e^{\widehat{K}}, \quad (28)$$

with

$$\widehat{K} = \sum_{p,q} \kappa_{pq} \hat{a}_p^\dagger \hat{a}_q, \quad (29)$$

where  $\widehat{K}$  is the orbital rotation operator and  $\kappa_{pq}$  is the orbital rotation parameter for orbitals  $p$  and  $q$ , which is an antisymmetric matrix ( $\kappa_{pq} = -\kappa_{qp}$ ). If the second order energy functional Eq. (19) is written as a function of the orbital rotation parameter  $\kappa_{pq}$ , it reads

$$\widetilde{E}_{\text{REMP}}^{(2)}(\kappa) = \langle \phi_0 | \widehat{H}^\kappa | \phi_0 \rangle + \langle \phi_0 | \{ \widehat{W}_N^\kappa \widehat{T}_2^{(1)} \}_c | \phi_0 \rangle + \langle \phi_0 | \left[ \widehat{\Lambda}_2^{(1)} \{ \widehat{W}_N^\kappa + \widehat{f}_N^\kappa \widehat{T}_2^{(1)} + (1-A) \widehat{W}_N^\kappa \widehat{T}_2^{(1)} \}_c \right] | \phi_0 \rangle. \quad (30)$$

The orbital gradient is given by

$$w_{pq} = \left. \frac{\partial \widetilde{E}_{\text{REMP}}^{(2)}(\kappa)}{\partial \kappa_{pq}} \right|_{\kappa=0} \quad (31)$$

and has to be brought to zero during the orbital optimization.

As elaborated for OCEPA(0),<sup>44</sup> the orbital gradient is computed from the asymmetry of the generalized Fock matrix, which involves sums over one- and two-particle density matrices. We adopted the density matrices of Bozkaya and Sherrill<sup>44,88</sup> and augmented them with the REMP scaling factor as necessary. The one-particle reduced density matrices  $\gamma_{pq}$  are given by

$$\gamma_{pq} = \gamma_{pq}^{\text{ref}} + \gamma_{pq}^{\text{corr}}, \quad (32)$$

with  $\gamma_{pq}^{\text{ref}}$  being the part originating from the reference and  $\gamma_{pq}^{\text{corr}}$  being the part originating from correlation. In detail,

$$\gamma_{pq}^{\text{ref}} = \delta_{pq}^{\text{occ}}, \quad (33)$$

$$\gamma_{pq}^{\text{corr}} = \langle 0 | \{ \widehat{\Lambda}_2^{(1)} \{ \{ \hat{a}_p^\dagger \hat{a}_q \} \widehat{T}_2^{(1)} \}_c \}_c | 0 \rangle. \quad (34)$$

The non-zero entries of  $\gamma_{pq}^{\text{corr}}$  are

$$\gamma_{ij}^{\text{corr}} = -\frac{1}{2} \sum_m \sum_{e,f} t_{ef}^{im(1)} \lambda_{jm}^{ef(1)} \quad (35)$$

and

$$\gamma_{ab}^{\text{corr}} = \frac{1}{2} \sum_{m,n} \sum_e t_{be}^{mn(1)} \lambda_{mm}^{ae(1)}, \quad (36)$$

where  $\delta_{pr}^{\text{occ}}$  is the Kronecker delta with the additional restriction that only orbitals that are occupied in the reference are considered. The general expression for the two-particle reduced density matrix  $\Gamma_{pqrs}$  reads

$$\Gamma_{pqrs} = \Gamma_{pqrs}^{\text{ref}} + \Gamma_{pqrs}^{\text{corr}} + \frac{1}{4} \delta_{pr}^{\text{occ}} \gamma_{qs}^{\text{corr}} + \frac{1}{4} \delta_{qs}^{\text{occ}} \gamma_{pr}^{\text{corr}} - \frac{1}{4} \delta_{ps}^{\text{occ}} \gamma_{qr}^{\text{corr}} - \frac{1}{4} \delta_{qr}^{\text{occ}} \gamma_{ps}^{\text{corr}}, \quad (37)$$

$$\Gamma_{pqrs}^{\text{ref}} = \frac{1}{4} (\delta_{pr}^{\text{occ}} \delta_{qs}^{\text{occ}} - \delta_{ps}^{\text{occ}} \delta_{qr}^{\text{occ}}), \quad (38)$$

$$\Gamma_{pqrs}^{\text{corr}} = \frac{1}{4} \langle 0 | \left( \left\{ \hat{a}_p^\dagger \hat{a}_q^\dagger \hat{a}_s \hat{a}_r \right\} \widehat{T}_2^{(1)} \right)_c | 0 \rangle + \frac{1}{4} \langle 0 | \left( \widehat{\Lambda}_2^{(1)} \left\{ \hat{a}_p^\dagger \hat{a}_q^\dagger \hat{a}_s \hat{a}_r \right\} \right)_c | 0 \rangle + (1-A) \frac{1}{4} \langle 0 | \left[ \widehat{\Lambda}_2^{(1)} \left( \left\{ \hat{a}_p^\dagger \hat{a}_q^\dagger \hat{a}_s \hat{a}_r \right\} \widehat{T}_2^{(1)} \right)_c \right] | 0 \rangle, \quad (39)$$

with the non-zero correlation contributions being

$$\Gamma_{ijkl}^{\text{corr}} = (1-A) \frac{1}{8} \sum_{e,f} t_{ef}^{ij(1)} \lambda_{kl}^{ef(1)}, \quad (40)$$

$$\Gamma_{ijab}^{\text{corr}} = t_{ab}^{ij(1)}, \quad (41)$$

$$\Gamma_{iajb}^{\text{corr}} = -(1-A) \frac{1}{4} \sum_m \sum_e t_{be}^{im(1)} \lambda_{jm}^{ae(1)}, \quad (42)$$

$$\Gamma_{abcd}^{\text{corr}} = (1-A) \frac{1}{8} \sum_{m,n} t_{cd}^{mn(1)} \lambda_{mn}^{ab(1)}. \quad (43)$$

As the  $\widehat{T}_2^{(1)}$  amplitudes solve the  $\lambda$  equations, the  $\widehat{\Lambda}_2^{(1)}$  amplitudes are replaced by the respective adjoint  $\widehat{T}_2^{(1)}$  amplitudes when forming density matrices. The correlated one-particle densities [Eqs. (35) and (36)] are not scaled as they originate from the term carrying the Fock operator in Eq. (30), which is equally contained in MP and RE. The densities as defined by Eqs. (32)–(43) are used to construct the generalized Fock matrix.<sup>35</sup> Actually, as proposed by Bozkaya and Sherrill in their seminal paper,<sup>44</sup> we do not construct the four-virtual two-particle density matrices if not needed but instead form an intermediate, which speeds up the computation drastically at no loss of accuracy.

Our generalized Fock matrix now has the same form as for OCEPA(0),

$$F_{pq} = \sum_r h_{pr} \gamma_{rq} + 2 \sum_{rst} \langle rs || tp \rangle \Gamma_{rstq}. \quad (44)$$

From the asymmetry of the generalized Fock matrix, the MO gradient  $w_{pq}$  is computed as

$$w_{pq} = 2(F_{pq} - F_{qp}). \quad (45)$$

The MO gradient is monitored for convergence, and as long as no sufficient convergence is achieved, orbital rotation parameters for

the  $n + 1$ st iteration are derived as a damped step into the opposite direction of the orbital gradient of the  $n$ th iteration,

$$\kappa_{pq}^{(n+1)} = -\frac{w_{pq}^n}{2(f_{pp} - f_{qq})}. \quad (46)$$

Orbital convergence can be accelerated by the direct inversion of the iterative subspace (DIIS) extrapolation<sup>118–120</sup> using the orbital rotation as the guess vector and the orbital gradient as the error vector. In doing so, care has to be taken that the orbital rotations of different iterations refer to a common basis, e.g., the initial orbitals. The total orbital rotation parameters of the  $n + 1$ st iteration will then be the sum of the individual rotations of all  $n$  preceding iterations.

Upon convergence of the orbital macroiterations, the MO basis Fock matrix will not be diagonal anymore; especially, the Brillouin theorem will not be fulfilled. As a consequence, the first-order wavefunction should also contain single excitations and there is also a correlation energy contribution by those single excitations. Including a perturbative singles correction was already tested by Neese *et al.*<sup>27</sup> for OO-SCS-MP2 where it was found that OO-MP2 does not benefit from doing so. Here, we investigate an analogous perturbative singles correction for OO-REMP. This correction is defined by the correlation energy added by the singles amplitudes that are obtained from solving the RO-REMP singles equations Eqs. (16) and (18) using the optimized orbitals as input. This ansatz will be denoted as OO-REMP+(S).

For UREMP and OO-REMP, an expression for the  $\langle \widehat{S}^2 \rangle$  expectation value according to Chen and Schlegel<sup>91</sup> was implemented. Specifically, Eq. (13) of Ref. 91 was used. Singles were ignored in all cases. We like to note that this expression is only an approximation and that one finds various expressions for the  $\langle \widehat{S}^2 \rangle$  expectation value of correlated wavefunctions in the literature, e.g., in Ref. 92.

### III. RESULTS

#### A. Computational details

All REMP calculations have been performed using a development version of the Bochum–Basel *ab initio* suite of programs (*waves*).<sup>48,55,60,93–96</sup> REMP, RO-REMP, UREMP, and OO-REMP have been implemented as an extension of the MC-CEPA (multi-configuration coupled electron pair approximation) program.<sup>60,96</sup> The implementation is inspired by the matrix-driven CI program of ORCA (*mdci*) and the orbital optimized coupled cluster code (OCC) of PSI4. REMP/OO-REMP energies always correspond to second order perturbation theory. All CCSD(T) calculations have been performed using ORCA<sup>97,98,121</sup> versions 4.2.0, 4.2.1, or 5.0.0. Basis sets have been used as stored in the TurboMole 6.5<sup>99</sup> basis set library or as deposited in ORCA.

The following abbreviations are used for statistical error descriptors: MSD denotes the mean signed deviation, i.e., the arithmetic mean of all deviations; MAD denotes the mean absolute deviation, i.e., the average of all absolute deviations;  $\Delta_{\text{min-max}}$  denotes the error spread, i.e., the largest positive minus the most negative error occurring;  $\sigma$  denotes the sample standard deviation; and RMSD denotes the root mean square deviation, i.e., the square root of the squared and averaged deviations.



## B. The W4-11 benchmark set and derived reactions

The W4-11 benchmark set<sup>100</sup> is a collection of 140 very accurate total atomization energies (TAE) of first- and second row main group molecules (TAE140). From this set, we selected the TAE\_nonMR124 subset defined in the same paper as a primary benchmark. This set contains those 124 atomization energies where none of the reactants exhibits severe multireference character. The reason for doing so is twofold: First of all, REMP and OO-REMP are single reference theories; we, therefore, do not expect (and do not obtain) reasonable performance for genuine multireference systems. Second, we observed convergence difficulties during orbital optimization with common multireference molecules, such as ozone or C<sub>2</sub>. Furthermore, as only electronic energies were calculated, results were compared against clamped-nuclei, nonrelativistic, zero-point exclusive values (TAE<sub>e</sub>). The reference atomization energies were taken from the supplementary material of Ref. 100 in Table SI-V. These reference numbers were calculated at the W4 level of theory or even better and were shown to be of excellent precision and accuracy.<sup>101</sup> In our previous study,<sup>55</sup> we used the CCSD(T) results of Bertels *et al.*<sup>10</sup> as reference. In this publication, we abandon CCSD(T) as a reference method for the W4-11 set, as we will show that plain CCSD(T) is not much more accurate than OO-REMP.

From the W4-11 set, four further benchmark sets were derived, the BDE99, HAT707, ISOMER20, and SN13 sets.<sup>100</sup> From these sets, we removed all reactions involving reactants not present in the TAE\_nonMR124 set, leaving 83 bond dissociation energies, 504 heavy atom transfers, 18 isomerizations, and 13 radicalic substitutions. Again, reference reaction energies were taken from Tables SI-VI to SI-XI from the columns marked as “TAE<sub>e</sub>” in Ref. 100.

Six different basis sets in conjunction with complete basis set (CBS) extrapolation were tested, namely, def2-TZVPPD, def2-QZVPPD, aug-cc-pVTZ, aug-cc-pVQZ, aug-cc-pwCVTZ, and aug-cc-pwCVQZ. This allows us to check the sensitivity of certain properties to the basis set size. It also allows us to identify Pauling points, i.e., method/basis combinations where fortuitous error cancellation of basis and method errors occurs. CBS extrapolation was performed as simple two-point extrapolation for SCF<sup>102–104</sup> and correlation energies.<sup>105</sup> SCF energies were extrapolated with an exponential function and an exponent<sup>106</sup> of  $\alpha = 1.6$ ; correlation energies were extrapolated with a polynomial function and an exponent of  $\beta = 3$ . As SCF energy for orbital optimized methods, the energy of the preceding RHF/ROHF/UHF calculation was used, respectively, for closed- and open-shell systems. The difference between the orbital optimized total energy and the respective Hartree–Fock energy was used as correlation energy for the extrapolation procedure. The extrapolation from def2-TZVPPD and def2-QZVPPD will be denoted as “CBS(3/4,def2),” the extrapolation from aug-cc-pVTZ and aug-cc-pVQZ will be denoted as “CBS(3/4,aVXZ),” and the extrapolation from aug-cc-pwCVTZ and aug-cc-pwCVQZ will be denoted as “CBS(3/4,awCVXZ).” Throughout the whole benchmark set, no electrons were kept frozen; instead, all electrons and all orbitals were always correlated.

The non-MR portion of the TAE140 set was already investigated in our previous paper<sup>55</sup> with CCSD(T)/aug-cc-pVTZ reference values where it showed error estimates of about 1 kcal mol<sup>-1</sup>. In the present work, we investigate complete basis set extrapolated

values with respect to W4 benchmark results, aiming to investigate the true accuracy of the REMP approaches themselves.

Figure 1 shows the root mean square deviation of the 124 total atomization energies of the TAE\_nonMR124 set when calculated with UREMP, RO-REMP, and OO-REMP. The most striking result is that every single curve exhibits a local minimum, indicating that the REMP “recipe” also works in all open shell variants.

As expected, increasing the basis set size from triple- $\zeta$  to quadruple- $\zeta$  leads to an improvement, except in the case of aug-cc-pVTZ and aug-cc-pVQZ where the minimal RMSDs are about equal but located at different  $A$  values. When only a single basis set is considered, a bit surprisingly, the def2-QZVPPD basis performs best for UREMP, RO-REMP, and OO-REMP. However, as the minima are found at 4.2, 3.4, and 2.2 kcal mol<sup>-1</sup>, respectively, for UREMP/RO-REMP/OO-REMP, none of these model chemistries is of any practical use for calculating atomization energies. Reliable results are only obtained if CBS extrapolation is used. One then finds that the def2 basis sets and the aVXZ basis sets perform about equally well, although with significantly different optimal RE/MP mixing ratios. The best performance is always delivered by the awCVXZ basis sets, which exhibit the lowest minima in all cases. The respective minima are found at  $A = 0.35$ , i.e., 35% MP2 in the unperturbed Hamiltonian [UREMP, 3.54 kcal mol<sup>-1</sup>, Fig. 1(a)], 40% MP2 [RO-REMP, 2.59 kcal mol<sup>-1</sup>, Fig. 1(b)], and 23% MP2 [OO-REMP, 1.15 kcal mol<sup>-1</sup>, Fig. 1(c)]. OO-REMP thus is clearly the most powerful of the three assessed methods. The performance of OO-REMP is even more impressive if one considers that the pure parent methods OO-RE and OO-MP2 exhibit RMSDs of 5.53 and 18.9 kcal mol<sup>-1</sup>, respectively. UCCSD(T)/CBS(3/4,aug-cc-pwCVXZ) delivers a RMSD of 0.79 kcal mol<sup>-1</sup> for the same set and is thus not vastly more accurate. On the other hand, both UREMP and RO-REMP can generally not be recommended for atomization energies. The variant based on restricted orbitals performs slightly better but not good enough. It should, however, be mentioned that both perform still significantly better than UCCSD(T)/CBS(3/4,aug-cc-pwCVXZ), which provides an RMSD of 9.87 kcal mol<sup>-1</sup>. These results can be compared to Karton’s results for the TAE\_nonMR124 set (Table 6 in Ref. 100). The only methods that perform equally well or even better are the W1, the ccCA, and the G4(MP2)-6X composite methods. All of these employ CCSD(T) calculations as components and exhibit, therefore, a less favorable computational scaling than OO-REMP. None of the density functionals investigated in Ref. 100 comes even close to an RMSD of 1 kcal mol<sup>-1</sup>.

The first subsets of reactions that may be formed from the W4-11 set are heavy-atom-transfer reactions (HAT\_nonMR504, Fig. 2). These are bimolecular reactions, such as C + CH<sub>3</sub>F → CF + CH<sub>3</sub>, where one heavy atom formally changes to the other reactant. Figure 2 depicts the RMSDs that can be achieved with UREMP, RO-REMP, and OO-REMP, respectively. Compared to Fig. 1, one finds some remarkable differences. The minima are less pronounced or even not present at all, the dependency on the mixing ratio is less pronounced, and the overall performance is poorer than before. UREMP turns out to be not reliable at all for these kinds of reactions, RO-REMP has a minimal RMSD of almost 5 kcal mol<sup>-1</sup>, and even OO-REMP exhibits a minimum RMSD of 2.15 kcal mol<sup>-1</sup> [ $A = 0.20$ , CBS(3/4,awCVXZ)]. The benefit of performing a CBS extrapolation is also smaller for this reaction set. It should, however, be mentioned that this set turns out to be exceedingly difficult as shown by the

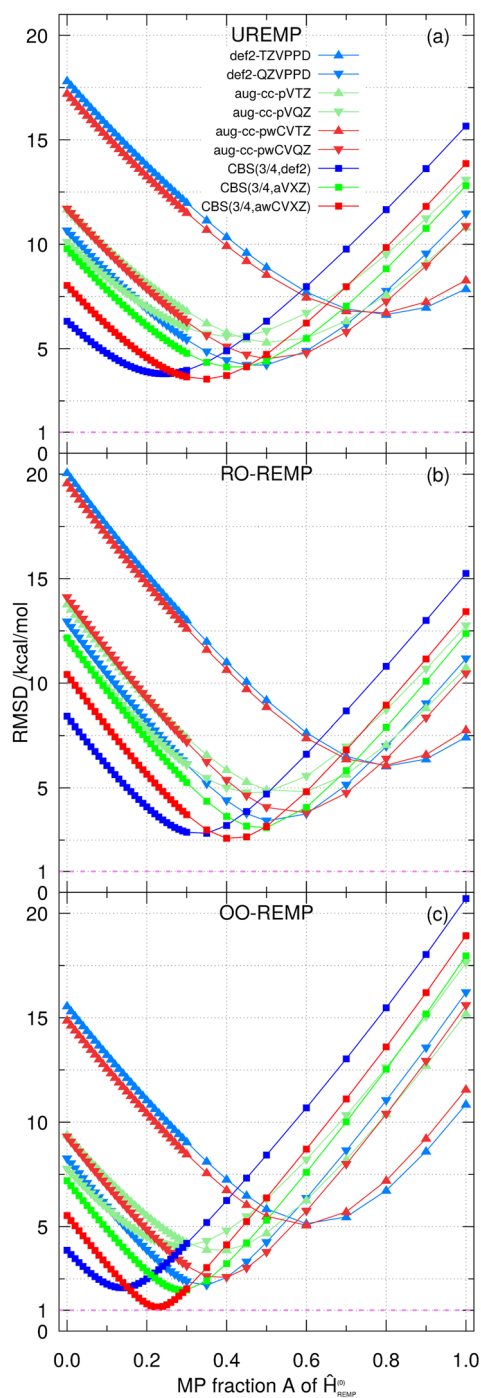


**FIG. 1.** Graphical representation of the RMSD averaged over 124 total atomization energies of the TAE\_nonMR124 subset of the W4-11 benchmark set as a function of the REMP mixing parameter  $A$  of  $\hat{H}_{\text{REMP}}^{(0)}$ . (a) UREMP, (b) RO-REM, and (c) OO-REM. The up-pointing triangles indicate triple- $\zeta$  basis sets; the down-pointing triangles indicate quadruple- $\zeta$  basis sets. The squares indicate results obtained via CBS extrapolation from the aforementioned basis sets. Ahlrichs basis sets (def2-XZVPPD) are shown in blue, Woon–Dunning basis sets (aug-cc-pVXZ) are shown in green, and Peterson–Dunning basis sets (aug-cc-pwCVXZ) are shown in red. See Tables S18–S44 for numerical values.

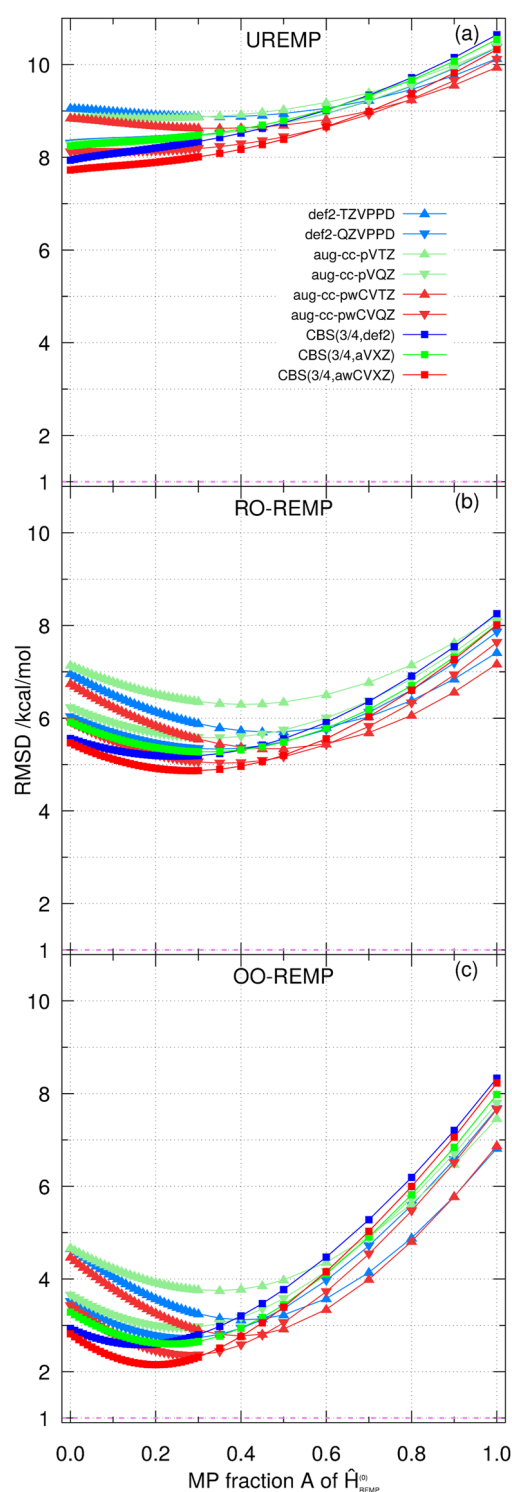


**FIG. 2.** Graphical representation of the RMSD averaged over 504 heavy atom transfer reaction energies of the HAT\_nonMR504 subset of the W4-11 benchmark set as a function of the REMP mixing parameter  $A$  of  $\hat{H}_{\text{REMP}}^{(0)}$ . (a) UREMP, (b) RO-REM, and (c) OO-REM. See Fig. 1 for further details and Tables S45–S71 for numerical values.

RMSD of UCCSD(T)/CBS(3/4,awCVXZ), which is  $1.81 \text{ kcal mol}^{-1}$ , and, thus, only marginally smaller than that of OO-REMP. For comparison, UCCSD/CBS(3/4,awCVXZ) performs relatively well with a RMSD of  $4.45 \text{ kcal mol}^{-1}$ .

The next subset that may be formed from the TAE\_nonMR124 set concerns bond dissociation energies (BDE\_nonMR83, Fig. 3). Here, one bond in molecules with three or more atoms is cleaved homolytically in various ways to form two fragments. Figure 3 shows the results obtained for this subset. As has been the case with atomization energies and heavy-atom-transfer reactions, neither UREMP nor RO-REMP is capable of describing these reactions satisfactorily. The only model chemistry that is reaching an RMSD below  $1 \text{ kcal mol}^{-1}$  is OO-REMP/CBS(3/4,awCVXZ). The minimum is located at  $A = 0.20$  with an RMSD of  $0.85 \text{ kcal mol}^{-1}$ . UCCSD(T)/CBS(3/4,awCVXZ) achieves an RMSD of  $0.77 \text{ kcal mol}^{-1}$  for the same set and is thus only slightly better.

The third set that can be formed consists of 18 isomerization energies (ISOMER\_nonMR18, Fig. 4). A typical reaction of this set would be propyne  $\rightarrow$  allene. As most systems are closed shell singlets, it is not surprising that UREMP and RO-REMP perform similar and that performance is already fairly good without orbital optimization. The overall performance is again improved by orbital optimization. Quite interestingly, now, the best performance is not found when CBS extrapolation is done. Instead, OO-REMP/aug-cc-pVQZ with  $A = 0.19$  provides the lowest RMSD ( $0.32 \text{ kcal mol}^{-1}$ ), followed by OO-REMP(0.23)/aug-cc-pwCVQZ ( $0.33 \text{ kcal mol}^{-1}$ ) and OO-REMP(0.19)/CBS(3/4,awCVXZ) ( $0.37 \text{ kcal mol}^{-1}$ ). A very similar behavior is found for CCSD(T), which achieves  $0.14/0.19/0.23 \text{ kcal mol}^{-1}$  with aug-cc-pVQZ/aug-cc-pwCVQZ/CBS(3/4,awCVXZ).

The last set of reactions consists of 13 radical substitution reactions (SN13); a prototypical example would be  $\text{CH}_3\text{F} + \text{OH} \rightarrow \text{F} + \text{CH}_3\text{OH}$ . The respective RMSDs are depicted in Fig. 5. Although all reactions involve radicals as reactants, both UREMP and RO-REMP perform remarkably well. Generally, the same trends as before are observed, namely, that REMP hybridization leads to a tremendous improvement over the parent methods. The most striking example here is probably again OO-REMP. While none of the parent methods regardless of the basis set comes even close to  $1 \text{ kcal mol}^{-1}$ , each of the curves in Fig. 5(c) shows a minimum roughly between  $A = 0.20$  and  $A = 0.40$ , and all of these minima are located clearly below  $1 \text{ kcal mol}^{-1}$ . It should be stressed that this improvement comes at no extra cost compared to OCEPA(0). The best overall performance is again achieved with OO-REMP(0.19)/CBS(3/4,awCVXZ) with an RMSD of  $0.37 \text{ kcal mol}^{-1}$ . CCSD(T)/CBS(3/4,awCVXZ) yields an RMSD of  $0.22 \text{ kcal mol}^{-1}$ .

Summarizing the above results, one finds that OO-REMP shows a performance that is qualitatively comparable to CCSD(T). The best performance is always found with an MP:RE mixing ratio of about 20:80. The only case where OO-REMP clearly misses the  $1 \text{ kcal mol}^{-1}$  criterion is the heavy atom transfer reaction set, where even CCSD(T) exhibits substandard performance. The performance of the variants building upon canonical UHF/ROHF determinants is much poorer especially in difficult cases. The restricted variant generally performs better than the unrestricted variant, but in difficult situations still not good enough.

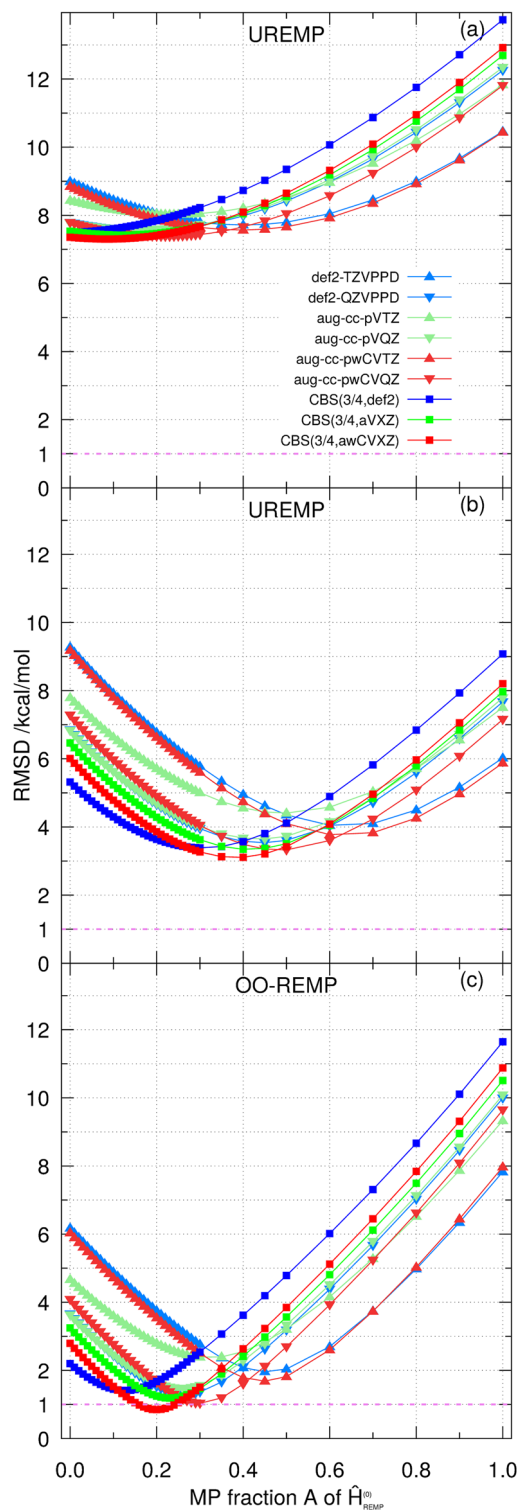


**FIG. 3.** Graphical representation of the RMSD averaged over 83 bond dissociation energies of the BDE\_nonMR83 subset of the W4-11 benchmark set as a function of the REMP mixing parameter  $A$  of  $\hat{H}_{\text{REMP}}^{(0)}$ . (a) UREMP, (b) RO-REMP, and (c) OO-REMP. See Fig. 1 for further details and Tables S72–S98 for numerical values.



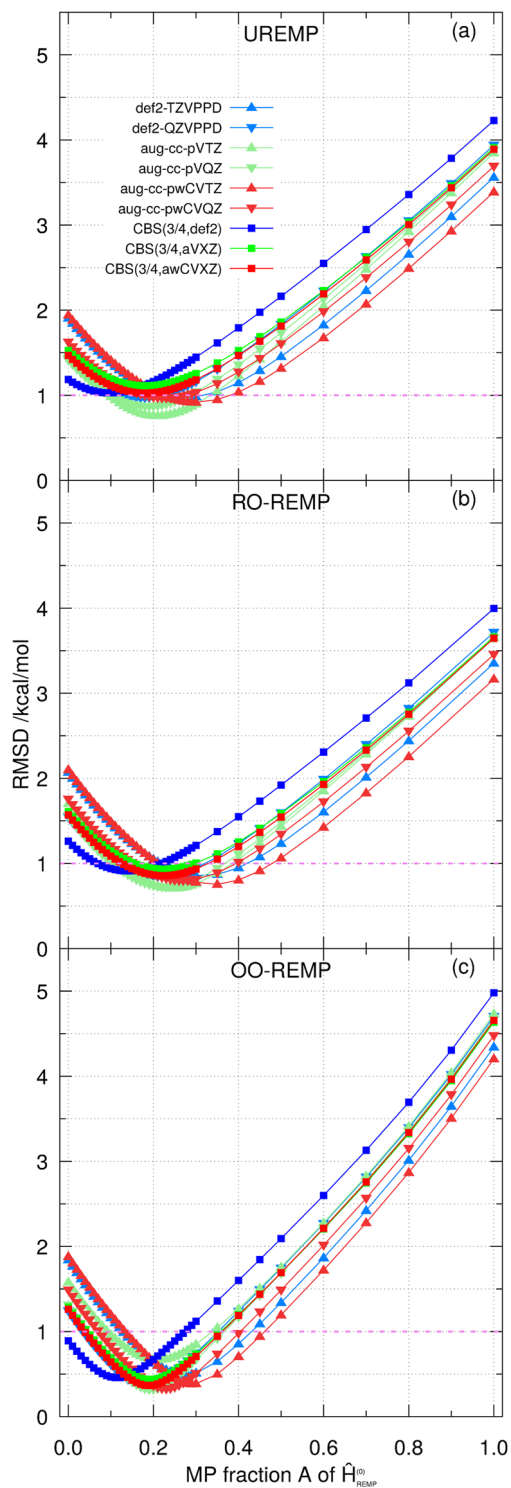


**FIG. 4.** Graphical representation of the RMSD averaged over 18 isomerization reaction energies of the ISOMER\_nonMR18 subset of the W4-11 benchmark set as a function of the REMP mixing parameter  $A$  of  $\hat{H}_{\text{REMP}}^{(0)}$ . (a) UREMP, (b) RO-REMP, and (c) OO-REMP. See Fig. 1 for further details and Tables S99–S125 for numerical values.

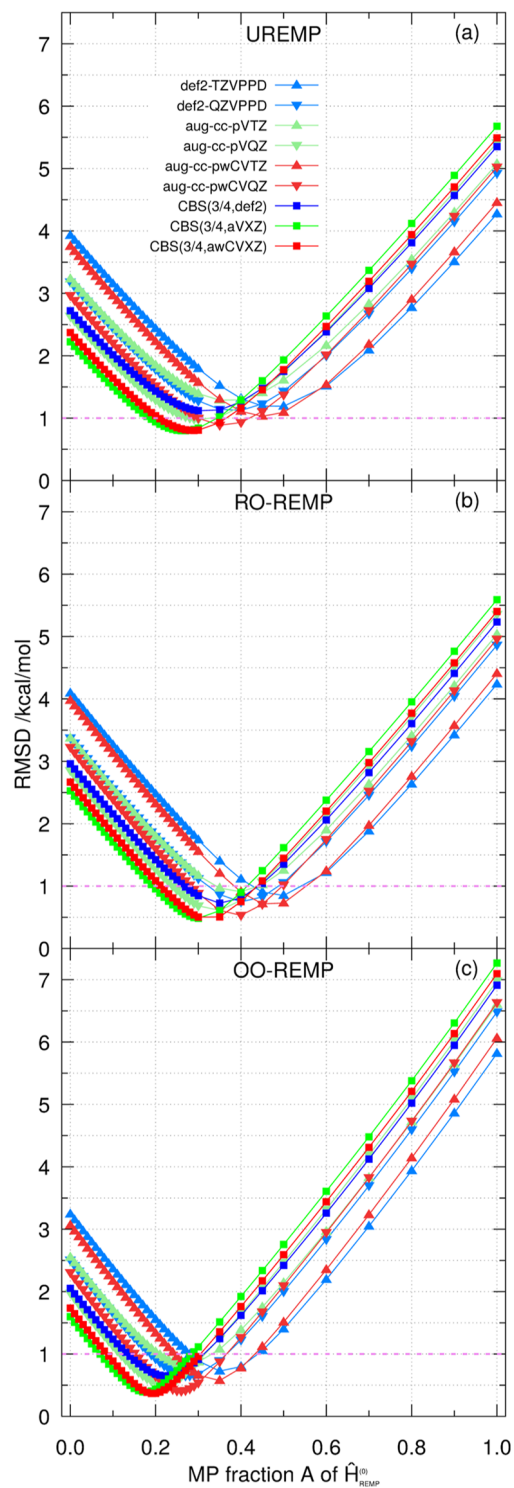


**FIG. 5.** Graphical representation of the RMSD averaged over 13 radical substitution reaction energies of the SN13 subset of the W4-11 benchmark set as a function of the REMP mixing parameter  $A$  of  $\hat{H}_{\text{REMP}}^{(0)}$ . (a) UREMP, (b) RO-REMP, and (c) OO-REMP. See Fig. 1 for further details and Tables S126–S152 for numerical values.

As the root mean square deviation is sensitive to outliers, the mean absolute deviation is considered as figure of merit, too. The corresponding graphs can be found in the [supplementary material](#), Figs. S1–S4. The mean absolute deviation graphs are very similar to the RMSD graphs and fully support the finding regarding the ordering of the REMP variants and the optimal mixing parameters.

Table I lists representative results for REMP variants and coupled cluster methods. The RMSDs of OO-REMP and CCSD(T) are correlated with each other, indicating that the success of OO-REMP does not originate from a random error cancellation of basis and method errors but can be attributed to the conceived internal error compensation. It can also be seen that OO-REMP is clearly superior to CCSD at comparable computational cost.

Furthermore, one finds that both REMP variants based on canonical orbitals (UREMP & RO-REMP) and CCSD show a strong bias toward underestimating total atomization energies (TAEs). OO-REMP and CCSD(T), on the other hand, exhibit no such trend;

**TABLE I.** Error measures obtained with the CBS(3/4,awCVXZ) extrapolation and various levels of theory on the non-multireference portion of the W4-11 set and its derived reaction sets. For a complete data collection and for error data of the remaining basis sets, see the [supplementary material](#). All errors in kcal mol<sup>-1</sup> relative to the electronic contribution of the W4 composite method or better.

	TAE	HAT	BDE	ISOMER	SUBST
Mean signed deviation (MSD)					
UREMP(0.20)	-3.19	3.25	1.52	0.06	-0.69
UREMP(0.25)	-2.40	3.41	1.94	0.20	-0.37
RO-REMP(0.20)	-4.86	0.63	-2.03	0.22	-0.84
RO-REMP(0.25)	-3.92	0.78	-1.54	0.37	-0.51
OO-REMP(0.20)	-0.83	0.85	0.11	0.14	0.05
OO-REMP(0.25)	0.06	0.96	0.53	0.29	0.41
CCSD	-8.35	1.15	-3.30	0.32	-1.35
CCSD(T)	0.48	0.63	0.43	0.06	0.19
Mean absolute deviation (MAD)					
UREMP(0.20)	3.35	4.95	3.69	0.76	0.76
UREMP(0.25)	2.75	4.98	3.64	0.82	0.63
RO-REMP(0.20)	4.93	3.81	2.89	0.66	0.85
RO-REMP(0.25)	4.04	3.71	2.52	0.68	0.55
OO-REMP(0.20)	1.08	1.21	0.61	0.29	0.30
OO-REMP(0.25)	0.92	1.21	0.76	0.41	0.49
CCSD	8.36	3.57	3.84	1.21	1.35
CCSD(T)	0.62	0.86	0.49	0.17	0.19
Root mean square deviation (RMSD)					
UREMP(0.20)	4.58	7.89	7.41	1.03	1.04
UREMP(0.25)	4.01	7.95	7.52	1.08	0.85
RO-REMP(0.20)	5.65	4.92	3.86	0.86	1.09
RO-REMP(0.25)	4.63	4.88	3.52	0.87	0.75
OO-REMP(0.20)	1.31	2.15	0.85	0.37	0.37
OO-REMP(0.25)	1.26	2.19	1.05	0.50	0.59
CCSD	9.87	4.45	4.85	1.73	1.66
CCSD(T)	0.79	1.81	0.77	0.23	0.22

here, the sign of the mean error rather depends on the basis set combination than on the method itself (see full tables in the [supplementary material](#)). The other class of reactions where an unambiguous direction can be assigned are the bond dissociation energies (BDE). Interestingly, UREMP and CCSD(T) now systematically overestimate the BDEs, while RO-REMP and CCSD underestimate them. In the HAT, ISOMER, and SUBST case, the sign is meaningless as it depends on a randomly chosen direction.

The MAD also listed in Table I has the advantage of being less susceptible to outliers than the RMSD. In general, one can draw the same conclusions as from the RMSD. CCSD(T) is the best performing method, but in difficult cases (TAE, HAT, and BDE), even CCSD(T) struggles if not used in conjunction with well-saturated basis sets.

### C. Closed-shell main group reaction energies—The SCS-MP2 calibration set

As in our previous publication,<sup>55</sup> we use a subset of the SCS-MP2 calibration set<sup>7</sup> as a closed shell reaction benchmark set. From Grimme's original set, all ionic systems, all open shell systems, the transition states, and the multireference systems were removed. This has both theoretical and practical reasons: In the case of ozone, e.g., the orbital optimization procedure did not converge for  $A < 0.15$ . For  $A \geq 0.15$ , the orbital optimization converged, but the results were extremely poor. Such behavior was, however, expected: orbital optimization is an extremely powerful tool as long as the reference wavefunction can be described by a single Slater determinant. It does not have to be a RHF/ROHF/UHF determinant, but it should be a single determinant. As the ground state of ozone is a genuine multireference case, it is almost certain that OO-REMP will fail, too. We like to note that this finding is also not an artifact of our implementation but fully reproducible with the OCEPA(0) codes of ORCA and PSI4.

Previously, it was shown that OO-REMP substantially improves upon REMP with canonical orbitals. The focus here is on assessing the performance of adding the missing single excitations in a perturbative fashion. The MSD, MAD, and RMSD upon scanning the  $A$  range are plotted in Fig. 6, and Table II lists some representative numbers.

As can be seen, both OO-REMP and OO-REMP+(S) lead to an improvement upon the parent methods indicated by a decreasing MAD and RMSD and an MSD close to zero with a small standard deviation. The results, however, show that adding single excitations in a perturbative fashion upon convergence does not lead to a further improvement. The worsening in Fig. 6(b) compared to Fig. 6(a) is not dramatic but noticeable. The minimal RMSD raises from 0.65 kcal mol<sup>-1</sup> (OO-REMP,  $A = 0.25$ ) to 0.86 kcal mol<sup>-1</sup> [OO-REMP+(S),  $A = 0.18$ ]. This is in line with the findings of Neese *et al.* for OO-MP2.<sup>27</sup> At least for closed shell cases, the perturbative singles according to Eqs. (16) and (18) thus do more harm than good when they are added on top of optimized orbitals. In the following, it will be investigated whether this conclusion also holds for open shell systems.

### D. The RSE43 set—Open shell reaction energies

The RSE43 benchmark set<sup>27,107</sup> consists of 43 radical stabilization energies. Those radical stabilization energies are defined as the

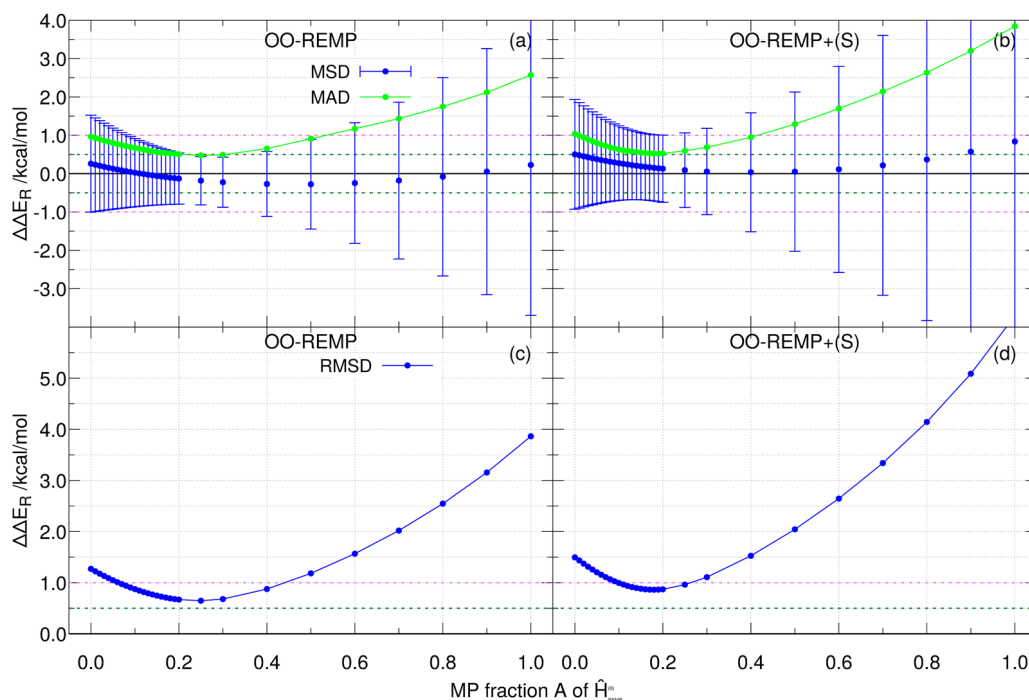


**FIG. 6.** Mean signed deviation (MSD), mean absolute deviation (MAD), and root mean square deviation (RMSD) averaged over 30 reactions of the SCS-MP2 calibration set as a function of the REMP mixing parameter  $A$  of  $\hat{H}_{\text{REMP}}^{(0)}$ . Error bars indicate one standard deviation. (a) MSD & MAD of OO-REMP, (b) MSD & MAD of OO-REMP+(S), (c) RMSD of OO-REMP, and (d) RMSD of OO-REMP+(S). All in  $\text{kcal mol}^{-1}$ . See Table S1 for numerical values.

reaction energy of the reaction of an organic radical with methane forming the methyl radical and an organic molecule carrying a hydrogen atom instead of the radical. Reaction 9, for example, features the abstraction of a hydrogen atom from the terminal methyl group of ethanol. This set or similar sets have already been used for benchmarking various orbital optimized methods.<sup>10,11,27,30,43</sup> As reference energies, the W1-F12 energies by Goerigk *et al.*<sup>108</sup> from the GMTKN55 database were chosen.

The strategy employed for the validation of the RSE43 set differs from that presented above for the W4-11 set. The focus here lies on testing a model chemistry, i.e., REMP/OO-REMP combined with a fixed basis set instead of employing a complete basis set extrapolation. As the reactions of the RSE43 set are loosely related to those of the SN subset of W4-11, the use of a valence quadruple zeta basis seems reasonable. Moreover, due to the size of the molecules involved, employing an even bigger basis set would not have been possible with our computational resources. The def2-QZVP basis set has thus been chosen as a reasonable compromise.

Figure 7 shows the MSD, MAD, and RMSD of the four tested REMP flavors. The outcome for the RSE43 set is distinctly different from the one of the W4-11 set. Considering UREMP first [Tables III and Fig. 7(a)], there is no minimum upon hybridization of the two different unperturbed Hamiltonians and the best result is delivered by pure RE. The systematic overestimation amounts to 2.7

$\text{kcal mol}^{-1}$ , and all radical stabilization energies are systematically overestimated.

While investigating the same set, Neese *et al.*<sup>27</sup> found a significant correlation between the spin contamination of the UHF reference determinant and the error of the reaction energy computed by MP2. A similar correlation is also found for RE. Figure 8 shows a graphical representation of the absolute errors of URE2 and UMP2 as a function of the largest occurring spin contamination in each reaction. It can be deduced that as soon as the spin contamination of the UHF reference of the open shell species rises above  $\approx 0.05$ , results at second order perturbation theory become completely unreliable. One thus either needs a method, which can cope with the spin contamination of a given reference, or one has to switch to another reference wavefunction. As both RE and MP are suffering from a poor reference in the same way, one cannot expect that REMP hybridization compensates for this error. Apparently, UREMP does not solve the issues arising from poor zeroth order wavefunctions.

Moving on to RO-REMP [Table IV and Fig. 7(b)], one already finds a tremendous improvement compared to UREMP. The mean deviation is in all cases well below  $1 \text{ kcal mol}^{-1}$ ; the standard deviation and the RMSD are smaller than in the UHF case, and for  $A > 0.1$ , the mean absolute deviation is below  $1 \text{ kcal mol}^{-1}$ , further dropping slowly to  $0.7 \text{ kcal mol}^{-1}$  for 100% MP. As an ROHF reference is always a pure  $\langle \hat{S}^2 \rangle$  eigenfunction, the natural explanation

**TABLE II.** Representative error descriptors for the SCS-MP2 calibration set [OO-REMP/def2-QZVP, all electrons correlated; reference: CCSD(T)/def2-QZVP, all electrons correlated]. All in kcal mol<sup>-1</sup>. The full table can be found in the [supplementary material](#) file (Table S1).

A	MSD	MAD	$\Delta_{\min-\max}$	$\sigma$	RMSD
OO-REMP					
0.00	0.26	0.97	6.08	1.27	1.27
0.12	-0.01	0.63	3.95	0.83	0.82
0.15	-0.06	0.56	3.45	0.76	0.75
0.18	-0.10	0.53	3.20	0.70	0.69
0.19	-0.12	0.52	3.19	0.68	0.68
0.20	-0.13	0.51	3.15	0.67	0.67
0.25	-0.18	0.48	3.02	0.63	0.65
0.30	-0.22	0.49	2.87	0.65	0.68
0.40	-0.27	0.65	3.55	0.85	0.88
1.00	0.23	2.57	19.21	3.92	3.86
OO-REMP+(S)					
0.00	0.50	1.04	7.03	1.43	1.49
0.12	0.24	0.59	4.88	0.92	0.94
0.15	0.19	0.55	4.62	0.87	0.88
0.18	0.15	0.52	4.44	0.86	0.86
0.19	0.14	0.52	4.40	0.87	0.87
0.20	0.13	0.53	4.52	0.88	0.87
0.25	0.09	0.60	5.21	0.97	0.96
0.30	0.06	0.69	6.00	1.13	1.11
0.40	0.04	0.95	7.89	1.55	1.53
1.00	0.84	3.84	31.11	6.27	6.22

for the improvement lies within the improved reference determinant, which is not suffering from spin contamination anymore. The overall shape of the RO-REMP MAD is rather unprecedented for REMP. There is no obvious minimum; instead, plain ROMP2 performs best. Yet, those mixing ratios performing best for the W4-11 set (30%–60% MP) also produce quite acceptable results on average for the RSE43 set with MADs consistently below 1 kcal mol<sup>-1</sup>.

Orbital optimized REMP has also been tested against the RSE43 benchmark set, and as shown in [Fig. 7\(c\)](#) and [Table V](#), it delivers excellent performance. The smallest mean absolute deviation and RMSD are found for  $A \approx 0.35$ . The best REMP mixing ratio has a mean absolute deviation of merely  $\approx 0.12$  kcal mol<sup>-1</sup> from the

**TABLE III.** UREMP: Representative error descriptors for the RSE43 benchmark set (UREMP/def2-QZVP, frozen core; reference: W1-F12). All in kcal mol<sup>-1</sup>. The full table can be found in [Table S2](#).

A	MSD	MAD	$\Delta_{\min-\max}$	$\sigma$	RMSD
0.00	2.69	2.69	19.41	3.88	4.69
0.12	2.76	2.74	20.09	4.06	4.86
0.15	2.75	2.75	20.25	4.10	4.90
0.20	2.76	2.76	20.56	4.18	4.97
1.00	3.27	3.27	27.08	5.77	6.57

**TABLE IV.** RO-REMP: Representative error descriptors for the RSE43 benchmark set (REMP/def2-QZVP, frozen core; reference: W1-F12). All in kcal mol<sup>-1</sup>. The full table can be found in [Table S3](#).

A	MSD	MAD	$\Delta_{\min-\max}$	$\sigma$	RMSD
0.00	0.64	1.05	8.70	1.34	1.47
0.12	0.76	0.98	6.65	1.01	1.25
0.15	0.77	0.97	6.29	0.95	1.22
0.30	0.79	0.94	5.00	0.77	1.09
0.40	0.77	0.90	4.55	0.70	1.03
0.90	0.59	0.71	3.86	0.60	0.83
1.00	0.54	0.69	3.82	0.61	0.81

W2-F12 reference. OO-REMP is thus probably within the error bar of the reference method. The parent methods OCEPA(0) and OO-MP2 already perform remarkably well with RMSDs of 0.40 and 0.73 kcal mol<sup>-1</sup>, but hybridizing both methods brings the RMSD down to 0.17 kcal mol<sup>-1</sup>. [Table V](#) also features results for some popular density functionals obtained with the same basis set taken from the GMTKN55 database.<sup>108</sup> Although the RSE43 set is not very challenging, none of the functionals listed comes even close to OO-REMP.

The perturbative singles correction of OO-REMP+(S) [see [Table VI](#) and [Fig. 7\(d\)](#)] again provides no improvement but deteriorates the extremely accurate OO-REMP results. Actually, OO-REMP+(S) is not more accurate than RO-REMP for the RSE43 set.

[Figures 7\(e\)–7\(h\)](#) show the RMSDs obtained from the four different REMP variants. In general, the conclusions that can be drawn are the same as before. UREMP is unreliable, RO-REMP performs best with 100% MP but is not very accurate, OO-REMP is very accurate over a wide parameter range yielding best results with  $A \approx 35\%$ , and OO-REMP+(S) exhibits a minimum but is by far not as reliable as OO-REMP. As the RMSD is especially prone to outliers, it relentlessly exposes the weaknesses of methods.

### E. The BH76 benchmark set

The performance of the four REMP variants was, furthermore, assessed with the BH76 benchmark set. BH76<sup>107</sup> is mostly a union of the HTBH38<sup>110</sup> and the NHTBH38<sup>111</sup> sets by Truhlar. The set consists of 76 reaction barrier heights for hydrogen and heavy atom transfer reactions. Reactions 1 and 2, for example, are  $H + N_2O \rightarrow [N_2OH]^{\ddagger} \rightarrow N_2 + OH$ . During the reaction, an oxygen atom is transferred from N<sub>2</sub>O to a hydrogen atom. Reactions 55 and 56 are the barriers for the abstraction of a hydrogen atom from H<sub>2</sub> by a fluorine atom. Goerigk *et al.*<sup>108</sup> computed new reference energies at the W2-F12<sup>112</sup> level of theory for this set, which are used in the following.

The BH76 set was already used in our previous publication<sup>55</sup> but with a different basis set and with different reference energies. Previously, we compared OO-REMP/aug-cc-pVTZ against CCSD(T)/aug-cc-pVTZ results by Bertels *et al.*<sup>10</sup> Here, we now compare REMP/def2-QZVP against W2-F12. Like with the RSE43 set, the focus now lies on comparing model chemistry to the best estimate instead of comparing two model chemistries.

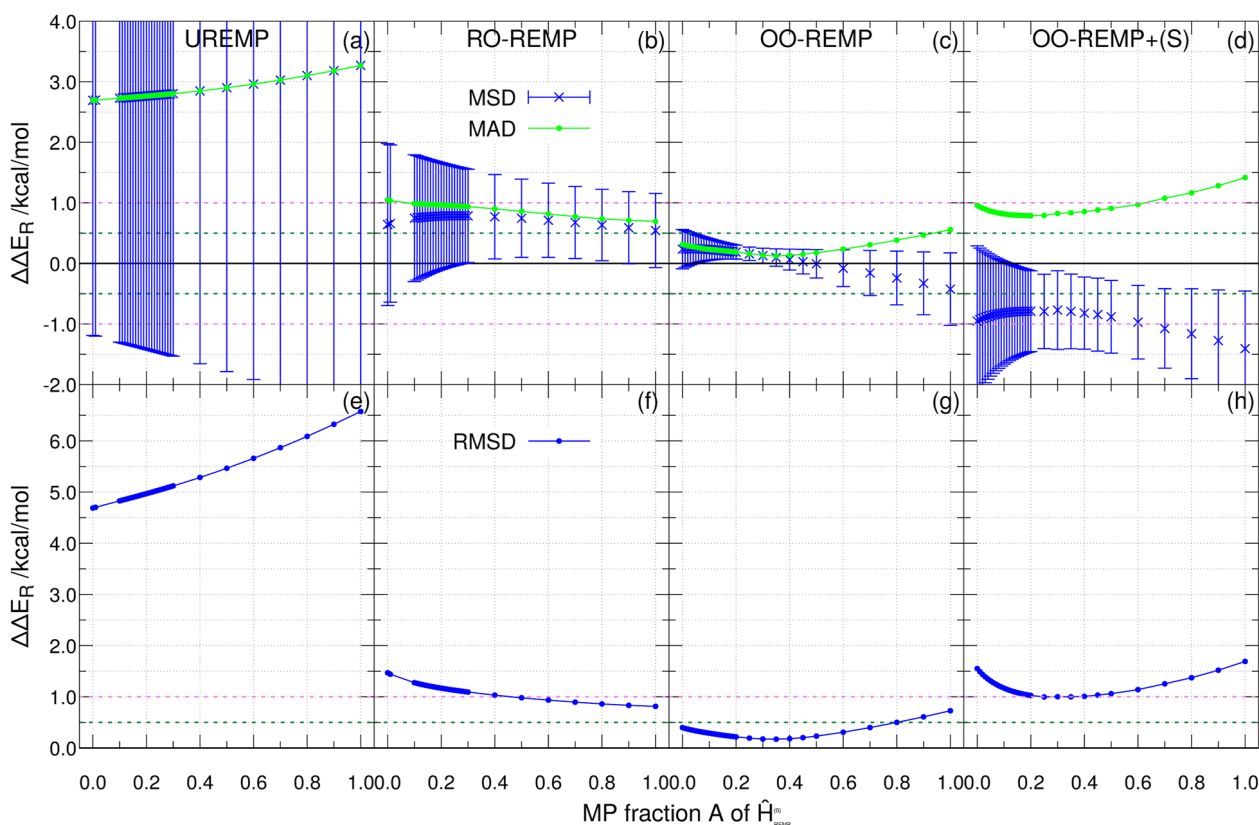


**FIG. 7.** Graphical representation of the MSD, MAD, and RMSD of four REMP variants for the RSE43 set as a function of the REMP mixing parameter  $A$  of  $\hat{H}_{\text{REMP}}^{(0)}$ . (a)–(d) MSD and MAD of UREMP/RO-REMP/OO-REMP/OO-REMP+(S). (e)–(h) RMSD of UREMP/RO-REMP/OO-REMP/OO-REMP+(S). All calculations use the def2-QZVP basis set. UREMP and RO-REMP make use of standard frozen cores, while OO-REMP and OO-REMP+(S) correlate all electrons. All errors with respect to the W2-F12 reference. See Tables S2–S5 for numerical values.

Figure 9 shows a graphical representation of the MSD and the MAD achieved with the different REMP variants for the BH76 set. Concentrating on UREMP first, Table VII collects some representative statistical descriptors. Especially those REMP mixing ratios

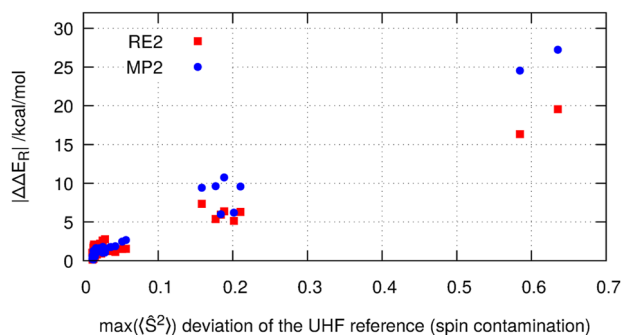


**FIG. 8.** Dependence of the absolute reaction energy errors of the RSE43 set on the spin contamination of the UHF reference of the radical species for pure RE and pure MP. See Table S6 for numerical values.

have been selected, which have been shown to deliver the best performance in the closed shell case. For all mixing ratios, all barriers are systematically overestimated by about  $4 \text{ kcal mol}^{-1}$ , and it is evident that variation of the REMP mixing parameter  $A$  leads to no improvement. In contrast, the mean signed deviation even has a shallow maximum between 0% and 100% MP. On average, the best performance is delivered by pure RE, but even pure RE overestimates the barriers by  $3.8 \text{ kcal mol}^{-1}$  and has error bars of the same size. The overall outcome here is the same as has been for the RSE43 set, namely, that UREMP is of no practical use for real-world open shell systems. The most probable explanation for the disastrous performance is again the large spin contamination of some of the employed UHF reference determinants.

Again, the spin contamination problem is most easily alleviated by using a restricted open shell HF (ROHF) determinant as the zeroth order wavefunction. RO-REMP results for the BH76 set are listed in Table VIII and Fig. 9(b). Indeed, as before, there is a substantial overall reduction of errors when a ROHF determinant instead of a UHF determinant is employed as the zeroth order wavefunction. Additionally, one finds a minimum in the mean absolute deviation curve at  $A \approx 0.30$ , which shows that REMP improves upon



**TABLE V.** Representative error descriptors for the RSE43 benchmark set (OO-REMP/def2-QZVP, all electrons correlated; reference: W1-F12). All in kcal mol<sup>-1</sup>. The full table can be found in Table S4.

A	MSD	MAD	$\Delta_{\min-\max}$	$\sigma$	RMSD
0.00	0.24	0.314	1.62	0.32	0.40
0.12	0.22	0.22	0.67	0.16	0.27
0.15	0.21	0.21	0.58	0.14	0.25
0.20	0.19	0.19	0.50	0.16	0.22
0.25	0.16	0.16	0.56	0.11	0.19
0.30	0.13	0.14	0.62	0.12	0.18
0.35	0.10	0.12	0.76	0.14	0.17
0.40	0.06	0.13	0.89	0.17	0.18
0.45	0.03	0.15	1.01	0.20	0.20
1.00	-0.42	0.56	2.31	0.60	0.73
<hr/>					
BP86-D3(0) <sup>a</sup>	-2.46	2.46	5.96	1.27	2.76
B3LYP-B3(0) <sup>a</sup>	-1.55	1.55	3.73	0.93	1.81
M062X-D3(0) <sup>a</sup>	-0.51	0.63	2.49	0.55	0.75
B2PLYP-D3(BJ) <sup>a</sup>	-0.51	0.57	3.31	0.54	0.73
PWPB95-D3(BJ) <sup>a</sup>	-0.97	0.97	2.57	0.60	1.14
DSD-PBEB95-D3(BJ) <sup>a</sup>	0.04	0.45	3.93	0.74	0.74
r2SCAN-3c <sup>a</sup>	-1.10	1.15	4.54	0.95	1.45

<sup>a</sup>Taken from Ref. 109.

pure RE and pure MP. Along with the MAD, the standard deviation also decreases. Nevertheless, the errors are still too large to satisfy the criterion of chemical accuracy. On the other hand, it should be mentioned that the reactions of this set are fairly difficult: commonly used DFT methods produce quite large mean absolute deviations<sup>113</sup> (see the lower part of Table IX).

Regarding the spin contamination problem, the BH76 set contains two rather delicate systems, namely, the reactants of reactions 75/76. Those reactions consist of the (degenerate) forth- and back

**TABLE VI.** Representative error descriptors for the RSE43 benchmark set [OO-REMP+(S)/def2-QZVP, all electrons correlated; reference: W1-F12]. All in kcal mol<sup>-1</sup>. The full table can be found in Table S5.

A	MSD	MAD	$\Delta_{\min-\max}$	$\sigma$	RMSD
0.00	-0.95	0.96	5.49	1.24	1.55
0.12	-0.81	0.81	3.30	0.80	1.13
0.15	-0.80	0.80	3.04	0.74	1.08
0.16	-0.79	0.79	2.96	0.72	1.07
0.17	-0.79	0.79	2.89	0.71	1.06
0.18	-0.79	0.79	2.82	0.69	1.05
0.19	-0.79	0.79	2.75	0.68	1.04
0.20	-0.79	0.79	2.69	0.67	1.03
0.25	-0.79	0.79	2.49	0.61	1.00
0.30	-0.77	0.83	3.77	0.65	1.00
1.00	-1.41	1.42	4.50	0.95	1.69

reaction C<sub>5</sub>H<sub>8</sub> → RKT22, which is the sigmatropic shift of one hydrogen atom from the methyl group of (Z)-pentadiene to the diene end. Both the reactant and the transition state are formal spin singlets, but the corresponding RHF determinants exhibit triplet instabilities and lead to UHF determinants of broken symmetry character. The corresponding  $\langle \hat{S}^2 \rangle$  expectation values of the UHF determinants of “C<sub>5</sub>H<sub>8</sub>”/“RKT22” are 0.358/0.543 (0.354/0.539) when calculated with the def2-QZVP (aug-cc-pVTZ) basis. At the ROHF level, such an open shell singlet cannot be represented by a single Slater determinant. Entries “C<sub>5</sub>H<sub>8</sub>” and “RKT22” have been treated as closed shell singlets at the RO-REMP level, whereas at the UREMP level, broken symmetry determinants obtained by a stability analysis were used. This is justified by an interesting observation that is made as soon as orbital optimization is operative. If the  $\langle \hat{S}^2 \rangle$  expectation value is calculated from the converged OO-REMP/aug-cc-pVTZ wavefunction, one finds that the initial UHF broken symmetry solution collapses back to a proper singlet

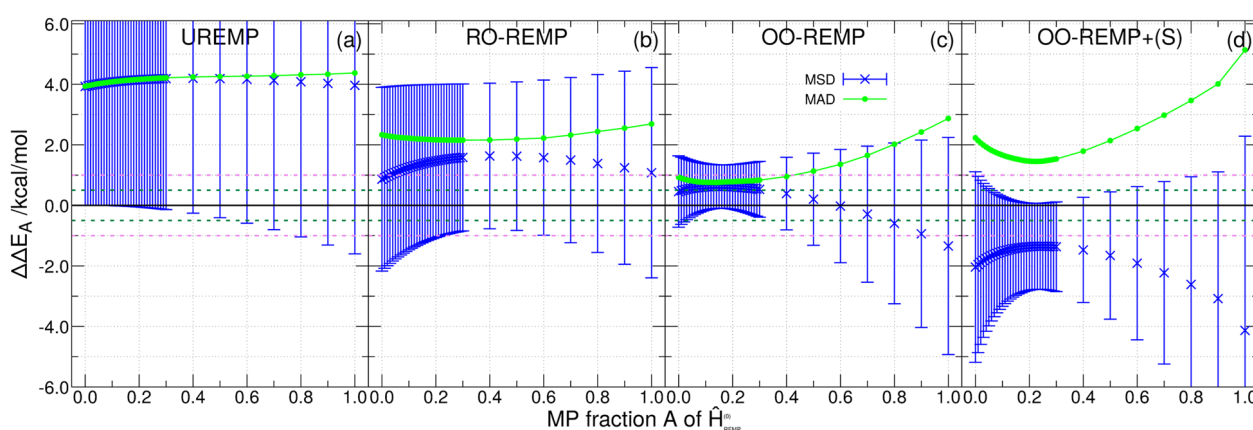


**FIG. 9.** Graphical representation of the MSD and the MAD of four REMP variants for the BH76 set as a function of the REMP mixing parameter  $A$  of  $\hat{H}_{\text{REMP}}^{(0)}$ . (a) UREMP, (b) RO-REMP, (c) OO-REMP, and (d) OO-REMP+(S). Error bars indicate one standard deviation. All calculations use the def2-QZVP basis set. UREMP and RO-REMP make use of standard frozen cores, while OO-REMP and OO-REMP+(S) correlate all electrons. All errors with respect to the W2-F12 reference. See Tables S7–S10 for numerical values.

**TABLE VII.** Representative error descriptors for the BH76 benchmark set (UREMP/def2-QZVP, frozen core; Reference: W2-F12). All values in kcal mol<sup>-1</sup>. The full table can be found in Table S7.

A	MSD	MAD	$\Delta_{\min-\max}$	$\sigma$	RMSD
0.00	3.93	3.93	21.73	3.92	5.53
0.01	3.95	3.95	21.97	3.94	5.56
0.12	4.09	4.10	23.84	4.11	5.78
0.15	4.12	4.13	24.19	4.15	5.83
0.20	4.15	4.16	24.70	4.21	5.89
1.00	3.97	4.37	31.06	5.57	6.81

determinant, and the resulting wavefunction is that of an exact spin singlet. This holds for both “C<sub>5</sub>H<sub>8</sub>” and “RKT22” and was found regardless of the mixing ratio.

Inspection of Fig. 9(c) and Table IX shows a significant improvement of OO-REMP upon the UREMP and RO-REMP results. As soon as orbital optimization is applied, the hybridization of the two perturbation theories again leads to a tremendous improvement as known from the W4-11 and the RSE43 set. For  $A \approx 0.14$ , the MAD becomes minimal and amounts to 0.76 kcal mol<sup>-1</sup>, well within the limit of chemical accuracy. Furthermore, the minimum in the MAD curve is rather flat, indicating that any mixture between  $A = 0.15$  and  $A = 0.30$  will suffice. The same holds for the RMSD, which becomes minimal for  $A \approx 0.16$ . Table IX also contains selected DFT results obtained with the same basis set. Assuming that the W2-F12 reference numbers are sufficiently accurate, none of the listed functionals reaches chemical accuracy on this set and one needs highly parameterized double hybrids to come close to an MAD of 1 kcal mol<sup>-1</sup>.

It should be noted that the def2-QZVP basis set as such is not adequate for all reactions of the BH76 set. When the whole set is further broken down into different reaction categories, one finds that especially the nucleophilic substitutions involving anions exhibit remarkably large errors. The reference method W2-F12<sup>112</sup> among others employs the cc-pVTZ-F12 and the cc-pVQZ-F12 basis sets. These possess more diffuse s, p, and d functions than def2-QZVP

**TABLE VIII.** RO-REMP: Representative error descriptors for the BH76 benchmark set (REMP/def2-QZVP, frozen core; reference: W2-F12). All in kcal mol<sup>-1</sup>. The full table can be found in Table S8.

A	MSD	MAD	$\Delta_{\min-\max}$	$\sigma$	RMSD
0.00	0.86	2.33	15.83	3.033	3.14
0.12	1.30	2.20	14.18	2.67	2.96
0.15	1.37	2.19	13.82	2.61	2.94
0.20	1.47	2.17	13.25	2.53	2.91
0.27	1.56	2.15	12.53	2.45	2.89
0.28	1.57	2.15	12.43	2.44	2.89
0.29	1.58	2.15	12.34	2.44	2.89
0.30	1.58	2.15	12.25	2.43	2.89
1.00	1.08	2.69	19.32	3.47	3.62

**TABLE IX.** Representative error descriptors for the BH76 benchmark set (OO-REMP/def2-QZVP, all electrons correlated; reference: W2-F12). All in kcal mol<sup>-1</sup>. The full table can be found in Table S9. DFT results were taken from the GMTKN55 homepage.<sup>113</sup>

A	MSD	MAD	$\Delta_{\min-\max}$	$\sigma$	RMSD
0.00	0.46	0.93	7.33	1.18	1.26
0.12	0.62	0.76	4.40	0.74	0.96
0.13	0.62	0.76	4.40	0.73	0.95
0.14	0.62	0.76	4.40	0.72	0.95
0.15	0.62	0.76	4.42	0.72	0.95
0.20	0.61	0.78	4.52	0.74	0.95
0.25	0.58	0.80	4.61	0.81	0.99
1.00	-1.34	2.87	26.39	3.57	3.81
BP86(noD)	-9.10	9.15			10.19
BP86(D3(BJ))	-9.81	9.86			10.82
B3LYP(noD)	-4.02	4.94			5.90
B3LYP(D3(BJ))	-4.81	5.70			6.45
M062X(noD)	0.70	2.33			7.29
BMK(noD)	-0.51	1.22			1.57
B2PLYP(noD)	-2.17	2.28			2.65
DSD-PBEB95(D3(BJ))	0.11	1.03			1.65

and are thus better suited for the description of anions in the gas phase. Our errors significantly decrease when the aug-cc-pVQZ basis set is used for these reactions. An example would be reaction 21 ( $F^- + CH_3Cl \rightarrow fch3clts$ ). With the def2-QZVP basis, OO-REMP(0.20) is off by -1.71 kcal mol<sup>-1</sup>, while the error decreases to 0.46 kcal mol<sup>-1</sup> with the aug-cc-pVQZ basis set. Furthermore, when considering the whole subset of reactions 13–28 from the BH76 set, the RMSD drops from 1.33 to 0.98 kcal mol<sup>-1</sup> when changing the basis from def2-QZVP to aug-cc-pVQZ. A comparison between def2-QZVP and aug-cc-pVQZ for the subset of reactions 13–28 can be found in Table S11 in the [supplementary material](#). The def2-QZVP basis set thus is not flexible enough for small anions. This assumption is supported by the fact that also the overall best DFT results for this set listed in the GMTKN55<sup>114</sup> show outliers for these reactions, indicating that DFT suffers from basis incompleteness exactly as REMP does. We, nevertheless, used this basis set for consistency reasons and for allowing a direct comparison of our numbers to the GMTKN55 results. Basis set incompleteness has not been an issue in our previous investigation<sup>55</sup> as the OO-REMP values and the CCSD(T) reference data were obtained with the same augmented basis set (aug-cc-pVTZ) such that ionic species are treated reasonably and on an equal footing.

It was again investigated whether OO-REMP is actually able to remove spin contamination from the reference determinant. One rather extreme example taken from the BH76 set is the transition state termed “ch3fclts,” which is formally a spin doublet but has a UHF ( $\bar{S}^2$ ) expectation value of 1.027. In the unrestricted case, the errors of reactions involving this transition state are always larger than 10 kcal mol<sup>-1</sup> regardless of the REMP mixing ratio. In the restricted open shell case, the largest occurring errors already drop

to 2.2 and 4.7 kcal mol<sup>-1</sup> for reactions 11 and 12, respectively (at  $A = 0.40$ ). As soon as orbital optimization is operative, the largest occurring absolute errors drop to 2.2 kcal mol<sup>-1</sup> ( $A = 1.00$ , i.e., pure OO-MP2) and the better mixing ratios reach sub-kcal mol<sup>-1</sup> accuracy. This improvement is again connected with an almost entire elimination of the spin contamination by orbital optimization: For all the tested REMP mixtures, OO-REMP calculations for “ch3fclts” have been performed using the def2-TZVP basis and  $\langle \hat{S}^2 \rangle$  was calculated upon convergence for both the reference and the total first order wavefunction.  $\langle \hat{S}^2 \rangle_{\Phi_{\text{UHF}}}$  was again 1.027. In the case of pure OO-RE, the  $\langle \hat{S}^2 \rangle$  expectation value of the optimized reference determinant  $|\phi_0\rangle$  is 0.7661 and the  $\langle \hat{S}^2 \rangle$  expectation value of the complete correlated wavefunction is 0.7499 [calculated with Eq. (13) of Ref. 91]. A graphical representation of  $\langle \hat{S}^2 \rangle$  as a function of  $A$  is shown in Fig. 10.

In this case, pure RE is most efficient in removing spin contamination from the reference during orbital optimization, resulting in an essentially spin-pure wavefunction. It is also interesting to note that MP2 delivers a better reference judged by  $\langle \hat{S}^2 \rangle$  but a worse total wavefunction as compared to RE2. The  $\langle \hat{S}^2 \rangle$  expectation values of both the reference and the total wavefunction, furthermore, show local maxima, which are not easily explicable. However, given that the spin contamination is always smaller than 0.005, all OO-REMP wavefunctions are of outstanding quality in this regard.

Inclusion of perturbative singles on top of OO-REMP was assessed for the BH76 test set; see Fig. 9(d) and Table X. As before, the perturbative singles do not improve the overall performance of the method. All error measures are worse than before, giving rise

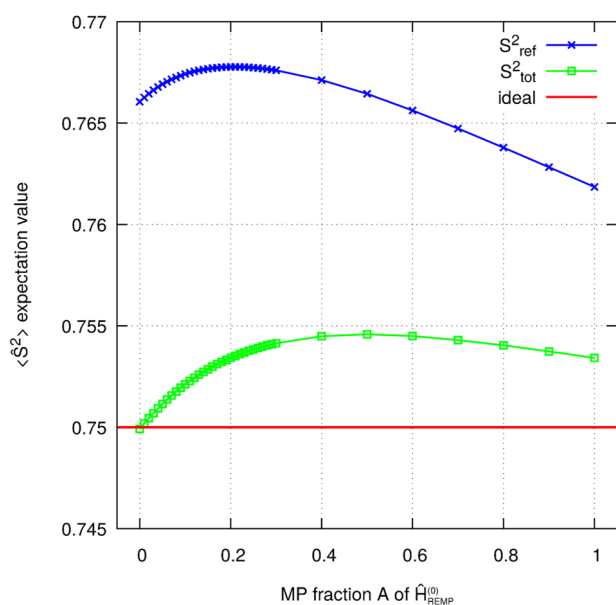


**FIG. 10.**  $\langle \hat{S}^2 \rangle$  of the optimized reference determinant (blue) and of the total first order OO-REMP wavefunction (green) as a function of the REMP mixing parameter  $A$ . Molecule: “ch3fclts” from the BH76 benchmark set, basis: def2-TZVP. See Table S17 for numerical values.

**TABLE X.** Representative error descriptors for the BH76 benchmark set [OO-REMP+(S)/def2-QZVP, all electrons correlated; reference: W2-F12]. All in kcal mol<sup>-1</sup>. The full table can be found in Table S10.

$A$	MSD	MAD	$\Delta_{\text{min-max}}$	$\sigma$	RMSD
0.00	-2.04	2.23	22.21	3.15	3.73
0.12	-1.48	1.60	11.25	1.69	2.23
0.13	-1.46	1.58	10.76	1.64	2.18
0.14	-1.44	1.56	10.30	1.59	2.14
0.15	-1.42	1.54	9.89	1.56	2.10
0.20	-1.37	1.46	8.58	1.44	1.98
0.23	-1.35	1.45	8.07	1.42	1.95
1.00	-4.13	5.13	36.34	6.42	7.60

to numbers not sufficient for chemical accuracy anymore. The error spread is more than three times larger than without perturbative singles. All findings are again confirmed by the RMSD (Fig. 11), which is more sensitive to outliers. OO-REMP is the only method capable of achieving an RMSD below 1 kcal mol<sup>-1</sup> and, thus, the only method that provides sufficient accuracy for this set.

Along with the BH76 set, the set of reaction energies accessible from the same data (BH76RC<sup>107</sup>) was also analyzed. In contrast to the activation barriers, one also finds that UREMP improves upon its parent methods (see Figs. 12 and 13). The smallest MAD is found for 25% MP (cf. Table XI), in reasonable qualitative agreement with the closed shell cases investigated. Unfortunately, even the best mixture exhibits errors that disqualify the method. Especially the error spread of 12 kcal mol<sup>-1</sup> is rather dissatisfying.

The restricted open-shell variant (cf. Table XII) provides a substantial improvement upon hybridization and also improves upon the unrestricted variant, although now the minimum seems to be located somewhere between 30% and 40% MP. The mean absolute error of the best mixture is slightly smaller compared to the unrestricted case but still larger than 1 kcal mol<sup>-1</sup>. The same holds for the RMSD.

After the inclusion of orbital optimization (see Table XIII), the mean absolute error drops to 0.67 kcal mol<sup>-1</sup> with 18% MP, and the RMSD is 1.10 kcal mol<sup>-1</sup> in this case. The reaction that exhibits by far the largest error ( $\approx 4$  kcal mol<sup>-1</sup>) is  $\text{F}^- + \text{CH}_3\text{Cl} \rightarrow \text{Cl}^- + \text{CH}_3\text{F}$ . This can again be attributed to the insufficiency of the def2-QZVP basis set for the involved ions as the error dramatically decreases as soon as the aug-cc-pVQZ basis is used: With the def2-QZVP basis set and  $A = 0.18$ , reactions 5–8 show absolute errors between 1.2 and 4.0 kcal mol<sup>-1</sup>. These errors drop to at most 0.85 kcal mol<sup>-1</sup> with the aug-cc-pVQZ basis set. A comparison of the results for reactions 5–8 can be found in Table S16.

If OO-REMP is compared to commonly used density functionals, one again finds that OO-REMP clearly outperforms these methods. As before, even the double-hybrid functional that performs best for this set gives slightly larger errors. Furthermore, it is interesting to note that in the case of that reaction where OO-REMP has the largest error, DSD-BLYP is also off by  $-2.87$  kcal mol<sup>-1</sup>.

In the case of the BH76RC set, inclusion of perturbative singles has only a minor influence (cf. Table XIV). The smallest error



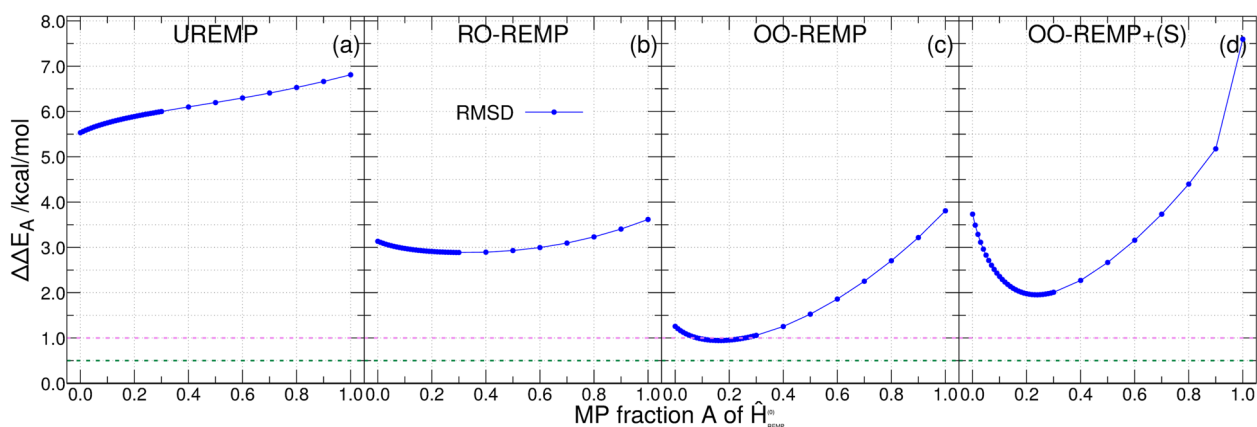


**FIG. 11.** Graphical representation of the RMSD of four REMP variants for the BH76 set as a function of the REMP mixing parameter  $A$  of  $\hat{H}_{\text{REMP}}^{(0)}$ . (a) UREMP, (b) RO-REM, (c) OO-REM, and (d) OO-REM+(S). All calculations use the def2-QZVP basis set. UREMP and RO-REM make use of standard frozen cores, while OO-REM and OO-REM+(S) correlate all electrons. All errors with respect to the W2-F12 reference. See Tables S7–S10 for numerical values.

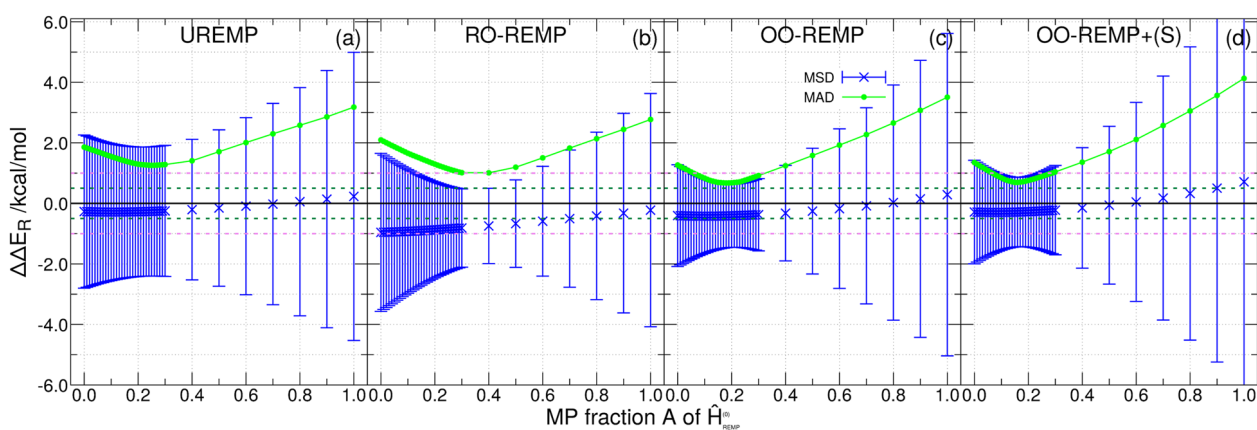


**FIG. 12.** Graphical representation of the MSD and the MAD of the four REMP variants for the BH76RC set as a function of the REMP mixing parameter  $A$  of  $\hat{H}_{\text{REMP}}^{(0)}$ . (a) UREMP, (b) RO-REM, (c) OO-REM, and (d) OO-REM+(S). Error bars indicate one standard deviation. All calculations use the def2-QZVP basis set. UREMP and RO-REM make use of standard frozen cores, while OO-REM and OO-REM+(S) correlate all electrons. All errors with respect to the W2-F12 reference. See Tables S12–S15 for numerical values.

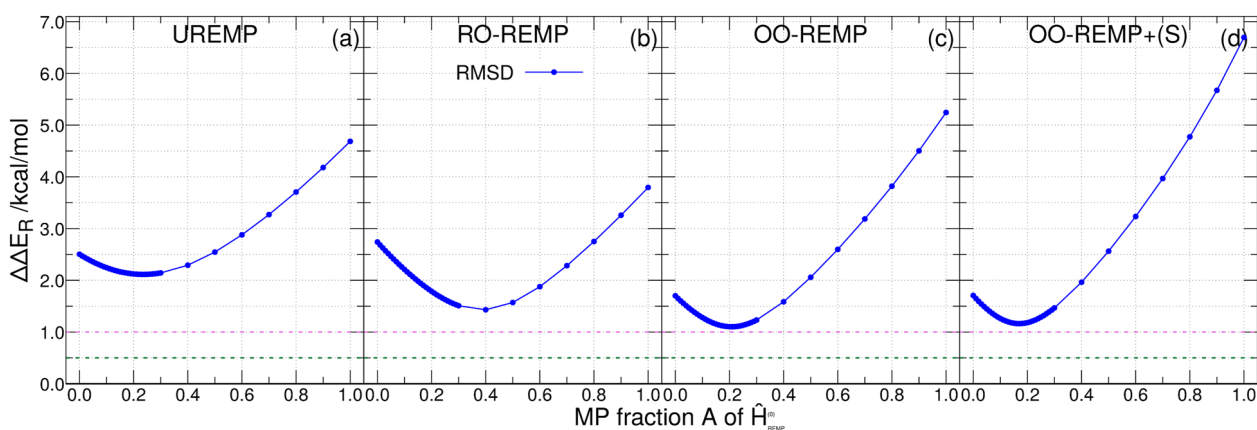


**FIG. 13.** Graphical representation of the RMSD of the four REMP variants for the BH76RC set as a function of the REMP mixing parameter  $A$  of  $\hat{H}_{\text{REMP}}^{(0)}$ . (a) UREMP, (b) RO-REM, (c) OO-REM, and (d) OO-REM+(S). All calculations use the def2-QZVP basis set. UREMP and RO-REM make use of standard frozen cores, while OO-REM and OO-REM+(S) correlate all electrons. All errors with respect to the W2-F12 reference. See Tables S12–S15 for numerical values.

**TABLE XI.** UREMP: Representative error descriptors for the BH76RC benchmark set (UREMP/def2-QZVP, frozen core; reference: W2-F12). All in kcal mol<sup>-1</sup>. The full table can be found in Table S12.

A	MSD	MAD	$\Delta_{\min-\max}$	$\sigma$	RMSD
0.00	-0.27	1.86	13.52	2.53	2.50
0.12	-0.29	1.49	12.43	2.23	2.21
0.15	-0.29	1.41	12.20	2.18	2.17
0.20	-0.28	1.30	12.52	2.14	2.12
0.24	-0.27	1.26	12.76	2.13	2.11
0.25	-0.26	1.26	12.82	2.13	2.11
1.00	0.23	3.18	23.98	4.76	4.69

**TABLE XII.** RO-REMP: Representative error descriptors for the BH76RC benchmark set (RO-REMP/def2-QZVP, frozen core; reference: W2-F12). All in kcal mol<sup>-1</sup>. The full table can be found in Table S13.

A	MSD	MAD	$\Delta_{\min-\max}$	$\sigma$	RMSD
0.00	-0.96	2.10	12.71	2.61	2.74
0.12	-0.92	1.58	8.68	1.94	2.12
0.15	-0.90	1.47	7.70	1.80	1.98
0.20	-0.88	1.30	6.09	1.58	1.79
0.30	-0.81	1.02	6.07	1.29	1.51
0.40	-0.75	1.01	6.59	1.24	1.43
0.50	-0.67	1.20	7.07	1.45	1.57
1.00	-0.22	2.77	19.11	3.85	3.79

is now found for 17% MP, and the error spread is larger; all other error measures are rather similar. Most importantly, also in this case, no improvement upon OO-REMP is found by adding perturbative singles.

**TABLE XIII.** Representative error descriptors for the BH76RC benchmark set (OO-REMP/def2-QZVP, all electrons correlated; reference: W2-F12). All in kcal mol<sup>-1</sup>. The full table can be found in Table S14. DFT data for comparison have been retrieved from the GMTKN55 homepage.

A	MSD	MAD	$\Delta_{\min-\max}$	$\sigma$	RMSD
0.00	-0.40	1.26	7.10	1.68	1.70
0.01	-0.41	1.22	6.75	1.63	1.65
0.12	-0.42	0.76	5.09	1.17	1.22
0.15	-0.42	0.69	4.95	1.09	1.16
0.18	-0.42	0.67	4.81	1.05	1.11
0.20	-0.41	0.68	4.72	1.04	1.10
1.00	0.29	3.51	29.97	5.33	5.24
BP86 [D3(BJ)]	-0.04	3.48			5.08
B3LYP [D3(BJ)]	-0.38	2.25			2.79
M06-2X [D3(0)]	-0.48	1.18			1.71
DSD-BLYP [D3(BJ)]	-0.21	0.81			1.21

**TABLE XIV.** Representative error descriptors for the BH76RC benchmark set [OO-REMP+(S)/def2-QZVP, all electrons correlated; reference: W2-F12]. All in kcal mol<sup>-1</sup>. The full table can be found in Table S15.

A	MSD	MAD	$\Delta_{\min-\max}$	$\sigma$	RMSD
0.00	-0.29	1.35	8.30	1.71	1.71
0.12	-0.30	0.77	6.84	1.20	1.21
0.15	-0.29	0.69	6.59	1.15	1.17
0.17	-0.28	0.70	6.45	1.15	1.16
0.20	-0.27	0.76	6.26	1.17	1.18
1.00	0.71	4.13	39.38	6.77	6.69

#### IV. SUMMARY AND OUTLOOK

We have investigated open-shell generalizations of the REMP hybrid perturbation theory and an orbital-optimized variant thereof. Opposite to the closed-shell counterpart, REMP with unrestricted reference determinants (UREMP) shows no systematic improvement upon the parent perturbation theories RE and MP. REMP based on restricted open-shell determinants (RO-REMP) improves upon its parent methods but does not fulfill the criteria for chemical accuracy. Orbital-optimized REMP (OO-REMP) improves upon both parent methods and systematically outperforms the non-orbital-optimized methods. It provides energies that are sufficiently accurate to reach chemical accuracy for both reaction energies and reaction barrier heights. Furthermore, it generates variationally optimized wavefunctions with small spin-contamination errors and approximately correct spin and spatial degeneracy. The perturbative inclusion of formally missing single excitations into OO-REMP leads to no improvement but worsens all considered results, similar to what has been found for OO-MP2.<sup>27</sup>

It was found that the choice of the mixing parameter *A* is robust over a wide range of investigated reaction types, especially in the case of OO-REMP. If the basis set is saturated enough for the problem under investigation, it was found that a mixing ratio of 20% MP:80% RE is always a good choice, performing similar to the individually best mixing ratio. With insufficient basis sets, one may observe error compensation by choosing significantly larger MP fractions, e.g., in the case of the atomization energies, but the results obtained that way are usually of no practical use. RO-REMP requires significantly larger MP fractions with the optimal mixing being about 40% MP:60% RE. UREMP shows no systematic behavior with pure unrestricted RE often being the best performing method.

There are several further developments that suggest themselves: First, orbital-optimized REMP delivers fully relaxed density matrices, which allows for the fast evaluation of first-order properties, such as electrical multipole moments or nuclear gradients. Analytical nuclear gradients were implemented as an extension in the PSI4 program package and successfully tested on a set of small molecules for which high-quality experimental data are available. Details will be presented in an upcoming publication.<sup>115</sup> The second extension is to modify the unperturbed Hamiltonian, e.g., by incorporating spin-dependent terms as in the S2-PT approach.<sup>23</sup> Using different mixings for the two CSF classes can be expected to give even better results. The third evident extension would be a multireference

generalization of the REMP partitioning. Work on all topics is in progress in our laboratory.

## SUPPLEMENTARY MATERIAL

See the [supplementary material](#) for all total energies that are provided as spreadsheets (.ods) or .csv files and complete versions of all tables and raw data for all graphs.

## ACKNOWLEDGMENTS

The authors acknowledge access to the high-performance computing resources of bwHPC, which was supported by the state of Baden-Württemberg and the German Research Foundation (DFG) through Grant No. INST 40/467-1 FUGG (bwForCluster JUSTUS) and Grant No. INST 40/575-1 FUGG (JUSTUS 2 cluster). The authors also acknowledge the Center for Light-Matter Interaction, Sensors and Analytics (LISA+) for providing them with computational resources. The authors would like to thank Dr. Elke Faßhauer and Marc Edelmann for proof-reading of the manuscript and for valuable suggestions.

## AUTHOR DECLARATIONS

### Conflict of Interest

The authors have no conflicts to disclose.

## DATA AVAILABILITY

The data that support the findings of this study are available within the article and its [supplementary material](#).

## REFERENCES

- <sup>1</sup>E. Schrödinger, "Quantisierung als Eigenwertproblem (dritte Mitteilung)," *Ann. Phys.* **385**, 437–490 (1926).
- <sup>2</sup>T. Helgaker, P. Jørgensen, and J. Olsen, *Molecular Electronic-Structure Theory*, reprinted ed. (Wiley, Chichester, New York, Weinheim, 2004).
- <sup>3</sup>I. Shavitt and R. J. Bartlett, *Many-Body Methods in Chemistry and Physics: MBPT and Coupled-Cluster Theory*, Cambridge Molecular Science (Cambridge University Press, 2009).
- <sup>4</sup>D. Cremer, "Møller-Plesset perturbation theory: From small molecule methods to methods for thousands of atoms," *Wiley Interdiscip. Rev.: Comput. Mol. Sci.* **1**, 509–530 (2011).
- <sup>5</sup>Á. Szabados, "Perturbation theory: Time-independent aspects of the theory applied in molecular electronic structure description," in *Reference Module in Chemistry, Molecular Sciences and Chemical Engineering* (Elsevier, 2017).
- <sup>6</sup>C. Møller and M. S. Plesset, "Note on an approximation treatment for many-electron systems," *Phys. Rev.* **46**, 618–622 (1934).
- <sup>7</sup>S. Grimme, "Improved second-order Møller-Plesset perturbation theory by separate scaling of parallel- and antiparallel-spin pair correlation energies," *J. Chem. Phys.* **118**, 9095–9102 (2003).
- <sup>8</sup>S. Grimme, L. Goerigk, and R. F. Fink, "Spin-component-scaled electron correlation methods," *Wiley Interdiscip. Rev.: Comput. Mol. Sci.* **2**, 886–906 (2012).
- <sup>9</sup>S. Grimme, "Improved third-order Møller-Plesset perturbation theory," *J. Comput. Chem.* **24**, 1529–1537 (2003).
- <sup>10</sup>L. W. Bertels, J. Lee, and M. Head-Gordon, "Third-order Møller-Plesset perturbation theory made useful? Choice of orbitals and scaling greatly improves accuracy for thermochemistry, kinetics, and intermolecular interactions," *J. Phys. Chem. Lett.* **10**, 4170–4176 (2019).
- <sup>11</sup>J. Lee and M. Head-Gordon, "Regularized orbital-optimized second-order Møller-Plesset perturbation theory: A reliable fifth-order-scaling electron correlation model with orbital energy dependent regularizers," *J. Chem. Theory Comput.* **14**, 5203–5219 (2018).
- <sup>12</sup>M. Pitoňák, P. Neogrády, J. Cerný, S. Grimme, and P. Hobza, "Scaled MP3 non-covalent interaction energies agree closely with accurate CCSD(T) benchmark data," *ChemPhysChem* **10**, 282–289 (2009).
- <sup>13</sup>R. Sedlak, T. Janowski, M. Pitoňák, J. Řezáč, P. Pulay, and P. Hobza, "Accuracy of quantum chemical methods for large noncovalent complexes," *J. Chem. Theory Comput.* **9**, 3364–3374 (2013).
- <sup>14</sup>A. Karton and L. Goerigk, "Accurate reaction barrier heights of pericyclic reactions: Surprisingly large deviations for the CBS-QB3 composite method and their consequences in DFT benchmark studies," *J. Comput. Chem.* **36**, 622–632 (2015).
- <sup>15</sup>P. S. Epstein, "The Stark effect from the point of view of Schrödinger's quantum theory," *Phys. Rev.* **28**, 695–710 (1926).
- <sup>16</sup>R. K. Nesbet, "Configuration interaction in orbital theories," *Proc. R. Soc. London, Ser. A* **230**, 312 (1955).
- <sup>17</sup>C. Murray and E. R. Davidson, "Different forms of perturbation theory for the calculation of the correlation energy," *Int. J. Quantum Chem.* **43**, 755–768 (1992).
- <sup>18</sup>P. R. Surján and Á. Szabados, "Appendix to 'studies in perturbation theory': The problem of partitioning," in *Fundamental World of Quantum Chemistry, A Tribute to the Memory of Per-Olov Löwdin*, edited by E. J. Brändas and E. S. Kryachko (Kluwer, Dordrecht, 2004), Vol. III, pp. 129–185.
- <sup>19</sup>C. Schmidt, M. Warken, and N. C. Handy, "The Feenberg series. An alternative to the Møller-Plesset series," *Chem. Phys. Lett.* **211**, 272–281 (1993).
- <sup>20</sup>P. Goldhammer and E. Feenberg, "Refinement of the Brillouin-Wigner perturbation method," *Phys. Rev.* **101**, 1233–1234 (1956).
- <sup>21</sup>E. Feenberg, "Invariance property of the Brillouin-Wigner perturbation series," *Phys. Rev.* **103**, 1116–1119 (1956).
- <sup>22</sup>Á. Szabados, "Theoretical interpretation of Grimme's spin-component-scaled second order Møller-Plesset theory," *J. Chem. Phys.* **125**, 214105 (2006).
- <sup>23</sup>R. F. Fink, "Spin-component-scaled Møller-Plesset (SCS-MP) perturbation theory: A generalization of the MP approach with improved properties," *J. Chem. Phys.* **133**, 174113 (2010).
- <sup>24</sup>P. R. Surján and Á. Szabados, "Optimized partitioning in perturbation theory: Comparison to related approaches," *J. Chem. Phys.* **112**, 4438–4446 (2000).
- <sup>25</sup>Á. Szabados and P. R. Surján, "Optimized partitioning in Rayleigh-Schrödinger perturbation theory," *Chem. Phys. Lett.* **308**, 303–309 (1999).
- <sup>26</sup>E. Soydaş and U. Bozkaya, "Accurate open-shell noncovalent interaction energies from the orbital-optimized Møller-Plesset perturbation theory: Achieving CCSD quality at the MP2 level by orbital optimization," *J. Chem. Theory Comput.* **9**, 4679–4683 (2013).
- <sup>27</sup>F. Neese, T. Schwabe, S. Kossmann, B. Schirmer, and S. Grimme, "Assessment of orbital-optimized, spin-component scaled second-order many-body perturbation theory for thermochemistry and kinetics," *J. Chem. Theory Comput.* **5**, 3060–3073 (2009).
- <sup>28</sup>T. N. Lan and T. Yanai, "Correlated one-body potential from second-order Møller-Plesset perturbation theory: Alternative to orbital-optimized MP2 method," *J. Chem. Phys.* **138**, 224108 (2013).
- <sup>29</sup>U. Bozkaya, "Orbital-optimized third-order Møller-Plesset perturbation theory and its spin-component and spin-opposite scaled variants: Application to symmetry breaking problems," *J. Chem. Phys.* **135**, 224103 (2011).
- <sup>30</sup>E. Soydaş and U. Bozkaya, "Assessment of orbital-optimized third-order Møller-Plesset perturbation theory and its spin-component and spin-opposite scaled variants for thermochemistry and kinetics," *J. Chem. Theory Comput.* **9**, 1452–1460 (2013).
- <sup>31</sup>C. Lasar and T. Klüner, "Explicitly correlated orbital optimized contracted pair correlation methods: Foundations and applications," *J. Theory Comput. Chem.* **17**, 1850024 (2018).

- <sup>32</sup>C. Lasar and T. Klüner, "Explicitly correlated orbital optimized contracted pair correlation methods: A short overview," *J. Phys. Chem. A* **121**, 4707–4711 (2017).
- <sup>33</sup>G. E. Scuseria and H. F. Schaefer, "The optimization of molecular orbitals for coupled cluster wavefunctions," *Chem. Phys. Lett.* **142**, 354–358 (1987).
- <sup>34</sup>C. D. Sherrill, A. I. Krylov, E. F. C. Byrd, and M. Head-Gordon, "Energies and analytic gradients for a coupled-cluster doubles model using variational Brueckner orbitals: Application to symmetry breaking in  $O_4^+$ ," *J. Chem. Phys.* **109**, 4171–4181 (1998).
- <sup>35</sup>U. Bozkaya, J. M. Turney, Y. Yamaguchi, H. F. Schaefer, and C. D. Sherrill, "Quadratically convergent algorithm for orbital optimization in the orbital-optimized coupled-cluster doubles method and in orbital-optimized second-order Møller-Plesset perturbation theory," *J. Chem. Phys.* **135**, 104103 (2011).
- <sup>36</sup>U. Bozkaya, A. Ünal, and Y. Alagöz, "Energy and analytic gradients for the orbital-optimized coupled-cluster doubles method with the density-fitting approximation: An efficient implementation," *J. Chem. Phys.* **153**, 244115 (2020).
- <sup>37</sup>R. C. Lochan and M. Head-Gordon, "Orbital-optimized opposite-spin scaled second-order correlation: An economical method to improve the description of open-shell molecules," *J. Chem. Phys.* **126**, 164101 (2007).
- <sup>38</sup>R. M. Razban, D. Stück, and M. Head-Gordon, "Addressing first derivative discontinuities in orbital-optimized opposite-spin scaled second-order perturbation theory with regularisation," *Mol. Phys.* **115**, 2102–2109 (2017).
- <sup>39</sup>U. Bozkaya and C. D. Sherrill, "Orbital-optimized MP2.5 and its analytic gradients: Approaching CCSD(T) quality for noncovalent interactions," *J. Chem. Phys.* **141**, 204105 (2014).
- <sup>40</sup>E. Soydaş and U. Bozkaya, "Assessment of orbital-optimized MP2.5 for thermochemistry and kinetics: Dramatic failures of standard perturbation theory approaches for aromatic bond dissociation energies and barrier heights of radical reactions," *J. Chem. Theory Comput.* **11**, 1564–1573 (2015).
- <sup>41</sup>U. Bozkaya, "Orbital-optimized MP3 and MP2.5 with density-fitting and Cholesky decomposition approximations," *J. Chem. Theory Comput.* **12**, 1179–1188 (2016).
- <sup>42</sup>U. Bozkaya, "Orbital-optimized linearized coupled-cluster doubles with density-fitting and Cholesky decomposition approximations: An efficient implementation," *Phys. Chem. Chem. Phys.* **18**, 11362–11373 (2016).
- <sup>43</sup>E. Soydaş and U. Bozkaya, "Assessment of the orbital-optimized coupled-electron pair theory for thermochemistry and kinetics: Improving on CCSD and CEPA(1)," *J. Comput. Chem.* **35**, 1073–1081 (2014).
- <sup>44</sup>U. Bozkaya and C. D. Sherrill, "Orbital-optimized coupled-electron pair theory and its analytic gradients: Accurate equilibrium geometries, harmonic vibrational frequencies, and hydrogen transfer reactions," *J. Chem. Phys.* **139**, 054104 (2013).
- <sup>45</sup>R. F. Fink, "The multi-reference retaining the excitation degree perturbation theory: A size-consistent, unitary invariant, and rapidly convergent wavefunction based *ab initio* approach," *Chem. Phys.* **356**, 39–46 (2009).
- <sup>46</sup>R. F. Fink, "Two new unitary-invariant and size-consistent perturbation theoretical approaches to the electron correlation energy," *Chem. Phys. Lett.* **428**, 461–466 (2006).
- <sup>47</sup>K. G. Dyall, "The choice of a zeroth-order Hamiltonian for second-order perturbation theory with a complete active space self-consistent-field reference function," *J. Chem. Phys.* **102**, 4909–4918 (1995).
- <sup>48</sup>S. Behnle and R. F. Fink, "REMP: A hybrid perturbation theory providing improved electronic wavefunctions and properties," *J. Chem. Phys.* **150**, 124107 (2019).
- <sup>49</sup>R. F. Fink, "Why does MP2 work?," *J. Chem. Phys.* **145**, 184101 (2016).
- <sup>50</sup>K. Raghavachari, G. W. Trucks, J. A. Pople, and M. Head-Gordon, "A fifth-order perturbation comparison of electron correlation theories," *Chem. Phys. Lett.* **157**, 479–483 (1989).
- <sup>51</sup>D. R. Nascimento and A. E. DePrince, "A parametrized coupled-pair functional for molecular interactions: PCPF-MI," *J. Chem. Theory Comput.* **10**, 4324–4331 (2014).
- <sup>52</sup>L. M. J. Huntington and M. Nooijen, "PCCSD: Parameterized coupled-cluster theory with single and double excitations," *J. Chem. Phys.* **133**, 184109–184127 (2010).
- <sup>53</sup>L. M. J. Huntington, A. Hansen, F. Neese, and M. Nooijen, "Accurate thermochemistry from a parameterized coupled-cluster singles and doubles model and a local pair natural orbital based implementation for applications to larger systems," *J. Chem. Phys.* **136**, 064101 (2012).
- <sup>54</sup>D. W. Small, "Remarkable accuracy of an  $O(N^6)$  perturbative correction to opposite-spin CCSD: Are triples necessary for chemical accuracy in coupled cluster?," *J. Chem. Theory Comput.* **16**, 4014–4020 (2020).
- <sup>55</sup>S. Behnle and R. F. Fink, "OO-REMP: Approaching chemical accuracy with second order perturbation theory," *J. Chem. Theory Comput.* **17**, 3259 (2021).
- <sup>56</sup>A. Szabo and N. S. Ostlund, *Modern Quantum Chemistry: Introduction to Advanced Electronic Structure Theory* (Dover Publications, Inc., 1996).
- <sup>57</sup>V. Fock, "Konfigurationsraum und zweite quantelung," *Z. Phys.* **75**, 622–647 (1932).
- <sup>58</sup>P. R. Surján, *Second Quantized Approach to Quantum Chemistry: An Elementary Introduction* (Springer, Berlin, Heidelberg, 1989), Vol. XII, p. 184.
- <sup>59</sup>N. C. Handy, P. J. Knowles, and K. Somasundram, "On the convergence of the Møller-Plesset perturbation series," *Theor. Chim. Acta* **68**, 87–100 (1985).
- <sup>60</sup>R. Fink and V. Staemmler, "A multi-configuration reference CEPA method based on pair natural orbitals," *Theor. Chim. Acta* **87**, 129–145 (1993).
- <sup>61</sup>W. Kutzelnigg, "Pair correlation theories," in *Modern Theoretical Chemistry*, edited by H. F. Schaefer III (Plenum Press, New York, 1977), pp. 129–188.
- <sup>62</sup>R. Ahlrichs, "Many body perturbation calculations and coupled electron pair models," *Comput. Phys. Commun.* **17**, 31–45 (1979).
- <sup>63</sup>S. Sharma and A. Alavi, "Multireference linearized coupled cluster theory for strongly correlated systems using matrix product states," *J. Chem. Phys.* **143**, 102815 (2015).
- <sup>64</sup>A. G. Taube and R. J. Bartlett, "Rethinking linearized coupled-cluster theory," *J. Chem. Phys.* **130**, 144112 (2009).
- <sup>65</sup>R. J. Bartlett, "Many-body perturbation theory and coupled cluster theory for electron correlation in molecules," *Annu. Rev. Phys. Chem.* **32**, 359–401 (1981).
- <sup>66</sup>J. Čížek, "On the correlation problem in atomic and molecular systems. Calculation of wavefunction components in urself-type expansion using quantum-field theoretical methods," *J. Chem. Phys.* **45**, 4256–4266 (1966).
- <sup>67</sup>J. Čížek, "On the correlation problem in atomic and molecular systems. Calculation of wavefunction components in urself-type expansion using quantum-field theoretical methods," *Adv. Quantum Chem.* **13**, 35–89 (1969).
- <sup>68</sup>R. J. Bartlett and I. Shavitt, "Comparison of high-order many-body perturbation theory and configuration interaction for  $H_2O$ ," *Chem. Phys. Lett.* **50**, 190–198 (1977).
- <sup>69</sup>R. J. Bartlett and I. Shavitt, "Comparison of high-order many-body perturbation theory and configuration interaction for  $H_2O$ ," *Chem. Phys. Lett.* **57**, 157–158 (1978).
- <sup>70</sup>W. Kutzelnigg and D. Mukherjee, "Normal order and extended Wick theorem for a multiconfiguration reference wave function," *J. Chem. Phys.* **107**, 432–449 (1997).
- <sup>71</sup>T. D. Crawford, H. F. Schaefer, and T. J. Lee, "On the energy invariance of open-shell perturbation theory with respect to unitary transformations of molecular orbitals," *J. Chem. Phys.* **105**, 1060–1069 (1996).
- <sup>72</sup>W. J. Lauderdale, J. F. Stanton, J. Gauss, J. D. Watts, and R. J. Bartlett, "Many-body perturbation theory with a restricted open-shell Hartree-Fock reference," *Chem. Phys. Lett.* **187**, 21–28 (1991).
- <sup>73</sup>Note that this is in contrast to Ref. 3 where "d" indicates only the actual diagonal of the Fock matrix.
- <sup>74</sup>P. J. Knowles, J. S. Andrews, R. D. Amos, N. C. Handy, and J. A. Pople, "Restricted Møller-Plesset theory for open-shell molecules," *Chem. Phys. Lett.* **186**, 130–136 (1991).
- <sup>75</sup>A. Hansen, "Development of efficient and accurate approximations to single reference correlation methods using pair natural orbitals," Ph.D. thesis, Rheinische Friedrich-Wilhelms-Universität Bonn, 2012, <http://hss.ulb.uni-bonn.de/2012/2976/2976.pdf>.
- <sup>76</sup>A. Hansen, D. G. Liakos, and F. Neese, "Efficient and accurate local single reference correlation methods for high-spin open-shell molecules using pair natural orbitals," *J. Chem. Phys.* **135**, 214102 (2011).
- <sup>77</sup>K. R. Glaesemann and M. W. Schmidt, "On the ordering of orbital energies in high-spin ROHF," *J. Phys. Chem. A* **114**, 8772–8777 (2010).



- <sup>78</sup>M. Jungen, "Hartree-Fock calculations for excited Rydberg states," *Theor. Chim. Acta* **60**, 369–377 (1981).
- <sup>79</sup>K. Fægri and R. Manne, "A new procedure for Roothaan's symmetry-restricted open-shell SCF method," *Mol. Phys.* **31**, 1037–1049 (1976).
- <sup>80</sup>B. N. Plakhotin, E. V. Gorelik, and N. N. Breslavskaya, "Koopmans' theorem in the ROHF method: Canonical form for the Hartree-Fock Hamiltonian," *J. Chem. Phys.* **125**, 204110 (2006).
- <sup>81</sup>B. Sandhoefer, S. Kossmann, and F. Neese, "Derivation and assessment of relativistic hyperfine-coupling tensors on the basis of orbital-optimized second-order Møller–Plesset perturbation theory and the second-order Douglas–Kroll–Hess transformation," *J. Chem. Phys.* **138**, 104102 (2013).
- <sup>82</sup>A. I. Krylov, C. D. Sherrill, E. F. C. Byrd, and M. Head-Gordon, "Size-consistent wave functions for nondynamical correlation energy: The valence active space optimized orbital coupled-cluster doubles model," *J. Chem. Phys.* **109**, 10669–10678 (1998).
- <sup>83</sup>A. I. Krylov, C. D. Sherrill, and M. Head-Gordon, "Excited states theory for optimized orbitals and valence optimized orbitals coupled-cluster doubles models," *J. Chem. Phys.* **113**, 6509–6527 (2000).
- <sup>84</sup>W. Kurlancheek and M. Head-Gordon, "Violations of N-representability from spin-unrestricted orbitals in Møller–Plesset perturbation theory and related double-hybrid density functional theory," *Mol. Phys.* **107**, 1223–1232 (2009).
- <sup>85</sup>S. Kossmann and F. Neese, "Correlated *ab initio* spin densities for larger molecules: Orbital-optimized spin-component-scaled MP2 method," *J. Phys. Chem. A* **114**, 11768–11781 (2010).
- <sup>86</sup>U. Bozkaya, "Analytic energy gradients and spin multiplicities for orbital-optimized second-order perturbation theory with density-fitting approximation: An efficient implementation," *J. Chem. Theory Comput.* **10**, 4389–4399 (2014).
- <sup>87</sup>U. Bozkaya, "Analytic energy gradients for the orbital-optimized third-order Møller–Plesset perturbation theory," *J. Chem. Phys.* **139**, 104116 (2013).
- <sup>88</sup>U. Bozkaya and C. D. Sherrill, "Analytic energy gradients for the orbital-optimized second-order Møller–Plesset perturbation theory," *J. Chem. Phys.* **138**, 184103 (2013).
- <sup>89</sup>T. D. Crawford and H. F. Schaefer III, "An introduction to coupled cluster theory for computational chemists," in *Reviews in Computational Chemistry* (John Wiley & Sons, 2000), pp. 33–136.
- <sup>90</sup>U. Bozkaya, "Orbital-optimized second-order perturbation theory with density-fitting and Cholesky decomposition approximations: An efficient implementation," *J. Chem. Theory Comput.* **10**, 2371–2378 (2014).
- <sup>91</sup>W. Chen and H. B. Schlegel, "Evaluation of  $S^2$  for correlated wave functions and spin projection of unrestricted Møller–Plesset perturbation theory," *J. Chem. Phys.* **101**, 5957–5968 (1994).
- <sup>92</sup>A. I. Krylov, "Spin-contamination of coupled-cluster wave functions," *J. Chem. Phys.* **113**, 6052–6062 (2000).
- <sup>93</sup>V. Staemmler and R. Jaquet, "CEPA calculations on open-shell molecules. I. Outline of the method," *Theor. Chim. Acta* **59**, 487–500 (1981).
- <sup>94</sup>U. Meier and V. Staemmler, "An efficient first-order CASSCF method based on the renormalized Fock-operator technique," *Theor. Chim. Acta* **76**, 95–111 (1989).
- <sup>95</sup>J. Wasilewski, "Graphical techniques in the configuration interaction approach based on pure Slater determinants," *Int. J. Quantum Chem.* **36**, 503–524 (1989).
- <sup>96</sup>R. Fink, "Entwicklung eines Mehrkonfigurations-CEPA-Programms unter Benutzung von PNO's und Anwendung auf organisch chemische Fragestellungen," Ph.D. dissertation (Ruhr-Universität Bochum, Bochum, Germany, 1991).
- <sup>97</sup>F. Neese, "The ORCA program system," *Wiley Interdiscip. Rev.: Comput. Mol. Sci.* **2**, 73–78 (2012).
- <sup>98</sup>F. Neese, "Software update: The ORCA program system, version 4.0," *Wiley Interdiscip. Rev.: Comput. Mol. Sci.* **8**, e1327 (2018).
- <sup>99</sup>TURBOMOLE V6.5 2013, a development of University of Karlsruhe and Forschungszentrum Karlsruhe GmbH, 1989–2007, TURBOMOLE GmbH, since 2007; available from <http://www.turbomole.com>, 2013.
- <sup>100</sup>A. Karton, S. Daon, and J. M. L. Martin, "W4-11: A high-confidence benchmark dataset for computational thermochemistry derived from first-principles W4 data," *Chem. Phys. Lett.* **510**, 165–178 (2011).
- <sup>101</sup>A. Karton, E. Rabinovich, J. M. L. Martin, and B. Ruscic, "W4 theory for computational thermochemistry: In pursuit of confident sub-kJ/mol predictions," *J. Chem. Phys.* **125**, 144108 (2006).
- <sup>102</sup>D. Feller, "Application of systematic sequences of wave functions to the water dimer," *J. Chem. Phys.* **96**, 6104–6114 (1992).
- <sup>103</sup>D. Feller, "The use of systematic sequences of wave functions for estimating the complete basis set, full configuration interaction limit in water," *J. Chem. Phys.* **98**, 7059–7071 (1993).
- <sup>104</sup>A. Halkier, T. Helgaker, P. Jørgensen, W. Klopper, and J. Olsen, "Basis-set convergence of the energy in molecular Hartree–Fock calculations," *Chem. Phys. Lett.* **302**, 437–446 (1999).
- <sup>105</sup>A. Halkier, T. Helgaker, P. Jørgensen, W. Klopper, H. Koch, J. Olsen, and A. K. Wilson, "Basis-set convergence in correlated calculations on Ne, N<sub>2</sub>, and H<sub>2</sub>O," *Chem. Phys. Lett.* **286**, 243–252 (1998).
- <sup>106</sup>The exponent  $\alpha = 1.60$  instead of  $\alpha = 1.63$  as recommended by Halkier *et al.*<sup>104</sup> was originally chosen by mistake. A later reevaluation of several data points revealed that this leads to negligible differences of less than 0.01 kcal mol<sup>-1</sup> in the statistical measures.
- <sup>107</sup>L. Goerigk and S. Grimme, "A general database for main group thermochemistry, kinetics, and noncovalent interactions - assessment of common and reparameterized (meta-)GGA density functionals," *J. Chem. Theory Comput.* **6**, 107–126 (2010).
- <sup>108</sup>L. Goerigk, A. Hansen, C. Bauer, S. Ehrlich, A. Najibi, and S. Grimme, "A look at the density functional theory zoo with the advanced GMTKN55 database for general main group thermochemistry, kinetics and noncovalent interactions," *Phys. Chem. Chem. Phys.* **19**, 32184–32215 (2017).
- <sup>109</sup>The Grimme Group at Bonn University, "DFT data for RSE43 from the GMTKN55 Homepage" (2017), <http://www.thch.uni-bonn.de/tc.old/downloads/GMTKN/GMTKN55/RSE43.html>.
- <sup>110</sup>Y. Zhao, B. J. Lynch, and D. G. Truhlar, "Multi-coefficient extrapolated density functional theory for thermochemistry and thermochemical kinetics," *Phys. Chem. Chem. Phys.* **7**, 43–52 (2005).
- <sup>111</sup>Y. Zhao, N. González-García, and D. G. Truhlar, "Benchmark database of barrier heights for heavy atom transfer, nucleophilic substitution, association, and unimolecular reactions and its use to test theoretical methods," *J. Phys. Chem. A* **109**, 2012–2018 (2005).
- <sup>112</sup>A. Karton and J. M. L. Martin, "Explicitly correlated  $W_n$  theory: W1-F12 and W2-F12," *J. Chem. Phys.* **136**, 124114 (2012).
- <sup>113</sup>The Grimme Group at Bonn University, "DFT data for BH76 from the GMTKN55 homepage" (2017), <http://www.thch.uni-bonn.de/tc.old/downloads/GMTKN/GMTKN55/RSE43.html>.
- <sup>114</sup>See e.g. <http://www.thch.uni-bonn.de/tc.old/downloads/GMTKN/GMTKN55/results/BH76/DSD-PBEB95/result.html> for Reactions 13–28.
- <sup>115</sup>S. Behnle, R. Richter, L. Voelkl, P. Idzko, U. Bozkaya, and R. F. Fink, "Benchmarking the REMP hybrid perturbation theory for molecular properties" (unpublished).
- <sup>116</sup>G. M. J. Barca, C. Bertoni, L. Carrington, D. Datta, N. De Silva, J. E. Deustua, D. G. Fedorov, J. R. Gour, A. O. Gunina, E. Guidez, T. Harville, S. Irle, J. Ivanic, K. Kowalski, S. S. Leang, H. Li, W. Li, J. J. Lutz, I. Magoulas, J. Mato, V. Mironov, H. Nakata, B. Q. Pham, P. Piecuch, D. Poole, S. R. Pruitt, A. P. Rendell, L. B. Roskop, K. Ruedenberg, T. Sattasathuchana, M. W. Schmidt, J. Shen, L. Slipchenko, M. Sosonkina, V. Sundriyal, A. Tiwari, J. L. Galvez Vallejo, B. Westheimer, M. Wloch, P. Xu, F. Zahariev, and M. S. Gordon, "Recent developments in the general atomic and molecular electronic structure system" *J. Chem. Phys.* **152**, 154102 (2020).
- <sup>117</sup>D. G. A. Smith, L. A. Burns, A. C. Simmonett, R. M. Parrish, M. C. Schieber, R. Galvelis, P. Kraus, H. Kruse, R. Di Remigio, A. Alenaizan, A. M. James,

S. Lehtola, J. P. Misiewicz, M. Scheurer, R. A. Shaw, J. B. Schriber, Y. Xie, Z. L. Glick, D. A. Sirianni, J. S. O'Brien, J. M. Waldrop, A. Kumar, E. G. Hohenstein, B. P. Pritchard, B. R. Brooks, H. F. Schaefer, A. Y. Sokolov, K. Patkowski, A. E. DePrince, U. Bozkaya, R. A. King, F. A. Evangelista, J. M. Turney, T. D. Crawford, and C. D. Sherrill, "PSI4 1.4: Open-source software for high-throughput quantum chemistry" *J. Chem. Phys.* **152**, 184108 (2020).

<sup>118</sup>P. Pulay, "Convergence acceleration of iterative sequences. the case of scf iteration," *Chem. Phys. Lett.* **73**, 393–398 (1980).

<sup>119</sup>P. Pulay, "Improved SCF convergence acceleration," *J. Comput. Chem.* **3**, 556–560 (1982).

<sup>120</sup>C. Hampel, K. A Peterson, and H.-J. Werner, "A comparison of the efficiency and accuracy of the quadratic configuration interaction (QCISD), coupled cluster (CCSD), and Brueckner coupled cluster (BCCD) methods," *Chem. Phys. Lett.* **190**, 1–12 (1992).

<sup>121</sup>F. Neese, "Software update: The ORCA program system—Version 5.0," *WIREs* (published online, 2022).

# Accurate property prediction by second order perturbation theory: The REMP and OO-REMP hybrids

Cite as: J. Chem. Phys. **157**, 104111 (2022); <https://doi.org/10.1063/5.0105628>

Submitted: 24 June 2022 • Accepted: 05 August 2022 • Accepted Manuscript Online: 05 August 2022 • Published Online: 08 September 2022

 Stefan Behnle, Robert Richter, Luca Völkl, et al.



View Online



Export Citation



CrossMark

## ARTICLES YOU MAY BE INTERESTED IN

### Density-functional theory vs density-functional fits

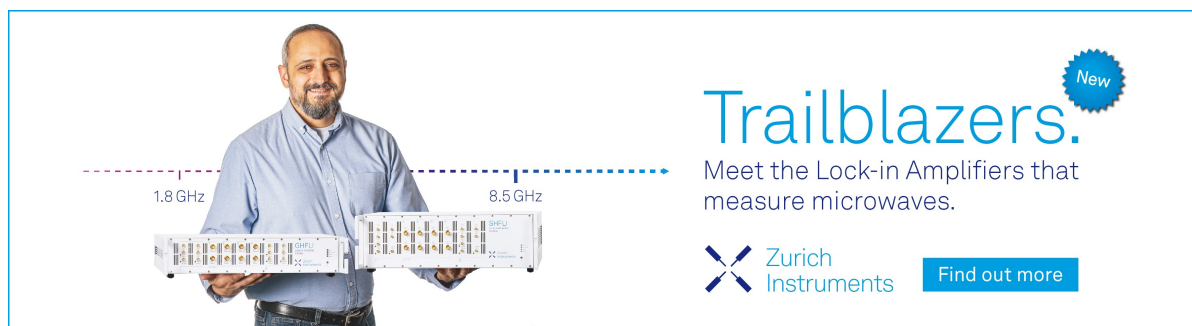
The Journal of Chemical Physics **156**, 214101 (2022); <https://doi.org/10.1063/5.0091198>


### Potential curves of the lower nine states of Li<sub>2</sub> molecule: Accurate calculations with the free complement theory and the comparisons with the SAC/SAC-CI results

The Journal of Chemical Physics **157**, 094109 (2022); <https://doi.org/10.1063/5.0101315>


### Extension of natural reaction orbital approach to multiconfigurational wavefunctions

The Journal of Chemical Physics **157**, 084118 (2022); <https://doi.org/10.1063/5.0098230>

**Trailblazers.** 

Meet the Lock-in Amplifiers that measure microwaves.

 Zurich Instruments [Find out more](#)

# Accurate property prediction by second order perturbation theory: The REMP and OO-REMP hybrids

Cite as: J. Chem. Phys. 157, 104111 (2022); doi: 10.1063/5.0105628

Submitted: 24 June 2022 • Accepted: 5 August 2022 •

Published Online: 8 September 2022






View Online



Export Citation



CrossMark

Stefan Behnle,<sup>1,a)</sup>  Robert Richter,<sup>1</sup> Luca Völkl,<sup>1</sup> Paul Idzko,<sup>1</sup> André Förstner,<sup>1</sup> Uğur Bozkaya,<sup>2,b)</sup>   
and Reinhold F. Fink<sup>1,c)</sup> 

## AFFILIATIONS

<sup>1</sup>Eberhard Karls University Tübingen, Institute for Physical and Theoretical Chemistry, Auf der Morgenstelle 18, 72076 Tübingen, Germany

<sup>2</sup>Department of Chemistry, Hacettepe University, Ankara 06800, Turkey

<sup>a)</sup>Electronic mail: stefan.behnle@uni-tuebingen.de

<sup>b)</sup>Electronic mail: ugur.bozkaya@hacettepe.edu.tr

<sup>c)</sup>Author to whom correspondence should be addressed: reinhold.fink@uni-tuebingen.de

## ABSTRACT

The prediction of molecular properties such as equilibrium structures or vibrational wavenumbers is a routine task in computational chemistry. If very high accuracy is required, however, the use of computationally demanding *ab initio* wavefunction methods is mandatory. We present property calculations utilizing Retaining the Excitation Degree – Møller–Plesset (REMP) and Orbital Optimized REMP (OO-REMP) hybrid perturbation theories, showing that with the latter approach, very accurate results are obtained at second order in perturbation theory. Specifically, equilibrium structures and harmonic vibrational wavenumbers and dipole moments of closed and open shell molecules were calculated and compared to the best available experimental results or very accurate calculations. OO-REMP is capable of predicting bond lengths of small closed and open shell molecules with an accuracy of 0.2 and 0.5 pm, respectively, often within the range of experimental uncertainty. Equilibrium harmonic vibrational wavenumbers are predicted with an accuracy better than 20 cm<sup>-1</sup>. Dipole moments of small closed and open shell molecules are reproduced with a relative error of less than 3%. Across all investigated properties, it turns out that a 20%:80% Møller–Plesset:Retaining the Excitation Degree mixing ratio consistently provides the best results. This is in line with our previous findings, featuring closed and open shell reaction energies.

Published under an exclusive license by AIP Publishing. <https://doi.org/10.1063/5.0105628>

## I. INTRODUCTION

Making accurate predictions for properties of unknown compounds is one of the main tasks of modern quantum chemical work. This requires methods with general applicability and high accuracy for a variety of properties.

While density functional theory in its various flavors is currently the method of choice for routine calculations, the situation was totally different only 30 years ago. Prior to the advent of hybrid functionals, most routine calculations were performed with wavefunction-based methods, especially configuration interaction (CI) and Møller–Plesset<sup>1–3</sup> (MP) perturbation theory. Due to its simplicity and favorable computational scaling, the second order MP (MP2) was for a long time the method of choice and often the

only affordable one with a predicational capacity better than the Hartree–Fock method. The Møller–Plesset partitioning utilizes the Hartree–Fock determinant as the unperturbed wavefunction and the diagonal blocks of the corresponding Fockian as the unperturbed Hamiltonian  $\hat{H}^{(0)}$ . Several attempts were made to improve the performance of the method while preserving the general structure of the working equations. The most notable modifications are (i) spin-component scaled (SCS)-MP2,<sup>4,5</sup> SCS-MP3,<sup>6</sup> or regularized MP variants,<sup>7,8</sup> which use empirically modified correlation energy expressions; (ii) fractional order perturbed energies as in MP2.5,<sup>9</sup> MP2.X,<sup>10</sup> or MP3.5;<sup>11</sup> (iii) orbital-optimized methods, which employ an iteratively optimized reference wavefunction, such as OO-MP2,<sup>12,13</sup> OB-MP2,<sup>14</sup> or OO-MP3.<sup>15</sup> Simultaneously applying several improvements as in OO-SOS-MP2,<sup>16,17</sup> OMP2.5,<sup>18–20</sup>



or the orbital-optimized and regularized MP-PT approaches  $\kappa$ - or  $\sigma$ -OOMP2<sup>8</sup> and MP2.8: $\kappa$ -OOMP2<sup>7</sup> turned out to be especially successful. Nevertheless, many of these methods suffer from the drawback that they are just recipes for obtaining energies so that there is no associated wavefunction or that there is a wavefunction, but the derivation of working equations for analytical derivatives becomes a major endeavor.

A completely different approach consists in abandoning the Møller–Plesset partitioning completely. Early approaches such as the Epstein–Nesbet (EN)<sup>21–24</sup> partitioning, however, turned out to be unsuccessful. The “Retaining the Excitation Degree” (RE)<sup>25,26</sup> method is an alternative partitioning of the Hamiltonian proposed by one of the present authors (R.F.F.). The zeroth order Hamiltonian contains all contributions of the second quantized Hamiltonian that do not change the number of electrons in occupied or virtual orbitals. It is related to Dyal’s active space Hamiltonian<sup>27</sup> and probably the most systematic definition of CEPA(0)/D [coupled electron pair approximation variant zero with doubles only] as it does not rely on arbitrary truncations of excitation operators or similar.

Based on a systematic investigation of the errors of the respective first order wavefunctions,<sup>28</sup> the present authors recently proposed the REMP hybrid perturbation theory scheme. REMP is defined by setting  $\hat{H}^{(0)}$  to a weighted mixture of the unperturbed Hamiltonians of MP and RE.<sup>29</sup> The hybridization of the two methods already at the wavefunction level allows us to alleviate systematic errors and provides better wavefunctions than each of the parent methods alone. Combining iterative orbital optimization and REMP mixing leads to a method termed OO-REMP, which was shown to systematically improve over the parent methods OCEPA and OO-MP2 as well as the corresponding canonical REMP variants using canonical Hartree–Fock reference wavefunctions, especially in open-shell cases.<sup>30,31</sup>

For the calculation of geometrical gradients, the availability of analytical gradients is always advantageous. Especially for larger molecules, the calculation of numerical gradients quickly becomes very tedious, requiring up to  $6N$  energy single point calculations on distorted geometries when two-sided numerical differentiation is used. Additionally, numerical gradients are noisy and depend on the chosen distortion. Analytical gradients, on the other hand, are often computationally efficient and free from artifacts of numerical differentiation. Analytical derivatives for MP2 were initially derived and implemented by Pople *et al.*<sup>32</sup> The working equations were later improved by various authors in several aspects.<sup>33–36</sup> Analytical gradients for CEPA(0)/D and OCEPA(0) were derived by Bozkaya and Sherrill.<sup>37</sup>

In contrast to thermochemical properties, there are still rather limited systematic data on the performance of commonly used methods for the prediction of equilibrium structures. There is also no equivalent to the GMTKN database<sup>38</sup> for molecular structures. Whenever there are performance benchmarks, the reference data seem to be arbitrarily selected, making the comparison of different methods cumbersome or impossible. Only recently, Brémond *et al.*<sup>39</sup> have published an assessment of a large number of density functionals for the prediction of equilibrium structures. They defined two benchmark sets consisting of small- and medium-sized organic molecules based on the work of Barone and co-workers.<sup>40,41</sup> It was found that the xDH-PBE0 functional exhibits the smallest mean absolute deviation (about 0.2 pm), closely followed by the

B2-PLYP family of functionals with mean absolute errors of around 0.3 pm. Interestingly, one of the results also was that full MP2 is more accurate than SCS-MP2 and SOS-MP2, indicating that the performance gain for thermochemical applications of spin component scaled methods seems to be traded off by performance losses for molecular structures, at least with the basis set used.

In the present work, we shall describe implementations of analytical first derivatives of the OO-REMP hybrid perturbation theory. Furthermore, we will assess the performance of REMP and OO-REMP for the prediction of equilibrium structures, harmonic vibrational frequencies, and static dipole moments. It will be shown that the performance of OO-REMP almost reaches that of the best widely applicable single reference method [coupled cluster with singles, doubles, and perturbative triples, CCSD(T)] while exhibiting a more favorable computational scaling.

## II. THEORY

### A. REMP perturbation theory

The general theory of REMP<sup>29</sup> and OO-REMP<sup>30</sup> has already been published, which is why we here only present those equations that are necessary for obtaining properties from REMP/OO-REMP wavefunctions.

Throughout this work, the commonly used indexing scheme for spin orbitals is used, i.e.,  $i, j, k, l$  are used for occupied,  $a, b, c, d$  are used for virtual, and  $p, q, r, s$  are used for arbitrary spin orbitals.  $\hat{a}_i$  denotes an annihilation operator from spin orbital  $i$ , while  $\hat{a}_i^\dagger$  denotes its adjoint creation operator.

In a nutshell, the unperturbed Hamiltonian of REMP ( $\hat{H}_{\text{REMP}}^{(0)}$ ) is a constrained linear combination of the unperturbed Hamiltonians of the Møller–Plesset perturbation theory and of the retaining the excitation degree perturbation theory,

$$\hat{H}_{\text{REMP}}^{(0)} = (1 - A) \cdot \hat{H}_{\text{RE}}^{(0)} + A \cdot \hat{H}_{\text{MP}}^{(0)}. \quad (1)$$

The mixing parameter  $A$  is the central parameter of the REMP approach; it specifies the Møller–Plesset fraction of  $\hat{H}^{(0)}$  and is the only empirical parameter involved. While  $\hat{H}_{\text{MP}}^{(0)}$  uses the Fockian as the unperturbed Hamiltonian,  $\hat{H}_{\text{RE}}^{(0)}$  keeps all contributions of the second quantized Hamiltonian, which preserve the excitation rank, i.e., it also contains terms that enter the fluctuating potential in MP-PT.  $A$  damps the contribution of the fluctuating potential to  $\hat{H}^{(0)}$ , which corresponds to a manipulation of perturbation-theoretical energy denominators associated with perturber functions.<sup>28,29</sup> In previous work, we provided numerical and analytical evidence that a choice of  $A$  between 0.1 and about 0.3 generally provides the best possible first order wavefunctions for the REMP partitioning. Roughly speaking, the large amount of  $\hat{H}_{\text{RE}}^{(0)}$  improves the interactions within double excitations, while the MP contribution of  $\hat{H}^{(0)}$  corrects for their interaction with singly, triply, and higher excited configurations. Further details can be found in Refs. 28–31.

The OO-REMP energy, first-order wavefunction, and relaxed one and two particle density matrices are obtained by minimizing the OO-REMP energy functional,

$$\begin{aligned} \tilde{E}_{\text{REMP}}^{(2)} = & \langle \phi_0 | \hat{H} | \phi_0 \rangle + \langle \phi_0 | \left\{ \widehat{W}_N \widehat{T}_2^{(1)} \right\}_c | \phi_0 \rangle \\ & + \langle \phi_0 | \left[ \widehat{\Lambda}_2^{(1)} \left\{ \widehat{W}_N + \widehat{f}_N \widehat{T}_2^{(1)} \right\} + (1-A) \widehat{W}_N \widehat{T}_2^{(1)} \right]_c | \phi_0 \rangle, \end{aligned} \quad (2)$$

where  $\widehat{T}_2^{(1)}$  are the first-order double excitations,  $\widehat{\Lambda}_2^{(1)}$  represents the adjoint deexcitations (Lagrangian multipliers), and  $\widehat{f}_N$  and  $\widehat{W}_N$  are the one- and two-electron contributions of the normal-ordered Hamiltonian (normal order with respect to the Fermi vacuum).  $\phi_0$  is the single determinantal reference wavefunction whose orbitals are iteratively optimized, and  $c$  indicates that only fully connected terms are considered. After convergence of the optimization procedure, one directly obtains relaxed reduced one- and two-particle density matrices  $\gamma_{pq}$  and  $\Gamma_{pqrs}$  without the need to solve an additional set of Z vector equations. These densities can directly be used for property evaluations.

The evaluation of one-electron properties, such as the permanent dipole moment, is straightforward. The one-particle density matrices  $\gamma_{pq}$  are transformed to the AO basis,

$$\gamma_{\lambda\sigma}^\alpha = \sum_{p,q} C_{\lambda p}^\alpha \gamma_{pq} C_{\sigma q}^\alpha = \mathbf{C}^\alpha \boldsymbol{\gamma} \mathbf{C}^{\alpha\dagger}. \quad (3)$$

Analogously for  $\gamma_{\lambda\sigma}^\beta$ , the alpha and beta densities are added up,

$$\gamma_{\lambda\sigma} = \gamma_{\lambda\sigma}^\alpha + \gamma_{\lambda\sigma}^\beta, \quad (4)$$

and the total density is contracted with the matrix elements of the requested operator to obtain the expectation value. For example, we obtain

$$\mu_{x,\text{el}} = -\text{Tr}(\boldsymbol{\gamma} \cdot \langle \mathbf{x} \rangle) = -\sum_{\lambda,\sigma} \gamma_{\lambda\sigma} \langle x \rangle_{\lambda\sigma}, \quad (5)$$

with  $\mu_{x,\text{el}}$  being the  $x$ , component of the electronic contribution to the dipole moment, while  $\langle x \rangle_{\lambda\sigma}$  is the matrixelement of the  $x$  operator in the AO basis functions  $\lambda$  and  $\sigma$ .

In combination with the nuclear contribution to the dipole moment ( $\vec{\mu}_{\text{nuc}} = \sum_I Z_I \vec{r}_I$ ), the total dipole moment is obtained. Care has to be taken if dipole moments of charged species (“electric monopoles”) are to be calculated. Whenever any of the multipole components below the one calculated is nonzero, it will become gauge dependent, i.e., it will depend on the choice of the origin. This is not an issue in this publication as only dipole moments of neutral species are investigated.

Calculating nuclear gradients is more involved, but the theory has been worked out by Bozkaya and Sherrill for OCEPA earlier.<sup>37</sup> The general expression for the nuclear gradient is given by

$$\frac{dE}{d\mathbf{x}} = \sum_{pq} \gamma_{pq} h_{pq}^x + \sum_{pqrs} \Gamma_{pqrs} g_{pqrs}^x - \sum_{pq} F_{pq} S_{pq}^x, \quad (6)$$

where  $h_{pq}^x$  is the derivative of a one-electron integral for coordinate  $x$ ,  $g_{pqrs}^x$  is the derivative of an antisymmetrized two-electron integral, and  $S_{pq}^x$  is the derivative of an overlap matrix element.  $F_{pq}$  is the generalized Fock matrix constructed during the orbital optimization, whose antisymmetry determines the MO gradient. Equation (6) is usually evaluated in the AO basis. As the REMP scaling is already included

in the densities, Eq. (6) can be used without further modifications for OO-REMP. Analytical OO-REMP gradients were implemented as a fork in the OCEPA code of PSI4. It makes use of the very same gradient machinery as OCEPA by just passing OO-REMP densities to the gradient engine instead. The correctness of the implementation was verified by comparing analytical OO-REMP gradients to the numerical ones. For canonical REMP, no analytical gradients were implemented. All REMP gradients were calculated numerically (see details below).

Regarding the computational scaling, the most expensive part of the REMP amplitude equations is the external exchange operator, which scales as  $\sigma^2 v^4$ , where  $\sigma$  and  $v$  are the number of correlated occupied and virtual orbitals, respectively. The one-particle density matrix scales as  $n^5$  and is, thus, negligibly expensive. The two-particle density matrices  $\Gamma_{ijkl}$ ,  $\Gamma_{iajb}$ , and  $\Gamma_{abcd}$  scale as  $\sigma^4 v^2$ ,  $\sigma^3 v^3$ , and  $\sigma^2 v^4$ , respectively, but the formation of the latter one can be avoided during orbital iterations<sup>37</sup> and is only needed for the structural gradient. The calculation of the gradient integrals and their contraction with densities scales with  $N_{\text{atom}} n^4$  and is, thus, inexpensive, and the same holds for the transformation of densities to the AO basis, which scales as  $n^5$ . The total computational cost of OREMP and its gradient, thus, scales with  $n^6$  ( $\sigma^2 v^4$ ) and is identical to that of OCEPA.<sup>37</sup>

### III. RESULTS

This paper is organized as follows: Sec. III B presents a detailed assessment of the predictational power for equilibrium structures of small main group single reference molecules. Section III C shows results for harmonic vibrations for a subset of the previously investigated molecules. Section III D finally provides results for static electric dipole moments of main-group molecules. Short summaries will be given at the end of each subsection, highlighting the most important results and take-home messages. As we shall show, REMP and OO-REMP with  $A = 0.20$  consistently provide very good results. Thus, these results will be singled out and compared with the performance of other quantum chemical methods.

#### A. Computational details

REMP, RO-REMP, UREMP, and OO-REMP have been implemented as an extension of the MC-CEPA program<sup>42,43</sup> and also as a modification of the PSI4 program package.<sup>44</sup> The implementation is inspired by the matrix-driven CI program of ORCA (mDCI) and the orbital optimized coupled cluster code (OCC) of PSI4. The REMP/OO-REMP energies considered here always correspond to second-order perturbation theory, while analytical properties are calculated from the first-order wavefunction. REMP and OO-REMP dipole moment calculations have been performed using a development version of the Bochum-Basel *ab initio* suite of programs (wawels).<sup>29,30,42,43,45–47</sup> REMP dipole moments were obtained by numerical differentiation of energies calculated with finite external electrical fields, while OO-REMP dipole moments were calculated fully analytically from relaxed density matrices. REMP and OO-REMP analytical and numerical gradients and vibrational wavenumbers were calculated using a local fork of the PSI4 quantum chemistry program package. The modified PSI4 version was made publicly available on GitHub<sup>48</sup> as the source code, and

the proposed changes were filed as a pull request to the official repository. CCSD(T) numerical gradients were calculated using ORCA<sup>49,50</sup> 5.0.2.

Basis sets have been used as stored in the TurboMole 6.5<sup>51</sup> basis set library (wavels) or as deposited in ORCA or PSI4.

The following abbreviations are used for statistical error descriptors: MSD denotes the Mean Signed Deviation, i.e., the arithmetic mean of all deviations; MAD denotes the Mean Absolute Deviation, i.e., the average of all absolute deviations;  $\Delta_{\min-\max}$  denotes the error spread, i.e., the largest positive minus the largest negative error occurring;  $\sigma$  denotes the sample standard deviation; and RMSD denotes the Root Mean Square Deviation, i.e., the square root of the squared and averaged deviations.

## B. Equilibrium structures of small molecules

To assess the performance for the prediction of equilibrium structures, a benchmark set consisting of small closed and open shell molecules was assembled. As REMP and especially OO-REMP are highly accurate methods, we tried to gather the most recent and accurate results for each molecule. When comparing experimental structures to the calculated ones, great caution has to be taken to avoid systematical errors. Experimental methods such as x-ray or electron diffraction provide  $r_0$  values, i.e., the bond lengths corresponding to the average bond length of the zeroth vibrational level. Quantum chemical methods, on the other hand, provide  $r_e$ , corresponding to the minimum of the potential energy surface. For low-level methods, it might be acceptable to mix these up but not for methods, which systematically provides sub-pm accuracy. There exist a number of protocols for determining  $r_e$  values from experimentally determined quantities. A very advanced procedure was described by Pawłowski *et al.*,<sup>52</sup> who combined experimental rotational constants  $B_0$  of different isotopologues and calculated rotation–vibration interaction constants  $\alpha_r^B$  in a fitting procedure to finally arrive at equilibrium bond lengths with statistical errors less than 0.1 pm and bond angles with errors less than 0.5°.

For reaching the basis set limit, normally complete basis set (CBS) extrapolation is the method of choice. It is usually straightforward to combine CBS extrapolation and numerical gradient calculations. CBS extrapolation of analytical gradients,<sup>53</sup> on the other hand, is still not well-established and not prominently available in major quantum chemistry packages. As analytical gradients are very often computationally much more efficient than the numerical ones, we assessed the performance of several basis set/method combinations (“model chemistries”) instead of trying to reach the basis set limit.

Table I collects experimental equilibrium bond lengths  $r_e$  with high accuracy. The set consists of 61 bond lengths and covers single, double, and triple bonds of neutral and ionic molecules. All members of this benchmark set were chosen by the requirement that the experimental uncertainty is significantly smaller than 0.1 pm and that the extrapolation to the minimum of the PES was done at a high level of sophistication. This ensures that the comparison of experimental and computed values is meaningful and that we are not just comparing one type of noise to the other. Given that the smallest occurring MAD [CCSD(T)/aug-cc-pwCVQZ] is actually smaller than 0.1 pm, our uncertainty choice is not an overly strict

criterion. A similar collection was compiled by Coriani *et al.*<sup>61</sup> but without a strict requirement for the uncertainty of the experimental data.

For the set of molecules in Table I, structural optimizations were performed with REMP, OO-REMP, and CCSD(T) for nine different basis sets. All electrons were always correlated, and no occupied or virtual orbitals were kept frozen. Convergence criteria were selected rather conservatively (REMP/OO-REMP: single point energy convergence:  $1.0 \cdot 10^{-9} E_h$ , residuum convergence:  $1.0 \cdot 10^{-8}$ , max. orbital gradient:  $1.0 \cdot 10^{-7}$ , rms orbital gradient:  $1.0 \cdot 10^{-8}$ , energy convergence for structural optimization:  $1.0 \cdot 10^{-7} E_h$ , largest displacement:  $1.0 \cdot 10^{-6} a_0$ , rms displacement:  $1.0 \cdot 10^{-7} a_0$ , largest gradient:  $1.0 \cdot 10^{-7} E_h/a_0$ , and rms gradient:  $1.0 \cdot 10^{-8} E_h/a_0$ ). CCSD(T) calculations employed the ORCA keywords `verytightscf` `verytightopt` corresponding to an energy convergence criterion of  $1.0 \cdot 10^{-9} E_h$  for the SCF and a residuum convergence criterion of  $1.0 \cdot 10^{-6}$  for CCSD(T) calculations. Convergence criteria for the geometry optimization were  $2.0 \cdot 10^{-7} E_h$  for the energy,  $3.0 \cdot 10^{-5} E_h/a_0$  for the largest gradient,  $8.0 \cdot 10^{-6} E_h/a_0$  for the rms gradient,  $2.0 \cdot 10^{-4} a_0$  for the largest displacement, and  $1.0 \cdot 10^{-4} a_0$  for the rms displacement. This ensures that all structures were converged to 0.01 pm, which is one order of magnitude smaller than the required precision of the experimental data. For singlet states, an RHF reference was chosen and the spin symmetry was also conserved during the orbital optimization procedure. Broken symmetry UHF singlets (given that the reference is unstable) were not considered as they usually lead to convergence problems. Moreover, they result in ill-defined multiplicities and lowered symmetries, thus spoiling comparability to the experiment. Doublet and triplet states used UHF references with one/two excess alpha spin electrons.

Figure 1 shows several error measures for bond lengths as a function of the mixing parameter  $A$ ; a relevant subset is collected in Table II. Complete tables for all other basis sets may also be found in the supplementary material. Not shown in Fig. 1 are results for double- $\zeta$  basis sets. The mean absolute deviations calculated with DZ basis sets were always larger than 1 pm regardless of  $A$  and the specific basis set, thus rendering such a level of theory useless for all but preoptimizations or very crude surveys.

Examining the mean signed deviation first, one common feature of REMP and OO-REMP is that starting from  $A = 0.0$  bonds are first getting shorter with the increasing MP fraction, reaching a minimum between  $0.2 \leq A \leq 0.4$ , and then start to increase again [Figs. 1(a) and 1(b)]. Bonds also systematically shorten by  $\approx 0.2$ – $0.3$  pm when going from a TZ to a QZ basis set. Inclusion of core polarization functions alone only has a small effect, while the addition of diffuse basis functions leads to a systematic bond length increase of 0.1–0.2 pm. Bond lengths predicted by canonical REMP tend to be systematically too short, while those predicted by OO-REMP tend to be on spot or slightly too short at the basis size limit. All in all, this confirms the trends already found by Helgaker *et al.*<sup>69</sup> 25 years ago. Said authors also found that an improved description of correlation [HF  $\rightarrow$  MP2  $\rightarrow$  CCSD(T)] leads on average to elongation of bonds, and this is also found when going from canonical REMP to orbital-optimized REMP.

Considering the MAD next, one finds no sizable improvement by hybridization in the case of canonical REMP [Fig. 1(c)]. Pure RE [i.e., CEPA(0)/D] performs best with most basis sets. The best

**TABLE I.** High-confidence experimental equilibrium bond lengths  $r_e$ . Uncertainties are as given in the literature and refer to one standard deviation.

Molecule	Electronic state	Bond	Value (pm)	Uncertainty (pm)	Source	Comment
BF	$^1\Sigma^+$	r(B-F)	126.686 5	0.000 2	54	$^{10}\text{B}^{19}\text{F}$
BO	$^2\Sigma^+$	r(B-O)	120.475	0.002	55	
$\text{C}_2^-$	$^2\Sigma^+$	r(C-C)	126.829	0.023	55	
$\text{C}_2\text{H}_2$ (ethyne)	$^1\Sigma_g^+$	r(C-H)	106.166	0.05	52	
		r(C-C)	120.356	0.057	52	
$\text{C}_2\text{H}_4$ (ethene)	$^1A_g$	r(C-H)	108.068	0.06	52	
		r(C-C)	133.074	0.08	52	
CF	$^2\Pi$	r(C-F)	127.217	0.043	55	
CH	$^2\Pi$	r(C-H)	111.791	0.002	55	
$^1\text{CH}_2$	$^1A_1$	r(C-H)	110.632	0.059	52	
$^3\text{CH}_2$	$^3B_1$	r(C-H)	107.530	0.011	56	
$\text{CH}_2\text{O}$ (formaldehyde)	$^1A_1$	r(C-H)	110.072	0.06	52	
		r(C-O)	120.465	0.07	52	
$\text{CH}_4$	$^1A_1$	r(C-H)	108.588	0.06	52	
CN	$^2\Sigma^+$	r(C-N)	117.180 74	0.000 04	57	
CNC	$^2\Pi$	r(C-N)	124.45	0.05	55	Linear structure
CO	$^1\Sigma^+$	r(C-O)	112.836	0.004	52	
$\text{CO}^+$	$^2\Sigma^+$	r(C-O)	111.522	0.002	55	
$\text{CO}_2$	$^1\Sigma_g^+$	r(C-O)	116.006	0.006	52	
CS	$^1\Sigma^+$	r(C-S)	153.481 75	0.000 27	58	
$\text{H}_2$	$^1\Sigma_g^+$	r(H-H)	74.149 1	0.013	52	
$\text{H}_2\text{O}$	$^1A_1$	r(O-H)	95.790 2	0.028	52	
$\text{H}_2\text{O}^+$	$^2B_1$	r(O-H)	99.92	0.06	55	
$\text{H}_2\text{O}_2$	$^1A$	r(O-H)	96.17	0.02	59	
		r(O-O)	145.24	0.03	59	
HBS	$^1\Sigma^+$	r(H-B)	116.98	0.04	60	
		r(B-S)	159.78	0.01	60	
HCl	$^1\Sigma^+$	r(H-Cl)	127.455 2	0.0006	54	$\text{H}^{35}\text{Cl}$
HCN	$^1\Sigma^+$	r(C-H)	106.528	0.012	52	
		r(C-N)	115.336	0.014	52	
HCP	$^1\Sigma^+$	r(C-H)	107.02	0.1	61	
		r(C-P)	153.99	0.02	61	
HF	$^1\Sigma^+$	r(H-F)	91.687 9	0.012	52	
$\text{HF}^+$	$^2\Pi$	r(H-F)	100.105	0.014	57	
HNC	$^1\Sigma^+$	r(N-H)	99.489	0.008	52	
		r(C-N)	116.875	0.01	52	
HNO	$^1A'$	r(N-H)	105.199	0.06	52	
		r(N-O)	120.859	0.069	52	
HOF	$^1A'$	r(O-H)	96.861 9	0.008	52	
		r(O-F)	143.447	0.011	52	
LiF	$^1\Sigma^+$	r(Li-F)	156.386 424	0.000 006 2	62	
LiH	$^1\Sigma^+$	r(Li-H)	159.491 31	0.000 08	54	
$\text{N}_2$	$^1\Sigma_g^+$	r(N-N)	109.773	0.005	52	
$\text{N}_2^+$	$^2\Sigma_g^+$	r(N-N)	111.641	0.005	57	
$(E)\text{-N}_2\text{H}_2$	$^1A_g$	r(N-H)	102.883	0.06	52	$\text{C}_{2h}$
		r(N-N)	124.575	0.07	52	
NF	$^3\Sigma^-$	r(N-F)	131.697 9	0.008 8	63	

TABLE I. (Continued.)

Molecule	Electronic state	Bond	Value (pm)	Uncertainty (pm)	Source	Comment
NH	$^3\Sigma^-$	r(N-H)	103.606 721	0.000 013	64	$r_e^{\text{BO}}$
NH <sup>+</sup>	$^2\Pi$	r(N-H)	106.898	0.006	55	
NH <sub>3</sub>	$^1A_1$	r(N-H)	101.139	0.06	52	
NO	$^2\Pi$	r(N-O)	115.078 4	0.001 4	55	
NO <sub>2</sub>	$2A_1$	r(N-O)	119.389	0.004	65	
O <sub>2</sub>	$^3\Sigma_g^-$	r(O-O)	120.752		66	
O <sub>2</sub> <sup>+</sup>	$^2\Pi_g$	r(O-O)	111.687	0.006	55	
OCS	$^1\Sigma^+$	r(C-O)	115.617	0.014	67	
		r(C-S)	156.140	0.014	67	
OF	$^2\Pi$	r(O-F)	135.410 78	0.000 001	55	
OH	$^2\Pi$	r(O-H)	96.966	0.009	55	
PH <sub>3</sub>	$^1A_1$	r(P-H)	141.16	0.06	68	
PN	$^1\Sigma^+$	r(P-N)	149.086 6	0.000 05	54	
SiO	$^1\Sigma^+$	r(Si-O)	150.973 75	0.000 02	54	

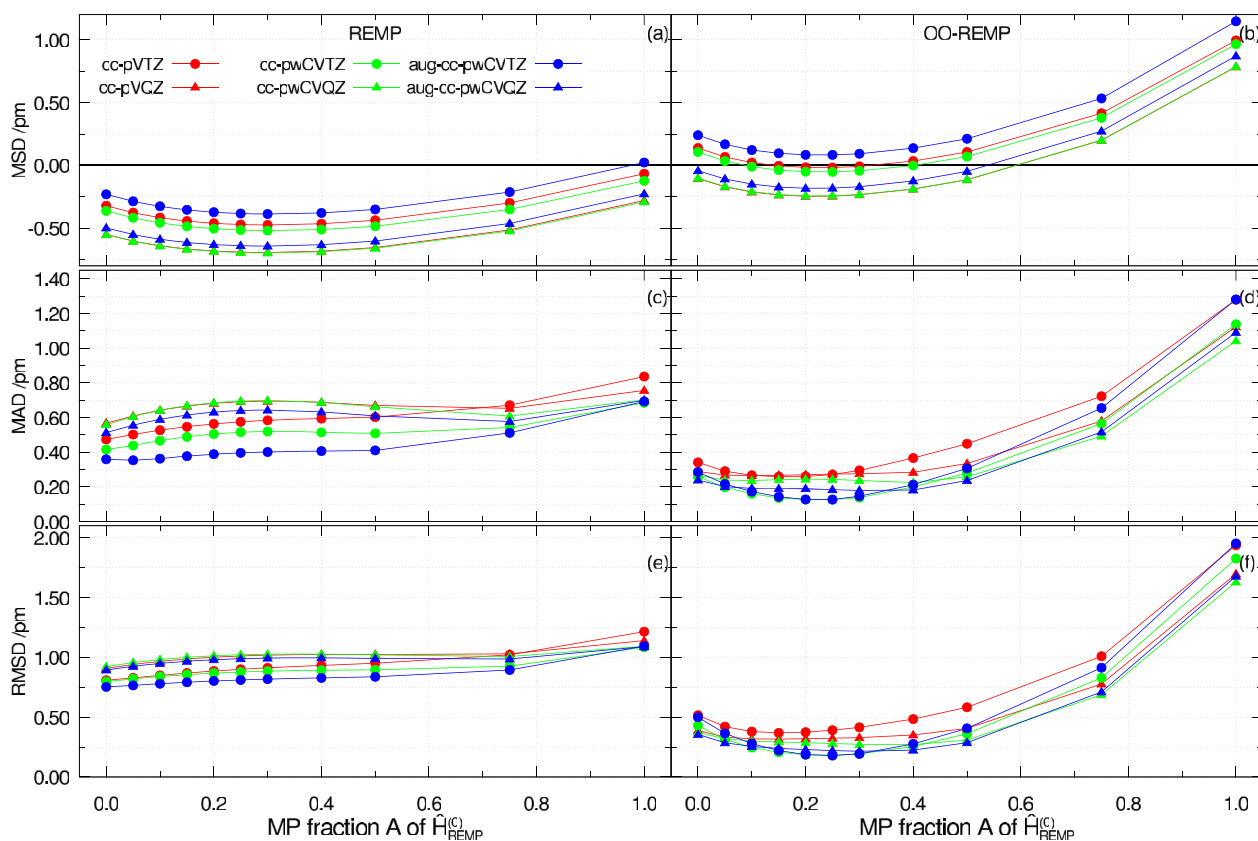


**FIG. 1.** Graphical representation of the bond length errors of REMP and OO-REMP for the high-confidence bond length set. Average over 61 equilibrium bond lengths. Reference: best available experimental/semi-experimental estimate. The dots indicate TZ basis sets; the triangles indicate QZ basis sets. The results for the cc-pVXZ family are shown in red, those for cc-pwCVXZ are shown in green, and those for aug-cc-pwCVXZ are shown in blue. (a), (c), and (e) REMP. (b), (d), and (f) OO-REMP.



**TABLE II.** Statistics for the high confidence bond length benchmark set, aug-cc-pwCVXZ basis set family. Average over the 61 bonds listed in Table I. All error measures are in pm. The complete tables can be found in the [supplementary material](#).

Method	A	MSD	MAD	$\sigma$	RMSD	Median	$ \Delta_{\max} $
aug-cc-pwCVTZ							
REMP	0.00	-0.230	0.359	0.722	0.753	-0.027	4.396
	0.15	-0.354	0.377	0.714	0.792	-0.170	4.543
	0.20	-0.373	0.388	0.717	0.803	-0.169	4.574
	0.25	-0.383	0.396	0.721	0.811	-0.190	4.602
	0.30	-0.387	0.401	0.726	0.818	-0.196	4.627
	1.00	0.023	0.692	1.102	1.094	-0.081	4.834
OO-REMP	0.00	0.240	0.285	0.441	0.499	0.151	2.504
	0.15	0.096	0.143	0.200	0.221	0.075	1.035
	0.20	0.084	0.127	0.169	0.187	0.068	0.799
	0.25	0.083	0.126	0.160	0.179	0.066	0.628
	0.30	0.093	0.146	0.172	0.194	0.068	0.513
	1.00	1.147	1.281	1.592	1.952	0.691	8.294
CCSD(T)		0.263	0.271	0.161	0.308	0.248	0.615
aug-cc-pwCVQZ							
REMP	0.00	-0.498	0.513	0.749	0.894	-0.315	4.646
	0.15	-0.614	0.614	0.754	0.967	-0.406	4.788
	0.20	-0.631	0.631	0.757	0.980	-0.410	4.818
	0.25	-0.640	0.640	0.760	0.989	-0.413	4.845
	0.30	-0.643	0.643	0.764	0.994	-0.439	4.868
	1.00	-0.227	0.699	1.074	1.089	-0.230	5.062
OO-REMP	0.00	-0.042	0.239	0.356	0.356	-0.060	1.721
	0.15	-0.173	0.189	0.167	0.239	-0.135	0.592
	0.20	-0.182	0.189	0.139	0.229	-0.146	0.616
	0.25	-0.181	0.183	0.127	0.221	-0.166	0.629
	0.30	-0.170	0.179	0.132	0.215	-0.164	0.632
	1.00	0.871	1.091	1.446	1.678	0.467	7.214
CCSD(T)		-0.016	0.081	0.121	0.121	0.025	0.441

results are obtained with the aug-cc-pwCVTZ basis, where all mixtures up to  $A = 0.5$  perform equally well with an MAD of 0.4 pm, but for  $A > 0.5$ , the performance significantly degrades. The finding that the aug-cc-pwCVTZ and over a wide range even the cc-pwCVTZ basis outperform the aug-cc-pwCVQZ basis suggests error cancellation of basis and method errors. In general, one finds that TZ basis sets deliver seemingly better results than the QZ basis sets. This is in line with the finding of Coriani *et al.*<sup>61</sup> where it was shown that MP2 and CCSD benefit from basis and method error cancellation if all electrons are correlated. With an MAD of  $\approx 0.5$  pm, REMP is about as accurate as CCSD for bond lengths.

In the case of OO-REMP, in contrast, one finds a significant improvement over the parent methods by hybridization [Fig. 1(d)]. Again, DZ basis sets deliver significantly larger errors than other basis sets and are not considered further. The best results are obtained with OO-REMP(0.25)/cc-pwCVTZ and OO-REMP(0.25)/aug-cc-pwCVTZ, which have MADs of merely

0.13 pm. This can be compared to OO-REMP(0.00)/aug-cc-pwCVTZ, i.e., OCEPA with an MAD of 0.29 pm and OO-REMP(1.00)/aug-cc-pwCVTZ, i.e., OO-MP2 with an MAD of 1.28 pm. Compared to the pure methods, the hybrid method, thus, improves by a factor of two or ten, respectively. Interestingly, when the results obtained with the cc-pwCVTZ and the aug-cc-pwCVTZ basis—which essentially yield the same MAD—around the minimum of the MAD are examined closer, one finds that the augmented basis leads to an overestimation that equals the underestimation of the non-augmented basis. OO-REMP/aug-cc-pwCVQZ exhibits a rather flat curve with a minimum at  $A = 0.30$  (MAD = 0.18 pm). The differences between TZ and QZ bases are smaller than in the canonical REMP case. While REMP(0.00)/aug-cc-pwCVTZ clearly seems to be just a Pauling point, it is less clear after orbital optimization is included. With the aug-cc-pwCVTZ basis, one rather reaches a saturation with respect to the basis size than a minimum. The largest error of OO-REMP(0.25)/aug-cc-pwCVTZ is

encountered for the O–F bond of HOF, which is overestimated by 0.63 pm. The RMSD [Figs. 1(e) and 1(f)] leads essentially to the same conclusions regarding the optimal choice of  $A$  and regarding the behavior with respect to basis set modifications. The smallest overall RMSD is found in the case of OO-REMP(0.25)/aug-cc-pwCVTZ (0.179 pm), but OO-REMP(0.25)/cc-pwCVTZ (0.182 pm), OO-REMP(0.20)/aug-cc-pwCVTZ (0.187 pm), and OO-REMP(0.20)/cc-pwCVTZ (0.186 pm) are virtually indistinguishable. One might conclude that the overall best mixture is located somewhere between an MP fraction of 20% and 25%, which is perfectly in accordance with our previous results. The RMSD obtained with the aug-cc-pwCVQZ basis is again rather flat and has a minimum at  $A = 0.30$  (0.215 pm) with  $A = 0.25$  and  $A = 0.20$  performing not much worse. Figure S1 in the [supplementary material](#) contains box plots for all basis sets. These plots independently corroborate our conclusions from a robust statistical point of view.

It is, furthermore, interesting to note that the optimal  $A$  value in the case of OO-REMP is much less basis set dependent than it was in our previous investigation featuring atomization energies.<sup>30</sup> Figures 1(d) and 1(f) show that regardless of the basis set, an  $A$  value in the range of 0.15–0.25 leads to the best results. It is, thus, not necessary to fine-tune this parameter for every basis set. Moreover, even a comparatively cheap model chemistry such as cc-pVTZ/OO-REMP(0.20) is able to provide equilibrium structures with mean absolute errors of 0.26 pm.

The REMP and OO-REMP results can be compared to CCSD(T) results listed in Table II. Again, the errors obtained with DZ basis sets are unacceptably large, as expected. In contrast to OO-REMP, one finds that systematically improving the basis set (TZ → QZ; addition of core polarization functions; addition of diffuse basis functions) always leads to a systematic improvement of the results. In agreement with the REMP and OO-REMP results and with literature data, one finds that increasing the cardinal number of the basis leads to shorter bonds, while adding core polarization and diffuse basis functions provides longer bonds. The smallest MAD of 0.081 pm is found in conjunction with the aug-cc-pwCVQZ basis set. Coriani *et al.*<sup>61</sup> found an MAD of 0.069 pm for CCSD(T)/cc-pwCVQZ, but for a different benchmark set. Nevertheless, this shows that CCSD(T) in combination with large enough basis sets is capable of predicting bond lengths with an error of less than 1 pm, on average even less than 0.1 pm. The largest error encountered belongs to the CN radical whose bond length is underestimated by 0.44 pm.

The residual error may be attributed to the basis set incompleteness, the neglect of higher excitations, and the neglect of relativistic corrections. It should, however, be mentioned that even without these corrections, the systematic and statistical errors of CCSD(T) and OO-REMP are smaller than the experimental accuracy typically achieved for larger molecules (cf. Table V).

It is further instructive to break down the dataset into spin singlets (41 entries) and systems with higher multiplicity (20 entries). As in earlier investigations, one finds that canonical REMP performs poor for open shell systems, while it delivers reasonable performance for closed shell systems. Considering only the aug-cc-pwCVTZ basis, one finds that REMP(0.05) delivers an MAD of 0.15 pm for closed shell systems, while REMP(0.00) achieves an MAD of 0.73 pm for open shell systems (the best results in each case). OO-REMP(0.25), on the other hand, achieves 0.14 pm for the

**TABLE III.** High-confidence experimental equilibrium bond angles  $\alpha_e$ . Uncertainties are as given in the literature and refer to one standard deviation.

Molecule	Angle	Value (deg)	Uncertainty (deg)	Source Comment
C <sub>2</sub> H <sub>4</sub>	a(H–C–C)	121.4	0.24	52
<sup>1</sup> CH <sub>2</sub>	a(H–C–H)	102.44	0.15	52
<sup>3</sup> CH <sub>2</sub>	a(H–C–H)	133.090 8	0.0021	56
CH <sub>2</sub> O	a(H–C–O)	121.63	0.24	52
H <sub>2</sub> O	a(H–O–H)	104.4	0.09	52
H <sub>2</sub> O <sub>2</sub>	a(H–O–O)	99.76	0.06	59
	d(H–O–O–H)	113.6	0.3	59
HNO	a(H–N–O)	108.26	0.18	52
HOF	a(H–O–F)	97.86	0.02	52
E-N <sub>2</sub> H <sub>2</sub>	a(H–N–N)	106.34	0.18	52
NH <sub>3</sub>	a(H–N–H)	107.17	0.18	52
NO <sub>2</sub>	a(O–N–O)	133.856 67	0.0033	65
PH <sub>3</sub>	a(H–P–H)	93.328	0.02	68

closed shell systems and even 0.09 pm for the open shell systems (the complete data can be found in the [supplementary material](#)). The excellent performance for open shell systems underlines the high quality of the OO-REMP approach, which was shown to avoid spin contamination errors. We note that the fortuitous error compensation of basis and method errors cannot be excluded for this small sample size. Furthermore, the systems included are rather well-behaved single reference cases. Nevertheless, for this set, OO-REMP(0.25)/aug-cc-pwCVTZ even outperforms CCSD(T)/aug-cc-pwCVQZ (MAD = 0.12 pm). As in our earlier investigation,<sup>31</sup> we conclude that performing an orbital optimization is mandatory for REMP in the case of the open shell systems, while the performance gain is less pronounced for closed shell systems. Moreover, in the case of OO-REMP, the minimum of the MAD is located at almost the same  $A$  value for closed (0.20) and open shell molecules (0.25). The proposed mixing ratio, thus, seems to be universal and applicable to single reference determinants of arbitrary multiplicity.

Along with the bond lengths, a set of 12 proper bond angles and one proper dihedral angle (see Table III) was evaluated. All angles listed in Table III belong to molecules in Table I, but not for all of these molecules highly accurate angles were available.

The behavior of REMP and OO-REMP for bond angles (cf. Fig. 2) is quite interesting and unprecedented. The only systematic trend is that RE [i.e., CEPA/0(D)] systematically overestimates bond angles, while MP2 underestimates them [see Fig. 2(a)]. In between, there is a smooth and flat transition. This trend is preserved upon activation of orbital optimization [see Fig. 2(b)], but additionally, all angles become smaller such that OO-REMP tends to underestimate bond angles, while canonical REMP is close on spot. The MAD of REMP [Fig. 2(c)] exhibits unprecedented double minima with a sharp dip at  $A = 0.05$  and rather flat minima toward  $A = 0.8 \dots 1.0$ . The flat minima at large  $A$  values are, however, not of interest as in this range, the bond length errors become unacceptably large. In the case of OO-REMP [Fig. 2(d)], no double minima occur, but the strong dip at  $A = 0.05$  mostly persists. In almost all cases, this can be attributed to singlet methylene, whose

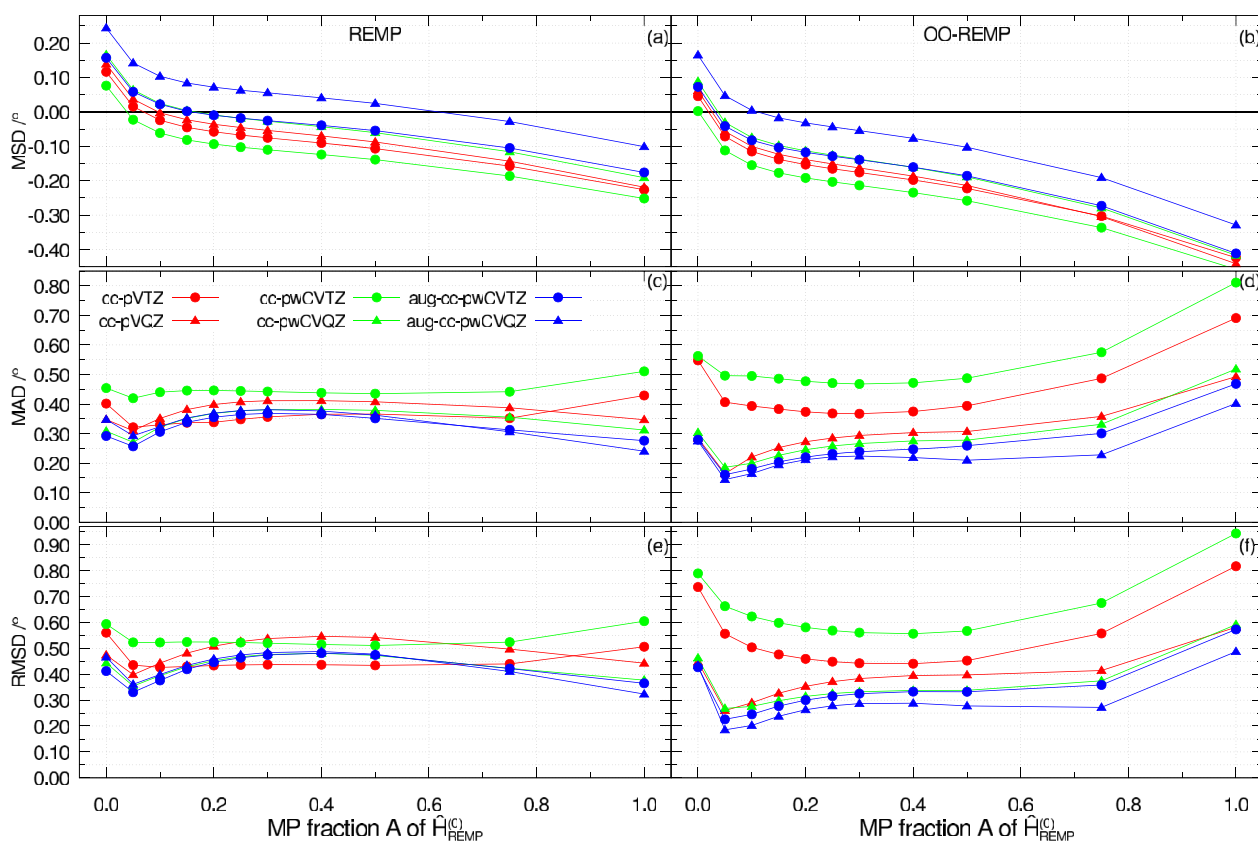


**FIG. 2.** Graphical representation of bond angle errors of REMP and OO-REMP for the high-confidence bond angle set. Average over 12 equilibrium bond angles. Reference: best available experimental/semi-experimental estimate. The dots indicate TZ basis sets; the triangles indicate QZ basis sets. The results for the cc-pVXZ family are shown in red, those for cc-pwCVXZ are shown in green, and those for aug-cc-pwCVXZ are shown in blue. (a), (c), and (e) REMP. (b), (d), and (f) OO-REMP.

bond angle is mispredicted at  $A = 0.0$  by about  $1^\circ$  with most basis sets, but already small Møller-Plesset fractions lead to great improvement. All in all, REMP is rather insensitive to both  $A$  and the basis set, with bond angle errors that amount to about  $0.4^\circ$  on average. Given that an uncertainty of  $0.5^\circ$  was allowed to enter the high confidence bond angle set, this is a pretty decent performance. It should be mentioned that the canonical method with the second smallest bond length error (REMP(0.05)/aug-cc-pwCVTZ) also delivers a bond angle MAD of only  $0.26^\circ$ , independently confirming the impressive performance of this Pauling point. The MAD of OO-REMP does not show pronounced double minima but flat minima around  $A = 0.35$  in the case of the cc-pVXZ bases and the mentioned sharp minimum at  $A = 0.05$  in all other cases. Additionally, one finds an almost textbook-like behavior with respect to improvements of the basis set [Fig. 2(d)]. The non-augmented valence basis sets perform worst; increasing the basis set cardinal number—which adds higher angular momentum functions—always leads to an improvement, and adding diffuse basis functions leads to a further improvement. The best results are now obtained with the aug-cc-pwCVQZ basis. This shows that an accurate prediction of bond angles seems to be crucially dependent on basis sets with

high angular momentum functions and augmented basis sets, which provide the necessary flexibility. Additionally, as changes in bond angles alter the distance between adjacent bonding electron pairs or lone pairs, bond angles are dependent on a balanced description of inter- and intra-pair correlation, which, in turn, requires complete enough basis sets. OO-REMP(0.05)/aug-cc-pwCVQZ has actually even significantly smaller errors than CCSD(T)/aug-cc-pwCVQZ, but its performance for bond lengths is inferior. It is a bit dissatisfying that in the case of OO-REMP, the minima with respect to  $A$  for bond lengths and bond angles do not coincide. On the other hand, one finds that OO-REMP(0.25)/aug-cc-pwCVTZ has an MAD of just  $0.23^\circ$ . Given that the average uncertainty in Table III amounts to  $0.13^\circ$ , this is an impressive performance sufficient for most routine calculations. Analyzing the CCSD(T) results for bond angles (cf. Table IV) shows that CCSD(T) is even slightly less accurate than OO-REMP: As in the case of the bond lengths, the lowest MAD is obtained with the aug-cc-pwCVQZ basis set, which is in line with the bond length results of CCSD(T) and the bond angle results of (OO)-REMP. The MAD of  $0.23^\circ$  is similar to that of OO-REMP(0.25)/aug-cc-pwCVTZ; only the MSD is smaller, indicating that CCSD(T) has a smaller systematic error, but the same statistical



**TABLE IV.** Statistics for the high-confidence bond angle benchmark set, aug-cc-pwCVXZ basis set family. Average over the 13 angles listed in Table III. All error measures are in degrees. The complete tables can be found in the [supplementary material](#).

Method	A	MSD	MAD	$\sigma$	RMSD	Median	$ \Delta_{\max} $
aug-cc-pwCVTZ							
REMP	0.00	0.157	0.292	0.397	0.412	0.103	1.051
	0.05	0.058	0.257	0.339	0.331	0.087	0.694
	0.20	-0.010	0.355	0.464	0.446	0.066	0.949
	0.25	-0.018	0.365	0.482	0.464	0.057	1.032
	0.30	-0.025	0.368	0.493	0.474	0.049	1.093
	1.00	-0.176	0.276	0.332	0.365	-0.143	0.833
OO-REMP	0.00	0.073	0.279	0.438	0.427	-0.018	1.122
	0.05	-0.042	0.161	0.231	0.226	-0.014	0.521
	0.20	-0.118	0.220	0.287	0.300	-0.011	0.627
	0.25	-0.129	0.232	0.300	0.315	-0.017	0.635
	0.30	-0.139	0.239	0.306	0.325	-0.025	0.664
	1.00	-0.412	0.469	0.415	0.573	-0.370	1.119
CCSD(T)		-0.138	0.241	0.342	0.356	-0.062	0.999
aug-cc-pwCVQZ							
REMP	0.00	0.244	0.348	0.413	0.466	0.224	1.214
	0.05	0.142	0.293	0.346	0.361	0.152	0.661
	0.20	0.072	0.369	0.472	0.459	0.057	0.914
	0.25	0.063	0.378	0.490	0.474	0.048	0.995
	0.30	0.055	0.381	0.500	0.484	0.040	1.054
	1.00	-0.101	0.240	0.320	0.323	-0.066	0.713
OO-REMP	0.00	0.165	0.275	0.418	0.434	0.082	1.288
	0.05	0.047	0.144	0.187	0.185	0.074	0.397
	0.20	-0.032	0.212	0.271	0.263	0.030	0.523
	0.25	-0.032	0.212	0.271	0.263	0.030	0.523
	0.30	-0.044	0.221	0.286	0.278	0.039	0.543
	1.00	-0.329	0.402	0.375	0.487	-0.248	0.980
CCSD(T)		-0.052	0.227	0.340	0.331	0.044	0.935

error. On the other hand, OO-REMP has a smaller largest absolute error than CCSD(T). Interestingly, the largest error of CCSD(T) of  $\approx -0.9^\circ$  belongs to the dihedral angle of  $\text{H}_2\text{O}_2$ , a closed shell molecule with no distinct multireference character.

All conclusions regarding basis sets drawn above equally apply to CCSD(T). Moreover, one can probably conclude that the CCSD(T) results are not yet converged with respect to the basis set and that even more accurate results may be obtained with 5Z basis sets.

All bond angle results should, however, be considered with a bit of caution. The statistical population is rather small, and the relative accuracy of the reference data is not as good as in the case of the bond length. If one has to choose a compromise for structural optimization, i.e., an  $A$  value that serves both bond lengths and bond angles, it is probably advantageous to select a value that primarily leads to minimal bond length errors. The variation of the error with

respect to a change in  $A$  is larger for the bond lengths, and an  $A$  value that produces good bond lengths still produces acceptable bond angles, while values that lead to minimal bond angle errors result in large bond length errors. Additionally, the evidence collected for lengths is much more robust than that for bond angles. Further breaking down the bond angle set into closed- and open-shell systems does make no sense in view of the already small sample size.

The second set consists of 28 bond lengths of small molecules where no experimental uncertainty was found or where the experimental uncertainty was clearly above 0.1 pm (see Table V). Furthermore, this set also features molecules for which only experimental structures averaged over the vibrational ground state were available ( $r_0$ ).

A graphical representation of the results for the low-confidence bond length set can be found in Fig. 3. Again, DZ basis sets were

**TABLE V.** Low-confidence experimental bond lengths  $r_e$  or  $r_0$ . Uncertainties are as given in the literature and refer to one standard deviation.

Molecule	Electronic state	Bond	Value (pm)	Uncertainty (pm)	Source	Comment
AlH	$^1\Sigma^+$	r(Al–H)	164.8		70	
BH	$^1\sigma^+$	r(B–H)	123.24		70	
BH <sup>+</sup>	$^2\Sigma^+$	r(B–H)	120.329	0.133	55	
BH <sub>2</sub>	$^2A_1$	r(B–H)	118.1		57	
CH <sub>3</sub>	$^2A_2''$	r(C–H)	107.6	0.1	55	
Cl <sub>2</sub>	$1\Sigma_g^+$	r(Cl–Cl)	198.7	0.9	66	<sup>35</sup> Cl <sub>2</sub>
ClOH	$^1A'$	r(O–H)	96.36	0.25	71	
		r(Cl–O)	169.08	0.10	71	
CO <sub>2</sub> <sup>+</sup>	$^2\Pi_g$	r(C–O)	117.68	0.74	55	$r_0$
CS <sub>2</sub>	$1\Sigma_g^+$	r(C–S)	155.259		61	
H <sub>2</sub> S	$^1A_1$	r(S–H)	133.56		72	
HC <sub>2</sub>	$^2\Sigma^+$	r(C–H)	106.51		73	
		r(C–C)	120.75		73	
HCO	$^2A'$	r(C–H)	111.91	0.5	55	
		r(C–O)	117.54	0.15	55	
HNF	$^2A''$	r(N–H)	103.5	0.3	74	
		r(N–F)	137.3	1	74	
HO <sub>2</sub>	$^2A''$	r(O–H)	97.07	0.2	55	
		r(O–O)	133.054	0.085	55	
HSiCl	$^1A'$	r(H–Si)	151.40		75	
		r(Si–Cl)	207.24		75	
Li <sub>2</sub>	$1\Sigma_g^+$	r(Li–Li)	267.29		70	
LiO	$^2\Pi$	r(Li–O)	169.449		54	$r_0$
N <sub>3</sub>	$^2\Pi_g$	r(N–N)	118.115		55	
NH <sub>2</sub>	$^2B_1$	r(N–H)	102.39		76	
SiH <sub>2</sub>	$^1A_1$	r(Si–H)	151.40		77	
SiH <sub>4</sub>	$^1A_1$	r(Si–H)	147.418		61	
SO <sub>3</sub>	$^1A_{1g}$	r(S–O)	141.75		78	

omitted as they lead to a systematic overestimation of more than 1 pm (see the respective tables in the [supplementary material](#)). Compared to the high-confidence bond lengths, the general trends concerning basis sets are preserved. One also finds that orbital optimization leads to longer bonds on average. In contrast to the high-confidence bond lengths, the MAD of REMP now shows some more distinct minima, which are located around  $A \approx 0.10$  [cf. [Fig. 3\(c\)](#)]. The best performance is again obtained with REMP(0.05)/aug-cc-pwCVTZ where the MAD amounts to 0.61 pm, which is almost twice as large as in the high-confidence case. The same general trends are also found in the RMSD [[Fig. 3\(e\)](#)].

OO-REMP again performs significantly better than canonical REMP. The smallest MAD is obtained with OO-REMP(0.10)/aug-cc-pwCVTZ and amounts to 0.29 pm [cf. [Fig. 3\(d\)](#)]. The previously best model chemistry—OO-REMP(0.25)/aug-cc-pwCVTZ—achieves a MAD of 0.35 pm. It should, however, be mentioned that the statistics for this set are mainly dominated by the results of the Li<sub>2</sub> molecule. The results are strongly dependent on the basis set and the  $A$  value. DZ basis sets lead to an overestimation of the bond length by up to 10 pm, and even with large augmented basis sets,

RE and OO-RE tend to underestimate the bond length by 1–2 pm, while MP2 and OO-MP2 tend to overestimate it by up to 5 pm (see the [supplementary material](#) for details). In between, there is only a small range around  $A = 0.05 \dots 0.15$  where the error is smaller than 1 pm. Although the reference value is of questionable quality, the molecule was retained in the set as CCSD(T) performed reasonably well with large basis sets. If the Li<sub>2</sub> molecule is removed from the set, essentially a very similar behavior as in the high-confidence case is recovered but with all curves shifted up to higher errors. The smallest errors are actually very similar to the ones when Li<sub>2</sub> is included. Given that the set contains data, which were presented with 0.1 pm accuracy or have uncertainties of 0.9 pm such as in the case of the Cl<sub>2</sub> molecule, the results should not be over-interpreted. In addition, as also CCSD(T)/aug-cc-pwCVQZ now produces a MAD of 0.19 pm (cf. [Table VI](#))—i.e., twice as large as with high-confidence reference data—the take-away message is rather that for benchmarking very precise methods, the reference data should be selected scrupulously.

Associated with the low-confidence bond length set, one can form a set of low-confidence bond angles (cf. [Table VII](#)). This set

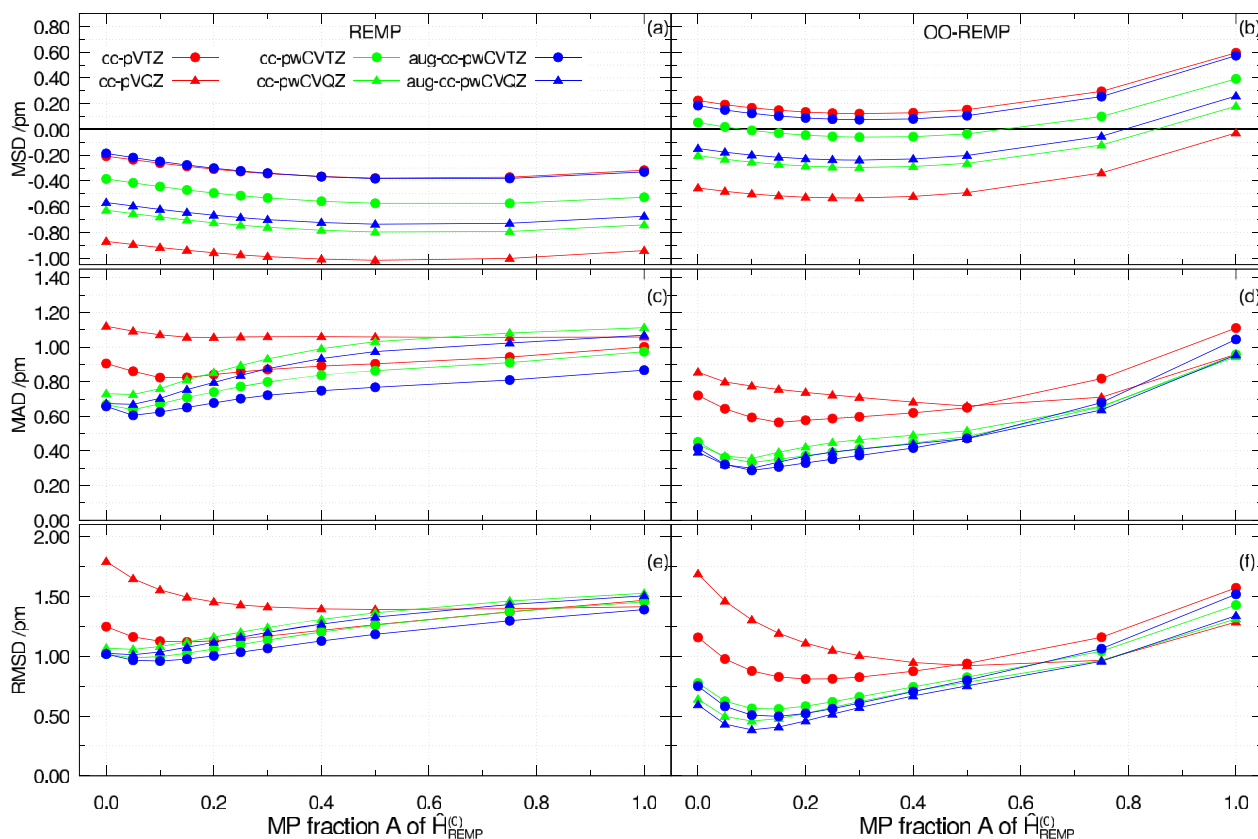


**FIG. 3.** Graphical representation of the bond length errors of REMP and OO-REM for the low-confidence bond length set. Average over 28 bond lengths. Reference: best available experimental/semi-experimental estimate. The dots indicate TZ basis sets; the triangles indicate QZ basis sets. The results for the cc-pVXZ family are shown in red, those for cc-pwCVXZ are shown in green, and those for aug-cc-pwCVXZ are shown in blue. (a), (c), and (e) REMP. (b), (d), and (f) OO-REM.

consists of bond angles for which either no uncertainty was given, the uncertainty was larger than  $0.5^\circ$ , or which were only provided as  $\alpha_0$ , i.e., angles of the vibrational ground state.

Figure 4 shows a graphical representation of the bond angle deviations for the low-confidence set. Numerical results are listed in Table VIII. As can be seen, neither REMP nor OO-REM seems to deliver a satisfactory performance for this set. The bond angles predicted by OO-REM are again systematically smaller than those predicted by REMP. In the case of canonical REMP, there is almost no dependence on the mixing parameter  $A$ , and on average, the bond angles are off by about  $0.5^\circ$  at least. There is also almost no basis set dependence judged by the MAD [Fig. 4(c)] and the RMSD [Fig. 4(e)]. The curves belonging to OO-REM, on the other hand, exhibit minima, which are located between  $A = 0.20$  and  $A = 0.40$ . Nevertheless, even the smallest average errors are larger than  $0.4^\circ$  and the RMSD of OO-REM is mostly even larger than the RMSD of REMP. There is a moderate basis dependency insofar as QZ basis sets deliver better results than TZ basis sets. The results obtained with CCSD(T) are seemingly similarly devastating: CCSD(T)/aug-cc-pwCVQZ achieves an MSD of  $-0.17^\circ$ , an MAD of  $0.56^\circ$ , and an RMSD of  $0.81^\circ$ . There is, however, a big caveat related to this analysis: The set is rather small, and the reference numbers are all

somehow flawed, either by the absence of error bars or by having  $\alpha_0$  values or by exceedingly large associated uncertainties. The bond angle of HNF, e.g., has an experimental uncertainty of  $1^\circ$ . Indeed, CCSD(T)/aug-cc-pwCVQZ predicts this angle to be  $1.85^\circ$  smaller. Given that this level of theory had an MAD of  $0.23^\circ$  against high-confidence reference data, it seems possible to improve this experimental value. Again, the take-home message is that a careful selection of the reference data is absolutely mandatory and not “cherry-picking.”

In addition to the systems listed in Table V, calculations for the Ar dimer have been performed. The data gathered, thus, have, however, been excluded from the statistical averaging. All basis sets except aug-cc-pwCVTZ and aug-cc-pwCVQZ almost always lead to errors larger than 10 pm, sometimes almost 40 pm. As these errors are 10–100 times larger than those encountered for all other cases, they would have dominated the statistics as dramatic outliers. Moreover, as even CCSD(T)/aug-cc-pwCVQZ is off by 3.5 pm, this system needs either even larger basis sets and/or more sophisticated correlation treatment or the available reference  $r_e$  is inaccurate. The respective data may be found in the supplementary material.

To summarize, it was found that with large enough basis sets, REMP(0.20) yields an MAD of 0.4–0.5 pm, while OO-REM(0.20)

**TABLE VI.** Statistics for the low-confidence bond length benchmark set, aug-cc-pwCVXZ basis set family. Average over the 28 bonds listed in Table V. All error measures are in pm. The complete tables can be found in the [supplementary material](#).

Method	A	MSD	MAD	$\sigma$	RMSD	Median	$ \Delta_{\max} $
aug-cc-pwCVTZ							
REMP	0.00	-0.186	0.658	1.019	1.017	-0.083	3.237
	0.05	-0.218	0.606	0.958	0.966	-0.117	3.300
	0.10	-0.249	0.625	0.944	0.959	-0.138	3.345
	0.20	-0.301	0.677	0.974	1.002	-0.228	3.412
	0.25	-0.322	0.702	1.000	1.033	-0.239	3.439
	1.00	-0.330	0.866	1.375	1.390	-0.481	5.100
OO-REMP	0.00	0.186	0.416	0.740	0.750	0.085	2.772
	0.05	0.151	0.322	0.571	0.581	0.056	2.414
	0.10	0.125	0.288	0.501	0.508	0.033	2.116
	0.20	0.089	0.331	0.523	0.521	-0.047	1.645
	0.25	0.080	0.353	0.566	0.561	-0.069	2.114
	1.00	0.573	1.044	1.431	1.518	0.240	5.141
CCSD(T)		0.216	0.281	0.393	0.442	0.108	1.641
aug-cc-pwCVQZ							
REMP	0.00	-0.568	0.674	0.868	1.024	-0.278	3.516
	0.05	-0.594	0.669	0.834	1.012	-0.307	3.581
	0.10	-0.620	0.704	0.844	1.036	-0.335	3.625
	0.20	-0.666	0.796	0.912	1.116	-0.444	3.691
	0.25	-0.684	0.836	0.952	1.158	-0.492	3.718
	1.00	-0.674	1.068	1.370	1.504	-0.630	4.642
OO-REMP	0.00	-0.148	0.393	0.586	0.594	-0.144	2.124
	0.05	-0.176	0.320	0.401	0.432	-0.172	1.087
	0.10	-0.199	0.300	0.336	0.385	-0.199	0.855
	0.20	-0.228	0.369	0.405	0.459	-0.256	1.321
	0.25	-0.235	0.394	0.467	0.516	-0.266	1.779
	1.00	0.260	0.954	1.337	1.339	-0.204	4.637
CCSD(T)		-0.109	0.189	0.227	0.248	-0.121	0.570

achieves an MAD of 0.1–0.2 pm. CCSD(T) was found to yield an MAD slightly below 0.1 pm with very large basis sets. Bond angles are predicted with an MAD of  $0.2^\circ$  by OO-REMP(0.20) and CCSD(T), while REMP(0.20) exhibits average errors of  $0.4^\circ$ .

**TABLE VII.** Low-confidence experimental equilibrium bond angles  $\alpha_e$ . Uncertainties are as given in the literature and refer to one standard deviation.

Molecule	Angle	Value (deg)	Uncertainty (deg)	Source	Comment
CLOH	a(Cl–O–H)	102.45		71	
H <sub>2</sub> O <sup>+</sup>	a(H–O–H)	110.5		79	
H <sub>2</sub> S	a(H–S–H)	92.11		72	
HCO	a(H–C–O)	124.95	0.25	80	$\alpha_0$
HNF	a(H–N–F)	102	1	74	
HO <sub>2</sub>	a(H–O–O)	104.1	2	81	
HSiCl	a(H–Si–Cl)	94.66		75	
NH <sub>2</sub>	a(H–N–H)	103.105		76	
SiH <sub>2</sub>	a(H–Si–H)	92.08		77	

### C. Harmonic vibrational wavenumbers of small molecules

For a subset of the molecules for which structural optimizations have been performed, harmonic vibrational wavenumbers were also calculated. The Hessian matrix was constructed by numerical differentiation of energies in the case of canonical REMP and by numerical differentiation of gradients in the case of OO-REMP. In both cases, a five-point formula was used as implemented in the FINDIF module of PSI4. If not mentioned otherwise, a geometrical distortion of  $5 \cdot 10^{-3} a_0$  was used. In each case, the structure optimized at exactly the same level of theory (method, basis, A parameter) was used as the unperturbed geometry.

In total, 81 normal modes of 43 molecules including some isotopologues were considered. Usually, the most abundant isotope was used for mass-weighting the Hessian prior to diagonalization. Isotopic masses were taken from the NIST database<sup>82</sup> and are tabulated in the [supplementary material](#). A full list of molecules together with the reference harmonic vibrational wavenumbers can be found in [Table IX](#).

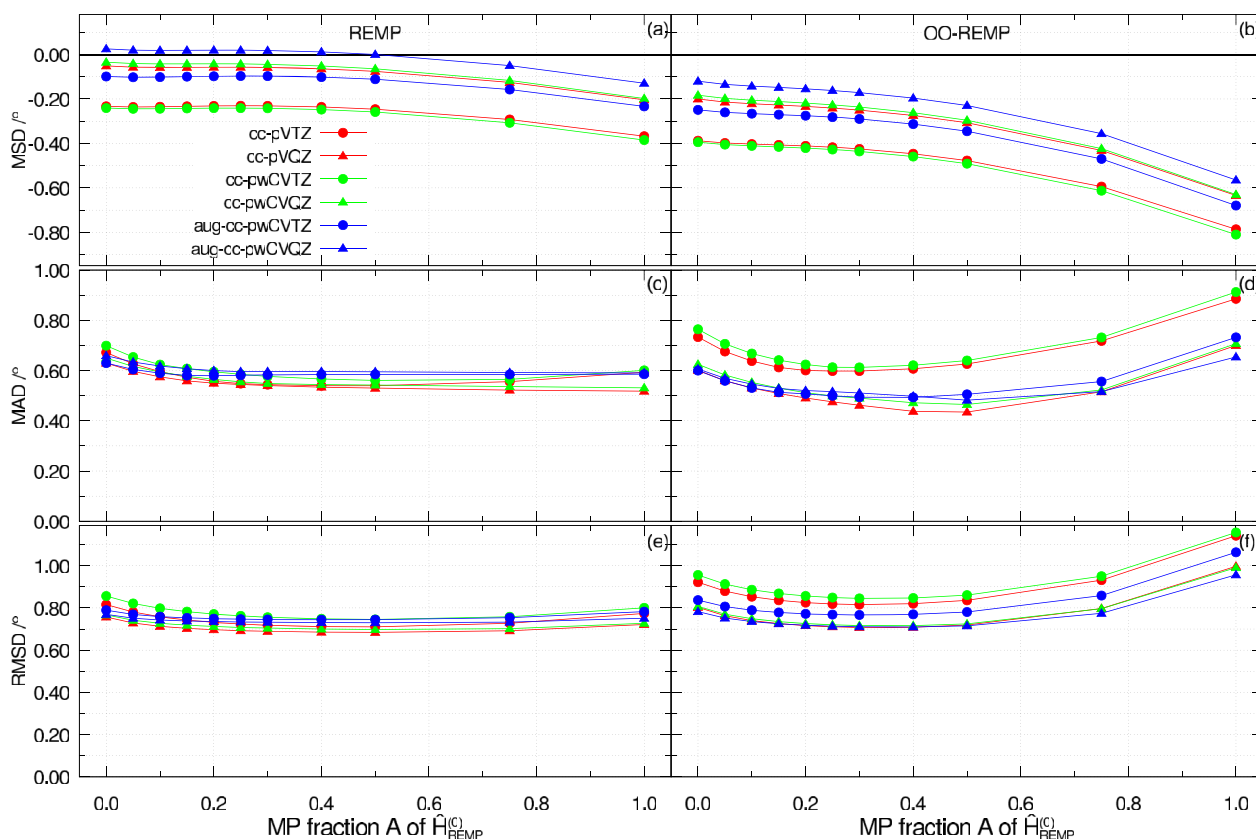


**FIG. 4.** Graphical representation of the bond angle errors of REMP and OO-REM for the low-confidence bond angle set. Average over nine bond angles from Table VII. Reference: best available experimental/semi-experimental estimate. The dots indicate TZ basis sets; the triangles indicate QZ basis sets. The results for the cc-pVXZ family are shown in red, those for cc-pwCVXZ are shown in green, and those for aug-cc-pwCVXZ are shown in blue. (a), (c), and (e) REMP. (b), (d), and (f) OO-REM.

From the available dataset, two outliers were removed, namely, the CN radical and the  $\text{CO}^+$  radical. Both molecules were sufficiently well described by OO-REM [OO-REM(0.20)/aug-cc-pwCVTZ is off by 9 and  $33\text{ cm}^{-1}$  for CN and  $\text{CO}^+$ , respectively], but dramatically overestimated by  $600\text{--}700\text{ cm}^{-1}$  by REMP.

Statistical descriptors for a selection of  $A$  values are presented in Table X; the complete table and tables for all smaller basis sets can be found in the supplementary material. Figure 5 shows statistical averages for the harmonic vibrational wavenumber benchmark set. The results for double zeta basis sets were again omitted but can be found in the supplementary material. The general trends with respect to basis set modifications are that increments of the basis set cardinal number from TZ to QZ generally lead to larger vibrational frequencies, while both the addition of core polarization functions and diffuse basis functions lead to a decrease of vibrational frequencies. One finds that the performance for harmonic vibrations closely resembles the one for the high-confidence bond length benchmark set (cf. Figs. 1 and 5). Looking at canonical REMP first [Fig. 5(a)], one finds that an increasing underestimation of bond lengths is correlated with an increasing overestimation of vibrational wavenumbers. Both errors can be traced back to bonds being too stiff. The mean absolute deviation [Fig. 5(a)] has no apparent

minimum for any basis set, instead, pure RE, i.e., CEPA/0(D) performs best. As in the case of bond lengths, the best results are obtained with the aug-cc-pwCVTZ basis set where one finds an MAD of  $17\text{ cm}^{-1}$ . Quite interestingly, REMP(0.00)/cc-pVTZ also delivers acceptable results with an MAD of  $24\text{ cm}^{-1}$ . The RMSD behaves similar to the only exception that REMP(0.00)/aug-cc-pwCVQZ is superior to REMP(0.00)/aug-cc-pwCVTZ by  $1\text{ cm}^{-1}$ . The correlation between bond length errors and wavenumber errors carries over to OO-REM. Consequently, as OO-REM leads to longer and weaker bonds, the associated force constants are smaller, leading to more accurate vibrations [cf. Fig. 5(b)]. The MAD exhibits minima for all basis sets [Fig. 5(d)], but compared to the bond lengths, these are shifted toward lower  $A$  values. The overall best results are obtained with OO-REM(0.10)/aug-cc-pwCVTZ (MAD =  $12\text{ cm}^{-1}$ ), but OO-REM(0.20)/aug-cc-pwCVTZ with an MAD of  $13\text{ cm}^{-1}$  is only slightly less accurate. The RMSD of OO-REM(0.10)/aug-cc-pwCVTZ amounts to only  $15\text{ cm}^{-1}$  and is, thus, only half as large as that of the best canonical method. The superiority of the orbital-optimized method is also reflected by the largest outliers of the respective best canonical and orbital-optimized methods. One finds that REMP(0.00)/aug-cc-pwCVTZ overestimates the OF stretch by  $292\text{ cm}^{-1}$ , while OO-REM(0.10)/aug-cc-pwCVTZ

**TABLE VIII.** Statistics for the low-confidence bond angle benchmark set, aug-cc-pwCVXZ basis set family. Average over the nine angles listed in Table VII. All error measures are in degrees. The complete tables can be found in the [supplementary material](#).

Method	$A$	MSD	MAD	$\sigma$	RMSD	Median	$ \Delta_{\max} $
aug-cc-pwCVTZ							
REMP	0.00	-0.099	0.630	0.831	0.789	0.182	1.644
	0.05	-0.102	0.604	0.809	0.769	0.185	1.620
	0.20	-0.098	0.579	0.788	0.749	0.103	1.583
	0.25	-0.097	0.581	0.785	0.747	0.123	1.578
	0.30	-0.097	0.583	0.784	0.745	0.140	1.577
	1.00	-0.233	0.586	0.792	0.783	0.017	1.777
OO-REMP	0.00	-0.249	0.600	0.847	0.837	0.121	1.900
	0.05	-0.260	0.559	0.809	0.806	0.134	1.877
	0.20	-0.275	0.507	0.765	0.772	-0.023	1.856
	0.25	-0.282	0.500	0.758	0.768	-0.005	1.861
	0.30	-0.290	0.494	0.753	0.767	0.010	1.871
	1.00	-0.679	0.732	0.868	1.064	-0.280	2.454
CCSD(T)		-0.286	0.559	0.835	0.837	0.052	2.013
aug-cc-pwCVQZ							
REMP	0.00	0.026	0.659	0.816	0.769	0.276	1.493
	0.05	0.020	0.634	0.797	0.751	0.235	1.470
	0.20	0.020	0.600	0.780	0.735	0.219	1.436
	0.25	0.019	0.596	0.778	0.734	0.237	1.433
	0.30	0.018	0.596	0.776	0.732	0.243	1.432
	1.00	-0.129	0.590	0.785	0.751	0.054	1.638
OO-REMP	0.00	-0.120	0.606	0.820	0.782	0.236	1.736
	0.05	-0.134	0.569	0.785	0.752	0.218	1.715
	0.20	-0.154	0.520	0.744	0.718	0.089	1.700
	0.25	-0.162	0.516	0.737	0.713	0.106	1.707
	0.30	-0.171	0.511	0.732	0.711	0.120	1.717
	1.00	-0.565	0.654	0.819	0.957	-0.169	2.304
CCSD(T)		-0.168	0.560	0.808	0.780	0.079	1.852

overestimates the antisymmetric HSiCl stretching vibration by only  $45\text{ cm}^{-1}$ . Further comparing orbital-optimized methods to their non-orbital-optimized counterparts, one finds that MP2 actually does not benefit from orbital optimization at all. Depending on the basis set, the largest outliers of OO-MP2 amount to almost  $-1100\text{ cm}^{-1}$  in the case of the  $\text{O}_2^+$  cation and the aug-cc-pwCVDZ basis set. This large error cannot only be attributed to the basis set as also the aug-cc-pwCVQZ basis leads to an underestimation of  $876\text{ cm}^{-1}$ . Canonical MP2 exhibits an error of “only”  $\approx -400\text{ cm}^{-1}$ . OO-REMP(0.10)/aug-cc-pwCVTZ, on the other hand, is off by only  $15\text{ cm}^{-1}$ , showing that the huge deviation can be attributed neither to a bad literature value nor to a general inapplicability of single reference methods. In a set of 81 entries, a single entry also does not have enough weight to completely distort the statistics and there are actually several cases where MP2 outperforms OO-MP2. That being said, one should keep in mind that canonical MP2 still

exhibits mean absolute errors of more than  $40\text{ cm}^{-1}$ . Pure RE [i.e., CEPA/0(D)], on the other hand, does benefit from orbital optimization. In the case of the aug-cc-pwCVTZ basis, the MAD is virtually the same ( $17\text{ cm}^{-1}$  in both cases), but the RMSD and the largest outlier decrease significantly upon orbital optimization: While REMF(0.0)/aug-cc-pwCVTZ overestimates the stretching vibration of the OF radical by  $292\text{ cm}^{-1}$ , OO-REMP(0.0)/aug-cc-pwCVTZ underestimates the same vibration by only  $88\text{ cm}^{-1}$ . For  $A > 0$ , the statistical descriptors of OO-REMP, furthermore, improve, while they deteriorate for canonical REMF, and up to  $A \approx 0.50$ , there is always a benefit associated with performing an orbital optimization.

To summarize the results, one finds that—depending on the required accuracy—both REMF and OO-REMP may be used for predicting harmonic vibrational frequencies but that OO-REMP delivers significantly better results. The optimal REMF mixture is



**TABLE IX.** Experimental reference data for the harmonic vibrational wavenumber benchmark set. If not mentioned otherwise, elemental symbols indicate the isotope with the highest natural abundance. Degenerate normal modes are given only once. The atomic masses used by us are given in the [supplementary material](#).

Molecule	$\omega$ (cm <sup>-1</sup> )	Source	Molecule	$\omega$ (cm <sup>-1</sup> )	Source
AlD	1211.774 02(15)	83	D <sub>2</sub>	3115.50(9)	83
AlH	1682.374 74(3)1	83	H <sub>2</sub> O	1648.47	84
Ar <sub>2</sub>	30.68(8)	85		3832.17	84
BF	1402.158 65(26)	83		3942.53	84
BH	2366.7296(16)	83	H <sub>2</sub> S	1214.5	86
C <sub>2</sub> H <sub>2</sub>	624.02	87		2721.9	86
	746.70	87		2733.4	86
	2010.70	87	DCl	2145.1326(11)	83
	3415.35	87	HCl	2990.9248(15)	83
	3496.91	87	HCN	727.24	88
C <sub>2</sub> H <sub>4</sub>	842.9	89		2128.18	88
	958.8	89		3440.05	88
	968.7	89	DF	3000.3	90
	1043.9	89	HF	4138.3850(7)	83
	1244.9	89	HSiCl	525.0	75
	1369.6	89		807.9	75
	1473.0	89		2004.3	75
	1654.9	89	Li <sub>2</sub>	351.4066(10)	83
	3146.9	89	LiF	910.572 72(10)	83
	3152.5	89	LiD	1054.939 73(32)	83
	3231.9	89	LiH	1405.498 05(7)6	83
	3234.3	89	LiO	814.62(15)	83
CF	1307.93(37)	83	N <sub>2</sub>	2358.57(9)	83
CH	2860.7508(98)	83	N <sub>2</sub> <sup>+</sup>	2207.0115(60)	83
CD	2101.051 93(55)	83	NF	1141.37(9)	83
CH <sub>2</sub> O	1190.9	91	ND	2399.126(30)	83
	1287.7	91	NH	3282.72(10)	83
	1562.6	91	NH <sub>3</sub>	1022	92
	1763.7	91		1691	92
	2944.3	91		3506	92
	3008.7	91		3577	92
CH <sub>4</sub>	1367.4	93	NO	1904.1346(18)	83
	1582.7	93	O <sub>2</sub>	1580.161(9)	83
	3025.5	93	O <sub>2</sub> <sup>+</sup>	1905.892(82)	83
	3156.8	93	OF	1053.0138(12)	83
Cl <sub>2</sub>	559.751(20)	83	OH	3737.76(18)	83
CN	2068.648(11)	83	PN	1336.948(20)	83
CO	2169.755 89(8)	83	SiH <sub>2</sub>	1020.49	94
CO <sup>+</sup>	2214.127(35)	83		2065.65	94
CS	1285.154 64(10)	83		2076.55	94
H <sub>2</sub>	4401.213(18)	83	SiO	1241.543 88(7)	83
HD	3813.15(18)	83			

in close agreement with the result for the structure benchmark, but poorer agreement with the thermochemistry benchmarks performed earlier. In contrast, the best mixture for thermochemistry [OO-REMP(0.20)] also delivers quite accurate vibrational frequencies in conjunction with sufficiently large basis sets.

A comparison to other methods and literature results is difficult as the current set has not been investigated previously. Byrd *et al.*<sup>57</sup>

defined a subset of their radical set, which contains only harmonic vibrational frequencies. For this set, they find that UMP2/cc-pVTZ delivers an MAD of 337 cm<sup>-1</sup>, while UB3LYP/cc-pVTZ achieves 71 cm<sup>-1</sup>, UCCSD(T)/cc-pVTZ yields 64 cm<sup>-1</sup>, and ROCCSD(T)/cc-pVTZ achieves 27 cm<sup>-1</sup>. Pawłowski *et al.*,<sup>95</sup> on the other hand, found that for a small set of small closed shell molecules, CCSD(T)/cc-pCVTZ reaches an MAD of 13.7 cm<sup>-1</sup>, while CCSD(T)/cc-pCVQZ

**TABLE X.** Statistics for the harmonic vibrational frequency benchmark set, aug-cc-pwCVXZ basis set family. Average over 81 of the 83 vibrations in Table IX (CN and CO<sup>+</sup> excluded). All error measures are in cm<sup>-1</sup>. The complete tables can be found in the [supplementary material](#).

Method	A	MSD	MAD	$\sigma$	RMSD	Median	$ \Delta_{\max} $
aug-cc-pwCVTZ							
REMP	0.00	7.7	17.3	36.9	37.4	1.7	320.0
	0.05	12.8	18.1	35.5	37.5	5.9	307.1
	0.10	16.6	20.4	34.7	38.3	13.0	298.6
	0.15	19.6	22.4	34.3	39.3	15.4	295.7
	0.20	22.1	24.2	34.2	40.5	18.6	294.3
	1.00	13.3	47.8	78.0	78.6	13.0	731.8
OO-REMP	0.00	-9.6	17.2	20.9	22.9	-9.4	131.8
	0.05	-3.3	13.1	16.9	17.2	-3.1	97.2
	0.10	1.3	11.8	15.3	15.3	2.2	77.2
	0.15	4.6	12.0	14.8	15.5	3.7	77.3
	0.20	7.0	13.1	15.3	16.7	6.4	79.9
	1.00	-23.6	64.7	135.4	136.6	5.7	1097.7
aug-cc-pwCVQZ							
REMP	0.00	14.7	19.6	33.6	36.5	6.3	267.7
	0.05	19.6	22.0	32.9	38.1	11.1	264.1
	0.10	23.7	25.4	33.1	40.6	17.4	262.5
	0.15	26.2	27.6	32.2	41.3	21.1	262.0
	0.20	28.4	29.7	32.0	42.6	24.8	262.5
	1.00	18.5	47.5	72.6	74.4	21.2	659.4
OO-REMP	0.00	-1.5	14.9	20.0	19.9	-4.5	141.9
	0.05	4.4	12.5	17.1	17.5	1.4	110.3
	0.10	8.8	13.2	15.8	18.0	6.8	88.9
	0.15	11.9	15.1	15.3	19.3	11.5	83.7
	0.20	14.3	16.9	15.4	20.9	15.4	86.2
	1.00	-16.2	62.1	124.8	125.1	7.6	987.4

even achieves 9.4 cm<sup>-1</sup>. Our results are similar to those of Bozkaya and Sherrill<sup>37</sup> who found slightly smaller mean absolute errors for CEPA/0(D) and OCEPA/0(D), but their set only comprised closed-shell molecules. They, furthermore, found an MAD of 8 cm<sup>-1</sup> for CCSD(T)/cc-pCVQZ on their benchmark set, which is only marginally better than the 12 cm<sup>-1</sup> of OO-REMP(0.10)/aug-cc-pwCVTZ on our probably more difficult benchmark set. Tentscher and Arey<sup>55</sup> calculated harmonic vibrational wavenumbers for a set of small radical species. The only method providing an MAD below 10 cm<sup>-1</sup> was an additive scheme termed CCSDTQex. They, furthermore, found that coupled cluster methods with perturbative triples based on ROHF of Brueckner orbitals provide significantly better results (MAD < 20 cm<sup>-1</sup>) than those employing UHF references (MAD > 40 cm<sup>-1</sup>). Coupled cluster methods with up to doubles and MP2 derivatives lead to MADs of at least 40 cm<sup>-1</sup>, and DFT with the exception of B2PLYPD performs even worse. Wennmohs and Neese<sup>96</sup> assessed the performance of a variety of coupled-pair type methods in conjunction with the QZVP basis on the basis of

small main-group diatomics. With the exception of CCSD(T), none of the tested methods was able to achieve an MAD below 20 cm<sup>-1</sup>. Bozkaya,<sup>97</sup> furthermore, benchmarked MP2, MP3, OMP3, CCSD, and CCSD(T) together with the cc-pCVQZ basis for a set of 17 open shell diatomics. For this rather difficult set, he found that even CCSD(T) yields an MAD of 52 cm<sup>-1</sup> and all other methods perform significantly worse. While these sets comprise harmonic vibrational frequencies of different molecules, the respective performance of canonical MP2 can be used for roughly standardizing the difficulty in the sets. It is fair to say that OO-REMP belongs to the top-performing methods with  $n^6$  scaling behavior for predicting harmonic vibrational frequencies.

No attempts were made to determine empirical scaling factors, which align calculated harmonic frequencies to experimental fundamental frequencies.

In short, it was found that REMP(0.20) provides an MAD of  $\approx 30$  cm<sup>-1</sup>, while OO-REMP(0.20) yields  $\approx 15$  cm<sup>-1</sup> depending on the basis set.



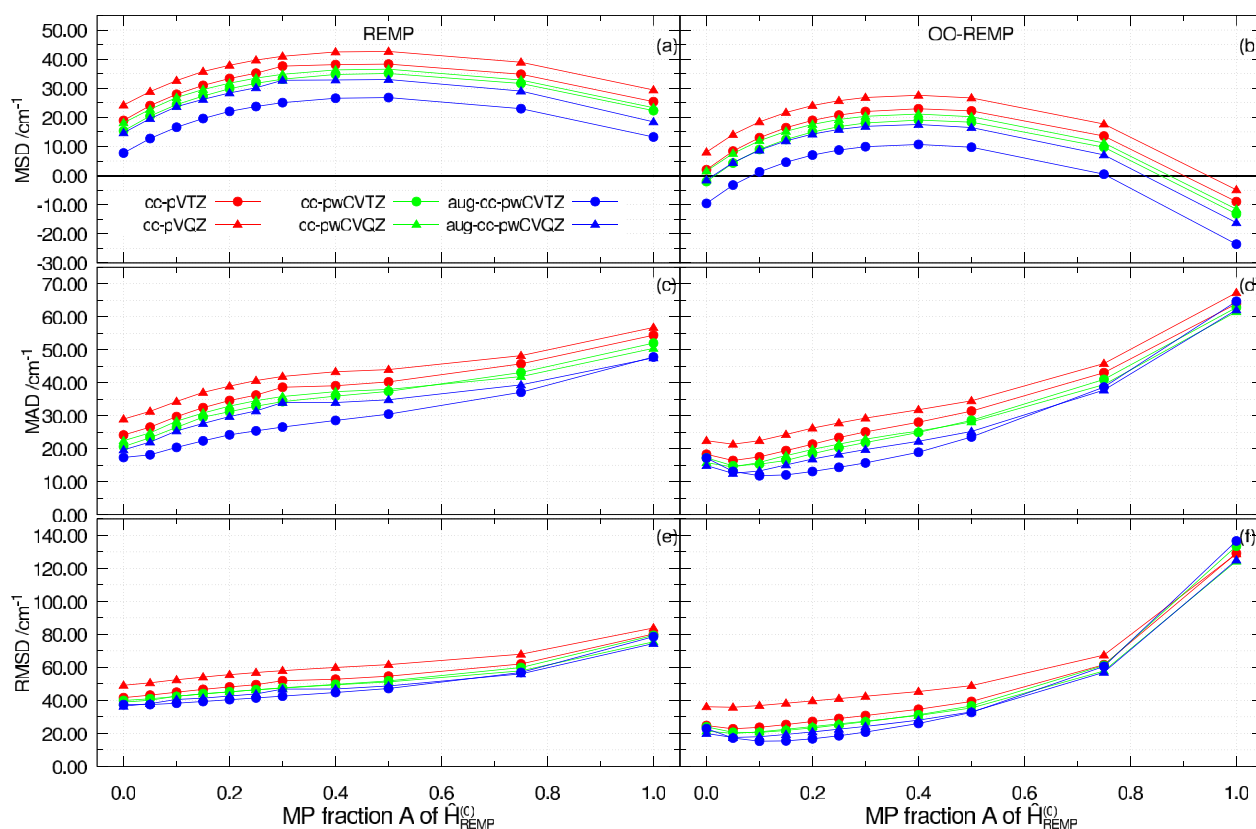


**FIG. 5.** Graphical representation of the harmonic vibrational wavenumber errors of REMP and OO-REMP for the vibrational frequency set. Average over 80 normal modes from Table IX excluding CN and CO<sup>+</sup>. Reference: best available experimental/semi-experimental estimate. The dots indicate TZ basis sets; the triangles indicate QZ basis sets. The results for the cc-pVXZ family are shown in red, those for cc-pwCVXZ are shown in green, and those for aug-cc-pwCVXZ are shown in blue. (a), (c), and (e) REMP. (b), (d), and (f) OO-REMP.

#### D. Dipole moments

If one is interested in the quality of an approximate wavefunction, the best reference would, of course, be a wavefunction computed by a high-level method, ideally full configuration interaction (FCI). We initially performed such a comparison for REMP wavefunctions and a set of small molecules.<sup>29</sup> The obvious drawback is that FCI and close-enough approximations are only in range for very small molecules. Moreover, it is not completely straightforward to directly compare two wavefunctions with each other.

It is, thus, convenient to analyze some substitute for the wavefunction. For the present purpose, the one-particle density and observable properties calculated thereof like the dipole moment represent an obvious choice. The molecular dipole moment can, thus, be used as a proxy measure to judge the quality of a wavefunction, as has been done before; see, e.g., Ref. 98. Note that for the reference data used in the following, we compare the absolute value of the dipole moment vector to its reference value.

The statistical analysis of the dipole moment error makes use of some additional relative measures: mean signed relative error (MSRE), mean absolute relative error (MARE), root mean square relative error (RMSRE), mean signed regularized relative error

(MSRRE), mean absolute regularized relative error (MARRE), and root mean square regularized relative error (RMSRRE). While the plain relative errors are always with respect to the reference value, the regularized errors are defined as  $\frac{\mu - \mu_{\text{ref}}}{\max(\mu_{\text{ref}}, 1 \text{ D})} \times 100\%$ , as proposed by Hait and Head-Gordon.<sup>99</sup>

The performance of REMP and OO-REMP to predict dipole moments was evaluated with two different benchmark sets. The first (and smaller) set is the S20 set by Bozkaya *et al.*<sup>100</sup> The set consists of 20 small and rather rigid closed shell molecules for which highly accurate experimental dipole moments are available. Bozkaya *et al.* computed CCSD(T)/CBS dipole moments from aug-cc-pVQZ and aug-cc-pV5Z results, showing that CCSD(T) is capable of reaching a mean absolute error as low as 0.016 D for this set, translating to a mean absolute relative error of 1.95%. We used their DF-CCSD(T)/aug-cc-pV5Z structures to compute REMP/aug-cc-pV5Z(-h) and OO-REMP/aug-cc-pV5Z(-h) dipole moments. REMP dipole moments were evaluated by numerical differentiation (three-point central differences) of the total energy with respect to an external electrical field using field increments of  $1.0 \cdot 10^{-4}$  a.u. ( $\approx 5.142 \cdot 10^7$  V m<sup>-1</sup>), while OO-REMP dipole moments were evaluated fully analytically from the converged one-particle density matrix.

**TABLE XI.** Errors for the S20 dipole moment benchmark set. All absolute errors are in debye relative to the experimental data given in Ref. 100; all relative errors are in %. The basis set for REMP/OO-REMP: aug-cc-pV5Z(-h). Complete tables and original data may be found in the [supplementary material](#). The average dipole moment in this set is 1.63 D, and six values are below and 14 above the regularization threshold of 1 D.

A	MSD (D)	MAD (D)	RMSD (D)	MSRE (%)	MARE (%)	RMSRE (%)	MSRRE (%)	MARRE (%)	RMSRRE (%)
REMP									
0.00	0.018	0.032	0.053	4.68	9.34	26.93	1.62	2.56	4.75
0.20	0.028	0.032	0.042	4.44	5.34	14.58	1.89	2.14	3.17
0.25	0.029	0.031	0.041	4.36	4.49	12.09	1.90	2.03	2.90
0.30	0.029	0.031	0.041	4.28	4.38	9.98	1.89	1.99	2.70
0.35	0.030	0.031	0.041	4.18	4.27	8.51	1.87	1.96	2.57
0.40	0.030	0.031	0.042	4.08	4.17	8.03	1.84	1.93	2.52
0.60	0.028	0.034	0.051	3.58	6.04	15.17	1.60	2.14	3.18
0.80	0.023	0.044	0.069	2.93	10.61	27.52	1.22	3.03	4.78
1.00	0.018	0.055	0.087	3.94	14.00	37.17	0.99	3.90	6.15
OO-REMP									
0.00	0.010	0.027	0.041	3.63	6.65	18.96	1.10	2.04	3.56
0.20	0.017	0.023	0.027	2.70	3.02	5.93	1.15	1.47	1.86
0.25	0.017	0.022	0.027	2.43	2.72	4.84	1.10	1.38	1.71
0.30	0.016	0.022	0.028	2.14	2.84	6.21	1.02	1.35	1.75
0.35	0.015	0.023	0.030	1.83	3.93	9.03	0.92	1.47	1.97
0.40	0.014	0.024	0.034	1.50	5.08	12.43	0.81	1.62	2.34
0.60	0.005	0.038	0.056	-0.14	10.52	28.42	0.17	2.69	4.58
0.80	0.003	0.045	0.068	4.83	9.82	28.89	0.39	2.94	4.57
1.00	-0.001	0.066	0.104	11.46	15.65	42.88	0.64	4.44	7.00
HF <sup>a</sup>	0.132	0.177	0.226	22.24	26.99	73.63	7.54	11.12	15.75
B3-LYP <sup>a</sup>	0.016	0.050	0.068	-2.41	6.16	13.66	0.21	3.09	4.41
CCSD <sup>a</sup>	0.028	0.042	0.061	4.39	9.21	24.21	1.69	2.97	4.69
CCSD(T) <sup>a</sup>	0.000	0.016	0.020	-0.70	1.95	3.68	0.00	1.01	1.39

<sup>a</sup>Data taken from Table 2 of Ref. 100.

Canonical REMP calculations employ standard frozen core settings, while OO-REMP calculations correlate all electrons. We also evaluated analytical dipole moments from unrelaxed REMP one-particle densities but found the errors to be almost as large as the Hartree-Fock ones, which is unacceptable. No result will, thus, be presented for this approach.

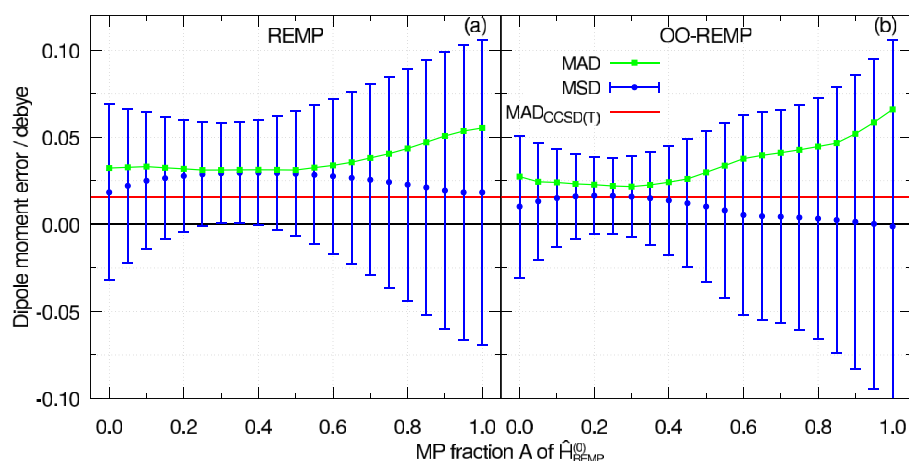
An overview of the results for REMP and OO-REMP and other methods is presented in Table XI.

Figure 6 shows a graphical representation of the performance of REMP and OO-REMP for the S20 benchmark set. Turning to canonical REMP first [Fig. 6(a)], one finds a very shallow minimum in the MAD spreading from  $A = 0$  to  $A = 0.6$  with a tiny maximum at  $A = 0.1$  and a very flat minimum at  $A = 0.5$ . On average, the REMP/aug-cc-pV5Z(-h) dipole moments in this range are off by  $\approx 0.03$  D. Compared to the results of Bozkaya *et al.*,<sup>100</sup> this is already better than all tested density functionals and CCSD (see Table XI). Interestingly, our MP2 results ( $A = 1.0$ ) almost coincide with those of Bozkaya *et al.* (0.055 vs 0.054 D) although we used CCSD(T) geometries for REMP, while they used MP2 geometries for MP2. The RMSD exhibits a more pronounced minimum located at  $A = 0.3$ . As the RMSD is usually dominated by outliers, it is interesting to identify these: Up to  $A = 0.25$ , it is  $\text{N}_2\text{O}$  that dominates the statistics

with errors of up to 0.18 D (at  $A = 0.00$ ). Above  $A = 0.25$ , it is the CS molecule whose error steadily increases up to 0.30 D at  $A = 1.00$ . At  $A = 0.25$ , the errors of both molecules are moderate (0.09 D for  $\text{N}_2\text{O}$  and 0.08 D for CS).

The optimal mixing ratio for canonical REMP ( $A = 0.30$ ) is not completely in line with what we found earlier<sup>29,30</sup> for the wavefunction itself, reaction energies, and transition barriers, where the optimal  $A$  rather turned out to be  $\approx 0.15$  with some scatter. If the dipole moment is considered as a proxy for the quality of the wavefunction itself, there is some discrepancy between our prior results<sup>29</sup> and the data presented herein, concerning the question of which choice of  $A$  leads to the smallest wavefunction error. On the other hand, does the S20 set feature quite some molecules that can be considered to be multireference species, thus distorting the analysis.

In contrast for OO-REMP [Fig. 6(b)], one finds that the minimum of the flat mean absolute deviation is located at  $A \approx 0.30$  and, thus, in rather close agreement with the best performing mixing ratio of our previous investigations. The MAD amounts to 0.022 D, which is better than the parent methods OCEPA (0.027 D) and OMP2 (0.066 D), better than any canonical REMP mixture, and close to CCSD(T)/CBS (0.016 D). Additionally, the previously best mixture



**FIG. 6.** Deviation of the calculated dipole moments of the S20 set from the experimental reference, absolute errors. The mean signed deviation is depicted by blue circles with the error bars indicating one standard deviation; the mean absolute deviation is depicted as green squares. The mean absolute deviation of CCSD(T)/CBS is indicated by the red solid line. (a) Canonical REMP/aug-cc-pV5Z(-h). (b) OO-REMP/aug-cc-pV5Z(-h). All errors are in debye. Numerical values can be found in the [supplementary material](#). Experimental and CCSD(T)/CBS dipole moments were taken from Ref. 100.

( $A = 0.20$ ) performs only insignificantly worse with an MAD of 0.023 D. Moreover, one finds that the RMSD has its minimum at  $A = 0.25$ . The RMSD is again mainly dominated by CS and  $N_2O$ . All in all, one finds that the findings of the previous investigations are confirmed regarding the optimal mixing and the overall accuracy.

The experimental dipole moments span almost two orders of magnitude, reaching from 0.11 D (CO) to 3.03 D ( $CH_3CN$ ). It is, thus, also crucial to investigate relative errors. Figure 7 depicts the relative signed (MSRE) and unsigned (MARE) errors of REMP and OO-REMP. Analyzing the relative errors leads to the same conclusions as before. Canonical REMP [Fig. 7(a)] exhibits again a flat minimum in the MARE curve reaching from  $A = 0.20$ – $0.50$ . The absolute relative error in this range amounts to 4%–5%, which is already fairly accurate. Orbital optimization [Fig. 7(b)] again improves on this by pushing the relative error down to 2.72% at  $A = 0.25$ . Quite satisfactorily, one finds that the regions where the absolute and relative errors become minimal coincide, showing that OO-REMP with appropriate mixing correctly predicts both small

and large dipole moments. For comparison, the mean absolute relative error of CCSD(T)/CBS amounts to 1.95%. Reanalyzing the data of Bozkaya *et al.*,<sup>100</sup> one finds that on a relative scale, CCSD and MP2 are off by at least 9% and that B3LYP is still the best-performing functional with a mean absolute relative error of 6.2%.

Hait and Head-Gordon<sup>99</sup> proposed to use regularized relative errors for assessing dipole moments to attenuate the influence of data points with small reference values. In addition to the plain relative errors, we computed regularized errors for both REMP and OO-REMP (cf. Fig. 8). As proposed in Ref. 99, a regularization parameter of 1 D was used. Regularization does not significantly change the general outcome. The mean absolute regularized relative error (MARRE) of REMP becomes minimal at  $A \approx 0.50$ , amounting to 1.88%, whereas the root mean square regularized relative error (RMSRRE) reaches its minimum of 2.52% at  $A = 0.40$ . OO-REMP achieves a MARRE of 1.35% at  $A = 0.30$  and a RMSRRE of 1.71% at  $A = 0.25$ . For comparison, CCSD(T)/CBS reaches a MARRE of 1.01% and an RMSRRE of 1.39%. The conclusions that can be drawn, thus, do not crucially depend on the weighting (by regularization)

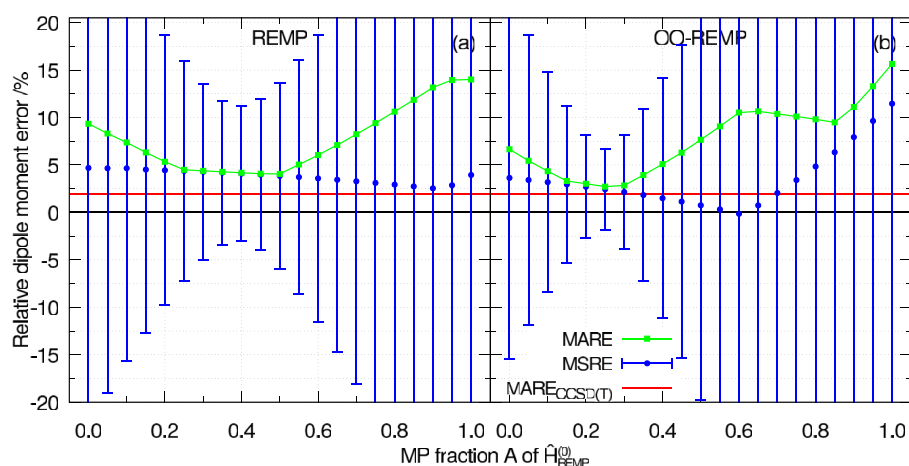


**FIG. 7.** Deviation of the calculated dipole moments of the S20 set from the experimental reference, relative errors. The mean signed relative error is depicted by blue circles with the error bars indicating one standard deviation; the mean absolute relative error is depicted as green squares. The mean absolute relative error of CCSD(T)/CBS is indicated by the red solid line. (a) Canonical REMP/aug-cc-pV5Z(-h). (b) OO-REMP/aug-cc-pV5Z(-h). All errors are in percent. Numerical values can be found in the [supplementary material](#). Experimental and CCSD(T)/CBS dipole moments were taken from Ref. 100.

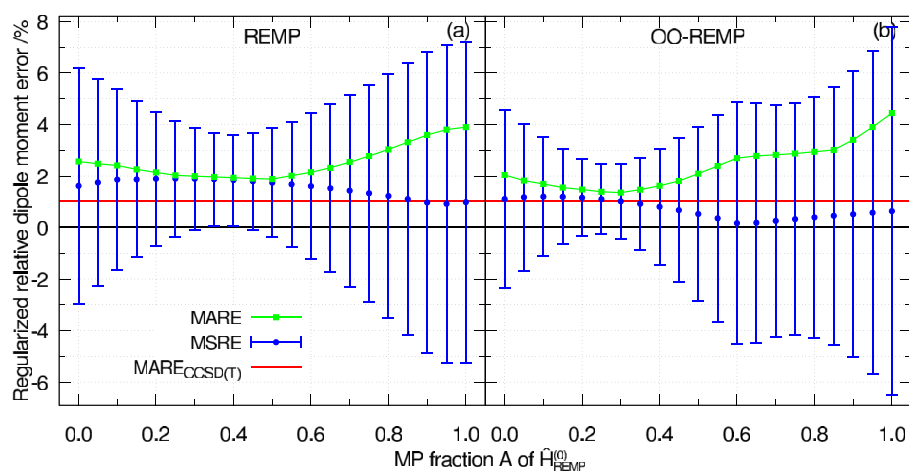


**FIG. 8.** Deviation of the calculated dipole moments of the S20 set from the experimental reference, regularized relative errors. The mean signed regularized relative error is depicted by blue circles with the error bars indicating one standard deviation; the mean absolute regularized relative error is depicted as green squares. The mean absolute regularized relative error of CCSD(T)/CBS is indicated as the red solid line. (a) Canonical REMP/aug-cc-pV5Z(-h). (b) OO-REMP/aug-cc-pV5Z(-h). All errors are in percent. Numerical values can be found in the [supplementary material](#). Experimental and CCSD(T)/CBS dipole moments were taken from Ref. 100.

of specific data points. The minima with respect to a change in the REMP mixing parameter  $A$  are found at essentially the same location regardless of whether regularized or “pure” relative errors are considered, but upon regularization, the performance of CCSD(T)/CBS and OO-REMP is even more similar. Compared to CCSD, the performance of OO-REMP is really impressive. Both methods do have a formal  $n^6$  scaling and require a similar number of FLOPs, but OO-REMP(0.25) is superior to CCSD in every single figure of merit shown in [Table XI](#).

Analyzing the sign of the errors, one finds that especially canonical REMP on average slightly overestimates dipole moments. This implies that REMP describes bonds on average as too ionic, implying that the too ionic Hartree–Fock reference is not corrected completely. Orbital optimization does a decent job here; at the mixing ratio where the MAD becomes minimal, the mean signed deviation of OO-REMP is significantly smaller than its canonical counterpart corresponding to a smaller systematic error. OO-REMP still overestimates the dipole moment but to a smaller extent than canonical REMP. Orbital optimization, thus, corrects the too ionic HF reference toward a more covalent picture.

All in all, one finds that CCSD(T) is still a little bit more accurate than OO-REMP regarding dipole moments although at the price of a higher computational cost. It, thus, seems to be legitimate to use CCSD(T) as a reference method for benchmarking OO-REMP when no experimental data are available although care has to be taken to not over-interpret the results.

The second test set investigated in this section is a large benchmark set by Hait and Head-Gordon, which previously was used to assess various density functionals.<sup>99</sup> It consists of 152 small closed and open shell molecules for which accurate reference dipole moments were calculated at the CCSD(T)/CBS level of theory. Given that orbital optimized REMP performed much better than canonical REMP for dipole moments, it was decided to only test the former with the larger benchmark set.

OO-REMP/aug-cc-pCVQZ dipole moments were calculated and compared to CCSD(T)/aug-cc-pCVQZ results [termed CCSD(T)/4Z] provided in Ref. 99. All structures and reference dipole moments were taken from Ref. 99. From the original set, two molecules had to be excluded. The first one is the ozone molecule,

which was excluded due to the known problem that the orbital optimization does not converge for  $A < 0.15$ . Ozone is a genuine multireference case, and it should be treated as such. The second molecule that was excluded is singlet methylene ( $^1\text{CH}_2$ ). There exists a broken symmetry determinant with  $m_z = 0$  originating from a stability analysis, which reproduces the UHF/aug-cc-pCVQZ dipole moment given by Hait and Head-Gordon. The  $\alpha$  and  $\beta$  spin HOMOs are roughly + and – linear combinations of the  $3a_1$  and  $1b_1$  orbitals, thus resembling the open shell singlet. This determinant, however, has an  $\bar{S}^2$  expectation value of 0.72 and is, thus, all but a pure spin singlet. It is questionable whether even CCSD(T) is able to cope with such an amount of spin contamination, thus questioning the validity of this dipole moment as a proper reference value for the dipole moment of singlet methylene. OO-REMP behaves non-deterministic as depending on the orbitals used to seed the orbital optimization (either said UHF orbitals or orbitals preoptimized with another  $A$  value), it fails to converge around  $A = 0.05$ , converges to a state that has still some spin contamination, or collapses to a pure closed-shell spin singlet with vastly too large dipole moment. For larger  $A$  values and if the orbitals stay spin-contaminated, the OO-REMP results coincide reasonably well with CCSD(T) (numbers are provided in the [supplementary material](#)). The whole set of (now) 150 molecules can be broken down into a subset consisting of proper closed shell singlet [molecules where a RHF determinant is stable, non-spin-polarized (NSP), 81 molecules] and molecules that possess an open shell ground state Hartree–Fock wavefunction, either due to having a higher multiplicity than singlet or because an RHF determinant exhibits a triplet instability, leading to a spin-contaminated open shell singlet [spin-polarized, (SP), 69 molecules].

The analysis was now focused around  $A = 0.20$  as the previous results have shown that this range provides the best results.

OO-REMP results for the complete set for a selection of mixing ratios are shown in [Table XII](#), [Tables XIII](#) and [XIV](#) list results for the NSP and SP subset, respectively.

[Figure 9](#) shows the average signed and absolute deviations of the OO-REMP/aug-cc-pCVQZ dipole moments from their CCSD(T)/aug-cc-pCVQZ counterparts. As can be seen, there is again a substantial improvement by hybridization compared to the

**TABLE XII.** Errors for the HHG152 dipole moment benchmark set. All absolute errors are in debye relative to the CCSD(T)/aug-cc-pCVQZ data given in Ref. 99; all relative errors are in %. The basis set for REMP/OO-REMP: aug-cc-pCVQZ. Complete tables and original data may be found in the [supplementary material](#). Average over 150 molecules. The average reference dipole moment amounts to 2.06 D; 51 values are below and 99 above the regularization threshold of 1 D.

A	MSD (D)	MAD (D)	RMSD (D)	MSRE (%)	MARE (%)	RMSRE (%)	MSRRE (%)	MARRE (%)	RMSRRE (%)
OO-REMP									
0.00	-0.005	0.031	0.054	-0.31	3.87	8.94	-0.33	1.96	3.39
0.20	0.004	0.021	0.035	-0.39	2.71	8.63	0.12	1.22	2.10
0.25	0.004	0.021	0.035	-0.26	2.66	8.29	0.16	1.23	2.17
0.30	0.004	0.021	0.036	0.13	2.47	6.26	0.17	1.27	2.31
0.35	0.004	0.022	0.039	0.52	2.59	6.59	0.17	1.34	2.51
0.40	0.003	0.024	0.042	0.93	3.19	9.49	0.15	1.45	2.75
0.60	-0.002	0.035	0.062	2.68	6.84	30.05	-0.07	2.27	4.06
0.80	-0.012	0.055	0.091	4.73	11.61	57.90	-0.51	3.52	5.85
1.00	-0.027	0.082	0.132	7.75	16.98	92.48	-1.20	5.11	8.22
MP2 <sup>a</sup>	0.155	0.207	0.688	17.43	27.50	109.71	8.22	11.96	36.54
CCSD <sup>a</sup>	0.035	0.045	0.062	4.47	7.47	28.88	1.93	2.71	3.83

<sup>a</sup>Data taken from the supplementary material of Ref. 99.

parent methods. Judged by the mean absolute deviation [Fig. 9(a)], OO-REMP(0.20) again delivers the best performance with an MAD of 0.021 D located in a shallow minimum ranging from  $A \approx 0.10$  to  $-0.30$ . The MAD is improved by almost a factor of two compared to OO-RE (0.034 D) and by a factor of four compared to OO-MP2 (0.082 D). The same conclusions hold if the set is decomposed into its subsets of 81 closed-shell and 69 spin-polarized systems. For the closed-shell molecules, the best performance is again provided by  $A = 0.24$  with an MAD of 0.012 D. The performance for spin-polarized molecules is significantly worse; the MAD becomes minimal at  $A = 0.19$  (0.030 D), but the minimum is extremely flat and the MAD is essentially the same up to  $A \approx 0.35$ . It is, furthermore, interesting to note that—analogously to the S20 set—dipole

moments of closed shell molecules are systematically overestimated, while dipole moments of open shell molecules are systematically underestimated.

Analyzing the root mean square deviation (which is more sensitive to outliers than the MAD) leads to essentially the same conclusions. The overall smallest RMSD is found at  $A = 0.22$ , while the individually smallest RMSDs for the two subsets are found at  $A = 0.22$  and  $A = 0.23$ . Judged by the RMSD, the closed-shell and the spin-polarized subsets do not demand a different treatment and the globally optimal mixing parameter works for both closed and open shell molecules.

Sarkar *et al.*<sup>101</sup> analyzed the performance of several wavefunction-based methods to predict ground state dipole

**TABLE XIII.** Errors for the closed shell (non-spin-polarized) molecules of the HHG152 dipole moment benchmark set (81 molecules). All absolute errors are in debye relative to the CCSD(T)/aug-cc-pCVQZ data given in Ref. 99; all relative errors are in %. The basis set for REMP/OO-REMP: aug-cc-pCVQZ. Complete tables and original data may be found in the [supplementary material](#).

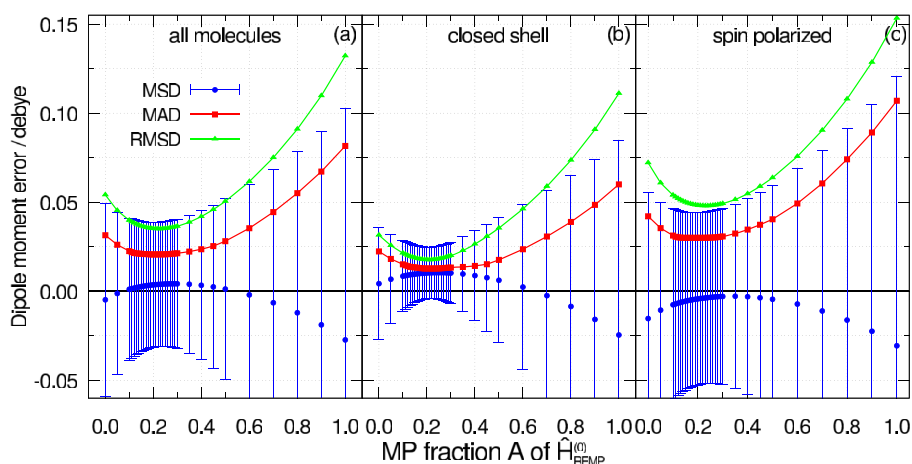
A	MSD (D)	MAD (D)	RMSD (D)	MSRE (%)	MARE (%)	RMSRE (%)	MSRRE (%)	MARRE (%)	RMSRRE (%)
OO-REMP									
0.00	0.004	0.022	0.032	-0.07	1.65	3.45	0.14	1.20	1.86
0.20	0.010	0.013	0.018	0.58	0.75	1.14	0.47	0.61	0.83
0.25	0.010	0.013	0.018	0.68	0.82	1.75	0.48	0.61	0.84
0.30	0.010	0.013	0.020	0.75	0.93	2.56	0.48	0.64	0.94
0.35	0.010	0.014	0.023	0.81	1.04	3.44	0.47	0.66	1.11
0.40	0.009	0.014	0.027	0.86	1.19	4.35	0.43	0.71	1.31
0.60	0.002	0.024	0.046	0.91	2.17	8.31	0.17	1.23	2.34
0.80	-0.009	0.039	0.074	0.78	3.49	12.81	-0.30	2.02	3.65
1.00	-0.025	0.060	0.111	0.46	5.14	18.01	-1.00	3.07	5.35
MP2 <sup>a</sup>	0.026	0.041	0.080	2.72	3.69	14.67	1.24	2.06	3.97
CCSD <sup>a</sup>	0.034	0.040	0.056	1.46	3.04	6.65	1.69	2.12	2.99

<sup>a</sup>Data taken from the supplementary material of Ref. 99.



**TABLE XIV.** Errors for the open shell (spin-polarized) molecules of the HHG152 dipole moment benchmark set (69 molecules). All absolute errors are in debye relative to the CCSD(T)/aug-cc-pCVQZ data given in Ref. 99; all relative errors are in %. The basis set for REMP/OO-REMP: aug-cc-pCVQZ. Complete tables and original data may be found in the [supplementary material](#).

A	MSD (D)	MAD (D)	RMSD (D)	MSRE (%)	MARE (%)	RMSRE (%)	MSRRE (%)	MARRE (%)	RMSRRE (%)
OO-REMP									
0.00	-0.015	0.042	0.072	-0.58	6.48	12.64	-0.88	2.88	4.57
0.20	-0.004	0.030	0.048	-1.54	5.02	12.66	-0.28	1.93	2.97
0.25	-0.003	0.030	0.048	-1.36	4.82	12.07	-0.23	1.95	3.06
0.30	-0.003	0.031	0.049	-0.61	4.28	8.81	-0.19	2.01	3.25
0.35	-0.003	0.032	0.051	0.18	4.40	8.97	-0.17	2.14	3.50
0.40	-0.003	0.035	0.055	1.01	5.54	13.17	-0.17	2.32	3.80
0.60	-0.007	0.049	0.076	4.75	12.32	43.39	-0.34	3.49	5.43
0.80	-0.016	0.074	0.108	9.37	21.15	84.23	-0.76	5.27	7.67
1.00	-0.031	0.107	0.153	16.31	30.89	134.95	-1.44	7.52	10.65
MP2 <sup>a</sup>	0.306	0.401	1.011	34.69	55.45	160.97	16.41	23.59	53.71
CCSD <sup>a</sup>	0.036	0.050	0.068	8.01	12.67	41.97	2.21	3.39	4.62

<sup>a</sup>Data taken from the supplementary material of Ref. 99.**FIG. 9.** Deviation of the calculated dipole moments of the Hait-Head-Gordon set from the CCSD(T)/aug-cc-pCVQZ reference, absolute errors. The mean signed deviation is depicted by blue circles with the error bars indicating one standard deviation; the mean absolute deviation is depicted as red squares. (a) Complete set of 151 molecules. (b) Closed shell molecules only. (c) Spin polarized/broken symmetry systems only. All errors are in debye. Numerical values can be found in the [supplementary material](#).

moments on a set of 16 small molecules. They found that CCSD/aug-cc-pVTZ (the best method with  $N^6$  scaling behavior investigated in this contribution) yields an MAD of 0.025 D against FCI/CBS. These results are qualitatively in line with the results from Table XII, given that the two sets are completely different, and with Bozkaya's results for the S2 benchmark set. As OO-REMP clearly outperforms CCSD in our investigations, it would also be interesting to assess its performance on the set of Sarkar *et al.*<sup>101</sup>

Again, relative errors were calculated and are depicted in Fig. 10. In the case of the relative errors, one finds a distinctly different behavior of the closed shell and the spin-polarized systems. While the closed-shell systems exhibit minimal MAREs of less than 1% (0.74% at  $A = 0.19$ ), the MARE of the spin-polarized systems does not drop below 4.37% at  $A = 0.11$ ; then, it raises again and exhibits again a minimum at  $A = 0.30$  (4.26%) after which it sharply raises. The reason for the double minimum is discussed below. This somewhat erratic behavior is caused by systems with small dipole

moment where small deviations lead to large relative errors. Nevertheless, the overall MARE stays constantly below 3% over a wide range of  $A$  values. For comparison, if the CCSD/aug-cc-pCVQZ and MP2/aug-cc-pCVQZ results provided with Ref. 99 are used to recalculate unregularized relative errors for the same selection of molecules, one finds relative errors of 7.5% and 27.5%, respectively. OO-REMP, thus, turns out to be robust for predicting small dipole moments.

Again, regularized relative errors were also computed to ameliorate the influence of small reference dipole moments (see Fig. 11). As a regularization parameter, again, 1 D was used. In contrast to the unregularized relative errors, the curves visualizing the  $A$  dependence are again completely smooth, showing that the somewhat erratic behavior of the raw relative errors can, indeed, be attributed to systems with small reference dipole moments. The regularized errors fully support the previous findings. The overall smallest mean absolute regularized relative error (MARRE) is

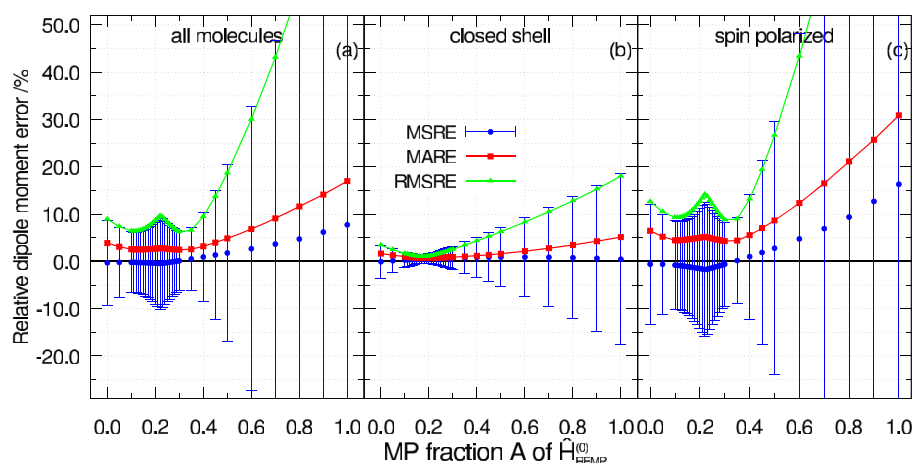


**FIG. 10.** Deviation of the calculated dipole moments of the Hait-Head-Gordon set from the CCSD(T)/aug-cc-pCVQZ reference, relative errors. The mean signed relative error is depicted by blue circles with the error bars indicating one standard deviation; the mean absolute relative error is depicted as red squares. (a) Complete set of 151 molecules. (b) Closed shell molecules only. (c) Spin polarized/broken symmetry systems only. All errors are in percent. Numerical values can be found in the [supplementary material](#).

found for  $A = 0.20$  (1.22%). Limited to the closed shell molecules, the smallest MARRE occurs at  $A = 0.25$  (0.58%), while the MARRE of the spin-polarized systems becomes minimal at  $A = 0.14$  (1.91%). This apparent discrepancy can be resolved by considering that the minima are very flat in both cases and essentially show the same behavior. Again, the root mean square regularized relative errors (RMSRREs) do not lead to very different conclusions. Overall, the minimum is found at  $A = 0.20$  (2.10%), while the best performance for the two subsets is obtained with  $A = 0.23$  (0.79%) and  $A = 0.18$  (2.96%).

In summary, one finds that OO-REMP is capable of predicting dipole moments for both non-spin-polarized and spin-polarized systems although not at the same accuracy. The optimal choice of the mixing parameter is essentially the same for both closed- and open-shell molecules and coincides with the range that has been shown to provide the best performance for other properties, namely,  $0.20 \leq A \leq 0.25$ . While—depending on the error measure—dipole moments of closed shell systems are predicted with an average error

of clearly less than 1%, the accuracy for open shell systems is about 2%. With respect to dipole moments, OO-REMP is, thus, clearly superior to even the best tested density functionals in Ref. 99, as well as MP2 and CCSD. So far, the only restriction is that it may only be applied to proper single reference cases.

When looking for outliers, there is only a handful of molecules where OO-REMP predicts dipole moments that are significantly off. In the case of OO-REMP(0.20), outliers with deviations larger than 0.05 D are BH (0.06), ClO<sub>2</sub> (−0.06), CN (−0.10), H<sub>2</sub>O–Li (0.07), HCHS (−0.05), HCP (0.05), HNO<sub>2</sub> (−0.07), HPO (−0.20), NaLi (−0.06), NO (0.06), NOCl (−0.15), NP (−0.09), PPO (0.15), PS (−0.11), and SiO (0.08). Outliers where the regularized relative error exceeds 5% are CN (−6.8%), HCP (5.4%), HPO (−7.5%), NaLi (−6.2%), NO (5.5%), NOCl (−7.5%), PPO (7.9%), and PS (−11.0%). Almost all of these are broken-symmetry cases where the success of the UCCSD(T) reference cannot be guaranteed. A closer inspection and comparison to experimental data provided by Hait and Head-Gordon in the supplementary material of Ref. 99 shows that

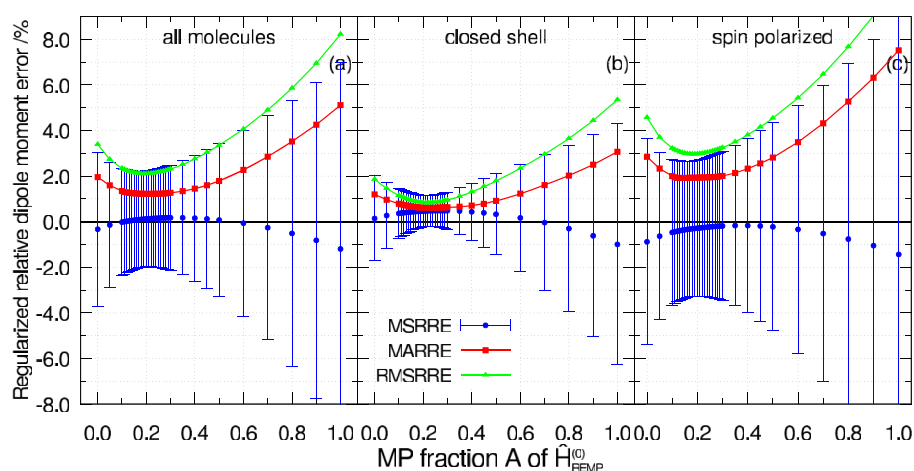


**FIG. 11.** Deviation of the calculated dipole moments of the Hait-Head-Gordon set from the CCSD(T)/aug-cc-pCVQZ reference, regularized relative errors. The mean signed regularized relative error is depicted by blue circles with the error bars indicating one standard deviation; the mean absolute regularized relative error is depicted as red squares. (a) Complete set of 151 molecules. (b) Closed shell molecules only. (c) Spin polarized/broken symmetry systems only. All errors are in percent. Numerical values can be found in the [supplementary material](#).

in some cases, there is no experimental value available to verify the UCCSD(T) result. In certain cases, the OO-REMP(0.20)/aug-cc-pCVQZ result is actually closer to the experimental value than CCSD(T)/CBS (HCHS, NaLi, NOCl, NP). It can also not be excluded completely that our initial Hartree–Fock calculations converged to the wrong state especially in broken symmetry cases although stability analyses was performed in doubt.

Both benchmark sets analyzed above do have a common weak point: The sets list only the absolute values of the dipole moment but not the components of the dipole vector. It is, thus, possible that in cases where the direction of the dipole moment is not completely determined by symmetry such as for CH<sub>3</sub>OH or CH<sub>3</sub>SH, a method may predict wrong components or the wrong direction of the dipole moment but the correct absolute value. This is all but unprecedented and, in fact, also happened in our investigation: for example, the dipole moment of the N<sub>2</sub>O molecule calculated with OO-REMP changed its sign while scanning through the *A* range, leading to a double minimum when only the length of the dipole vector is compared (*A* = 0.30 and *A* = 0.85). Given that *A* = 0.85 gives rather substandard performance in other cases, we assume that *A* = 0.30 here provides the right answer for the right reason. The ambiguity introduced by the loss of the sign/direction of the dipole vector manifests as kinks in the curves of Figs. 6 and 7 or as double minima. The error seemingly decreases, but the results are actually worse than indicated by the error measure as the dipole moment now has the right length but the wrong direction.

Broken down to the most important results, it was found that REMP(0.20) has a relative error of ≈5%, while OREMP(0.20) and CCSD(T) achieve 3% and 2%, respectively.

#### IV. SUMMARY AND OUTLOOK

We have investigated the capabilities of REMP and OO-REMP to predict first-order properties of small closed- and open-shell main-group molecules. It was found that, in principle, both REMP and OO-REMP are capable of accurately predicting equilibrium structures of these molecules. In the case of canonical REMP, the best results are obtained with pure RE, but small admixtures of MP do not lead to much worse results. Depending on the basis set, the smallest achieved MAD was ≈0.3 pm. In the case of OO-REMP, one finds significant improvements by hybridization and the smallest MAD—obtained with a 80:20 mixture of RE:MP—amounts to 0.13 pm. It was found that CCSD(T) is only slightly more accurate. For bond angles, one finds a somewhat erratic behavior, which can partly be attributed to the lower reliability of the reference data. Again, one finds that the orbital-optimized variant outperforms the canonical variant, leading to mean absolute deviations of 0.2°.

In the case of harmonic vibrational frequencies, one again finds no improvement by hybridization in the canonical case, but in the orbital-optimized case, although the optimal mixture has a slightly different composition. Both REMP and OO-REMP lead to minimal MADs of less than 20 cm<sup>-1</sup> with OO-REMP reaching an MAD as low as 12 cm<sup>-1</sup>.

In the case of static dipole moments, both REMP and OO-REMP benefit from hybridization with the latter being again

superior. It is shown that OO-REMP clearly outperforms B3LYP and CCSD for dipole moments, yielding relative errors as low as 3%, which is again almost as accurate as CCSD(T).

Although the optimal mixing ratio varies from property to property, it is possible to identify a parameter range, which leads to the best result. As the error curves as functions of the mixing parameter *A* exhibit different slopes, it is possible to come up with a globally optimal compromise. In the case of OO-REMP, such a compromise would be *A* = 0.20 as it leads to optimal bond lengths and dipole moments without sacrificing much accuracy for bond angles. This choice also turned out to be essentially optimal for thermochemistry<sup>30,31</sup> and has, therefore, the potential to be universally applicable.

During the course of this work, we found it difficult to compile a set of molecules with high-quality experimental equilibrium bond lengths and, especially, bond angles. Many structures that one finds on the first attempt, e.g., in the NIST Computational Chemistry Comparison and Benchmark DataBase (CCCBDB) do not have a sufficient number of decimal places, are not given with an experimental uncertainty, are of dubious provenance, or represent averages of the vibrational ground state. The situation is especially poor for bond angles. As they are naturally more flexible than bonds, the respective errors are usually larger. Nevertheless, some authors only publish bond lengths even if all necessary data for bond angles would be available, too. We think that it is overdue to augment the existing databases with high-quality (semiempirical) equilibrium structures and their assigned errors if available.

In this and the preceding works, we have demonstrated that OO-REMP has a predictational capacity nearly approaching that of the gold standard of quantum chemistry [CCSD(T)]. This may be of particular interest for the predictions of accurate molecular structures and properties as the relaxed densities determined in OO-REMP allow for an efficient evaluation of gradients and other first order properties, where the computational demand for these properties is typically only a small fraction of the time required for the energy evaluation. As a characteristic example, an OO-REMP energy calculation of the ethene molecule in C<sub>1</sub> symmetry with the cc-pVTZ basis set required 121 s of CPU time, while the gradient took only 20 s additionally [timings obtained on a single core of an Intel Xeon E6252 Gold (Cascade Lake) processor of the JUSTUS2 high-performance compute cluster]. The computationally most dominant steps for the gradient evaluation are the formation of the two-particle density matrix with four external indices, its transformation to the AO basis, and sorting of the density matrix in the AO basis.

Additionally, the REMP and OO-REMP approaches have clear potential for further improvement. As before and in line with the present observations, REMP tends to underestimate the absolute correlation energy by 2%–5%.<sup>29</sup> Thus, a modification of the unperturbed Hamiltonian that overcomes this small but systematic deficiency, e.g., by incorporating spin-dependent terms as in the S2-PT approach,<sup>102</sup> seems to be an interesting research topic. Even more, due to the success of the RE partitioning in multireference perturbation theory,<sup>25,103–106</sup> a multireference OO-REMP approach has a high potential for becoming a very accurate and broadly applicable quantum chemical approach. Ultimately, the implementation of analytical derivatives<sup>107–110</sup> for such an approach seems to be promising. Work on these topics is in progress in our laboratory.



A third extension would be second-order properties, such as NMR shieldings, or frequency-dependent properties, such as excitation energies or frequency-dependent polarizabilities. Last but not least, higher orders in perturbation theory (REMP3 and OO-REMP3) are viable as long as the perturbed wavefunction is restricted to double excitations at most and might lead to even more accurate results.

The REMF and OO-REMF implementation based on the PSI4 program package was made publicly available on GitHub<sup>48</sup> as the source code for everyone able to compile PSI4 from the source.

*Note added in proof:* The implementation of REMF and OO-REMF in PSI4 without density fitting was meanwhile merged into the master branch of PSI4 and will be available with the 1.7 release. The implementation which makes use of density fitting for the two-electron integrals was not yet merged but is also scheduled for the 1.7 release version.

## SUPPLEMENTARY MATERIAL

See the [supplementary material](#) for the complete versions of all tables and raw data for all graphs and further box plots for the bond length, bond angle, and harmonic vibration sets. All optimized structures for all methods are available as XMol .xyz files. Raw data are available as .ods spreadsheets. Further raw data (output files, etc.) are available upon request from the authors.

## ACKNOWLEDGMENTS

The authors acknowledge the support from the state of Baden-Württemberg through bwHPC and the German Research Foundation (DFG) through Grant No. INST 40/467-1 FUGG (bwForCluster JUSTUS) and Grant No. INST 40/575-1 FUGG (JUSTUS 2 cluster). The authors also acknowledge the Center for Light-Matter Interaction, Sensors & Analytics (LISA+) for providing them with computational resources.

## AUTHOR DECLARATIONS

### Conflict of Interest

The authors have no conflicts to disclose.

## Author Contributions

**Stefan Behnle:** Conceptualization (equal); Data curation (equal); Investigation (equal); Methodology (equal); Software (equal); Visualization (equal); Writing – original draft (equal); Writing – review & editing (equal). **Robert Richter:** Investigation (equal); Writing – review & editing (equal). **Luca Völk:** Investigation (equal); Writing – review & editing (equal). **Paul Idzko:** Investigation (equal); Writing – review & editing (equal). **André Förstner:** Investigation (equal). **Uğur Bozkaya:** Conceptualization (equal); Software (lead); Writing – review & editing (equal). **Reinhold F. Fink:** Conceptualization (equal); Funding acquisition (equal); Investigation (equal); Methodology (equal); Project administration (equal); Resources (equal); Software (equal); Supervision (equal); Writing – original draft (equal); Writing – review & editing (equal).

## DATA AVAILABILITY

The data that support the findings of this study are available within the article and its [supplementary material](#).

## REFERENCES

- C. Möller and M. S. Plesset, “Note on an approximation treatment for many-electron systems,” *Phys. Rev.* **46**, 618–622 (1934).
- T. Helgaker, P. Jørgensen, and J. Olsen, *Molecular Electronic-Structure Theory*, repr. ed. (Wiley, Chichester; New York; Weinheim, 2004).
- D. Cremer, “Møller–Plesset perturbation theory: From small molecule methods to methods for thousands of atoms,” *Wiley Interdiscip. Rev.: Comput. Mol. Sci.* **1**, 509–530 (2011).
- S. Grimme, “Improved second-order Møller–Plesset perturbation theory by separate scaling of parallel- and antiparallel-spin pair correlation energies,” *J. Chem. Phys.* **118**, 9095–9102 (2003).
- S. Grimme, L. Goerigk, and R. F. Fink, “Spin-component-scaled electron correlation methods,” *Wiley Interdiscip. Rev.: Comput. Mol. Sci.* **2**, 886–906 (2012).
- S. Grimme, “Improved third-order Møller–Plesset perturbation theory,” *J. Comput. Chem.* **24**, 1529–1537 (2003).
- L. W. Bertels, J. Lee, and M. Head-Gordon, “Third-order Møller–Plesset perturbation theory made useful? Choice of orbitals and scaling greatly improves accuracy for thermochemistry, kinetics, and intermolecular interactions,” *J. Phys. Chem. Lett.* **10**, 4170–4176 (2019).
- J. Lee and M. Head-Gordon, “Regularized orbital-optimized second-order Møller–Plesset perturbation theory: A reliable fifth-order-scaling electron correlation model with orbital energy dependent regularizers,” *J. Chem. Theory Comput.* **14**, 5203–5219 (2018).
- M. Pitonák, P. Neogrady, J. Cerný, S. Grimme, and P. Hobza, “Scaled MP3 non-covalent interaction energies agree closely with accurate CCSD(T) benchmark data,” *ChemPhysChem* **10**, 282–289 (2009).
- R. Sedlak, T. Janowski, M. Pitonák, J. Řezáč, P. Pulay, and P. Hobza, “Accuracy of quantum chemical methods for large noncovalent complexes,” *J. Chem. Theory Comput.* **9**, 3364–3374 (2013).
- A. Karton and L. Goerigk, “Accurate reaction barrier heights of pericyclic reactions: Surprisingly large deviations for the CBS-QB3 composite method and their consequences in DFT benchmark studies,” *J. Comput. Chem.* **36**, 622–632 (2015).
- E. Soydaş and U. Bozkaya, “Accurate open-shell noncovalent interaction energies from the orbital-optimized Møller–Plesset perturbation theory: Achieving CCSD quality at the MP2 level by orbital optimization,” *J. Chem. Theory Comput.* **9**, 4679–4683 (2013).
- F. Neese, T. Schwabe, S. Kossmann, B. Schirmer, and S. Grimme, “Assessment of orbital-optimized, spin-component scaled second-order many-body perturbation theory for thermochemistry and kinetics,” *J. Chem. Theory Comput.* **5**, 3060–3073 (2009).
- T. N. Lan and T. Yanai, “Correlated one-body potential from second-order Møller–Plesset perturbation theory: Alternative to orbital-optimized MP2 method,” *J. Chem. Phys.* **138**, 224108 (2013).
- E. Soydaş and U. Bozkaya, “Assessment of orbital-optimized third-order Møller–Plesset perturbation theory and its spin-component and spin-opposite scaled variants for thermochemistry and kinetics,” *J. Chem. Theory Comput.* **9**, 1452–1460 (2013).
- R. C. Lochan and M. Head-Gordon, “Orbital-optimized opposite-spin scaled second-order correlation: An economical method to improve the description of open-shell molecules,” *J. Chem. Phys.* **126**, 164101 (2007).
- R. M. Razban, D. Stück, and M. Head-Gordon, “Addressing first derivative discontinuities in orbital-optimized opposite-spin scaled second-order perturbation theory with regularisation,” *Mol. Phys.* **115**, 2102–2109 (2017).
- U. Bozkaya and C. D. Sherrill, “Orbital-optimized MP2.5 and its analytic gradients: Approaching CCSD(T) quality for noncovalent interactions,” *J. Chem. Phys.* **141**, 204105 (2014).

- <sup>19</sup>E. Soydaş and U. Bozkaya, "Assessment of orbital-optimized MP2.5 for thermochemistry and kinetics: Dramatic failures of standard perturbation theory approaches for aromatic bond dissociation energies and barrier heights of radical reactions," *J. Chem. Theory Comput.* **11**, 1564–1573 (2015).
- <sup>20</sup>U. Bozkaya, "Orbital-optimized MP3 and MP2.5 with density-fitting and cholesky decomposition approximations," *J. Chem. Theory Comput.* **12**, 1179–1188 (2016).
- <sup>21</sup>P. S. Epstein, "The Stark effect from the point of view of Schroedinger's quantum theory," *Phys. Rev.* **28**, 695–710 (1926).
- <sup>22</sup>R. K. Nesbet, "Configuration interaction in orbital theories," *Proc. R. Soc. London, Ser. A* **230**, 312 (1955).
- <sup>23</sup>C. Murray and E. R. Davidson, "Different forms of perturbation theory for the calculation of the correlation energy," *Int. J. Quantum Chem.* **43**, 755–768 (1992).
- <sup>24</sup>P. R. Surján and Á. Szabados, "Appendix to 'studies in perturbation theory': The problem of partitioning," in *Fundamental World of Quantum Chemistry, A Tribute to the Memory of Per-Olov Löwdin*, edited by E. J. Brändas and E. S. Kryachko (Kluwer, Dordrecht, 2004), Vol. III, pp. 129–185.
- <sup>25</sup>R. F. Fink, "The multi-reference retaining the excitation degree perturbation theory: A size-consistent, unitary invariant, and rapidly convergent wavefunction based *ab initio* approach," *Chem. Phys.* **356**, 39–46 (2009).
- <sup>26</sup>R. F. Fink, "Two new unitary-invariant and size-consistent perturbation theoretical approaches to the electron correlation energy," *Chem. Phys. Lett.* **428**, 461–466 (2006).
- <sup>27</sup>K. G. Dyall, "The choice of a zeroth-order Hamiltonian for second-order perturbation theory with a complete active space self-consistent-field reference function," *J. Chem. Phys.* **102**, 4909–4918 (1995).
- <sup>28</sup>R. F. Fink, "Why does MP2 work?," *J. Chem. Phys.* **145**, 184101 (2016).
- <sup>29</sup>S. Behnle and R. F. Fink, "REMP: A hybrid perturbation theory providing improved electronic wavefunctions and properties," *J. Chem. Phys.* **150**, 124107 (2019).
- <sup>30</sup>S. Behnle and R. F. Fink, "OO-REMP: Approaching chemical accuracy with second-order perturbation theory," *J. Chem. Theory Comput.* **17**, 3259 (2021).
- <sup>31</sup>S. Behnle and R. F. Fink, "UREMP, RO-REMP, and OO-REMP: Hybrid perturbation theories for open-shell electronic structure calculations," *J. Chem. Phys.* **156**, 124103 (2022).
- <sup>32</sup>J. A. Pople, R. Krishnan, H. B. Schlegel, and J. S. Binkley, "Derivative studies in Hartree-Fock and Møller-Plesset theories," *Int. J. Quantum Chem.* **16**, 225–241 (1979).
- <sup>33</sup>N. C. Handy, R. D. Amos, J. F. Gaw, J. E. Rice, and E. D. Simandiras, "The elimination of singularities in derivative calculations," *Chem. Phys. Lett.* **120**, 151–158 (1985).
- <sup>34</sup>R. J. Harrison, G. B. Fitzgerald, W. D. Laidig, and R. J. Barteltt, "Analytic MBPT(2) second derivatives," *Chem. Phys. Lett.* **124**, 291–294 (1986).
- <sup>35</sup>P. Jørgensen and T. Helgaker, "Møller-Plesset energy derivatives," *J. Chem. Phys.* **89**, 1560–1570 (1988).
- <sup>36</sup>T. Helgaker, P. Jørgensen, and N. C. Handy, "A numerically stable procedure for calculating Møller-Plesset energy derivatives, derived using the theory of Lagrangians," *Theor. Chim. Acta* **76**, 227–245 (1989).
- <sup>37</sup>U. Bozkaya and C. D. Sherrill, "Orbital-optimized coupled-electron pair theory and its analytic gradients: Accurate equilibrium geometries, harmonic vibrational frequencies, and hydrogen transfer reactions," *J. Chem. Phys.* **139**, 054104 (2013).
- <sup>38</sup>L. Goerigk, A. Hansen, C. Bauer, S. Ehrlich, A. Najibi, and S. Grimme, "A look at the density functional theory zoo with the advanced GMTKN55 database for general main group thermochemistry, kinetics and noncovalent interactions," *Phys. Chem. Chem. Phys.* **19**, 32184–32215 (2017).
- <sup>39</sup>É. Brémond, M. Savarese, N. Q. Su, Á. J. Pérez-Jiménez, X. Xu, J. C. Sancho-García, and C. Adamo, "Benchmarking density functionals on structural parameters of small-/medium-sized organic molecules," *J. Chem. Theory Comput.* **12**, 459–465 (2016).
- <sup>40</sup>M. Piccardo, E. Penocchio, C. Puzzarini, M. Biczysko, and V. Barone, "Semi-experimental equilibrium structure determinations by employing B3LYP/SNSD anharmonic force fields: Validation and application to semirigid organic molecules," *J. Phys. Chem. A* **119**, 2058–2082 (2015).
- <sup>41</sup>E. Penocchio, M. Piccardo, and V. Barone, "Semiexperimental equilibrium structures for building blocks of organic and biological molecules: The B2PLYP route," *J. Chem. Theory Comput.* **11**, 4689–4707 (2015).
- <sup>42</sup>R. Fink and V. Staemmler, "A multi-configuration reference CEPA method based on pair natural orbitals," *Theor. Chim. Acta* **87**, 129–145 (1993).
- <sup>43</sup>R. Fink, "Entwicklung eines Mehrkonfigurations-CEPA-Programms unter Benutzung von PNO's und Anwendung auf organisch chemische Fragestellungen," Ph.D. dissertation (Ruhr-Universität Bochum, Bochum, Germany, 1991).
- <sup>44</sup>D. G. A. Smith, L. A. Burns, A. C. Simmonett, R. M. Parrish, M. C. Schieber, R. Galvelis, P. Kraus, H. Kruse, R. Di Remigio, A. Alenaizan, A. M. James, S. Lehtola, J. P. Misiewicz, M. Scheurer, R. A. Shaw, J. B. Schriber, Y. Xie, Z. L. Glick, D. A. Sirianni, J. S. O'Brien, J. M. Waldrop, A. Kumar, E. G. Hohenstein, B. P. Pritchard, B. R. Brooks, H. F. Schaefer, A. Y. Sokolov, K. Patkowski, A. E. DePrince, U. Bozkaya, R. A. King, F. A. Evangelista, J. M. Turney, T. D. Crawford, and C. D. Sherrill, "PSI4 1.4: Open-source software for high-throughput quantum chemistry," *J. Chem. Phys.* **152**, 184108 (2020).
- <sup>45</sup>V. Staemmler and R. Jaquet, "CEPA calculations on open-shell molecules. I. Outline of the method," *Theor. Chim. Acta* **59**, 487–500 (1981).
- <sup>46</sup>U. Meier and V. Staemmler, "An efficient first-order CASSCF method based on the renormalized Fock-operator technique," *Theor. Chim. Acta* **76**, 95–111 (1989).
- <sup>47</sup>J. Wasilewski, "Graphical techniques in the configuration interaction approach based on pure Slater determinants," *Int. J. Quantum Chem.* **36**, 503–524 (1989).
- <sup>48</sup>REMP-enhanced fork of the psi4 repository, 2022.
- <sup>49</sup>F. Neese, "The ORCA program system," *Wiley Interdiscip. Rev.: Comput. Mol. Sci.* **2**, 73–78 (2012).
- <sup>50</sup>F. Neese, "Software update: The ORCA program system, version 4.0," *Wiley Interdiscip. Rev.: Comput. Mol. Sci.* **8**, e1327 (2018).
- <sup>51</sup>TURBOMOLE V6.5 2013, a development of University of Karlsruhe and Forschungszentrum Karlsruhe GmbH, 1989–2007, TURBOMOLE GmbH, since 2007, available at <http://www.turbomole.com>, 2013.
- <sup>52</sup>F. Pawłowski, P. Jørgensen, J. Olsen, F. Hegelund, T. Helgaker, J. Gauss, K. L. Bak, and J. F. Stanton, "Molecular equilibrium structures from experimental rotational constants and calculated vibration-rotation interaction constants," *J. Chem. Phys.* **116**, 6482–6496 (2002).
- <sup>53</sup>C. E. Warden, D. G. A. Smith, L. A. Burns, U. Bozkaya, and C. D. Sherrill, "Efficient and automated computation of accurate molecular geometries using focal-point approximations to large-basis coupled-cluster theory," *J. Chem. Phys.* **152**, 124109 (2020).
- <sup>54</sup>F. J. Lovas, E. Tiemann, J. S. Coursey, S. A. Kotochigova, J. Chang, v. Olsen, and R. A. Dragoset, Diatomic spectral database–NIST standard reference database 114, 2005.
- <sup>55</sup>P. R. Tentscher and J. S. Arey, "Geometries and vibrational frequencies of small radicals: Performance of coupled cluster and more approximate methods," *J. Chem. Theory Comput.* **8**, 2165–2179 (2012).
- <sup>56</sup>P. Jensen and P. R. Bunker, "The potential surface and stretching frequencies of  $\tilde{X}^3B_1$  methylene ( $\text{CH}_2$ ) determined from experiment using the morse oscillator-rigid bender internal dynamics Hamiltonian," *J. Chem. Phys.* **89**, 1327–1332 (1988).
- <sup>57</sup>E. F. C. Byrd, C. D. Sherrill, and M. Head-Gordon, "The theoretical prediction of molecular radical species: A systematic study of equilibrium geometries and harmonic vibrational frequencies," *J. Phys. Chem. A* **105**, 9736–9747 (2001).
- <sup>58</sup>J. A. Coxon and P. G. Hajigeorgiou, "On the direct determination of analytical diatomic potential energy functions from spectroscopic data: The  $X^1\Sigma^+$  electronic states of NaF, LiI, CS, and SiS," *Chem. Phys.* **167**, 327–340 (1992).
- <sup>59</sup>J. H. Baraban, P. B. Changala, and J. F. Stanton, "The equilibrium structure of hydrogen peroxide," *J. Mol. Spectrosc.* **343**, 92–95 (2018).
- <sup>60</sup>P. Turner and I. Mills, "The infrared spectrum, equilibrium structure and harmonic and anharmonic force field of thiobromine, HBS," *Mol. Phys.* **46**, 161–170 (1982).

- <sup>61</sup>S. Coriani, D. Marchesan, J. Gauss, C. Hättig, T. Helgaker, and P. Jørgensen, "The accuracy of *ab initio* molecular geometries for systems containing second-row atoms," *J. Chem. Phys.* **123**, 184107 (2005).
- <sup>62</sup>D. M. Bittner and P. F. Bernath, "Line lists for LiF and LiCl in the  $X^1\Sigma^+$  ground state," *Astrophys. J., Suppl. Ser.* **235**, 8 (2018).
- <sup>63</sup>K. Kobayashi and S. Saito, "The microwave spectrum of the NF radical in the second electronically excited ( $b^1\Sigma^+$ ) state: Potentials of three low-lying states ( $X^3\Sigma^-, a^1\Delta, b^1\Sigma^+$ )," *J. Chem. Phys.* **108**, 6606–6610 (1998).
- <sup>64</sup>M. Melosso, L. Bizzocchi, F. Tamassia, C. Degli Esposti, E. Canè, and L. Dore, "The rotational spectrum of  $^{15}\text{ND}$ . Isotopic-independent Dunham-type analysis of the imidogen radical," *Phys. Chem. Chem. Phys.* **21**, 3564–3573 (2019).
- <sup>65</sup>Y. Morino, M. Tanimoto, S. Saito, E. Hirota, R. Awata, and T. Tanaka, "Microwave spectrum of nitrogen dioxide in excited vibrational states—Equilibrium structure," *J. Mol. Spectrosc.* **98**, 331–348 (1983).
- <sup>66</sup>*NIST Standard Reference Database 69: NIST Chemistry Webbook* (National Institute of Standards and Technology, 2022).
- <sup>67</sup>J.-G. Lahaye, R. Vandenhoute, and A. Fayt, " $\text{CO}_2$  laser saturation Stark spectra and global rovibrational analysis of the main isotopic species of carbonyl sulfide ( $\text{OC}^{34}\text{S}$ ,  $\text{O}^{13}\text{CS}$ , and  $^{18}\text{OCS}$ )," *J. Mol. Spectrosc.* **123**, 48–83 (1987).
- <sup>68</sup>D. A. Helms and W. Gordy, "Forbidden rotational spectra of symmetric-top molecules:  $\text{PH}_3$  and  $\text{PD}_3$ ," *J. Mol. Spectrosc.* **66**, 206–218 (1977).
- <sup>69</sup>T. Helgaker, W. Klopper, H. Koch, and J. Noga, "Basis-set convergence of correlated calculations on water," *J. Chem. Phys.* **106**, 9639–9646 (1997).
- <sup>70</sup>K. P. Huber and G. Herzberg, *Molecular Spectra and Molecular Structure* (Springer, Boston, MA, 1979), p. 716.
- <sup>71</sup>W. D. Anderson, M. C. L. Gerry, and R. W. Davis, "The microwave spectrum of isotopically substituted hypochlorous acid: Determination of the molecular structure," *J. Mol. Spectrosc.* **115**, 117–130 (1986).
- <sup>72</sup>T. H. Edwards, N. K. Moncur, and L. E. Snyder, "Ground-state molecular constants of hydrogen sulfide," *J. Chem. Phys.* **46**, 2139–2142 (1967).
- <sup>73</sup>P. G. Szalay, L. S. Thøgersen, J. Olsen, M. Kállay, and J. Gauss, "Equilibrium geometry of the ethynyl (CCH) radical," *J. Phys. Chem. A* **108**, 3030–3034 (2004).
- <sup>74</sup>J. Chen and P. J. Dagdigan, "The DNF  $\tilde{A}^2A'-\tilde{X}^2A''$  band system: Rotational analysis of the origin band and partial analysis of several higher bands," *J. Mol. Spectrosc.* **162**, 152–167 (1993).
- <sup>75</sup>J. Vázquez and J. F. Stanton, "Theoretical investigation of the structure and vibrational spectrum of the electronic ground state  $\tilde{X}(^1A')$  of  $\text{HSiCl}_2$ ," *J. Phys. Chem. A* **106**, 4429–4434 (2002).
- <sup>76</sup>J. Demaison, L. Margulès, and J. E. Boggs, "Equilibrium structure and force field of  $\text{NH}_2$ ," *Phys. Chem. Chem. Phys.* **5**, 3359–3363 (2003).
- <sup>77</sup>C. Yamada, H. Kanamori, E. Hirota, N. Nishiwaki, N. Itabashi, K. Kato, and T. Goto, "Detection of the silylene  $\text{V}_2$  band by infrared diode laser kinetic spectroscopy," *J. Chem. Phys.* **91**, 4582–4586 (1989).
- <sup>78</sup>V. Meyer, D. H. Sutter, and H. Dreizler, "The centrifugally induced pure rotational spectrum and the structure of sulfur trioxide. A microwave Fourier transform study of a nonpolar molecule," *Z. Naturforsch., A* **46**, 710–714 (1991).
- <sup>79</sup>H. Lew and I. Heiber, "Spectrum of  $\text{H}_2\text{O}^+$ ," *J. Chem. Phys.* **58**, 1246–1247 (1973).
- <sup>80</sup>J. M. Brown and D. A. Ramsay, "Axis switching in the transition of  $\text{HCO}$ : Determination of molecular geometry," *Can. J. Phys.* **53**, 2232–2241 (1975).
- <sup>81</sup>Y. Beers and C. J. Howard, "The spectrum of  $\text{DO}_2$  near 60 GHz and the structure of the hydroperoxyl radical," *J. Chem. Phys.* **64**, 1541–1543 (1976).
- <sup>82</sup>J. S. Coursey, D. J. Schwab, J. J. Tsai, and R. A. Dragoset, "Atomic weights and isotopic compositions (version 4.1)," National Institute of Standards and Technology, Gaithersburg, MD; Available at <http://physics.nist.gov/Com>.
- <sup>83</sup>K. K. Irikura, "Experimental vibrational zero-point energies: Diatomic molecules," *J. Phys. Chem. Ref. Data* **36**, 389–397 (2007).
- <sup>84</sup>W. S. Benedict, N. Gailar, and E. K. Plyler, "Rotation-vibration spectra of deuterated water vapor," *J. Chem. Phys.* **24**, 1139–1165 (1956).
- <sup>85</sup>P. R. Herman, P. E. LaRocque, and B. P. Stoicheff, "Vacuum ultraviolet laser spectroscopy. V. Rovibronic spectra of  $\text{AR}_2$  and constants of the ground and excited states," *J. Chem. Phys.* **89**, 4535–4549 (1988).
- <sup>86</sup>R. L. Cook, F. C. De Lucia, and P. Helminger, "Molecular force field and structure of hydrogen sulfide: Recent microwave results," *J. Mol. Struct.* **28**, 237–246 (1975).
- <sup>87</sup>G. Strey and I. M. Mills, "Anharmonic force field of acetylene," *J. Mol. Spectrosc.* **59**, 103–115 (1976).
- <sup>88</sup>W. Quapp, "A redefined anharmonic potential energy surface of HCN," *J. Mol. Spectrosc.* **125**, 122–127 (1987).
- <sup>89</sup>J. L. Duncan, D. C. McKean, and P. D. Mallinson, "Infrared crystal spectra of  $\text{C}_2\text{H}_4$ ,  $\text{C}_2\text{D}_4$ , and *as*- $\text{C}_2\text{H}_2\text{D}_2$  and the general harmonic force field of ethylene," *J. Mol. Spectrosc.* **45**, 221–246 (1973).
- <sup>90</sup>H. Müller, R. Franke, S. Vogtner, R. Jaquet, and W. Kutzelnigg, "Toward spectroscopic accuracy of *ab initio* calculations of vibrational frequencies and related quantities: A case study of the HF molecule," *Theor. Chem. Acc.* **100**, 85–102 (1998).
- <sup>91</sup>M. M. Wohar and P. W. Jagodzinski, "Infrared spectra of  $\text{H}_2\text{CO}$ ,  $\text{H}_2^{13}\text{CO}$ ,  $\text{D}_2\text{CO}$ , and  $\text{D}_2^{13}\text{CO}$  and anomalous values in vibrational force fields," *J. Mol. Spectrosc.* **148**, 13–19 (1991).
- <sup>92</sup>G. E. Scuseria, A. C. Scheiner, J. E. Rice, T. J. Lee, and H. F. Schaefer III, "Analytic evaluation of energy gradients for the single and double excitation coupled cluster (CCSD) wave function: A comparison with configuration interaction (CCSD, CISDT, and CISDTQ) results for the harmonic vibrational frequencies, infrared intensities, dipole moment, and inversion barrier of ammonia," *Int. J. Quantum Chem.* **32**, 495–501 (1987).
- <sup>93</sup>T. J. Lee, J. M. L. Martin, and P. R. Taylor, "An accurate *ab initio* quartic force field and vibrational frequencies for  $\text{CH}_4$  and isotopomers," *J. Chem. Phys.* **102**, 254–261 (1995).
- <sup>94</sup>E. Hirota and H. Ishikawa, "The vibrational spectrum and molecular constants of silicon dihydride  $\text{SiH}_2$  in the ground electronic state," *J. Chem. Phys.* **110**, 4254–4257 (1999).
- <sup>95</sup>F. Pawłowski, A. Halkier, P. Jørgensen, K. L. Bak, T. Helgaker, and W. Klopper, "Accuracy of spectroscopic constants of diatomic molecules from *ab initio* calculations," *J. Chem. Phys.* **118**, 2539–2549 (2003).
- <sup>96</sup>F. Wennmohs and F. Neese, "A comparative study of single reference correlation methods of the coupled-pair type," *Chem. Phys.* **343**, 217–230 (2008).
- <sup>97</sup>U. Bozkaya, "Analytic energy gradients for the orbital-optimized third-order Møller–Plesset perturbation theory," *J. Chem. Phys.* **139**, 104116 (2013).
- <sup>98</sup>T. Bodenstein and S. Kvaal, "A state-specific multireference coupled-cluster method based on the bivariational principle," *J. Chem. Phys.* **153**, 024106 (2020).
- <sup>99</sup>D. Hait and M. Head-Gordon, "How accurate is density functional theory at predicting dipole moments? An assessment using a new database of 200 benchmark values," *J. Chem. Theory Comput.* **14**, 1969–1981 (2018).
- <sup>100</sup>U. Bozkaya, E. Soydaş, and B. Filiz, "State-of-the-art computations of dipole moments using analytic gradients of high-level density-fitted coupled-cluster methods with focal-point approximations," *J. Comput. Chem.* **41**, 769–779 (2020).
- <sup>101</sup>R. Sarkar, M. Boggio-Pasqua, P.-F. Loos, and D. Jacquemin, "Benchmarking TD-DFT and wave function methods for oscillator strengths and excited-state dipole moments," *J. Chem. Theory Comput.* **17**, 1117–1132 (2021).
- <sup>102</sup>R. F. Fink, "Spin-component-scaled Møller–Plesset (SCS-MP) perturbation theory: A generalization of the MP approach with improved properties," *J. Chem. Phys.* **133**, 174113 (2010).
- <sup>103</sup>H. R. Larsson, H. Zhai, K. Gunst, and G. K.-L. Chan, "Matrix product states with large sites," *J. Chem. Theory Comput.* **18**, 749–762 (2022).
- <sup>104</sup>M. Saitow and T. Yanai, "A multireference coupled-electron pair approximation combined with complete-active space perturbation theory in local pair-natural orbital framework," *J. Chem. Phys.* **152**, 114111 (2020).
- <sup>105</sup>S. Sharma, G. Knizia, S. Guo, and A. Alavi, "Combining internally contracted states and matrix product states to perform multireference perturbation theory," *J. Chem. Theory Comput.* **13**, 488–498 (2017).
- <sup>106</sup>G. Jeanmairet, S. Sharma, and A. Alavi, "Stochastic multi-reference perturbation theory with application to the linearized coupled cluster method," *J. Chem. Phys.* **146**, 044107 (2017).

<sup>107</sup>P. Celani and H.-J. Werner, “Multireference perturbation theory for large restricted and selected active space reference wave functions,” *J. Chem. Phys.* **112**, 5546–5557 (2000).

<sup>108</sup>P. Celani and H.-J. Werner, “Analytical energy gradients for internally contracted second-order multireference perturbation theory,” *J. Chem. Phys.* **119**, 5044–5057 (2003).

<sup>109</sup>Y. Nishimoto, S. Battaglia, and R. Lindh, “Analytic first-order derivatives of (X)MS, XDW, and RMS variants of the CASPT2 and RASPT2 methods,” *J. Chem. Theory Comput.* **18**, 4269 (2022).

<sup>110</sup>J. W. Park, “Analytical gradient theory for strongly contracted (SC) and partially contracted (PC) *N*-electron valence state perturbation theory (NEVPT2),” *J. Chem. Theory Comput.* **15**, 5417–5425 (2019).